Catalytic Asymmetric Synthesis of Benzofuran Derivatives and Desymmetrization Reactions to Generate Chiral Pyrrole Compounds

A Dissertation

Submitted in Partial Fulfilment of the

Requirements for the Degree of

Doctor of Philosophy

by

Rupkumar Khuntia

(Roll No.- 196122026)

Department of Chemistry

Indian Institute of Technology Guwahati

Guwahati, Assam, 781039

APRIL 2025

Dedicated to

My Family

Indian Institute of Technology Guwahati

Department of Chemistry

Guwahati, Assam-781039

STATEMENT

I, hereby declared that the work comprised in this thesis entitled "***Catalytic Asymmetric Synthesis of Benzofuran Derivatives and Desymmetrization Reactions to Generate Chiral Pyrrole Compounds***" is the outcome of the research work carried out by me under the supervision of **Prof. Subhas Chandra Pan**, Department of Chemistry, Indian Institute of Technology Guwahati, India, for the award of the degree of Doctor of Philosophy.

In harmony with the general practice of reporting scientific observations, due acknowledgements have been made if the work is established on the findings of other investigators.

Rupkumar Khuntia.

Guwahati

April 2025

Rupkumar Khuntia

Roll No.- 196122026

Department of chemistry

IIT Guwahati

Indian Institute of Technology Guwahati

Department of Chemistry

Guwahati, Assam-781039, India

Tel. No.: +91-361-25833004

Prof. Subhas Chandra Pan **e-mail: span@iitg.ac.in**

Professor

CERTIFICATE

This is to certify that the work incorporated in the thesis entitled "***Catalytic Asymmetric Synthesis of Benzofuran Derivatives and Desymmetrization Reactions to Generate Chiral Pyrrole Compounds***" which is being submitted to the Indian Institute of Technology Guwahati for the award of ***Doctor of Philosophy*** in Chemistry by ***Mr. Rupkumar Khuntia*** (Roll No: 196122026) was carried out by him under my supervision at this institute. The work presented in his thesis is original and that has not been submitted elsewhere for a degree.

Subhas Ch. Pan

Guwahati
April 2025

Prof. Subhas Chandra Pan
Professor, Department of Chemistry
IIT Guwahati

Acknowledgements

I would like to appreciate all the peoples around me who have assisted and guided me throughout my academic journey. It would have been impossible to finish all the work presented in this thesis without the help of many individuals.

First of all, I would like to express my sincere gratitude to my supervisor **Prof. Subhas Chandra Pan** for giving me an opportunity to work in such a beautiful research environment and for introducing me to this challenging yet fascinating field of asymmetric catalysis. I am extremely grateful to him for his inspiring guidance, support, helpful discussions throughout my research work.

I would like to acknowledge my doctoral committee members **Prof. Bhisma Kumar Patel** (Chairman), **Prof. Dipankar Srimani** and **Dr. Akshai Kumar A. S.** (member) for their valuable suggestions and encouragements which helped a lot to improve my thesis.

I extend my sincere thanks to the **Dr. Lisa Roy** from ICT IOC Bhubaneswar and **Dr. Kalishankar Bhattacharyya** from IIT Guwahati for his collaborative assistance during my research work.

I am thankful to IIT Guwahati for the fellowship and also thankful to IIT Guwahati, Department of Chemistry and Central Instruments Facilities (CIF) for providing research facilities and instrumental facilities. I will always remain thankful to the staff members of CIF and department of chemistry.

My deepest gratitude to my dear lab mates Dr. Subas Chandra Sahoo, Dr. Megha Balha, Dr. Chandan Gharui, Dr. Nimisha Bania, Dr. Chandrakanta Parida, Dr. Amit Shikari, Subhankar Biswas, Dipankar Barman, Jyotish Barman, Ramji Meher, Gaurav Jaiswal, Dipali Digangana Sahoo, Sujan Sarkar and Dwiti Krishna Mishra for their great support during my Ph.D. period. I sincerely thank to my project student Subhrajit Karmakar, Diptendu Maity, Rujuma Begum, Ankita Roy for her contribution in my works.

I am thankful to all NMR, XRD and HRMS operators especially Abhay Pratap Singh for help in solving crystal structure.

I am grateful to all my teachers throughout my academic career for their constant encouragement and guidance starting from my school life, until today.

My special thanks to K V Mahendra, Subhrajyoti Ghosh, Hirendranath Dhara, Aniket Banerjee and, my Ph.D. batch mates, seniors and juniors who helped during my work and for making a friendly environment.

I could not have completed my PhD endeavour without the endless love, support, and blessings from my parents. I am deeply grateful to my father, **Paltu Khuntia**, my mother, **Gita Rani Khuntia**, and my elder brother, **Rajkumar Khuntia**. I would also like to extend my heartfelt appreciation to my aunt, **Monorama Maity**, who raised me as her own son. Without her nurturing, I would not have been able to reach this significant milestone. I would like to praise my thanks to my grandparents **late Bhagaban Chandra Maity, Ms. Manjurani Maity**, **Uncle Santosh Maity**. I feel truly blessed to have these pillars of strength in my life. I thank the Almighty for making all this possible and giving me strength and determination to work.

Sincerely,

Rupkumar Khuntia

Table of content

Abbreviation

Ac	Acetyl
AcOH	Acetic acid
anh.	Anhydrous
aq.	Aqueous
Å	Angstrom
Ar	Aryl
BINOL	1,1'-Bi-2-naphthol
br.	Broad
Bn	Benzyl
Boc	tert-Butyloxycarbonyl
Bu	Butyl
CCDC	Cambridge crystallographic data
COSY	Correlation spectroscopy
CPME	Cyclopentyl methyl ether
Cy	Cyclohexyl
°C	Degree celsius
d	Doublet or day
δ	Chemical shift or delta
DACH	*trans*-(1,2)-Diaminocyclohexane
DBU	1,8-Diazabicyclo[5.4.0]undec-7-
DCE	Dichloroethane
DCM	Dichloromethane
DDQ	2,3-Dichloro-5,6-dicyano-1,4-
DIPEA	N,N-Diisopropylethylamine
DME	Dimethoxyethane
DME	Dimethoxyethane
DMF	N,N-Dimethylformamide
DMAP	4-(Dimethylamino)pyridine
DMSO	Dimethylsulfoxide
dr	Diastereomeric ratio
δ	Delta
EtOAc	Ethyl acetate
ee	Enantiomeric excess
er	Enantiomeric ratio
equiv.	Equivalent
ESI	Electrospray ionization
Et	Ethyl
EWG	Electron withdrawing group
EDG	Electron donating group
FT-IR	Fourier-transform infrared
g	Grams
γ	Gamma
h	Hours
H-bonding	Hydrogen-bonding
HOMO	Highest occupied molecular

HPLC	High performance liquid
HRMS	High resolution mass
Hz	Hertz
i	Iso
J	Coupling constant
LUMO	Lowest unoccupied molecular
m	Multiplet
m	*Meta*
mCPBA	*meta*-Chloroperoxybenzoic acid
Me	Methyl
mg	Miligram
mL	Mililitre
mmol	Milimole
m.p.	Melting point
MS	Molecular seives
MTBE	Methy tertiary butyl ether
NHC	N-Heterocyclic carbene
NMR	Nuclear magnetic resonance
NOESY	Nuclear overhauser
o	*Ortho*
ORTEP	Oak ridge thermal ellipsoid plot
p	*Para*
PG	Protecting group
Ph	Phenyl
Pr	propyl
ppm	Parts per million
p-TSA	*p-Toluenesulfonic acid*
q	Quartet
rac	Racemic
RCM	Ring-closing metathesis
rt	Room temperature
s	Singlet
THF	Tetrahydrofuran
t	Triplet
TBS	*tert-Butyldimethylsilyl*
TES	*tert-Butyldiethylsilyl*
TFA	Trifluoroacetic acid
TLC	Thin-layer chromatography
TMS	Tetramethylsilane
Ts	*p-Tolylsulfonyl*
uv	Ultra violet
XRD	X-ray diffraction

Abstract

The thesis entitled ***"Catalytic Asymmetric Synthesis of Benzofuran Derivatives and Desymmetrization Reactions to Generate Chiral Pyrrole Compounds"*** has divided into five chapters based on the results achieved from the experimental works performed during the entire course of the Ph.D. research programme.

Chapter 1: It is the introduction part. The chapter contains a brief discussion of asymmetric catalysis. Particularly, asymmetric organocatalysis and silver/organocatalyst combined catalysis. This part also described a desymmetrization reactions.

Chapter 2: Structurally divergent enantioselective synthesis of benzofuran fused azocine derivatives and spiro-cyclopentanone benzofurans enabled by sequential catalysis

A protocol for the structurally divergent synthesis of benzofuran fused azocine derivatives and spiro-cyclopentanone benzofurans has been developed via chiral bifunctional urea catalyzed reaction between aurone-derived α,β- unsaturated imine and ynone followed by switchable divergent annulation reactions by Lewis base catalysts (DBU and PPh3). Furthermore, the mechanism study revealed, a concomitant epimerization is responsible for high dr and ees.

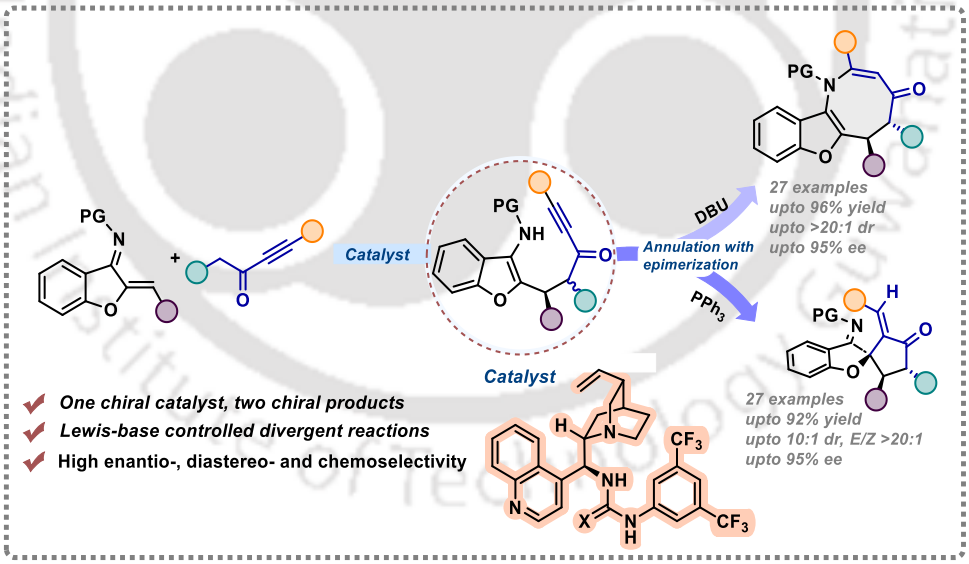

Chapter 3: Organocatalytic Regio- and Enantioselective Friedel-Crafts Alkylation of N-Aryl Anilines with Aurone-Derived Azadienes: Access to Benzofuran Embedded Triarylmethanes

Herein, we have disclosed a catalytic asymmetric Friedel-Crafts alkylation of N-aryl anilines with azadienes for the synthesis of benzofuran containing triarylmethanes. In this method, (R)-TRIP, was found to be effective for this reaction. The triarylmethanes with

benzofuran motif were obtained in moderate yields with high regio- and good to high enantioselectivities (upto 95% ee).

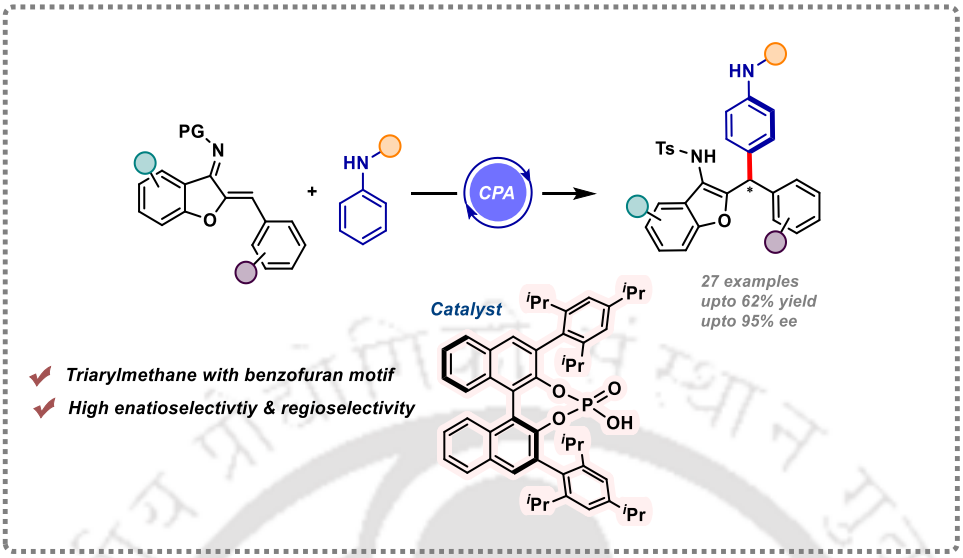

Chapter 4: Catalytic Asymmetric de novo Synthesis of Chiral Pyrroles through Desymmetrizing Oxidative [3+2]-Cycloaddition and the Van Leusen Reaction

Herein, we reported the first catalytic enantioselective de novo construction of centrally chiral pyrroles through desymmetrizing oxidative [3+2]-cycloaddition of meso cyclohexedione with isocyanoacete by employing silver catalysis. Furthermore, to introduce a more diverse set of substituents, we developed the first catalytic asymmetric the Van Leusen reaction with α–substituted TosMIC for the synthesis of centrally chiral pyrroles. In both cases, high to excellent yield and excellent ee were observed.

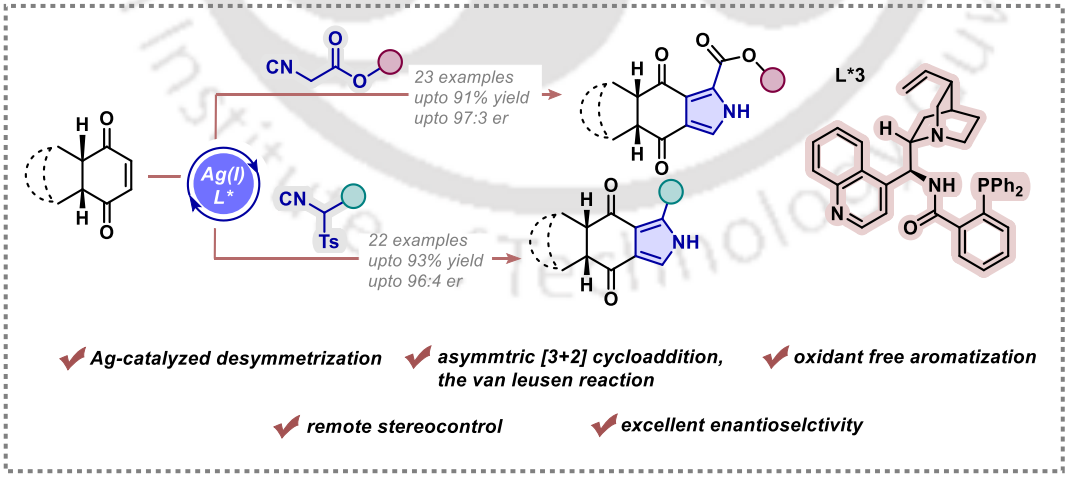

Chapter 5: Organocatalytic Asymmetric Desymmetrizing Friedel-Crafts Reaction of Prochiral 3,4-Fused Pyrroles

In this chapter, we have demonstrated the first catalytic enantioselective desymmetrizing Friedel-Crafts reaction of prochiral 3,4-fused pyrroles. Using BINOL-based substituted cyclohexylarene phosphoric acid, prochiral 3,4-fused pyrroles underwent a highly regioselective and enantioselective F-C reaction with allenamide without creating any judicious sereocenter. The mechanistic study revealed that, an ion pair mechanism felicitates the stereocontrol of the desymmetrization reaction.

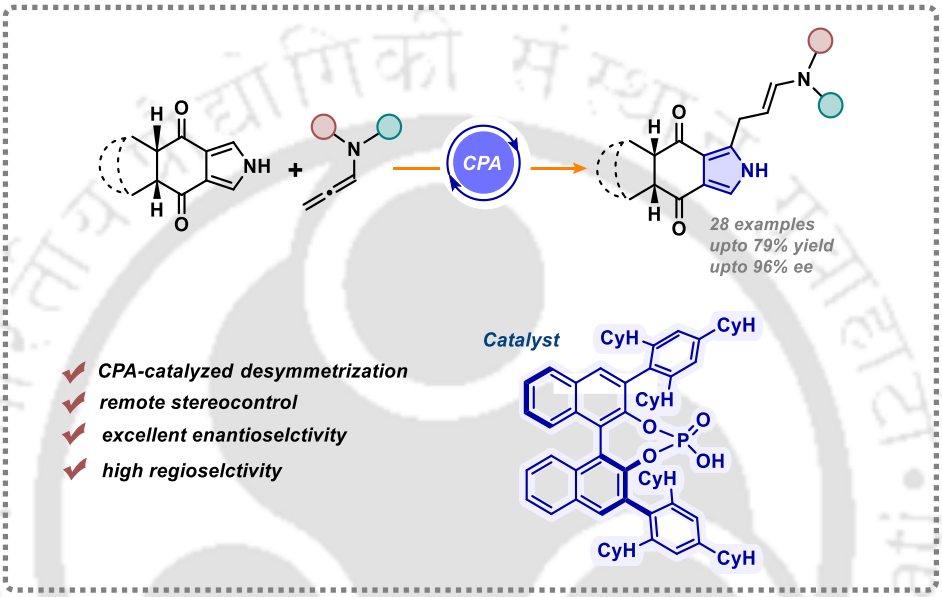

Chapter 1

Introduction

1.1 Introduction:

The word "asymmetric" merely indicates that some components or features of something aren't equal or comparable. This concept can be applied to many different objects, such as chemicals, nature, or even human bodies. René Just Haüy, a French mineralogist, initially identified the idea of chirality in 1801 while researching quartz crystals. Later, in 1847, when Louis Pasteur took things a step further by exploring paratartrate crystals.[1] He discovered that tartaric acid could exist in two different forms, which turned out to be mirror images of each other—these forms are called enantiomers.

Molecular chirality is a big deal in the field of stereochemistry and plays a crucial role in understanding living things. Although enantiomers have the same chemical and physical properties when they're in an environment without chiral influences, they behave differently in a chiral environment. For example, they differ in attributes like melting point, boiling point, color, and density.

When it comes to interacting with plane-polarized light, one enantiomer—known as dextrorotatory (d-(+))—rotates the light to the right, while the other one, called levorotatory (l-(-)), turns it to the left. However, both enantiomers cause the same amount of rotation, but in opposite directions.

An example is lavender-like aroma and scent of Japanese honeysuckle, they smell different, despite being made of the left- and right-handed versions of the same molecule, called Linalool (Fig. 1).[2] In short, enantiomers are like chiral twins that are non-superimposable structure with each other.

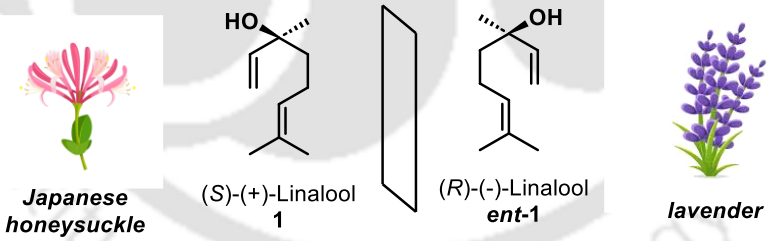

Fig. 1: The enantiomer of Linalool.

Another example, where (*S*)-(-)-asparagine possesses a bitter taste, but (*R*)-(+)-asparagine is characterized by its sweetness (Fig. 2). [3]

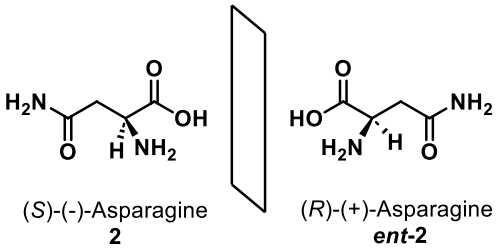

Fig. 2: The enantiomer of aspergine.

Enzymes within biological systems are chiral and predominantly exist in a single enantiomeric form, which makes them to differentiate between enantiomers. It's crucial to remember that a compound's enantiomer may produce a beneficial therapeutic effect while its opposite may have detrimental side effects. In Parkinson's disease, for example, dopamine is a successful treatment. Only (*S*)-Dopa can restore nerve function, whereas (*R*)-Dopa is known to be toxic (Fig. 3).[4]

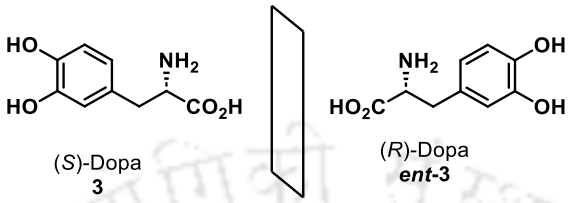

Fig. 3: The enantiomer of Dopa.

Many natural examples show that opposite enantiomers can have differing effects on biological systems. Therefore, to guarantee that natural products and therapeutic molecules have the appropriate physical, chemical, and biological qualities, they must be prepared in enantiomerically pure forms. In modern chemistry, several crucial procedures are essential, particularly in the pharmaceutical industry. Asymmetric synthesis is one important feature that favours the production of one stereoisomer (either an enantiomer or a diastereomer) over another. Four primary categories of asymmetric synthesis exist: The four types of approaches are (1) substrate-controlled, (2) auxiliary-controlled, (3) reagent-controlled, and (4) catalyst-controlled.

(1) **Substrate-controlled method:** It is a diastereoselective processes in which an existing chiral center in the substrate influences the formation of a new chiral center.

(2) **Auxiliary-controlled method:** An essential tool in organic chemistry is a chiral auxiliary, also known as a chiral molecular unit, which forms a transient bond with an achiral substrate to generate one of two stereoisomers. Only the intended reaction pathway can proceed since these optically active chemicals introduce chirality and block one attack pathway. Steric factors subsequently determine the resulting chiral center's stereochemistry.

(3) **Reagent-controlled method:** A chiral reagent controlled the formation of predominant stereoisomer.

(4) **Catalyst-controlled method:** The first three methods are costly because they required expensive chiral reagents or chiral substrates in stoichiometric quantities. In contrast, in this method, the stereochemistry of chemical reactions is largely controlled by chiral catalysts, which efficiently promote the creation of particular enantiomers, or mirror images.

Based on the catalysts' nature, The *catalyst-controlled* asymmetric synthesis categorized into three major parts.

(1) **Bio-catalysis**: It is the chemical catalytic reaction by which enzymes or other biological active catalysts carry out stereoselective, chemo-, and regio-transformations.[5] Typically, modest reaction conditions are needed for this technique. Biocatalysts do have several drawbacks, though, including substrate selectivity, sensitivity to high pH and temperature, and—above all—the inability to synthesize the opposite enantiomer because enzymes only exist in one enantiomeric form in nature.

(2) **Metal-catalysis**: Metal catalysis,[6] especially the application of organometallic catalysts, has emerged as a significant area of study because of the extraordinary transformations they facilitate, including asymmetric hydrogenation, epoxidation, and dihydroxylation of olefins, along with cross-coupling reactions and olefin metathesis. Metal catalysis has several advantages, but it also has significant drawbacks, including toxicity and the challenge of removing trace metal pollutants associated with transition-metal catalysis.

(3) **Organocatalysis:** Between these two earlier approaches, a third technique known as organocatalysis has emerged.[7] Chemical synthesis has been significantly impacted by this method. Organocatalysis is a method that uses a sub-stoichiometric amount of organic molecules without metal elements in their active regions to speed up chemical reactions.

1.2. Asymmetric Organocatalysis:

Asymmetric organocatalysis uses tiny organic molecules to promote organic processes in an economical and environment-friendly manner. This technique bypasses many of the issues typically linked to transition-metal catalysis and biocatalysis. Organocatalysts present various benefits: they are generally easy to manage, durable, stable at ambient temperatures, affordable, and in certain instances, can be purchased commercially. Particularly within the last 20 years, this discipline has advanced quickly because of the emergence of novel ideas and techniques.[8] Many distinguished awards have been given in recognition of this progress, such as 2021 Nobel prize in chemistry awarded jointly to Benjamin List and David W.C. MacMillan "for the development of asymmetric organocatalysis".

1.2.1. Mechanisms for organocatalytic reactions:

Although there are many other kinds of activation in the field of organocatalytic techniques, two main mechanistic types may be distinguished:

(1) *covalent organocatalysis* and (2) *non-covalent organocatalysis*.

These novel approaches not only increase reaction efficiency, but also open up new path for creative chemical transformation. Covalent-based activation approaches use an organic catalyst's reversible binding to a substrate to form a reactive intermediate capable of engaging in a range of reactions with high enantioselectivity (Fig. 4). Chiral primary and secondary amines are one form of catalyst. Enolizable aldehydes and ketones are

transformed into nucleophilic enamines (**I**),[9] unsaturated carbonyl compounds into electrophilic iminium ions (**II**),[10] and enamines are single-electron oxidized with a chemical oxidant to

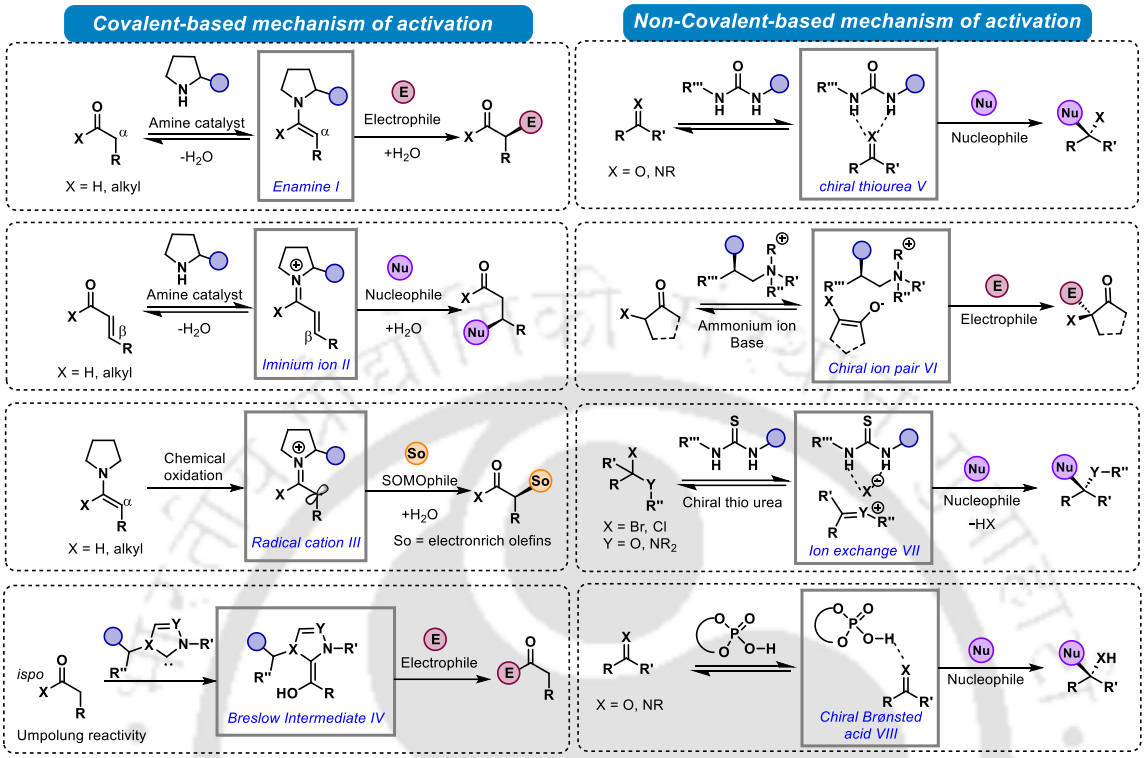

Fig 4. Reactivity of various organocatalysts.

produce α-iminyl radical cation intermediates (**III**),[11] which activate carbonyl substrates. N-heterocyclic carbene catalysts (**IV**)[12] offer aldehydes another method of activation. They alter the typically electrophilic carbonyl carbon atom's characteristic reactivity, which causes the formation of the Breslow intermediate **IV**[13] to have an umpolung reactivity. This intermediate serves as an analogue of an acyl anion.[14,15] The ipso, α, and β positions of unmodified carbonyl compounds can be stereoselectively functionalized due to activation mechanisms that rely on strong, directed interactions.

Non-covalent approaches rely on the of several weak attractive interactions between the catalyst and basic functional groups on the substrates.[16] Although these catalyst–substrate interactions are generally weaker and less directed than their covalent counterparts, they work together to achieve a high level of organization in the transition state, leading to a significant enhancement of enantioselectivity. Strategies such as hydrogen-bonding activation (**V**),[17] phase-transfer catalysis (**VI**),[18] anion-binding activation (**VII**),[19] and Brønsted acid catalysis (**VIII**)[20] are all effective organocatalytic methods for synthesizing chiral molecules.[21]

1.2.2. Hydrogen-bonding catalysis:

In the past decades, a variety of H-bonding catalysts have been synthesized and used for a broad range of asymmetric organic transformations; these catalysts can be easily divided into three groups based on their activation patterns:

i) double hydrogen bond catalyst, ii) single hydrogen bond catalyst, iii) acid/base bifunctional catalyst.

In the context of *double hydrogen bond catalysts*, the concurrent donation of dual hydrogen bonds represents an effective strategy for the activation of electrophiles (Fig. 5). A seminal example of this approach is the Schiff base developed by Jacobsen in 1998, which was designed to promote asymmetric Strecker reaction.[22] This type of catalyst was first synthesized, intended to be a possible ligand for a Lewis acidic metal catalysis. However, it was discovered that without a metal addition, an effective enantioselective catalytic Strecker reaction could be achieved. This unexpected finding greatly expanded the field of asymmetric catalysis with hydrogen bond catalysts and later attracted a lot of attention from the scientific community.

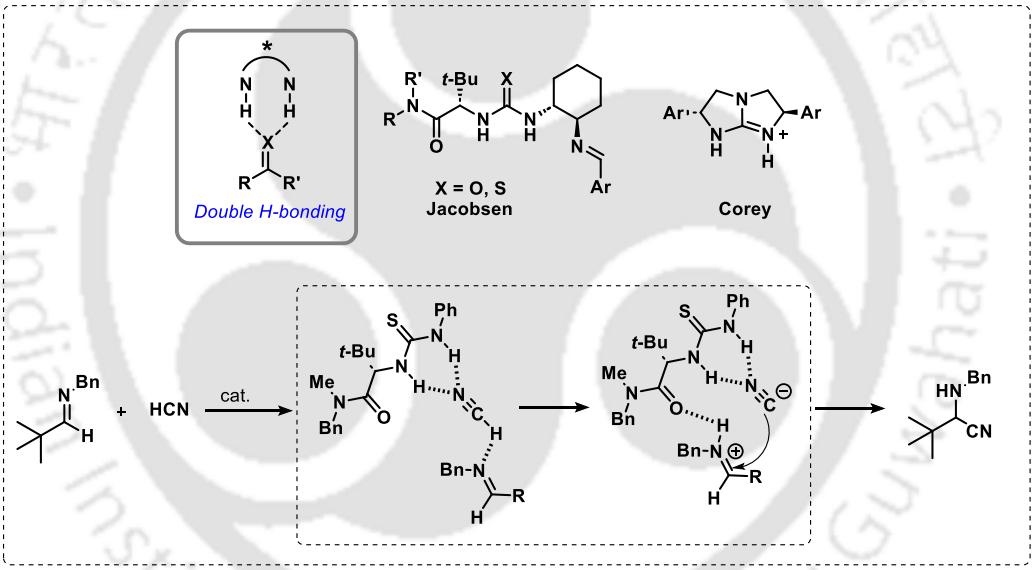

Fig. 5: double hydrogen bond catalysts reactivity and example

Double hydrogen bonding in asymmetric reactions is more common than *single hydrogen bond activation*. Excellent examples of intramolecular hydrogen bonding are chiral diol catalysts, like TADDOL[23] that effectively promotes a variety of asymmetric syntheses. For substrate binding, one of the alcohol group's hydrogen atoms donates hydrogen bonds while the other forms an intramolecular bond. While the other hydrogen atom in the alcohol group forms an intramolecular bond, the other hydrogen atom forms hydrogen bonds with the substrate (Fig. 6). X-ray crystallographic research was used to study this phenomenon. TADDOL was employed by Rawal and associates as a chiral "BBA catalyst" (Brønsted acid-assisted Brønsted acid catalyst).[24, 25] They found that only one of the intended product's enantiomers was produced by the highly enantioselective hetero-Diels-Alder reaction when axially chiral biaryl diol was present.[26]

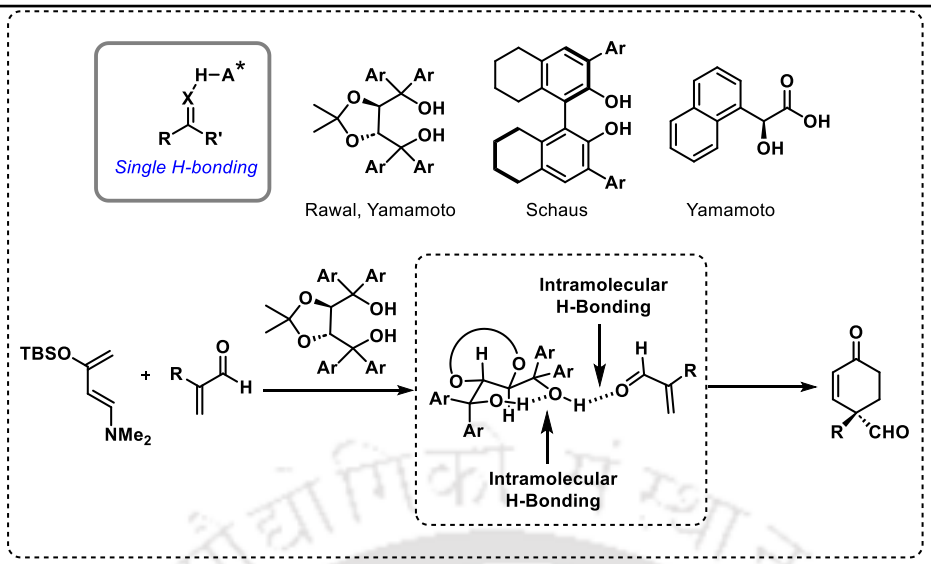

Fig. 6: Single hydrogen bonding catalysts reactivity and example.

Recently, the simultaneous activation of electrophiles and nucleophiles employing Brønsted base and acid moieties has been a major focus of hydrogen bonding catalysis (Fig. 7). This method, which began with natural catalysts such as proline[27] and cinchona alkaloids,[28] resulted in improvements in *chiral acid/base bifunctional catalysts*. The asymmetric Michael addition of 1,3-dicarbonyl compounds to nitroolefins via Takemoto's thiourea[29] catalyst is a good illustration. Two processes for this catalysis have recently been postulated, one by experimental methods[30] and the other through quantum chemical calculations,[31] both of which produce the identical product, as demonstrated.

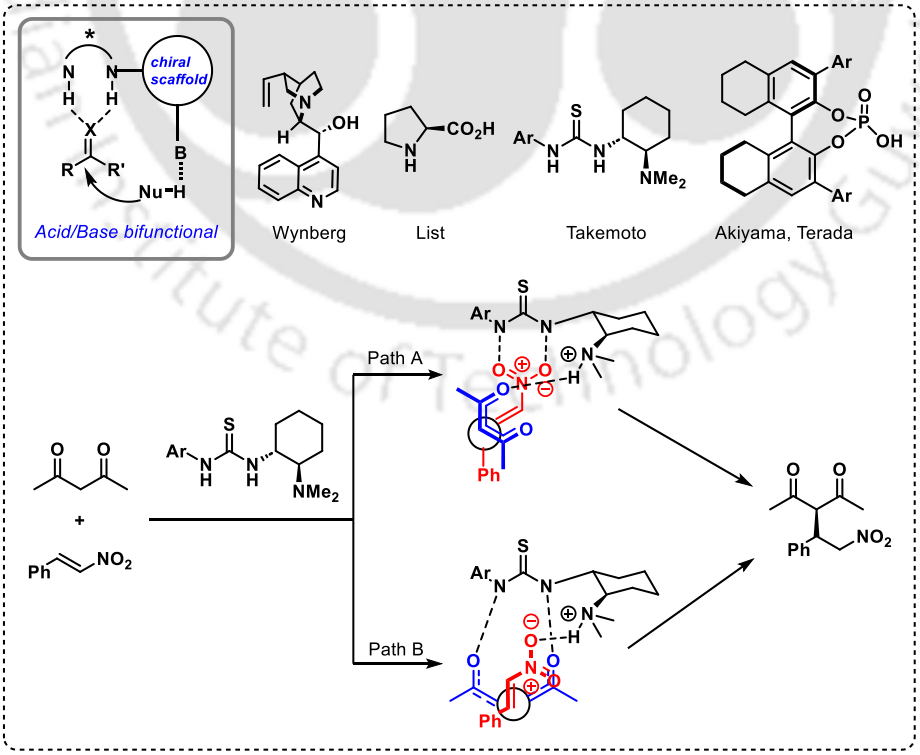

Fig. 7. Bifunctional catalysts reactivity and example.

1.2.3. Asymmetric Michael reaction:

The Michael reaction is a key process in organic chemistry, highlighting the addition of carbon nucleophiles to conjugate acceptor systems. Discovered by Arthur Michael in 1887, this reaction is well-known as the Michael addition (Scheme 1).[32]

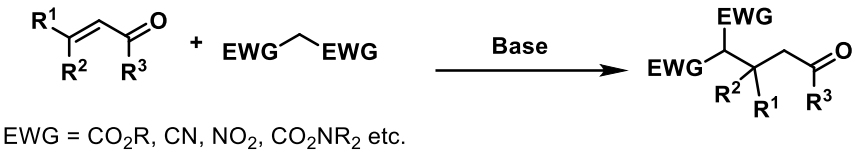

Scheme 1: Michael reaction.

Wynberg made a pivotal discovery in 1975 by introducing the first asymmetric Michael reaction (Scheme 2).[33] Using optically active quinine as a catalyst, he facilitated the addition of 1-oxo-2-indanecarboxylate to methyl vinyl ketone, achieving a moderate enantiomeric excess (ee) of 68%.

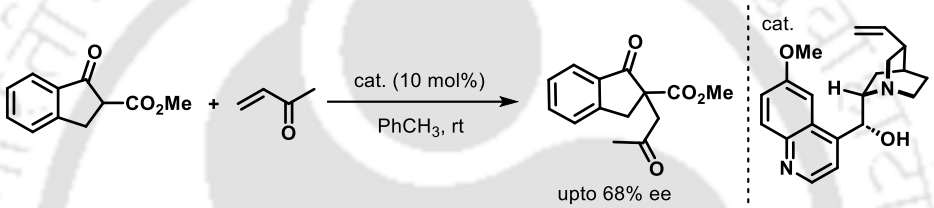

Scheme 2: First organocatalyzed Michael reaction.

1.2.4. Asymmetric Friedel−Crafts reaction:

In 1877, Charles Friedel and James Mason Crafts introduced the Friedel-Crafts reaction, a pivotal method for forming carbon−carbon bonds that requires a catalyst.[34] Traditional catalysts include Lewis acids such as $AlCl_3$, $FeCl_3$, and $TiCl_4$, as well as Brønsted acids like HF and H_2SO_4, and acidic oxide catalysts such as silica-alumina.[35] A breakthrough occurred in 2001 when MacMillan group reported the first organocatalytic asymmetric Friedel-Crafts reaction.[36] They achieved enantioselective alkylation of pyrroles with α,β-unsaturated aldehydes, generating β-pyrrolyl carbonyls with an impressive enantiomeric excess of 93% (Scheme 3). This advancement showcases the evolving potential of organocatalysis in organic synthesis.

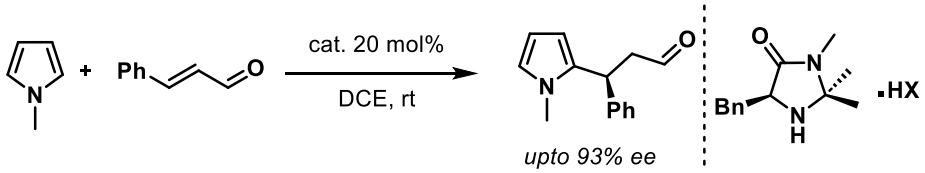

Scheme 3: First organocatalyzed Asymmetric Friedel−Crafts reaction.

1.3. Asymmetric transition-metal/organocatalyst combined catalysis:

1.3.1. Introduction:

Asymmetric transition-metal/organocatalyst combined catalysis is a promising strategy introduced 20 years ago,[37] utilizing chiral transition-metal complexes and organocatalysts. Recognized with Nobel Prizes in 2001 and 2021, asymmetric transition-metal/organocatalyst combined catalysis aims to achieve new reactivity and selectivity, including regio-, chemo-, diastereo-, and enantioselectivity, for producing single enantiomers from achiral or racemic substrates.[38] By carefully choosing a specific pair of organocatalysts and metal complexes, we can combine different and compatible bond-activation methods into a single bond-forming process, known as cooperative catalysis (Figure 8a).[39] Alternatively, these can also be utilized in a series of catalytic transformations before the final products are released, referred to as relay catalysis (Figure 8b).[40] The metal-ligand cooperation hampered by the bond length and geometry of the transition state, which may not provide an optimal chiral environment for forging new bonds.[41] However, combining a metal complex with an organocatalyst (one that does not impact metal complexation) can simplify the complicated process of creating bifunctional artificial catalysts. This combination provides additional flexibility and opens new opportunities for building reactions.

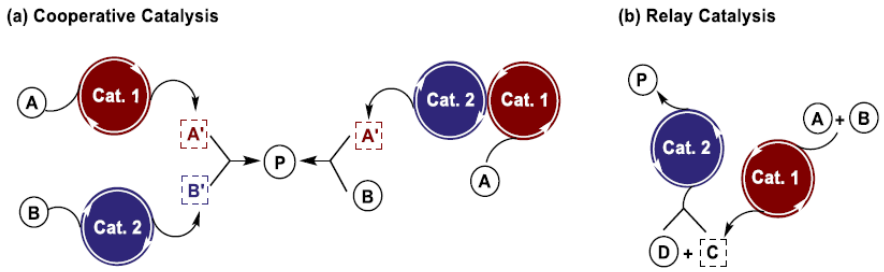

Fig. 8: Modes of Asymmetric transition-metal/organocatalyst combined catalysis.

1.3.2. Ag(I)/organocatalyst combined catalysis:

Silver(I) salts are moderately acidic Lewis compounds that serve as catalysts in organic reactions. Examples include $AgNO_3$, $AgClO_4$, $AgBF_4$, and AgOTf, which facilitate cycloadditions, rearrangements, and glycosylation by interacting well with halogen and sulfur groups, as well as carbon–carbon multiple bonds.[42] In 1990, Ito and his collaborators, first report a chiral silver(I)-catalyzed asymmetric reaction. They described that chiral ferrocenylphosphine–silver(I) complexes function as highly effective chiral catalysts in asymmetric aldol-type reactions involving isocyanoacetates or tosylmethyl isocyanide and aldehydes.[43] These have resulted in an increasing number of unique enantioselective silver-catalyzed reactions of various types (Fig. 9). There are five types of Ag(I)/organocatalyst combined catalysis available:[44] Ag(I)/Bronsted acid, Ag(I)/chiral amine, Ag(I)/bifunctional squaramide, Ag(I)/alkaloid derived phosphines and Ag(I)/chiral 2-amino pyridines. The catalysis majorly involved in silver-catalyzed asymmetric aldol-

type reaction, silver-catalyzed asymmetric Mannich reactions, silver-catalyzed asymmetric Michael reactions, asymmetric 1,3-dipolar cycloadditions, asymmetric alkynylations, asymmetric allylations, asymmetric cyclizations reaction, asymmetric aminations, asymmetric domino and tandem reactions.

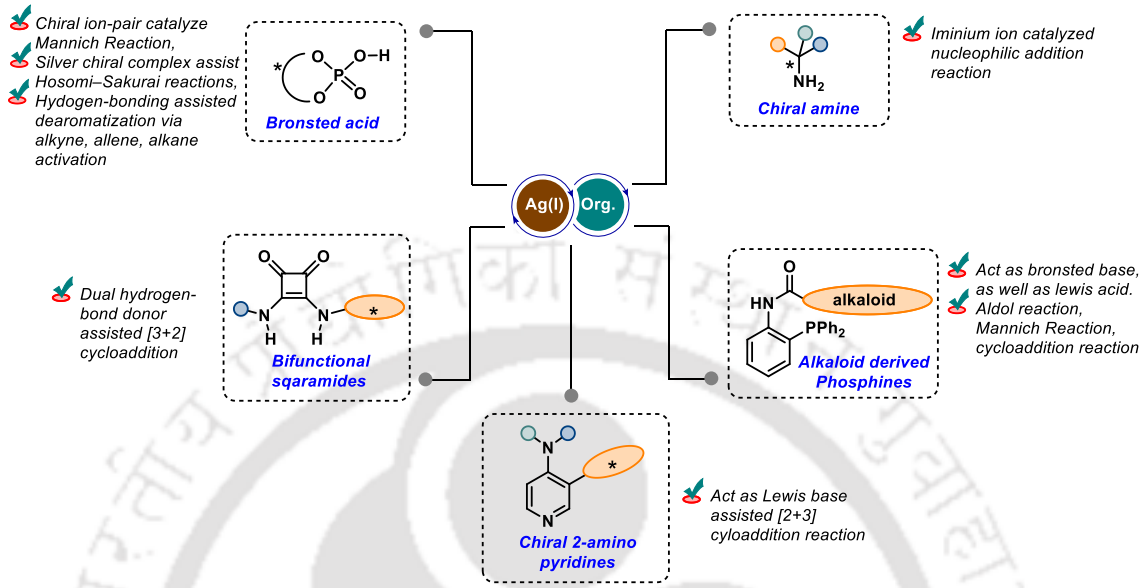

Fig. 9: Types of Ag(I)/organocatalyzed catalysis

Ag(I)/Bronsted acid catalysis: In this catalysis, Bronsted acid and silver (I) together used as chiral ion pair catalyst. It acts as hydrogen bond donor or chiral anion donor.

In 2012, Hui and co-workers reported a chiral phosphoric acid anion and silver combination as synergic ion-pair catalysis for an aza-Mannich reaction.[45] Under the catalytic conditions, substituted oxazolone and tosyl-imine gone through a Mannich reaction to afford quaternary α,β-diamino acid in high yields, excellent dr and ees (Scheme 4).

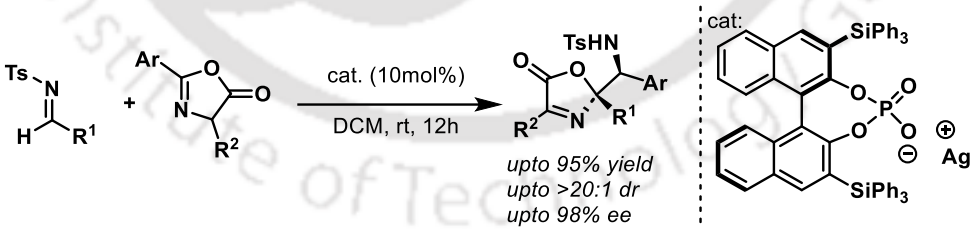

Scheme 4: Asymmetric silver catalyzed aza-Mannich reaction.

In 2011, Kobayashi and co-workers explored an Ag(I)-catalyzed asymmetric Hosomi−Sakurai reaction.[46] in the presence of catalytic silver BINOL-derived phosphate and InCl at room temperature. Under these conditions, allylboronate reacted with N,O-aminals to afford homoallylamides in excellent yields and ees (Scheme 5). The authors proposed that chiral silver-complexes operate as chiral anion donors. The mechanism went through an S_N1 mechanism to produce an iminium intermediate, which is required for the chiral counter anion.

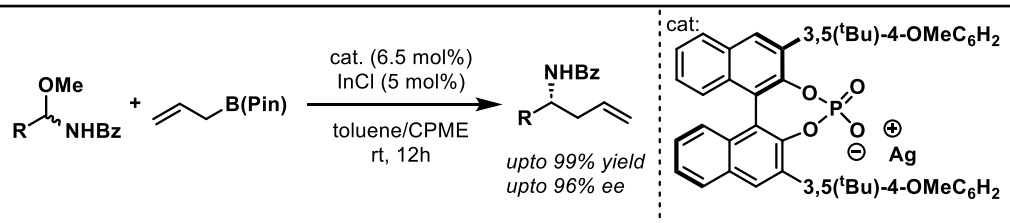

Scheme 5: Silver catalyzed asymmetric Hosomi−Sakurai reaction.

Taylor and Unsworth then described a silver-catalyzed spiro-cyclization of indoles. Intermolecular dearomative cyclization of indolyl ynones was achieved with excellent yields and modest ees utilizing Ag(I)-chiral BINOL phosphates (Scheme 6).[47] This process involves dual activation by silver and phosphoric acid. Silver activates the alkyne and phosphate components involved in sterocontrolled dearomatization.

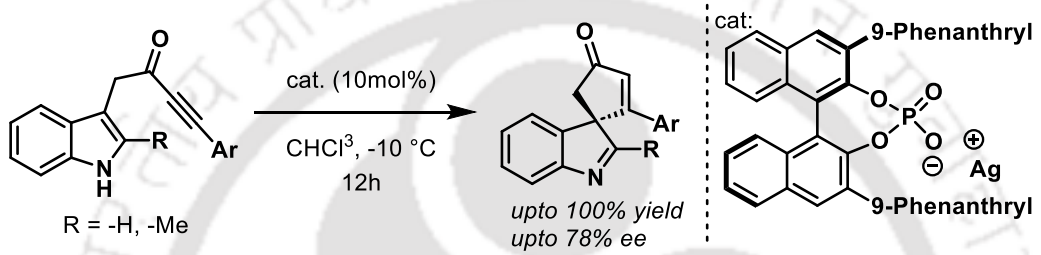

Scheme 6: Silver catalyzed dearomatization reaction.

Ag(I)-chiral amine catalysis: In this catalysis, silver acts as a Lewis acid, while chiral amine forms an enamine species to facilitate a nucleophilic addition.

In 2014, Enders et al. explored a chiral amine and silver catalysed one-pot method for a sequential Michael addition/hydroalkoxylation.[48] In this process, initially 4-hydroxycoumarin underwent a Michael addition to enynone using chiral enamine catalysis. Then, further addition of silver(I) carbonate gave chiral cumarone devivatives by 5-exo-dig cyclization (Scheme 7).

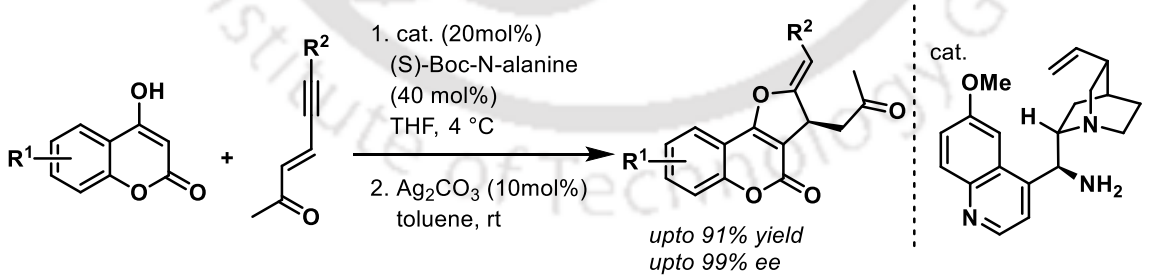

Scheme 7: Silver-chiral amine catalyzed one-pot Michael Addition/Hydroalkoxylation reaction.

Ag(I)/bifunctional squaramide catalysis: In this catalysis, bifunctional catalyst acts as hydrogen bond donor and silver(I) acts as lewis acid, to activate isocyanoacetates, alkynes, alkene.

In 2012, Shi et al, devised a highly diastereo- and enantioselective asymmetric [3+2] cycloaddition reaction of α-aryl isocyanoacetates with N-aryl maleimides using Ag(I)/cinchona alkaloid-derived squaramide cooperative catalysis.[49] The author described,

due to chelation of isocyanate carbon with silver(I), bifunctional amine easily deprotonates α-proton of isocyanoacetate to facilitate Michael addition to hydrogen bonded N-aryl maleimide. Finally, a 5-endo-dig cyclization with electrophilic silver isocyanide gave [3+3] cycloaddition product in excellent yields, dr and ees (Scheme 8).

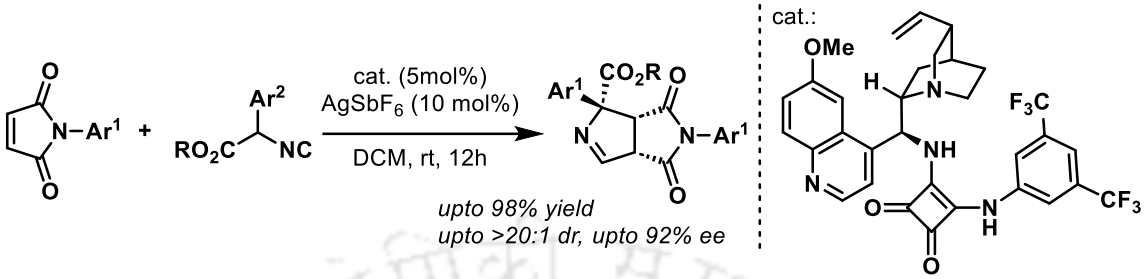

Scheme 8: Ag-bifunctional catalyzed [3+2] cycloaddition reaction.

Ag(I)/ alkaloid derived phosphines: In this catalysis, alkaloid derived phopsphines acts as bronsted base, H-bond donor and Lewis base. Whereas silver can involve in elctrophile activation.

Dixon et al. reported the first diastereoselective aldol reaction using Ag(I)-hydrochinchona-derived phosphine catalysis in 2011 (Scheme 9). The catalyst is based on a precatalyst hydrochinchona-derived phosphine with Brønsted and Lewis basic sites and a hydrogen-bond donor near a chiral pocket.[50] The combination of soft acid Ag(I) and precatalyst effectively accelerates the nucleophilicity of isocyanoacetates that have undergone an asymmetric Mannich-type addition/cyclization. Under catalytic conditions, isocyanoacetate and aldehydes produced chiral oxazoline derivatives with outstanding yields, dr, and ees.

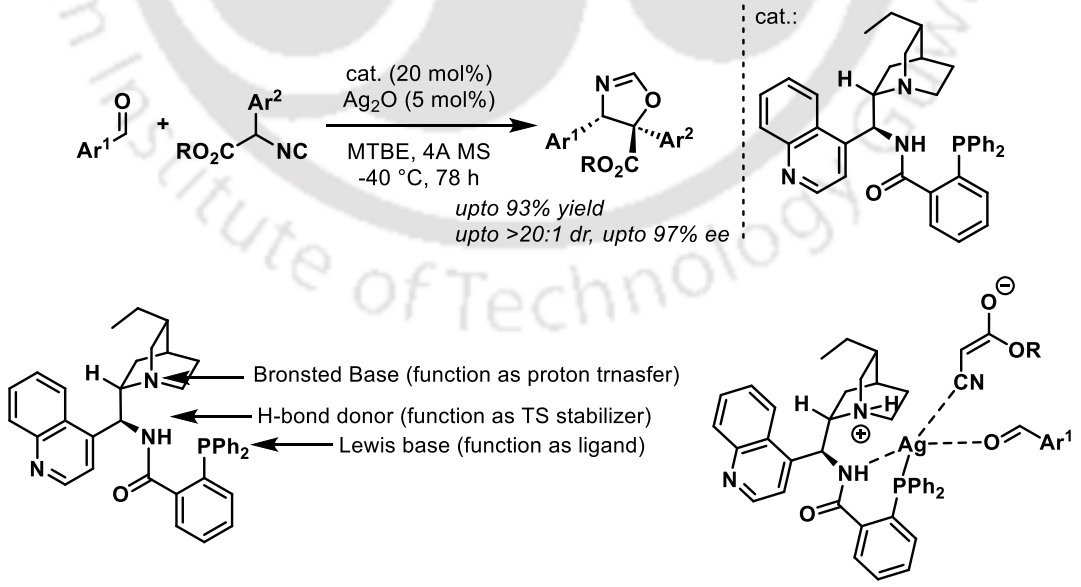

Scheme 9: Silver-alkaloid derived phosphine catalyzed aldol reaction and reactivity.

Later, in 2014 and 2015, Dixon et al. reported a Mannich-type addition/cyclization and aldol/cyclization reaction of acetaldehyde using Ag(I) and hydroquinine-derived

phosphines, involving acetophenones and isocyanoacetate as a pronucleophile (Scheme 10).[51] These catalytic process follows the same pathway as the Ag(I)-hydrochinchona-derived phosphine catalysis. Under optimal conditions, the cyclization reaction produced chiral imidazoline and oxazoline derivatives in good yields with excellent diastereomeric and enantiomeric ratios respectively.

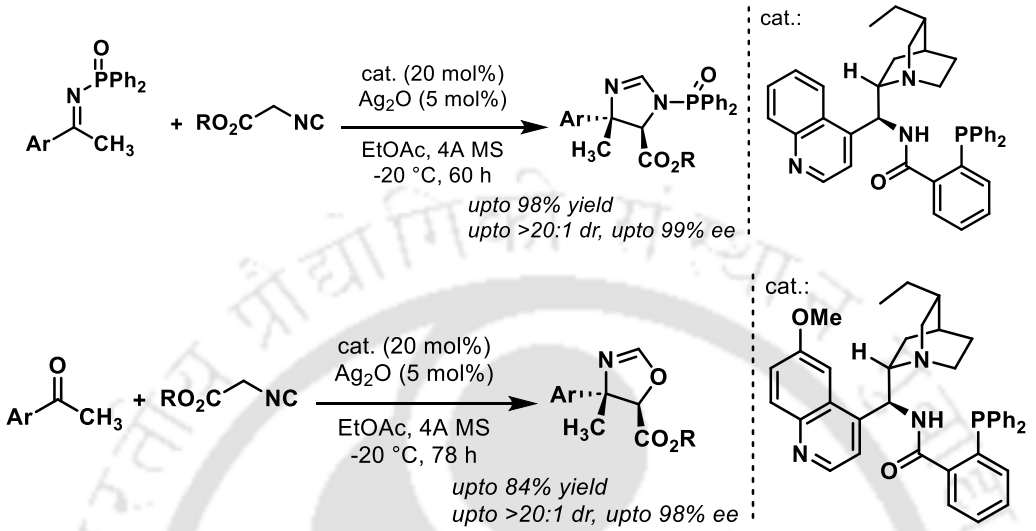

Scheme 10: Silver-alkaloid derived phosphine catalyzed aldol and Mannich-type addition.

Ag(I)/chiral 2-amino pyridines catalysis: This catalysis uses silver to activate alkynes, alkenes, and allenes. Whereas chiral 2-amino pyridine functions as a Lewis base, it can covalently connect to substrates and activates their reactivity.

In 2023, Han and Zhan et al. reported a dual catalytic system involving 4-aminopyridine and silver metal.[52] A metal/Lewis base relay catalytic system featuring silver acetate and a modified chiral pyrrolidinopyridine (PPY) applied in the cycloisomerization/(2 + 3) cycloaddition reaction of enynamides. In this relay catalysis, silver activates the ynamide substrate to create an unsaturated ketimine intermediate, which reacted with PPY activated allylic ylide intermediate (generated from edaravone-derived MBH carbonate) to give bispirocyclopentene derivatives in excellent yields and ees (Scheme 11).

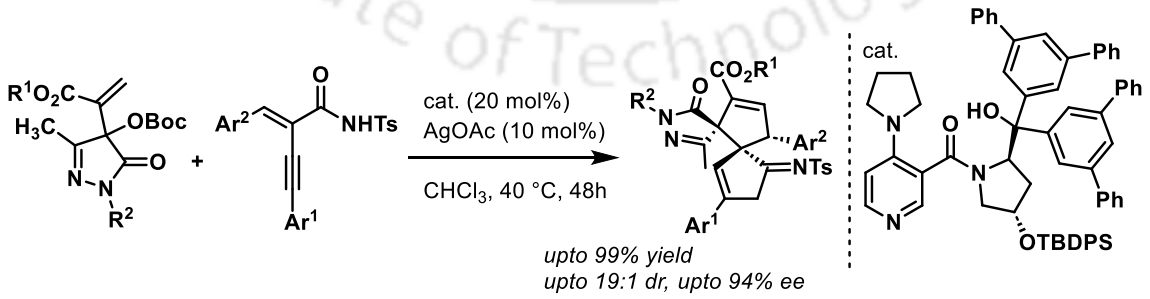

Scheme 11: Ag(I)-PPY catalyzed spiro cyclization reaction.

1.4. Asymmetric desymmetrization reactions:

Desymmetrization of prochiral or meso-substrates that already have stereogenic centers has proven to be a useful and effective synthetic chemistry technique. This method has

received a lot of interest because of its capacity to make complicated compounds easier to assemble, especially in an enantioselective and diastereoselective manner (Fig. 10). Simultaneously, organocatalysis has clearly evolved into a powerful toolbox in asymmetric catalysis since it was first developed, capable of bringing up new possibilities for desymmetrizing reactions. Furthermore, with correct substrate and catalyst design, numerous stereocenters can be created in a single process while maintaining excellent diastereocontrol, resulting in high value and desymmetrization feasibility.[53,54] Desymmetrization separates enantiocontrol from restricted enantiofacial distinction, making it a promising prospect for applying various types of catalytic reactions in enantioselective synthesis.

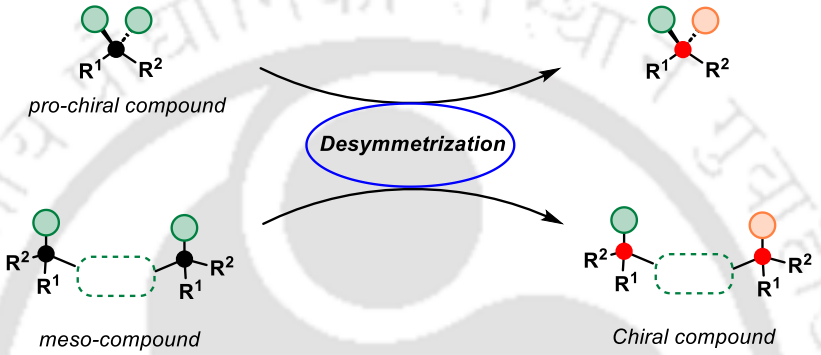

Fig 10: Desymmetrization Strategy.

A meso-compound is an achiral compound that contains many stereogenic centers and a symmetric plane.[55] When comparing desymmetrization of one prochiral-containing meso-compound to numerous prochiral centre-containing meso-compounds, it is more effective at producing optically active multiple stereocenter-containing compounds in a single step. A novel desymmetrization strategy should not produce any judicious stereogenic center that has low diastereoselctivity. This judicious desymmetrization can be resolved by producing several stereogenic centers without creating any additional stereocenter. This strategy can be employed by functionalization of C-sp^2 carbon center or a substitution dependent aromatization.

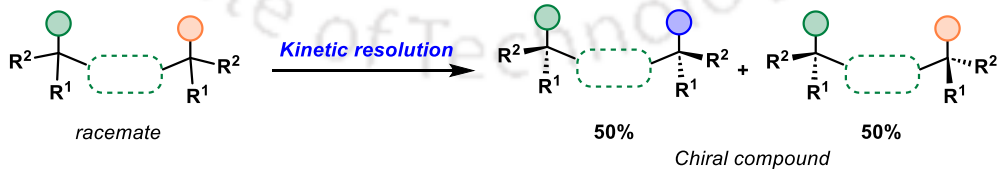

Fig. 11.: Kinetic resolution.

Desymmetrization of meso-compounds is associated with kinetic resolution of racemates. However, the desymmetrization technique outperforms kinetic resolution as the maximum theoretical yield is limited to 50% (Fig. 11). Desymmetrization can result in a high optical purity, but this may come at the cost of lower chemical yield, even with a moderately selective catalyst. However, overreaction can create a bis-functionalized product (Fig. 12),

Horeau-Langenbeck type amplification).[56-58] Whereas kinetic resolution eliminates the minor enantiomer by catalyst control. Desymmetrization of meso-compounds could also produce both enantiomers from the same chiral reagent or catalyst through selective functional group rearrangement. Therefore, the desymmetrization strategy is commonly used in natural product synthesis.[59] In the recent years, this strategy becomes a common method for the synthesis of axially chiral C-C, C-N, N-N, C-O and C-B molecules.[60]

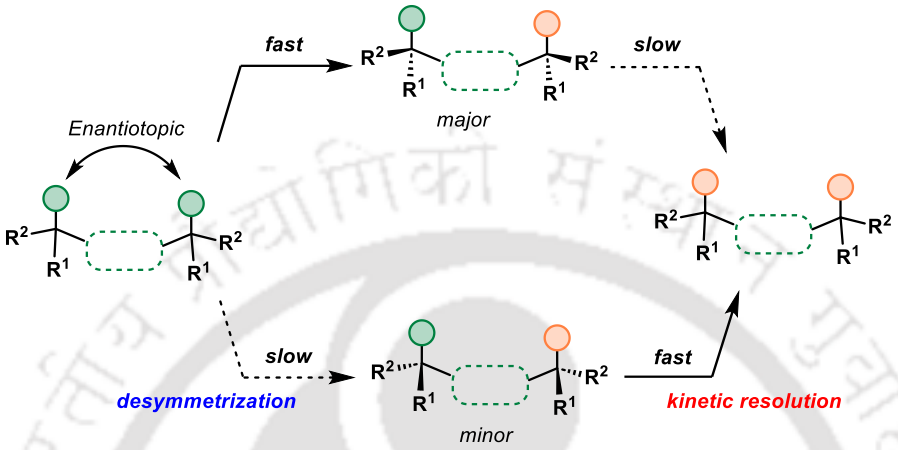

Fig. 12: Desymmetrization of enantiotopic-meso compounds.

1.4.1. Desymmetrization reactions by de novo aromatization:

Desymmetrization reactions can be achieved by substituted aromatization strategy. This strategy not only creates one stereoisomer but also the other isomer can be achieved by just changing the substitution position. This strategy is one of the pillars for the synthesis of axial, quaternary, and multiple chiral center synthesis.

Another approach reported in 1994 by Mori et al. showed that prochiral triynes could be desymmetrized enantioselectively by Ni-catalysis (Scheme 12).[61] They successfully constructed the arene ring with high enantioselectivity using a two-component [2+2+2] cycloaddition reaction.

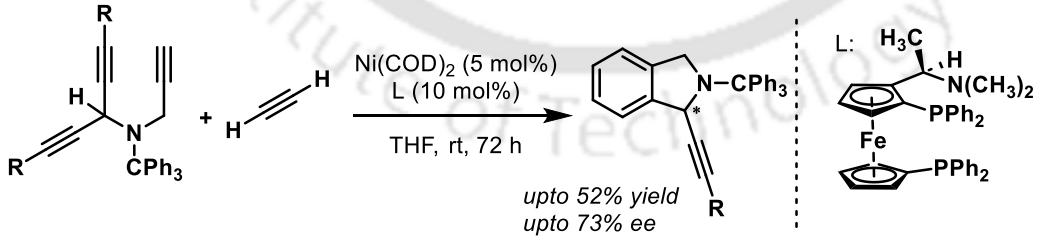

Scheme 12: Ni-catalyzed desymmetric two-component [2+2+2] cycloaddition reaction.

Using a [2+2+2] cycloaddition of symmetrical dialkynylphosphine oxides with 1,6-diynes, Tanaka et al. created an enantioselective synthesis of P-stereogenic alkynylphosphine oxides in 2008.[62] A cationic rhodium(I) complex attached to a chiral BINAP ligand catalyzes this reaction. Furthermore, a C2-symmetric P-stereogenic bis(alkynylphosphine oxide) can be produced using this technique (Scheme 13).

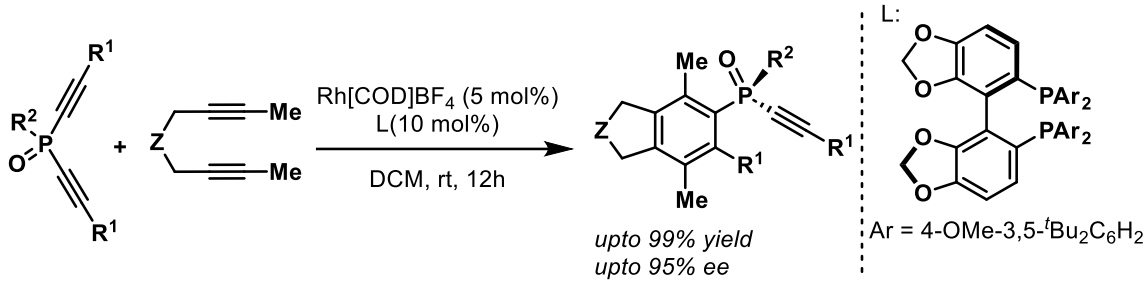

Scheme 13: Rh-catalyzed [2+2+2] cycloaddition for the synthesis of P-stereogenic phosphine oxides.

In 2019, Chi et al. reported a strategy for synthesizing substituent-dependent, centrally chiral arenes using N-heterocyclic carbene (NHC) catalysis.[63] This method presented a one-step organic catalytic approach that involved an NHC-catalyzed cycloaddition reaction between achiral indanone and α,β-unsaturated aldehydes (Scheme 14). The process enabled the direct construction of an aryl ring and resulted in the formation of optically active 1,3-indandiones in high yields and with excellent enantiomeric excesses.

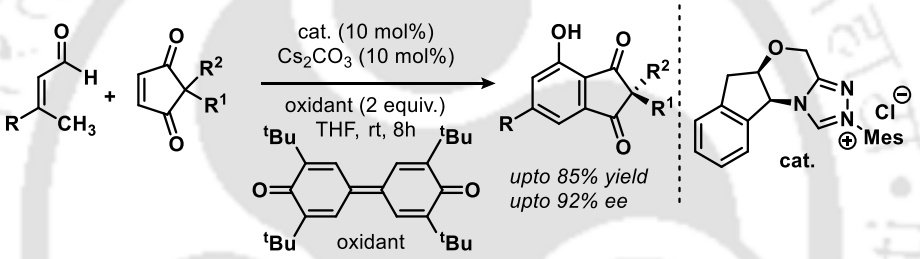

Scheme 14. Chiral NHC catalyzed desymmetrization strategy for chiral arene synthesis.

In 2022, Mukherjee and co-workers developed a desymmetrizing *de novo* method using diphenylprolinol silyl ether to create centrally chiral arenes (Scheme 15).[64] This process works through a dienamine intermediate, which allows for a [4+2] cycloaddition between polycyclic meso-cyclohexenediones and α,β-unsaturated aldehydes. Then, the Diels-Alder adduct underwent *de novo* oxidation to afford centrally chiral arenes with high yields and excellent enantiomeric excesses.

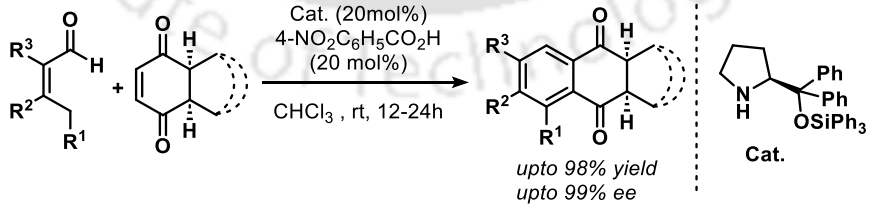

Scheme 15. Desymmetrization reaction for chiral arene synthesis via dienamine catalysis.

In 2022, Oh et al. reported that a chiral silver catalyst could be used in the Van Leusen pyrrole synthesis to catalytically asymmetrically desymmetrize cyclohexadienones (Scheme 16). A suitable surrogate isocyanomethyl sulfone (NasMIC) is responsible for the development of chiral-fused pyrrole derivatives. Excellent yields and ees were obtained from chiral cyclohexanones under ideal conditions.[65]

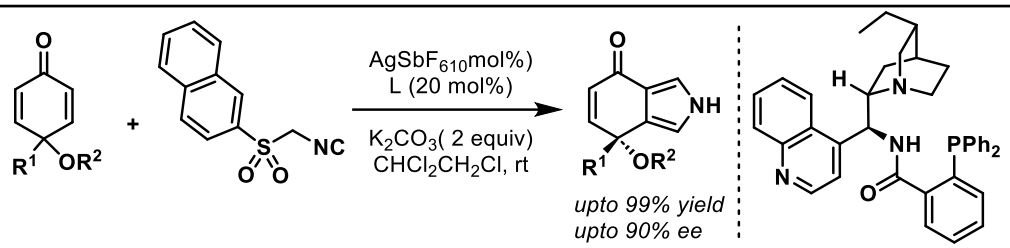

Scheme 16. Ag(I) catalyzed desymmetric the Van-Leusen reaction.

In 2017, Tan and co-workers reported catalytic asymmetric Paal–Knorr reaction for the synthesis of axially chiral arylpyrroles.[66] High yields and excellent to outstanding enantioselectivities were achieved in the synthesis of a wide variety of C-N axially chiral arylpyrroles (Scheme 17). The authors described, to achieve effective enantiocontrol, a combined-acid catalytic system that includes both a Lewis acid and a chiral phosphoric acid.

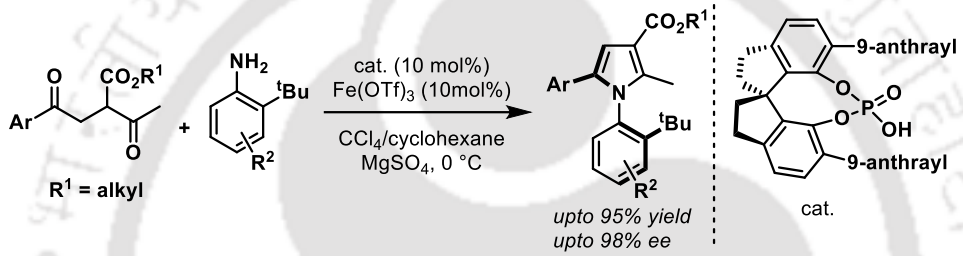

Scheme 17: Asymmetric Paal–Knorr reaction for the synthesis of axially chiral arylpyrroles.

1.4.2. Desymmetrization reaction by C(sp²)−H functionalization:

In 2015, Mukherjee et al. described a desymmetrization of prochiral 2,2-disubstituted cyclopentene-1,3-diones with C(sp²)−H functionalization.[67] In this process, a urea derivative based on dihydroquinine serves as a catalyst. Nitroalkanes, which are inexpensive, readily available, and air-stable, are used as the alkylating agent in this process. This method creates compounds with a central carbon atom that has four distinct groups attached to it by altering a particular carbon-hydrogen bond (C(sp²)−H) (Scheme 18). This method gave chiral cyclopentene-1,3-diones in excellent enantioselectivities and in good to excellent yields.

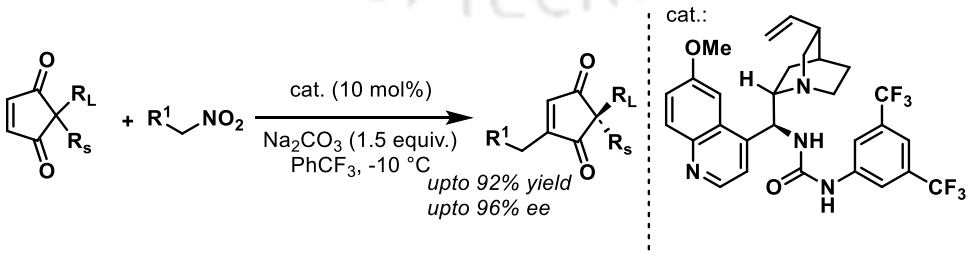

Scheme 18: Organocatalytic Enantioselective Formal C(sp2)−H Alkylation.

Using bifunctional catalyzed C(sp²)−H functionalization, in 2016 Mukherjee et al. reported desymmetrization of meso-cyclohexadiones with nitro methane (Scheme 19).[68]

The method uses nitroalkanes as alkylating agents and is catalyzed by a tertiary amino-thiourea derivative, yields densely functionalized products with excellent enantioselectivity and at least four contiguous stereogenic centers distant from the reaction site.

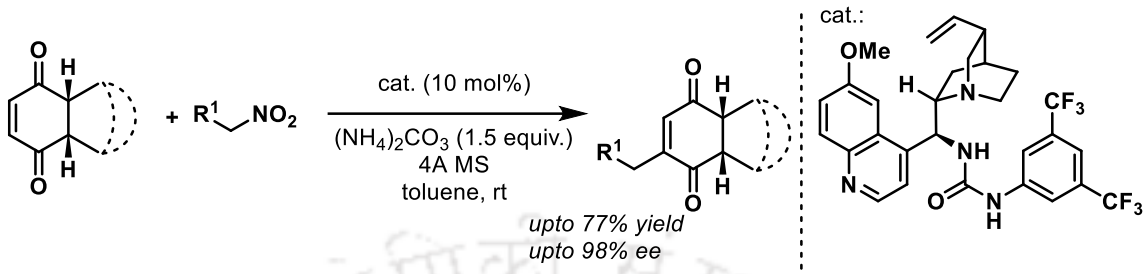

Scheme 19: Formal C(sp^2)–H Alkylation enabled desymmetrization of meso- cyclohexadiones.

Whereas, in 2020 Tse and Yeung reported that desymmetrizing catalytic asymmetric halogenation of BPOL (bisphenol) with NBS (N – bromosuccinimide) as the halogen source.[69] According to the authors, the bifunctional catalyst (S)-BINOL-amine derivative uses intermolecular hydrogen bonds to increase the hydroxyl proton's acidity. By forming hydrogen bonds with the acidic proton, this amino organocatalyst can simultaneously activate the halogen source and the phenol substrate, enabling the halogen atom to be delivered in enantioselective fashion (Scheme 20).

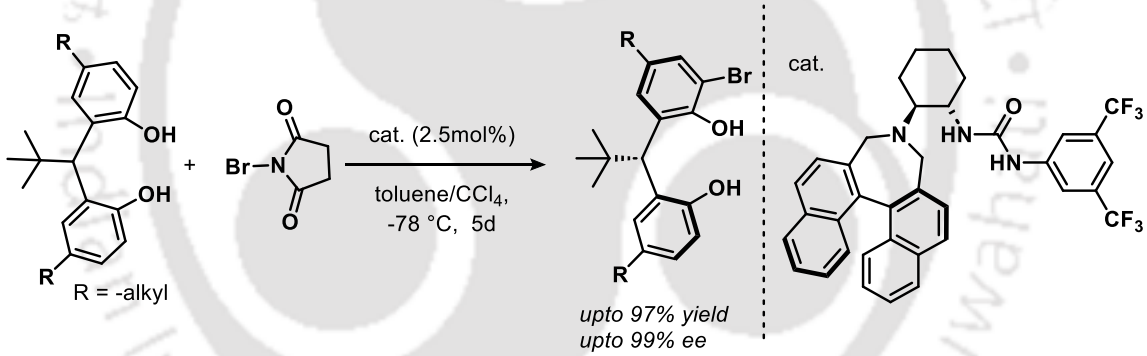

Scheme 20: Desymmetrization of BPOL with Asymmetric Ortho-Selective Halogenation.

1.5. Conclusion and Focal Theme of the Present Work:

The focal theme of this thesis is to utilize bifunctional tertiary amine thiourea, squaramide, chiral phosphoric acid catalysts and organo/Ag(I)-combined catalysis in various cascade reactions. Chapter I is an introduction part that explained the organocatalysis and silver(I)/organocatalyst conbined catalysis. It also discussed about desymmetrization of meso-compounds. Chapter II includes a sequential bifunctional and Lewis acid catalyzed divergent synthesis of benzofuran-based azocines and spiro-cyclopentane derivatives. Chapter III describes chiral phosphoric acid catalyzed highly chemo- and regio-selective para-C-H functionalization of N-aryl anilines with aurone derived azadienes to afford chiral triarylmethanes. Chapter IV discussed a Ag(I)/cinchonidine-derived phosphine catalyzed de novo synthesis of substituent dependent chiral pyrroles through

desymmetrization reaction of meso-cyclohexediones via [3+2]-cycloaddition and the Van-Leusen reaction. Lastly chapter V described a chiral phosphoric acid catalyzed Friedel-Craft reaction of prochiral pyrroles with allenamides.

1.6. References:

1. L. Pasteur, *Ann. Chim. Phys*. **1848**, *24*, 442.
2. A. C. Aprotosoaie, M. Hăncianu, I.-I. Costache, A. Miron, *Flavour Fragr. J*. **2014**, *29*, 193.
3. H. B. Vickery, G. W. Pucher, C. G. Deuber, *J. Biol. Chem*. **1942**, *145*, 45.
4. P. Warot, *Lille médical: journal de la Faculté de médecine et de pharmacie de l'Université de Lille* **1971**, *17*, 329.
5. M. T. Reetz, *J. Am. Chem. Soc*. **2013**, *135*, 12480.
6. E. N. Jacobsen, A. Pfaltz, H. Yamamoto, *Comprehensive Asymmetric Catalysis, Volume I to III*; Springer: Berlin, Heidelberg, **1999**.
7. (a) B. List, *Chem. Rev*. **2007**, *107*, 5413. (b) P. Renzi, M. Bella, *Chem. Commun*. **2012**, *48*, 6881.
8. O. G. Mancheño, M. Waser, *Eur. J. Org. Chem.* **2023**, *26*, e202200950.
9. (a) B. List, R. A. Lerner, C. F. Barbas, *J. Am. Chem. Soc.* **2000**, *122*, 239. (b) S. Mukherjee, J. W. Yang, S. Hoffmann, B. List, *Chem. Rev*. **2007**, *107*, 5471.
10. (a) K. A. Ahrendt, C. J. Borths, D. W. C. MacMillan, *J. Am. Chem. Soc*. **2000**, *122*, 4243. (b) G. Lelais, D. W. C. MacMillan, *Aldrichimica Acta,* **2006**, *39*, 79.
11. T. D. Beeson, A. Mastracchio, J.-B. Hong, K. Ashton, D. W. C. Macmillan, *Science*, **2007**, *316*, 582.
12. D. Enders, O. Niemeier, A. Henseler, *Chem. Rev.* **2007**, *107*, 5606.
13. R. Breslow, *J. Am. Chem. Soc*. **1958**, *80*, 3719.
14. J. Sheehan, T. Hara, *J. Org. Chem.* **1974**, *39*, 1196.
15. D. Enders, U. Kallfass, *Angew. Chem. Int. Ed.* **2002**, *41*, 1743.
16. R. R. Knowles, E. N. Jacobsen, *Proc. Natl Acad. Sci. USA* **2010**, *107*, 20678.
17. (a) M. S. Taylor, E. N. Jacobsen, *Angew. Chem. Int. Ed.* **2006**, *45*, 1520. (b) M. Sigman, & E. N. Jacobsen, *J. Am. Chem. Soc.* **1998**, *120*, 4901.
18. (a) U. H. Dolling, P. Davis, E. J. J. Grabowski, *J. Am. Chem. Soc.* **1984**, *106*, 446. (b) S. Shirakawa, K Maruoka, *Angew. Chem. Int. Ed.* **2013**, *52*, 4312.
19. S. E. Reisman, A. G. Doyle, E. N. Jacobsen, *J. Am. Chem. Soc*. **2008**, *130*, 7198.

20. (a) T. Akiyama, J. Itoh, K. Yokota, K. Fuchibe, *Angew. Chem. Int. Ed.* **2004**, *43*, 1566. (b) D. Uraguchi, M. Terada, *J. Am. Chem. Soc.* **2004**, *126*, 5356. (c) D. Parmar, E. Sugiono, S. Raja, M. Rueping, *Chem. Rev*. **2014**, *114*, 9047.

21. K. Brak, E. N. Jacobsen, *Angew. Chem. Int. Ed*. **2013**, *52*, 534.

22. M. S. Sigman, E. N. Jacobsen, *J. Am. Chem. Soc*. **1998**, *120*, 4901.

23. For a review on TADDOL, see: D. Seebach, A. K. Beck, A. Heckel, *Angew. Chem. Int. Ed.* **2001**, *40*, 92.

24. H. Yamamoto, K. Futatsugi, *Angew. Chem. Int. Ed.* **2005**, *44*, 1924.

25. Y. Huang, A. K. Unni, A. N. Thadani, V. H. Rawal, *Nature* **2003**, *424*, 146.

26. A. K. Unni, N. Takenaka, H. Yamamoto, V. H. Rawal, *J. Am. Chem. Soc.* **2005**, *127*, 1336.

27. B. List, R. A. Lerner, C. F. Barbas, *J. Am. Chem. Soc*. **2000**, *122*, 2395.

28. (a) Cinchona Alkaloids in Synthesis and Catalysis (C. E. Song, Ed.), *Wiley-VCH,* Weinheim, **2009**; (b) T. Marcelli, H. Hiemstra, *Synthesis* **2010**, 1229.

29. T. Okino, Y. Hoashi, Y. Takemoto, *J. Am. Chem. Soc.* **2003**, *125*, 12672.

30. T. Azuma, Y. Kobayashi, K. Sakata, T. Sasamori, N. Tokitoh, Y. Takemoto, *J. Org. Chem.* **2014**, *79*, 1805.

31. A. Hamza, G. Schubert, T. Soós, I. Pápai, *J. Am. Chem. Soc*. **2006**, *128*, 13151.

32. A. Michael, *J. Prakt. Chem*. **1887**, *35*, 349.

33. H. Wynberg, R. Helder, *Tetrahedron Lett*. **1975**, *16*, 4057.

34. For a historical introduction to Friedel and Crafts, see for example, G. A. Olah, R. E. A Dear,. In Friedel-Crafts and Related Reactions; Olah, G. A., Ed.; Wiley and Sons: New York, **1963**, p 1.

35. G. A. Olah, Friedel-Crafts Chemistry; Wiley and Sons: New York, **1973**.

36. N. A. Paras, D. W. C. MacMillan, *J. Am. Chem. Soc*. **2001**, *123*, 4370.

37. (a) G.-S. Chen, Y.-J. Deng, L.-Z. Gong, A.-Q. Mi, X. Cui, Y.-Z. Jiang, M. C. K.; Choi, A. S. C. Chan, *Tetrahedron-Asymmetry* **2001**, *12*, 1567−1571. (b) M. Nakoji, T. Kanayama, T. Okino, Y. Takemoto, *Org. Lett.* **2001**, *3,* 3329−3331.

38. (a) Z.-H. Shao, H.-B. Zhang, *Chem. Soc. Rev.* **2009**, *38*, 2745−2755. (b) Z. T. Du, Z.-H. Shao, *Chem. Soc. Rev.* **2013**, *42*, 1337−1378. (c) B. A. Arndtsen, L.-Z. Gong, *Springer Nature*: Cham, Switzerland, **2020**. (d) L.-Z. Gong, *Wiley-VCH: Weinheim, Germany*, **2021**.

39. (a) G. M. Sammis, H. Danjo, E. N. Jacobsen, *J. Am. Chem. Soc***. 2004**, *126*, 9928−9929. (b) B. M. Trost, X. Luan, *J. Am. Chem. Soc*. **2011**, 133, 1706−1709. (c) A. E. Allen, D. W. C. MacMillan, *Chem. Sci.* **2012**, *3*, 633−658.

40. D.-F. Chen, Z.-Y. Han, X.-L. Zhou, L.-Z. Gong, *Acc. Chem. Res*. **2014**, *47*, 2365−2377.

41. T. Ikariya, M. Shibasaki, *Springer: Berlin, Heidelberg*, **2011**.

42. (a) D. R. Rae *Encyclopedia of Reagents for Organic Synthesis,* L. A. PaquetteJohn Wiley & Sons, Chichester, **1995**, p. 4461. (b) J. C. Lanter *Encyclopedia of Reagents for Organic Synthesis*, L. A. PaquetteJohn Wiley & Sons, Chichester, **1995**, p. 4469. (c) L.-G. Wistrand Encyclopedia of Reagents for Organic Synthesis, L. A. PaquetteJohn Wiley & Sons, Chichester, **1995**, p. 4472. (d) T. H. Black, Encyclopedia of Reagents for Organic Synthesis, L. A. PaquetteJohn Wiley & Sons, Chichester, **1995**, p. 4476.

43. (a) M. Sawamura, H. Hamashima and Y. Ito, *J. Org. Chem.*, **1990**, *55*, 5935. (b) T. Hayashi, Y. Uozumi, Y.Yamazaki, M. Sawamura, H. Hamashima, Y. Ito, *Tetrahedron Lett.*, **1991**, *32*, 2799.

44. (a) M. Naodovic, H. Yamamoto, *Chem. Rev.* **2008,** *108,* 3132. (b) H. Pellissier, *Chem. Rev*. **2016**, *116*, 14868−14917.

45. S.-H. Shi, F.-P. Huang, P. Zhu, Z.-W. Dong, X.-P. Hui, *org lett*, **2012**, *14*, 2010.

46. Y.-Y. Huang, A. Chakrabarti, N. Morita, U. Schneider, S. Kobayashi, *Angew. Chem., Int. Ed*. **2011**, *50*, 11121.

47. M. J. James, J. D. Cuthbertson, P. O'Brien, R. J. K. Taylor, W. P. Unsworth, *Angew. Chem., Int. Ed.* **2015**, *54*, 7640−7643.

48. D. Hack, P. Chauhan, K. Deckers, G. N. Hermann, L. Mertens, G. Raabe, D. Enders, *Org. Lett*. **2014**, *16*, 5188−5191.

49. M.-X. Zhao, D.-K. Wei, F.-H. Ji, X.-L. Zhao, M. Shi, *Chem. - Asian J.* **2012**, *7*, 2777−2781.

50. F. Sladojevich, A. Trabocchi, A. Guarna, D. J. Dixon, *J. Am. Chem. Soc*. **2011**, *133*, 1710−1713.

51. (a) I. Ortin, D. J. Dixon, *Angew. Chem., Int. Ed*. **2014**, *53*, 3462−3465. (b) R. de la Campa, I. Ortin, D. J. Dixon, *Angew. Chem., Int. Ed*. **2015**, *54*, 4895−4898.

52. J. Jiang, J. Zhou, Y. Li, C. Peng, G. He, W. Huang, G. Zhan, B. Han, *Communications Chemistry*, **2023**, *6*, 128.

53. M.C. Willis, *J. Chem. Soc. Perkin Trans*., **1999**, *1*, 1765-1784.

54. M.D. Díaz-de-Villegas, *Chem. Soc. Rev*., **2011**, *40,* 5564-5587.

55. For selected recent reviews, see:a) A. Borissov, T. Q. Davies, S. R. Ellis,T. A. Fleming, M. S. W. Richardson, D. J. Dixon, *Chem. Soc. Rev*. **2016**, *45*,5474; b) X.-P. Zeng, Z.-Y. Cao, Y.-H. Wang, F. Zhou, J. Zhou, *Chem. Rev*.**2016**, *116*, 7330; c) M. A. Horwitz, J. S. Johnson, *Eur. J. Org. Chem*. **2017**, *11*, 1381; d) M. D. Díaz De Villegas, J. A. Gálvez, P. Etayo, R. Badorrey, P.López-Ram-De-Víu, *Chem. Soc. Rev*. **2011**, *40*,

5564; e) Y. Xu, T.-Y. Zhai, Z.Xu, L.-W. Ye, *Trends Chem*. **2022**, *4*, 191; f) C. Nájera, F. Foubelo, J. M.Sansano, M. Yus, *Tetrahedron* **2022**, 106–107, 132629.
56. W. Langenbeck, GZ. Physik Triem, *Chem.* **1936**, *177*, 401.
57. J.P. Vigneron, M. Dhaenens, A. Horeau, *Tetrahedron.* **1973**, *29*, 1055.
58. V. Rautenstrauch, *Bull Soc Chim Fr*. **1994**, 131, 515.
59. M. A. Horwitz, J. S. Johnson, *Eur. J. Org. Chem*. **2017**, 1381–1390.
60. J. Moon, S. Kim, S. Lee, H.-A. Cho, A. Kim, M. K. Ham, S. H. Kim, J. Jung, Y. Kwon, *ChemCatChem* **2024**, *16*, e202400690.
61. T. Zhu, Y. Liu, M. Smetankova, S. Zhuo, C. Mou, H. Chai, Z. Jin, Y. R. Chi, *Angew. Chem. Int. Ed.* **2019**, *58*, 15778.
62. B. Ghosh, M. S. Harariya, S. Mukherjee, *Angew. Chem. Int. Ed.* **2022**, *61*, e202204523.
63. M. A. Abozeid, H. Y. Kim, K. Oh, *Org. Lett.* **2022**, *24*, 1812.
64. L. Zhang, J. Zhang, J. Ma, D.-J. Cheng, B. Tan, *J. Am. Chem. Soc*. **2017**, *139*, 1714.
65. Y. Sato, T. Nishimata, M. Mori, *J. Org. Chem*. **1994**, *59*, 6133-6135.
66. G. Nishida, K. Noguchi, M. Hirano, K. Tanaka*, Angew. Chem., Int. Ed*. **2008**, *47*, 3410-3413.
67. M. S. Manna, S. Mukherjee, *J. Am. Chem. Soc*. **2015**, *137*, 130−133.
68. R. Sarkar, S. Mukherjee, *Org. Lett*. **2016**, *18*, 6160−6163.
69. X. Xiong, T. Zheng, X. Wang, Y.-L. Steve Tse, Y.-Y. Yeung, *Chem* **2020**, *6*, 919–932.

Chapter 2

Structurally divergent enantioselective synthesis of benzofuran fused azocine derivatives and spiro-cyclopentanone benzofurans enabled by sequential catalysis

Abstract: An important objective in organic synthesis and medicinal chemistry is the capacity to access structurally varied and complex molecules rapidly and affordably from easily available starting materials. In this chapter, a protocol for the structurally divergent synthesis of benzofuran fused azocine derivatives and spiro-cyclopentanone benzofurans has been developed via chiral bifunctional urea catalyzed reaction between aurone-derived α,β-unsaturated imine and ynone followed by switchable divergent annulation reactions by Lewis base catalysts (DBU and PPh_3) with concomitant epimerization. The skeletally diversified products were formed in high yields with high diastereo- and enantioselectivities.

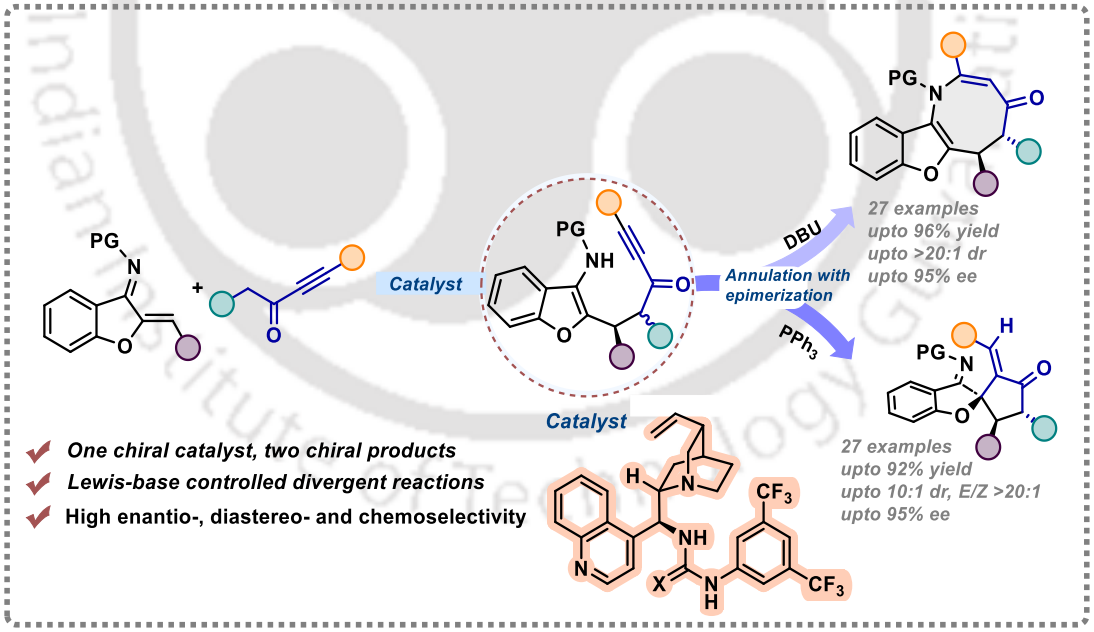

2.1. Introduction:

In recent years, significant attention has been given to the development of concise, green and efficient methodologies for the preparation of target molecules.[1] Also, for drug and probe discovery, it is crucial to develop switchable chemo-, regio-, or diastereodivergent reactions that allow for the production of two or more structurally and stereogenically distinct types of chiral products from identical starting materials. Switchable divergent asymmetric synthesis refers to selective transformations that efficiently produce two or more distinct products with varying chemo-, regio-, or diastereoselectivity from the same starting materials under easily adjustable conditions (Fig 1).[2] In fact, synthesis of two or more structurally and stereogenically different types of chiral products via a divergent strategy is quite attractive.[2c] Apart from chiral metal complex-based catalysts, several organocatalytic systems have been utilized widely, including chiral Lewis bases, chiral primary and secondary amines, chiral Brønsted bases, and chiral Brønsted acids. There are four most effective methods that have been used: cycle-specific cascade reactions, the use of organocatalysts with different structures, different additives, or synergistic catalysis.[3]

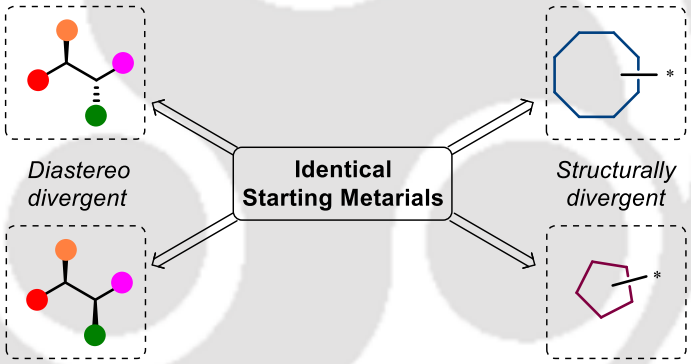

Fig. 1: Divergent synthesis strategies.

The principal strategy that has been used to synthesize structurally different products employing different chiral catalysts via different chiral intermediates.[3d-s] On the other hand, it is quite challenging to obtain structurally different compounds using the same chiral catalyst and with different additives or reagents or varying reaction conditions (additive or reagent controlled).[3a–c,t–x] Benzofuran or indole-fused eight membered rings containing a nitrogen atom (azocines) are important structural motifs that are prevalent in many natural products and biologically active molecules such as PKD inhibitor kb-NB96-53, balasubramide, grandilodine A, etc.[4] The efficient construction of eight-membered rings in such molecular structures is a fundamental synthetic challenge. Similarly, spiro-cyclopentane benzofuran motifs are present in many bioactive natural products such as laurentristich-4-ol,

spiroapplanatumine K and involucratustone B.[5] However, only a few catalytic asymmetric syntheses of spiro-cyclopentanone benzofurans are known. Thus, an efficient route for the preparation of such a motif in enantioselective fashion is highly desirable.

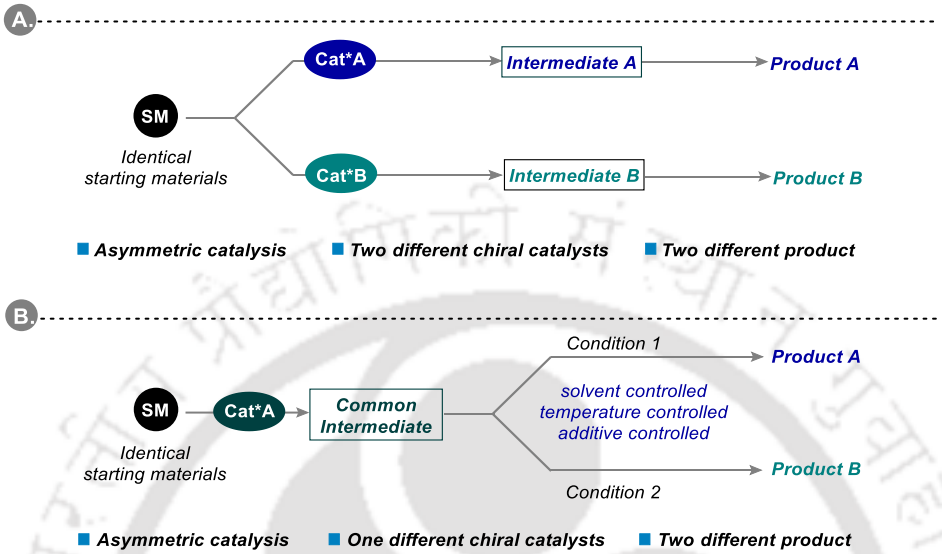

Fig. 2: A. Catalyst controlled asymmetric divergent Synthesis. B. Additive controlled asymmetric divergent Synthesis.

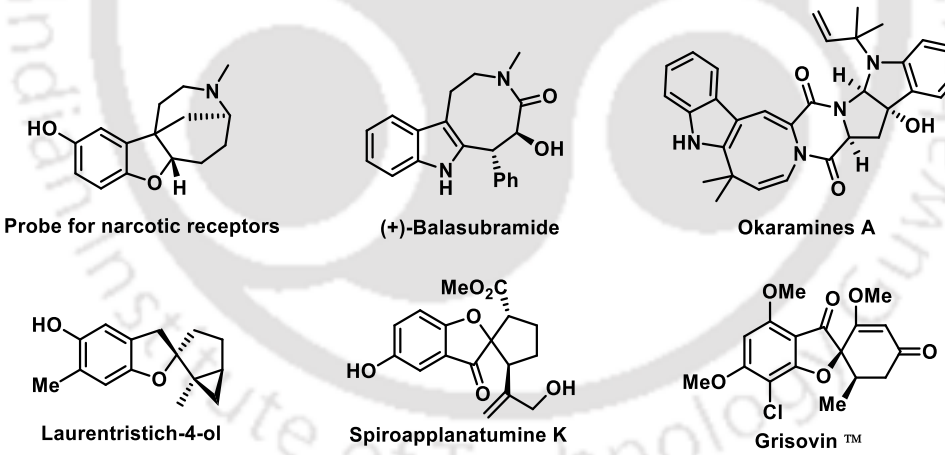

Fig. 3: Selected biologically active molecules.

2.2. Previous Study:

2.2.1. Organocatalytic asymmetric additive/solvent controlled divergent synthesis:

In 2006, Jørgensen and coworkers reported an additive-controlled divergent synthesis of tetrahydrothiophenes using a diaryl prolinol TMS ether catalyst.[6] Interestingly, the authors described a novel organocatalytic Michael-aldol domino reactions, and by selecting suitable additives, one can influence the regioselectivity of these domino reactions. This reaction

results in the formation of diastereomerically pure (tetrahydrothiophen-2-yl)phenyl methanones using PhCOOH as base and tetrahydrothiophene carbaldehydes with $NaHCO_3$. In both cases, favorable yields and with outstanding enantioselectivities reach up to 96% ee.

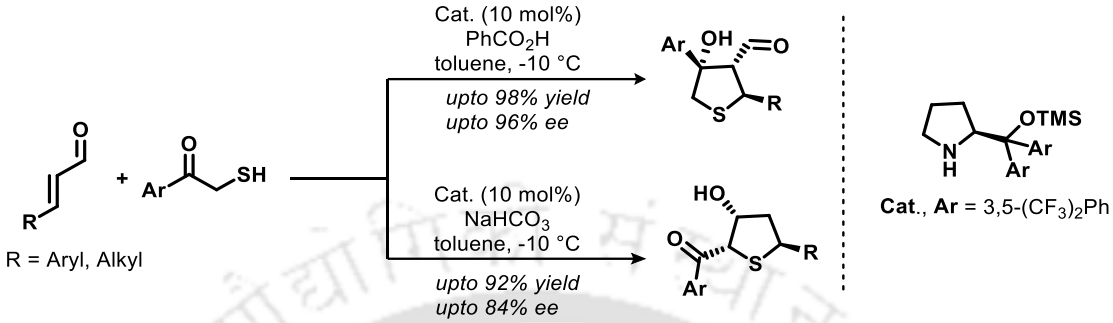

Scheme 1: Base controlled asymmetric divergent reaction.

In the year 2010, Feng and co-workers described a temperature-controlled cycloaddition reaction.[7] The author described an enantioselective Diels–Alder (DA) reaction and inverse-electron-demand hetero-Diels–Alder reaction with β,γ-unsaturated α-ketoesters and cyclopentadiene using chiral N,N′-dioxide–$Cu(OTf)_2$ complexes as catalysts. The selectivity of the DA and HDA adducts was enhanced by controlling the reaction temperature. DA adducts exhibited good to high selectivity when the reaction was conducted at room temperature, while moderate selectivity for the HDA adducts was observed at -20°C. However, in both cases excellent ees were observed.

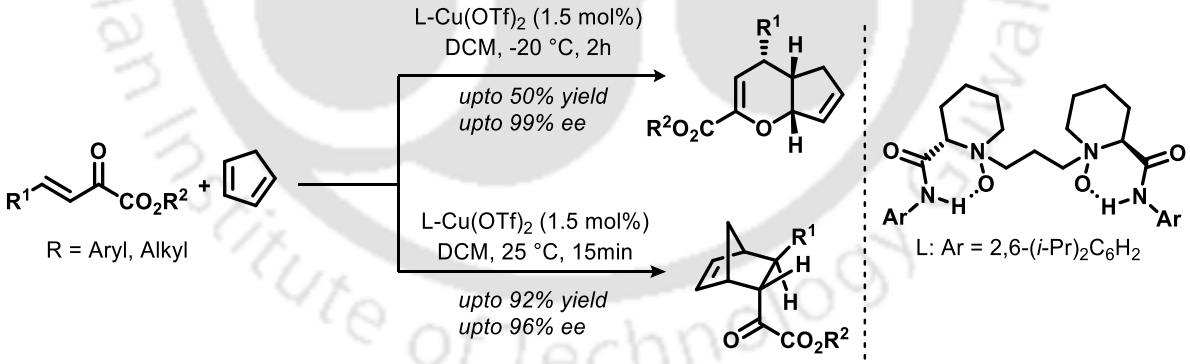

Scheme 2: Temperature-controlled asymmetric DA and HAD reaction.

Then, In the year 2020, Wang and co-workers has been established a double divergent process for the reaction between α-enaminones and quinones by easily adjusting the catalyst and additive, resulting in structurally divergent adduct.[8] In this method, the incorporation of phosphoric acid in the reaction altered the pathway, promoting the effective generation of various N-substituted indoles in excellent yield (upto 99%). On the other hand, the introduction of 4Å molecular sieves redirected the reaction pathway, resulting in the

enantioselective production of 2,3-dihydrobenzofurans with outstanding yields and upto 99% enantioselectivities under mild conditions.

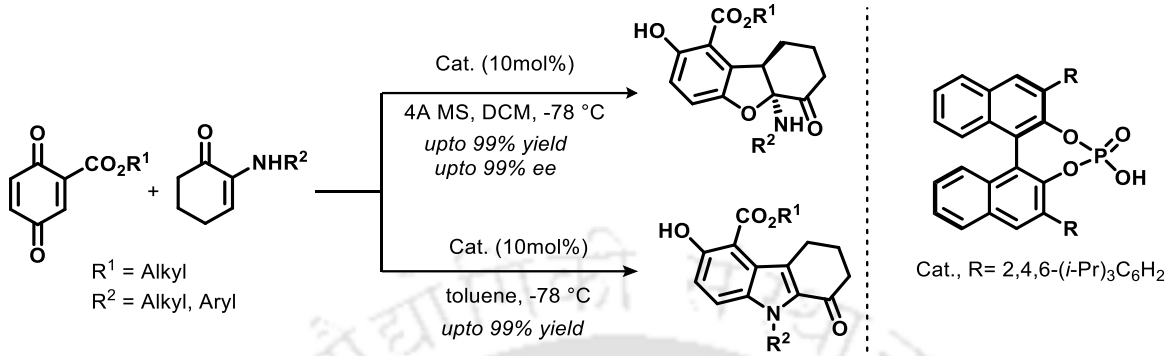

Scheme 3: Additive-controlled structurally-divergent reaction.

In the year 2021, Xu and co-workers described a solvent directed structurally divergent synthesis of β-lactams and α-amino acid derivatives.[9] Under isothiourea (ITU) catalysis imine and C(1)-ammonium enolate underwent a stereospecific Mannich reaction, resulting in the formation of zwitterionic intermediates. This intermediate underwent intramolecular lactamization in ACN/DCM solvent yielding β-lactam derivatives in excellent yield and enantioselectivities. Again, when ethanol was employed as the solvent, the intermediates participated in an intermolecular esterification to give chiral α-amino acids in good yield and enantioselctivities.

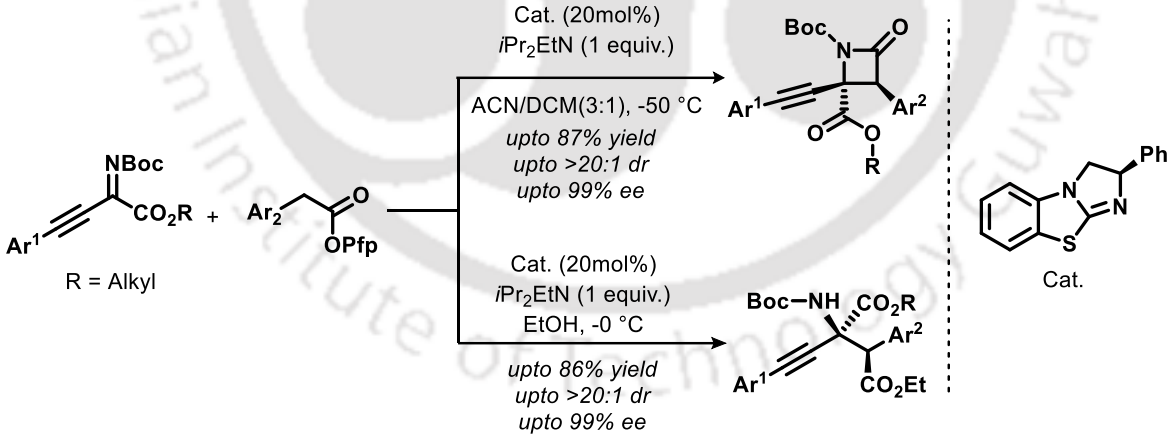

Scheme 4: Solvent-controlled structurally-divergent reaction.

2.2.2. Organocatalytic achiral divergent reactions with aurone-derived *α,β*-unsaturated imine:

In the year 2018, Huang and co-workers developed base-controlled divergent domino reaction with crotonate-derived sulfur ylides and azadienes.[10] In presence of 3 equiv. DABCO, the reaction underwent to form benzofuran fused six-membered rings in excellent yield.

Again, in presence of 3 equiv. K_2CO_3, the reaction afforded benzofuran fused seven-membered rings in excellent yield. In this divergent domino reaction, crotonate-derived sulfur ylides acts as a C2 or C3 synthon through the straightforward modification of the base.

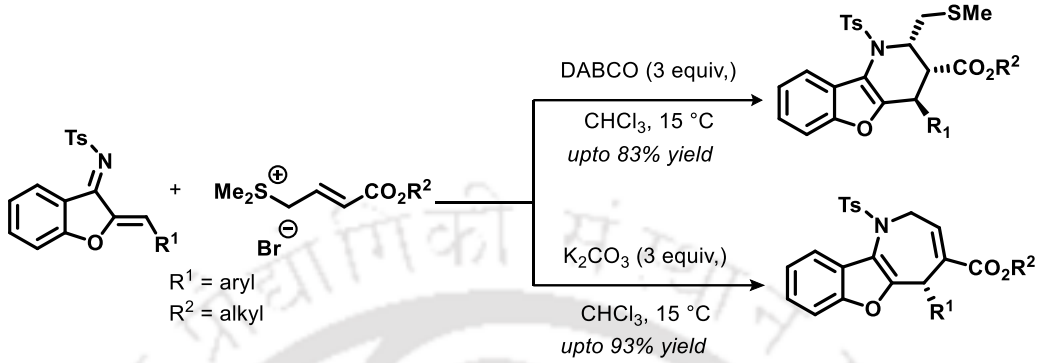

Scheme 5: Base-controlled structurally-divergent synthesis of benzofurans.

In the year 2010, Zhai and co-workers reported annulation reactions involving aurone-derived α,β-unsaturated imines and activated terminal alkynes has afforded a diverse set of 1,4-dihydrobenzofuro[3,2-b]pyridines.[11] The reaction afforded 4,5-substituted 1,4-dihydrobenzofuro[3,2-b]pyridines in presence of triethylamine in good yield. Again, in presence of triphenylphosphine afforded tri-substituted 1,4-dihydrobenzofuro[3,2-b]pyridines in excellent yield.

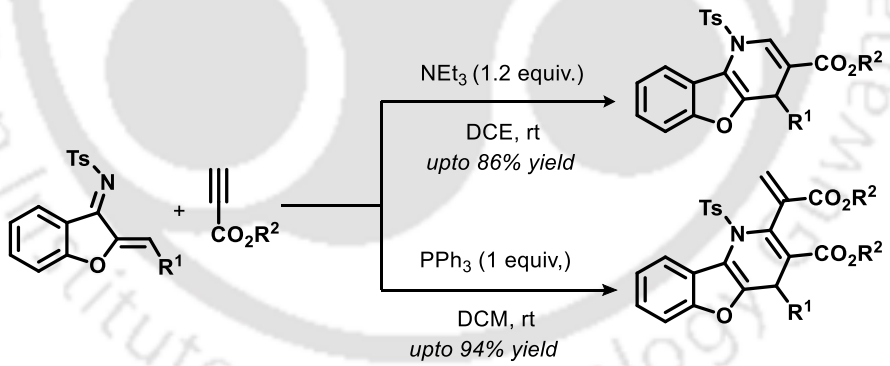

Scheme 6: Lewis-base controlled synthesis of diversely substituted benzofuro pyridines.

2.2.3. Selected example of synthesis of Azocine and spiro-benzofuran derivatives:

In the year 2017, Ullah and Lu unveiled a phosphine-catalyzed, enantioselective formal [4+4] annulation method for synthesizing eight-membered ring structures.[12] Utilizing amino-acid-derived phosphines catalyst, the formal [4+4] annulations between aurone-derived α,β-unsaturated imines and allene ketones occurred smoothly, resulting in a diverse array of benzofuran- or indole-fused azocines with high yields and outstanding enantioselectivities within 12h.

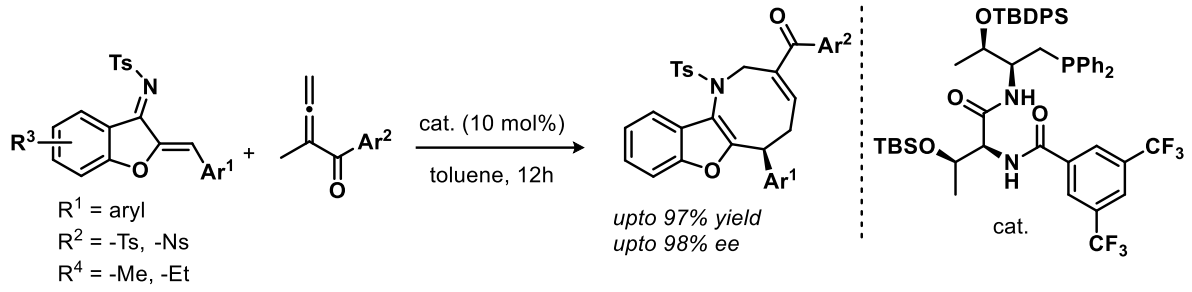

Scheme 7: Chiral phosphine catalyzed synthesis of azocines.

In the year 2020, Liu and Li reported an efficient method to synthesize spiro-indanones under bifunctional catalysis.[13] The authors described the reaction of spiro-annulation involving 2-(tosylmethyl)phenols and α-thiocyanato indanones is catalyzed by quinine-derived squramide catalyst. Under an optimized condition, 2-(tosyl methyl)phenols produce an intermediate o-quinonemethide. The intermediate underwent asymmetric 1,4-addition with α-thiocyanato indanones, followed by a spiro-cyclization, to obtain spiro-benzofuran compounds in high diastereoselectivity, outstanding yield, and enantioselectivities.

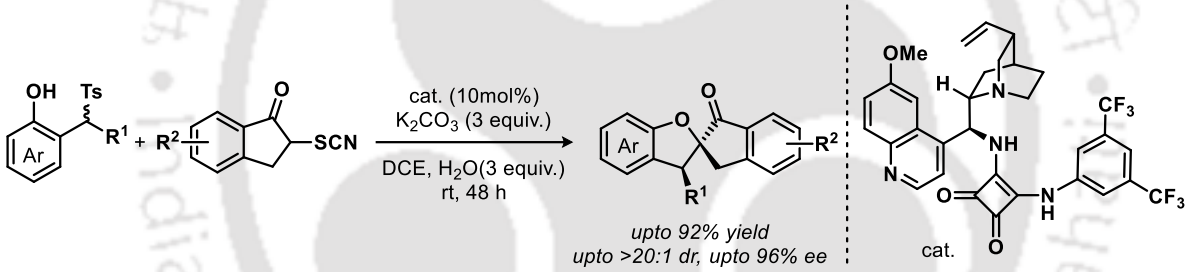

Scheme 8: Chiral bifunctional-catalyzed synthesis of spiro-benzofurans.

In the year 2019, Wang and co-workers presented an approach for the construction of highly diastereo- and enantioselective spiro-2,3-dihydrobenzofurans. Under bifunctional phosphonium salt catalysis *ortho*-quinone methides and α-bromoketones underwent [4+1] cycloaddition reactions to afford spiro-benzofuran derivatives in high yield and excellent diastreo-, enantioselectivities.

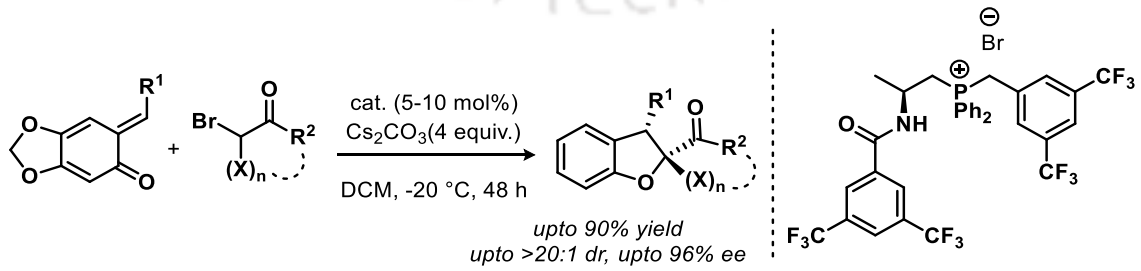

Scheme 9: Chiral Phosphine catalyzed synthesis of Spiro-benzofurans.

In the year 2019, Banerjee and co-workers reported that a formal [3 + 2] cycloaddition reaction catalyzed by MgI_2 takes place between donor-acceptor cyclopropanes and azadienes which felicitate spiro-benzofuran derivatives under mild condition. Under this condition, the reaction affords the chemoselective product in good yield.

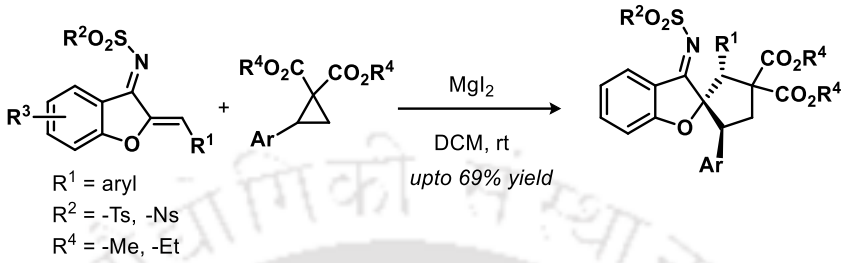

Scheme 10: MgI_2-catalyzed Synthesis of spiro-benzofuran.

2.3. Objective:

In the current work, we describe a unique divergent process by sequential catalysis[16] where the first step uses a bifunctional catalyst and in the second step, the chiral intermediate participates in Lewis base controlled divergent annulation reactions. This method presents organocatalytic cycle-varying cascade. We envisioned that a benzofuran/indole-derived nitrogen-containing electrophilic partner such as aurone derived α,β-unsaturated imine[17] could be coupled with alkynyl ketones[18] to deliver azocines and spiro-cyclopentanone benzofurans. We speculated that such a motif can be generated by reacting only the C=C of aurone-derived α,β-unsaturated imine. Herein, we would like to disclose our extensive explorations on these issues.

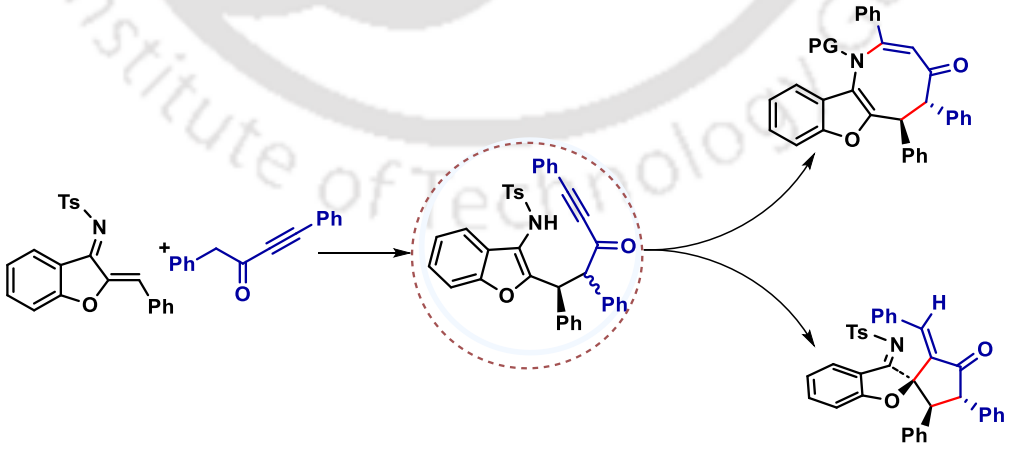

Scheme 11: Objective of the reaction.

2.4. Results and discussion:

2.4.1. Catalyst, solvent and temperature optimization for synthesis of azocine:

The initial experiment involved performing the reaction between N-sulfonyl 1-azadiene 1a and ynone **2a** with bifunctional urea catalyst **I** in toluene at room temperature (Table 1, entry 1). A smooth conversion was observed in 12 hours to provide intermediate **A** with 1.7:1 dr, which after short column chromatography was treated with DBU. This resulted in an annulation reaction with concomitant epimerization[19] for the formation of thermodynamically stable trans benzofuran fused azocine derivative **3a** with 88% yield, >20:1 dr and 84% ee. Interestingly, Takemoto catalyst **II** with a thiourea motif afforded **3a** with much less enantioselectivity (Table 1, entry 2). A good enantioselectivity of 80% was detected with *t*-leucine derived bifunctional urea catalyst **III** but thiourea derivative **IV** was not effective (Table 1, entries 3–4). Then we screened *t*-leucine derived bifunctional squaramide catalyst **V** in the reaction and moderate enantioselectivity was obtained (Table 1, entry 5). Then we turned our attention to employ cinchona alkaloid derived bifunctional urea and thiourea catalysts and this proved to be effective.[20] Cinchonidine derived bifunctional urea catalyst **VI** promoted the reaction with 90% yield and 88% ee was observed (Table 1, entry 6). Thiourea derivative **VII** was not effective (Table 1, entry 7). Similar trends of enantioselectivities were observed with quinine derived bifunctional urea and thiourea catalysts **VIII** and **IX** (Table 1, entries 8–9). Bifunctional squaramide catalyst **X** also was not suitable for the reaction (Table 1, entry 10).

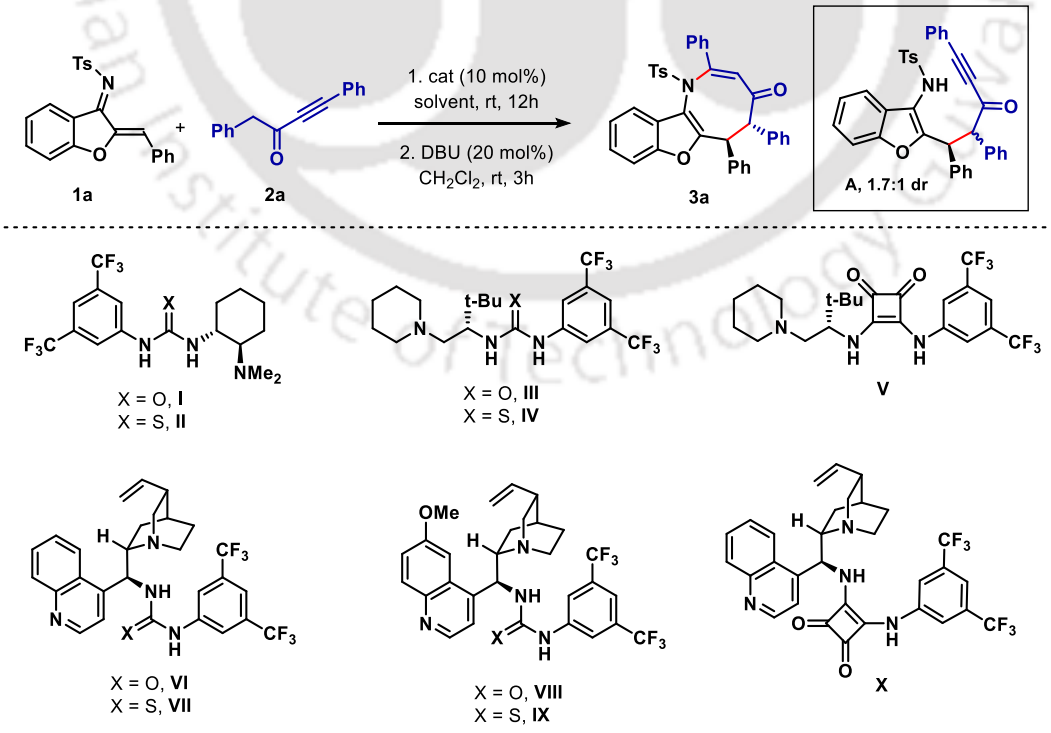

Table 1. ***Optimization of catalysts for chiral azocine:***

Entry[a]	Catalyst	Solvent	Yield(3a)[b]	d.r(3a)[c]	*ee*(3a)[d]
1	**I**	toluene	88%	>20:1	84%
2	**II**	toluene	57%	>20:1	33%
3	**III**	toluene	89%	>20:1	80%
4	**IV**	toluene	90%	>20:1	5%
5	**V**	toluene	90%	>20:1	67%
6	**VI**	toluene	90%	>20:1	88%
7	**VII**	toluene	30%	>20:1	12%
8	**VIII**	toluene	92%	>20:1	77%
9	**IX**	toluene	55%	>20:1	47%
10	**X**	toluene	<5%	n.d.	n.d.
11	**VI**	mesitylen	91%	>20:1	82%
12	**VI**	*o*-xylene	77%	>20:1	82%
13	**VI**	DCM	89%	>20:1	79%
14	**VI**	DCE	88%	>20:1	83%
15	**VI**	MTBE	89%	>20:1	76%
16[e]	**VI**	toluene	88%	>20:1	88%
17[f]	**VI**	toluene	91%	>20:1	92%
18[g]	**VI**	toluene	<5%	n.d.	n.d.

[a] Reactions were carried out with 0.1 mmol of **1a** with 0.11 mmol of **2a** in 1 ml solvent at rt. Then, the isolated intermediate **A** was treated with DBU (0.02 mmol) in DCM (1 mL) at rt for 3 h. [b] Isolated yield after silica gel column chromatography. [c] Determined by ^{1}H NMR. [d] Determined by chiral HPLC. [e] Reaction was run at 0 °C. [f] Reaction was run at -10 °C and for 2d. [g] Reaction was run at -20 °C for 72 hr.

Then we focused on the solvent optimization with catalyst **VI** (Table 1, entries 11–15). Slightly lower enantioselectivities were found in mesitylene and *o*-xylene solvents. However, no improvement was observed in DCM, DCE or MTBE solvents. Then the reaction was run in toluene at lower temperatures (Table 1, entries 16–17). Though the enantioselectivity did not change at 0 °C, the enantioselectivity improved to 92% ee after running the reaction at −10 °C for 2 days. Further lowering of temperature to -20 °C did not gave the desired product. Under the optimal conditions, the diastereomeric ratio of intermediate **A** was found to be 1.7:1

and the enantioselectivities of the major and minor diastereomers were 92% and 88% ees, respectively. A one-pot reaction was also performed but the product **3a** was obtained in lower enantioselectivity (90% yield and 83% ee).

2.4.2. Scope for the synthesis of azocines:

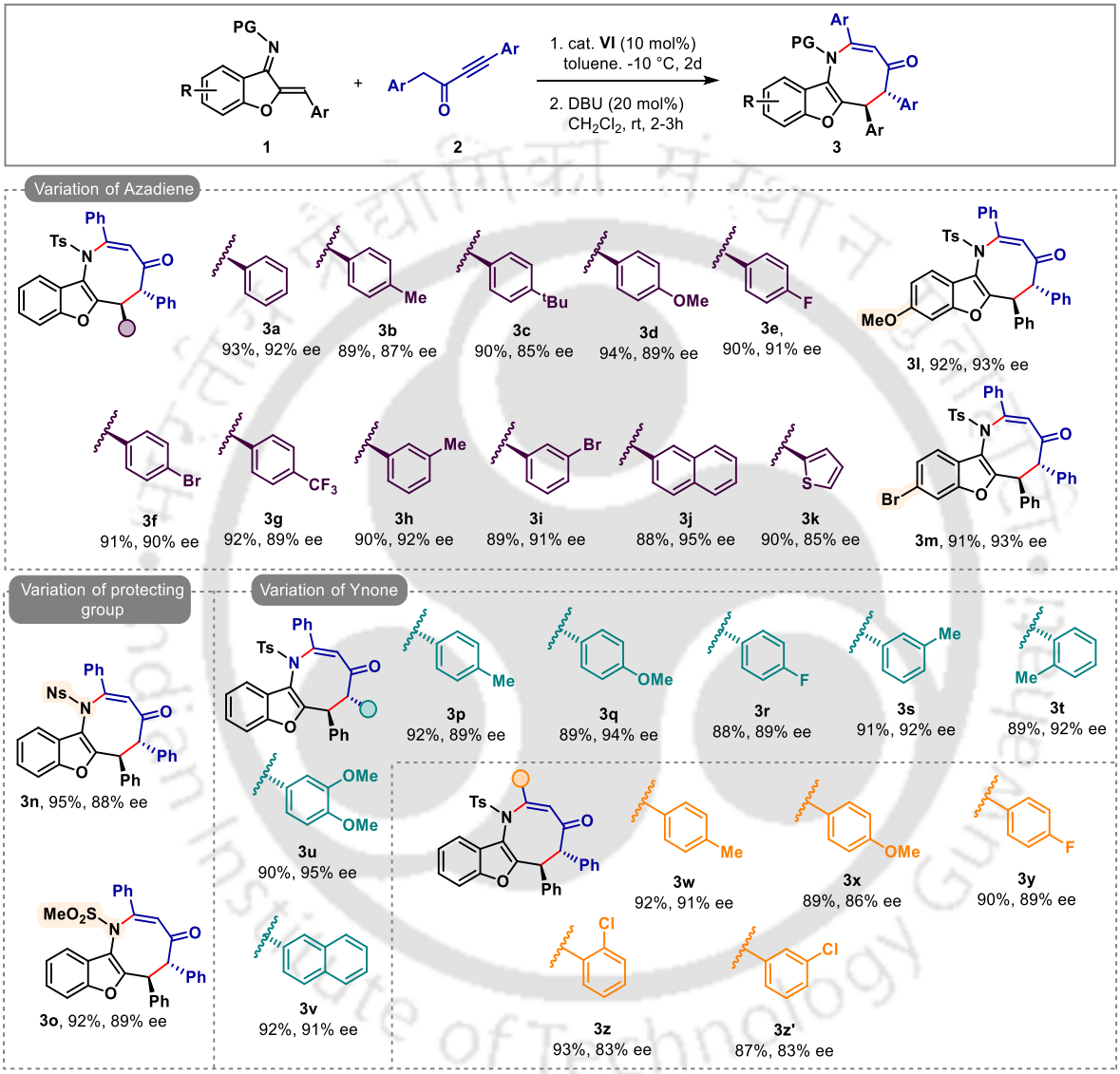

Scheme 12: Scope of chiral azocines.

After finalizing the optimal reaction conditions, we set out to determine the substrate range for this new [4 + 4] annulation. Initially, the scope of azadiene **1** was checked and gratifyingly good results were obtained. As shown in Scheme 12, high to excellent enantioselectivities and good to high yields were obtained for a variety of azadienes with substitutions in the *ortho*, *meta*, and *para* positions of the phenyl group. 4-Methyl and 4- methoxy substituted azadienes **1b** and **1d** provided products **3b** and **3d** in 87% and 89% ees, respectively. Slightly lower

enantioselectivity was detected for product **3c** having 4-*t*-butyl substitution. Halo substitutions were also tolerated and high enantioselectivities were observed for products **3e** and **3f** having 4-fluoro and 4-bromo substitutions, respectively. A smooth conversion was also detected for compound **2g** having 4-CF_3 substitution and the desired product **3g** was isolated in 92% yield with 89% ee. The reaction outcome did not change with meta-substituted aryl group containing azadienes **1h** and **1i**, and high enantioselectivities were attained for products **3h** and **3i**. 2-Naphthyl containing azadiene **1j** also participated in the reaction to deliver product **3j** in 95% ee. Finally, 2-thienyl containing azadiene **1k** was engaged in the reaction and a good result was obtained for product **3k**. Then substitutions in the benzofuran motif were examined, and pleasingly, methoxy- and bromo-substituted azadienes **1l** and **1m** reacted smoothly to provide products **3l** and **3m**, respectively, in 93% ee. Other groups, such as N-Ns and N–SO_2Me groups, could be used in place of the N-Ts group; and high enantioselectivities were found for **3n** and **3o**. Then the scope of ynone **2** was examined and encouragingly positive outcomes were found. Initially the aryl group close to the carbonyl group was varied. Here also, different substitutions at the *ortho*-, *meta*- and *para*-positions were tolerated and excellent enantioselectivities were detected for the products **3p**–**3t**. High enantioselectivity was detected for compound **3u** having a 3,4-disubstituted aryl group. The reaction outcome did not change with 2-naphthyl substitution and product **3v** was isolated in 92% yield with 91% ee. Then the substitutions on the aryl group attached to the triple bond in **2** were checked. To our delight, good results were observed for products **3w**–**3y** having different para-substituted aryl groups. Slightly lower enantioselectivities were detected for products **3z** and **3z′** having *ortho*- and *meta*-substitutions, respectively.

2.4.3. Scope for the synthesis of spiro-cyclopentanone benzofurans:

Next, the chiral intermediate **A** (dr = 1.7:1) formed from the reaction of **1a** and **2a** was treated with 20 mol% triphenylphosphine in CH_2Cl_2. To our delight, after stirring for 12 hours, spiro-cyclopentanone benzofuran **4a** with a stereogenic quaternary centre was isolated in 90% yield with 7:1 dr and 92% ee (Scheme 13). Here also epimerization was observed. A one-pot reaction was also performed but spiro-benzofuran **4a** was isolated in 83% yield with 77% ee. The minor diastereomer originates from the creation of a stereogenic quaternary centre. Then a variety of azadienes **1** were examined under sequential conditions, and encouragingly positive results were found. When several *para*-substitutions were first tested, the results for products **4b**–**4g** were pleasingly high in terms of diastereoselectivities and excellent in terms of enantioselectivities (Scheme 13). The outcome did not change with *meta*-substitutions and the products **4h** and **4i** were obtained in 92% and 91% ees, respectively. Naphthyl and thienyl substitutions were also tolerated and good results were detected for products **4j** and **4k**. Then,

the benzofuran motif's substitutions were looked at, and it was pleasing to see that the methoxy- and bromo-substituted azadienes **1l** and **1m** reacted smoothly to produce products **4l** and **4m** in 93% ee. Next, other imine protective groups were examined, and it was discovered that N-Ns and N–SO_2Me groups containing azadienes produced positive results for the products **4n**–**4o**. Then the scope of ynone **2**

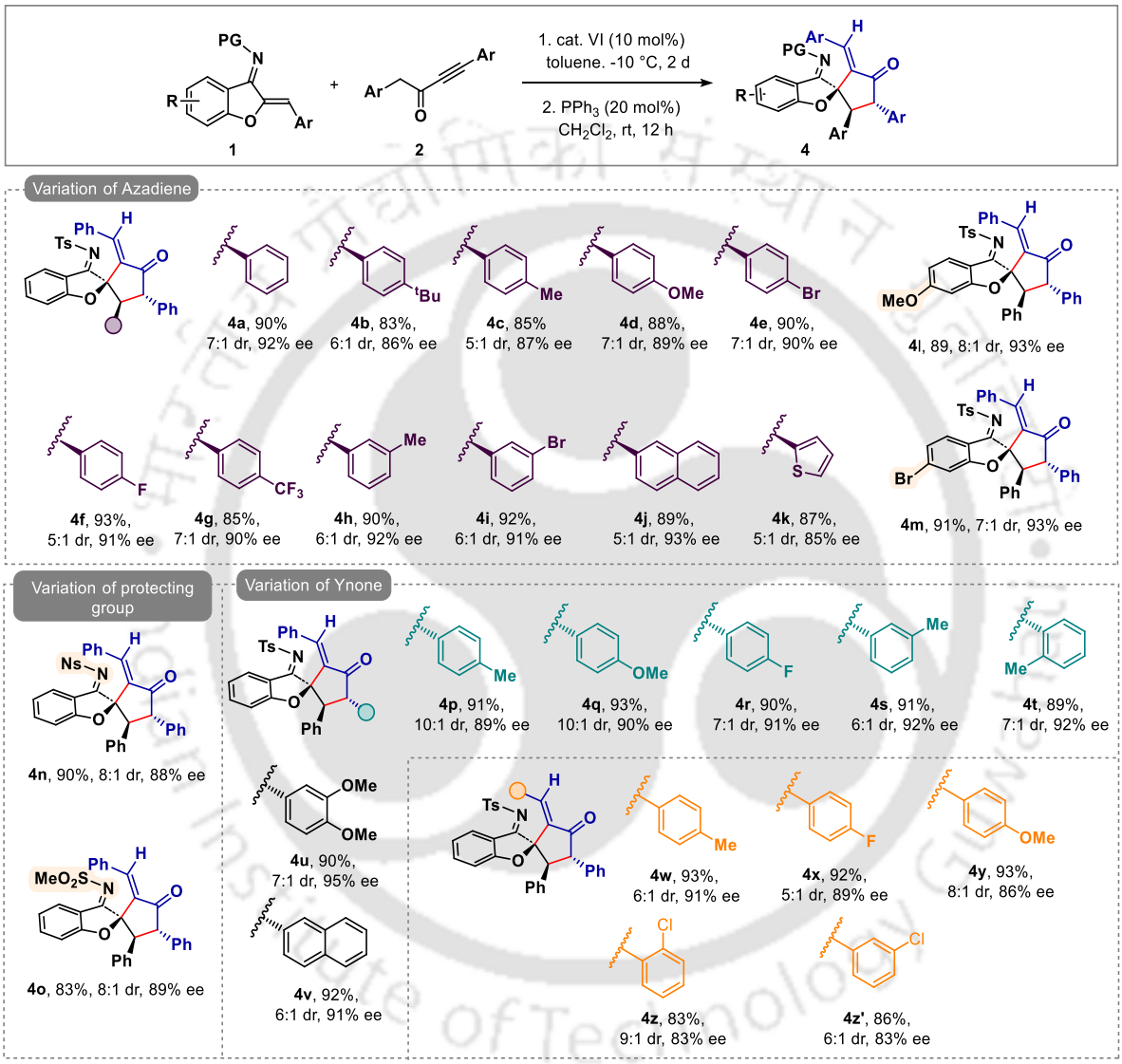

Scheme 13: Scope of chiral spiro-cyclopentanone benzofurans.

was checked and here also excellent results were found with different aryl group variations incorporated at the a-position of the carbonyl group of **2**. In fact, 89–92% ees were observed for products **4p**–**4v**. Then different substitutions on the aryl group attached to the triple bond in **2** were checked and excellent results were achieved for products **4w**–**4y** having different para-substitutions. The enantioselectivities slightly dropped with *ortho*- and *meta*-substitutions (both **4z** and **4z′** in 83% ee).

2.5. Determination of absolute configurations:

The absolute configuration of **3f** and **4k** was determined by single crystal X-ray crystallography. The absolute configuration of compound **3f** was determined to be (5*S*, 6*S*). Thus, other azocine derivatives **3** are expected to have same configuration. Similarly, the absolute configuration of **4k** was found to be (4'*S*, 5'*S*). Thus, other benzofurans **4** will have same configuration.

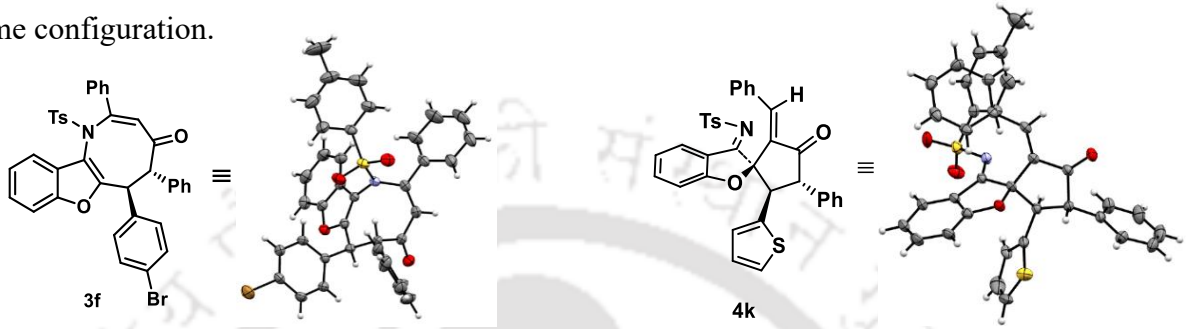

Scheme 14: ORTEP diagram of **3f** and **4k** with thermal ellipsoid probability 30%.

2.6. Synthetic transformation:

Then, azocine **3a** was subjected to a variety of organic transformations to further demonstrate the usefulness of our technique (Scheme 15). Initially, **3a** was treated with sodium borohydride and cerous chloride to provide **5** with an alcohol group in high diastereoselectivity and the enantioselectivity was almost retained. Then a chlorination reaction was performed with trichloroisocyanuric acid (TCCA). This resulted in the formation of **6** in 99% yield and both diastereo- and enantioselectivity were unchanged. Then, allylation of **3a** was carried out with allyl magnesium bromide in THF. To our delight, the reaction proceeded smoothly to provide compound **7** as a single diastereomer with high enantioselectivity. Finally, deprotection of the N-tosyl group was performed and product **8** was formed without erosion in enantioselectivity.

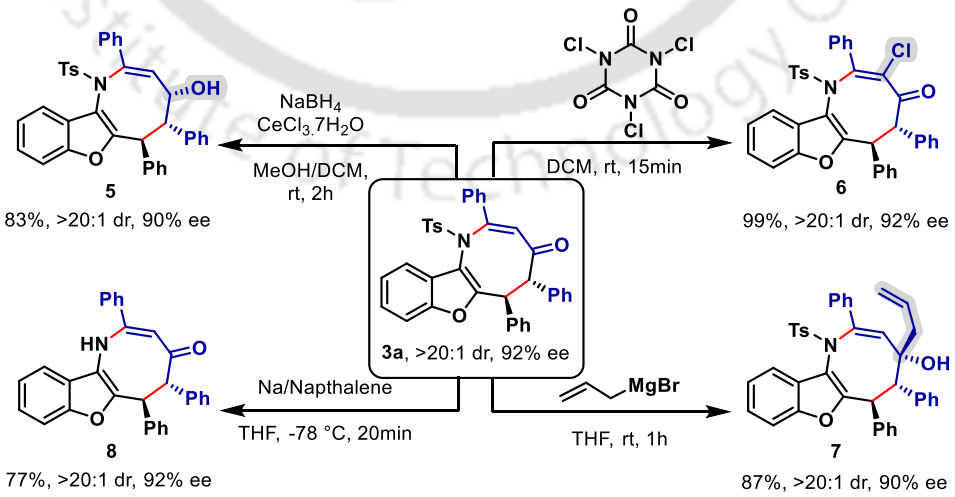

Scheme 15: Synthetic transformation of 3a.

2.7. Mechanism:

2.7.1. Control experiment:

To get insight of the mechanism, we carried out deuteration experiments with the intermediate **A** (Scheme 6). At first, **A** (1.7:1 dr) was treated with DBU (20 mol%) and D_2O (20 equiv) in CH_2Cl_2 at room temperature. ^1H nuclear magnetic resonance (NMR) analysis of **3a** revealed 85% deuterium incorporation at the C3- position and 75% deuterium incorporation at the C5-position. When **3a** was stirred under similar conditions, no H/D exchange was detected. Similarly, deuteration reaction was performed with intermediate A, PPh_3 (20 mol%) and D_2O (20 equiv) and in fact 80% deuterium incorporation was found at the olefin carbon and 64% deuterium incorporation was detected at the C4'-position of **4a**. No H/D exchange was noticed when **4a** was agitated in the same manner. This suggests, in both cases C2-center of **A** underwent an epimerization to deliver the stereoisomers in favour of the thermodynamically more stable *trans*-isomer.

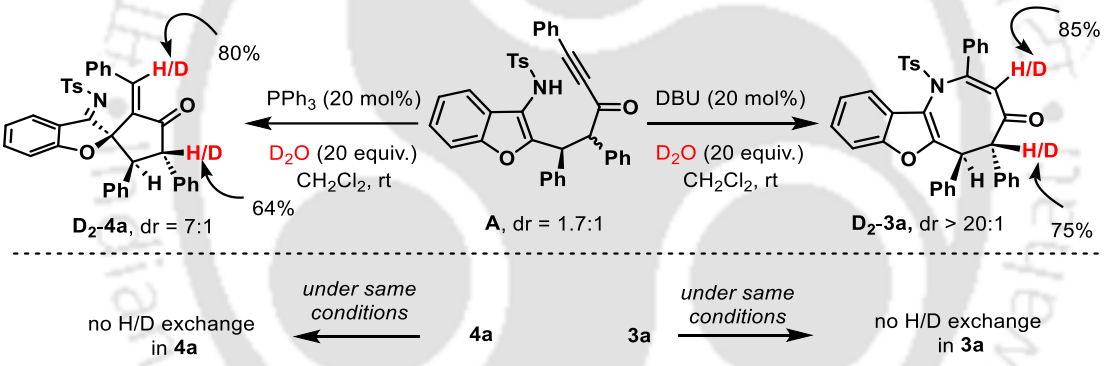

Scheme 16: Deuterium exchange experiment.

2.7.2. Proposed enantio-determining step:

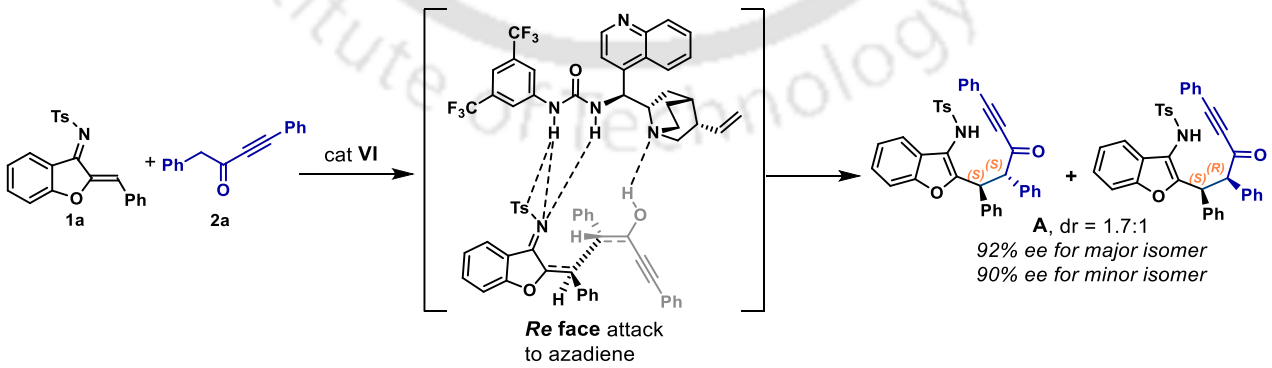

Scheme 17: Proposed transition state.

Based on the absolute configurations of **3f** and **4k**, we hypothesized that a favorable 1,4-Michael addition occurred at the *Re*-face of the 1-azadiene, resulting in intermediate **A** with a diastereomeric ratio of 1.7:1. This advantageous attack yielded intermediate **A** with 92% ee for the major isomer and 90% ee for the minor isomer. These findings were supported by theoretical calculations.

2.7.3. Proposed Mechanism for synthesis of azocine derivatives:

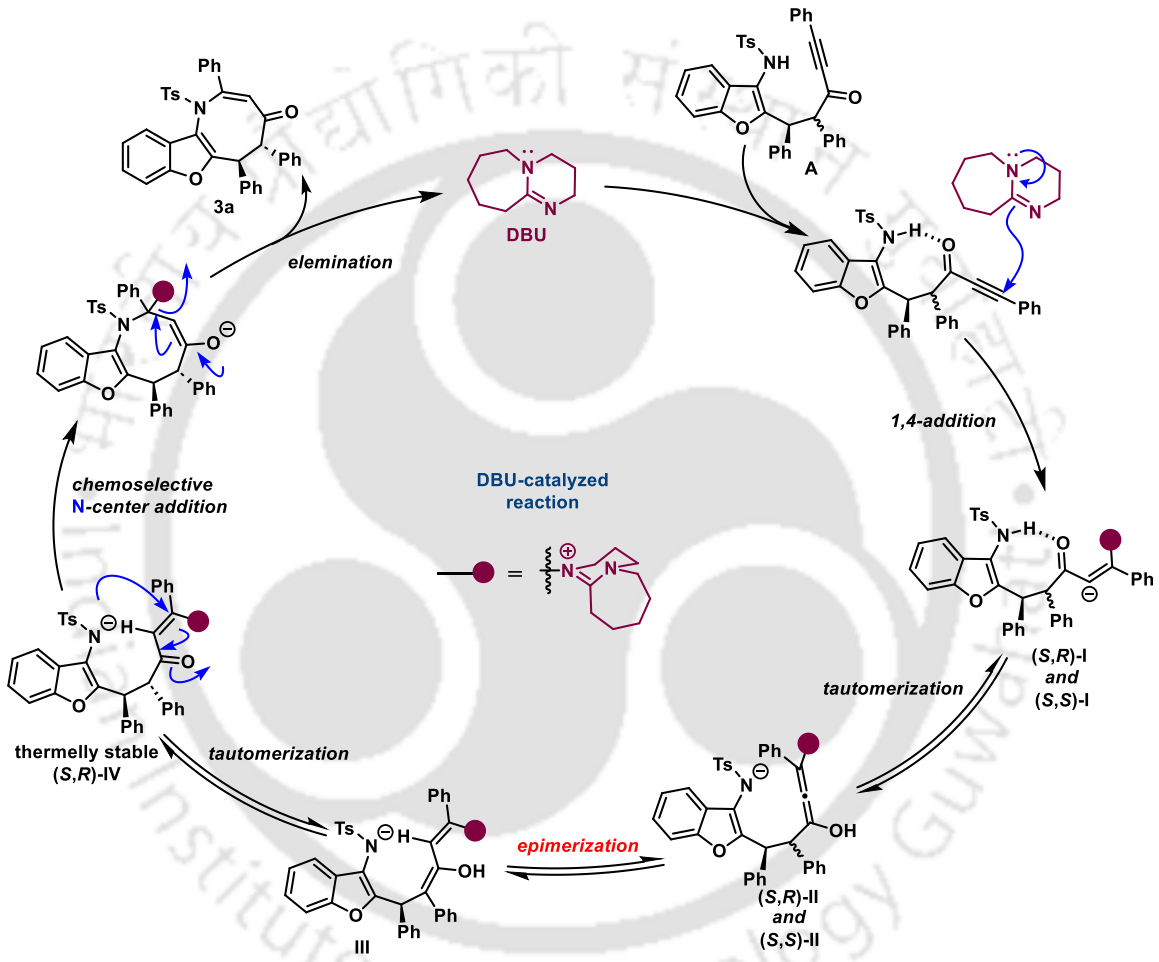

Scheme 18: Proposed catalytic cycle for azocine formation.

Based on the control experiment, we propose that DBU initially undergoes a 1,4-addition reaction with the diastereomers (*S*,*R*)-**A** and (*S*,*S*)-**A**, resulting in the formation of intermediate **II** through keto–enol tautomerization. Following this, the intermediates (*S*,*R*)-**II** and (*S*,*S*)-**II** undergo epimerization to yield a standard intermediate **III**. This intermediate **III** subsequently tautomerizes to form the thermally stable (*S*,*R*)-**IV**. This step promotes the generation of compound **3a** with high diastereoselectivity. Finally, the pathway leading to the formation of the eight-membered cyclized azocine derivative **3a** involves a stepwise intramolecular

nucleophilic attack by the nitrogen center on the electrophilic β-sp² carbon center, resulting in the release of DBU.

2.7.4. Proposed Mechanism for synthesis of spiro-benzofuran derivatives:

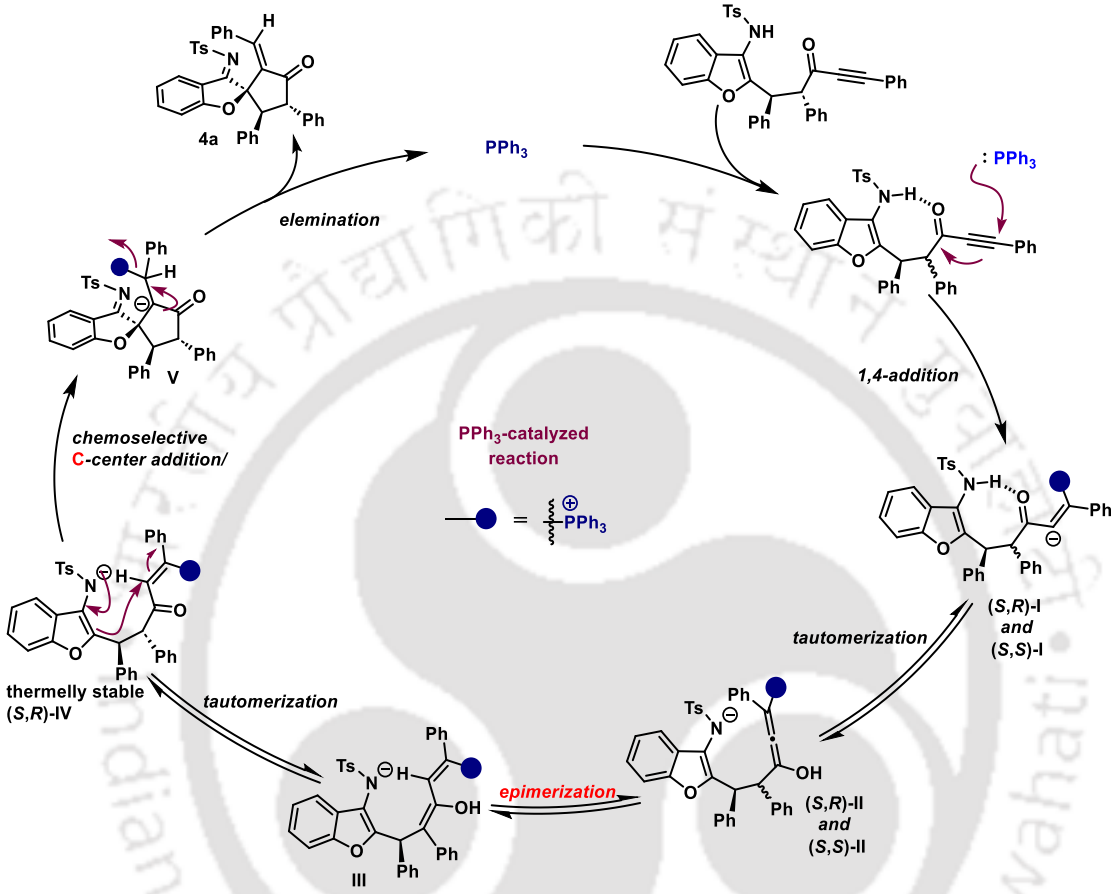

Scheme 19: Proposed catalytic cycle for spiro-cyclopentanone benzofuran formation.

In the PPh_3-catalyzed reaction, PPh_3 first undergoes a 1,4-addition reaction with the diastereomers (*S*,*R*)-**I** and (*S*,*S*)-**I**, leading to the formation of intermediate **II** through tautomerization. The intermediates (*S*,*R*)-**II** and (*S*,*S*)-**II** then undergo epimerization to yield a standard intermediate **III**. This intermediate **III** subsequently tautomerizes to form the thermally stable compound (*S*,*R*)-**IV**. This process enhances the generation of compound **4a** with high diastereoselectivity. Ultimately, the delocalization of the anionic electrons from the nitrogen atom to the C1 atom creates an intrinsic nucleophilic center next to the oxygen in the furan ring. This alteration facilitates an intramolecular nucleophilic umpolung attack on the α-sp^2 carbon center, resulting in the formation of a chiral spiro intermediate **V** through proton transfer. Following this, elimination of PPh_3 leads to the generation of the five-membered chiral spiro compound **4a**.

2.8. Conclusion:

We have developed a divergent pathway for the catalytic asymmetric synthesis of skeletally different benzofuran fused azocine derivatives and spiro-cyclopentanone benzofurans. The methodology involves sequential catalysis of chiral bifunctional urea catalysed reaction between aurone-derived α,β-unsaturated imine and ynone followed by Lewis base catalyzed divergent annulation reactions. In both cases, epimerization leads to high diastereoselctivity. Few synthetic transformations have also been performed. Given the significant medicinal value of azocines and spiro-cyclopentanone benzofurans, the pharmaceutical sector may find our procedure valuable.

2.9. Experimental Section:

2.9.1. General Information:

All dry solvents were dried using activated 4Å molecular sieves and stored under argon. For thin layer chromatography (TLC), silica gel plates with fluorescence indicator 254 nm were used and compounds were visualized by irradiation with UV light and/or by I_2. Celite® 512 medium was used for filtrations. Flash column chromatography was performed using 100-200 or 230-400 mesh silica gel. Petroleum ether and ethyl acetate for flash chromatography were acquired from commercial sources and were used without purification. NMR spectra were acquired on a Bruker 400 MHz, 500 MHz and 600 MHz spectrometer. Chemical shifts (δ) are reported in ppm relative to residual solvent signals ($CDCl_3$, 7.26 ppm for ^1H NMR and 77.23 ppm for ^{13}C NMR respectively. ^{13}C spectra were acquired on a broad band decoupled mode. For ^1H-NMR, data are reported as follows: chemical shift, multiplicity (s = singlet, d = doublet, dd = double doublet, ddd = doublet of doublet of doublets, t = triplet, q = quartet, dt = doublet of triplets, m = multiplet), coupling constants (Hz) and integration. Using ESI mode HRMS spectra were recorded. Enantiomeric ratios were determined by HPLC analysis performed on Chiral Columns using a Daicel Chiralpak IA, ID and IE Column.

2.9.2. General Procedure for synthesis of 1-azadiene:

The derivatives of azadiene were synthesized following reported literature procedure.[21]

2.9.3. General Procedure for synthesis of ynone:

The derivatives of ynone were synthesized following reported literature procedure.[22]

2.9.4. General Procedure for synthesis of various catalyst:

All the catalysts were synthesized according to the reported literature procedure.[23]

2.9.5. General Procedure for the Synthesis of chiral azocines derivatives:

To a stirred solution of 1-azadienes **1a** (0.1 mmol) and ynones **2a** (0.11 mmol) in dry toluene (1 mL) at -10 °C, were added catalyst **VI** 10 mol%, and the reaction was allowed to run at the same temperature for 2 days. After full consumption of starting materials, solvents were evaporated and the reaction mixture was subjected to a short column chromatography (petroleum ether : ethyl acetate = 95:5) to afford intermediate **A.** Then the intermediate **A** dissolved in 1ml DCM, and DBU (20 mol%) was added subsequently. The reaction mixture was stirred at room temperature until the complete conversion of intermediate **A** was detected. The solvents were removed under reduced pressure and purified by flash column chromatography (petroleum ether : ethyl acetate = 95:5) to give azocines (**3a-z'**).

2.9.6. General Procedure for the Synthesis of chiral Spiro-Cyclopentane Benzofurans:

To a stirred solution of 1-azadienes **1a** (0.1 mmol) and freshly prepared ynones **2a** (0.11 mmol) in toluene solvent (1 mL) at -10 °C, were added 10 mol% catalyst **VI**. The reaction was allowed to run in the same temperature for 2 days. After full consumption of starting materials, solvents were evaporated and the reaction mixture was subjected to a short column chromatography (petroleum ether : ethyl acetate = 90:10) to afford intermediate **A.** Then the intermediate **A** dissolved in 1ml DCM, and PPh_3 (20 mol%) was added subsequently. The reaction mixture was stirred at room temperature until the complete conversion of intermediate was detected. The solvents were removed under reduced pressure and purified by flash column chromatography (petroleum ether : ethyl acetate = 95:5 to 90:10) to give Spiro-Cyclopentane Benzofurans (**4a-z'**).

2.9.7. Procedure for the synthesis of compound 5:

In an oven dried 10 mL round-bottom flask, **3a** (59.5 mg, 0.1 mmol, 1.0 equiv) was taken along with 1.5 mL of MeOH and 1.5 mL of DCM. The resulting solution was cooled to 0 °C using an ice-bath, followed by portion-wise addition of $CeCl_3.7H_2O$ (73.9mg, 0.3 mmol, 3 equiv) and $NaBH_4$ (18.9 mg, 0.5 mmol, 5 equiv) separately. The resulting mixture was stirred at 0 °C. After complete consumption of **3a**, H_2O (5 mL) was added dropwise. The resulting mixture was diluted with 5 mL of DCM. The organic layer was separated, and the aqueous layer was extracted with DCM (3 × 5 mL). Combined organic layer was washed with brine (3 × 5 mL), dried over anhydrous Na_2SO_4 and concentrated under reduced pressure. The residue was purified by flash column chromatography (petroleum ether : ethyl acetate = 95:5) to give product **5**.

2.9.8. Procedure for the synthesis of compound 6:

In an oven dried 5ml vial, **3a** (59.5 mg, 0.1 mmol) was taken in 0.5 ml DCM. In that resulting solution, trichloroisocyanuric acid (TCCA) (23.2 mg, 0.1 mmol) was added and

stirred at room temperature until **3a** fully consumed. At the end of the reaction, the solvent was removed in vacuo. The residue was purified by flash column chromatography (petroleum ether : ethyl acetate = 95:5) to give product **6**.

2.9.9. Procedure for the synthesis of compound 7:

In an oven dried 10 mL round-bottom flask, **3a** (59.5 mg, 0.1 mmol, 1.0 equiv) was taken in 1.5 mL dry THF under argon atmosphere. The resulting solution was cooled to 0 °C using ice-bath, followed by dropwise addition of allyl magnesium bromide (1 M in Et_2O; 0.60 mL, 0.60 mmol, 4.0 equiv) over 5 minutes. The resulting mixture was allowed to attain ambient temperature. After complete consumption of **3a**, sat. aqueous NH_4Cl (3 mL) was added. The resulting mixture was dilute with EtOAc (5 mL). The organic layer was separated, and the aqueous layer was extracted with EtOAc (3 × 5 mL). Combined organic layer was washed with brine (2 × 5 mL), dried over anhydrous Na_2SO_4 and concentrated under reduced pressure. Purification by flash column chromatography (petroleum ether : ethyl acetate = 95:5) afforded **7**.

2.9.10. Procedure for the synthesis of compound 8:

To a solution of Napthalene(76.8mg, 0.6mmol, 6eqiv.) in 2ml THF was added sodium(13.6mg, 06mmol, 6equiv.) at room temperature under argon atmosphere. The colourless solution was stirred until becomes dark-green solution. After that, this solution was added over a solution of **3a** (59.5mg, 0.1mmol, 1equiv.) in 1ml THF at -78 °C for 10 min. The reaction mixture was stirred at the same temperature for 20 min. After, consumption of **3a**, sat. aq. NH_4Cl (3ml) was added. The mixture was diluted with EtOAc (5ml). The organic layer was separated, and the aqueous layer was extracted with EtOAc (3 × 5 mL). Combined organic layer was washed with brine (2 × 5 mL), dried over anhydrous Na_2SO_4 and concentrated under reduced pressure. Purification by flash column chromatography (petroleum ether : ethyl acetate = 90:15) afforded **8**.

2.10. Single crystal X-ray diffraction analysis:

The compound **3f** was dissolved in minimum amount of hot *n*-hexane/ethyl acetate (3:1) and kept the solution at room temperature for 4 days to give block like crystal. The crystallographic refinement parameters are given below:

CCDC	2235079		
Bond precision:	C-C = 0.0068 Å		Wavelength = 0.71073
Cell:	a = 8.8558(7) Å	b = 17.2619(11) Å	c = 10.4540(8) Å
	α = 90°	β = 91.877°	γ = 90°
Temperature:	296 K		

Volume (Å^3)	1597.2(2)
Space group	*P*21
Crystal system	*Monoclinic*
Moiety formula	$C_{38}H_{28}BrNO_4S$
Formula Weight	674.58
Density (g cm^{-3})	1.403
Z	2
Absorption coefficient, μ (mm^{-1})	1.394
F000	692.0
Index ranges	$-10 \leq h \leq 10$,$-20 \leq k$ 20,$-12 \leq l \leq 12$
Independent reflections	5612
T_{min},T_{max}	0.647,0.696
$T_{min'}$	0.634
Data completeness	1.93/1.00
θ range for data collection	1.949 to 24.996°
Final R indexes [$I \geq 2\sigma$ (I)]	R_1 = 0.0321, ωR_2 = 0.0658
Final R indexes [all data]	R_1 = 0.0444, ωR_2 = 0.0710
Goodness-of-fit on F^2	1.041
Data/restraints/parameters	5612/1/407
Flack parameter	0.023

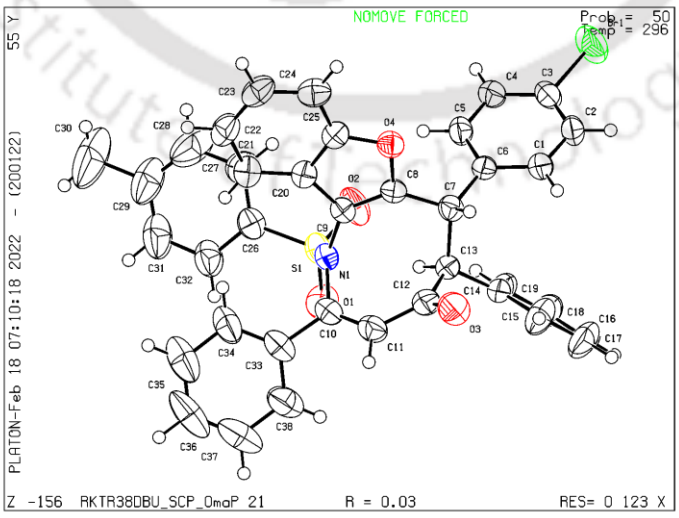

The compound **4k** was dissolved in minimum amount of hexane/chloroform (3:1) and kept the solution at room temperature for 7 days to give block like crystal. The crystallographic refinement parameters are given below:

CCDC	**2235267**		
Bond precision:	C-C = 0.0093 Å		Wavelength = 0.71073
Cell:	a = 10.022(4) Å	b = 11.611(5) Å	c = 30.123(13) Å
	α = 90°	β = 90°	γ = 90°
Temperature:	296 K		

Volume (Å^3)	3505(3)
Space group	*P*212121
Crystal system	*Orthorhombic*
Moiety formula	$C_{36}H_{27}NO_4S_2$
Formula Weight	721.07
Density (g cm^{-3})	1.366
Z	4
Absorption coefficient, μ (mm^{-1})	0.421
F000	1488.0
Index ranges	$-11 \le h \le 11$,$-13 \le k$ 13,$-35 \le l \le 35$
Independent reflections	6128
T_{min},T_{max}	0.922, 0.959
$T_{min'}$	0.912
Data completeness	1.76/0.99
θ range for data collection	1.35 to 25.00°
Final *R* indexes [$I \ge 2\sigma$ (I)]	R_1 = 0.0770, ωR_2 = 0.2148
Final *R* indexes [all data]	R_1 = 0.0935, ωR_2 = 0.2402
Goodness-of-fit on F^2	1.008
Data/restraints/parameters	6128/0/425
Flack parameter	0.05

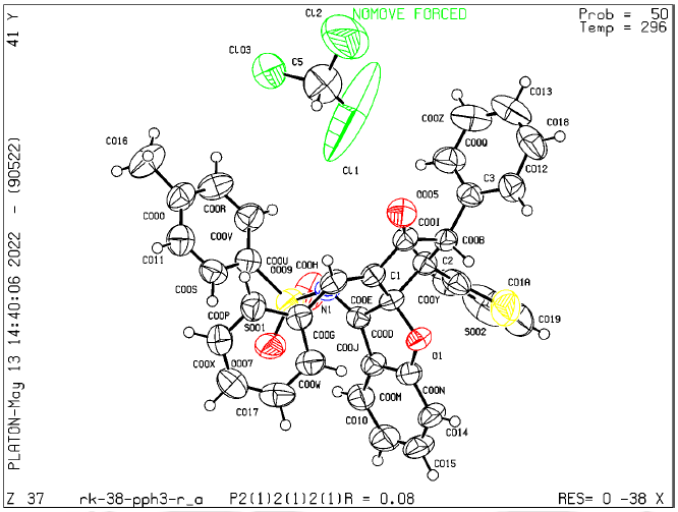

2.11. Characterization of the products:

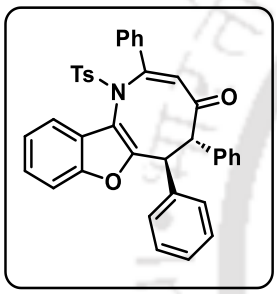

(5*S*,6*S*,*Z*)-2,5,6-triphenyl-1-tosyl-5,6-dihydrobenzofuro[3,2-b]azocin-4(1*H*)-one(3a): White solid, 55.4 mg, 93% yield, >20:1 *dr*, 92% *ee*; R_f = 0.5 (petroleum ether/ethyl acetate = 95:5)

^{1}H NMR (400 MHz, Chloroform-d) δ 7.58 (d, J = 7.3 Hz, 2H), 7.55 – 7.52 (m, 3H), 7.50 (s, 1H), 7.48 – 7.43 (m, 1H), 7.38 (d, J = 8.2 Hz, 1H), 7.33 (t, J = 7.6 Hz, 2H), 7.29 – 7.23 (m, 2H), 7.21 (d, J = 7.8 Hz, 2H), 7.17 – 7.13 (m, 5H), 7.09 (d, J = 7.3 Hz, 1H), 7.07 – 7.03 (m, 3H), 6.05 (d, J = 13.1 Hz, 1H), 5.92 (s, 1H), 4.88 (d, J = 13.1 Hz, 1H), 2.42 (s, 3H).**^{13}C NMR** (126 MHz, Chloroform-d) δ 201.13, 158.44, 154.88, 152.64, 144.85, 137.64, 136.98, 136.57, 136.21, 130.36, 130.22, 130.04, 129.95, 129.35, 129.11, 128.53, 128.35, 128.26, 127.51, 127.34, 126.88, 126.26, 125.31, 123.23, 120.54, 119.29, 112.24, 54.23, 49.51, 21.85. **HRMS (ESI$^+$) *m/z*:** $[M+H]^+$ calculated for $C_{38}H_{29}NO_4S$: 596.1890, found: 596.1893; **HPLC:** The enantiomeric excess was determined using CHIRALPAK ID column (*n*-Hexane/ *i*-PrOH=90:10, flow rate=1.0 mL/min, λ= 220 nm, τ_{major} = 22.6 min, τ_{minor} = 36.0 min).

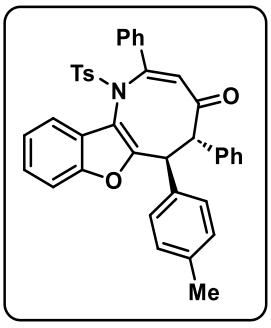

(5*S*,6*S*,*Z*)-2,5-diphenyl-6-(*p*-tolyl)-1-tosyl-5,6-dihydrobenzofuro [3,2-b]azocin-4(1*H*)-one (3b): White solid, 54.2 mg, 89% yield, >20:1 *dr*, 87% *ee*; R_f = 0.5 (petroleum ether/ethyl acetate = 95:5. MHz, Chloroform-d) δ 7.54 (t, J = 8.0 Hz, 4H), 7.49 – 7.44 (m, 3H), 7.38 (d, J = 8.3 Hz, 1H), 7.34 (t, J = 7.6 Hz, 2H), 7.28 – 7.23 (m, 4H), 7.18 – 7.13 (m, 4H), 7.06 – 7.04 (m, 3H), 6.99 (d, J = 7.8 Hz, 2H), 6.07 (d, J = 13.1 Hz, 1H), 5.92 (s, 1H), 4.88 (d, J = 13.1 Hz, 1H), 2.42 (s, 3H), 2.20 (s, 3H). **13C NMR** (126 MHz, Chloroform-d) δ 201.24, 158.69,

154.89, 152.59, 144.80, 136.98, 136.83, 136.53, 136.33, 134.49, 130.33, 130.18, 129.93, 129.84, 129.32, 129.10, 129.07, 128.51, 128.26, 127.46, 126.79, 126.27, 125.21, 123.18, 120.34, 119.21, 112.23, 54.22, 48.93, 21.84, 21.26. **HRMS (ESI$^+$) *m/z*:** $[M+Na]^+$ calculated for $C_{38}H_{29}NO_4S$: 632.1866, found: 632.1853; **HPLC:** The enantiomeric excess was determined using CHIRALPAK ID column (*n*-Hexane/ *i*-PrOH =90:10, flow rate=1.0 mL/min, λ= 254 nm, τ_{major} = 23.0 min, τ_{minor} = 29.4 min).

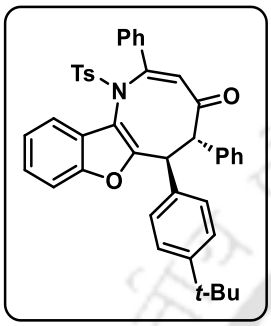

(5*S*,6*S*,*Z*)-6-(4-(*tert*-butyl)phenyl)-2,5-diphenyl-1-tosyl-5,6-dihydrobenzofuro[3,2-b]azocin-4(1*H*)-one: White solid, 60.9 mg, 90% yield, >20:1 *dr*, 85% *ee*; R_f = 0.5 (petroleum ether/ethyl acetate = 95:5). **^{1}H NMR** (500 MHz, Chloroform-d) *δ* 7.54 – 7.49 (m, 4H), 7.47 – 7.43 (m, 3H), 7.39 (d, *J* = 8.2 Hz, 1H), 7.33 (t, *J* = 7.6 Hz, 2H), 7.25 – 7.24 (m, 2H), 7.22 (t, *J* = 7.5 Hz, 2H), 7.18 – 7.13 (m, 6H), 7.05 (t, *J* = 9.2 Hz, 3H), 6.02 (d, *J* = 13.1 Hz, 1H), 5.90 (s, 1H), 4.86 (d, *J* = 13.2 Hz, 1H), 2.42 (s, 3H), 1.19 (s, 9H). **^{13}C NMR** (126 MHz, Chloroform-d) *δ* 201.37, 158.83, 154.79, 152.62, 149.86, 144.78, 137.07, 134.43, 130.31, 130.19, 129.97, 129.52, 129.34, 129.10, 128.51, 128.22, 127.38, 126.83, 126.34, 125.25, 123.20, 120.45, 119.25, 112.26, 54.40, 48.99, 34.53, 31.44, 21.86. **HRMS (ESI$^+$) *m/z*:** $[M+H]^+$ calculated for $C_{42}H_{37}NO_4S$: 652.2517, found: 652.2517; **HPLC:** The enantiomeric excess was determined using CHIRALPAK ID column (*n*-Hexane/ *i*-PrOH =90:10, flow rate=1.0 mL/min, λ= 254 nm, τ_{major} = 13.6 min, τ_{minor} = 19.7 min).

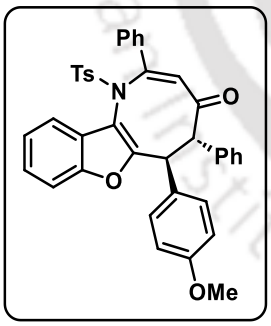

(5*S*,6*S*,*Z*)-6-(4-methoxyphenyl)-2,5-diphenyl-1-tosyl-5,6-dihy*dro* benzofuro[3,2-b]azocin-4(1*H*)-one (3d): White solid, 58.7 mg, 94% yield, >20:1 *dr*, 90% *ee*; R_f = 0.5 (petroleum ether/ethyl acetate = 95:5);

1H NMR (500 MHz, Chloroform-d) δ 7.51 (q, J = 8.0 Hz, 6H), 7.44 (t, J = 7.4 Hz, 1H), 7.37 (d, J = 8.2 Hz, 1H), 7.32 (t, J = 7.6 Hz, 2H), 7.24 – 7.21 (m, 3H), 7.16 – 7.12 (m, 4H), 7.03 (t, J = 7.3 Hz, 3H), 6.70 (d, J = 8.6 Hz, 2H), 6.02 (d, J = 13.1 Hz, 1H), 5.90 (s, 1H), 4.84 (d, J = 13.1 Hz, 1H), 3.66 (s, 3H), 2.40 (s, 3H). **13C NMR** (126 MHz, Chloroform-d) δ 201.21, 158.76, 158.69, 154.81, 152.59, 144.82, 136.98, 136.53, 136.35, 131.03, 130.33, 130.19, 129.92, 129.74, 129.33, 129.07, 128.51, 128.27, 127.47, 126.83, 126.27, 125.23, 123.20, 120.33, 119.23, 113.76, 112.20, 55.20, 54.46, 48.70, 21.82. **HRMS (ESI$^+$) *m/z*:** $[M+H]^+$ calculated for $C_{39}H_{31}NO_5S$: 626.1996, found: 626.1996; **HPLC:** The enantiomeric excess was determined using CHIRALPAK ID column (*n*-Hexane/ *i*-PrOH =90:10, flow rate=1.0 mL/min, λ= 254 nm, τ_{major} = 13.6 min, τ_{minor} = 19.7 min).

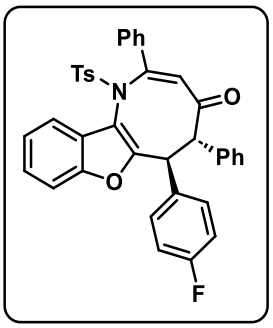

(5*S*,6*S*,*Z*)-6-(4-fluorophenyl)-2,5-diphenyl-1-tosyl-5,6-dihydro benzofuro[3,2-b]azocin-4(1*H*)-one (3e): White solid, 55.1 mg, 90% yield, >20:1 *dr*, 91% *ee*; R_f = 0.5 (petroleum ether/ethyl acetate = 95:5)

^{1}H NMR (500 MHz, Chloroform-d) δ 7.58 – 7.51 (m, 6H), 7.47 (t, J = 7.4 Hz, 1H), 7.40 (d, J = 8.2 Hz, 1H), 7.34 (t, J = 7.5 Hz, 2H), 7.30 – 7.23 (m, 4H), 7.20 – 7.17 (m, 2H), 7.13 (d, J = 8.1 Hz, 2H), 7.05 (d, J = 8.0 Hz, 3H), 6.87 (t, J = 8.7 Hz, 2H), 6.03 (d, J = 13.1 Hz, 1H), 5.93 (s, 1H), 4.88 (d, J = 13.1 Hz, 1H), 2.43 (s, 3H). **^{13}C NMR** (126 MHz, Chloroform-d) δ 200.95, 163.03, 161.07, 158.13, 154.88, 152.63, 144.94, 136.86, 136.42, 136.04, 133.43, 133.41, 131.63, 131.57, 130.41, 130.16, 129.93, 129.37, 129.07, 128.56, 128.37, 127.64, 126.80, 126.14, 125.44, 123.32, 120.58, 119.32, 115.35, 115.18, 112.22, 54.28, 48.77, 21.86. **HRMS (ESI$^+$) *m/z*:** $[M+K]^+$ calculated for $C_{38}H_{28}FNO_4S$: 652.1355, found: 652.1358; **HPLC:** The enantiomeric excess was determined using CHIRALPAK ID column (*n*-Hexane/ *i*-PrOH =90:10, flow rate=1.0 mL/min, λ= 254 nm, τ_{major} = 17.5 min, τ_{minor} = 27.0 min).

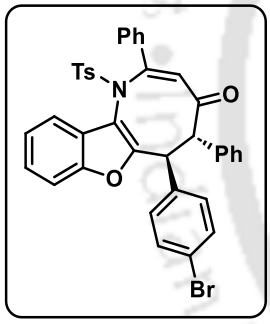

(5*S*,6*S*,*Z*)-6-(4-bromophenyl)-2,5-diphenyl-1-tosyl-5,6-dihy*dro* benzofuro[3,2-b]azocin-4(1*H*)-one (3f): White solid, 61.3 mg, 91% yield, >20:1 *dr*, 90% *ee*; R_f = 0.5 (petroleum ether/ethyl acetate = 95:5)

^{1}H NMR (400 MHz, Chloroform-d) δ 7.54 – 7.51 (m, 3H), 7.50 – 7.47 (m, 2H), 7.46 – 7.44 (m, 2H), 7.39 (d, J = 8.2 Hz, 1H), 7.34 (d, J = 7.6 Hz, 2H), 7.32 – 7.28 (m, 3H), 7.24 – 7.23 (m, 2H), 7.20 – 7.15 (m, 2H), 7.14 – 7.10 (m, 2H), 7.05 – 7.02 (m, 3H), 6.03 (d, J = 13.2 Hz, 1H), 5.92 (s, 1H), 4.85 (d, J = 13.2 Hz, 1H), 2.42 (s, 3H). **^{13}C NMR** (101 MHz, Chloroform-d) δ 200.79, 157.78, 154.92, 152.65, 144.96, 136.83, 136.67, 136.41, 135.88, 131.73, 131.53, 130.44, 130.11, 129.93, 129.38, 129.07, 128.57, 128.47, 127.76, 126.75, 126.09, 125.50, 123.36, 121.53, 120.66, 119.31, 112.24, 53.93, 48.82, 21.88. **HRMS (ESI$^+$) *m/z*:** $[M+H]^+$ calculated for $C_{38}H_{28}BrNO_4S$: 674.0995, found: 674.1024; **HPLC:** The enantiomeric excess was determined using CHIRALPAK ID column (*n*-Hexane/ *i*-PrOH =90:10, flow rate=1.0 mL/min, λ= 254 nm, τ_{major} = 19.8 min, τ_{minor} = 29.0 min).

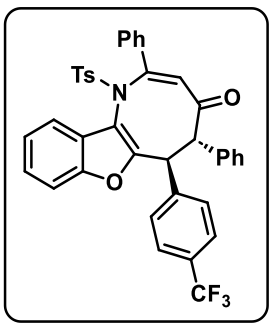

(5*S*,6*S*,*Z*)-2,5-diphenyl-1-tosyl-6-(4-(trifluoromethyl)phenyl)-5,6-dihydrobenzofuro[3,2-b]azocin-4(1*H*)-one (3g): White solid, 60.9

mg, 92% yield, >20:1 *dr*, 89% *ee*; R_f = 0.5 (petroleum ether/ethyl acetate = 95:5)

^{1}H NMR (500 MHz, Chloroform-d) δ 7.72 (d, J = 8.1 Hz, 2H), 7.54 – 7.51 (m, 4H), 7.46 - 7.43 (m, 3H), 7.39 (d, J = 8.2 Hz, 1H), 7.34 (t, J = 7.7 Hz, 2H), 7.31 – 7.27 (m, 1H), 7.25 – 7.22 (m, 2H), 7.17 (q, J = 7.5 Hz, 2H), 7.12 (d, J = 8.3 Hz, 2H), 7.06 – 7.03 (m, 3H), 6.08 (d, J = 13.2 Hz, 1H), 5.94 (s, 1H), 4.95 (d, J = 13.1 Hz, 1H), 2.43 (s, 3H). **^{13}C NMR** (126 MHz, Chloroform-d) δ 200.41, 157.26, 154.75, 141.43, 135.51, 130.26, 130.18, 129.87, 129.73, 129.19, 128.87, 128.38, 128.30, 127.62, 126.54, 125.41, 125.15, 125.12, 123.22, 120.71, 119.16, 112.06, 53.63, 48.94, 21.66. **HRMS (ESI$^+$) *m/z*:** $[M+H]^+$ calculated for $C_{39}H_{28}F_3NO_4S$: 664.1764, found: 664.1797; **HPLC:** The enantiomeric excess was determined using CHIRALPAK IA column (*n*-Hexane/ *i*-PrOH =90:10, flow rate=1.0 mL/min, λ= 220 nm, τ_{major} = 10.73 min, τ_{minor} = 15.5 min).

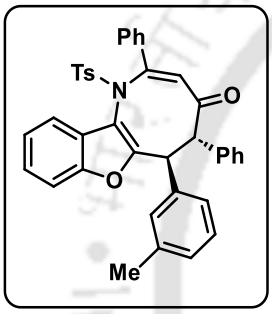

(5*S*,6*S*,*Z*)-2,5-diphenyl-6-(*m*-tolyl)-1-tosyl-5,6-dihydro benzofuro[3,2-b]azocin-4(1*H*)-one (3h): White solid, 54.8 mg, 90% yield, >20:1 *dr*, 92% *ee*; R_f = 0.5 (petroleum ether/ethyl acetate = 95:5)

^{1}H NMR (500 MHz, Chloroform-d) δ 7.54 (d, J = 6.9 Hz, 2H), 7.50 (d, J = 7.0 Hz, 2H), 7.47 – 7.43 (m, 1H), 7.41 – 7.36 (m, 3H), 7.33 (t, J = 7.6 Hz, 2H), 7.28 – 7.27 (m, 1H), 7.26 – 7.25 (m, 1H), 7.23 – 7.20 (m, 2H), 7.17 – 7.14 (m, 4H), 7.08 (s, 1H), 7.05 (dd, J = 8.1, 6.4 Hz, 3H), 6.89 (d, J = 7.5 Hz, 1H), 6.02 (d, J = 13.1 Hz, 1H), 5.90 (s, 1H), 4.83 (d, J = 13.1 Hz, 1H), 2.42 (s, 3H), 2.23 (s, 3H). **^{13}C NMR** (126 MHz, Chloroform-d) δ 201.21, 158.61, 154.82, 152.65, 144.79, 137.83, 137.48, 137.10, 136.62, 136.31, 130.88, 130.31, 130.24, 129.97, 129.34, 129.13, 128.51, 128.20, 128.17, 128.11, 127.47, 127.00, 126.91, 126.37, 125.25, 123.21, 120.57, 119.27, 112.27, 54.35, 49.47, 21.84, 21.56. **HRMS (ESI$^+$) *m/z*:** $[M+H]^+$ calculated for $C_{39}H_{31}NO_4S$: 610.2047, found: 610.2050; **HPLC:** The enantiomeric excess was determined using CHIRALPAK ID column (*n*-Hexane/ *i*-PrOH=90:10, flow rate=1.0 mL/min, λ= 254 nm, τ_{major} = 23.0 min, τ_{minor} = 28.1 min).

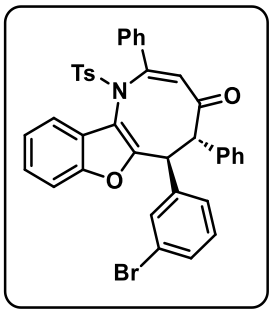

(5*S*,6*S*,*Z*)-6-(3-bromophenyl)-2,5-diphenyl-1-tosyl-5,6-dihydro benzofuro[3,2-b]azocin-4(1*H*)-one (3i): White solid, 59.9 mg, 89% yield, >20:1 *dr*, 91% *ee*; R_f = 0.5 (petroleum ether/ethyl acetate = 95:5)

^{1}H NMR (400 MHz, Chloroform-d) δ 7.77 – 7.76 (m, 1H), 7.53 – 7.46 (m, 6H), 7.43 (d, J = 7.6 Hz, 1H), 7.39 (d, J = 8.2 Hz, 1H), 7.33 (d, J = 7.6 Hz, 2H), 7.31 – 7.26 (m, 1H), 7.26-7.21 (m, 3H), 7.20 – 7.18 (m,

1H), 7.17 – 7.11 (m, 4H), 7.04 – 6.99 (m, 4H), 5.98 (d, *J* = 13.2 Hz, 1H), 5.90 (s, 1H), 4.81 (d, *J* = 13.1 Hz, 1H), 2.41 (s, 3H). **^{13}C NMR** (126 MHz, Chloroform-d) *δ* 200.66, 157.59, 154.89, 152.71, 144.93, 139.93, 136.89, 136.52, 135.82, 133.11, 130.53, 130.42, 130.17, 129.94, 129.87, 129.38, 129.13, 128.60, 128.56, 128.43, 127.75, 126.83, 126.17, 125.54, 123.38, 122.36, 120.92, 119.37, 112.30, 54.07, 49.16, 21.85. **HRMS (ESI$^+$) *m/z*:** $[M+H]^+$ calculated for $C_{38}H_{28}BrNO_4S$: 674.0995, found: 674.1001; **HPLC:** The enantiomeric excess was determined using CHIRALPAK ID column (*n*-Hexane/ *i*-PrOH =90:10, flow rate=1.0 mL/min, λ= 254 nm, τ_{major} = 22.7 min, τ_{minor} = 33.8 min).

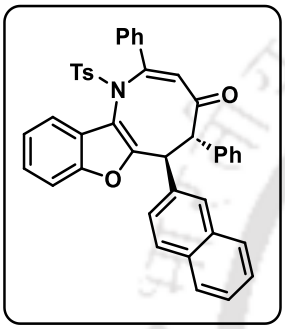

(5*S*,6*S*,*Z*)-6-(naphthalen-2-yl)-2,5-diphenyl-1-tosyl-5,6-dihydro benzofuro[3,2-b]azocin-4(1*H*)-one (3j): White solid, 56.7 mg, 88% yield, >20:1 *dr*, 95% *ee*; R_f = 0.5 (petroleum ether/ethyl acetate = 95:5)

^{1}H NMR (500 MHz, Chloroform-d) *δ* 8.10 (s, 1H), 7.78 – 7.77 (m, 1H), 7.74 – 7.72 (m, 1H), 7.69 – 7.67 (m, 1H), 7.64 (d, *J* = 8.6 Hz, 1H), 7.57 – 7.54 (m, 4H), 7.48 – 7.45 (m, 1H), 7.39 – 7.33 (m, 5H), 7.26 – 7.23 (m, 1H), 7.19 – 7.13 (m, 5H), 7.10 – 7.03 (m, 4H), 6.16 (d, *J* = 13.1 Hz, 1H), 5.94 (s, 1H), 5.05 (d, *J* = 13.1 Hz, 1H), 2.42 (s, 3H). **^{13}C NMR** (126 MHz, Chloroform-d) *δ* 201.08, 158.39, 154.92, 152.68, 144.87, 137.01, 136.61, 136.14, 135.27, 133.51, 132.73, 130.38, 130.19, 129.99, 129.53, 129.37, 129.16, 128.55, 128.30, 127.95, 127.67, 127.64, 127.56, 126.92, 126.30, 125.88, 125.34, 123.26, 119.30, 112.24, 54.32, 49.57, 21.85. **HRMS (ESI$^+$) *m/z*:** $[M+K]^+$ calculated for $C_{42}H_{31}NO_4S$: 684.1606, found: 684.1611; **HPLC:** The enantiomeric excess was determined using CHIRALPAK ID column (*n*-Hexane/ *i*-PrOH=90:10, flow rate=1.0 mL/min, λ= 254 nm, τ_{major} = 33.4 min, τ_{minor} = 40.5 min).

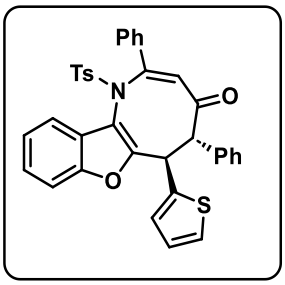

(5*S*,6*R*,*Z*)-2,5-diphenyl-6-(thiophen-2-yl)-1-tosyl-5,6-dihydro benzofuro[3,2-b]azocin-4(1*H*)-one (3k): White solid, 54.0 mg, 90% yield, >20:1 *dr*, 85% *ee*; R_f = 0.5 (petroleum ether/ethyl acetate = 95:5)

1H NMR (400 MHz, Chloroform-d) *δ* 7.57 – 7.42 (m, 4H), 7.46 – 7.42 (m, 2H), 7.35 (d, *J* = 7.5 Hz, 2H), 7.33 – 7.28 (m, 4H), 7.25 (d, *J* = 5.9 Hz, 1H), 7.19 – 7.14 (m, 4H), 7.11 (d, *J* = 7.8 Hz, 1H), 7.05 (d, *J* = 7.7 Hz, 2H), 6.81 - 6.79 (m, 1H), 5.90 (d, *J* = 12.9 Hz, 1H), 5.88 (s, 1H), 5.15 (d, *J* = 13.0 Hz, 1H), 2.42 (s, 3H).

^{13}C NMR (101 MHz, Chloroform-d) δ 200.55, 157.62, 144.89, 139.85, 136.83, 136.55, 136.17, 130.43, 130.18, 129.84, 129.41, 129.05, 128.53, 128.44, 127.93, 127.90, 126.71, 126.45, 125.54, 125.19, 123.43, 119.31, 112.33, 55.42, 44.20, 21.85. **HRMS (ESI$^+$) *m/z*:** $[M+H]^+$ calculated for $C_{36}H_{27}NO_4S_2$: 602.1450, found: 602.1450; **HPLC:** The enantiomeric excess was determined using CHIRALPAK ID column (*n*-Hexane/ *i*-PrOH =90:10, flow rate=1.0 mL/min, λ= 254 nm, τ_{major} = 32.4 min, τ_{minor} = 45.8 min).

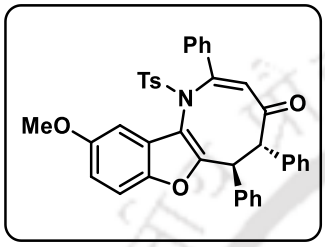

(5*S*,6*S*,*Z*)-10-methoxy-2,5,6-triphenyl-1-tosyl-5,6-dihy*dro* benzofuro[3,2-b]azocin-4(1*H*)-one (3l): White solid, 57.5 mg, 92% yield, >20:1 *dr*, 93% *ee*; R_f = 0.5 (petroleum ether/ethyl acetate = 95:5)

^{1}H NMR (500 MHz, Chloroform-d) δ 7.64 – 7.61 (m, 4H), 7.56 – 7.55 (m, 2H), 7.51 (t, *J* = 7.4 Hz, 1H), 7.39 (t, *J* = 7.7 Hz, 2H), 7.31 – 7.24 (m, 4H), 7.22 – 7.17 (m, 5H), 7.14 (d, *J* = 7.4 Hz, 1H), 7.10 (d, *J* = 8.1 Hz, 2H), 6.88 (dd, *J* = 8.9, 2.5 Hz, 1H), 6.42 (d, *J* = 2.5 Hz, 1H), 6.11 (d, *J* = 13.1 Hz, 1H), 5.98 (s, 1H), 4.90 (d, *J* = 13.1 Hz, 1H), 3.67 (s, 3H), 2.44 (s, 3H). **^{13}C NMR** (126 MHz, Chloroform-d) δ 201.10, 159.09, 156.17, 154.85, 147.56, 144.82, 137.70, 137.08, 136.76, 136.19, 130.29, 130.23, 130.03, 129.90, 129.36, 129.23, 128.49, 128.34, 128.24, 127.49, 127.31, 127.24, 126.62, 120.54, 114.00, 112.77, 101.88, 55.61, 54.23, 49.69, 21.77. **HRMS (ESI$^+$) *m/z*:** $[M+H]^+$ calculated for $C_{39}H_{31}NO_5S$: 626.1996, found: 626.2004; **HPLC:** The enantiomeric excess was determined using CHIRALPAK ID column (*n*-Hexane/ *i*-PrOH =90:10, flow rate=1.0 mL/min, λ= 254 nm, τ_{major} = 26.8 min, τ_{minor} = 30.3 min).

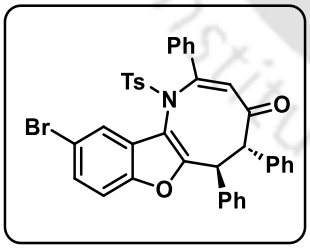

(5*S*,6*S*,*Z*)-10-bromo-2,5,6-triphenyl-1-tosyl-5,6-dihy*dro* benzofuro[3,2-b]azocin-4(1*H*)-one (3m): White solid, 61.3 mg, 91% yield, >20:1 *dr*, 93% *ee*; R_f = 0.5 (petroleum ether/ethyl acetate = 95:5)

^{1}H NMR (500 MHz, Chloroform-d) δ 7.55 (d, *J* = 8.7 Hz, 3H), 7.49 (d, *J* = 7.2 Hz, 4H), 7.46 (d, *J* = 7.3 Hz, 1H), 7.34 (t, *J* = 7.5 Hz, 2H), 7.28 – 7.26 (m, 2H), 7.21 (q, *J* = 6.6, 5.8 Hz, 3H), 7.17 – 7.15 (m, 2H), 7.11 (d, *J* = 7.8 Hz, 3H), 7.05 (d, *J* = 8.0 Hz, 2H), 6.86 (d, *J* = 8.3 Hz, 1H), 6.01 (d, *J* = 13.0 Hz, 1H), 5.93 (s, 1H), 4.84 (d, *J* = 13.0 Hz, 1H), 2.43 (s, 3H). **^{13}C NMR** (126 MHz, Chloroform-d) δ 200.97, 159.14, 154.59, 152.87, 145.10, 137.25, 136.74, 136.45, 135.97, 130.46, 130.18, 129.98, 129.83, 129.45, 129.05, 128.61, 128.41, 128.29, 127.58, 127.46, 126.99, 126.72, 125.35, 120.43, 120.22, 118.59, 115.69, 54.11, 49.45, 21.88. **HRMS (ESI$^+$) *m/z*:** $[M+H]^+$ calculated for $C_{38}H_{28}BrNO_4S$:

674.0995, found: 674.0961; **HPLC:** The enantiomeric excess was determined using CHIRALPAK ID column (*n*-Hexane/ *i*-PrOH =90:10, flow rate=1.0 mL/min, λ= 254 nm, τ_{major} = 22.7 min, τ_{minor} = 33.8 min).

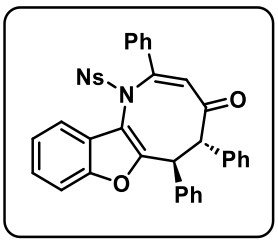

(5*S*,6*S*,*Z*)-1-((4-nitrophenyl)sulfonyl)-2,5,6-triphenyl-5,6-di hydrobenzofuro[3,2-b]azocin -4(1*H*)-one (3n): Yellow solid, 34.1 mg, 95% yield, >20:1 *dr*, >99% *ee*; R_f = 0.5 (petroleum ether/ethyl acetate = 90:10);

^{1}H NMR (600 MHz, Chloroform-d) δ 8.06 (d, J = 8.8 Hz, 2H), 7.58 (d, J = 7.3 Hz, 2H), 7.53 - 7.50 (m, 5H), 7.44 (d, J = 8.2 Hz, 1H), 7.41 – 7.38 (m, 2H), 7.35 (t, J = 7.6 Hz, 2H), 7.33 – 7.30 (m, 1H), 7.24 (t, J = 7.5 Hz, 2H), 7.20 – 7.16 (m, 4H), 7.13 – 7.10 (m, 1H), 6.95 (d, J = 7.8 Hz, 1H), 6.04 (d, J = 13.2 Hz, 1H), 6.00 (s, 1H), 4.93 (d, J = 13.2 Hz, 1H). **^{13}C NMR** (151 MHz, Chloroform-d) δ 200.88, 158.93, 153.46, 152.77, 150.53, 145.51, 137.14, 136.13, 135.82, 130.83, 130.28, 130.10, 130.00, 129.96, 128.84, 128.45, 128.42, 127.74, 127.73, 127.54, 125.76, 125.67, 123.74, 123.62, 119.62, 118.45, 112.72, 54.41, 49.50. **HRMS (ESI$^+$) *m/z*:** $[M+H]^+$ calculated for $C_{37}H_{26}N_2O_6S$: 649.1404, found: 649.1409; **HPLC:** The enantiomeric excess was determined using CHIRALPAK ID column (*n*-Hexane/ *i*-PrOH =90:10, flow rate=1.0 mL/min, λ= 254 nm, τ_{major} = 16.4 min, τ_{minor} = 25.7 min)

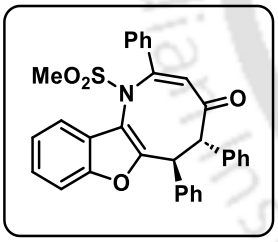

(5*S*,6*S*,*Z*)-1-(methylsulfonyl)-2,5,6-triphenyl-5,6-dihydro benzofuro[3,2-b]azocin-4(1*H*)-one(3o): White solid, 47.8 mg, 92% yield, >20:1 *dr*, >89% *ee*; R_f = 0.5 (petroleum ether/ethyl acetate = 95:5)

^{1}H NMR (500 MHz, Chloroform-d) *δ* 7.82 – 7.80 (m, 2H), 7.77 (d, *J* = 7.6 Hz, 1H), 7.60 – 7.54 (m, 3H), 7.50 - 7.47 (m, 4H), 7.43 (t, *J* = 7.3 Hz, 1H), 7.39 (d, *J* = 7.5 Hz, 1H), 7.36 – 7.33 (m, 1H), 7.21 (t, *J* = 7.4 Hz, 2H), 7.14 (t, *J* = 7.8 Hz, 3H), 7.07 (t, *J* = 7.3 Hz, 1H), 5.97 (s, 1H), 5.90 (d, *J* = 13.1 Hz, 1H), 4.88 (d, *J* = 13.1 Hz, 1H), 3.01 (s, 3H). **^{13}C NMR** (126 MHz, Chloroform-d) *δ* 201.14, 158.54, 153.91, 137.31, 136.92, 135.95, 130.80, 130.13, 129.92, 129.53, 129.09, 128.34, 128.31, 127.59, 127.39, 127.06, 126.21, 125.62, 124.04, 119.61, 117.91, 112.74, 54.46, 49.44, 44.02. **HRMS (ESI$^+$) *m/z*:** $[M+H]^+$ calculated for $C_{32}H_{25}NO_4S$: 520.1578, found: 520.1578; **HPLC:** The enantiomeric excess was determined using CHIRALPAK ID column (*n*-Hexane/ *i*-PrOH =90:10, flow rate=1.0 mL/min, λ= 254 nm, τ_{major} = 19.9 min, τ_{minor} = 34.4 min).

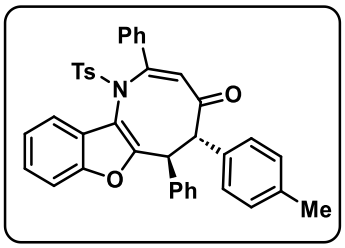

(5*S*,6*S*,*Z*)-2,6-diphenyl-5-(*p*-tolyl)-1-tosyl-5,6-dihydro benzofuro[3,2-b]azocin-4(1*H*)-one(3p): White solid, 56.0 mg, 92% yield, >20:1 *dr*, 89% *ee*; R_f = 0.5 (petroleum ether/ethyl acetate = 95:5)

^{1}H NMR (500 MHz, Chloroform-d) δ 7.60 (d, J = 7.8 Hz, 2H), 7.54 (d, J = 7.6 Hz, 2H), 7.45 (t, J = 7.4 Hz, 1H), 7.40 - 7.37 (m, 3H), 7.34 (t, J = 7.5 Hz, 2H), 7.28 – 7.25 (m, 2H), 7.19 (t, J = 7.5 Hz, 2H), 7.17 – 7.13 (m, 3H), 7.11 (t, J = 7.4 Hz, 1H), 7.05 (q, J = 8.8, 7.3 Hz, 5H), 6.03 (d, J = 13.1 Hz, 1H), 5.91 (s, 1H), 4.88 (d, J = 13.1 Hz, 1H), 2.42 (s, 3H), 2.25 (s, 3H). **^{13}C NMR** (126 MHz, Chloroform-d) δ 201.37, 158.59, 154.74, 152.65, 144.81, 137.74, 137.08, 136.62, 133.15, 130.31, 130.08, 129.98, 129.94, 129.34, 129.11, 129.03, 128.51, 128.34, 127.29, 126.88, 126.30, 125.26, 123.21, 120.49, 119.28, 112.22, 53.87, 49.34, 21.83, 21.26. **HRMS (ESI$^+$) *m/z*:** $[M+H]^+$ calculated for $C_{39}H_{31}NO_4S$: 610.2047, found: 610.2056; **HPLC:** The enantiomeric excess was determined using CHIRALPAK ID column (*n*-Hexane/ *i*-PrOH =90:10, flow rate=1.0 mL/min, λ= 254 nm, τ_{major} = 24.3 min, τ_{minor} = 39.0 min).

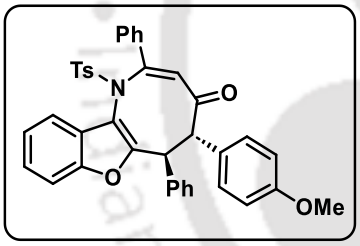

(5*S*,6*S*,*Z*)-5-(4-methoxyphenyl)-2,6-diphenyl-1-tosyl-5,6-dihydrobenzofuro[3,2-b]azocin-4(1*H*)-one(3q): White solid, 55.6 mg, 89% yield, >20:1 *dr*, 94% *ee*; R_f = 0.5 (petroleum ether/ethyl acetate = 95:5)

^{1}H NMR (500 MHz, Chloroform-d) δ 7.58 (d, J = 7.6 Hz, 2H), 7.54 (d, J = 7.6 Hz, 2H), 7.47 - 7.71 (m, 3H), 7.38 (d, J = 8.2 Hz, 1H), 7.33 (t, J = 7.6 Hz, 2H), 7.28 - 7.25 (m, 1H), 7.19 (t, J = 7.6 Hz, 2H), 7.16 – 7.13 (m, 3H), 7.10 (t, J = 7.3 Hz, 1H), 7.06 - 7.03 (m, 3H), 6.76 (d, J = 8.3 Hz, 2H), 5.99 (d, J = 13.1 Hz, 1H), 5.92 (s, 1H), 4.84 (d, J = 13.1 Hz, 1H), 3.73 (s, 3H), 2.42 (s, 3H). **^{13}C NMR** (126 MHz, Chloroform-d) δ 201.57, 159.02, 158.55, 154.77, 152.65, 144.82, 137.77, 137.04, 136.63, 131.15, 130.32, 130.08, 129.94, 129.34, 129.12, 128.52, 128.37, 127.30, 126.92, 126.29, 125.28, 123.21, 120.54, 119.28, 113.75, 112.23, 55.35, 53.43, 49.58, 21.83. **HRMS (ESI$^+$) *m/z*:** $[M+Na]^+$ calculated for $C_{39}H_{31}NO_5S$: 648.1816, found: 648.1820; **HPLC:** The enantiomeric excess was determined using CHIRALPAK ID column (*n*-Hexane/ *i*-PrOH =90:10, flow rate=1.0 mL/min, λ= 254 nm, τ_{major} = 23.6 min, τ_{minor} = 43.7 min).

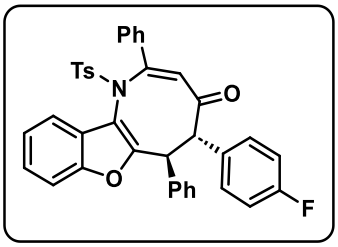

(5*S*,6*S*,*Z*)-5-(4-fluorophenyl)-2,6-diphenyl-1-tosyl-5,6-dihydrobenzofuro[3,2-b]azocin-4(1*H*)-one(3r): White solid, 53.9 mg, 88% yield, >20:1 *dr*, 89% *ee*; R_f = 0.5 (petroleum ether/ethyl acetate = 95:5)

^{1}H NMR (500 MHz, Chloroform-d) δ 7.53 (t, J = 8.3 Hz, 4H), 7.47 - 7.42 (m, 3H), 7.36 (d, J = 8.2 Hz, 1H), 7.32 (t, J = 7.6 Hz, 2H), 7.24 - 7.23 (m, 1H), 7.17 (t, J = 7.5 Hz, 2H), 7.14 – 7.11 (m, 3H), 7.09 (t, J = 7.4 Hz, 1H), 7.03 – 7.01 (m, 3H), 6.88 (t, J = 8.5 Hz, 2H), 6.04 (d, J = 13.1 Hz, 1H), 5.91 (s, 1H), 4.78 (d, J = 13.1 Hz, 1H), 2.40 (s, 3H). **^{13}C NMR** (126 MHz, Chloroform-d) δ 200.91, 163.32, 161.37, 158.22, 155.18, 152.67, 144.93, 137.57, 136.95, 136.55, 132.09, 132.06, 131.76, 131.70, 130.44, 130.02, 129.95, 129.38, 129.14, 128.56, 128.47, 127.45, 126.83, 126.22, 125.37, 123.28, 120.63, 119.29, 115.21, 115.04, 112.27, 53.39, 49.83, 21.84. **HRMS (ESI$^+$) *m/z*:** $[M+Na]^+$ calculated for $C_{38}H_{28}FNO_4S$: 636.1616, found: 636.1605; **HPLC:** The enantiomeric excess was determined using CHIRALPAK ID column (*n*-Hexane/ *i*-PrOH =90:10, flow rate=1.0 mL/min, λ= 254 nm, τ_{major} = 17.9 min, τ_{minor} = 28.0 min).

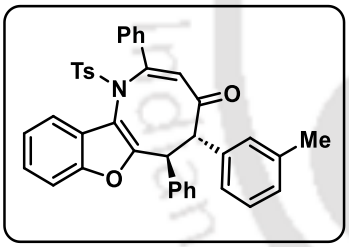

(5*S*,6*S*,*Z*)-2,6-diphenyl-5-(*m*-tolyl)-1-tosyl-5,6-dihydro benzofuro[3,2-b]azocin-4(1*H*)-one(3s): White solid, 55.4 mg, 91% yield, >20:1 *dr*, 92% *ee*; R_f = 0.5 (petroleum ether/ethyl acetate = 95:5)

^{1}H NMR (500 MHz, Chloroform-d) δ 7.58 (d, J = 7.3 Hz, 2H), 7.54 (d, J = 6.9 Hz, 2H), 7.45 (t, J = 7.4 Hz, 1H), 7.37 (d, J = 8.2 Hz, 1H), 7.33 (t, J = 7.8 Hz, 3H), 7.28 (d, J = 7.4 Hz, 1H), 7.25 – 7.24 (m, 1H), 7.19 – 7.13 (m, 5H), 7.11 – 7.07 (m, 2H), 7.04 (t, J = 8.5 Hz, 3H), 6.95 (d, J = 7.6 Hz, 1H), 6.00 (d, J = 13.2 Hz, 1H), 5.91 (s, 1H), 4.88 (d, J = 13.1 Hz, 1H), 2.41 (s, 3H), 2.28 (s, 3H). **^{13}C NMR** (126 MHz, Chloroform-d) δ 201.24, 158.59, 154.71, 152.66, 144.82, 137.73, 137.69, 137.05, 136.63, 136.06, 130.92, 130.32, 130.05, 129.96, 129.35, 129.12, 128.52, 128.31, 128.28, 128.12, 127.30, 127.20, 126.93, 126.31, 125.28, 123.22, 120.51, 119.29, 112.23, 54.18, 49.39, 21.83, 21.60. **HRMS (ESI$^+$) *m/z*:** $[M+H]^+$ calculated for $C_{39}H_{31}NO_4S$: 610.2047, found: 610.2053; **HPLC:** The enantiomeric excess was determined using CHIRALPAK ID column (*n*-Hexane/ *i*-PrOH =90:10, flow rate=1.0 mL/min, λ= 254 nm, τ_{major} = 18.5 min, τ_{minor} = 30.3 min).

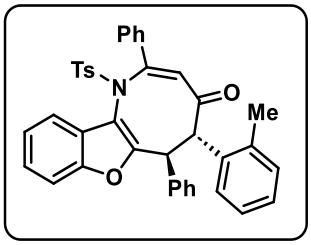

(5*S*,6*S*,*Z*)-2,6-diphenyl-5-(*o*-tolyl)-1-tosyl-5,6-dihydro benzofuro[3,2-b]azocin-4(1*H*)-one(3t): White solid, 54.2 mg, 89% yield, >20:1 *dr*, 92% *ee*; R_f = 0.5 (petroleum ether/ethyl acetate = 95:5)

^{1}H NMR (500 MHz, Chloroform-d) δ 7.71 (d, J = 7.9 Hz, 1H), 7.63 (d, J = 7.6 Hz, 2H), 7.52 (d, J = 7.5 Hz, 2H), 7.48 (t, J = 7.5 Hz, 1H), 7.40 – 7.34 (m, 3H), 7.24 (d, J = 7.6 Hz, 2H), 7.19 (t, J = 7.6 Hz, 2H), 7.15 – 7.09 (m, 3H), 7.07 – 7.00 (m, 5H), 6.85 (d, J = 7.9 Hz, 1H), 6.50 (d, J = 13.1 Hz, 1H), 5.92 (s, 1H), 4.98 (d, J = 13.1 Hz, 1H), 2.59 (s, 3H), 2.41 (s, 3H). **^{13}C NMR** (126 MHz, Chloroform-d) δ 201.12, 158.74, 154.80, 152.66, 144.85, 137.63, 137.43, 137.04, 136.61, 134.55, 130.30, 130.27, 129.99, 129.89, 129.55, 129.27, 129.21, 128.59, 128.35, 127.39, 127.11, 127.01, 126.02, 126.00, 125.26, 123.09, 120.19, 119.29, 112.23, 48.94, 48.89, 21.86, 21.14. **HRMS (ESI$^+$) *m/z*:** $[M+H]^+$ calculated for $C_{39}H_{31}NO_4S$: 610.2047, found: 610.2047; **HPLC:** The enantiomeric excess was determined using CHIRALPAK ID column (*n*-Hexane/ *i*-PrOH =90:10, flow rate=1.0 mL/min, λ= 254 nm, τ_{major} = 11.6 min, τ_{minor} = 18.8 min).

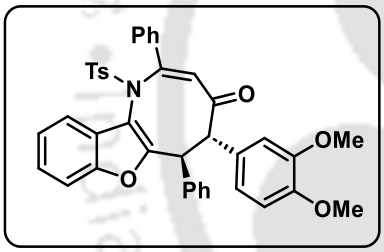

(5*S*,6*S*,*Z*)-5-(3,4-dimethoxyphenyl)-2,6-diphenyl-1-tosyl-5,6-dihydrobenzofuro[3,2-b]azocin-4(1*H*)-one(3u): White solid, 58.9 mg, 90% yield, >20:1 *dr*, 95% *ee*; R_f = 0.5 (petroleum ether/ethyl acetate = 95:5)

^{1}H NMR (400 MHz, Chloroform-d) δ 7.57 - 7.53 (m, 4H), 7.45 (t, J = 7.4 Hz, 1H), 7.38 – 7.31 (m, 3H), 7.26 (t, J = 7.7 Hz, 1H), 7.20 – 7.13 (m, 5H), 7.10 – 7.09 (m, 2H), 7.04 (d, J = 8.0 Hz, 3H), 7.01 - 6.99 (m, 1H), 6.69 (d, J = 8.3 Hz, 1H), 5.97 (d, J = 13.0 Hz, 1H), 5.92 (s, 1H), 4.82 (d, J = 13.0 Hz, 1H), 3.87 (s, 3H), 3.80 (s, 3H), 2.42 (s, 3H). **^{13}C NMR** (101 MHz, Chloroform-d) δ 201.52, 158.50, 154.71, 152.64, 148.78, 148.52, 144.85, 137.79, 137.00, 136.60, 130.34, 130.00, 129.93, 129.35, 129.11, 128.75, 128.53, 128.39, 127.35, 126.92, 126.26, 125.31, 123.23, 122.83, 120.57, 119.28, 113.19, 112.23, 110.79, 56.19, 55.95, 53.65, 49.88, 21.84. **HRMS (ESI$^+$) *m/z*:** $[M+Na]^+$ calculated for $C_{40}H_{28}NO_6S$: 678.1921, found: 678.1928; **HPLC:** The enantiomeric excess was determined using CHIRALPAK ID column (*n*-Hexane/ *i*-PrOH =90:10, flow rate=1.0 mL/min, λ= 254 nm, τ_{major} = 51.4 min, τ_{minor} = 84.6 min).

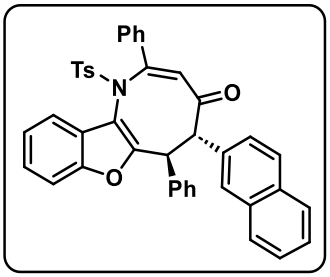

(5*S*,6*S*,*Z*)-5-(naphthalen-2-yl)-2,6-diphenyl-1-tosyl-5,6-dihydrobenzofuro[3,2-b]azocin-4(1*H*)-one(3v): White solid, 59.3 mg, 92% yield, >20:1 *dr*, 91% *ee*; R_f = 0.5 (petroleum ether/ethyl acetate = 95:5)

^{1}H NMR (400 MHz, Chloroform-d) δ 7.92 (s, 1H), 7.82 – 7.80 (m, 1H), 7.75 – 7.70 (m, 3H), 7.64 (d, J = 7.3 Hz, 2H), 7.57 (d, J = 7.0 Hz, 2H), 7.47 (t, J = 7.6 Hz, 1H), 7.43 – 7.39 (m, 3H), 7.35 (t, J = 7.5 Hz, 2H), 7.29 (d, J = 7.4 Hz, 1H), 7.19 – 7.11 (m, 5H), 7.06 (d, J = 8.0 Hz, 3H), 7.02 (t, J = 7.4 Hz, 1H), 6.25 (d, J = 13.1 Hz, 1H), 5.94 (s, 1H), 5.03 (d, J = 13.1 Hz, 1H), 2.44 (s, 3H). **^{13}C NMR** (101 MHz, Chloroform-d) δ 201.07, 158.52, 155.00, 152.70, 144.89, 137.52, 137.03, 136.61, 133.86, 133.36, 132.93, 130.39, 130.03, 129.98, 129.52, 129.39, 129.16, 128.56, 128.41, 128.16, 127.86, 127.72, 127.68, 127.39, 126.88, 126.29, 125.98, 125.94, 125.33, 123.26, 120.54, 119.31, 112.28, 54.35, 49.38, 21.87. **HRMS (ESI$^+$) *m/z*:** $[M+K]^+$ calculated for $C_{42}H_{33}NO_4S$: 684.1606, found: 684.1607; **HPLC:** The enantiomeric excess was determined using CHIRALPAK ID column (*n*-Hexane/ *i*-PrOH =90:10, flow rate=1.0 mL/min, λ= 254 nm, τ_{major} = 33.2 min, τ_{minor} = 52.7 min).

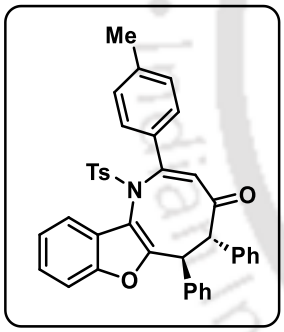

(5*S*,6*S*,*Z*)-5,6-diphenyl-2-(*p*-tolyl)-1-tosyl-5,6-dihydro benzofuro[3,2-b]azocin-4(1*H*)-one(3w): White solid, 56 mg, 92% yield, >20:1 *dr*, 91% *ee*; R_f = 0.5 (petroleum ether/ethyl acetate = 95:5)

^{1}H NMR (600 MHz, Chloroform-d) δ 7.58 (d, J = 7.6 Hz, 2H), 7.50 (d, J = 7.3 Hz, 2H), 7.42 (d, J = 7.8 Hz, 2H), 7.38 (d, J = 8.2 Hz, 1H), 7.28 – 7.25 (m, 2H), 7.21 (t, J = 7.5 Hz, 2H), 7.18 (d, J = 8.0 Hz, 3H), 7.17 – 7.15 (m, 2H), 7.13 (d, J = 7.9 Hz, 2H), 7.08 (d, J = 7.4 Hz, 2H), 7.06 (d, J = 8.0 Hz, 2H), 6.04 (d, J = 13.1 Hz, 1H), 5.90 (s, 1H), 4.87 (d, J = 13.1 Hz, 1H), 2.43 (s, 6H). **^{13}C NMR** (151 MHz, Chloroform-d) δ 201.14, 158.35, 155.02, 152.54, 144.80, 140.80, 137.64, 136.94, 136.21, 133.68, 130.18, 129.98, 129.82, 129.26, 129.16, 129.09, 128.34, 128.22, 127.46, 127.32, 126.28, 126.20, 125.27, 123.22, 120.48, 119.23, 112.20, 54.05, 49.35, 21.89, 21.69. **HRMS (ESI$^+$) *m/z*:** $[M+H]^+$ calculated for $C_{39}H_{31}NO_4S$: 610.2047, found: 610.2054; **HPLC:** The enantiomeric excess was determined using CHIRALPAK ID column (*n*-Hexane/ *i*-PrOH =90:10, flow rate=1.0 mL/min, λ= 254 nm, τ_{major} = 19.9 min, τ_{minor} = 34.4 min).

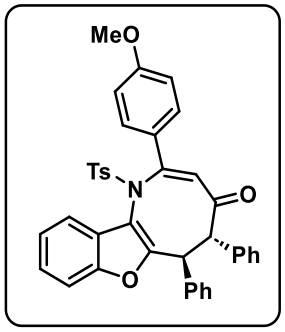

(5*S*,6*S*,*Z*)-2-(4-methoxyphenyl)-5,6-diphenyl-1-tosyl-5,6-dihydrobenzofuro[3,2-b]azocin-4(1*H*)-one(3x): White solid, 55.6 mg, 89% yield, >20:1 *dr*, 86% *ee*; R_f = 0.5 (petroleum ether/ethyl acetate = 95:5)

^{1}H NMR (400 MHz, Chloroform-d) δ 7.56 (d, J = 7.5 Hz, 2H), 7.49 (d, J = 7.0 Hz, 2H), 7.46 (d, J = 8.7 Hz, 2H), 7.37 (d, J = 8.2 Hz, 1H), 7.28 – 7.22 (m, 4H), 7.19 (d, J = 8.2 Hz, 2H), 7.16 – 7.11 (m, 4H), 7.08 (d, J = 7.3 Hz, 3H), 6.82 (d, J = 8.7 Hz, 2H), 6.03 (d, J = 13.1 Hz, 1H), 5.86 (s, 1H), 4.86 (d, J = 13.1 Hz, 1H), 3.87 (s, 3H), 2.42 (s, 3H). **^{13}C NMR** (101 MHz, Chloroform-d) δ 200.92, 161.65, 158.51, 154.74, 152.66, 144.75, 137.77, 137.27, 136.38, 131.47, 130.26, 130.04, 129.35, 129.16, 129.04, 128.33, 128.20, 127.43, 127.29, 126.44, 125.70, 125.27, 123.25, 120.58, 119.22, 113.94, 112.25, 55.71, 54.07, 49.50, 21.85. **HRMS (ESI$^+$) *m/z*:** $[M+H]^+$ calculated for $C_{39}H_{31}NO_5S$: 626.1996, found: 626.1996; **HPLC:** The enantiomeric excess was determined using CHIRALPAK ID column (*n*-Hexane/ *i*-PrOH =90:10, flow rate=1.0 mL/min, λ= 254 nm, τ_{major} = 15.6 min, τ_{minor} = 25.2 min).

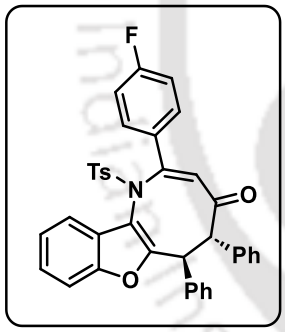

(5*S*,6*S*,*Z*)-2-(4-fluorophenyl)-5,6-diphenyl-1-tosyl-5,6-dihydrobenzofuro[3,2-b]azocin-4(1*H*)-one(3y): White solid, 55.1 mg, 90% yield, >20:1 *dr*, 89% *ee*; R_f = 0.5 (petroleum ether/ethyl acetate = 95:5)

^{1}H NMR (500 MHz, Chloroform-d) δ 7.57 – 7.49 (m, 6H), 7.39 (d, J = 8.2 Hz, 1H), 7.28 (d, J = 7.5 Hz, 3H), 7.21 (q, J = 6.9, 6.4 Hz, 4H), 7.17 – 7.13 (m, 4H), 7.11 - 7.07 (m, 3H), 7.05 – 7.02 (m, 3H), 6.02 (d, J = 13.1 Hz, 1H), 5.89 (s, 1H), 4.87 (d, J = 13.1 Hz, 1H), 2.44 (s, 3H). **^{13}C NMR** (126 MHz, Chloroform-d) δ 200.94, 165.16, 163.16, 158.56, 153.65, 152.67, 145.15, 137.57, 137.04, 136.14, 132.87, 132.85, 131.94, 131.87, 130.21, 130.03, 129.47, 129.06, 128.37, 128.29, 127.56, 127.38, 126.90, 126.27, 125.39, 123.33, 120.42, 119.06, 115.74, 115.57, 112.35, 54.24, 49.57, 21.86.

HRMS (ESI$^+$) *m/z*: $[M+K]^+$ calculated for $C_{38}H_{28}FNO_4S$: 652.1355, found: 652.1355;

HPLC: The enantiomeric excess was determined using CHIRALPAK ID column (*n*-Hexane/ *i*-PrOH =90:10, flow rate=1.0 mL/min, λ= 254 nm, τ_{major} = 17.2 min, τ_{minor} = 27.2 min).

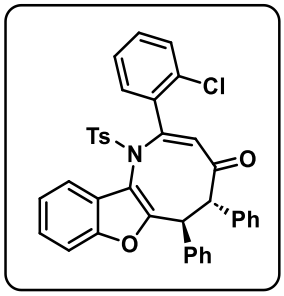

(5*S*,6*S*,*Z*)-2-(2-chlorophenyl)-5,6-diphenyl-1-tosyl-5,6-dihydrobenzofuro[3,2-b]azocin-4(1*H*)-one(3z): White solid, 58.5 mg, 93% yield, >20:1 *dr*, 83% *ee*; R_f = 0.5 (petroleum ether/ethyl acetate = 95:5)

^{1}H NMR (600 MHz, Chloroform-d) δ 7.58 (d, *J* = 7.2 Hz, 2H), 7.55 (d, *J* = 8.1 Hz, 1H), 7.53 – 7.50 (m, 3H), 7.39 (t, *J* = 8.0 Hz, 2H), 7.24 (t, *J* = 7.8 Hz, 3H), 7.20 - 7.16 (m, 4H), 7.16 – 7.13 (m, 2H), 7.12 – 7.08 (m, 2H), 7.04 (d, *J* = 8.0 Hz, 2H), 6.94 (d, *J* = 7.7 Hz, 1H), 6.06 (d, *J* = 13.2 Hz, 1H), 5.95 (s, 1H), 4.92 (d, *J* = 13.2 Hz, 1H), 2.41 (s, 3H).**^{13}C NMR** (151 MHz, Chloroform-d) δ 201.27, 158.64, 152.61, 149.38, 144.97, 137.39, 136.70, 136.08, 135.01, 134.71, 132.34, 131.01, 130.95, 130.01, 129.95, 129.43, 129.01, 128.93, 128.40, 127.58, 127.40, 126.37, 125.89, 125.29, 123.02, 119.85, 112.19, 54.52, 48.98, 21.85. **HRMS (ESI$^+$) *m/z*:** $[M+H]^+$ calcd for $C_{38}H_{29}ClNO_4S$: 630.1501, found: 630.1501; **HPLC:** The enantiomeric excess was determined using CHIRALPAK ID column (*n*-Hexane/ *i*-PrOH =90:10, flow rate=1.0 mL/min, λ= 254 nm, τ_{major} = 24.2 min, τ_{minor} = 45.3 min).

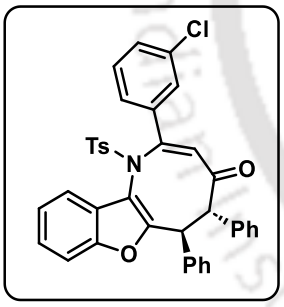

(5*S*,6*S*,*Z*)-2-(3-chlorophenyl)-5,6-diphenyl-1-tosyl-5,6-dihydrobenzofuro[3,2-b]azocin-4(1*H*)-one(3z'): White solid, 54.8 mg, 87% yield, >20:1 *dr*, 83% *ee*; R_f = 0.5 (petroleum ether/ethyl acetate = 95:5)

^{1}H NMR (500 MHz, Chloroform-d) δ 7.58 (d, *J* = 7.6 Hz, 2H), 7.51 (d, *J* = 7.6 Hz, 2H), 7.47 (d, *J* = 5.9 Hz, 2H), 7.43 - 7.38 (m, 2H), 7.33 (t, *J* = 7.9 Hz, 1H), 7.28 (d, *J* = 7.6 Hz, 1H), 7.24 - 7.21 (m, 4H), 7.21 - 7.15 (m, 4H), 7.14 - 7.08 (m, 3H), 7.04 (d, *J* = 7.8 Hz, 1H), 6.05 (d, *J* = 13.1 Hz, 1H), 5.95 (s, 1H), 4.89 (d, *J* = 13.1 Hz, 1H), 2.45 (s, 3H). **^{13}C NMR** (126 MHz, Chloroform-d) δ 200.99, 158.59, 153.20, 152.65, 145.38, 138.21, 137.49, 136.67, 136.03, 134.50, 130.36, 130.18, 130.03, 129.82, 129.56, 128.96, 128.37, 128.31, 128.06, 127.58, 127.39, 127.34, 126.12, 125.40, 123.40, 120.27, 119.04, 112.32, 54.25, 49.56, 21.85. **HRMS (ESI$^+$) *m/z*:** $[M+H]^+$ calcd for $C_{38}H_{29}ClNO_4S$: 630.1501, found: 630.1498; **HPLC:** The enantiomeric excess was determined using CHIRALPAK ID column (*n*-Hexane/ *i*-PrOH =90:10, flow rate=1.0 mL/min, λ= 254 nm, τ_{major} = 15.5 min, τ_{minor} = 22.0 min).

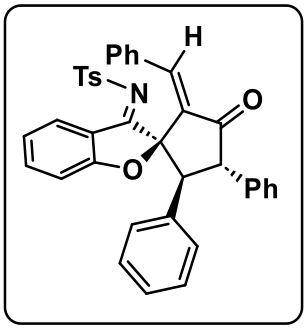

***N*-((2*R*,4'*S*,5'S,*E*)-2'-((*E*)-benzylidene)-3'-oxo-4',5'-diphenyl-3*H*-spiro[benzofuran-2,1'-cyclopentan]-3-ylidene)-4-methyl benzenesulfonamide (4a):** Pale yellow Solid, 53.5 mg, 90% yield, 92% *ee*, the measured *dr* is 7:1 from ^{1}H NMR: 4.65-4.62(*minor*), 4.54-4.52(*major*), E/Z = >20:1; R_f = 0.4 (petroleum ether/ethyl acetate = 90:10)

^{1}H NMR (500 MHz, $CDCl_3$): δ 8.32 – 8.17 (m, 1H), 8.01 (s, 1H), 7.52 (d, *J* = 7.9 Hz, 2H), 7.47-7.43 (m, 1H), 7.29 – 7.23 (m, 5H), 7.19 (t, *J* = 7.4 Hz, 5H), 7.08 (t, *J* = 7.7 Hz, 2H), 7.02 (t, *J* = 7.6 Hz, 3H), 6.99 – 6.93 (m, 3H), 6.91 (d, *J* = 7.7 Hz, 1H), 6.85 (d, *J* = 8.4 Hz, 1H), 4.53 (d, *J* = 13.9 Hz, 1H), 3.95 (d, *J* = 13.6 Hz, 1H), 2.45 (s, 3H). **^{13}C NMR (126 MHz, $CDCl_3$)** (*major*+*minor*): δ 201.28, 200.70, 181.73, 179.61, 171.22, 167.91, 144.06, 143.58, 140.81, 139.01, 138.95, 138.72, 138.51, 135.79, 135.77, 135.07, 134.61, 133.77, 133.14, 132.43, 132.35, 132.29, 132.13, 130.92, 130.80, 130.02, 129.92, 129.76, 129.47, 129.35, 129.22, 129.08, 129.05, 128.87, 128.81, 128.78, 128.64, 128.38, 128.35, 128.31, 128.17, 128.15, 128.08, 127.61, 127.19, 127.07, 122.65, 122.27, 121.05, 117.60, 112.69, 111.90, 95.20, 94.11, 61.67, 57.86, 56.62, 54.49, 22.86, 21.81. **HRMS (ESI$^+$) (*m/z*):** $[M+Na]^+$ calcd for $C_{38}H_{29}NO_4S$: 618.1710, found: 618.1715; **HPLC:** The enantiomeric excess was determined using CHIRALPAK IA column (*n*-Hexane/ *i*-PrOH = 90:30, flow rate = 1.0 mL/min, λ =254 nm, τ_{major} = 23.5 min, τ_{minor} = 49.7 min).

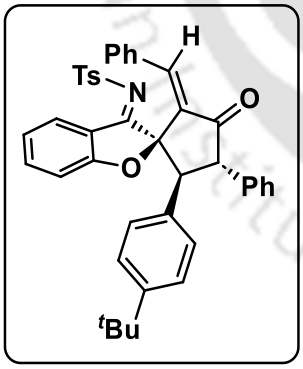

***N*-((2*R*,4'*S*,5'*S*,*E*)-2'-((*E*)-benzylidene)-5'-(4-(tert-butyl)phenyl)-3'-oxo-4'-phenyl-3*H*-spiro[benzofuran-2,1'-cyclopentan]-3-ylidene)-4-methylbenzenesulfonamide(4b):** Yellow solid, 54 mg, 83% yield, 6:1 *dr* and 85% *ee*, the measured *dr* is 6:1 from ^{1}H NMR: 4.65-4.62(*minor*), 4.54-4.51(*major*), E/Z = >20:1; R_f = 0.5 (petroleum ether/ethyl acetate = 90:10);

^{1}H NMR (500 MHz, Chloroform-d) δ 8.23 (s, 1H), 8.00 (s, 1H), 7.50 (d, *J* = 7.9 Hz, 2H), 7.39 (t, *J* = 7.8 Hz, 1H), 7.28 – 7.25 (m, 6H), 7.22 – 7.20 (m, 3H), 7.08 (d, *J* = 8.0 Hz, 3H), 7.01 (s, 1H), 6.99 – 6.96 (m, 3H), 6.89 (t, *J* = 7.7 Hz, 1H), 6.78 (d, *J* = 8.5 Hz, 1H), 4.53 (d, *J* = 13.8 Hz, 1H), 3.96 (s, 1H), 2.45 (s, 3H), 1.08 (s, 9H). **^{13}C NMR** (126 MHz, Chloroform-d) δ 201.55, 179.92, 167.89, 151.06, 143.52, 138.59, 136.01, 134.24, 133.85, 130.84, 129.91, 129.44, 129.15, 129.09, 128.81, 128.79, 128.70, 127.59, 127.20, 124.89, 122.04, 112.79, 94.31, 61.53, 56.27, 31.28, 21.81. **HRMS (ESI$^+$) (*m/z*):** $[M+H]^+$ calcd for $C_{42}H_{37}NO_4S$: 652.2517, found: 652.2517; **HPLC:** The

enantiomeric excess was determined using CHIRALPAK IA column (*n*-Hexane/ *i*-PrOH = 90:30, flow rate = 1.0 mL/min, λ =254 nm, τ_{major} = 12.8 min, τ_{minor} = 21.0 min).

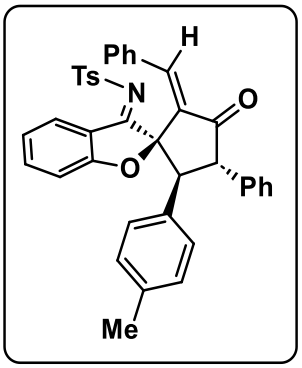

***N*-((2*R*,4'*S*,5'*S*,*E*)-2'-((*E*)-benzylidene)-3'-oxo-4'-phenyl-5'-(*p*-tolyl)-3*H*-spiro [benzofuran-2,1'-cyclopentan]-3-ylidene)-4-methylbenzene sulfonamide (4c):**Pale yellow solid, 51.7 mg, 85% yield, 87% *ee*, the measured *dr* is 5:1 from ^{1}H NMR: 4.63-4.59(*minor*), 4.51-4.48(*major*), E/Z = >20:1; R_f = 0.4 (petroleum ether/ethyl acetate = 90:10)

^{1}H NMR (400 MHz, Chloroform-d) δ 8.23 (s, 1H), 8.00 (s, 1H), 7.53 (d, J = 7.9 Hz, 2H), 7.50 – 7.44 (m, 1H), 7.27 (d, J = 7.1 Hz, 3H), 7.25 -7.22(m, 2H), 7.20-7.16 (m, 3H), 7.06 (d, J = 7.8 Hz, 4H), 6.93 (dd, J = 7.8, 5.2 Hz, 3H), 6.86 (d, J = 8.4 Hz, 1H), 6.82 (d, J = 7.8 Hz, 2H), 4.49 (d, J = 14.0 Hz, 1H), 3.94 (s, 1H), 2.45 (s, 3H), 2.08 (s, 3H). **^{13}C NMR** (101 MHz, Chloroform-d) δ 201.39, 179.75, 168.04, 150.00, 143.54, 143.43, 138.95, 138.65, 137.69, 135.95, 134.89, 133.84, 130.72, 129.74, 129.48, 129.08, 128.89, 128.79, 128.62, 127.56, 127.21, 122.25, 112.73, 94.23, 61.34, 56.82, 21.81, 21.13. **HRMS (ESI$^+$) (*m/z*):** $[M+H]^+$ calcd for $C_{39}H_{31}NO_4S$: 610.2047, found: 610.2036; **HPLC:** The enantiomeric excess was determined using CHIRALPAK IA column (*n*-Hexane/ *i*-PrOH=90:30, flow rate=1.0 mL/min, λ= 254 nm, τ_{major} = 28.5 min, τ_{minor} = 42.3 min).

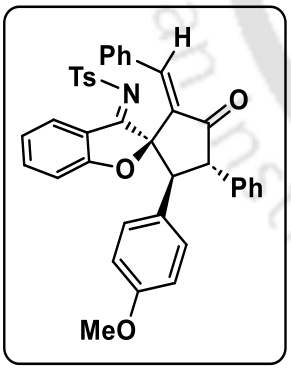

***N*-((2*R*,4'*S*,5'*S*,*E*)-2'-((*E*)-benzylidene)-5'-(4-methoxyphenyl)-3'-oxo-4'-phenyl-3*H*-spiro[benzofuran-2,1'-cyclopentan]-3-ylidene)-4-methylbenzenesulfonamide(4d):** Pale yellow solid**,** 55mg, 88% yield, 90% *ee*. The measured *dr* is 7:1 from ^{1}H NMR: 4.61-4.58 (*minor*), 4.48-4.44(*major*), E/Z = >20:1; R_f = 0.4 (petroleum ether/ethyl acetate = 90:10)

^{1}H NMR (400 MHz, $CDCl_3$): δ 8.25 (s, 1H), 8.00 (s, 1H), 7.57 – 7.44 (m, 3H), 7.25 (t, J = 9.3 Hz, 5H), 7.21 – 7.14 (m, 3H), 7.13 – 7.05 (m, 4H), 6.98 – 6.91 (m, 3H), 6.88 (d, J = 8.4 Hz, 1H), 6.57 (dd, J = 7.3, 4.9 Hz, 2H), 4.46 (d, J = 14.0 Hz, 1H), 3.91(s, 1H), 3.59 (s, 3H), 2.45 (s, 3H). **^{13}C NMR (101 MHz, $CDCl_3$)**: δ 201.35, 179.79, 168.01, 159.26, 143.55, 139.10, 138.56, 135.88, 134.75, 133.80, 130.75, 130.27, 129.74, 129.47, 129.06, 128.78, 128.62, 127.57, 127.17, 124.33, 122.29, 113.64, 112.71, 94.24, 61.15, 56.90, 55.24, 21.80. **HRMS (ESI$^+$) (*m/z*):** $[M+H]^+$ calcd for $C_{39}H_{31}NO_5S$: 626.1996, found: 618.1997; **HPLC:** The enantiomeric excess was determined

using CHIRALPAK IA column (*n*-Hexane/ ^{i}PrOH=90:30, flow rate=1.0 mL/min, λ = 254 nm, τ_{major} = 32.0 min, τ_{minor} = 50.7 min).

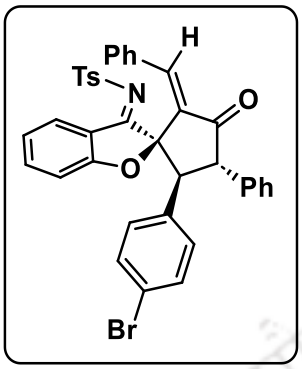

***N*-((2*R*,4'*S*,5'*S*,*E*)-2'-((*E*)-benzylidene)-5'-(4-bromophenyl)-3'-oxo-4'-phenyl-3*H*-spiro[benzofuran-2,1'-cyclopentan]-3-ylidene)-4-methyl benzenesulfonamide(4e):** Pale yellow solid, 60.6 mg, 90% yield, 90% *ee*, the measured *dr* is 7:1 from ^{1}H NMR: 4.59-4.56(*minor*), 4.47-4.44(*major*), E/Z = >20:1; R_f = 0.4 (petroleum ether/ethyl acetate = 90:10)

^{1}H NMR (500 MHz, Chloroform-d): *δ* 8.26 (s, 1H), 8.01 (s, 1H), 7.61 – 7.47 (m, 3H), 7.29 – 7.23 (m, 4H), 7.21 (m, 1H), 7.19 – 7.11 (m, 4H), 7.10 – 7.05 (m, 4H), 7.02 – 6.96 (m, 2H), 6.93 (d, *J* = 7.3Hz, 2H), 6.89 (d, *J* = 8.4 Hz, 1H), 4.45 (d, *J* = 13.9 Hz, 1H), 3.89 (d, *J* = 13.5 Hz, 1H), 2.45 (s, 3H). **^{13}C NMR** (126 MHz, Chloroform-d) (*major*+*minor*): *δ* 200.76, 179.21, 171.14, 167.79, 144.21, 143.91, 143.70, 141.11, 139.40, 139.28, 138.55, 138.35, 135.42, 134.83, 134.42, 133.66, 133.02, 132.34, 132.18, 131.61, 131.41, 131.10, 130.90, 130.85, 130.41, 129.72, 129.51, 129.30, 128.97, 128.92, 128.67, 128.19, 127.80, 127.19, 127.05, 122.97, 122.64, 122.43, 122.22, 120.75, 117.46, 112.70, 111.90, 94.90, 93.83, 61.15, 57.42, 56.74, 54.69, 21.83. **HRMS (ESI^{+}) (*m/z*):** $[M+H]^{+}$ calcd for $C_{38}H_{28}BrNO_4S$: 674.0995, found: 674.0956; **HPLC:** The enantiomeric excess was determined using CHIRALPAK IA column (*n*-Hexane/ ^{i}PrOH=90:30, flow rate=1.0 mL/min, λ= 274 nm, τ_{major} = 44.7 min, τ_{minor} = 80.2 min)

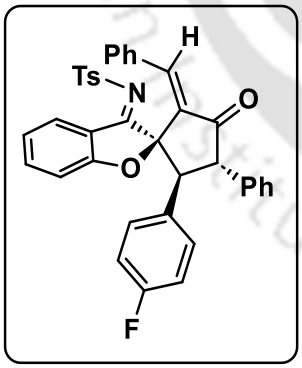

***N*-((2*R*,4'*S*,5'*S*,*E*)-2'-((*E*)-benzylidene)-5'-(4-fluorophenyl)-3'-oxo-4'-phenyl-3*H*-spiro [benzofuran-2,1'-cyclopentan]-3-ylidene)-4-methylbenzenesulfonamide(4f):** Pale yellow solid, 57 mg, 93% yield, 91% *ee*, the measured *dr* is 5:1 from ^{1}H NMR: 4.60-4.57(*minor*), 4.20-4.17(*major*), E/Z = >20:1; R_f = 0.4 (petroleum ether/ethyl acetate = 90:10)

^{1}H NMR (500 MHz, Chloroform-d) *δ* 8.26 (s, 1H), 8.01 (s, 1H), 7.53-7.49 (m, 3H), 7.31 – 7.27 (m, 4H), 7.25 (d, *J* = 5.3 Hz, 2H), 7.19-7.15 (m, 4H), 7.11 – 7.06 (m, 2H), 6.95 (t, *J* = 7.5 Hz, 3H), 6.88 (d, *J* = 8.4 Hz, 1H), 6.73 (t, *J* = 8.5 Hz, 2H), 4.45 (d, *J* = 14.0 Hz, 1H), 3.94 (s, 1H), 2.46 (s, 3H). **^{13}C NMR** (126 MHz, Chloroform-d) *δ* 200.88, 179.37, 167.83, 163.47, 161.50, 143.76, 143.68, 139.27, 138.45, 135.58, 134.47, 133.74, 130.87, 130.81, 129.97, 129.76, 129.51, 129.36, 129.02, 128.94, 128.89, 128.68, 128.26, 128.20, 127.75, 127.20, 127.05, 122.51, 115.32, 115.15, 112.66, 94.00, 61.01, 56.92, 21.82. **HRMS (ESI^{+}) (*m/z*):** $[M+K]^{+}$ calcd for $C_{38}H_{28}FNO_4S$: 652.1355,

found: 652.1352; **HPLC:** The enantiomeric excess was determined using CHIRALPAK IA column (*n*-Hexane/ ^{i}PrOH=90:30, flow rate=1.0 mL/min, λ_{max}= 254 nm, τ_{major} = 32.6 min, τ_{minor} = 72.7 min).

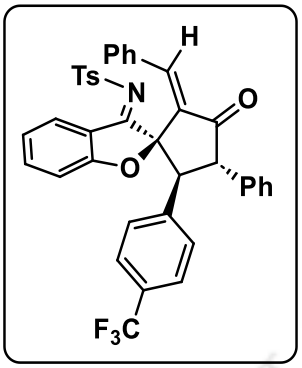

***N*-((2*R*,4'*S*,5'*S*,*E*)-2'-((*E*)-benzylidene)-3'-oxo-4'-phenyl-5'-(4-(trifluoromethyl)phenyl)-3*H*-spiro[benzofuran-2,1'-cyclopentan]-3-ylidene)-4-methylbenzenesulfonamide(4g):** Pale yellow solid, 56.3 mg, 85% yield, 92% *ee*, the measured *dr* is 7:1 from ^{1}H NMR: 4.65-4.62(*minor*), 4.54-4.51(*major*), E/Z = >20:1; R_f = 0.4 (petroleum ether/ethyl acetate = 90:10)

^{1}H NMR (500 MHz, Chloroform-d) δ 8.25 (s, 1H), 8.03 (s, 1H), 7.52 (d, *J* = 7.9 Hz, 2H), 7.47 (t, *J* = 7.8 Hz, 1H), 7.33 (d, *J* = 8.2 Hz, 2H), 7.28 (dd, *J* = 7.9 Hz, 7H), 7.22 (d, *J* = 7.1 Hz, 1H), 7.16 (d, *J* = 7.5 Hz, 2H), 7.08 (t, *J* = 7.6 Hz, 2H), 6.94 (d, *J* = 7.6 Hz, 3H), 6.84 (d, *J* = 8.4 Hz, 1H), 4.53 (d, *J* = 13.9 Hz, 1H), 4.01 (s, 1H), 2.45 (s, 3H). **^{13}C NMR** (126 MHz, Chloroform-d) δ 200.48, 178.99, 167.66, 144.08, 143.76, 139.30, 138.36, 135.32, 134.20, 133.65, 130.95, 130.45, 130.19, 129.76, 129.65, 129.53, 129.33, 129.24, 128.97, 128.70, 128.40, 128.22, 127.88, 127.21, 127.06, 125.12 , 122.88, 122.66, 112.64, 93.85, 61.35, 56.63, 21.81. **HRMS (ESI^{+}) (*m/z*):** $[M+K]^{+}$ calcd for $C_{39}H_{28}F_3NO_4S$: 702.1323, found: 702.1259; **HPLC:** The enantiomeric excess was determined using CHIRALPAK IA column (*n*-Hexane/ ^{i}PrOH=90:30, flow rate=1.0 mL/min, λ= 254 nm, τ_{major} = 39.4 min, τ_{minor} = 64.3 min).

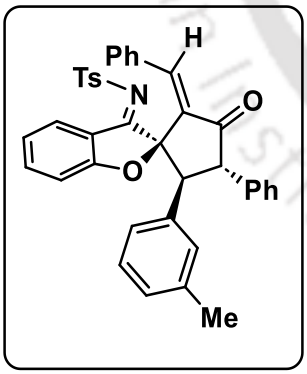

***N*-((2*R*,4'*S*,5'*S*,*E*)-2'-((*E*)-benzylidene)-3'-oxo-4'-phenyl-5'-(*m*-tolyl)-3*H*-spiro[benzofuran-2,1'-cyclopentan]-3-ylidene)-4-methylbenzenesulfonamide(4h):** Pale yellow solid, 54.8 mg, 90% yield, 92% *ee*, the measured *dr* is 6:1 from ^{1}H NMR: 4.62-4.58(*minor*), 4.51-4.48(*major*), E/Z = >20:1; R_f = 0.4 (petroleum ether/ethyl acetate = 90:10)

^{1}H NMR (400 MHz, Chloroform-d) δ 8.25 (d, *J* = 8.2 Hz, 1H), 8.02 (s, 1H), 7.54 (d, *J* = 8.1 Hz, 2H), 7.46 (d, *J* = 8.5, 1H), 7.28 (d, *J* = 8.2 Hz, 2H), 7.22 – 7.18 (m, 2H), 7.14 (t, *J* = 7.8 Hz, 2H), 7.11 – 7.06 (m, 3H), 7.05 – 6.98 (m, 6H), 6.97 – 6.94 (m, 3H), 6.85 (d, *J* = 8.4 Hz, 1H), 4.50 (d, *J* = 13.9 Hz, 1H), 3.97 (d, *J* = 13.7 Hz, 1H), 2.46 (s, 3H), 2.27 (s, 3H). **^{13}C NMR** (126 MHz, Chloroform-d) (*major*+*minor*) δ 201.37, 200.8, 181.83, 179.68, 171.21, 167.94, 143.98, 143.52, 140.71, 138.89, 138.83, 138.55, 137.94, 137.68, 135.86, 135.00, 134.52, 133.78, 133.15, 132.14, 130.85, 130.77, 130.21, 130.02, 129.88, 129.76, 129.44, 129.39, 129.04, 128.95, 128.83, 128.77, 128.71,

128.63, 128.13, 127.96, 127.55, 127.14, 127.01, 126.02, 125.97, 122.57, 122.16, 121.08, 117.63, 112.58, 111.80, 95.23, 94.17, 61.62, 57.78, 56.37, 54.34, 21.82, 21.78, 21.37, 21.30. **HRMS (ESI$^+$) (*m/z*):** $[M+H]^+$ calcd for $C_{39}H_{31}NO_4S$: 610.2047, found: 610.2035; **HPLC:** The enantiomeric excess was determined using CHIRALPAK IA column (*n*-Hexane/ ^{i}PrOH=90:30, flow rate=1.0 mL/min, $\lambda = 254$ nm, $\tau_{major} = 17.3$ min, $\tau_{minor} = 23.9$ min).

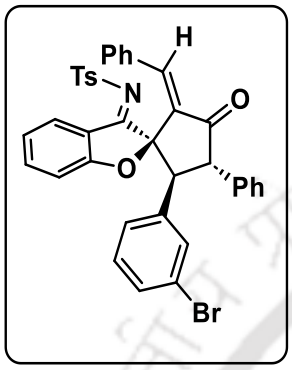

***N*-((2*R*,4'*S*,5'*S*,*E*)-2'-((*E*)-benzylidene)-5'-(3-bromophenyl)-3'-oxo-4'-phenyl-3*H*-spiro [benzofuran-2,1'-cyclopentan]-3-ylidene)-4-methylbenzenesulfonamide(4i):** pale yellow solid, 62 mg, 92% yield, 91% *ee*, the measured *dr* is 6:1 from ^{1}H NMR: 4.60-4.57(*minor*), 4.51-4.48(*major*), E/Z = >20:1; $R_f = 0.4$ (petroleum ether/ethyl acetate = 90:10)

^{1}H NMR (400 MHz, Chloroform-d) δ 8.33 (s, 1H), 8.06 (s, 1H), 7.58 – 7.54 (m, 2H), 7.50-7.49 (m, 1H), 7.36 – 7.29 (m, 5H), 7.21 (d, $J = 7.5$ Hz, 3H), 7.14 (dd, $J = 9.6$, 7.2 Hz, 3H), 7.11 – 7.05 (m, 2H), 7.00 (d, $J = 7.8$ Hz, 3H), 6.97 (d, $J = 8.3$ Hz, 1H), 6.92 (t, $J = 7.8$ Hz, 1H), 4.50 (d, $J = 13.9$ Hz, 1H), 3.94 (s, 1H), 2.50 (s, 3H). **^{13}C NMR** (101 MHz, Chloroform-d) (*major*+*minor*) δ 200.62, 200.1, 181.19, 179.04, 171.11, 167.75, 144.15, 144.10, 143.89, 143.68, 141.27, 139.26, 139.22, 138.61, 138.40, 135.42, 134.98, 134.95, 134.69, 134.16, 133.69, 132.34, 132.08, 131.84, 131.43, 131.22, 131.04, 130.92, 130.12, 129.98, 129.93, 129.90, 129.79, 129.51, 129.34, 129.02, 129.00, 128.93, 128.88, 128.70, 128.43, 128.38, 128.20, 127.81, 127.21, 127.18, 122.94, 122.56, 122.28, 117.51, 112.67, 111.91, 94.88, 93.86, 61.34, 57.41, 56.62, 54.33, 21.86, 21.82. **HRMS (ESI$^+$) (*m/z*):** $[M+H]^+$ calcd for $C_{38}H_{28}BrNO_4S$: 674.0995, found: 674.1002; **HPLC:** The enantiomeric excess was determined using Churalpak IA column (*n*-Hexane/ ^{i}PrOH=90:30, flow rate=1.0 mL/min, $\lambda = 254$ nm, $\tau_{major} = 29.4$ min, $\tau_{minor} = 31.8$ min).

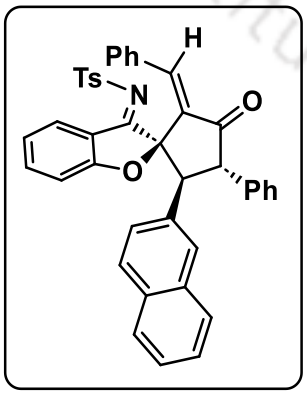

***N*-((2*R*,4'*S*,5'*S*,*E*)-2'-((*E*)-benzylidene)-5'-(naphthalen-2-yl)-3'-oxo-4'-phenyl-3*H*-spiro [benzofuran-2,1'-cyclopentan]-3-ylidene)-4-methylbenzenesulfonamide(4j):** Yellow solid, 34.1 mg, 89% yield, 93% *ee*, the measured *dr* is 5:1 from ^{1}H NMR: 4.84-4.81(*minor*), 4.73-4.70(*major*), E/Z = >20:1; $R_f = 0.4$ (petroleum ether/ethyl acetate = 90:10)

^{1}H NMR (500 MHz, Chloroform-d) δ 8.23 (s, 1H), 8.09 (s, 1H), 7.70 (d, $J = 10.3$ Hz, 2H), 7.63 (t, $J = 7.7$ Hz, 3H), 7.57 (d, $J = 8.4$ Hz, 1H), 7.41 (d, $J = 8.7$ Hz, 2H), 7.42-7.33 (m, 5H), 7.32 – 7.27 (m, 3H), 7.23 – 7.16 (m, 2H), 7.12 (t, $J = 7.8$ Hz, 2H), 7.00 (d, $J = 7.7$ Hz, 2H), 6.82 (t, $J = 8.8$ Hz, 2H), 4.71 (d, $J =$

13.9 Hz, 1H), 4.29 – 4.09 (m, 1H), 2.51 (s, 3H). **^{13}C NMR** (101 MHz, Chloroform-d) (*major*+minor) δ 201.21, 200.66, 179.66, 167.84, 144.08, 143.61, 140.84, 138.97, 138.60, 135.78, 134.76, 133.79, 133.00, 132.94, 132.33, 130.79, 130.36, 130.03, 129.96, 129.89, 129.75, 129.52, 129.35, 129.04, 129.02, 128.88, 128.83, 128.68, 128.64, 128.17, 128.11, 127.82, 127.63, 127.49, 127.23, 127.10, 126.55, 126.19, 126.11, 126.05, 122.68, 122.29, 112.48, 111.85, 95.36, 94.36, 62.80, 58.22, 56.78, 54.97, 22.90, 21.83. **HRMS (ESI$^+$) (*m/z*):** $[M+Na]^+$ calcd for $C_{42}H_{31}NO_4S$: 668.1866, found: 668.1849; **HPLC:** The enantiomeric excess was determined using CHIRALPAK IA column (*n*-Hexane/ ^{i}PrOH=90:30, flow rate=1.0 mL/min, λ = 254 nm, τ_{major} = 33.0 min, τ_{minor} = 61.1 min).

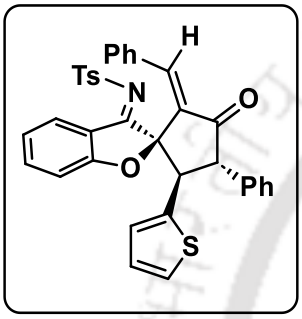

***N*-((2*R*,4'*S*,5'*R*,*E*)-2'-((*E*)-benzylidene)-3'-oxo-4'-phenyl-5'-(thiophen-2-yl)-3*H*-spiro [benzofuran-2,1'-cyclopentan]-3-ylidene)-4-methylbenzenesulfonamide(4k):** yellow solid, 52.2 mg, 87% yield, 85% *ee* (98% *ee* after crystallization), the measured *dr* is 5:1 from ^{1}H NMR: 4.53-4.49(*minor*), 4.37-4.33(*major*), E/Z = >20:1; R_f = 0.4 (petroleum ether/ethyl acetate = 90:10)

^{1}H NMR (400 MHz, Chloroform-d) δ 8.30 (s, 1H), 8.01 (s, 1H), 7.59 – 7.48 (m, 3H), 7.31 – 7.26 (m, 4H), 7.26 – 7.18 (m, 4H), 7.10 (q, *J* = 7.6, 6.6 Hz, 2H), 7.04 – 6.93 (m, 5H), 6.69 (d, *J* = 3.4 Hz, 1H), 6.63 – 6.55 (m, 1H), 4.35 (d, *J* = 13.6 Hz, 1H), 4.18 (s, 1H), 2.45 (s, 3H). **^{13}C NMR** (101 MHz, Chloroform-d) δ 200.46, 179.34, 168.09, 153.64, 143.78, 143.61, 139.07, 138.54, 135.69, 135.30, 134.54, 133.73, 130.84, 129.75, 129.49, 129.12, 128.85, 128.66, 128.40, 128.15, 127.80, 127.22, 126.60, 125.62, 122.49, 113.02, 93.68, 59.19, 57.48, 21.81. **HRMS (ESI$^+$) (*m/z*):** $[M+H]^+$ calcd for $C_{36}H_{27}NO_4S_2$: 602.1455, found: 602.1460; **HPLC:** The enantiomeric excess was determined using CHIRALPAK IA column (*n*-Hexane/ ^{i}PrOH=90:30, flow rate=1.0 mL/min, λ = 254 nm, τ_{major} = 23.4 min, τ_{minor} = 64.6 min).

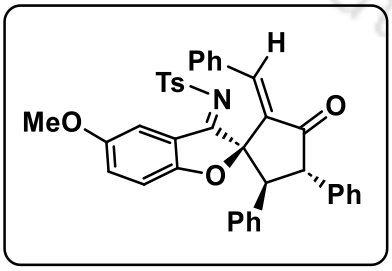

***N*-((2*R*,4'*S*,5'*S*,*E*)-2'-((*E*)-benzylidene)-6-methoxy-3'-oxo-4',5'-diphenyl-3*H*-spiro [benzofuran-2,1'-cyclopentan]-3-ylidene)-4-methylbenzenesulfonamide(4l):** Pale yellow solid, 55.6 mg, 89% yield, 93% *ee*, the measured *dr* is 8:1 from ^{1}H NMR: 4.66-4.63(*minor*), 4.53-4.49(*major*), E/Z = >20:1; R_f = 0.4 (petroleum ether/ethyl acetate = 90:10)

^{1}H NMR (400 MHz, Chloroform-d) (*major*) δ 8.00 (s, 1H), 7.68 (s, 1H), 7.53 (d, *J* = 7.9 Hz, 2H), 7.26 (dd, *J* = 9.3, 7.5 Hz, 5H), 7.22 – 7.16 (m, 5H), 7.10 (ddd, *J* = 7.9, 4.9, 2.0 Hz, 3H),

7.07 – 7.02 (m, 2H), 7.02 – 6.99 (m, 1H), 6.98 – 6.94 (m, 2H), 6.76 (d, *J* = 9.1 Hz, 1H), 4.51 (d, *J* = 13.9 Hz, 1H), 3.95 (s, 1H), 3.74 (s, 3H), 2.45 (s, 3H). **^{13}C NMR** (101 MHz, Chloroform-d) *δ* 201.32, 179.84, 163.48, 154.62, 143.51, 138.66, 135.93, 134.69, 133.77, 132.52, 132.29, 130.72, 129.82, 129.66, 129.48, 129.23, 129.08, 128.80, 128.61, 128.38, 128.17, 128.10, 127.59, 127.14, 113.42, 94.72, 61.70, 56.11, 21.80. **HRMS (ESI$^+$) *m/z*:** $[M+H]^+$ calcd for $C_{39}H_{31}NO_5S$: 626.1996, found: 626.2002; **HPLC:** The enantiomeric excess was determined using CHIRALPAK IA column (*n*-Hexane/ ^{i}PrOH=90:30, flow rate=1.0 mL/min, λ = 254 nm, τ_{major} = 41.0 min, τ_{minor} = 53.8 min).

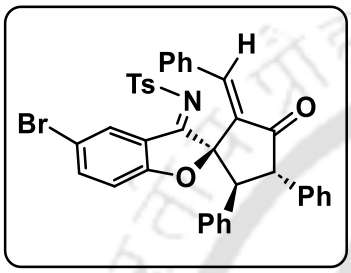

***N*-((2*R*,4'*S*,5'*S*,*E*)-2'-((*E*)-benzylidene)-6-bromo-3'-oxo-4',5'-diphenyl-3*H*-spiro [benzofuran-2,1'-cyclopentan]-3-ylidene)-4-methylbenzenesulfonamide(4m):** yellow solid, 61.3 mg, 91% yield, 93% *ee*, the measured *dr* is 7:1 from ^{1}H NMR: 4.61-4.58(*minor*), 4.52-4.49(*major*), E/Z = >20:1; R_f = 0.4 (petroleum ether/ethyl acetate = 90:10)

^{1}H NMR (500 MHz, Chloroform-d) *δ* 8.11 (s, 1H), 8.02 (s, 1H), 7.51 (d, *J* = 7.9 Hz, 2H), 7.25-7.28 (d, *J* = 8.3 Hz, 3H), 7.26-7.24 (m, 2H), 7.19 (dd, *J* = 13.1, 7.0 Hz, 5H), 7.15 – 7.10 (m, 3H), 7.05 (q, *J* = 6.3 Hz, 4H), 6.93 (d, *J* = 7.6 Hz, 2H), 4.51 (d, *J* = 13.9 Hz, 1H), 3.94 (d, *J* = 14.1 Hz, 1H), 2.46 (s, 3H). **^{13}C NMR** (126 MHz, Chloroform-d) *δ* 200.98, 178.17, 167.83, 144.01, 143.83, 138.12, 135.58, 134.31, 133.88, 133.73, 132.06, 130.93, 129.65, 129.54, 129.16, 129.02, 128.84, 128.75, 128.38, 128.34, 127.68, 127.23, 126.03, 116.08, 95.02, 62.00 – 61.24 (m), 56.46, 21.84. **HRMS (ESI$^+$) *m/z*:** $[M+H]^+$ calcd for $C_{38}H_{28}BrNO_4S$: 674.0995, found: 674.0978; **HPLC:** The enantiomeric excess was determined using CHIRALPAK IE column (*n*-Hexane/ ^{i}PrOH=90:30, flow rate=1.0 mL/min, λ = 254 nm, τ_{major} = 16.1 min, τ_{minor} = 60.2 min).

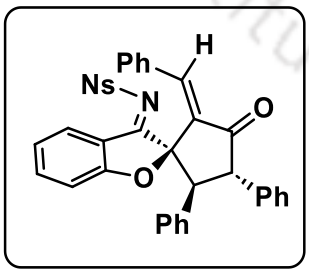

***N*-((2*R*,4'*S*,5'*S*,*E*)-2'-((*E*)-benzylidene)-3'-oxo-4',5'-diphenyl-3*H*-spiro[benzofuran-2,1'-cyclopentan]-3-ylidene)-4-nitrobenzenesulfonamide(4n):** Pale yellow solid, 56.3 mg, 90% yield, 88% *ee*, the measured *dr* is 8:1 from ^{1}H NMR: 4.29-4.26(*minor*), 3.94(*major*), E/Z = >20:1; R_f = 0.4 (petroleum ether/ethyl acetate = 90:10)

^{1}H NMR (500 MHz, Chloroform-d) *δ* 8.32 (d, *J* = 8.5 Hz, 2H), 8.18 (d, *J* = 8.0 Hz, 1H), 8.02 (s, 1H), 7.77 (d, *J* = 8.5 Hz, 2H), 7.53 (t, *J* = 7.8 Hz, 1H), 7.34 (t, *J* = 7.7 Hz, 1H), 7.25 (t, *J* = 7.4 Hz, 3H), 7.21 – 7.19 (m, 2H), 7.17 (d, *J* = 7.7 Hz, 2H), 7.12 (t, *J* = 7.6 Hz, 2H), 7.05 (t, *J* = 7.5 Hz, 2H), 7.00 (d, *J* = 7.6 Hz, 1H), 6.98 – 6.95 (m, 2H), 6.91 (d, *J* = 8.4 Hz, 1H), 4.55 (d,

J = 14.0 Hz, 1H), 3.94 (s, 1H). **^{13}C NMR** (126 MHz, Chloroform-d) *δ* 200.82, 181.58, 168.40, 150.31, 146.86, 143.49, 139.97, 135.59, 134.07, 133.67, 132.32, 132.08, 131.11, 129.87, 129.18, 128.97, 128.87, 128.83, 128.53, 128.49, 128.47, 128.32, 128.30, 127.75, 124.20, 122.66, 113.06, 94.48, 62.00, 56.56. **HRMS (ESI$^+$) *m/z*:** $[M+Na]^+$ calcd for $C_{37}H_{26}N_2O_6S$: 649.1404, found: 649.1410; **HPLC:** The enantiomeric excess was determined using CHIRALPAK IA column (*n*-Hexane/ ^{i}PrOH=90:30, flow rate=1.0 mL/min, λ = 274 nm, τ_{major} = 14.8 min, τ_{minor} = 21.8 min).

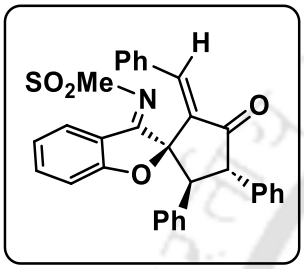

***N*-((2*R*,4'*S*,5'*S*,*E*)-2'-((*E*)-benzylidene)-3'-oxo-4',5'-diphenyl-3*H*-spiro[benzofuran-2,1'-cyclopentan]-3-ylidene)methanesulfonamide(4o):** Pale yellow solid, 43 mg, 83% yield, 89% *ee*, the measured *dr* is 7:1 from ^{1}H NMR: 5.11-5.08(*minor*), 4.62-4.60(*major*), E/Z = >20:1; R_f = 0.4 (petroleum ether/ethyl acetate = 90:10)

^{1}H NMR (500 MHz, Chloroform-d) *δ* 8.17 (s, 1H), 8.08 (d, *J* = 8.2 Hz, 1H), 7.51-7.47 (m, 1H), 7.33 (d, *J* = 7.5 Hz, 2H), 7.31 – 7.26 (m, 4H), 7.26 – 7.22 (m, 2H), 7.11 (t, *J* = 7.6 Hz, 2H), 7.08 – 7.03 (m, 4H), 7.03 – 6.99 (m, 1H), 6.93 (t, *J* = 7.7 Hz, 1H), 6.89 (d, *J* = 8.4 Hz, 1H), 4.61 (d, *J* = 14.0 Hz, 1H), 4.06 (d, *J* = 14.0 Hz, 1H), 2.93 (s, 3H). **^{13}C NMR** (126 MHz, Chloroform-d) *δ* 201.21, 180.28, 167.90, 143.80, 139.15, 135.76, 134.98, 134.00, 133.37, 132.27, 131.18, 130.80, 130.05, 129.49, 129.45, 129.18, 129.09, 129.07, 129.04, 128.88, 128.78, 128.74, 128.64, 128.20, 128.13, 127.70, 127.45, 124.91, 123.78, 122.27, 120.84, 120.12, 112.73, 94.02, 61.80, 56.65, 42.56. **HRMS (ESI$^+$) *m/z*:** $[M+H]^+$ calcd for $C_{32}H_{25}NO_4S$: 520.1578, found: 520.1579; **HPLC:** The enantiomeric excess was determined using CHIRALPAK IE column (*n*-Hexane/ ^{i}PrOH=90:30, flow rate=1.0 mL/min, λ = 274 nm, τ_{major} = 13.8 min, τ_{minor} = 16.4 min).

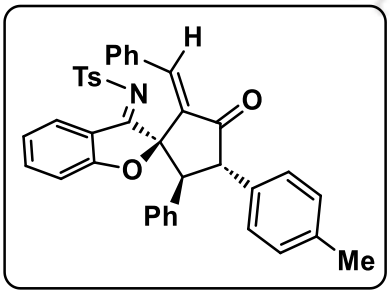

***N*-((2*R*,4'*S*,5'*S*,*E*)-2'-((*E*)-benzylidene)-3'-oxo-5'-phenyl-4'-(p-tolyl)-3*H*-spiro [benzofuran-2,1'-cyclopentan]-3-ylidene)-4-methylbenzenesulfonamide(4p):** Pale yellow solid, 55.4 mg, 91% yield, 89% *ee*, the measured *dr* is 10:1 from ^{1}H NMR: 4.57-4.55(*minor*), 4.46-4.44(*major*), E/Z = >20:1; R_f = 0.4 (petroleum ether/ethyl acetate = 90:10)

^{1}H NMR (500 MHz, Chloroform-d) *δ* 8.19 (s, 1H), 7.96 (s, 1H), 7.49 (d, *J* = 7.9 Hz, 2H), 7.41 (t, *J* = 7.8 Hz, 1H), 7.24-7.22 (m, 4H), 7.15 (d, *J* = 7.5 Hz, 2H), 7.05-7.02 (m, 5H), 6.98 (t, *J* = 7.5 Hz, 2H), 66.94-6.86 (m, 4H), 6.80 (d, *J* = 8.4 Hz, 1H), 4.45 (d, *J* = 14.0 Hz, 1H), 3.90

(s, 1H), 2.42 (s, 3H), 2.21 (s, 3H). **^{13}C NMR** (126 MHz, Chloroform-d) δ 201.50, 179.69, 167.98, 143.56, 143.47, 138.96, 138.63, 137.25, 134.74, 133.86, 132.79, 132.49, 130.74, 129.91, 129.76, 129.58, 129.48, 129.34, 129.28, 128.91, 128.64, 128.17, 128.05, 127.22, 127.11, 122.25, 112.69, 94.17, 61.74, 56.40, 21.81, 21.27. **HRMS (ESI$^+$) *m/z*:** $[M+H]^+$ calcd for $C_{39}H_{31}NO_4S$: 610.2047, found: 610.2056; **HPLC:** The enantiomeric excess was determined using CHIRALPAK IA column (*n*-Hexane/ ^{i}PrOH=90:30, flow rate=1.0 mL/min, λ = 254 nm, τ_{major} = 23.3 min, τ_{minor} = 38.3 min).

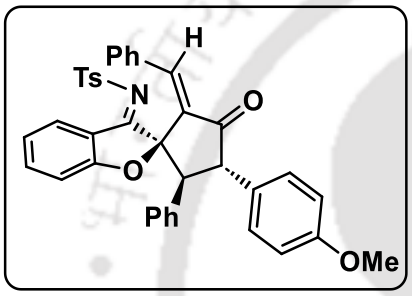

***N*-((2*R*,4'*S*,5'*S*,*E*)-2'-((*E*)-benzylidene)-4'-(4-methoxy phenyl)-3'-oxo-5'-phenyl-3*H*-spiro[benzofuran-2,1'-cyclopentan]-3-ylidene)-4 methylbenzenesulfonamide(4q):** Pale yellow solid, 58.1 mg, 93% yield, 90% *ee*, the measured *dr* is 10:1 from ^{1}H NMR: 4.61-4.59(*minor*), 4.50-4.47(*major*), E/Z = >20:1; R_f = 0.4 (petroleum ether/ethyl acetate = 90:10).

^{1}H NMR (500 MHz, Chloroform-d) δ 8.25 (s, 1H), 8.02 (s, 1H), 7.54 (d, J = 7.9 Hz, 2H), 7.46 (t, J = 7.8 Hz, 1H), 7.28 (d, J = 8.1 Hz, 3H), 7.20 (d, J = 7.5 Hz, 2H), 7.10 (t, J = 8.4 Hz, 3H), 7.03 (t, J = 7.5 Hz, 3H), 6.99-6.91 (m, 4H), 6.85 (d, J = 8.4 Hz, 1H), 6.79 (d, J = 8.2 Hz, 2H), 4.49 (d, J = 14.0 Hz, 1H), 3.89 (d, J = 27.8 Hz, 1H), 3.72 (s, 3H), 2.46 (s, 3H). **^{13}C NMR** (126 MHz, Chloroform-d) δ 201.65, 179.67, 167.93, 159.03, 143.56, 138.98, 138.55, 134.62, 133.80, 132.46, 130.75, 130.05, 129.75, 129.46, 129.25, 128.62, 128.16, 128.05, 127.82, 127.18, 114.34, 112.68, 94.08, 61.80, 55.95, 55.36, 21.79. **HRMS (ESI$^+$) *m/z*:** $[M+H]^+$ calcd for $C_{39}H_{31}NO_5S$: 626.1996, found: 626.1996; **HPLC:** The enantiomeric excess was determined using CHIRALPAK IA column (*n*-Hexane/ ^{i}PrOH=90:30, flow rate=1.0 mL/min, λ = 254 nm, τ_{major} = 37.8 min, τ_{minor} = 68.8 min).

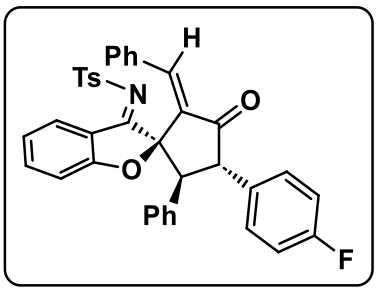

***N*-((2*R*,4'*S*,5'*S*,*E*)-2'-((*E*)-benzylidene)-4'-(4-fluorophenyl)-3'-oxo-5'-phenyl-3*H*-spiro [benzofuran-2,1'-cyclopentan]-3-ylidene)-4-methylbenzenesulfonamide(4r):** Pale yellow solid, 55.1 mg, 90% yield, 91% *ee*, the measured *dr* is 7:1 from ^{1}H

NMR: 4.64-4.62(*minor*), 4.53-4.51(*major*), E/Z = >20:1; R_f = 0.4 (petroleum ether/ethyl acetate = 90:10)

^{1}H NMR (600 MHz, Chloroform-d) δ 8.25 (d, J = 7.3 Hz, 1H), 8.02 (s, 1H), 7.52 (d, J = 7.9 Hz, 2H), 7.48 – 7.45 (m, 1H), 7.32 – 7.26 (m, 3H), 7.18 (d, J = 7.6 Hz, 2H), 7.15 (t, J = 6.2 Hz, 2H), 7.11 – 7.07 (m, 2H), 7.05 – 7.01 (m, 3H), 6.99 (d, J = 7.3 Hz, 1H), 6.96 – 6.93 (m, 4H), 6.86 (d, J = 8.4 Hz, 1H), 4.52 (d, J = 13.9 Hz, 1H), 3.89 (s, 1H), 2.45 (s, 3H). **^{13}C NMR** (151 MHz, Chloroform-d) δ 201.05, 167.90, 163.10, 161.47, 143.64, 139.06, 138.47, 134.38, 133.69, 132.17, 131.43, 130.89, 130.64, 130.58, 129.79, 129.48, 129.18, 128.67, 128.26, 128.21, 127.20, 122.34, 115.86, 115.71, 112.68, 93.97, 61.75, 55.85, 21.81. **HRMS (ESI$^+$) (*m/z*):** $[M+Na]^+$ calcd for $C_{38}H_{28}FNO_4S$: 636.1616, found: 636.1602; **HPLC:** The enantiomeric excess was determined using CHIRALPAK IA column (*n*-Hexane/ ^{i}PrOH=90:30, flow rate=1.0 mL/min, λ = 254 nm, τ_{major} = 28.9 min, τ_{minor} = 51.3 min).

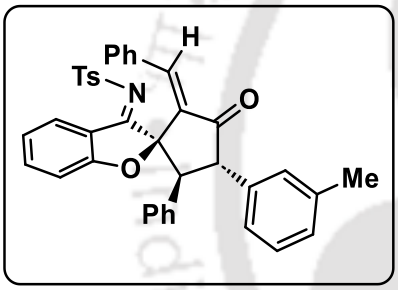

***N*-((2*R*,4'*S*,5'*S*,*E*)-2'-((*E*)-benzylidene)-3'-oxo-5'-phenyl-4'-(m-tolyl)-3*H*-spiro [benzofuran-2,1'-cyclopentan]-3-ylidene)-4-methylbenzenesulfonamide(4s):** Pale yellow solid, 55.4 mg, 91% yield, 92% *ee*, the measured *dr* is 6:1 from ^{1}H NMR: 4.62-4.58(*minor*), 4.51-4.48(*major*), E/Z = >20:1; R_f = 0.4 (petroleum ether/ethyl acetate = 90:10)

^{1}H NMR (400 MHz, Chloroform-d) δ 8.25 (d, J = 8.2 Hz, 1H), 8.02 (s, 1H), 7.54 (d, J = 8.1 Hz, 2H), 7.48-7.43 (m, 1H), 7.43 – 7.39 (m, 1H), 7.28 (d, J = 8.2 Hz, 3H), 7.20 (d, J = 7.0 Hz, 2H), 7.14 (t, J = 7.8 Hz, 2H), 7.11 – 7.06 (m, 3H), 7.05-6.99 (m, 6H), 6.98 – 6.94 (m, 4H), 6.92 (d, J = 7.7 Hz, 1H), 6.85 (d, J = 8.4 Hz, 1H), 4.50 (d, J = 13.9 Hz, 1H), 3.97 (d, J = 13.7 Hz, 1H), 2.46 (s, 3H), 2.27 (s, 3H). **^{13}C NMR** (101 MHz, Chloroform-d) (*major*+*minor*) δ 201.51, 200.96, 181.73, 179.69, 171.23, 167.94, 144.02, 143.57, 140.72, 138.99, 138.92, 138.74, 138.54, 138.44, 138.37, 138.32, 135.76, 135.10, 134.63, 133.79, 133.18, 132.50, 132.41, 132.31, 132.14, 130.92, 130.77, 129.99, 129.91, 129.85, 129.76, 129.62, 129.46, 129.35, 129.24, 129.00, 128.78, 128.74, 128.68, 128.63, 128.50, 128.33, 128.26, 128.14, 128.03, 127.18, 127.08, 126.15, 126.02, 122.62, 122.25, 112.69, 111.90, 95.24, 94.15, 61.71, 57.94, 56.70, 54.55, 21.84, 21.80, 21.72, 21.64. **HRMS (ESI$^+$) *m/z*:** $[M+H]^+$ calcd for $C_{39}H_{31}NO_4S$: 610.2047, found: 610.2054; **HPLC:** The enantiomeric excess was determined using CHIRALPAK IA column (*n*-Hexane/ ^{i}PrOH=90:30, flow rate=1.0 mL/min, λ = 254 nm, τ_{major} = 21.2 min, τ_{minor} = 39.5 min).

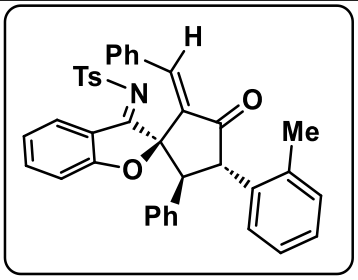

***N*-((2*R*,4'*S*,5'*S*,*E*)-2'-((*E*)-benzylidene)-3'-oxo-5'-phenyl-4'-(o-tolyl)-3*H*-spiro [benzofuran-2,1'-cyclopentan]-3-ylidene)-4-methylbenzenesulfonamide(4t):** yellow solid, 54.2 mg, 89% yield, 92% *ee*, the measured *dr* is 7:1 from ^{1}H NMR: 5.02-4.99(*minor*), 4.80-4.77(*major*), E/Z = >20:1; R_f = 0.4 (petroleum ether/ethyl acetate = 90:10)

^{1}H NMR (500 MHz, Chloroform-d) (*major*) δ 8.24 (s, 1H), 7.99 (s, 1H), 7.55 (d, J = 7.9 Hz, 2H), 7.46 (t, J = 7.8 Hz, 1H), 7.28 (d, J = 8.0 Hz, 3H), 7.18 (d, J = 7.5 Hz, 2H), 7.14 (d, J = 7.4 Hz, 1H), 7.10 – 7.05 (m, 4H), 7.01 (t, J = 7.1 Hz, 3H), 6.95 (dd, J = 11.8, 7.6 Hz, 4H), 6.88 (d, J = 8.4 Hz, 1H), 4.79 (d, J = 14.1 Hz, 1H), 4.09 (d, J = 14.3 Hz, 1H), 2.46 (s, 3H), 2.40 (s, 3H). **^{13}C NMR** (126 MHz, Chloroform-d) (*major*+*minor*) δ 201.00, 199.97, 181.45, 179.69, 171.28, 167.98, 144.06, 143.58, 140.46, 139.04, 138.84, 138.53, 134.95, 134.74, 134.38, 133.80, 133.66, 133.19, 132.45, 132.32, 130.96, 130.82, 130.75, 129.87, 129.84, 129.69, 129.48, 129.26, 129.22, 128.75, 128.63, 128.33, 128.14, 128.10, 127.56, 127.20, 127.16, 126.44, 122.71, 122.30, 117.53, 112.68, 111.95, 95.23, 94.24, 60.89, 56.22, 21.83, 20.46. **HRMS (ESI+) *m/z***: [M+H]+ calcd for C39H31NO4S: 610.2047, found: 610.2054; **HPLC:** The enantiomeric excess was determined using CHIRALPAK IA column (*n*-Hexane/ ^{i}PrOH=90:30, flow rate=1.0 mL/min, λ = 254 nm, τ_{major} = 20.1 min, τ_{minor} = 32.5 min).

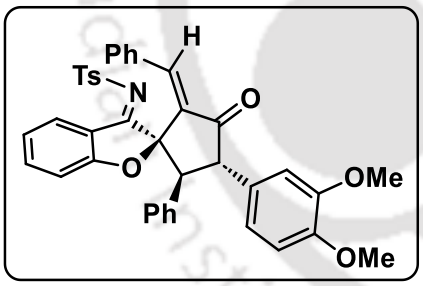

***N*-((2*R*,4'*S*,5'*S*,*E*)-2'-((*E*)-benzylidene)-4'-(3,4-dimethoxy phenyl)-3'-oxo-5'-phenyl-3*H*-spiro[benzofuran-2,1'-cyclopentan]-3-ylidene)-4-methylbenzenesulfonamide (4u):** Yellow solid, 58.9 mg, 90% yield, 95% *ee*, the measured *dr* is 7:1 from ^{1}H NMR: 4.61-4.57(*minor*), 4.49-4.45(*major*), E/Z = >20:1; R_f = 0.4 (petroleum ether/ethyl acetate = 90:10)

^{1}H NMR (400 MHz, Chloroform-d) δ 8.25 (d, J = 8.2 Hz, 1H), 8.02 (s, 1H), 7.53 (d, J = 8.0 Hz, 2H), 7.48 – 7.42 (m, 1H), 7.29 – 7.23 (m, 3H), 7.22 – 7.17 (m, 2H), 7.10 – 7.00 (m, 5H), 6.99-6.64 (m, 3H), 6.91 (t, J = 7.6 Hz, 1H), 6.84 (d, J = 8.4 Hz, 1H), 6.75 – 6.70 (m, 2H), 4.47 (d, J = 13.9 Hz, 1H), 3.92 (s, 1H), 3.78 (s, 3H), 3.76 (s, 3H), 2.44 (s, 3H). **^{13}C NMR** (101 MHz, Chloroform-d) δ 201.42, 179.68, 167.92, 149.12, 148.54, 143.59, 139.00, 138.53, 134.61, 133.74, 132.56, 132.27, 132.23, 130.74, 129.73, 129.45, 129.24, 128.80, 128.76, 128.65, 128.59, 128.35, 128.33, 128.17, 128.07, 127.14, 122.26, 121.19, 112.66, 112.38, 111.49, 93.99, 62.82, 56.20, 56.02, 55.96, 21.76. **HRMS (ESI$^+$) *m/z*:** [M+Na]$^+$ calcd for $C_{40}H_{33}NO_6S$: 678.1921, found: 678.1928; **HPLC:** The enantiomeric excess was determined

using CHIRALPAK IA column (*n*-Hexane/ ^{i}PrOH=90:30, flow rate=1.0 mL/min, λ = 254 nm, τ_{major} = 36.4 min, τ_{minor} = 63.1 min).

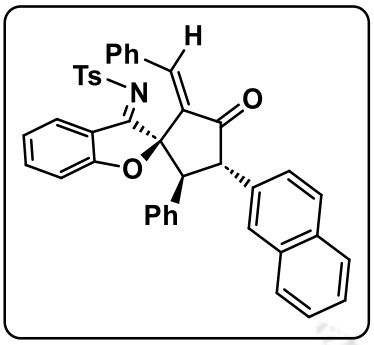

***N*-((2*R*,4'*S*,5'*S*,*E*)-2'-((*E*)-benzylidene)-4'-(naphthalen-2-yl)-3'-oxo-5'-phenyl-3*H*-spiro [benzofuran-2,1'-cyclopentan]-3-ylidene)-4-methylbenzenesulfonamide(4v):** Yellow solid, 59.3 mg, 92% yield, 91% *ee*, the measured *dr* is 6:1 from ^{1}H NMR: 4.85-4.81(*minor*), 4.74-4.71(*major*), E/Z = >20:1; R_f = 0.4 (petroleum ether/ethyl acetate = 90:10)

^{1}H NMR (400 MHz, Chloroform-d) *δ* 8.29 (d, *J* = 8.2 Hz, 1H), 8.07 (s, 1H), 7.78-7.73 (m, 3H), 7.65 (s, 1H), 7.57 (d, *J* = 8.1 Hz, 2H), 7.52 – 7.46 (m, 1H), 7.45 – 7.40 (m, 2H), 7.34-7.28 (m, 4H), 7.25 (d, *J* = 7.2 Hz, 2H), 7.11 (t, *J* = 7.6 Hz, 2H), 7.06-6.97 (m, 5H), 6.97-6.93 (m, 1H), 6.90 (d, *J* = 8.4 Hz, 1H), 4.72 (d, *J* = 13.9 Hz, 1H), 4.11 (s, 1H), 2.48 (s, 3H). **^{13}C NMR** (101 MHz, Chloroform-d) *δ* 201.36, 179.64, 167.98, 143.72, 143.62, 140.96, 139.03, 138.57, 134.67, 133.79, 133.57, 133.38, 132.92, 132.34, 130.84, 129.82, 129.51, 129.26, 128.67, 128.61, 128.54, 128.21, 128.13, 128.00, 127.80, 127.24, 126.57, 126.22, 126.09, 122.31, 112.72, 94.21, 61.73, 56.99, 21.82. **HRMS (ESI^{+}) (*m/z*):** $[M+H]^{+}$ calcd for $C_{42}H_{31}NO_4S$: 646.2047, found: 646.2046; **HPLC:** The enantiomeric excess was determined using CHIRALPAK IA column (*n*-Hexane/ ^{i}PrOH=90:30, flow rate=1.0 mL/min, λ = 254 nm, τ_{major} = 40.9 min, τ_{minor} = 66.4 min).

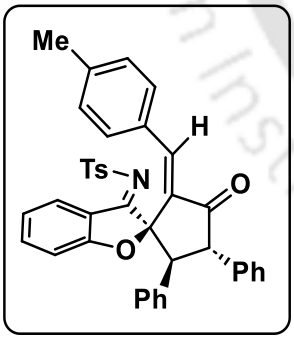

4-methyl-*N*-((2*R*,4'*S*,5'*S*,*E*)-2'-((*E*)-4-methylbenzylidene)-3'-oxo-4',5'-diphenyl-3*H*-spiro [benzofuran-2,1'-cyclopentan]-3-ylidene)benzenesulfonamide(4w): Pale yellow solid, 56.6 mg, 93% yield, 91% *ee*, the measured *dr* is 6:1 from ^{1}H NMR: 4.64-4.61(*minor*), 4.52-4.49(*major*), E/Z = >20:1; R_f = 0.4 (petroleum ether/ethyl acetate = 90:10)

^{1}H NMR (500 MHz, Chloroform-d) *δ* 8.26 (s, 1H), 7.97 (s, 1H), 7.50 (d, *J* = 7.9 Hz, 2H), 7.44 (t, *J* = 7.9 Hz, 1H), 7.24 (t, *J* = 7.3 Hz, 4H), 7.19 (d, *J* = 8.2 Hz, 5H), 7.02 (t, *J* = 7.5 Hz, 2H), 6..97-6.63 (m, 2H), 6.89-6.86 (m, 3H), 6.85 – 6.81 (m, 1H), 4.51 (d, *J* = 13.9 Hz, 1H), 3.97 (s, 1H), 2.44 (s, 3H), 2.28 (s, 3H). **^{13}C NMR** (126 MHz, Chloroform-d) (*major*+*minor*) *δ* 201.34, 179.79, 168.05, 143.79, 143.50, 141.65, 138.93, 138.60, 135.97, 133.16, 132.50, 130.85, 130.18, 129.43, 129.29, 129.11, 129.08, 128.84, 128.79, 128.15, 128.05, 127.56, 127.16, 122.23, 112.71, 94.41, 61.89, 56.64, 21.80, 21.74. **HRMS (ESI^{+}) *m/z*:** $[M+H]^{+}$ calcd for $C_{39}H_{31}NO_4S$: 610.2047, found: 610.2055; **HPLC:** The enantiomeric

excess was determined using CHIRALPAK IE column (*n*-Hexane/ ^{i}PrOH=90:30, flow rate=1.0 mL/min, λ = 254 nm, τ_{major} = 21.0 min, τ_{minor} = 59.3 min).

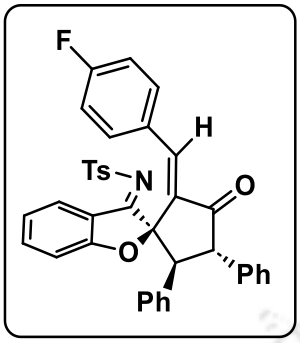

***N*-((2*R*,4'*S*,5'*S*,*E*)-2'-((*E*)-4-fluorobenzylidene)-3'-oxo-4',5'-diphenyl-3*H*-spiro [benzofuran-2,1'-cyclopentan]-3-ylidene)-4-methylbenzenesulfonamide(4x):** Pale yellow solid, 56.3 mg, 92% yield, 89% *ee*, the measured *dr* is 5:1 from ^{1}H NMR: 4.64-4.60 (*minor*), 4.53-4.50(*major*), E/Z = >20:1; R_f = 0.4 (petroleum ether/ethyl acetate = 90:10)

^{1}H NMR (400 MHz, Chloroform-d) *δ* 8.26 (s, 1H), 7.95 (s, 1H), 7.59 (d, *J* = 7.9 Hz, 2H), 7.49 – 7.43 (m, 1H), 7.31 – 7.26 (m, 3H), 7.26 – 7.23 (m, 2H), 7.20-7.17 (m, 4H), 7.06 – 6.98 (m, 3H), 6.97 – 6.89 (m, 3H), 6.84 (d, *J* = 8.4 Hz, 1H), 6.74 (t, *J* = 8.7 Hz, 2H), 4.52 (d, *J* = 14.0 Hz, 1H), 3.98 (s, 1H), 2.46 (s, 3H). **^{13}C NMR** (101 MHz, Chloroform-d) (*major*) *δ* 201.13, 179.54, 167.96, 143.72, 142.28, 139.16, 138.51, 135.76, 134.62, 132.31, 131.94, 131.86, 131.61, 129.98, 129.95, 129.56, 129.24, 129.06, 128.90, 128.85, 128.41, 128.23, 128.15, 127.66, 127.21, 127.09, 122.45, 116.03, 115.82, 112.69, 94.09, 61.62, 56.69, 21.82. **HRMS (ESI^{+}) (*m/z*):** $[M+K]^{+}$ calcd for $C_{38}H_{28}FNO_4S$: 618.1710, found: 618.1715; **HPLC:** The enantiomeric excess was determined using CHIRALPAK IA column (*n*-Hexane/ ^{i}PrOH=90:30, flow rate=1.0 mL/min, λ = 254 nm, τ_{minor} = 22.7 min, τ_{major} = 56.9 min).

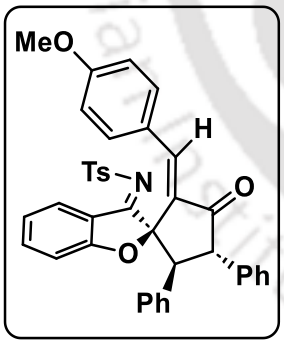

***N*-((2*R*,4'*S*,5'*S*,*E*)-2'-((*E*)-4-methoxybenzylidene)-3'-oxo-4',5'-diphenyl-3*H*-spiro [benzofuran-2,1'-cyclopentan]-3-ylidene)-4-methylbenzenesulfonamide(4y):** Pale yellow solid, 58.1 mg, 93% yield, 86% *ee*, the measured *dr* is 8:1 from ^{1}H NMR: 4.62-4.60(*minor*), 4.52-4.49(*major*), E/Z = >20:1; R_f = 0.4 (petroleum ether/ethyl acetate = 90:10)

^{1}H NMR (500 MHz, Chloroform-d) *δ* 8.31 (s, 1H), 7.94 (d, *J* = 2.6 Hz, 1H), 7.50 (d, *J* = 8.0 Hz, 2H), 7.44 (t, *J* = 7.8 Hz, 1H), 7.24 (dd, *J* = 7.7, 4.9 Hz, 4H), 7.21 – 7.15 (m, 5H), 7.03-7.00 (m, 3H), 6.97-6.92 (m, 4H), 6.83 (d, *J* = 8.5 Hz, 1H), 6.60 (d, *J* = 8.3 Hz, 1H), 4.50 (d, *J* = 14.0 Hz, 1H), 3.91 (d, *J* = 36.8 Hz, 1H), 3.72 (d, *J* = 15.7 Hz, 3H), 2.43 (s, 3H).**^{13}C NMR** (126 MHz, Chloroform-d) (*major*+*minor*) *δ* 201.34, 200.73, 200.08, 181.71, 180.02, 171.13, 168.07, 162.16, 161.65, 143.98, 143.89, 143.49, 140.86, 138.98, 138.73, 138.57, 136.09, 135.22, 132.55, 132.38, 131.46, 130.99, 129.93, 129.88, 129.83, 129.81, 129.61, 129.43, 129.29, 129.12, 129.08, 128.85, 128.83, 128.76, 128.32, 128.26, 128.13, 128.02, 127.52, 127.26, 127.12, 127.03, 126.77, 126.16, 125.51, 122.65, 122.21,

114.34, 113.88, 113.81, 112.79, 112.11, 95.75, 94.71, 62.13, 58.41, 56.59, 55.66, 55.51, 54.35, 21.82, 21.78. **HRMS (ESI$^+$) *m/z*:** $[M+H]^+$ calcd for $C_{39}H_{31}NO_5S$: 626.1996, found: 626.1990; **HPLC:** The enantiomeric excess was determined using CHIRALPAK IA column (*n*-Hexane/ ^{i}PrOH=90:30, flow rate=1.0 mL/min, λ_{max}= 254 nm, τ_{minor} = 22.7 min, τ_{major} = 56.9 min).

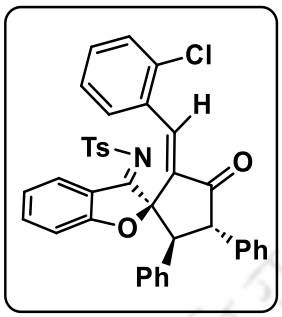

***N*-((2*R*,4'*S*,5'*S*,*E*)-2'-((*E*)-2-chlorobenzylidene)-3'-oxo-4',5'-diphenyl-3H-spiro[benzofuran-2,1'-cyclopentan]-3-ylidene)-4-methylbenzene sulfonamide(4z):** Pale yellow solid, 52.2 mg, 83% yield, 83% *ee*, the measured *dr* is 9:1 from ^{1}H NMR: 4.65-4.63(*minor*), 4.56-4.54(*major*), E/Z = >20:1; R_f = 0.4 (petroleum ether/ethyl acetate = 90:10)

^{1}H NMR (600 MHz, Chloroform-d) δ 8.14 (d, *J* = 8.3 Hz, 1H), 8.12 (s, 1H), 7.78 – 7.73 (m, 2H), 7.47 - 7.45 (m, 1H), 7.36 (t, *J* = 7.7 Hz, 3H), 7.27-7.26 (m, 1H), 7.26 - 7.25 (m, 2H), 7.21 - 7.19 (m, 6H), 7.04 (t, *J* = 7.7 Hz, 2H), 7.00 – 6.97 (m, 1H), 6.91 – 6.86 (m, 2H), 6.61 – 6.55 (m, 2H), 4.55 (d, *J* = 14.0 Hz, 1H), 3.99 (d, *J* = 13.7 Hz, 1H), 2.48 (s, 3H).**^{13}C NMR** (151 MHz, Chloroform-d) (*major*+*minor*) δ 200.67, 179.31, 167.73, 143.74, 140.28, 139.51, 139.07, 138.44, 137.60, 137.33, 135.42, 135.38, 134.78, 132.72, 132.17, 131.70, 130.31, 130.10, 129.96, 129.77, 129.64, 129.12, 129.03, 128.82, 128.26, 128.15, 127.67, 127.32, 127.10, 126.46, 125.23, 122.62, 122.28, 120.72, 114.28, 112.59, 93.73, 60.85, 56.55, 53.64, 22.91, 21.87. **HRMS (ESI$^+$) *m/z*:** $[M+H]^+$ calcd for $C_{38}H_{29}ClNO_4S$: 630.1501, found: 630.1501; **HPLC:** The enantiomeric excess was determined using CHIRALPAK IA column (*n*-Hexane/ ^{i}PrOH=90:30, flow rate=1.0 mL/min, λ_{max}= 254 nm, τ_{major} = 24.7 min, τ_{minor} = 52.1min).

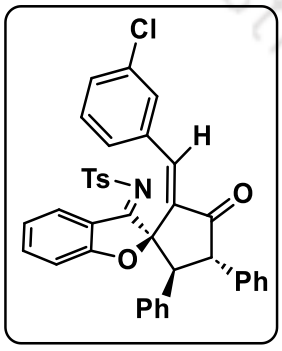

***N*-((2*R*,4'*S*,5'*S*,*E*)-2'-((*E*)-3-chlorobenzylidene)-3'-oxo-4',5'-diphenyl-3*H*-spiro[benzofuran-2,1'-cyclopentan]-3-ylidene)-4-methylbenzenesulfonamide(4z'):** Pale yellow solid, 54.1 mg, 86% yield, 83% *ee*, the measured *dr* is 6:1 from ^{1}H NMR: 4.65-4.63(*minor*), 4.56-4.54(*major*), E/Z = >20:1; R_f = 0.4 (petroleum ether/ethyl acetate = 90:10)

^{1}H NMR (500 MHz, CDCl3) δ 8.277 (s, 1H), 7.92 (s, 1H), 7.59 (d, J = 7.8 Hz, 2H), 7.45 (t, J = 7.8 Hz, 1H), 7.28 (d, J = 8.0 Hz, 2H), 7.24 (d, J = 6.8 Hz, 2H), 7.19 (d, J = 7.3 Hz, 4H), 7.04 - 7.00 (m, 4H), 6.85 - 6.82 (m, 3H), 6.83 (t, J = 6.9 Hz, 3H), 4.51 (d, J = 13.9 Hz, 1H), 3.98 (s, 1H), 2.44 (s, 3H). **^{13}C NMR** (126 MHz, CDCl3) (*major*+*minor*) δ 200.86, 200.26, 181.22, 179.16, 170.88, 167.78, 143.95,

143.55, 141.70, 139.02, 138.98, 138.93, 138.48, 138.21, 136.73, 135.91, 135.72, 135.53, 134.99, 133.45, 133.29, 132.14, 132.05, 131.94, 130.79, 130.74, 130.43, 130.16, 129.74, 129.68, 129.36, 129.04, 128.86, 128.71, 128.65, 128.57, 128.44, 128.23, 128.19, 128.04, 127.97, 127.48, 127.03, 126.89, 122.64, 122.30, 120.59, 117.39, 114.08, 112.45, 111.71, 94.88, 93.77, 61.35, 57.52, 56.50, 54.39, 21.65, 21.62. **HRMS (ESI$^+$) *m/z*:** $[M+H]^+$ calcd for $C_{38}H_{29}ClNO_4S$: 630.1501, found: 630.1498; **HPLC:** The enantiomeric excess was determined using CHIRALPAK IA column (*n*-Hexane/ ^{i}PrOH=90:30, flow rate=1.0 mL/min, λ_{max}= 254 nm, τ_{minor} = 17.9 min, τ_{major} = 20.9 min)

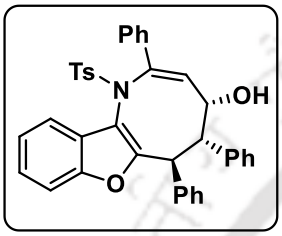

5: white solid, 49.5 mg, 83% yield, >20:1 *dr*, 90% *ee*. R_f = 0.4 (petroleum ether/ethyl acetate = 90:10). **^{1}H NMR** (500 MHz, Chloroform-d) δ 7.50 (d, J = 7.7 Hz, 2H), 7.41 – 7.20 (m, 17H), 7.15 (t, J = 7.3 Hz, 2H), 7.05 (d, J = 8.0 Hz, 2H), 5.30 (s, 1H), 5.14 (s, 1H), 4.60 (s, 1H), 4.30 (s, 1H), 2.38 (s, 3H). **^{13}C NMR** (126 MHz, Chloroform-d) δ 153.52, 144.09, 138.73, 137.42, 129.44, 129.28, 129.11, 128.80, 128.60, 128.53, 128.45, 128.18, 127.29, 127.06, 126.71, 124.75, 123.43, 119.72, 112.22, 71.63, 46.39, 31.79, 21.77. **HRMS (ESI$^+$) (*m/z*):** $[M+H]^+$ calcd for $C_{38}H_{31}NO_4S$: 598.2047, found: 598.2053; **HPLC:** HPLC: The enantiomeric excess was determined using CHIRALPAK ID column (*n*-Hexane/ *i*-PrOH=90:10, flow rate=1.0 mL/min, λ_{max}= 254 nm, τ_{major} = 13.4 min, τ_{minor} = 20.9 min).

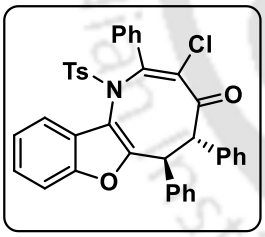

6: White solid, 57.96 mg, 92% yield, >20:1 *dr*, 92% *ee*. **^{1}H NMR** (500 MHz, Chloroform-d) δ 7.60 (d, J = 7.6 Hz, 2H), 7.57 (d, J = 7.5 Hz, 4H), 7.49 (t, J = 7.6 Hz, 1H), 7.41 (t, J = 9.1 Hz, 3H), 7.28 (d, J = 6.9 Hz, 1H), 7.24 (d, J = 8.4 Hz, 2H), 7.18 (d, J = 7.4 Hz, 3H), 7.11 (t, J = 7.8 Hz, 2H), 6.94 (q, J = 8.1 Hz, 4H), 6.79 (d, J = 7.8 Hz, 1H), 6.25 (d, J = 13.1 Hz, 1H), 5.00 (d, J = 13.1 Hz, 1H), 2.39 (s, 3H). **^{13}C NMR** (126 MHz, Chloroform-d) δ 197.27, 158.89, 152.76, 150.93, 144.79, 136.83, 136.69, 135.84, 134.77, 131.43 – 131.04 (m), 130.67, 130.19, 129.29, 128.90, 128.61, 128.52, 128.37, 127.88, 127.52, 125.62, 125.53, 123.30, 120.80, 119.37, 112.36, 54.65, 49.79, 21.80. **HRMS (ESI$^+$) (*m/z*):** $[M+Na]^+$ calcd for $C_{38}H_{28}ClNO_4S$: 652.1320, found: 652.1320; **HPLC:** HPLC: The enantiomeric excess was determined using CHIRALPAK ID column (*n*-Hexane/ *i*-PrOH=90:10, flow rate=1.0 mL/min, λ_{max}= 254 nm, τ_{major} = 13.4 min, τ_{minor} = 20.9 min).

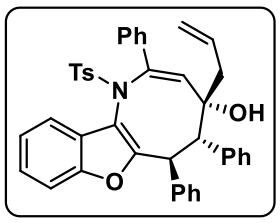

7: white solid, 52.87mg, 87% yield, >20:1 *dr*, 90% *ee*. **^{1}H NMR** (400 MHz, Chloroform-d) δ 7.46 (t, J = 6.9 Hz, 3H), 7.34 (t, J = 7.4 Hz, 3H), 7.29 – 7.25 (m, 3H), 7.22 – 7.20 (m, 3H), 7.15 - 7.08 (m, 4H), 7.01 – 6.96 (m, 5H), 6.93 – 6.90 (m, 1H), 6.60 (d, J = 7.9 Hz, 1H), 6.02 – 5.92 (m, 1H), 5.78 (s, 1H), 5.20 (d, J = 10.0 Hz, 1H), 5.09 (s, 2H), 5.02 (d, J = 17.0 Hz, 1H), 2.54 - 2.49 (m, 1H), 2.43 (s, 3H), 2.13 - 2.08 (m, 1H). **^{13}C NMR** (126 MHz, Chloroform-d) δ 158.84, 153.30, 144.29, 141.83, 140.63, 140.38, 139.67, 137.82, 133.53, 133.19, 130.37, 129.64, 129.49, 129.17, 128.81, 128.73, 128.33, 127.81, 127.68, 127.66, 126.34, 126.13, 126.04, 124.33, 122.75, 120.70, 120.06, 119.63, 111.91, 50.41, 49.87, 47.67, 21.82. **HRMS (ESI$^+$) (*m/z*):** $[M+K]^+$ calcd for $C_{41}H_{35}NO_4S$: 676.1919, found: 676.1922; **HPLC:** The enantiomeric excess was determined using CHIRALPAK ID column (*n*-Hexane/ ^{i}PrOH=90:10, flow rate=1.0 mL/min, λ_{max}= 254 nm, τ_{minor} = 23.2 min, τ_{major} = 25.9 min).

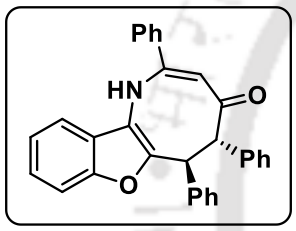

8: white solid, 33.9mg, 77% yield, >20:1 dr, 92% ee. **^{1}H NMR** (600 MHz, DMSO-d_6) δ 9.23 (s, 1H), 8.01 – 7.98 (m, 2H), 7.93 (d, J = 7.5 Hz, 1H), 7.67 – 7.61 (m, 3H), 7.47 (d, J = 8.0 Hz, 1H), 7.44 – 7.41 (m, 2H), 7.40 - 7.38 (m, 1H), 7.36 - 7.33 (m, 1H), 7.30 – 7.27 (m, 2H), 7.18 (t, J = 7.6 Hz, 2H), 7.15 – 7.09 (m, 3H), 7.06 – 7.02 (m, 1H), 5.22 (s, 1H), 5.19 (d, J = 12.9 Hz, 1H), 4.77 (d, J = 12.9 Hz, 1H). **^{13}C NMR** (151 MHz, DMSO-d_6) δ 198.21, 158.31, 153.62, 150.98, 140.34, 137.76, 136.77, 131.29, 129.55, 129.08, 128.92, 128.28, 128.09, 127.61, 126.87, 126.64, 126.22, 125.37, 123.11, 121.83, 119.49, 111.18, 103.82, 55.68, 44.99. **HRMS (ESI$^+$) (*m/z*):** $[M+H]^+$ calcd for $C_{31}H_{23}NO_2$: 442.1802, found: 442.1802; **HPLC:** The enantiomeric excess was determined using CHIRALPAK ID column (*n*-Hexane/ ^{i}PrOH=90:30, flow rate=1.0 mL/min, λ_{max}= 254 nm, τ_{major} = 8.9 min, τ_{minor} = 19.0 min).

2.12. NMR Spectra and HPLC chromatogram:

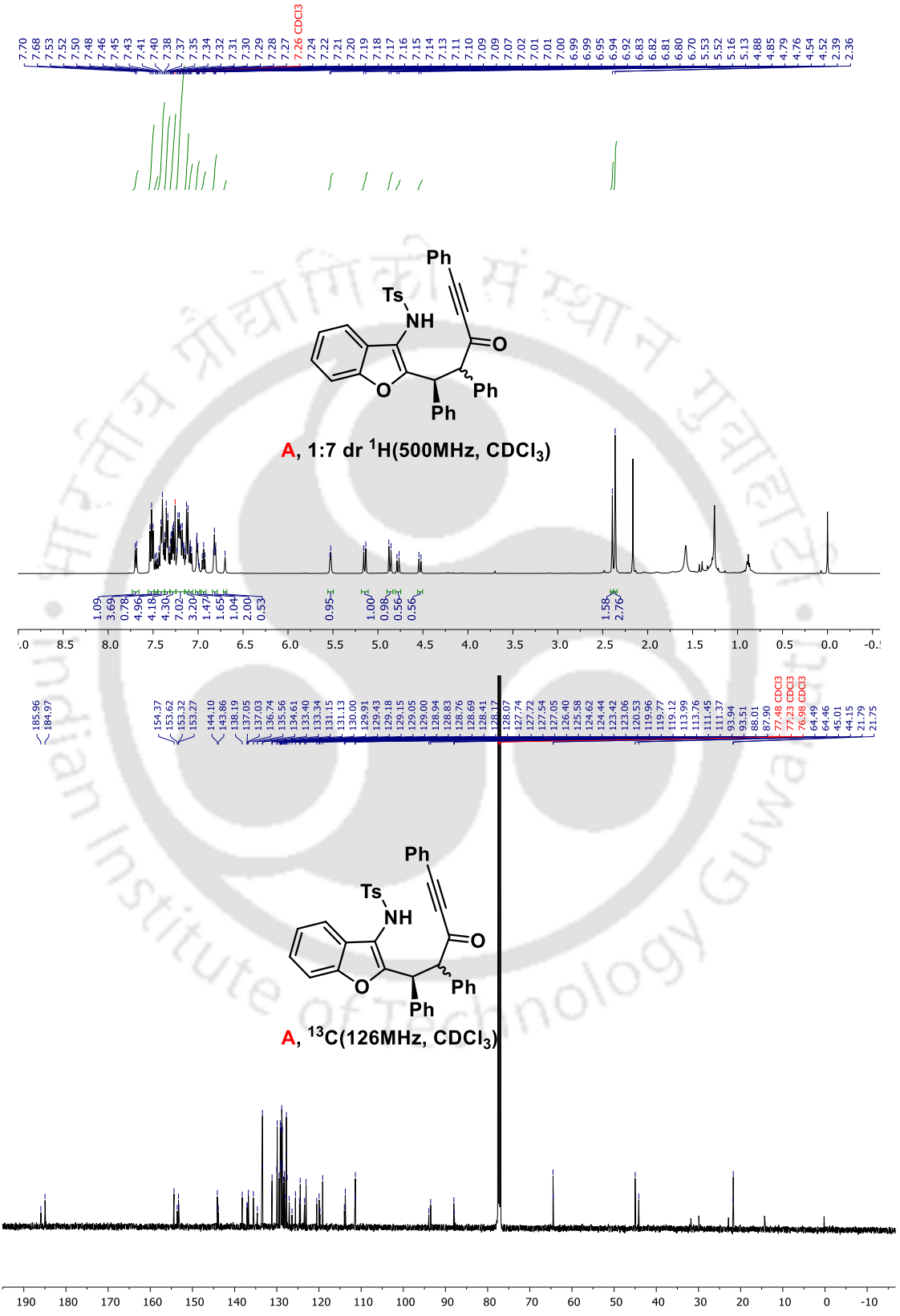

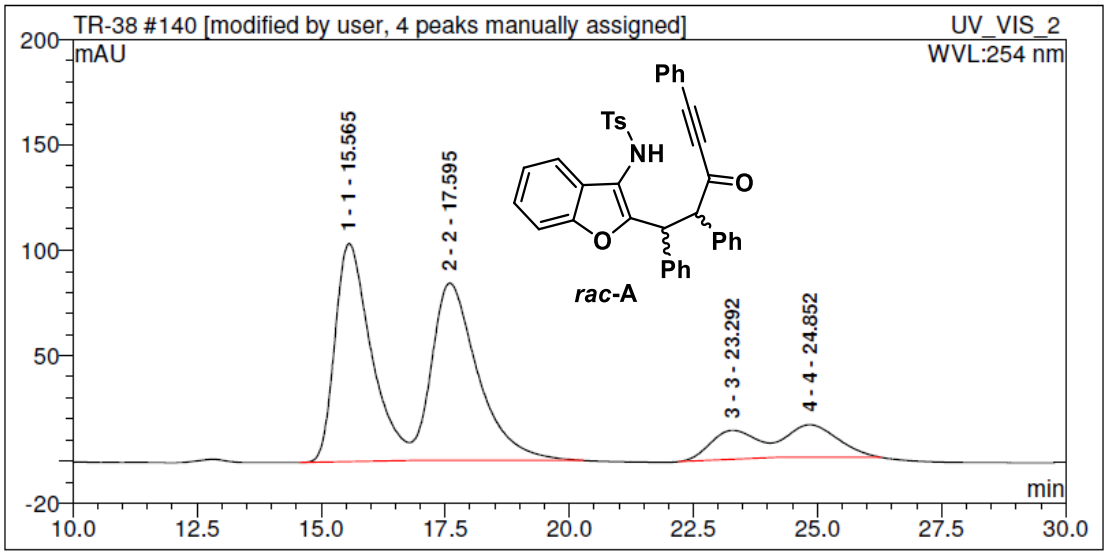

Peak Name	Ret.Time (detected) min	Area mAU*min	Rel.Area(ident.) %	Height mAU	Amount
1 1	15.57	88.15827	41.49711319	103.3562	n.a.
2 2	17.60	90.30376	42.50702045	84.13357	n.a.
3 3	23.29	16.16849	7.610694519	13.71956	n.a.
4 4	24.85	17.814	8.385171843	15.455	n.a.

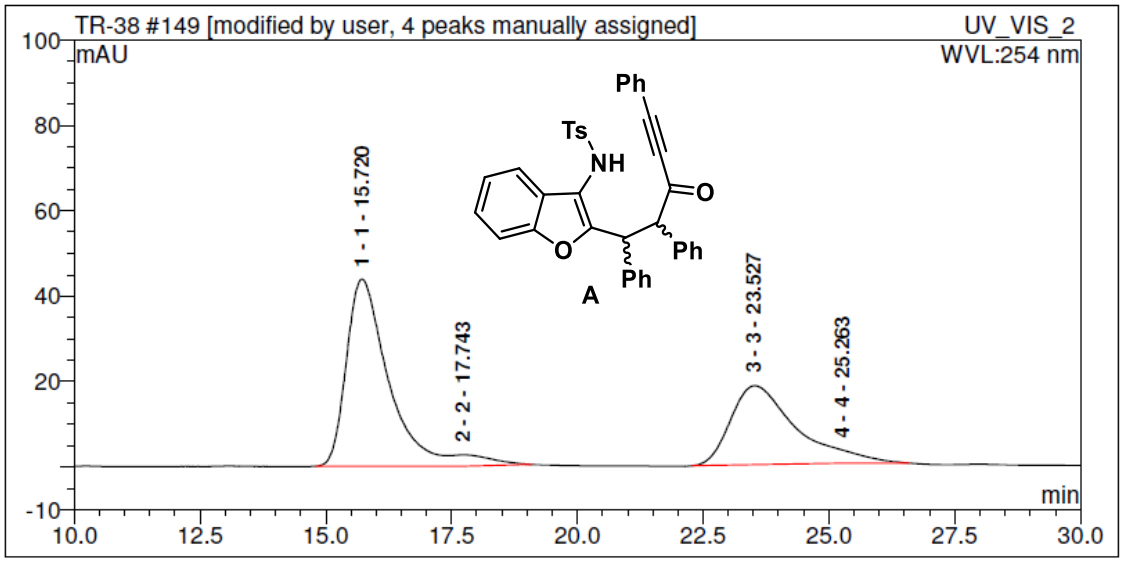

Peak Name	Ret.Time (detected) min	Area mAU*min	Rel.Area(ident.) %	Height mAU	Amount
1 1	15.72	42.09199	58.55196375	43.7907	n.a.
2 2	17.74	1.870579	2.602064032	2.63749	n.a.
3 3	23.53	26.31776	36.60925896	18.46781	n.a.
4 4	25.26	1.608	2.236713253	3.090	n.a.

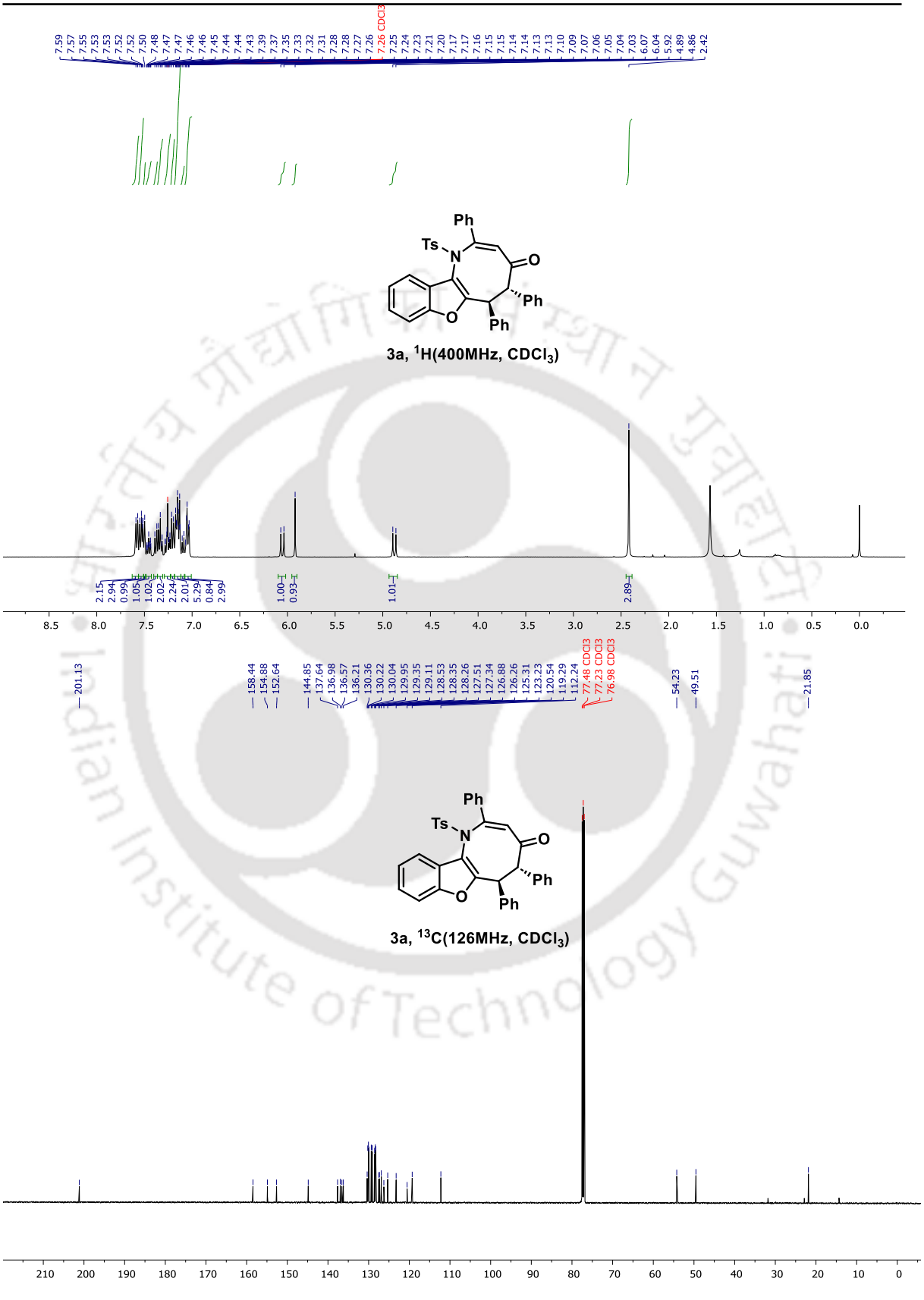

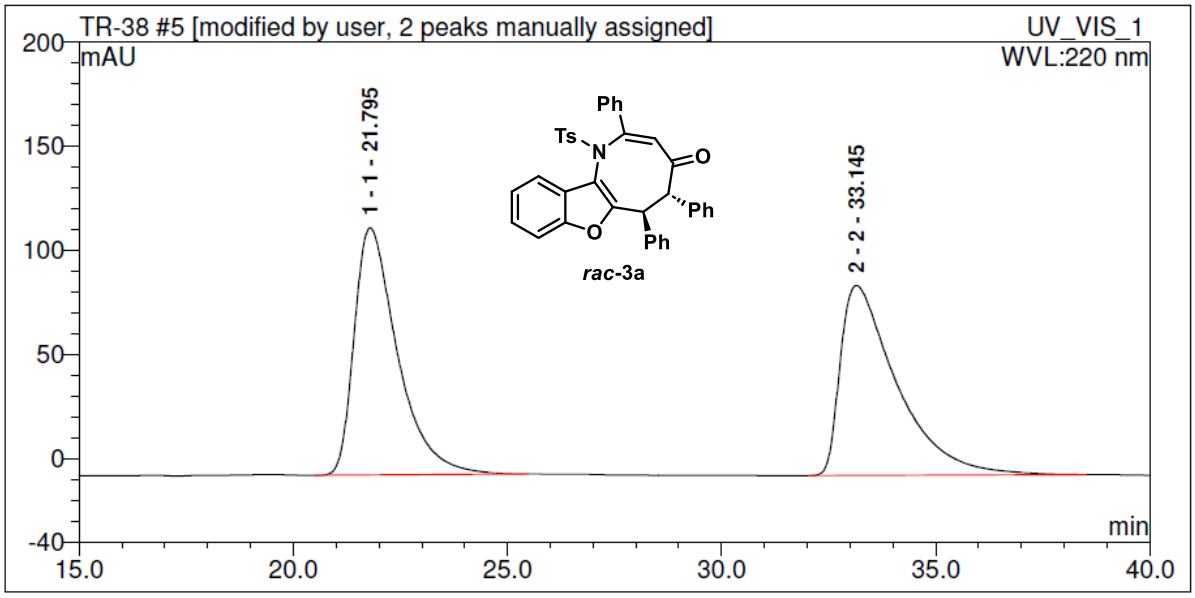

	Peak Name	Ret.Time (detected) min	Area mAU*min	Rel.Area(ident.) %	Height mAU	Amount
1	1	21.80	138.8226	49.83190877	118.6878	n.a.
2	2	33.15	139.759	50.16809123	91.203	n.a.

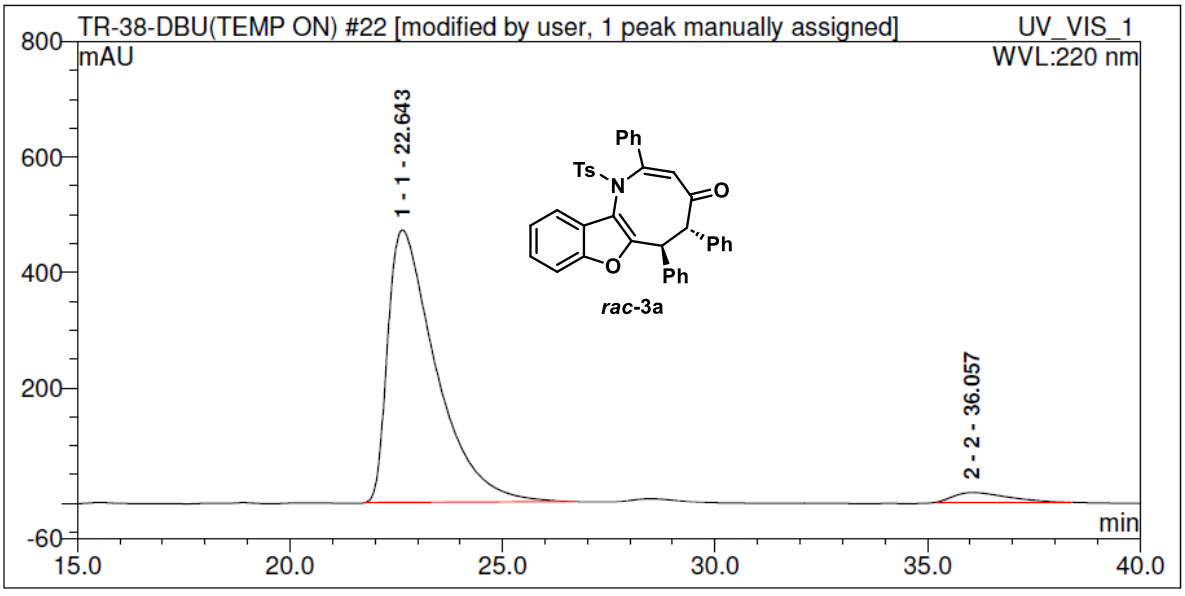

	Peak Name	Ret.Time (detected) min	Area mAU*min	Rel.Area(ident.) %	Height mAU	Amount
1	1	22.64	620.7385	96.14471419	471.9738	n.a.
2	2	36.06	24.891	3.855285815	17.045	n.a.

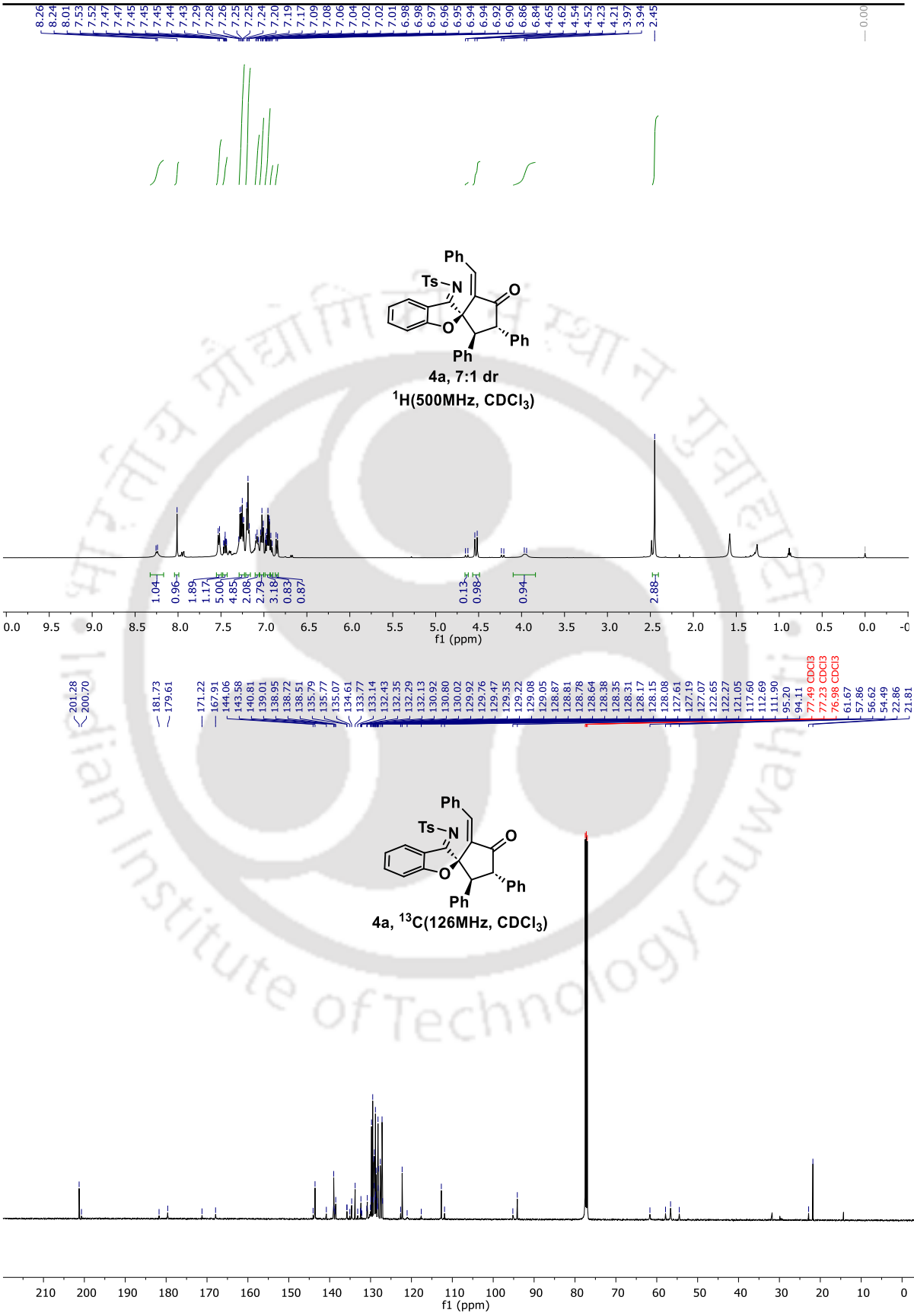

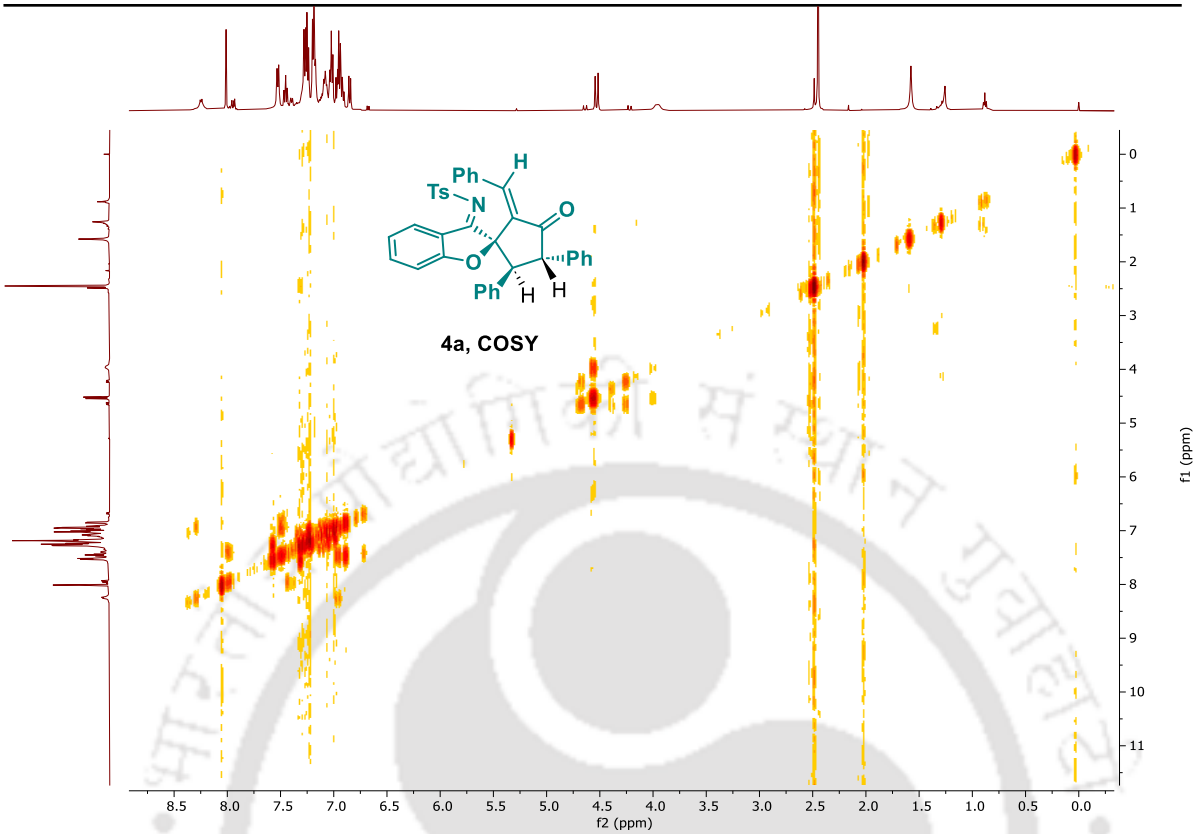

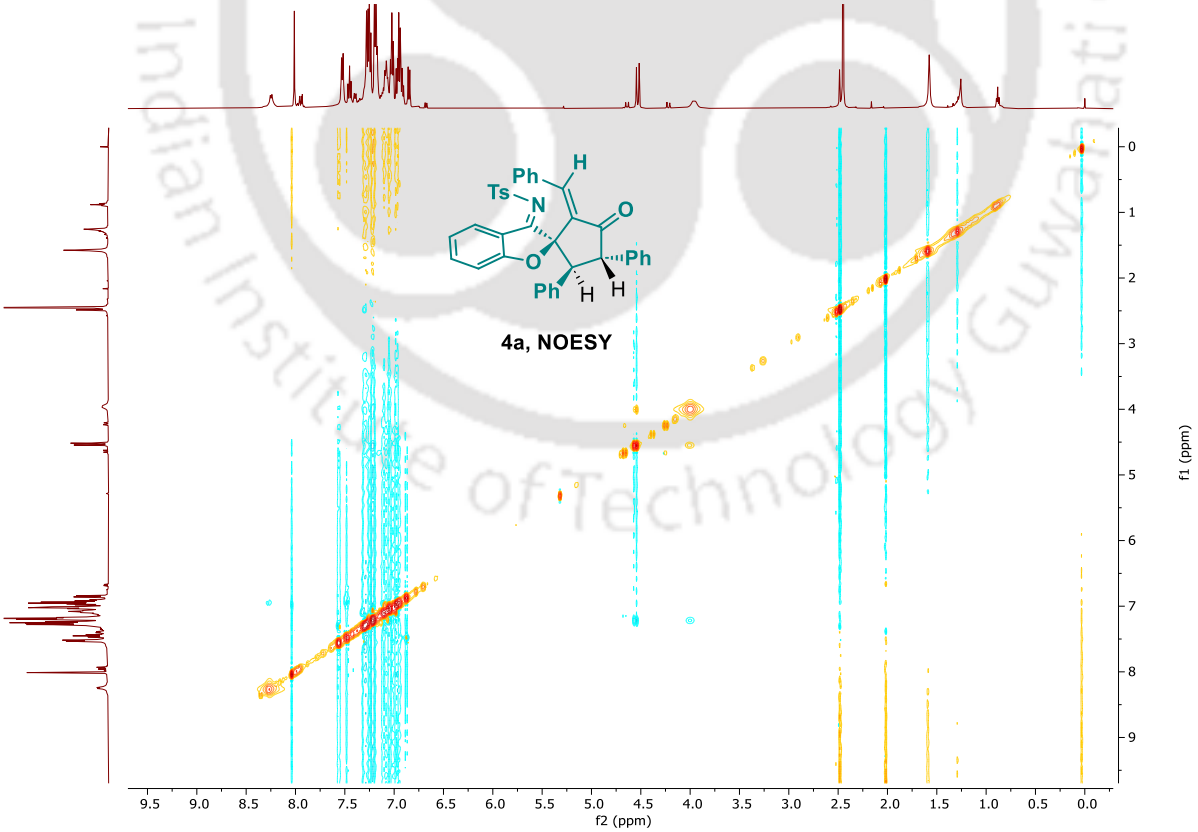

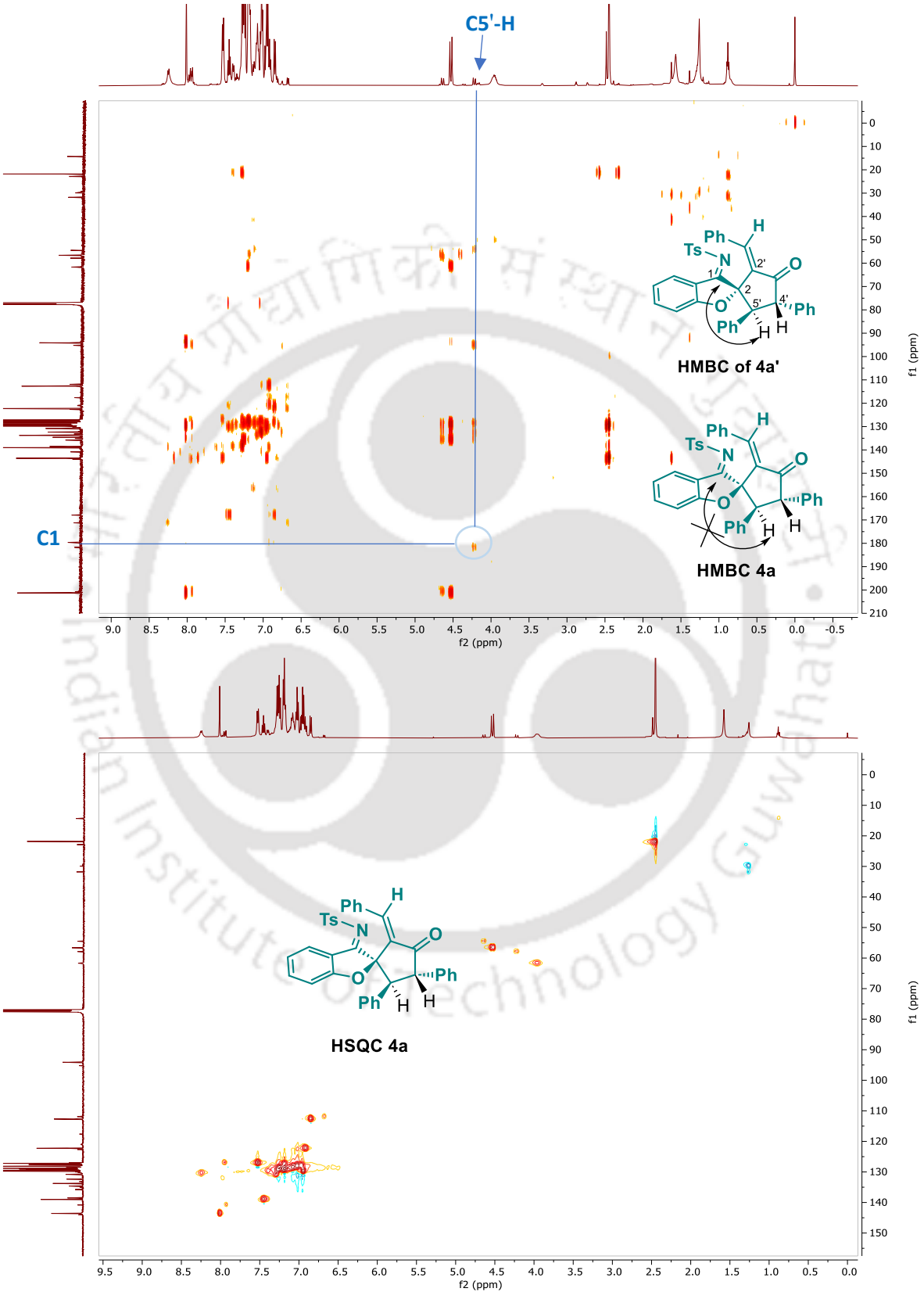

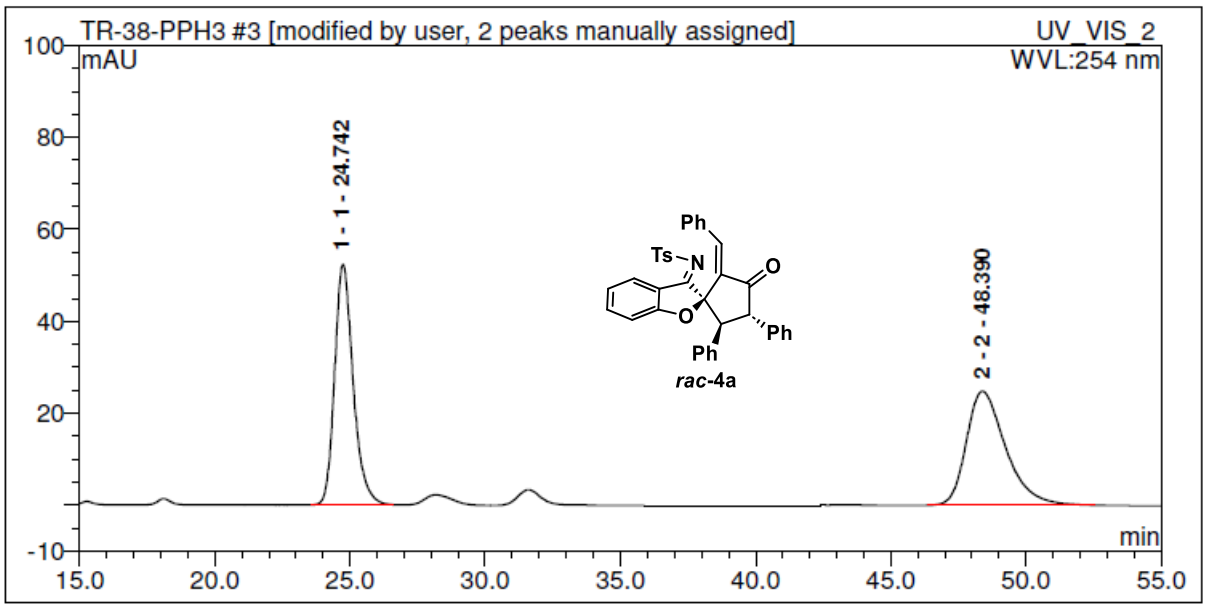

Peak Name	Ret.Time (detected) min	Area mAU*min	Rel.Area(ident.) %	Height mAU	Amount
1 1	24.74	41.55797	49.91453761	52.22303	n.a.
2 2	48.39	41.700	50.08546239	24.754	n.a.

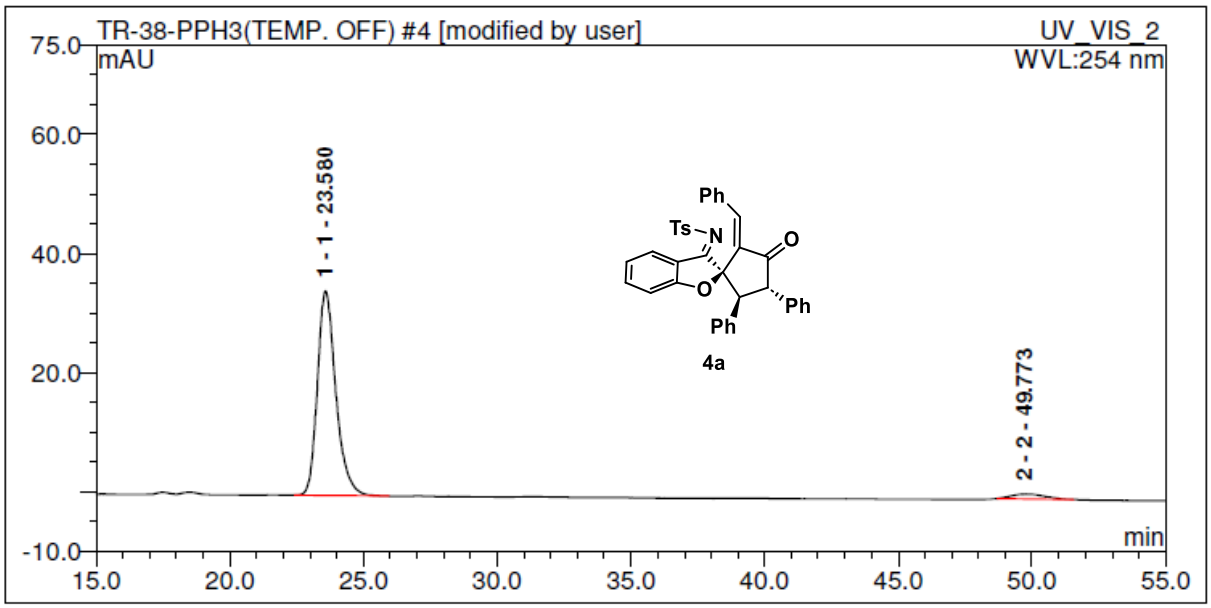

Peak Name	Ret.Time (detected) min	Area mAU*min	Rel.Area(ident.) %	Height mAU	Amount
1 1	23.58	27.43192	95.86291217	34.29574	n.a.
2 2	49.77	1.184	4.137087826	0.830	n.a.

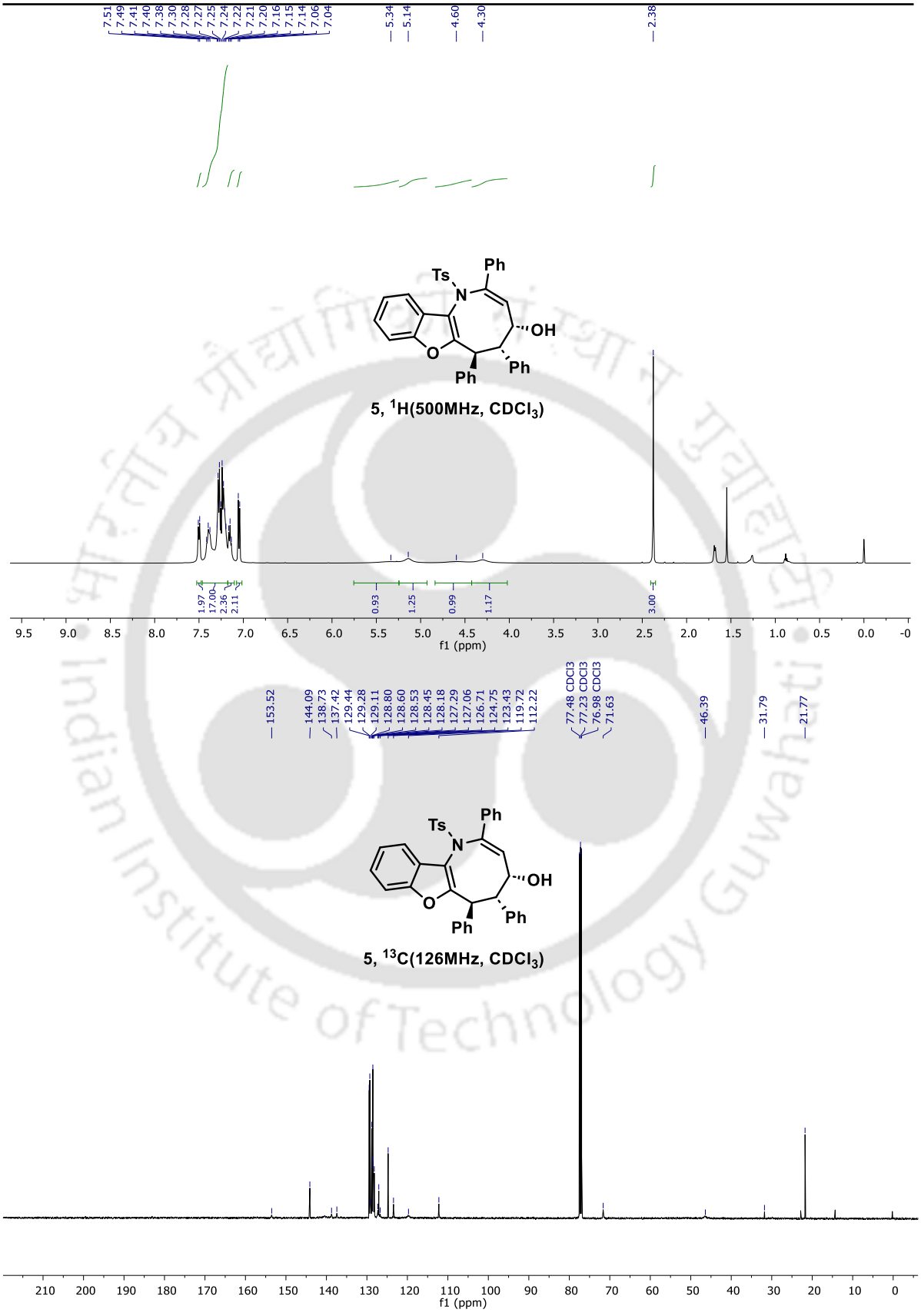

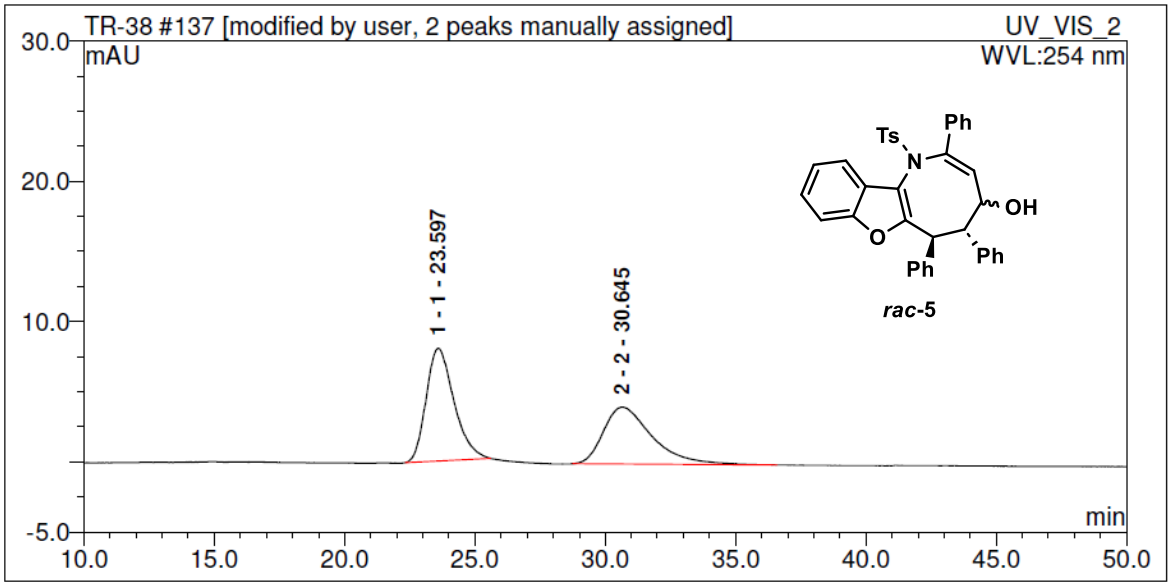

	Peak Name	Ret.Time (detected) min	Area mAU*min	Rel.Area(ident.) %	Height mAU	Amount
1	1	23.60	9.915024	53.11033727	8.01853	n.a.
2	2	30.65	8.754	46.88966273	4.054	n.a.

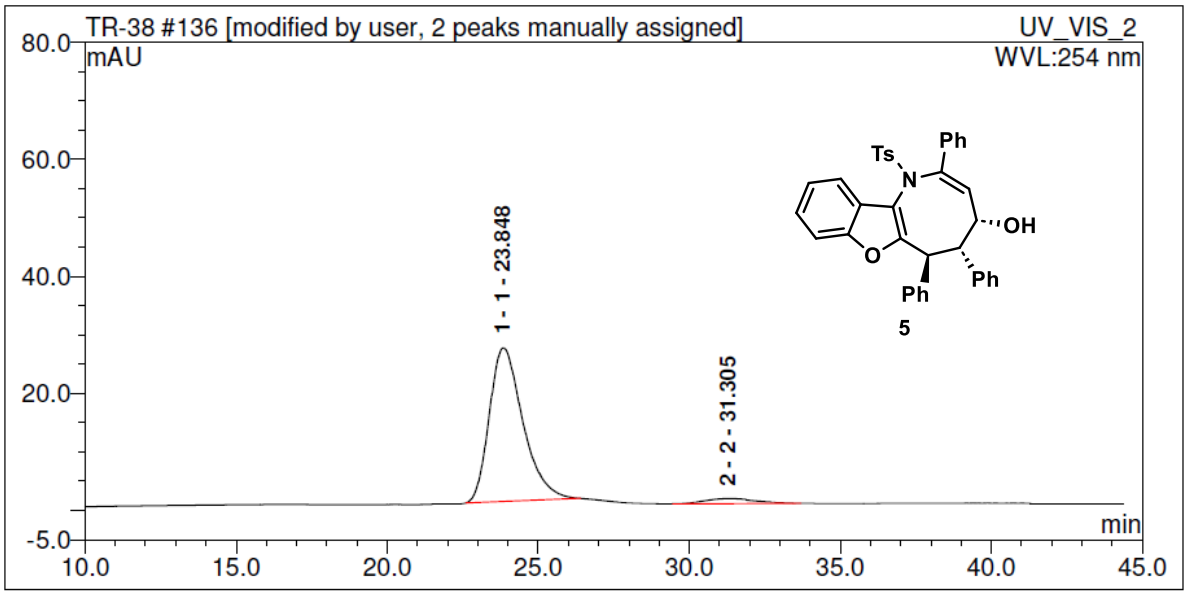

	Peak Name	Ret.Time (detected) min	Area mAU*min	Rel.Area(ident.) %	Height mAU	Amount
1	1	23.85	33.87526	95.4346562	26.25407	n.a.
2	2	31.31	1.621	4.565343802	0.865	n.a.

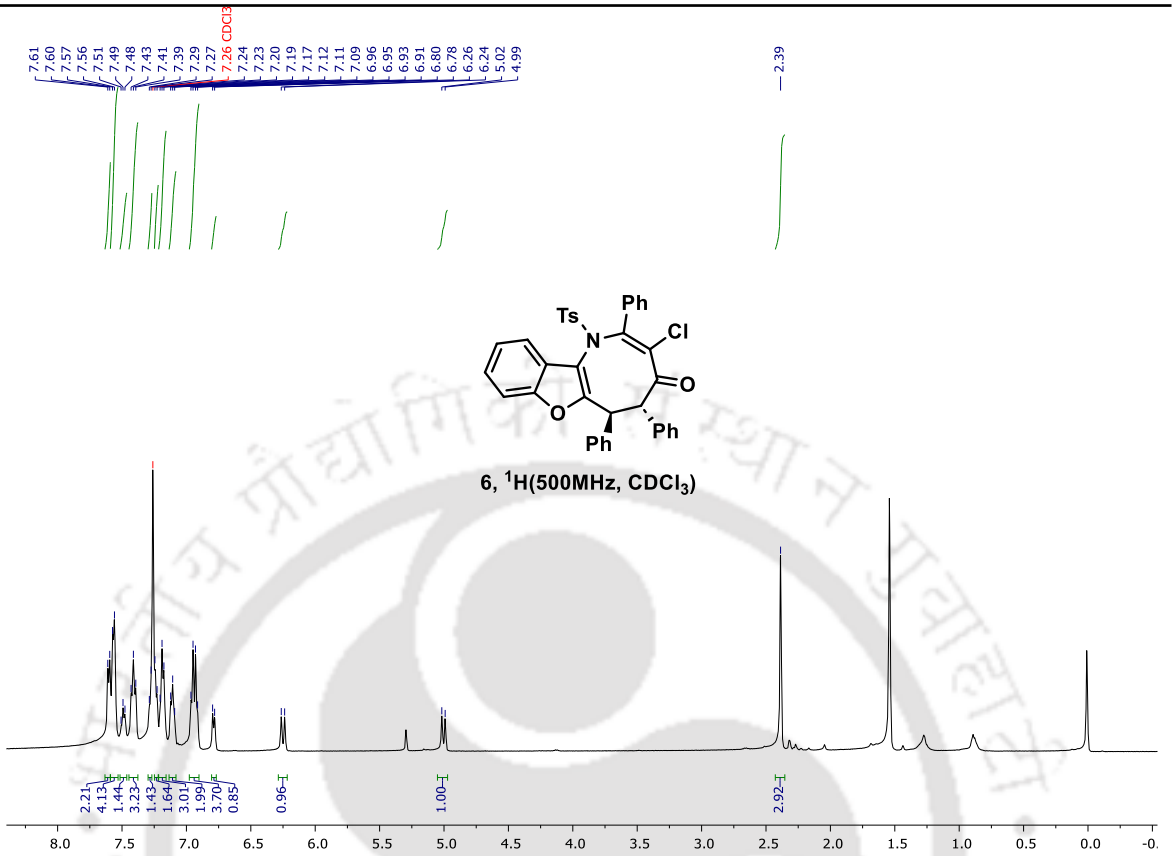

6, ^{1}H(500MHz, $CDCl_3$)

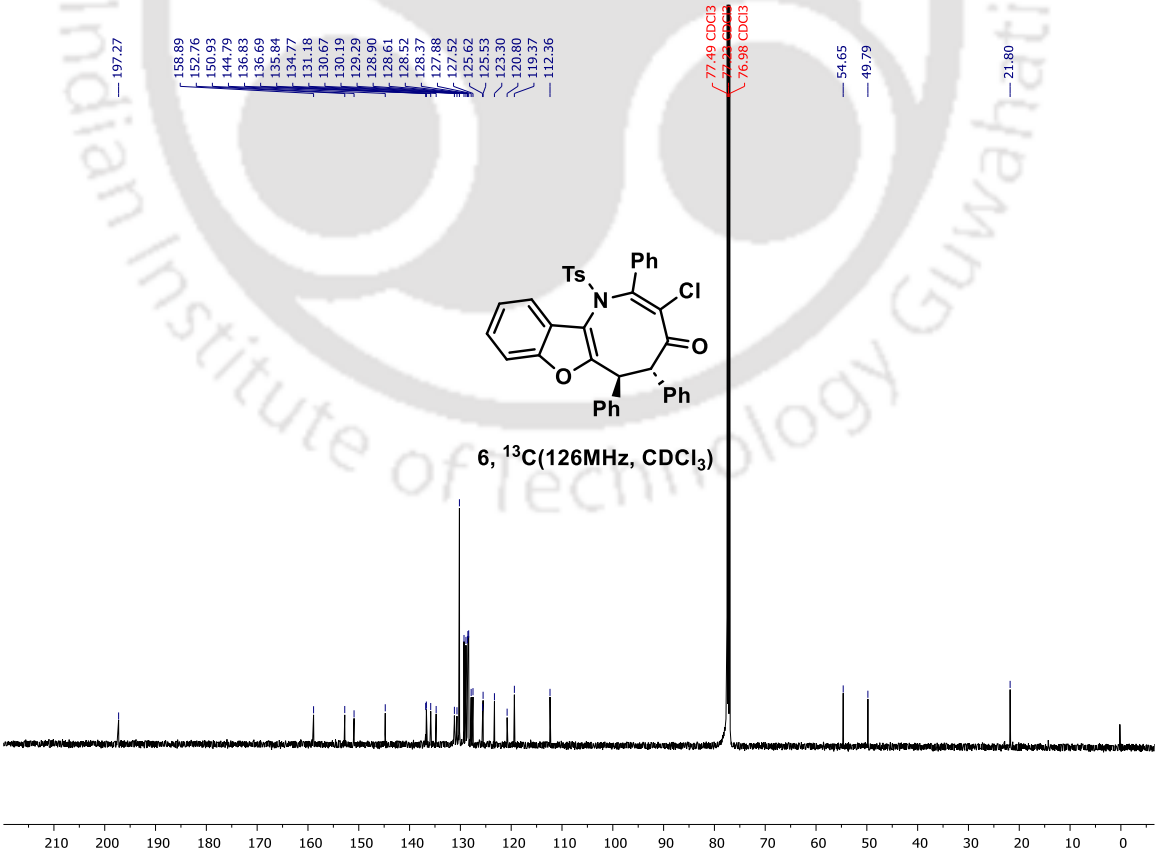

6, ^{13}C(126MHz, $CDCl_3$)

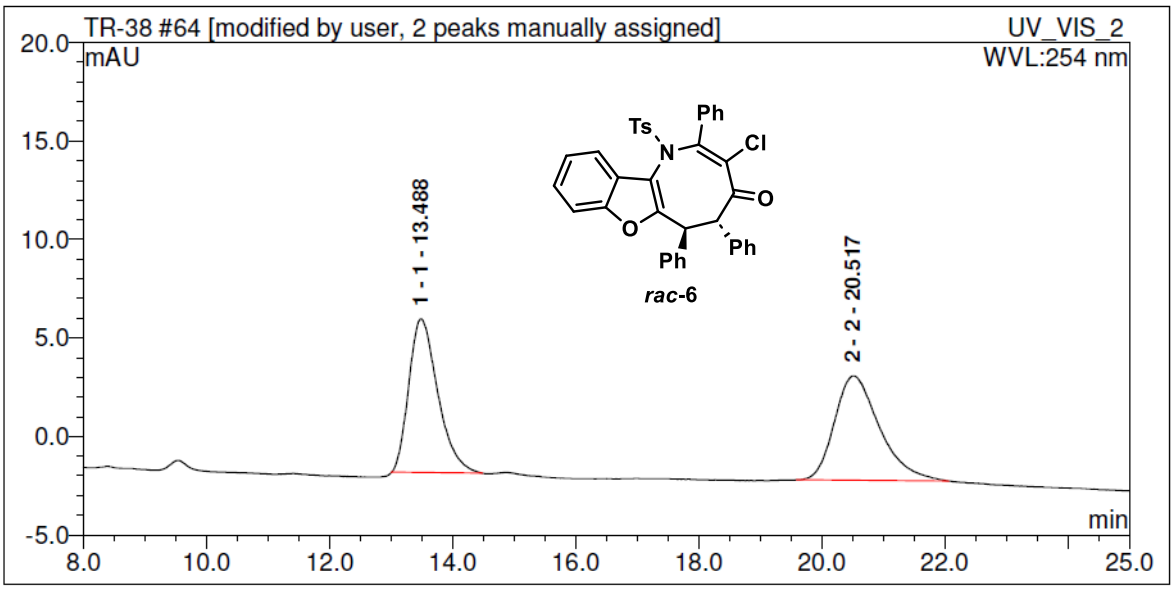

	Peak Name	Ret.Time (detected) min	Area mAU*min	Rel.Area(ident.) %	Height mAU	Amount
1	1	13.49	4.259287	48.69296571	7.80147	n.a.
2	2	20.52	4.488	51.30703429	5.293	n.a.

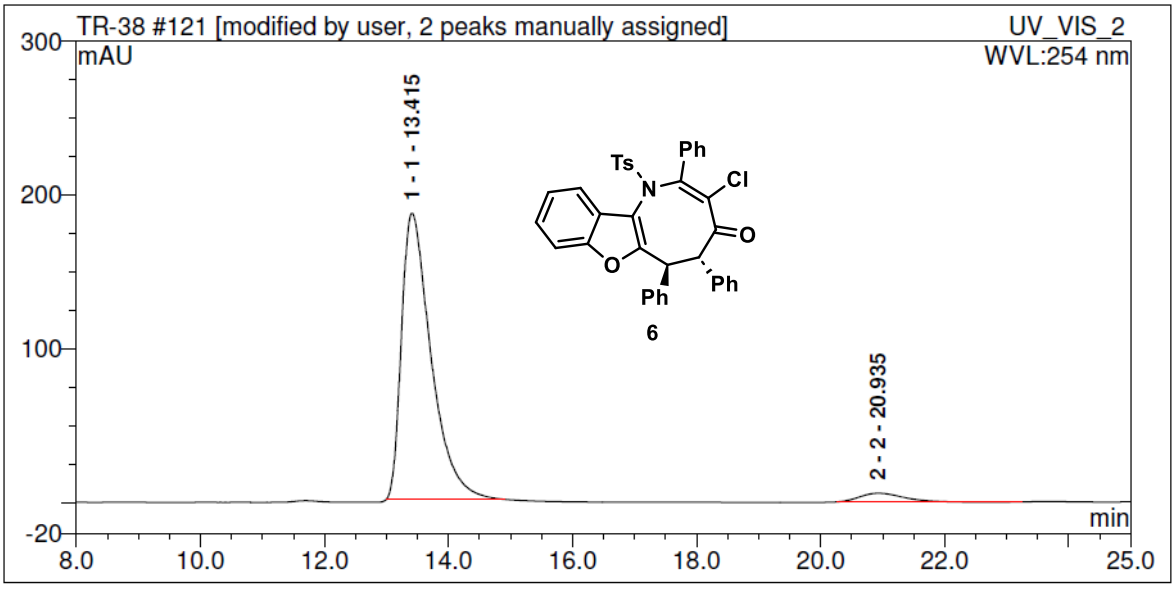

	Peak Name	Ret.Time (detected) min	Area mAU*min	Rel.Area(ident.) %	Height mAU	Amount
1	1	13.42	102.5229	95.96243862	185.8448	n.a.
2	2	20.94	4.314	4.037561376	5.571	n.a.

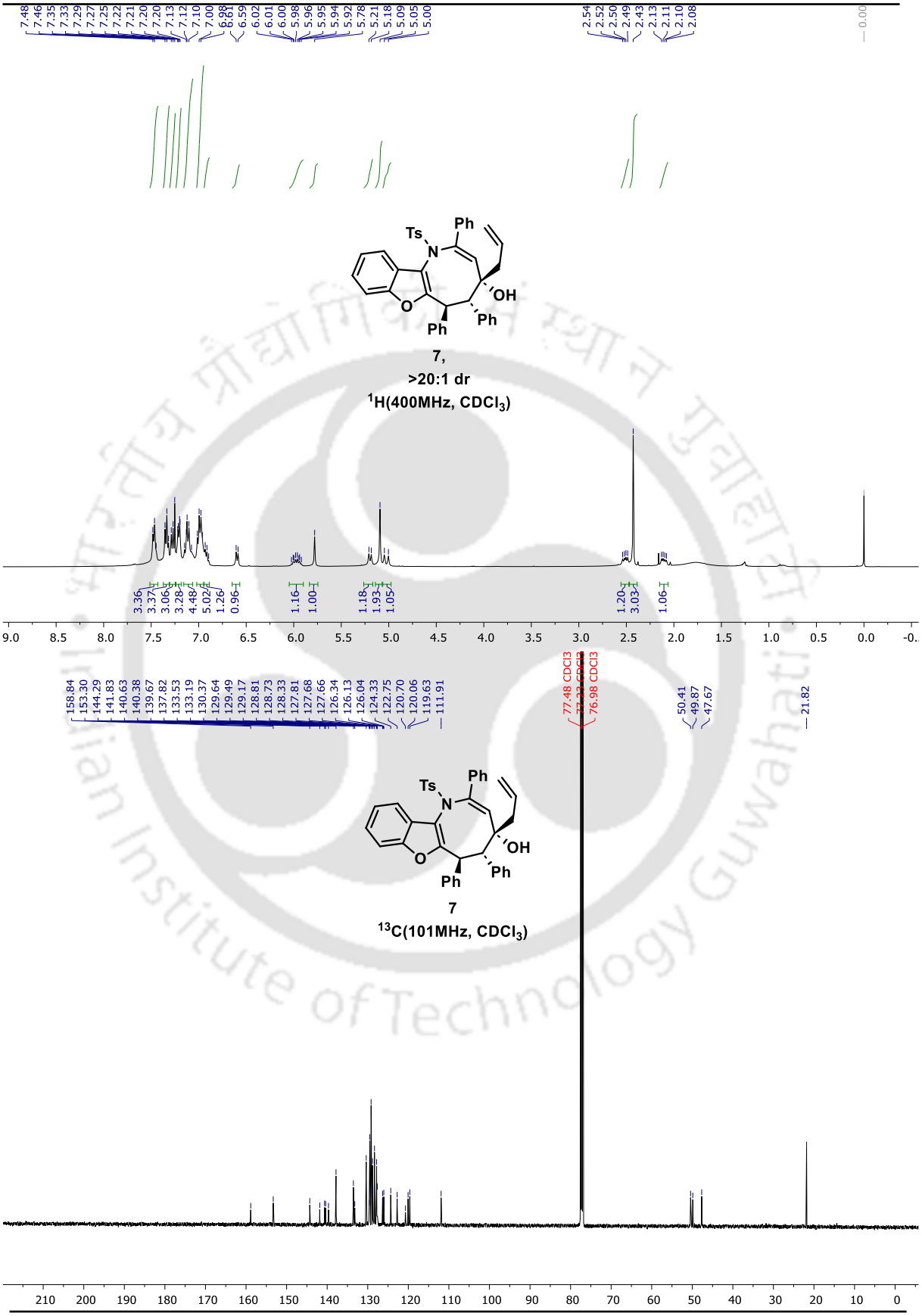

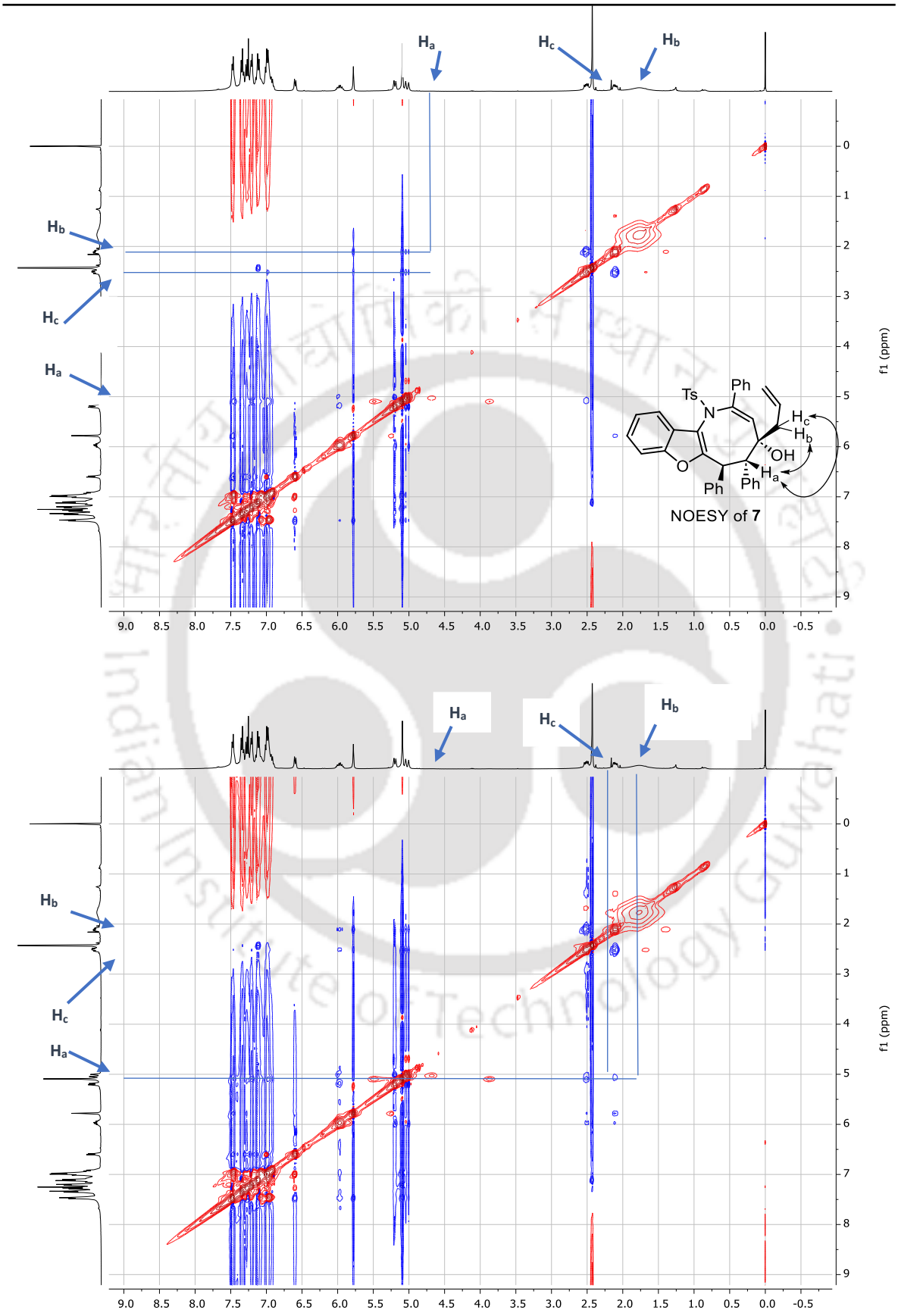

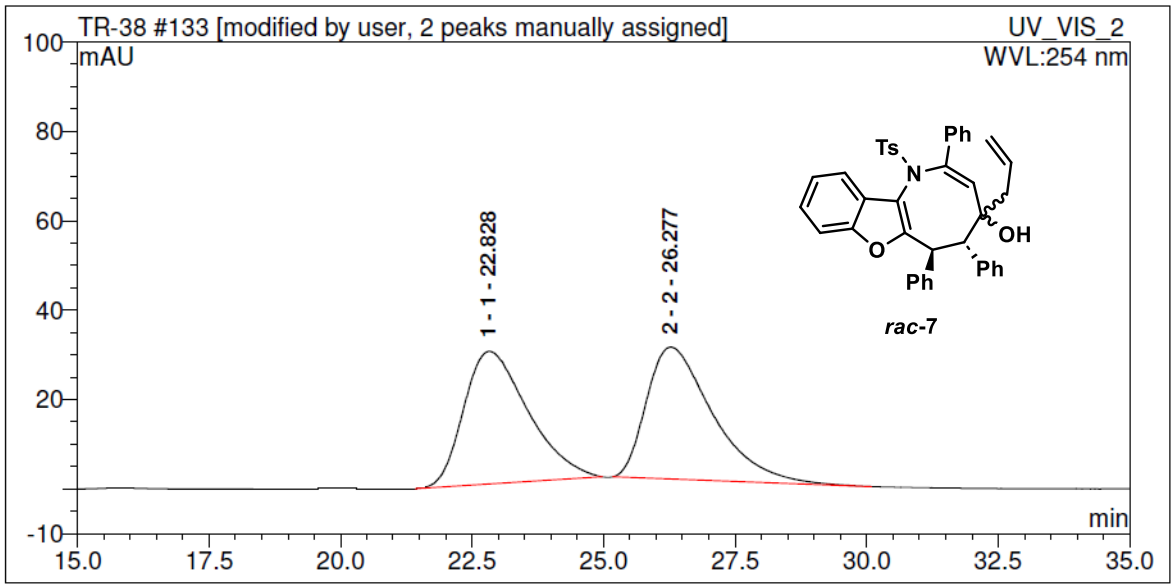

Peak Name	Ret.Time (detected) min	Area mAU*min	Rel.Area(ident.) %	Height mAU	Amount
1 1	22.83	41.96408	49.29883068	29.65025	n.a.
2 2	26.28	43.158	50.70116932	29.517	n.a.

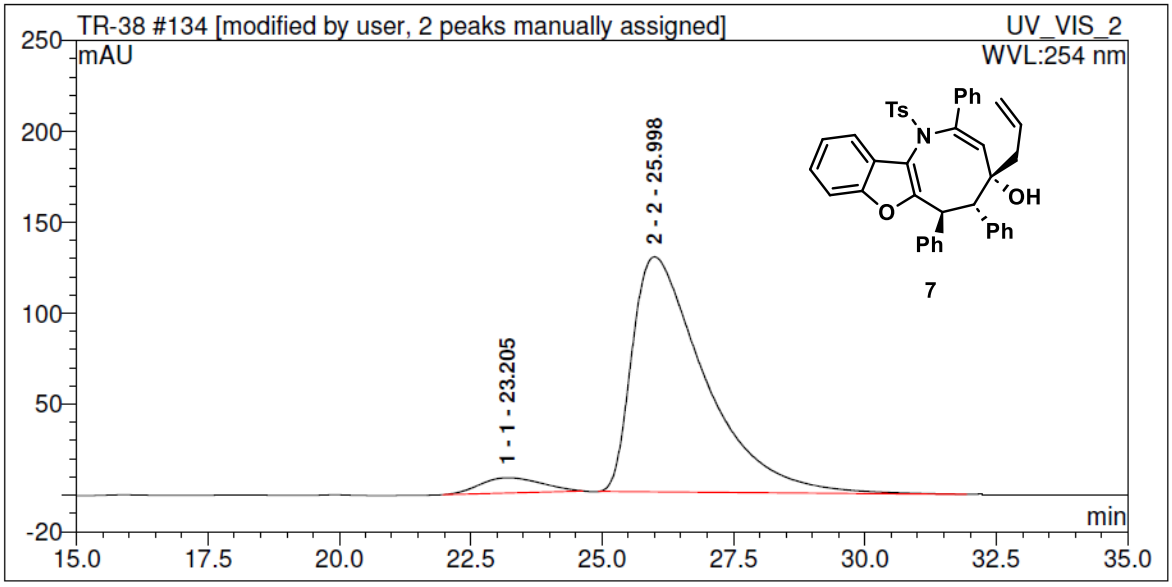

Peak Name	Ret.Time (detected) min	Area mAU*min	Rel.Area(ident.) %	Height mAU	Amount
1 1	23.21	11.29338	5.13931689	8.38958	n.a.
2 2	26.00	208.451	94.86068311	129.256	n.a.

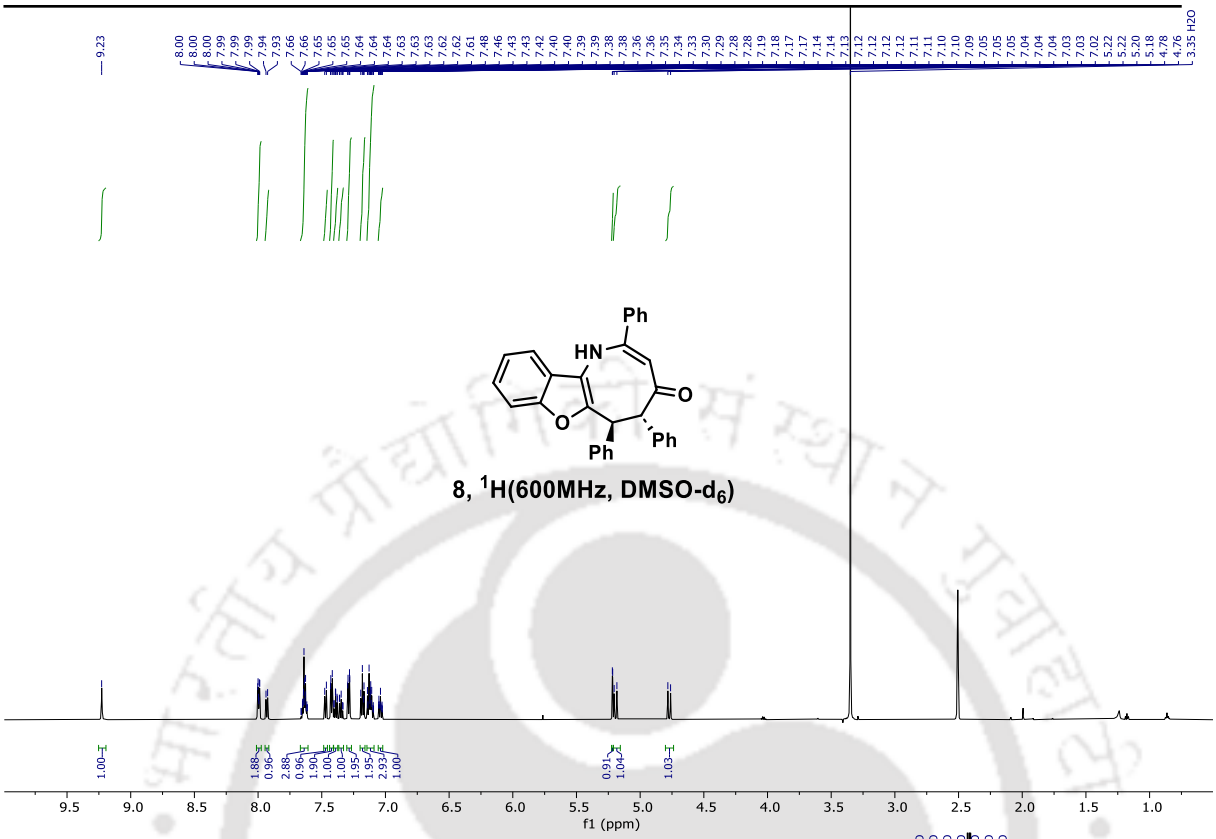

8, ^{1}H(600MHz, DMSO-d_6)

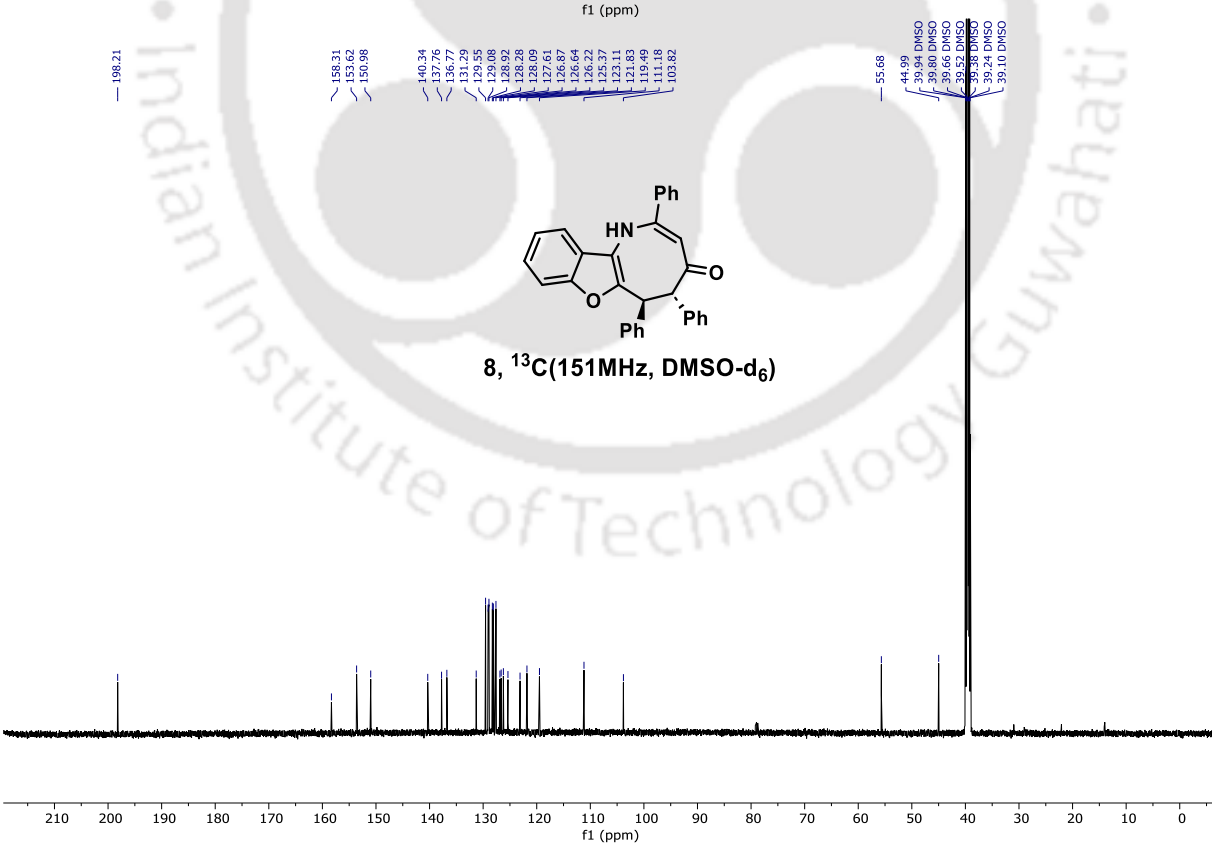

8, ^{13}C(151MHz, DMSO-d_6)

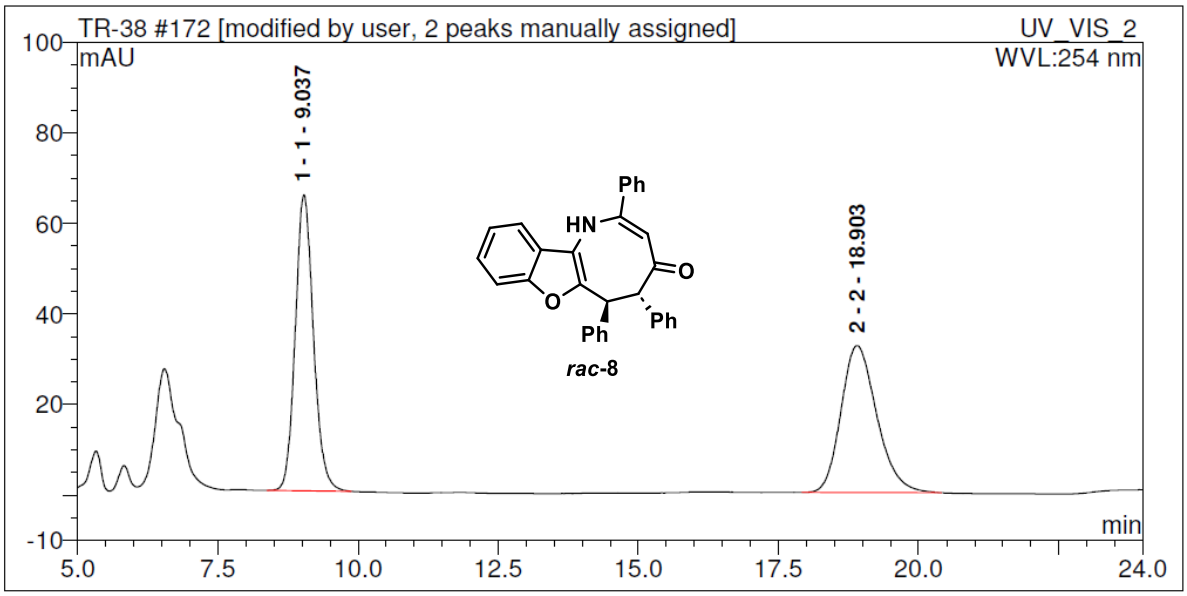

	Peak Name	Ret.Time (detected) min	Area mAU*min	Rel.Area(ident.) %	Height mAU	Amount
1	1	9.04	24.60834	50.57557064	65.36341	n.a.
2	2	18.90	24.048	49.42442936	32.472	n.a.

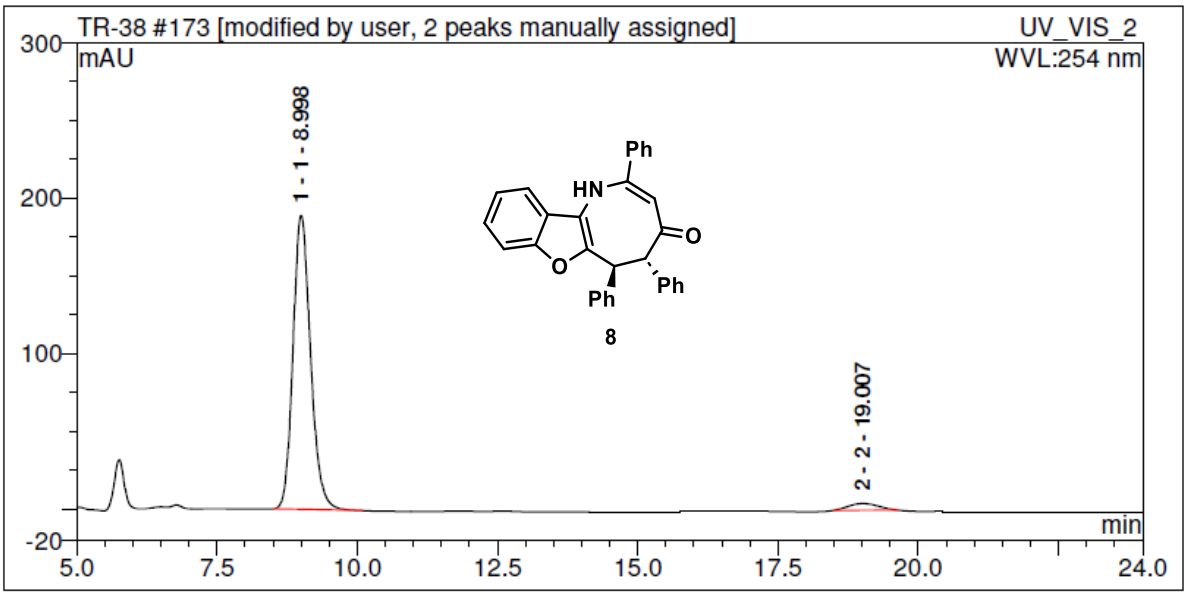

	Peak Name	Ret.Time (detected) min	Area mAU*min	Rel.Area(ident.) %	Height mAU	Amount
1	1	9.00	68.65999	96.23084124	188.926	n.a.
2	2	19.01	2.689	3.769158756	4.386	n.a.

2.13. References:

1. R. S. Doerksen, C. C. Meyer and M. J. Krische, *Angew. Chem. Int. Ed.*, **2019**, *58*, 14055; (b) A. H. Hoveyda, Y. Zhou, Y. Shi, M. K. Brown, H. Wu and S. Torker, *Angew. Chem. Int. Ed.*, **2020**, *59*, 21304; (c) S. Rej, Y. Ano and N. Chatani, *Chem. Rev*., **2020**, *120*, 1788.
2. For selected reviews, see: (a) L. C. Miller and R. Sarpong, *Chem. Soc. Rev*., **2011**, *40*, 4550; (b) J. Mahatthananchai, A. M. Dumas and J. W. Bode, *Angew. Chem. Int. Ed.*, **2012**, *51*, 10954; (c) G. Zhan, W. Du and Y.-C. Chen, *Chem. Soc. Rev*., **2017**, *46*, 1675; (d) L. Lin and X. Feng, *Chem.–Eur. J*., **2017**, *23*, 6464; (e) Y.-C. Lee, K. Kumar and H. Waldmann, *Angew. Chem. Int. Ed.*, **2018**, *57*, 5212; (f) L. Li, Z. Chen, X. Zhang and Y. Jia, *Chem. Rev*., **2018**, *118*, 3752; (g) I. P. Beletskaya, C. N´ajera and M. Yus, *Chem. Rev*., **2018**, *118*, 5080; (h) M. Viji, S. Lanka, J. Sim, C. Jung, H. Lee, M. Vishwanath and J.-K. Jung, *Catalysis*, **2021**, *11*, 1013.
3. For selected examples, see: (a) X. Tian, C. Cassani, Y. Liu, A. Moran, A. Urakawa, P. Galzerano, E. Arceo and P. Melchiorre, *J. Am. Chem. Soc*., **2011**, *133*, 17934; (b) H. Shang, Y. Wang, Y. Tian, J. Feng and Y. Tang, *Angew. Chem. Int. Ed.*, **2014**, *53*, 5662; (c) J.-Y. Liao, P.-L. Shao and Y. Zhao, *J. Am. Chem. Soc*., **2015**, 137, 628; (d) W. Du, Q. Gu, Z. Li and D. Yang, *J. Am. Chem. Soc*., **2015**, *137*, 1130; (e) H. V. Adcock, E. Chatzopoulou and P. W. Davies, *Angew. Chem. Int. Ed.*, **2015**, *54*, 15525; (f) L. Næsborg, K. S. Halskov, F. Tur, S. M. N. Mønsted and K. A. Jørgensen, *Angew. Chem. Int. Ed.*, **2015**, *54*, 10193; (g) T. Hashimoto, H. Nakatsu and K. Maruoka, *Angew. Chem. Int. Ed.*, **2015**, *54*, 4617; (h) G. Zhan, M.-L. Shi, Q. He, W.-J. Lin, Q. Ouyang, W. Du and Y.-C. Chen, *Angew. Chem. Int. Ed.*, **2016**, *55*, 2147; (i) J.-J. Feng, T.-Y. Lin, C.-Z. Zhu, H. Wang, H.-H. Wu and J. Zhang, *J. Am. Chem. Soc*., **2016**, *138*, 2178; (j) Q.-Q. Cheng, J. Yedoyan, H. Arman and M. P. Doyle, *J. Am. Chem. Soc*., **2016**, *138*, 44; (k) Q.-Q. Cheng, M. Lankelma, D. Wherritt, H. Arman and M. P. Doyle, *J. Am. Chem. Soc*., **2017**, *139*, 9839; (l) L. Wang, S. Li, M. Blgmel, R. Puttreddy, A. Peuronen, K. Rissanen and D. Enders, *Angew. Chem. Int. Ed.*, **2017**, *56*, 8516; (m) Y. Deng, L. A. Massey, Y. A. Rodriguez N´u˜nez, H. Arman, M. P. Doyle, *Angew. Chem. Int. Ed.,* **2017**, *56*, 12292; (n) D. Uraguchi, R. Shibazaki, N. Tanaka, K. Yamada, K. Yoshioka and T. Ooi, *Angew. Chem. Int. Ed.*, **2018**, *57*, 8927; (o) Z. Liu, P. Sivaguru, G. Zanoni, E. A. Anderson and X. Bi, *Angew. Chem. Int. Ed.*, **2018**, *57*, 8927; (p) S. Wei, L. Yin, S. R. Wang and Y. Tang, *Org. Lett*., **2019**, *21*, 1458; (q) Y.-H. Wang, J.-S. Tian, P.-W. Tan, Q. Cao, X.-X. Zhang, Z.-Y. Cao, F. Zhou, X. Wang and J. Zhou, *Angew. Chem. Int. Ed.*, **2020**, *59*, 1634; (r) H.-K. Liu, S. R. Wang, X.-Y. Song, L.-P. Zhao, L. Wang and Y. Tang, *Angew. Chem. Int. Ed.*, **2019**, *58*, 4345; (s) G. Lin, Y. Zhang, H. Zeng, X. Feng, Z. Su and L. Lin, *Chem. Sci*.,

2022, *13*, 4313; (t) Q.-Z. Li, Y.-L. Guan, Q.-W. Huang, T. Qi, P. Xiang, X. Zhang, H.-J. Leng and J.-L. Li, *ACS Catal*., **2023**, *13*, 1164.

4. (a) I. Nakamura, Y. Sato, K. Takeda and M. Terada, *Chem.– Eur. J*., **2014**, *20*, 10214; (b) B. Riemer, O. Hofer and H. Greger, *Phytochemistry*, **1997**, *45*, 337; (c) Y. Shiono, K. Akiyama and H. Hayashi, *Biosci. Biotechnol, Biochem*., **2000**, *64*, 1519; (d) K. M. George, M. Frantz, K. BravoAltamirano, C. R. LaValle, M. Tandon, S. Leimgruber, E. R. Sharlow, J. S. Lazo, Q. J. Wang and P. Wipf, *Pharmaceutics*, **2011**, *3*, 186; (e) F. Li, J. E. Folk, K. Cheng, M. Kurimura, J. A. Deck, J. R. Deschamps, R. B. Rothman, C. M. Dersch, A. E. Jacobson and K. C. Rice, *Bioorg. Med. Chem*., **2011**, *19*, 4330.
5. (a) P. Chen, J. Wang, K. Liu and C. Li, *J. Org. Chem*., **2008**, *73*, 339; (b) Q.-M. Li, J.-G. Luo, Y.-M. Zhang, Z.-R. Li, X.-B. Wang, M.-H. Yang, J. Luo, H.-B. Sun, Y.-J. Chen and L.-Y. Kong, *Chem.–Eur. J*., **2015**, *21*, 13206; (c) Q. Luo, X.-Y. Wei, J. Yan, J.-F. Luo, R. Liang, Z.-C. Tu and Y.-X. Cheng, *J. Nat. Prod*., **2017**, *80*, 61.
6. S. Brandau, E. Maerten and K. A. Jørgensen, *J. Am. Chem. Soc*., **2006**, *128*, 14986.
7. Y. Zhu, X. H. Chen, M. S. Xie, S. X. Dong, Z. Qiao, L. L. Lin, X. H. Liu and X. M. Feng, *Chem.–Eur. J*., **2010**, *16*, 11963.
8. W. Luo, Z. Sun, E. H. N. Fernando, V. N. Nesterov, T. R. Cundari and H. Wang, *Chem. Sci.*, **2020**, *11*, 9386.
9. D.-S. Ji, H. Liang, K.-X. Yang, Z.-T. Feng, Y.-C. Luo, G.-Q. Xu, Y. Gu and P.-F. Xu, *Chem. Sci*., **2022**, *13*, 1801.
10. J. Chen, P. Jia and Y. Huang, *Org. Lett*., **2018**, *20*, 6715.
11. B. Cheng, H. Li, X. Zhu, X. Zhang, Y. He, H. Sun, T. Wang and H. Zhai, *Chem. Commun*., **2021**, *57*, 7701.
12. W. Zheng, W. Yao, N. Ullah, Y. Lu, *Angew. Chem. Int. Ed*., **2017**, *56*, 14222.
13. X. Liu, K. Wang, Y. Liu, C. Li, *Chem. Eur. J.*, **2021**, *27*, 735.
14. S. Zhang, X. Yu, J. Pan, C. Jiang, H. Zhanga, T. Wang, *Org. Chem. Front*., **2019**, *6*, 3799.
15. K. Verma, I. M. Taily, P. Banerjee, *Org. Biomol. Chem*., **2019**, *17*, 8149.
16. For selected recent reports, see: (a) J. Masson-Makdissi, L. Prieto, X. Abel-Snape, M. Lautens, *Angew. Chem. Int. Ed*., **2021**, *60*, 16932; (b) V. Corti, R. Riccioli, A. Martinelli, S. Sandri, M. Fochi. L. Bernardi, *Chem. Sci*., **2021**, *12*, 10233; (c) C. Portolani, G. Centoze, S. Luciani, A. Pellegrini, P. Righi, A. Mazzanti, A. Ciogli, A. Sorato, G. Bencivenni, *Angew. Chem. Int. Ed*., **2022**, *61*, e202209895; (d) X. Chang, X. Cheng, X.-T. Liu, C. Fu, W.-Y. Wang, C.-J. Wang, *Angew. Chem. Int. Ed*., **2022**, *61*, e202206517; (e) J.-H. Xie, Y.-M. Hou, Z. Feng, S.-L. You, *Angew. Chem. Int. Ed*., **2023**, *62*, e202216396.

17. For selected examples, see: (a) Z.-Q. Rong, M. Wang, C. H. E Chow, Y. Zhao, *Chem. Eur. J.*, **2016**, *22*, 9483; (b) Z-Q. Rong, L.-C. Yang, S. Liu, Z. Yu, Y.-N. Wang, Z. Y. Tan, R.-Z. Huang, Y. Lan, Y. Zhao, *J. Am. Chem. Soc*., 2017, *139*, 15304; (c) K.-Q. Chen, Z.-H. Gao, S. Ye, *Org. Chem. Front*., **2019**, *6*, 405; (d) B. M. Trost, Z. Zuo, *Angew. Chem. Int. Ed*., **2021**, *60*, 5806.
18. For a review, see: L. Wang, H. Zhu, T. Peng, D. Yang, *Org. Biomol. Chem*., **2021**, *19*, 2110.
19. (a) D. B. Ramachary, C. Venkaiah and P. M. Krishna, *Chem. Commun*., **2012**, *48*, 2252; (b) D. B. Ramachary, C. Venkaiah and R. Madhavachary, *Org. Lett*., **2013**, *15*, 3042; (c) H. M. Carder, Y. Wang, A. E. Wendlandt, *J. Am. Chem. Soc*. **2022**, *144*, 11870; (d) C. Che, Y.-N. Lu, C.-J. Wang, *J. Am. Chem. Soc*. **2023**, *145*, 2779.
20. For reviews, see: a) S. J. Connon, *Chem. Commun*., **2008**, 2499; (b) W.-Y. Siau, J. Wang, *Catal. Sci. Technol*. **2011**, *1*, 1298.
21. (a) R. Löser, M. Chlupacova, A. Marecek, V. Opletalova, M. Gütschow, *Helv. Chim. Acta*, **2004**, *87*, 2597; (b) M. Morimoto, H. Fukumoto, T. Nozoe, A. Hagiwara, K. Komai, J. Agric, *Food Chem*. **2007**, *55*, 700; (c) Z-Q. Rong, M. Wang, C. H. E. Chow, Y. Zhao, *Chem. Eur. J.* **2016**, *22*, 9483.
22. (a) J. Xie, P. Xu, Y. Zhu, J. Wang, W-C. C. Lee, X. P. Zhang; *J. Am. Chem. Soc.* **2021**, *143*, 11670; (b) H. Wang, J. R. Denton, H. M. L. Davies, *Org. Lett*. **2011**, *13*, 4316; (c) Y. Sadamitsu, K. Komatsuki, K. Saito, T. Yamada, *Org. Lett*. **2017**, *19*, 3191.
23. (a) M. S. Manna, V. Kumar, S. Mukherjee, *Chem. Commun*. **2012**, *48*, 5193. (b) K. Bera, I. N. N. Namboothiri, *Org. Biomol. Chem*. **2014**, *12*, 6425.

Chapter 3

Organocatalytic Regio- and Enantioselective Friedel-Crafts Alkylation of N-Arylanilines with Aurone-Derived Azadienes: Access to Benzofuran Embedded Triarylmethanes

Abstract: Herein we disclose a catalytic asymmetric Friedel-Crafts alkylation of N-arylanilines with azadienes for the synthesis of benzofuran containing triarylmethanes. An easily available chiral phosphoric acid, TRIP, was found to be effective for this reaction. The triarylmethanes with benzofuran motif were obtained in moderate yields with high regio- and good to high enantioselectivities. The scope of the reaction was broad and few synthetic transformations have been demonstrated.

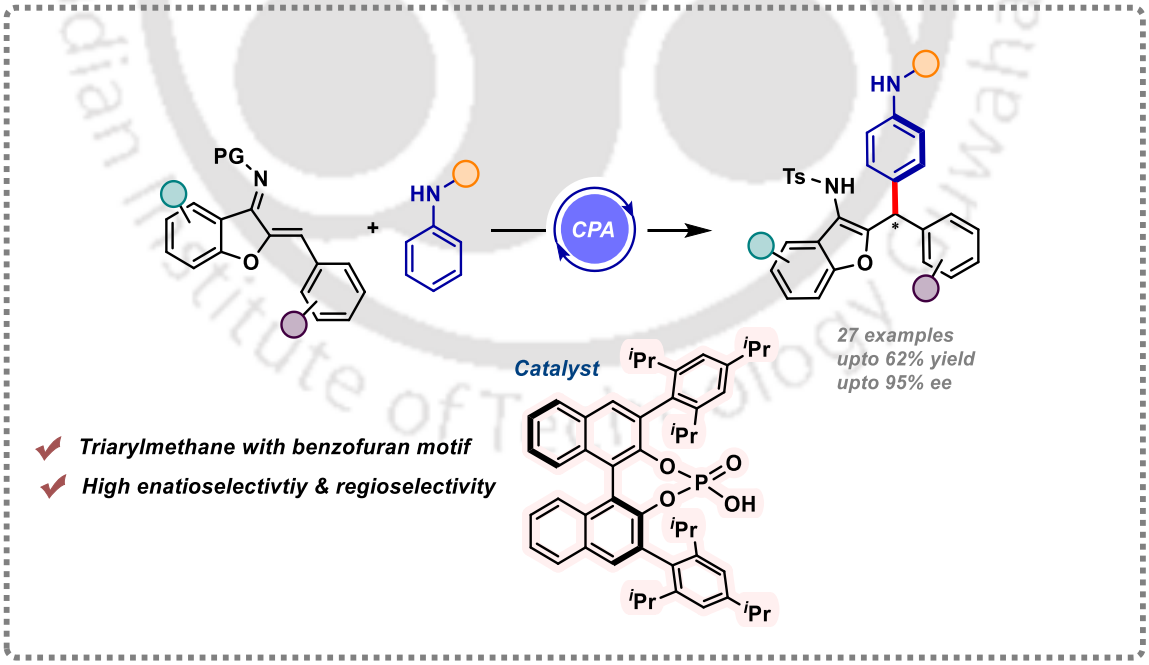

3.1. Introduction:

Aniline and its derivatives are useful compounds in synthetic chemistry due to their wide applications in pharmaceutical agents, fluorescent dyes, and functional materials.[1] Consequently, the regio- and enantioselective functionalization of anilines has drawn attention to organic chemists and during the past few decades; and considerable efforts have been made in this intensely researched area.[2] The efficient functionalization of anilines using metal-catalyzed C-H functionalization was one of them. However, the majority of studies on the C-H functionalization of anilines have depended on the nitrogen atom's directing group to produce the ortho-functionalized products (Fig. 1).[3] Asymmetric variants are also exceedingly challenging to implement. Related study indicates that the catalytic asymmetric version of the relevant distant *para* C-H functionalization, in particular, is still a difficult task for the synthetic community to complete. Only a few examples of catalytic asymmetric aromatic *para* C-H functionalization of aniline derivatives have been successfully accomplished in recent years using Friedel-Crafts procedures.[4] Also a few enantioselective Friedel-Crafts alkylations of anilines using Lewis acid or Brønsted acid catalysis have been successful.[8-15] But, in the asymmetric reactions, only a small number of *N,N*-disubstituted anilines could be used, severely limiting the variety of products. Enantioselective and chemoselective functionalization of N-monosubstituted anilines is often a very difficult job due to the increased nucleophilicity of the aniline NH bond (Fig. 1).[5] Therefore, it is very important and in high demand to create a direct method for *para*-C-H functionalization of anilines that include the N-H bond.

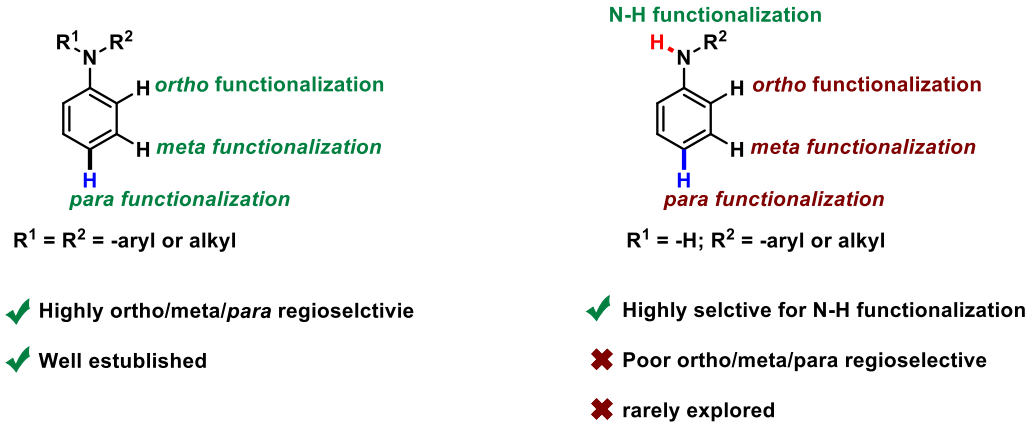

Fig. 1: Functionalization of Aniline.

Chiral triarylmethane structures are important components with a wide range of uses in organic synthesis, functional materials, pharmaceuticals, and biologically active substances. Over the past few decades, significant advancements have been made in the enantioselective

synthesis of chiral triarylmethanes,[6] however the synthesis of chiral triarylmethanes with heterocyclic motif is less explored despite such structure is present in bioactive compounds (Fig. 2).[7] Thus, we became interested to develop a catalytic asymmetric variant for the synthesis of triarylmethanes having a benzofuran motif.

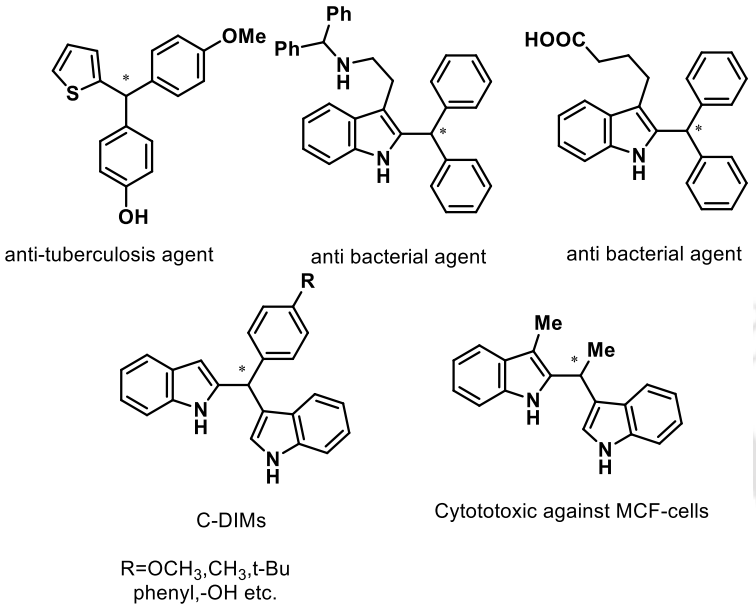

Fig. 1: Biologically active chiral triarylmethane.

3.2. Previous Study:

3.2.1. Asymmetric *para*-C-H functionalization of *N,N*-disubstituted anilines:

In 2000, Jørgensen and co-workers first reported a Friedel-Crafts *para* functionalization of *N,N*-disubstituted anilines. Under the catalytic system of chiral bisoxazoline−copper(II) complexes, *N,N*-disubstituted anilines and glyoxylate gave highly regio- and enantioselective *para* functionalized product in excellent yield and ee.[8]

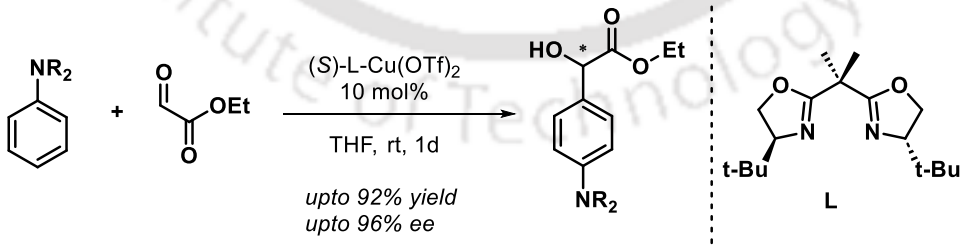

Scheme 1: First Friedel-Crafts alkylation of aniline.

MacMillan et al., later in 2002, reported a Friedel-Crafts *para* functionalization of *N,N*-disubstituted anilines with unsaturated aldehydes. With the use of iminium catalysis, they construct benzylic stereogenicity. In presence of (2*S*,5*S*)-5-benzyl-2-*tert*-

butylimidazolidinone amine catalyst anilines underwent a conjugate addition to unsaturated aldehydes to afford the products in excellent yields and ees.[9]

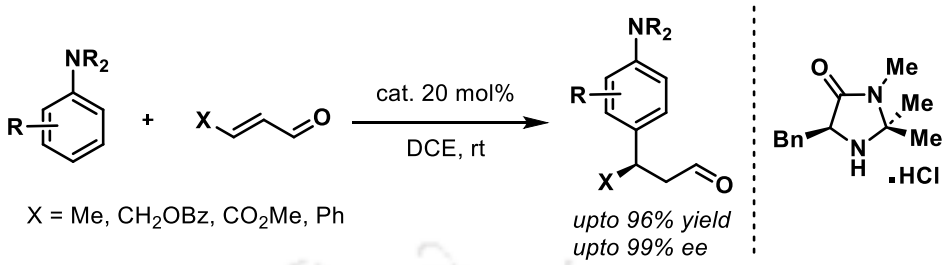

Scheme 2: *Para* C-H functionalization of *N,N*-disubstituted aniline by iminium catalysis.

In 2004, Ding and co-workers reported a chiral titanium(IV) complex catalysed asymmetric synthesis of aminomandelic acid derivatives. Catalysis of the titanium complexes of BINOL derivatives gave ethyl esters of *para*-*N,N*-dialkylaminomandelic acids with outstanding yields and high ees *via* Friedel-Crafts functionalization of *N,N*-disubstituted anilines with ethyl glyoxylate.[10]

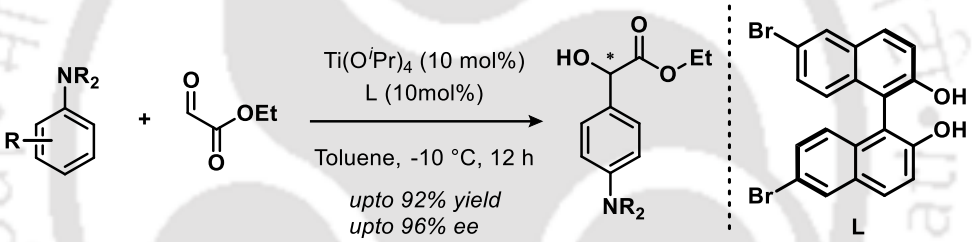

Scheme 3: *Para* C-H functionalization of *N,N*-disubstituted aniline by chiral Ti(IV)-complex.

In 2005, Leighton and co-workers explored a chiral simple strained silacycle reagent promoted Friedel-Crafts alkylation of anilines. N,N-disubstituted aniline underwent Friedel-Crafts alkylation with benzoylhydrazone of isopropyl glyoxylate in the presence of stoichiometric amount of chiral silane Lewis acid to provide chiral benzylamines in good yields and high ees.[11]

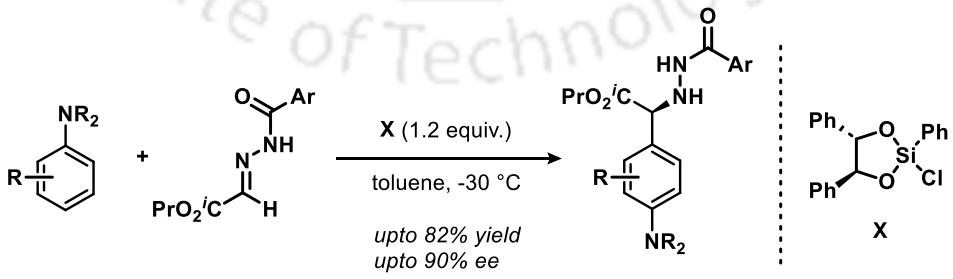

Scheme 4: Chiral silane Lewis acid mediated Friedel-Craftsalkylation of anilines.

Later, in 2014, Hu et al. explored a three component Rh(II)/chiral phosphoric acid catalyzed Friedel-Crafts reaction of *N,N*-disubstituted anilines. Under the optimized conditions, aniline, methyl phenyldiazoacetate and *N*-benzylideneaniline in the presence of both $[Rh_2(TFA)_4]$ (1 mol %) and chiral phosphoric acid (2 mol%) gave *para*-C-H functionalized aniline bearing α,α-diaryl benzylic quaternary stereocenters in excellent yields, dr and ees through a metal carbene involved zwitterion intermediate.[12]

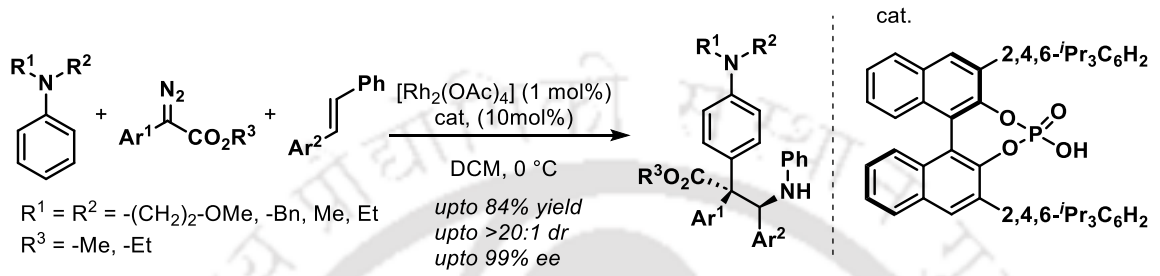

Scheme 5: Rh(II)-CPA catalyzed three component *para*-C-H alkylation of *N,N*-disubstituted aniline.

Then, Zhou et al. in 2015 reported a facile synthesis of chiral diaryl carboxylates by Friedel-Crafts alkylation of anilines. Also, in this case, a Rh(II)/chiral phosphoric acid complex gave a zwitterion intermediate with *N,N*-disubstituted anilines and methyl aryldiazoacetate to afford the target products in excellent yields and ees.[13]

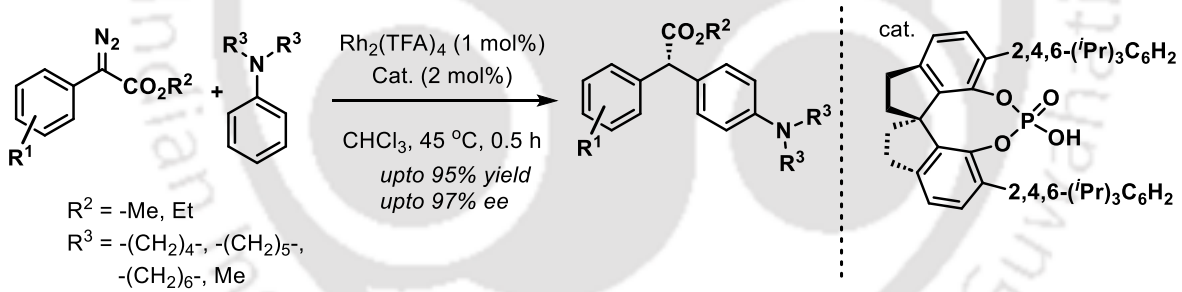

Scheme 6: Rh(II)-CPA catalyzed ara-C-H alkylation of *N,N*-disubstituted aniline.

Next, in 2018 Chen and Fan together reported rhodium/chiral ligand catalyzed ring opening reaction with *N,N*-disunstituted anilines *via* Friedel-Crafts reaction. Using $Rh(COD)_2SbF_6$ as metal catalyst and (R)-difluoroPhos as ligand, they achieved *para*-selective C-H functionalization of anilines, following asymmetric arylative ring-opening reactions of heterobicyclic alkenes with excellent yields and ees. [14]

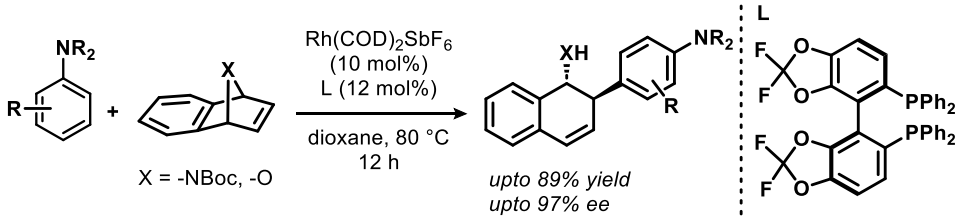

Scheme 7: Rh(II)-Phosphine ligand catalyzed *para*-C-H alkylation of aniline.

Recently, in 2021, Zhang et al. explored Co(II)/chiral PyBOX ligand catalyzed Friedel-Crafts alkylation of anilines. The method involves generation of an intermediate with base and it further reacts with N,N-disubstituted anilines in the presence of Co(II)-PyBOX complex to afford chiral quaternary canter bearing isatine derivatives in high yields and excellent ees.[15]

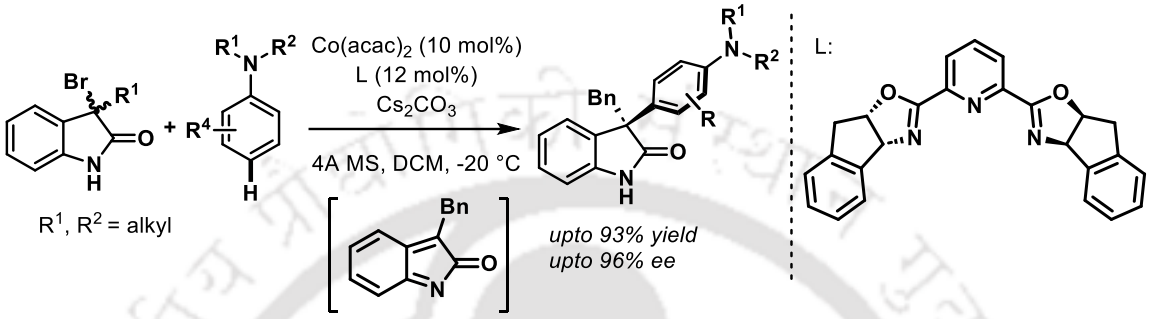

Scheme 8: Co(I)-PyBOX ligand catalyzed *para*-C-H alkylation of aniline.

3.2.2. Asymmetric *para*-C-H functionalization N-monosubstituted anilines:

In 2020, Zhang and Zhu reported the first organocatalyzed *para*-C-H functionalization of N-monosubstituted anilines. Using chiral BINOL-based phosphoric acid as the catalyst, they found that N-monosubstituted anilines undergo Friedel-Crafts reactions with isatin-derived ketimines, resulting in aryl-containing quaternary amines with excellent yields and enantioselectivities. The authors proposed a dual-hydrogen-bonding stereocontrol model involving chiral phosphoric acids and hydroxyl groups, along with a potential π–π interaction, which is responsible for the *para*-selective functionalization while disfavoring N-H functionalization of aniline.[16]

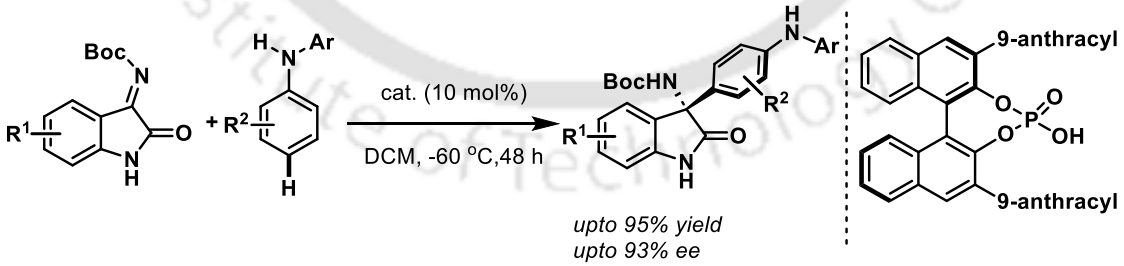

Scheme 9: Chiral phosphoric acid catalyzed *para*-C-H alkylation of N-monosubstituted aniline.

Then, in 2023, Sun and Shen explored another example of chiral phosphoric acid-catalyzed *para*-C-H functionalization of N-monosubstituted anilines to synthesize various ranges of chiral triarylamines. Under chiral phosphoric acid catalysis, N-monosubstituted aniline

performs conjugate addition to in-situ formed *o*-quinone methide to afford chiral triarylmethanes in outstanding yield and ees.[17s]

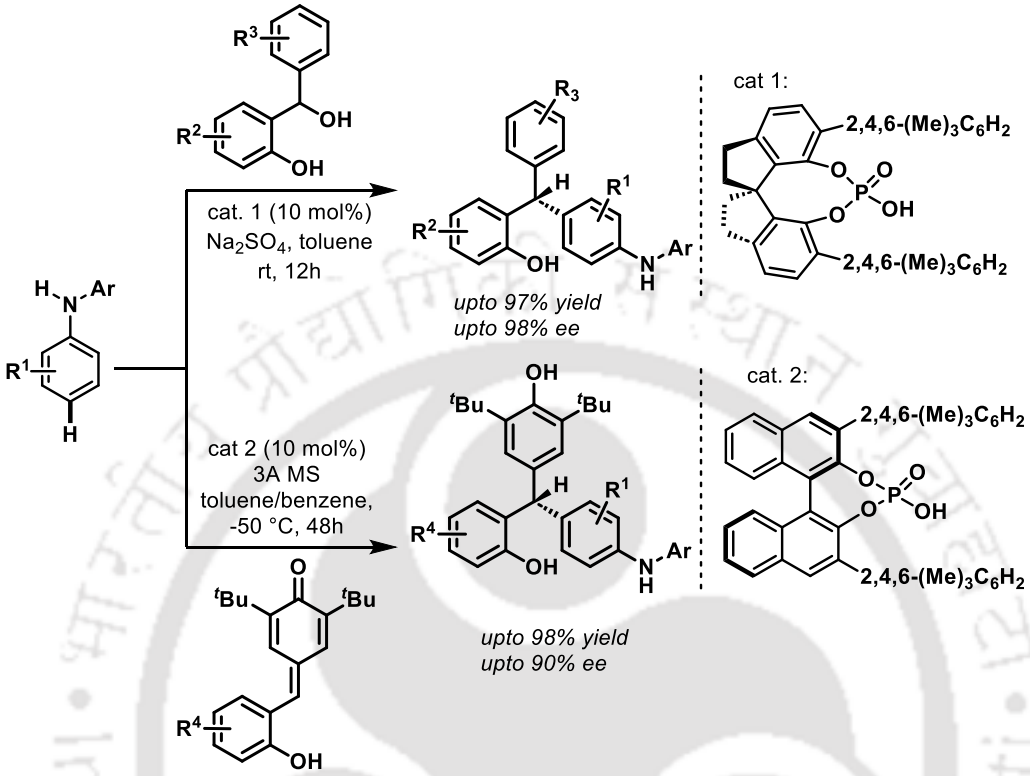

Scheme 10: Catalytic *para*-C-H alkylation of N-monosubstituted anilines with *o*-quinone methides.

3.3. Objective:

As previously, there were no reports of synthesis of triarylmethanes with N-monosubstituted anilines. We envisioned a reaction between N-monosubstituted aniline and aurone-derived azadiene[18] could deliver a benzofuran embedded chiral triarylmethane compound (Fig 3).

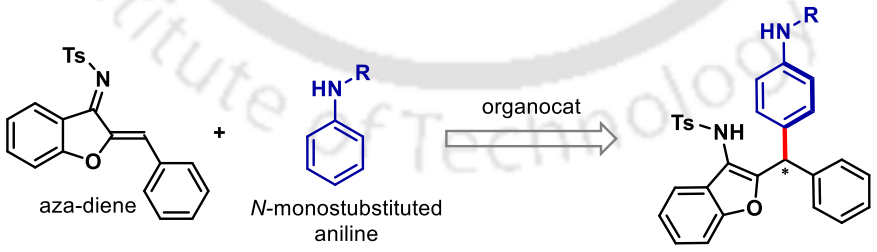

Fig. 3. Objective.

3.4. Results and discussion:

3.4.1. Catalyst, solvent and temperature optimization for synthesis of azocine:

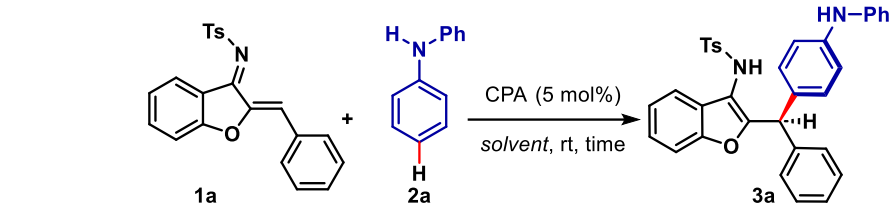

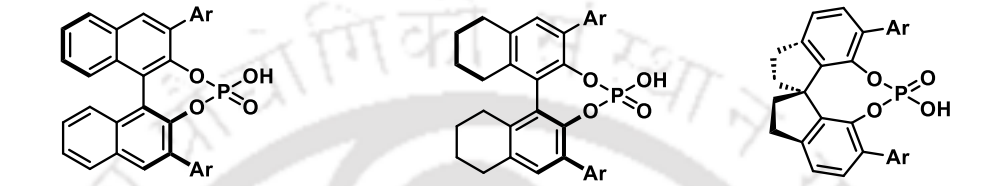

I, Ar = 1-naphthyl;
II, Ar = 2-naphthyl; **III**, Ar = 3,5-$(CF_3)_2C_6H_3$;
IV, Ar = 9-anthracenyl; **V**, Ar = 2,4,6-$(^iPr)_3C_6H_2$

VI, Ar = 2,4,6-$(^iPr)_3C_6H_2$

VII, Ar = 2,4,6-$(^iPr)_3C_6H_2$

Table 1. ***Optimization of catalysts:***

Entry[a]	Catalyst	Solvent	Time	Yield(3a)[b]	*ee*(3a)[c]
1	**I**	DCM	3h	89%	31%
2	**II**	DCM	3h	88%	22%
3	**III**	DCM	3h	90%	12%
4	**IV**	DCM	3h	95%	3%
5	**V**	DCM	3h	92%	32%
6	**VI**	DCM	3h	72%	3%
7	**VII**	DCM	3h	90%	racemic
8	**V**	Toluene	12h	88%	53%
9[d]	**V**	*o*-xylene	24h	82%	61%
10[d]	**V**	Mesitylene	24h	85%	77%
11	**V**	CCl_4	3h	92%	22%
12	**V**	Et_2O	12h	77%	22%
13	**V**	cyclohexane	5d	78%	83%
14	***V***	*n-Hexane*	*5d*	*60%*	*92%*

[a] Reactions were carried out with 0.1 mmol of **1a** with 0.11 mmol of **2a** in 1 ml solvent at rt. [b] Isolated yield after silica gel column chromatography. [c] Determined by ^{1}H NMR. [d] Determined by chiral HPLC. [e] Reaction was run at 40 °C.

To test our hypothesis, we first explored a model reaction between azadiene **1a** and diphenylamine (**2a**) in dichloromethane at room temperature with 1-naphthyl substituted phosphoric acid catalyst **I** (Table 1). Delightfully, the intended triaryl product **3a** was achieved in 89% yield with 31% ee after stirring for 3h at room temperature (Table 1, entry 1). The enantioselectivity of **3a** got slightly decreased with phosphoric acid **II** having 2-naphthyl substituents (Table 1, entry 2). Catalysts **III** and **IV** having 3,5-di trifluoromethylphenyl and 9-anthracenyl substituents respectively were not suitable for the reaction (Table 1, entries 3-4). Moderate enantioselectivity of 32% was achieved with TRIP catalyst **V** (Table 1, entry 5). Other catalysts such as H_8-TRIP and Spiro-TRIP were not suitable for the reaction (Table 1, entries 6-7). Then, various solvents were tested in an effort to increase the enantioselectivity, and the results showed promise (Table 1, entries 8-14). The enantioselectivity got increased in toluene and *o*-xylene (Table 1, entries 8-9). Also, 77% ee was detected in mesitylene (Table 1, entry 10). However, no further improvements were seen using CCl_4 and Et_2O (table 1, entries 11-12). The enantioselectivity got further improved to 83% ee in cyclohexane solvent and reaction time was increased (Table 1, entry 13). Finally, hexane turned out to be the best solvent providing 92% ee of the product **3a** though yield got slightly decreased (Table 1, entry 14).

3.4.2. Scope of the reaction:

After the ideal conditions were established, the process's scope was investigated. Initially, azadienes **1a**-**1k** having different substituents at the phenyl group were screened (Scheme 11). Initially, substitutions at the *para*-position were checked and gratifyingly positive outcomes were found. The enatioselectivity slightly dropped for *para*-^{t}butyl substituted product **3b** (Scheme 11). Halo-substitutions were also tolerated and acceptable enantioselectivity of 81% ee was achieved for compounds **3c** and **3d** having 4-fluoro and 4-chloro substitutions respectively. The enantioselectivity got improved for compound **3e** having 4-bromo substitution. Triflormethyl substituted compound **1f** also took part in the reaction to provide product **3f** in 93% ee. Then *meta*-substitutions were checked and gratifyingly the products **3g** and **3h** were obtained in high enantioselectivities. The reaction outcome did not change much with *ortho*-substitutions and products **3i** and **3j** were isolated in moderate yields and with good enantioselectivities. A 2,4-disubstituted phenyl group containing azadiene **1k** also participated in the reaction and delivered product **3k** in 89% ee. The reaction outcome did not change much

with naphthyl substituted product **3l**. When the benzofuran motif substitutions were looked at, it was found that the methoxy- and bromo-substituted azadienes **1m** and **1n**, respectively, reacted smoothly to produce products **3m** and **3n** in 84% ee and 91% ee respectively. The N-Ts group could be replaced with N-Ns group and the desired product **3o** was isolated in 85% ee.

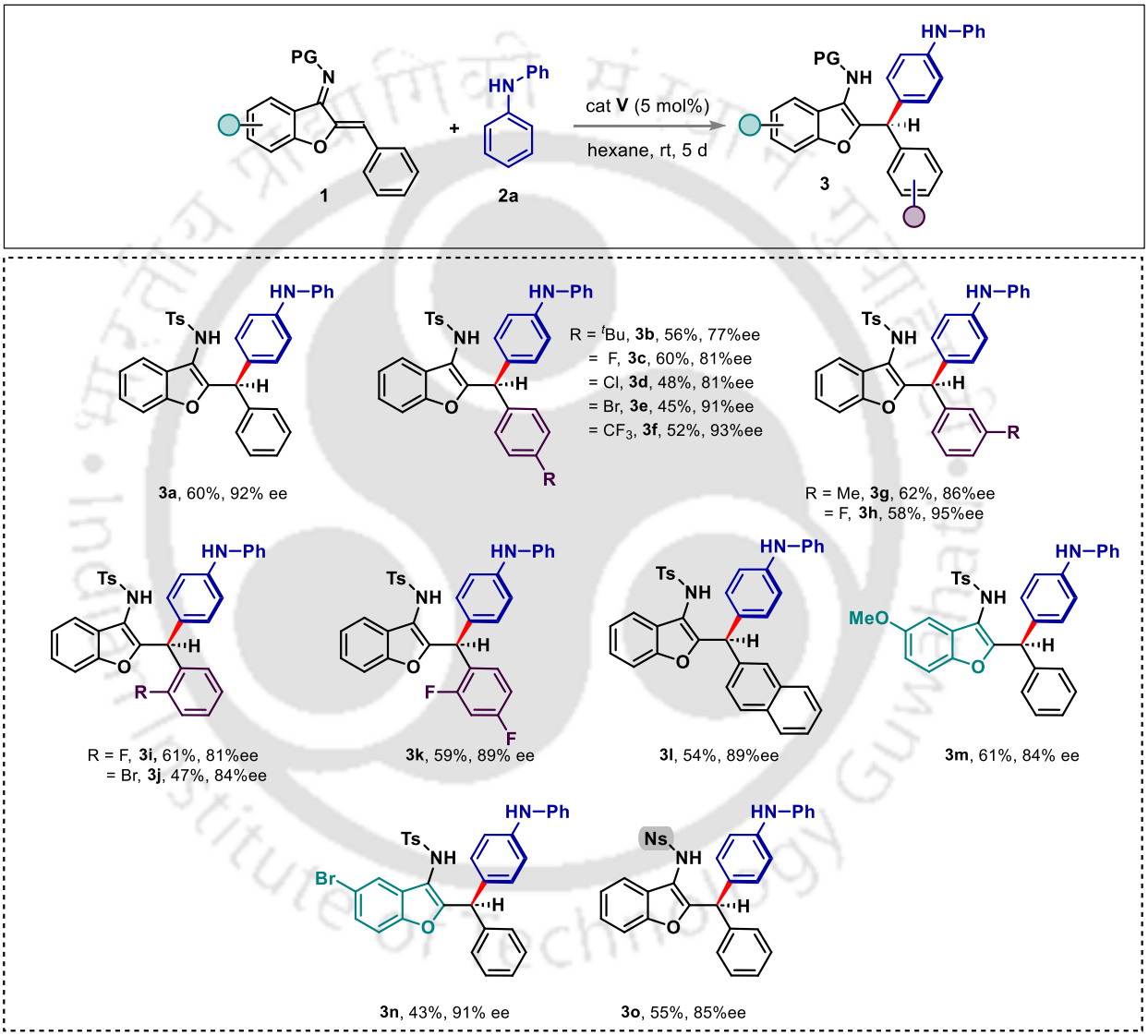

Scheme 11: Scope of 1-Azadiene.

Then diphenylamines **2** having different substitutions at one of the phenyl groups were tested in the reaction (Scheme 12). Initially, substitutions at the *para*-position were checked and gratifyingly good results were obtained for the products **3p-3t** with different electron-neutral, electron-rich, or electron-poor groups. In particular, product **3r** having trifluoromethyl

substituent was isolated with 90% ee. Then 2,4-disubstitutions were checked and delightfully the reactions progressed smoothly with **1u** and **1v** to provide **3u** and **3v** respectively in acceptable enantioselectivities. Similar outcome was observed for product **3w** having 3,4-dimethyl substitutions**.** Then amine **2x** with biphenyl substituent and amine **2y** with phenylacetylene motif were tested in the reaction**.** We were pleased to find that in both situations, good enantioselectivity of 85% was achieved.

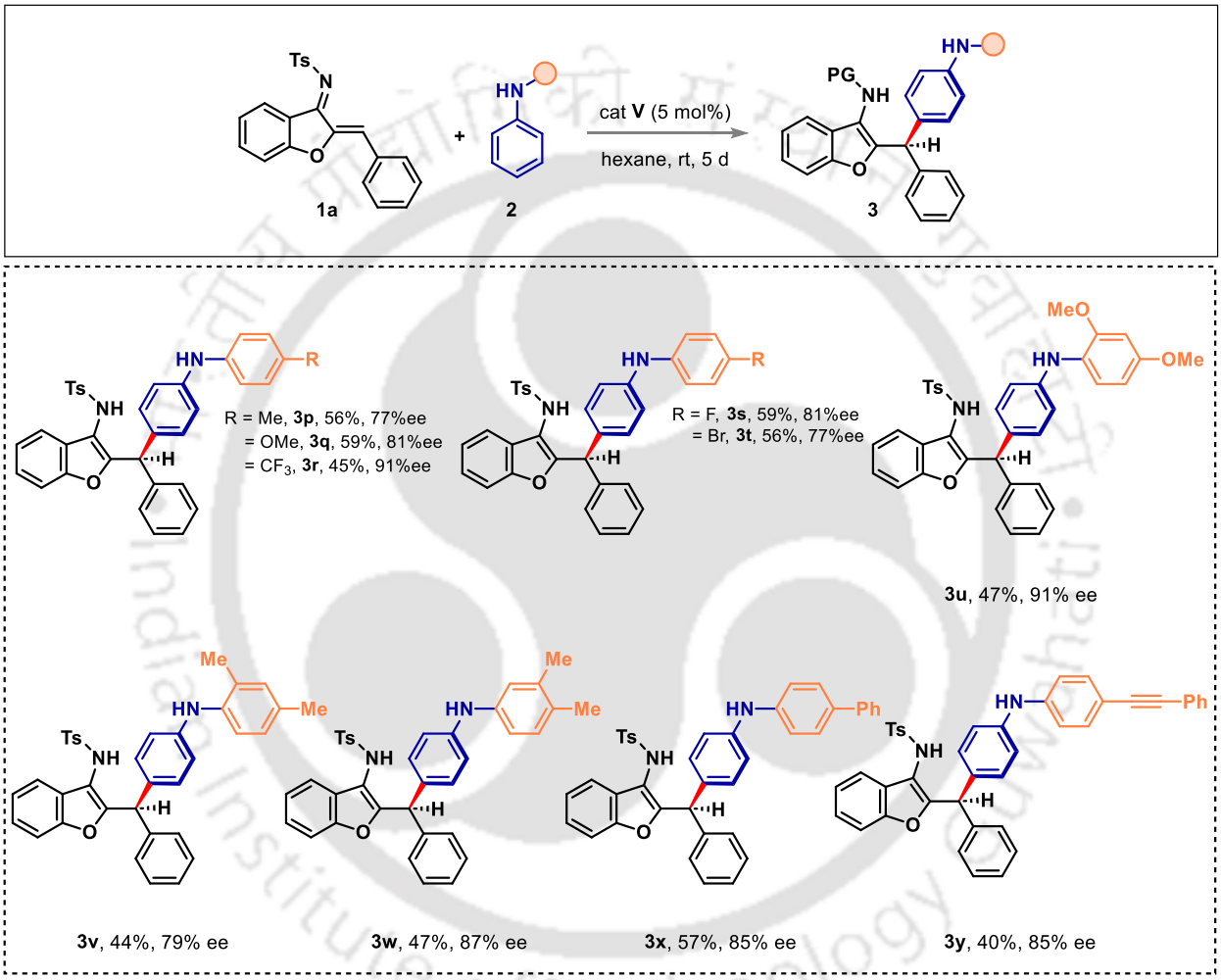

Scheme 12: Scope of diphenylamines.

3.5. Absolute configuration determination by electronic circular dichroism:

For determination of the absolute configuration of the herein synthesized **3a**, the computed ECD-spectrum of (*R*)-**3a** was compared with the experimental spectrum (c = 10^{-4} M, CH_3CN). We have optimized both the *R* and *S* conformers using B3LYP D4 /Def2-TZVP level of theory. Full Time Dependent Density Functional Theory (TDDFT) calculation has been

carried out using same level of theory without considering the Tamm-Dancoff approximation (TDA) to evaluate the ECD spectrum. By normalizing with the experimental data, we have found that ***R***-conformer of **3a** is best fitted with the experimental results (Fig. 4).

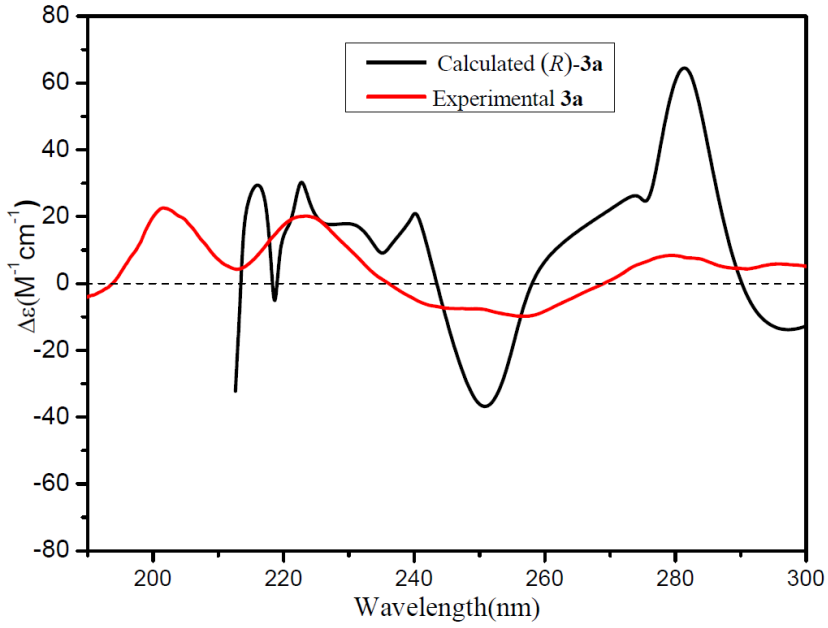

Fig. 4: Experimental and calculated ECD spectra for **3a**.

3.6. Scale-up reaction and Synthetic application:

Then a scale-up reaction was performed on 1 mmol scale of **1a** and to our delight the desired product **3a** was isolated in 55% yield with 92% ee (Scheme 2). After that, a few synthetic transformations were carried out on **3a** (Scheme 2). Initially methylation of N-tosyl group of **3a** was performed with methyl iodide and compound **4** was formed in 88% yield with retention of enantioselectivity. Then N-tosyl protection was carried out on **3a**. This led to the formation of **5** in 92% yield without erosion in enantioselectivity.

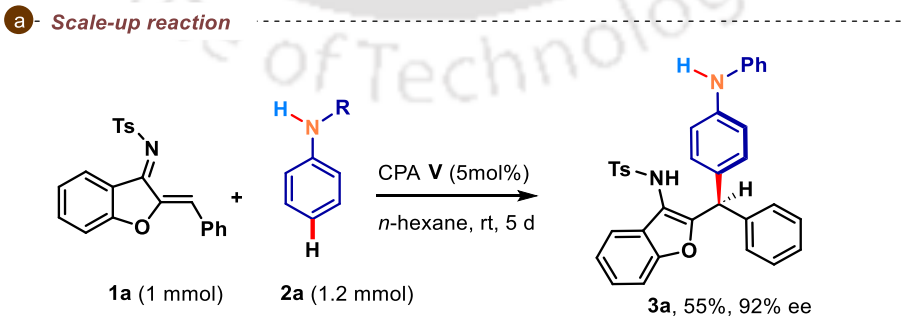

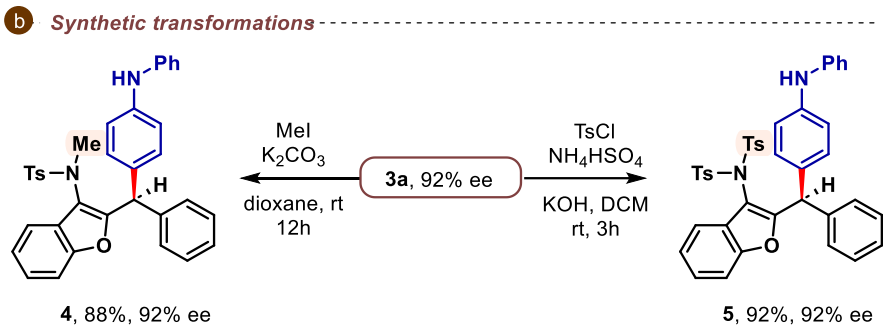

Scheme 12: (a) Scale-up reaction, (b) Synthetic transformation of **3a**.

3.7. Mechanism:

3.7.1. Control experiment:

To comprehend the reaction's mechanism, a few control tests were conducted (Scheme 13). Initially, the reaction between azadiene **1a** and *N,N*-dimethylaniline (**6**) was carried out, but no product was formed. To understand the role of phenyl group, other N-monosubstituted aninlines **7** and **8** were reacted with **1a**. Lower yields and poor enantioselectivities were observed for the products **9** and **10**. This indicates a possible π-π interaction between the phenyl group of aniline **2** and aryl group of catalyst **V**.

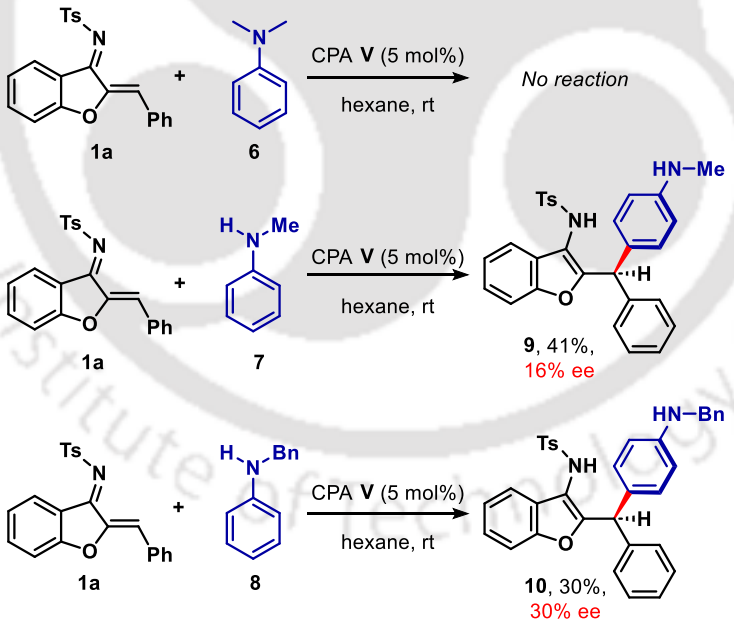

Scheme 13: Control experiment.

3.7.2. Proposed transition state:

The absolute configuration of **3a** was confirmed to be (*R*) by comparison of experimental and calculated electronic circular dichroism. Based on the absolute configuration, a plausible TS

has been drawn in Scheme 14. The catalyst blocks the *Re*-face of the double bond of azadiene **1a** and thus attack takes place on the *Si*-face.

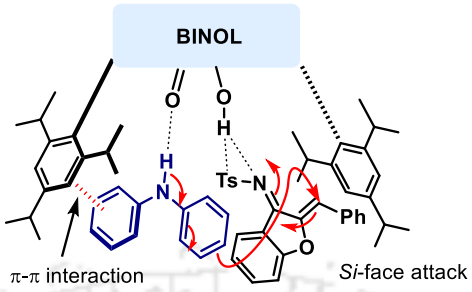

Scheme 14: Proposed transition state.

3.8. Conclusion:

In conclusion, we present an organocatalytic regio- and enantioselective Friedel-Crafts alkylation of *N*-arylanilines with azadienes for the synthesis of benzofuran containing triarylmethanes. Using readily accessible TRIP catalyst, the desired products were produced under ambient reaction conditions in moderate yields with good to high enantioselectivities. Few synthetic transformations have been demonstrated. Given the significant medicinal value of triarylmethanes, the pharmaceutical industry might find our approach useful.

3.9. Experimental Section:

3.9.1. General Information:

All dry solvents were dried using activated 4Å molecular sieves and stored under argon. For thin layer chromatography (TLC), silica gel plates with fluorescence indicator 254 nm were used and compounds were visualized by irradiation with UV light and/or iodine and/or phosphomolybdic acid stain. Celite® 512 medium was used for filtrations. Column chromatography was performed using 100-200 mesh silica gel. Hexane, ethyl acetate, acetone and dichloromethane for column chromatography were acquired from commercial sources and were used without purification. NMR spectra were acquired on a Bruker 400 MHz, 500 MHz and 600 MHz spectrometer. Chemical shifts (δ) are reported in ppm relative to residual solvent signals (Chloroform-d, 7.26 ppm for ^{1}H NMR and 77.23 ppm for ^{13}C NMR; DMSO-d^{6} ,2.52 ppm for ^{1}H NMR and 40.45 ppm for ^{13}C NMR respectively. ^{13}C spectra were acquired on a broad band decoupled mode. For ^{1}H-NMR, data are reported as follows: chemical shift, multiplicity (s = singlet, d = doublet, dd = double doublet, ddd = doublet of doublet of doublets, t = triplet, q = quartet, dt = doublet of triplets, m = multiplet), coupling constants (Hz) and integration. Using ESI positive mode HRMS spectra were recorded. Enantiomeric excesses were determined by HPLC analysis performed on Chiral Columns using a Daicel Chiralpak IA, ID, AD-H and Chiral-Select OM column.

3.9.2. General Procedure for synthesis of 1-azadiene:

The derivatives of azadiene were synthesized following reported literature procedure.[19]

3.9.3. General Procedure for synthesis of diphenyl amine:

The derivatives of ynone were synthesized following reported literature procedure.[20]

3.9.4. General Procedure for synthesis of various catalyst:

All the catalysts were synthesized according to the reported literature procedure.[21]

3.9.5. General Procedure for the Synthesis of chiral triarylmethane derivatives:

In an oven-dried screw cap *via*l equipped with a magnetic stir bar was charged with **1**(0.1 mmol, 1 equiv.), **V** catalyst (0.005 mmol, 5 mol%). Then, 1mL n-hexane was added in the mixture. After that, diphenyl amine **2** (0.11mmol, 1.1 equiv.) was added to the mixture and stirred at room temperature with 300 rpm. After stirring for 5 days, the crude mixture was loaded in column chromatography (petroleum ether : EtOAc = 90:10) to afford **3**.

3.9.6. Procedure for the synthesis of 4:

In an oven dried 10 mL round-bottom flask, **3a** (54.4 mg, 0.1 mmol, 1.0 equiv) in dioxane (2.5 mL), K_2CO_3 (1.5 equiv.) added. The reaction mixture cooled to 0 ℃ and the mixture was allowed to stir for 5min. Then, methyl iodide (1.2 equiv.) was added dropwise at this temperature. The mixture was stirred at room temperature, until full consumption of starting materials observed, H_2O added and extracted with Et_2O. Combined organic layer was washed with brine (3 × 5 mL), dried over anhydrous Na_2SO_4 and concentrated under reduced pressure. The residue was purified by flash column chromatography (n-hexane : ethyl acetate = 85:15) to give product **4.**

3.9.6. Procedure for the synthesis of 5:

In an oven dried 10 mL round-bottom flask, **3a** (54.4 mg, 0.1 mmol, 1.0 equiv) in dichloromethane (1 mL), KOH (8.4 mg, 0.15 mmol, 1.5 equiv.) and tetrabutylammonium hydrogensulfate (3.39 mg, 10 mol%) were added, and the mixture was allowed to stir for 15 min followed by addition of a solution of sulfonyl chloride (23 mg, 0.12mmol, 1.2 equiv.) in dichloromethane (0.5 mL), and the mixture was stirred at room temperature until the starting material was consumed. Then, water (20 mL) was added and the aqueous layer was extracted with EtOAc (3 × 20 mL). The combined organic layer was dried (Na_2SO_4) and concentrated, which upon flash chromatography (n-hexane : EtOAc = 85:15) gave **5**.

3.10. Characterization of the products:

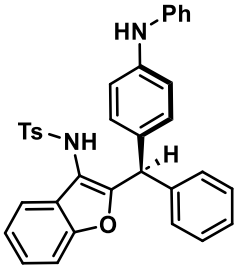

(*R*)-4-methyl-*N*-(2-(phenyl(4-(phenylamino)phenyl)methyl) benzofuran-3-yl)benzenesulfonamide (3a): Brown solid, 32 mg, 60% yield, 92% ee; R_f = 0.5 (petroleum ether : ethyl acetate = 85:15). **^{1}H NMR** (500 MHz, DMSO-d^6) δ 10.02 (s, 1H), 8.13 (s, 1H), 7.57 (d, J = 8.0 Hz, 2H), 7.48 (d, J = 8.2 Hz, 1H), 7.30 – 7.16 (m, 10H), 7.14 (t, J = 7.5 Hz, 1H), 7.07 (t, J = 8.3 Hz, 4H), 6.98 (d, J = 8.4 Hz, 2H), 6.92 (d, J = 8.3 Hz, 2H), 6.81 (t, J = 7.3 Hz, 1H), 5.57 (s, 1H), 2.28 (s, 3H). **^{13}C NMR** (126 MHz, DMSO-d^6) δ 154.91, 153.63, 144.27, 144.07, 142.89, 142.07, 137.82, 132.63, 130.46, 130.15, 130.02, 129.31, 129.11, 127.70, 127.34, 126.59, 125.23, 123.69, 120.74, 120.48, 117.54, 117.39, 114.98, 112.22, 46.35, 21.90. **HRMS (ESI$^+$) *m/z*:** $[M+H]^+$ calculated for $C_{34}H_{28}N_2O_3S$: 545.1894, found: 545.1885; **HPLC:** The enantiomeric excess was determined using Chiral-Select OM column (*n*-Hexane/ *i*-PrOH=80:20, flow rate=1.0 mL/min, λ= 220 nm, τ_{major} = 20.7 min, τ_{minor} = 25.7 min).

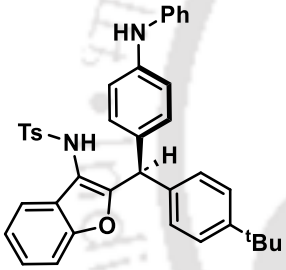

(*R*)-*N*-(2-((4-(tert-butyl)phenyl)(4-(phenylamino)phenyl)methyl) benzofuran-3-yl)-4-methylbenzenesulfonamide (3b): Brown solid, 33 mg, 56% yield, 77% ee; R_f = 0.5 (petroleum ether : ethyl acetate = 85:15)

^{1}H NMR (400 MHz, DMSO-d^6) δ 9.99 (s, 1H), 8.13 (s, 1H), 7.58 (d, J = 8.3 Hz, 2H), 7.47 (d, J = 7.9 Hz, 1H), 7.31 – 7.26 (m, 2H), 7.23 – 7.19 (m, 6H), 7.14 – 7.09 (m, 1H), 7.06 – 7.03 (m, 2H), 7.02 – 6.99 (m, 2H), 6.98 – 6.95 (m, 2H), 6.92 – 6.88 (m, 2H), 6.80 (t, J = 7.3 Hz, 1H), 5.51 (s, 1H), 2.29 (s, 3H), 1.25 (s, 9H). **^{13}C NMR** (101 MHz, DMSO-d^6) δ 155.23, 153.59, 149.65, 144.33, 144.09, 142.81, 139.08, 137.94, 130.51, 130.13, 130.04, 129.06, 127.77, 126.61, 125.90, 125.21, 123.70, 120.67, 120.44, 117.46, 114.86, 112.25, 45.98, 35.03, 32.05, 21.95. **HRMS (ESI$^+$) *m/z*:** $[M+H]^+$ calculated for $C_{38}H_{36}N_2O_3S$: 601.2520, found: 601.2508; **HPLC:** The enantiomeric excess was determined using Chirapak AD-H column (*n*-Hexane/ *i*-PrOH=70:30, flow rate=1.0 mL/min, λ= 274 nm, τ_{major} = 11.8 min, τ_{minor} = 38.4 min).

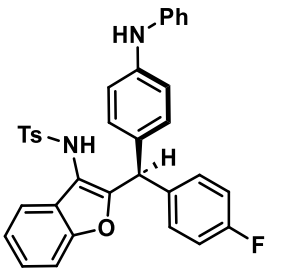

(*S*)-*N*-(2-((4-fluorophenyl)(4-(phenylamino)phenyl)methyl) benzofuran-3-yl)-4-methylbenzenesulfonamide (3c): Purple solid, 34 mg, 60% yield, 81% ee; R_f = 0.5 (petroleum ether : ethyl acetate = 85:15)

^{1}H NMR (500 MHz, DMSO-d^6) δ 10.06 (s, 1H), 8.16 (s, 1H), 7.55 (d, J = 8.2 Hz, 2H), 7.49 (d, J = 8.2 Hz, 1H), 7.31 – 7.27 (m, 1H), 7.27 –

7.20 (m, 3H), 7.17 (t, J = 7.7 Hz, 3H), 7.13 – 7.04 (m, 6H), 6.97 (d, J = 8.5 Hz, 2H), 6.90 (d, J = 8.6 Hz, 2H), 6.81 (t, J = 7.3 Hz, 1H), 5.56 (s, 1H), 2.27 (s, 3H).**^{13}C NMR** (126 MHz, DMSO-d^6) δ 161.77 (d, $^1J_{C-F}$ = 243Hz), 154.52, 153.69, 144.23, 144.12, 143.00, 138.25 (d, $^4J_{C-F}$ = 2.5 Hz), 137.68, 132.49, 131.1 (d, $^3J_{C-F}$ = 7.5 Hz), 130.48, 130.12, 130.06, 127.71, 126.57, 125.37, 123.80, 120.87, 120.56, 117.61, 117.39, 115.89 (d, $^2J_{C-F}$ = 21.5Hz), 115.07, 112.29, 45.56, 21.90. **HRMS (ESI$^+$) *m/z*:** $[M+H]^+$ calculated for $C_{34}H_{27}FN_2O_3S$: 563.1800, found: 563.1799; **HPLC:** The enantiomeric excess was determined using Chiralpak IA column (*n*-Hexane/ *i*-PrOH=70:30, flow rate=1.0 mL/min, λ= 254 nm, τ_{major} = 18.6 min, τ_{minor} = 42.2 min).

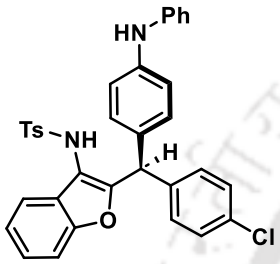

(*S*)-*N*-(2-((4-chlorophenyl)(4-(phenylamino)phenyl)methyl) benzofuran-3-yl)-4-methylbenzenesulfonamide (3d): Yellow solid, 32 mg, 60% yield, 81% ee; R_f = 0.5 (petroleum ether : ethyl acetate = 85:15)

^{1}H NMR (500 MHz, DMSO-d^6) δ 10.07 (s, 1H), 8.15 (s, 1H), 7.57 – 7.52 (m, 2H), 7.49 (d, J = 8.2 Hz, 1H), 7.34 - 7.32 (m, 3H), 7.28 – 7.19 (m, 3H), 7.18 - 7.15 (m, 3H), 7.07 - 7.04 (m, 4H), 6.98 (d, J = 7.5 Hz, 2H), 6.92 (d, J = 8.6 Hz, 2H), 6.82 (t, J = 7.3 Hz, 1H), 5.56 (s, 1H), 2.27 (s, 3H). **^{13}C NMR** (126 MHz, DMSO-d^6) δ 154.08, 153.71, 144.17, 144.09, 143.07, 141.08, 137.60, 132.17, 132.06, 131.04, 130.41, 130.15, 130.02, 129.08, 127.66, 126.54, 125.38, 123.78, 120.90, 120.57, 117.64, 117.36, 115.23, 112.25, 45.66, 21.87. **HRMS (ESI$^+$) *m/z*:** $[M+H]^+$ calculated for $C_{34}H_{27}ClN_2O_3S$: 579.1504, found: 579.1489; **HPLC:** The enantiomeric excess was determined using Chiral-Select OM column (*n*-Hexane/ *i*-PrOH=80:20, flow rate=1.0 mL/min, λ= 254 nm, τ_{major} = 23.8 min, τ_{minor} = 28.8 min).

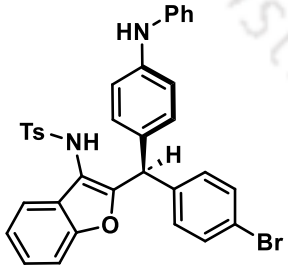

(*S*)-*N*-(2-((4-bromophenyl)(4-(phenylamino)phenyl)methyl) benzofuran-3-yl)-4-methylbenzenesulfonamide (3e): Yellow solid, 28 mg, 45% yield, 91% ee; R_f = 0.5 (petroleum ether : ethyl acetate = 85:15)

^{1}H NMR (400 MHz, DMSO-d^6) δ 10.09 (s, 1H), 8.18 (s, 1H), 7.54 (d, J = 8.2 Hz, 2H), 7.50 - 7.45 (m, 3H), 7.33 (d, J = 7.2 Hz, 1H), 7.29 – 7.18 (m, 4H), 7.17 - 7.15 (m, 3H), 7.05 (d, J = 7.4 Hz, 2H), 6.99 - 6.96 (m, 4H), 6.91 (d, J = 8.7 Hz, 2H), 6.81 (t, J = 7.3 Hz, 1H), 5.52 (s, 1H), 2.27 (s, 3H). **^{13}C NMR** (101 MHz, DMSO-d^6) δ 153.99, 153.74, 144.18, 144.15, 143.09, 141.54, 137.55, 132.14, 132.05, 131.45, 130.46, 130.21, 130.08, 127.70, 126.56, 125.44, 123.85, 120.95, 120.63, 120.60, 117.64, 117.36, 115.27, 112.31, 45.73, 21.96. **HRMS (ESI$^+$) *m/z*:** $[M+H]^+$ calculated for $C_{34}H_{27}BrN_2O_3S$:

623.0999, found: 623.0987; **HPLC:** The enantiomeric excess was determined using Chiral-Select OM column (*n*-Hexane/ *i*-PrOH=80:20, flow rate=1.0 mL/min, λ= 220 nm, τ_{major} = 23.8 min, τ_{minor} = 28.8 min).

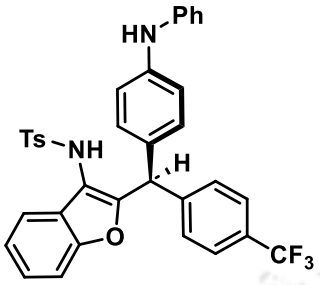

(*R*)-4-methyl-*N*-(2-((4-(phenylamino)phenyl)(4-(trifluoromethyl)phenyl)methyl) benzofuran-3-yl)benzenesulfonamide (3f): Pale yellow solid, 32 mg, 52% yield, 93% ee; R_f = 0.5 (petroleum ether : ethyl acetate = 85:15)

^{1}H NMR (400 MHz, DMSO-d^6) δ 10.11 (s, 1H), 8.18 (s, 1H), 7.65 (d, J = 8.2 Hz, 2H), 7.55 (d, J = 8.3 Hz, 2H), 7.50 (d, J = 8.3 Hz, 1H), 7.33 (d, J = 7.9 Hz, 1H), 7.29 – 7.21 (m, 5H), 7.21 – 7.19 (m, 1H), 7.17 - 7.14 (m, 3H), 7.08 – 7.04 (m, 2H), 6.99 (d, J = 8.7 Hz, 2H), 6.93 (d, J = 8.7 Hz, 2H), 6.82 (t, J = 7.3 Hz, 1H), 5.63 (s, 1H), 2.24 (s, 3H). **^{13}C NMR** (101 MHz, DMSO-d^6) δ 153.78, 153.60, 146.79, 144.11, 144.07, 143.22, 137.57, 131.78, 130.46, 130.27, 130.06, 130.04, 127.71, 126.50, 126.07 (q, J = 4Hz), 125.52, 123.89, 120.97, 120.65, 117.71, 117.36, 115.54, 112.34, 46.14, 21.81. **HRMS (ESI$^+$) *m/z*:** $[M+H]^+$ calculated for $C_{35}H_{27}F_3N_2O_3S$: 613.1768, found: 613.1745; **HPLC:** The enantiomeric excess was determined using Chiralpak IA column (*n*-Hexane/ *i*-PrOH=70:30, flow rate=1.0 mL/min, λ= 254 nm, τ_{major} = 14.9 min, τ_{minor} = 40.7 min).

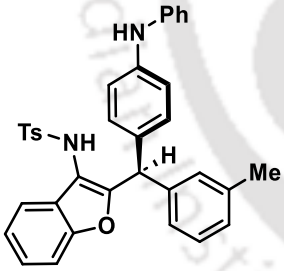

(*S*)-4-methyl-*N*-(2-((4-(phenylamino)phenyl)(*m*-tolyl)methyl)benzofuran-3-yl)benzenesulfonamide (3g): Brown solid, 34 mg, 62% yield, 86% ee; R_f = 0.5 (petroleum ether : ethyl acetate = 85:15)

^{1}H NMR (500 MHz, DMSO-d^6) δ 10.04 (s, 1H), 8.15 (s, 1H), 7.58 (d, J = 8.0 Hz, 2H), 7.49 (d, J = 8.3 Hz, 1H), 7.28 (d, J = 7.8 Hz, 1H), 7.25 - 7.20 (m, 3H), 7.19 (d, J = 8.1 Hz, 2H), 7.16 -7.13 (m, 2H), 7.06 (d, J = 7.9 Hz, 2H), 7.03 (d, J = 7.6 Hz, 1H), 6.98 (d, J = 8.4 Hz, 2H), 6.93 – 6.89 (m, 3H), 6.88 (d, J = 7.8 Hz, 1H), 6.81 (t, J = 7.3 Hz, 1H), 5.53 (s, 1H), 2.27 (s, 3H), 2.25 (s, 3H). **^{13}C NMR** (126 MHz, DMSO-d^6) δ 154.99, 153.65, 144.29, 144.03, 142.84, 142.06, 138.13, 137.83, 132.73, 130.44, 130.18, 130.04, 129.91, 129.03, 128.04, 127.71, 126.67, 126.45, 125.23, 123.72, 120.79, 120.47, 117.52, 117.37, 114.90, 112.26, 46.30, 22.03, 21.92. **HRMS (ESI$^+$) *m/z*:** $[M+H]^+$ calculated for $C_{35}H_{30}N_2O_3S$: 559.2050, found: 559.2039; **HPLC:** The enantiomeric excess was determined using Chiralpak ID column (*n*-Hexane/ *i*-PrOH=80:20, flow rate=1.0 mL/min, λ= 254 nm, τ_{major} = 19.8 min, τ_{minor} = 22.5 min).

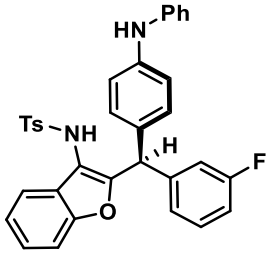

(S)-N-(2-((3-fluorophenyl)(4-(phenylamino)phenyl)methyl) benzofuran-3-yl)-4-methylbenzenesulfonamide (3h): Pale yellow solid, 32 mg, 58% yield, 95% ee; R_f = 0.5 (petroleum ether : ethyl acetate = 85:15)

^{1}H NMR (500 MHz, Chloroform-d) δ 7.82 (d, J = 8.3 Hz, 2H), 7.56 (d, J = 8.3 Hz, 1H), 7.46 – 7.36 (m, 4H), 7.33 - 7.29 (m, 3H), 7.28 (d, J = 7.4 Hz, 1H), 7.25 – 7.22 (m, 2H), 7.22 – 7.18 (m, 2H), 7.16 – 7.13 (m, 2H), 7.12 - 7.07 (m, 3H), 6.95 (d, J = 10.2 Hz, 1H), 6.46 (s, 1H), 5.88 (s, 1H), 5.70 (s, 1H), 2.53 (s, 3H). **^{13}C NMR** (126 MHz, Chloroform-d) δ 163.96 (d, $^1J_{C-F}$ = 246Hz), 155.30, 153.59, 144.36, 143.45, 143.40, 142.97, 142.51, 136.48, 132.14, 130.32, 130.03, 129.96, 129.91, 129.88, 129.55, 127.80, 125.86, 124.76, 124.70, 124.67, 123.38, 121.44, 119.49, 118.28, 117.90, 117.67, 116.1 (d, $^2J_{C-F}$ = 22.7 Hz), 114.0 (d, $^2J_{C-F}$ = 21.4 Hz), 113.95, 113.84, 111.84, 46.59, 21.71. **HRMS (ESI$^+$) *m/z*:** $[M+H]^+$ calculated for $C_{34}H_{27}FN_2O_3S$: 563.1800, found: 563.1780; **HPLC:** The enantiomeric excess was determined using Chiral-Select OM column (*n*-Hexane/ *i*-PrOH=80:20, flow rate=1.0 mL/min, λ= 254 nm, τ_{major} = 21.1 min, τ_{minor} = 25.5 min).

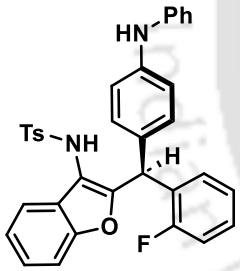

(S)-N-(2-((2-fluorophenyl)(4-(phenylamino)phenyl)methyl) benzofuran-3-yl)-4-methylbenzenesulfonamide (3i): Pale yellow solid, 34 mg, 61% yield, 92% ee; R_f = 0.5 (petroleum ether : ethyl acetate = 85:15)

^{1}H NMR (400 MHz, DMSO-d^6) δ 10.09 (s, 1H), 8.14 (s, 1H), 7.52 - 7.49 (m, 3H), 7.34 - 7.30 (m, 2H), 7.29 – 7.22 (m, 2H), 7.22 – 7.15 (m, 4H), 7.14 - 7.12 (m, 4H), 7.04 (d, J = 7.9 Hz, 2H), 6.98 – 6.93 (m, 2H), 6.90 (d, J = 8.5 Hz, 2H), 6.80 (t, J = 7.3 Hz, 1H), 5.80 (s, 1H), 2.25 (s, 3H). **^{13}C NMR** (101 MHz, DMSO-d^6) δ 160.48 (d,$^1J_{C-F}$ = 248.0 Hz), 153.89, 153.76, 144.22, 144.00, 143.04, 137.60, 131.60, 130.38, 130.06, 129.83, 129.67 (d, $^3J_{C-F}$ = 8.0 Hz), 128.93 (d, $^2J_{C-F}$ = 14.0 Hz), 127.56, 126.62, 125.44, 125.23, 123.86, 120.90, 120.54, 117.58, 117.38, 116. (d, $^2J_{C-F}$ = 21.1 Hz), 115.05, 112.34, 37.16, 21.98. **HRMS (ESI$^+$) *m/z*:** $[M+H]^+$ calculated for $C_{34}H_{27}FN_2O_3S$: 563.1800, found: 563.1801; **HPLC:** The enantiomeric excess was determined using Chiralpak IA column (*n*-Hexane/ *i*-PrOH=70:30, flow rate=1.0 mL/min, λ= 254 nm, τ_{major} = 31.5 min, τ_{minor} = 40.1 min).

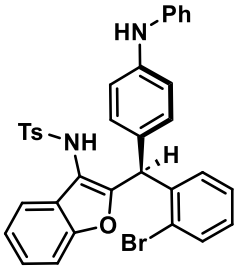

(*S*)-*N*-(2-((2-bromophenyl)(4-(phenylamino)phenyl)methyl) benzofuran-3-yl)-4-methylbenzenesulfonamide (3j): Brown solid, 29 mg, 47% yield, 86% ee; R_f = 0.5 (petroleum ether : ethyl acetate = 85:15)

^{1}H NMR (500 MHz, DMSO-d^6) δ 10.33 (s, 1H), 8.37 (s, 1H), 7.85 (d, J = 8.0 Hz, 1H), 7.78 -7.74 (m, 3H), 7.61 – 7.54 (m, 2H), 7.52 – 7.45 (m, 6H), 7.42 (t, J = 7.5 Hz, 1H), 7.38 (d, J = 8.0 Hz, 2H), 7.30 (d, J = 7.9 Hz, 2H), 7.21 (d, J = 8.4 Hz, 2H), 7.10 (d, J = 8.4 Hz, 2H), 7.06 (t, J = 7.3 Hz, 1H), 6.16 (s, 1H), 2.52 (s, 3H). **^{13}C NMR** (126 MHz, DMS-d^6) δ 154.48, 153.73, 144.22, 143.82, 142.91, 140.98, 137.75, 133.90, 131.20, 130.55, 130.36, 130.31, 130.01, 129.54, 128.64, 127.50, 126.77, 125.39, 124.96, 123.81, 120.85, 120.50, 117.58, 117.29, 115.09, 112.29, 46.22, 21.95. **HRMS (ESI$^+$) *m/z*:** $[M+H]^+$ calculated for $C_{34}H_{27}BrN_2O_3S$: 623.0999, found: 623.0980; **HPLC:** The enantiomeric excess was determined using Chiral-Select OM column (*n*-Hexane/ *i*-PrOH=80:20, flow rate=1.0 mL/min, λ= 220 nm, τ_{major} = 26.8 min, τ_{minor} = 42.6 min).

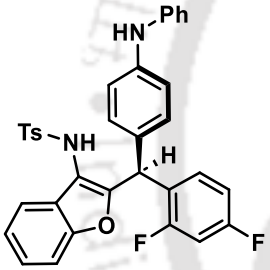

(S)-N-(2-((2,4-difluorophenyl)(4-(phenylamino)phenyl)methyl) benzofuran-3-yl)-4-methylbenzenesulfonamide (3k): Brown solid, 34 mg, 59% yield, 89% ee; R_f = 0.5 (petroleum ether : ethyl acetate = 85:15).

^{1}H NMR (500 MHz, DMSO-d^6) δ 10.12 (s, 1H), 8.14 (s, 1H), 7.52 - 7.48 (m, 3H), 7.38 (d, J = 7.7 Hz, 1H), 7.27 (t, J = 7.9 Hz, 1H), 7.22 - 7.15 (m, 5H), 7.13 (d, J = 8.2 Hz, 2H), 7.06 - 6.99 (m, 3H), 6.96 (d, J = 8.2 Hz, 2H), 6.90 (d, J = 8.3 Hz, 2H), 6.81 (t, J = 7.5 Hz, 1H), 5.74 (s, 1H), 2.26 (s, 3H). **^{13}C NMR** (126 MHz, DMSO-d^6) δ 159.39, 153.80, 153.36, 144.16, 143.97, 143.14, 137.48, 131.30, 130.31, 130.04, 129.74, 127.53, 126.59, 125.51, 125.29, 123.90, 121.04, 120.58, 117.64, 117.35, 115.15, 112.33, 112.21, 112.05, 105.08, 104.87, 104.67, 39.47, 21.86. **HRMS (ESI$^+$) *m/z*:** $[M+H]^+$ calculated for $C_{34}H_{26}F_2N2O_3S$: 581.1705, found: 581.1699; **HPLC:** The enantiomeric excess was determined using Chiralpak IA column (*n*-Hexane/ *i*-PrOH=70:30, flow rate=1.0 mL/min, λ= 254 nm, τ_{major} = 26.4 min, τ_{minor} = 31.2 min).

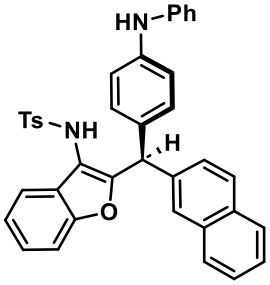

(S)-4-methyl-N-(2-(naphthalen-2-yl(4-(phenylamino)phenyl) methyl)benzofuran-3-yl)benzenesulfonamide (3l): Pale yellow solid, 32 mg, 54% yield, 89% ee; R_f = 0.5 (petroleum ether : ethyl acetate = 85:15)

^{1}H NMR (500 MHz, Methanol-d^4) δ 7.95 (d, J = 8.3 Hz, 1H), 7.88 (d, J = 7.2 Hz, 1H), 7.79 (d, J = 8.2 Hz, 1H), 7.53 – 7.46 (m, 2H), 7.46 –

7.41 (m, 2H), 7.36 (m, 3H), 7.25 – 7.19 (m, 2H), 7.19 – 7.09 (m, 3H), 7.04 (d, J = 7.9 Hz, 2H), 6.95 (d, J = 2.2 Hz, 4H), 6.85 (d, J = 8.0 Hz, 2H), 6.83 – 6.78 (m, 1H), 6.31 (s, 1H), 2.13 (s, 3H). **^{13}C NMR** (126 MHz, Methanol-d^4) δ 157.78, 155.89, 146.05, 145.69, 144.88, 139.38, 139.34, 136.41, 134.55, 133.73, 131.63, 131.35, 131.03, 130.73, 129.58, 129.12, 128.74, 128.30, 127.95, 127.49, 127.20, 126.36, 126.31, 124.84, 122.06, 121.81, 119.34, 119.01, 116.05, 113.11, 45.46, 22.42. **HRMS (ESI$^+$) *m/z*:** $[M+H]^+$ calculated for $C_{38}H_{30}N_2O_3S$: 595.2050, found: 595.2050; **HPLC:** The enantiomeric excess was determined using Chiral-Select OM column (*n*-Hexane/ *i*-PrOH=80:20, flow rate=1.0 mL/min, λ= 254 nm, τ_{major} = 14.2 min, τ_{minor} = 18.6 min).

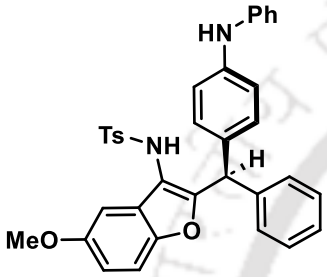

(R)-N-(5-methoxy-2-(phenyl(4-(phenylamino)phenyl)methyl)benzofuran-3-yl)-4-methylbenzenesulfonamide (3m): Yellow solid, 35 mg, 61% yield, 84% ee; R_f = 0.5 (petroleum ether : ethyl acetate = 85:15)

^{1}H NMR (500 MHz, DMSO-d^6) δ 9.92 (s, 1H), 8.15 (s, 1H), 7.61 (d, J = 7.9 Hz, 2H), 7.38 (d, J = 9.0 Hz, 1H), 7.30 (t, J = 7.5 Hz, 2H), 7.26 – 7.20 (m, 5H), 7.13 (d, J = 7.6 Hz, 2H), 7.06 (d, J = 7.9 Hz, 2H), 7.01 – 6.98 (m, 4H), 6.84 – 6.75 (m, 2H), 6.48 (s, 1H), 5.64 (s, 1H), 3.60 (s, 3H), 2.30 (s, 3H). **^{13}C NMR** (126 MHz, DMSO-d^6) δ 156.51, 156.33, 148.40, 144.28, 144.14, 142.91, 142.11, 138.14, 132.65, 130.53, 130.20, 130.02, 129.35, 129.15, 127.82, 127.37, 127.08, 120.47, 117.53, 117.44, 115.02, 113.97, 112.91, 102.50, 56.16, 46.48, 21.86. **HRMS (ESI$^+$) *m/z*:** $[M+H]^+$ calculated for $C_{35}H_{30}N2O_{3S}$: 575.2000, found: 575.2000; **HPLC:** The enantiomeric excess was determined using Chiral-Select OM column (*n*-Hexane/ *i*-PrOH=80:20, flow rate=1.0 mL/min, λ= 254 nm, τ_{major} = 18.1min, τ_{minor} = 28.6 min).

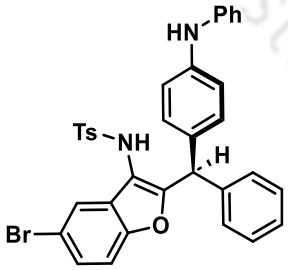

(R)-N-(5-bromo-2-(phenyl(4-(phenylamino)phenyl) methyl)benzofuran-3-yl)-4-methylbenzenesulfonamide (3n): Brown solid, 27 mg, 43% yield, 91% ee; R_f = 0.5 (petroleum ether : ethyl acetate = 85:15)

^{1}H NMR (500 MHz, DMSO-d^6) δ 10.02 (s, 1H), 8.16 (s, 1H), 7.57 (d, J = 8.0 Hz, 2H), 7.48 (d, J = 8.8 Hz, 1H), 7.36 (d, J = 8.7, 1H), 7.31 - 7.28 (m, 2H), 7.24 - 7.21 (m, 5H), 7.11 (d, J = 7.5 Hz, 2H), 7.07 - 7.06 (m, 3H), 7.01 – 6.93 (m, 4H), 6.82 (t, J = 7.3 Hz, 1H), 5.64 (s, 1H), 2.32 (s, 3H). **^{13}C NMR** (126 MHz, DMSO-d^6) δ 157.09, 152.42, 144.51, 144.20, 143.06, 141.71, 137.52, 132.17, 130.59, 130.19, 130.04, 129.32, 129.23, 128.57, 127.85, 127.82, 127.50, 122.93, 120.56, 117.63, 117.40, 116.22, 114.50, 114.44, 46.39, 21.98. **HRMS (ESI$^+$) *m/z*:** $[M+H]^+$ calculated for $C_{34}H_{27}BrN_2O_3S$:

623.0999, found: 623.0999; **HPLC:** The enantiomeric excess was determined using Chiral-Select OM column (*n*-Hexane/ *i*-PrOH=80:20, flow rate=1.0 mL/min, λ= 254 nm, τ_{major} = 21.3 min, τ_{minor} = 32.2 min).

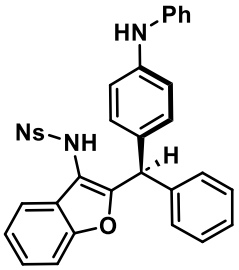

(R)-4-nitro-N-(2-(phenyl(4-(phenylamino)phenyl)methyl) benzofuran-3-yl)benzenesulfonamide (3o): Colourless solid, 32 mg, 55% yield, 85% ee; R_f = 0.5 (petroleum ether : ethyl acetate = 85:15)

^{1}H NMR (500 MHz, DMSO-d^6) δ 10.60 (s, 1H), 8.16 – 8.06 (m, 3H), 7.91 – 7.87 (m, 2H), 7.53 (d, J = 8.2 Hz, 1H), 7.43 (d, J = 7.8 Hz, 1H), 7.29 (t, J = 7.8 Hz, 1H), 7.26 – 7.18 (m, 5H), 7.13 (t, J = 7.2 Hz, 1H), 7.06 – 6.99 (m, 4H), 6.94 – 6.89 (m, 4H), 6.82 (t, J = 7.3 Hz, 1H), 5.45 (s, 1H). **^{13}C NMR** (126 MHz, DMSO-d^6) δ 154.80, 153.81, 150.36, 145.71, 144.12, 143.04, 141.98, 132.44, 130.08, 129.98, 129.24, 129.08, 129.05, 127.28, 126.51, 125.55, 125.36, 124.05, 120.80, 120.57, 117.75, 117.08, 114.32, 112.39, 46.13. **HRMS (ESI$^+$) *m/z*:** $[M+H]^+$ calculated for $C_{33}H_{25}N3O_5S$: 576.1588, found: 576.1588; **HPLC:** The enantiomeric excess was determined using Chiralpak IA column (*n*-Hexane/ *i*-PrOH=70:30, flow rate=1.0 mL/min, λ= 254 nm, τ_{major} = 20.9 min, τ_{minor} = 30.5 min).

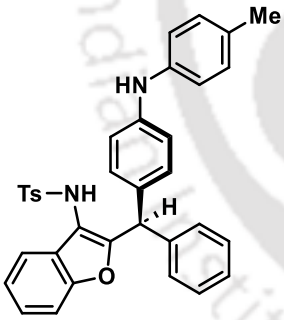

(*R*)-4-methyl-*N*-(2-(phenyl(4-(p-tolylamino)phenyl)methyl) benzofuran-3-yl)benzenesulfonamide (3p): Brown solid, 31 mg, 56% yield, 90% ee; R_f = 0.5 (petroleum ether : ethyl acetate = 85:15)

^{1}H NMR (400 MHz, DMSO-d^6) δ 10.04 (s, 1H), 8.01 (s, 1H), 7.57 (d, J = 8.2 Hz, 2H), 7.48 (d, J = 8.2 Hz, 1H), 7.28 – 7.22 (m, 4H), 7.22 – 7.17 (m, 3H), 7.14 (t, J = 7.4 Hz, 1H), 7.07- 7.03 (m, 4H), 6.97 (d, J = 8.3 Hz, 2H), 6.93 – 6.86 (m, 4H), 5.55 (s, 1H), 2.28 (s, 3H), 2.23 (s, 3H). **^{13}C NMR** 13C NMR (101 MHz, DMSO-d^6) δ 154.99, 153.64, 144.11, 143.54, 142.16, 141.54, 137.80, 131.97, 130.48, 130.16, 129.55, 129.33, 129.13, 127.73, 127.34, 126.61, 125.25, 123.72, 120.76, 118.33, 116.59, 114.94, 112.25, 46.33, 21.95, 21.20. **HRMS (ESI$^+$) *m/z*:** $[M+H]^+$ calculated for $C_{38}H_{30}N_2O_3S$: 559.2050, found: 559.2059; **HPLC:** The enantiomeric excess was determined using Chiralpak IA column (*n*-Hexane/ *i*-PrOH=70:30, flow rate=1.0 mL/min, λ= 254 nm, τ_{major} = 28.1 min, τ_{minor} = 38.3 min).

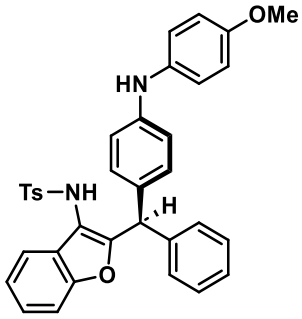

(R)-N-(2-((4-((4-methoxyphenyl)amino)phenyl) (phenyl)methyl)benzofuran-3-yl)-4-methylbenzenesulfonamide (3q): Brown solid, 34 mg, 59% yield, 89% ee; R_f = 0.5 (petroleum ether : ethyl acetate = 85:15)

^{1}H NMR (400 MHz, DMSO-d^6) δ 10.03 (s, 1H), 8.16 (s, 1H), 7.56 (d, J = 8.0 Hz, 2H), 7.50 (d, J = 8.5 Hz, 1H), 7.29 – 7.10 (m, 8H), 7.06 (d, J = 8.0 Hz, 2H), 6.97 (d, J = 8.6 Hz, 2H), 6.91 (d, J = 8.4 Hz, 2H), 6.81 (t, J = 5.7 Hz, 2H), 6.65 (t, J = 6.3 Hz, 2H), 5.53 (s, 1H), 3.70 (s, 3H), 2.27 (s, 3H). **^{13}C NMR** (101 MHz, DMSO-d^6) δ 159.98, 154.86, 153.62, 144.27, 144.10, 143.59, 142.89, 137.76, 132.46, 130.46, 130.18, 130.13, 130.05, 127.68, 126.59, 125.29, 123.74, 121.69, 120.75, 120.49, 117.54, 117.37, 115.71, 114.98, 112.26, 112.21, 55.86, 46.26, 21.91. **HRMS (ESI$^+$) *m/z*:** $[M+H]^+$ calculated for $C_{35}H_{30}N2O_{3S}$: 575.2000, found: 575.1981; **HPLC:** The enantiomeric excess was determined using Chirapak IA column (*n*-Hexane/ *i*-PrOH=70:30, flow rate=1.0 mL/min, λ= 220 nm, τ_{major} = 41.9 min, τ_{minor} = 48.1 min).

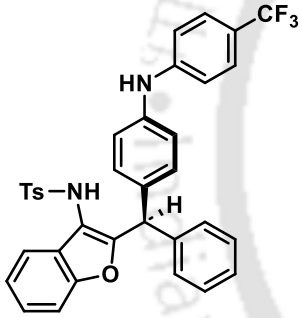

(R)-4-methyl-N-(2-(phenyl(4-((4-(trifluoromethyl)phenyl) amino)phenyl) methyl)benzofuran-3-yl)benzenesulfonamide (3r): Brown solid, 27 mg, 45% yield, 76% ee; R_f = 0.5 (petroleum ether : ethyl acetate = 85:15)

^{1}H NMR (400 MHz, DMSO-d^6) δ 10.06 (s, 1H), 8.70 (s, 1H), 7.57 (d, J = 8.0 Hz, 2H), 7.52 - 7.49 (m, 3H), 7.32 – 7.22 (m, 5H), 7.22 – 7.16 (m, 3H), 7.14 (d, J = 8.3 Hz, 2H), 7.08 (d, J = 7.8 Hz, 4H), 6.99 (d, J = 8.3 Hz, 2H), 5.61 (s, 1H), 2.28 (s, 4H).**^{13}C NMR** (101 MHz, DMSO-d^6) δ 158.68, 157.72, 152.39, 148.16, 145.90, 145.01, 141.82, 138.83, 134.54, 134.35, 133.41, 133.25, 131.76, 131.51, 130.61, 129.38, 127.82, 124.83, 123.75, 119.56, 119.21, 116.33, 50.46, 25.98. **HRMS (ESI$^+$) *m/z*:** $[M+H]^+$ calculated for $C_{35}H_{27F3}N2O_{3S}$: 613.1768, found: 613.1747; **HPLC:** The enantiomeric excess was determined using Chiralpak IA column (*n*-Hexane/ *i*-PrOH=70:30, flow rate=1.0 mL/min, λ= 254 nm, τ_{major} = 12.8 min, τ_{minor} = 20.9 min).

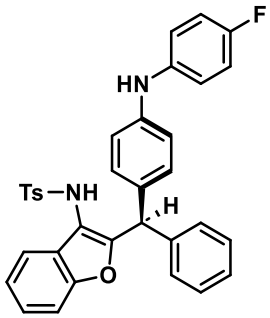

(R)-N-(2-((4-((4-fluorophenyl)amino)phenyl)(phenyl) methyl)benzofuran-3-yl)-4-methylbenzenesulfonamide (3s): Brown solid, 33 mg, 59% yield, 81% ee; R_f = 0.5 (petroleum ether : ethyl acetate = 85:15)

^{1}H NMR (500 MHz, DMSO-d^6) δ 10.01 (s, 1H), 8.08 (s, 1H), 7.57 (d, J = 8.0 Hz, 2H), 7.48 (d, J = 8.2 Hz, 1H), 7.30 – 7.21 (m, 5H), 7.19 (d, J = 8.1 Hz, 2H), 7.14 (t, J = 7.5 Hz, 1H), 7.07 (t, J = 5.3 Hz, 6H), 6.91

(s, 4H), 5.57 (s, 1H), 2.28 (s, 3H). **^{13}C NMR** (126 MHz, Chloroform-d) 13C NMR (126 MHz, DMSO-d^6) δ 162.21 (d, $^1J_{C-F}$ = 235.6 Hz), 158.93, 157.62, 148.07, 147.39, 146.07, 144.61 (d, $^4J_{C-F}$ = 2.5 Hz), 141.82, 136.41, 134.45, 134.21, 133.29, 133.10, 131.69, 131.33, 130.59, 129.22, 127.69, 124.73, 123.66 (d , $^3J_{C-F}$ = 8.8 Hz), 120.74, 120.52 (d, $^2J_{C-F}$ = 22.7 Hz), 118.97, 116.21, 50.33, 25.90. **HRMS (ESI$^+$) *m/z*:** $[M+H]^+$ calculated for $C_{34}H_{27}FN_2O_3S$: 563.1800, found: 563.1790; **HPLC:** The enantiomeric excess was determined using Chiral-Select OM column (*n*-Hexane/ *i*-PrOH=80:20, flow rate=1.0 mL/min, λ= 254 nm, τ_{major} = 18.4 min, τ_{minor} = 24.7 min).

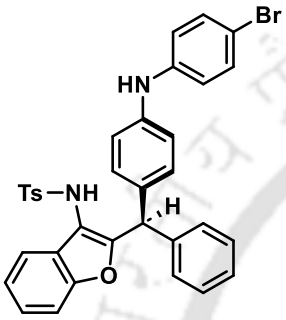

(R)-N-(2-((4-((4-bromophenyl)amino)phenyl)(phenyl) methyl)benzofuran-3-yl)-4-methylbenzenesulfonamide (3t): Brown solid, 35 mg, 56% yield, 87% ee; R_f = 0.5 (petroleum ether : ethyl acetate = 85:15)

^{1}H NMR (400 MHz, DMSO-d6) δ 10.04 (s, 1H), 8.31 (s, 1H), 7.56 (d, J = 8.4 Hz, 2H), 7.48 (d, J = 8.2 Hz, 1H), 7.34 (d, J = 8.8 Hz, 2H), 7.27 – 7.22 (m, 4H), 7.22 – 7.16 (m, 3H), 7.13 (t, J = 7.6 Hz, 1H), 7.06 (d, J = 7.0 Hz, 2H), 7.02 – 6.95 (m, 4H), 6.93 (d, J = 8.6 Hz, 2H), 5.58 (s, 1H), 2.26 (s, 3H). **^{13}C NMR** (101 MHz, DMSO-d6) δ 154.79, 153.67, 144.12, 143.87, 142.11, 141.99, 137.78, 133.46, 132.70, 130.50, 130.27, 129.35, 129.18, 127.73, 127.42, 126.59, 125.31, 123.76, 120.79, 118.95, 118.10, 115.08, 112.28, 110.92, 46.37, 21.95. **HRMS (ESI$^+$) *m/z*:** $[M+H]^+$ calculated for $C_{34}H_{27}BrN_2O_3S$: 623.0999, found: 623.0989; **HPLC:** The enantiomeric excess was determined using Chiralpak IA column (*n*-Hexane/ *i*-PrOH=70:30, flow rate=1.0 mL/min, λ= 254 nm, τ_{major} = 21.7 min, τ_{minor} = 39.9 min).

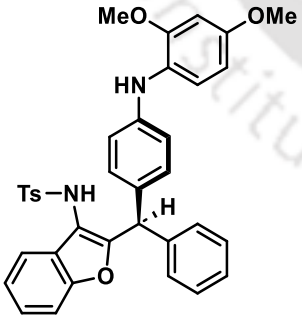

(R)-N-(2-((4-((2,4-dimethoxyphenyl)amino)phenyl)(phenyl) methyl)benzofuran-3-yl)-4-methylbenzenesulfonamide (3u): Brown solid, 28 mg, 47% yield, 91% ee; R_f = 0.5 (petroleum ether : ethyl acetate = 85:15)

^{1}H NMR (400 MHz, DMSO-d6) δ 10.02 (s, 1H), 7.57 - 7.55 (m, 2H), 7.47 (d, J = 8.3 Hz, 1H), 7.27 – 7.21 (m, 4H), 7.21 – 7.16 (m, 3H), 7.16 – 7.12 (m, 1H), 7.12 – 7.07 (m, 2H), 7.06 – 7.01 (m, 2H), 6.83 – 6.78 (m, 2H), 6.71 – 6.66 (m, 2H), 6.63 (t, J = 2.2 Hz, 1H), 6.47 (d, J = 8.6 Hz, 1H), 5.51 (s, 1H), 3.76 (s, 3H), 3.74 (s, 3H), 2.28 (s, 3H). **^{13}C NMR** (101 MHz, DMSO-d6) δ 156.67, 155.24, 153.76, 153.62, 145.67, 144.15, 142.33, 137.84, 130.55, 130.51, 129.97, 129.30, 129.10, 127.75, 127.29, 126.64, 125.21, 123.71, 123.35, 120.74, 115.06, 114.82, 112.25, 105.25, 100.48, 56.40, 56.22, 46.31, 21.95. **HRMS (ESI$^+$) *m/z*:** $[M+H]^+$ calculated

for $C_{36}H_{32}N2O_{5S}$: 605.2105, found: 605.2106; **HPLC:** The enantiomeric excess was determined using Chiralpak IA column (*n*-Hexane/ *i*-PrOH=70:30, flow rate=1.0 mL/min, λ= 254 nm, τ_{major} = 54.6 min, τ_{minor} = 66.6 min).

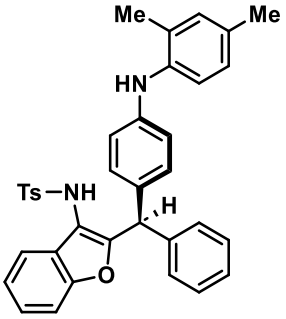

(R)-N-(2-((4-((2,4-dimethylphenyl)amino)phenyl)(phenyl) methyl)benzofuran-3-yl)-4-methylbenzenesulfonamide (3v): Brown solid, 25 mg, 44% yield, 74% ee; R_f = 0.5 (petroleum ether : ethyl acetate = 85:15)

^{1}H NMR (400 MHz, DMSO-d^6) δ 10.02 (s, 1H), 8.12 (s, 1H), 7.50 - 7.48 (m, 3H), 7.32 (d, J = 7.7 Hz, 1H), 7.26 – 7.21 (m, 2H), 7.19 - 7.13 (m, 3H), 7.09 (d, J = 7.9 Hz, 2H), 7.03 (d, J = 8.0 Hz, 2H), 6.95 - 6.92 (m, 5H), 6.83 - 6.77 (m, 3H), 5.62 (s, 1H), 2.26 (s, 3H), 2.25 (s, 3H), 2.05 (s, 3H). **^{13}C NMR** (101 MHz, DMSO-d^6) δ 155.41, 153.70, 144.34, 143.93, 142.71, 137.70, 137.41, 136.43, 136.36, 132.28, 132.04, 130.26, 130.15, 130.06, 128.53, 127.50, 127.27, 126.91, 125.16, 123.74, 120.82, 120.41, 117.45, 117.43, 114.54, 112.24, 43.10, 21.95, 21.52, 20.23. **HRMS (ESI$^+$) *m/z*:** $[M+H]^+$ calculated for $C_{36}H_{32}N2O_{3S}$: 573.2207, found: 573.2207; **HPLC:** The enantiomeric excess was determined using Chiralpak IA column (*n*-Hexane/ *i*-PrOH=70:30, flow rate=1.0 mL/min, λ= 254 nm, τ_{major} = 17.9 min, τ_{minor} = 39.8 min).

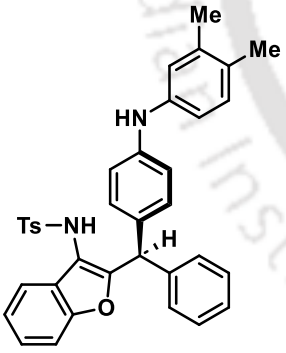

(R)-N-(2-((4-((3,4-dimethylphenyl)amino)phenyl)(phenyl) methyl)benzofuran-3-yl)-4-methylbenzenesulfonamide (3w): Yellow solid, 27 mg, 47% yield, 83% ee; R_f = 0.5 (petroleum ether : ethyl acetate = 85:15)

^{1}H NMR (400 MHz, DMSO-d^6) δ 9.98 (s, 1H), 8.08 (s, 1H), 7.46 - 7.44 (m, 3H), 7.28 (d, J = 7.7 Hz, 1H), 7.16 (m, 5H), 7.05 (d, J = 7.9 Hz, 2H), 6.99 (d, J = 8.0 Hz, 2H), 6.91 - 6.88 (m, 5H), 6.79 - 6.73 (m, 3H), 5.58 (s, 1H), 2.22 (s, 3H), 2.21 (s, 3H), 2.01 (s, 3H).**^{13}C NMR** (101 MHz, DMSO-d^6) δ 155.82, 154.12, 144.76, 144.34, 143.12, 138.11, 137.83, 136.84, 136.78, 132.69, 132.45, 130.68, 130.57, 130.47, 128.95, 127.92, 127.68, 127.33, 125.57, 124.16, 121.24, 120.83, 117.87, 117.85, 114.96, 112.66, 43.52, 22.36, 21.94, 20.65. **HRMS (ESI$^+$) *m/z*:** $[M+H]^+$ calculated for $C_{36}H_{32}N2O_{3S}$: 573.2207, found: 573.2236; **HPLC:** The enantiomeric excess was determined using Chiralpak IA column (*n*-Hexane/ *i*-PrOH=70:30, flow rate=1.0 mL/min, λ= 254 nm, τ_{major} = 24.2 min, τ_{minor} = 45.3 min).

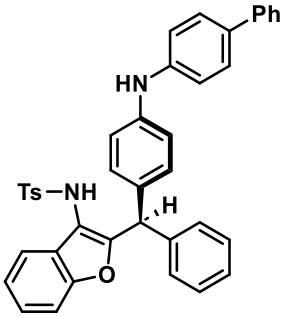

(R)-N-(2-((4-([1,1'-biphenyl]-4-ylamino)phenyl) (phenyl)methyl)benzofuran-3-yl)-4-methylbenzenesulfonamide (3x): Pale yellow solid, 35 mg, 57% yield, 89% ee; R_f = 0.5 (petroleum ether : ethyl acetate = 85:15)

^{1}H NMR (500 MHz, DMSO-d^6) δ 10.04 (s, 1H), 8.32 (s, 1H), 7.62 - 7.57 (m, 4H), 7.55 (d, J = 8.3 Hz, 2H), 7.49 (d, J = 8.2 Hz, 1H), 7.42 (t, J = 7.7 Hz, 2H), 7.30- 7.25 (m, 4H), 7.24 (d, J = 7.4 Hz, 2H), 7.20 (d, J = 8.1 Hz, 2H), 7.17 – 7.13 (m, 3H), 7.09 (d, J = 7.6 Hz, 2H), 7.04 (d, J = 8.3 Hz, 2H), 6.96 (d, J = 8.2 Hz, 2H), 5.60 (s, 1H), 2.29 (s, 3H).**^{13}C NMR** (126 MHz, DMSO-d^6) δ 154.44, 153.22, 143.66, 143.48, 142.10, 141.62, 140.54, 137.38, 132.56, 131.58, 130.04, 129.79, 129.29, 128.90, 128.70, 127.82, 127.28, 126.93, 126.82, 126.22, 126.17, 124.82, 123.28, 120.33, 117.38, 117.12, 114.60, 111.81, 45.95, 21.50. **HRMS (ESI$^+$) *m/z*:** $[M+H]^+$ calculated for $C_{40}H_{32}N2O_{3S}$: 621.2207, found: 621.2189; **HPLC:** The enantiomeric excess was determined using Chiralpak IA column (*n*-Hexane/ *i*-PrOH=70:30, flow rate=1.0 mL/min, λ= 220 nm, τ_{major} = 10.7 min, τ_{minor} = 15.5 min).

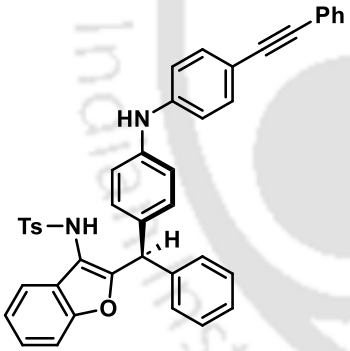

(R)-4-methyl-N-(2-(phenyl(4-((4-(phenylethynyl) phenyl)amino)phenyl)methyl) benzofuran-3-yl)benzenesulfonamide (3y): Brown solid, 26 mg, 40% yield, 86% ee; R_f = 0.5 (petroleum ether : ethyl acetate = 85:15).

^{1}H NMR (500 MHz, DMSO-d^6) δ 10.05 (s, 1H), 8.53 (s, 1H), 7.58 (d, J = 8.0 Hz, 2H), 7.50 (t, J = 7.3 Hz, 3H), 7.41 - 7.37 (m, 5H), 7.31 – 7.27 (m, 3H), 7.27 – 7.23 (m, 3H), 7.20 (d, J = 7.9 Hz, 2H), 7.11 – 7.07 (m, 2H), 7.00 - 7.05 (m, 4H), 6.98 (d, J = 8.4 Hz, 2H), 5.61 (s, 1H), 2.28 (s, 3H). **^{13}C NMR** (126 MHz, DMSO-d^6) δ 154.28, 153.23, 144.74, 143.66, 141.49, 141.06, 137.36, 133.58, 133.10, 131.49, 130.04, 129.82, 129.15, 128.91, 128.73, 127.28, 126.98, 126.14, 126.09, 124.86, 123.49, 123.30, 120.34, 118.51, 115.81, 114.67, 112.30, 111.82, 90.86, 88.05, 45.96, 21.49. **HRMS (ESI$^+$) *m/z*:** $[M+H]^+$ calculated for $C_{42}H_{32}N_2O_3S$: 645.2207, found: 645.2192; **HPLC:** The enantiomeric excess was determined using Chiralpak AD-H column (*n*-Hexane/ *i*-PrOH=70:30, flow rate=1.0 mL/min, λ= 254 nm, τ_{major} = 12.8 min, τ_{minor} = 21.0 min).

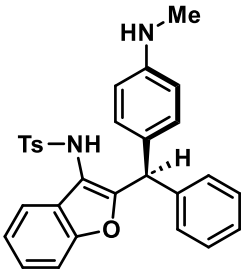

(R)-4-methyl-N-(2-((4-(methylamino)phenyl)(phenyl) methyl)benzofuran-3-yl)benzenesulfonamide (9): Brown solid, 19.7 mg, 41% yield, 16% ee; R_f = 0.5 (petroleum ether : ethyl acetate = 85:15).

^{1}H NMR (500 MHz, DMSO-d^6) δ 9.97 (s, 1H), 7.56 (d, J = 8.2 Hz, 2H), 7.46 (d, J = 8.6 Hz, 1H), 7.26 - 7.17 (m, 7H), 7.12 (t, J = 7.4 Hz, 1H), 7.06 – 7.00 (m, 2H), 6.80 (d, J = 8.3 Hz, 2H), 6.49 – 6.37 (m, 2H), 5.56 (d, J = 5.1 Hz, 1H), 5.49 (s, 1H), 2.64 (d, J = 4.9 Hz, 3H), 2.29 (s, 3H). **^{13}C NMR** (126 MHz, DMSO-d^6) δ 155.54, 153.37, 149.46, 142.54, 137.85, 130.47, 130.03, 129.03, 129.326, 129.00, 128.36, 127.7, 126.65, 125.13, 123.64, 120.54, 114.65, 112.29, 112.18, 80.17, 79.90, 79.64, 46.22, 30.68, 21.93. **HRMS (ESI$^+$) *m/z*:** $[M+H]^+$ calculated for $C_{29}H_{26}N_2O_3S$: 483.1737, found: 483.1719; **HPLC:** The enantiomeric excess was determined using Chiralpak IA column (*n*-Hexane/ *i*-PrOH=80:20, flow rate=1.0 mL/min, λ= 254 nm, τ_{major} = 26.0 min, τ_{minor} = 29.1 min).

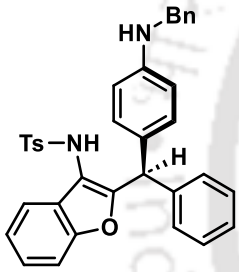

(R)-N-(2-((4-(benzylamino)phenyl)(phenyl)methyl)benzofuran-3-yl)-4-methyl benzenesulfonamide (10): Yellow solid, 16.5 mg, 30% yield, 30% ee; R_f = 0.5 (petroleum ether : ethyl acetate = 85:15).

^{1}H NMR (400 MHz, DMSO-d^6) δ 9.98 (s, 1H), 7.55 (d, J = 8.2 Hz, 2H), 7.46 (d, J = 7.9 Hz, 1H), 7.38 – 7.29 (m, 4H), 7.26 – 7.18 (m, 6H), 7.16 (d, J = 8.0 Hz, 2H), 7.12 (t, J = 7.0 Hz, 1H), 7.00 (d, J = 7.0 Hz, 2H), 6.73 (d, J = 8.5 Hz, 2H), 6.46 (d, J = 8.7 Hz, 2H), 6.25 (t, J = 6.0 Hz, 1H), 5.44 (s, 1H), 4.23 (d, J = 5.9 Hz, 2H), 2.27 (s, 3H). **^{13}C NMR** (126 MHz, DMSO-d^6) δ 154.99, 153.65, 144.29, 144.03, 142.84, 142.06, 138.13, 137.83, 132.73, 130.44, 130.18, 130.04, 129.91, 129.03, 128.04, 127.71, 126.67, 126.45, 125.23, 123.72, 120.79, 120.47, 117.52, 117.37, 114.90, 112.26, 46.30, 22.03, 21.92. **HRMS (ESI$^+$) *m/z*:** $[M+H]^+$ calculated for $C_{35}H_{30}N2O_{3S}$: 559.2050, found: 559.2056; **HPLC:** The enantiomeric excess was determined using Chiralpak AD-H column (*n*-Hexane/ *i*-PrOH=70:30, flow rate=1.0 mL/min, λ= 254 nm, τ_{major} = 13.1min, τ_{minor} = 15.8 min).

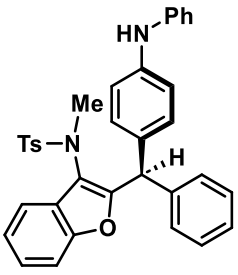

4: Brown solid (49.1 mg, 88% yield, 92% ee). **^{1}H NMR** (500 MHz, DMSO-d^6) δ 8.10 (s, 1H), 7.53 (d, *J* = 8.0 Hz, 2H), 7.44 (d, *J* = 8.3 Hz, 1H), 7.23 (d, *J* = 7.8 Hz, 1H), 7.18 (q, *J* = 8.0 Hz, 3H), 7.14 (d, *J* = 8.1 Hz, 2H), 7.13 - 6.87 (m, 2H), 7.01 (d, *J* = 7.9 Hz, 2H), 6.98 (d, *J* = 7.6 Hz, 1H), 6.93 (d, *J* = 8.4 Hz, 2H), 6.88 – 6.84 (m, 3H), 6.83 (d, *J* = 7.8 Hz, 1H), 6.76 (t, *J* = 7.3 Hz, 1H), 5.48 (s, 1H), 2.22 (s, 3H), 2.20 (s, 3H). ^{13}C NMR (126 MHz, DMSO-d^6) δ 154.74, 153.39, 144.04, 143.78, 142.59, 141.81, 137.87,

137.58, 132.48, 130.19, 129.93, 129.79, 129.66, 128.78, 127.79, 127.46, 126.42, 126.20, 124.98, 123.46, 120.53, 120.22, 117.27, 117.12, 114.65, 112.01, 46.05, 21.78, 21.67. **HRMS (ESI+) (m/z):** [M+H]+ calcd for $C_{35}H_{30}N_2O_3S$: 559.2050, found: 559.2037; **HPLC:** The enantiomeric excess was determined using Chiral-select OM column (n-Hexane/ i-PrOH=80:20, flow rate=1.0 mL/min, λmax= 254 nm, τmajor = 13.4 min, τminor = 20.9 min).

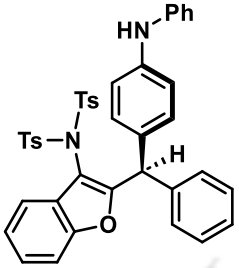

5: Yellow solid (64 mg, 92% yield, 92% ee). **^{1}H NMR** (400 MHz, DMSO-d^6) δ 8.22 (s, 1H), 7.64 - 7.61 (m,, 3H), 7.58 (d, J = 8.3 Hz, 2H), 7.38 - 7.33 (m, 4H), 7.33 – 7.26 (m, 4H), 7.25 - 7.19 (m, 2H), 7.20 – 7.14 (m, 2H), 7.13 – 7.07 (m, 3H), 7.06 - 6.98 (m, 4H), 6.83 (t, J = 7.4 Hz, 1H), 6.60 (d, J = 7.8 Hz, 1H), 5.49 (s, 1H), 2.40 (d, J = 2.3 Hz, 6H). **^{13}C NMR** (101 MHz, DMSO-d^6) δ150.46,146.75,144.15, 143.27, 141.99, 135.92, 132.09, 130.78, 130.37, 130.68, 130.08, 129.51, 129.38, 129.31, 127.78, 126.19, 125.94, 124.68, 120.67, 119.81, 117.71, 117.40, 113.34, 112.90, 47.04, 22.17. **HRMS (ESI+) (m/z):** [M+H]+ calcd for $C_{15}H_{34}N_2O_5S_2$: 699.1982, found: 699.1961; **HPLC:** The enantiomeric excess was determined using Chiral-select OM column (n-Hexane/ i-PrOH=80:20, flow rate=1.0 mL/min λmax= 254 nm, τmajor = 11.6 min, τminor = 18.8 min).

3.11. NMR Spectra and HPLC chromatograms:

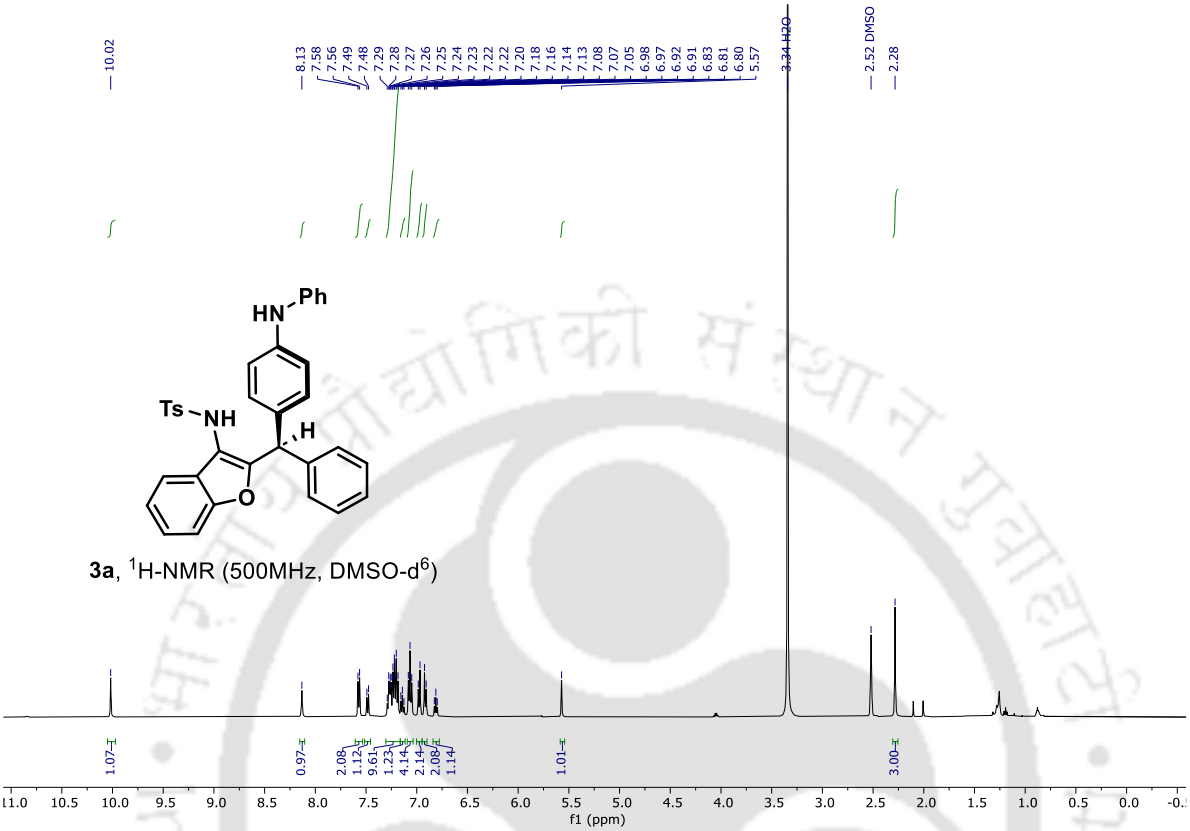

3a, ^{1}H-NMR (500MHz, DMSO-d^{6})

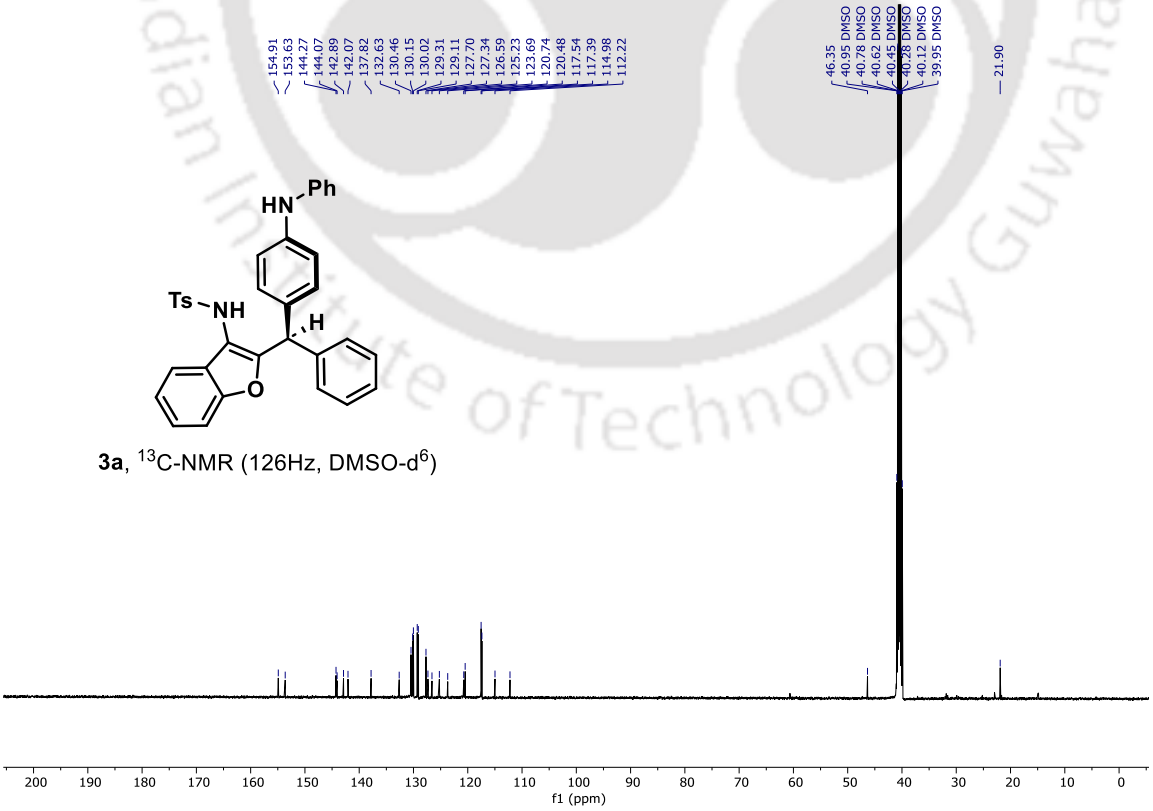

3a, ^{13}C-NMR (126Hz, DMSO-d^{6})

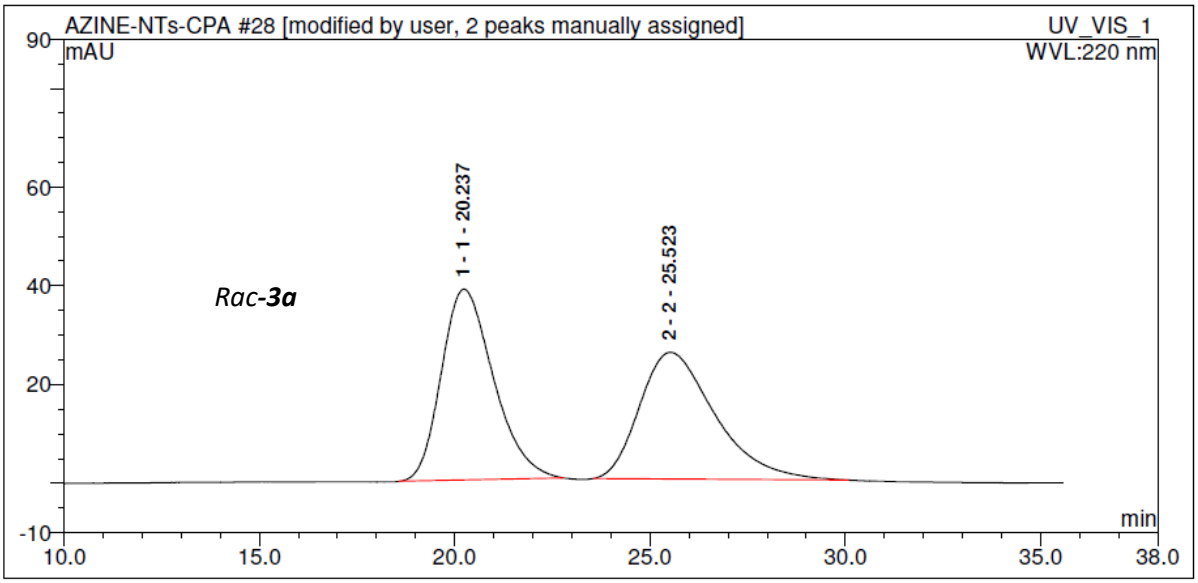

	Peak Name	Ret.Time (detected) min	Area mAU*min	Rel.Area(ident.) %	Height mAU	Amount
1	1	20.23666667	59.83955	51.0815009	38.64492	n.a.
2	2	25.52333333	57.30569	48.9184991	25.64917	n.a.

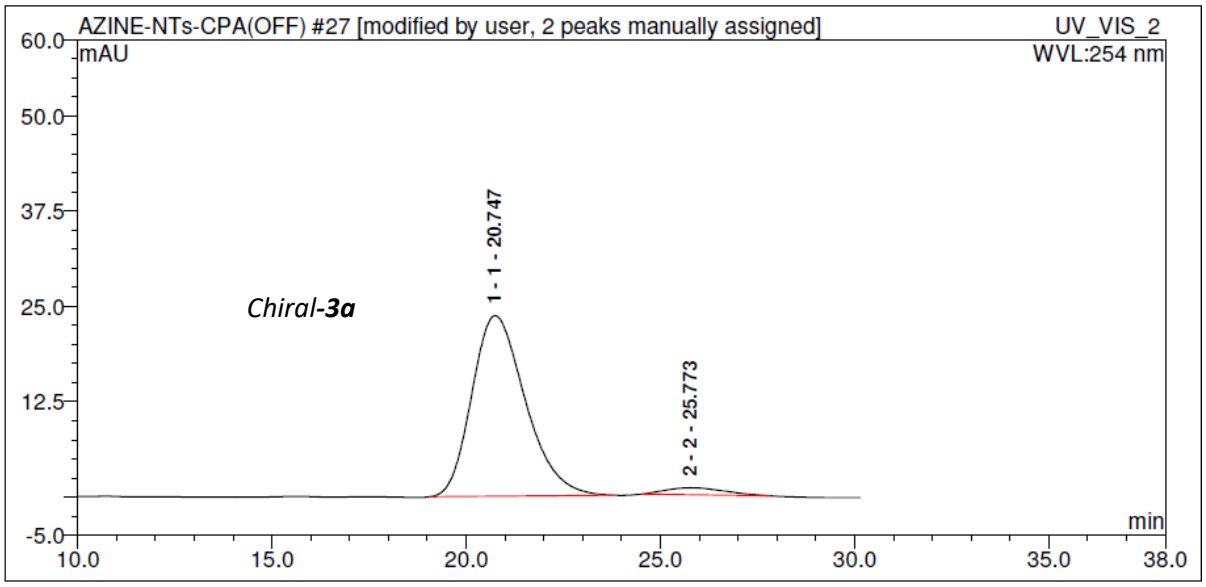

	Peak Name	Ret.Time (detected) min	Area mAU*min	Rel.Area(ident.) %	Height mAU	Amount
1	1	20.74666667	37.86632	95.89683569	23.68565	n.a.
2	2	25.77333333	1.620197	4.103164312	0.90871	n.a.

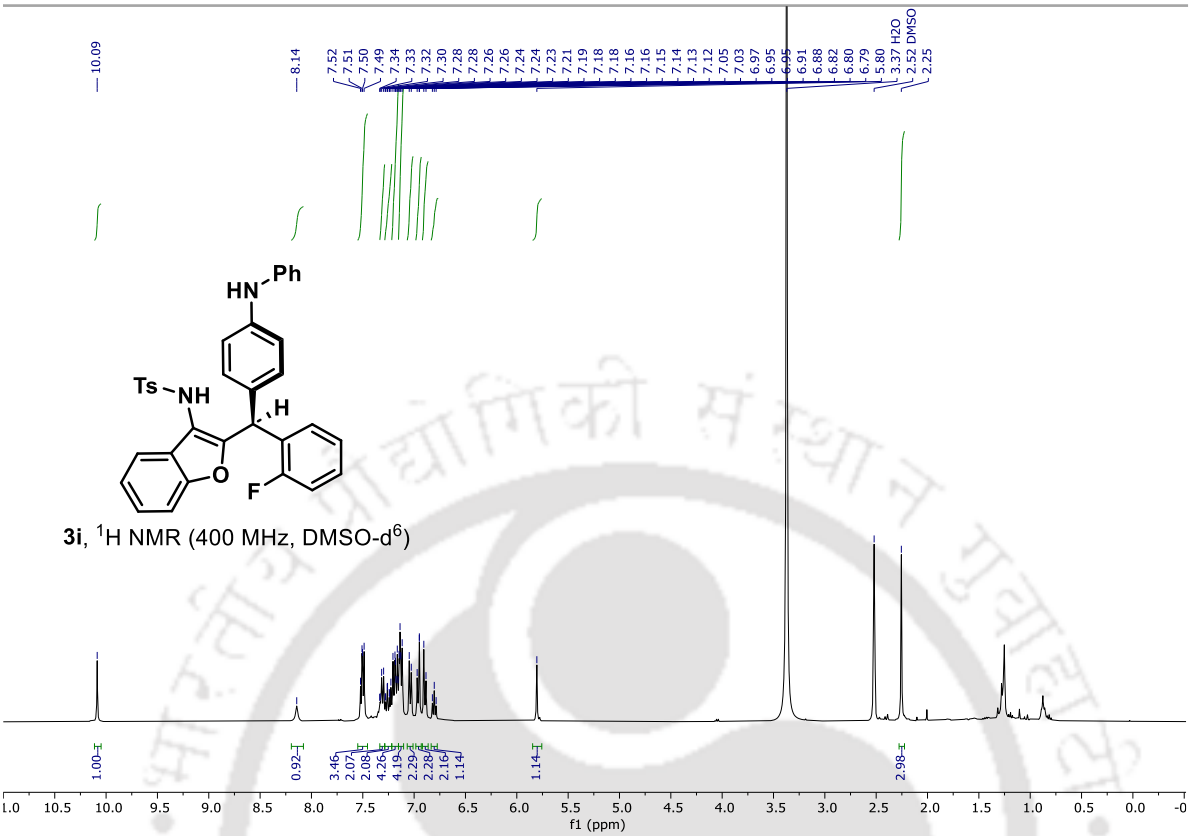

3i, ^{1}H NMR (400 MHz, DMSO-d^{6})

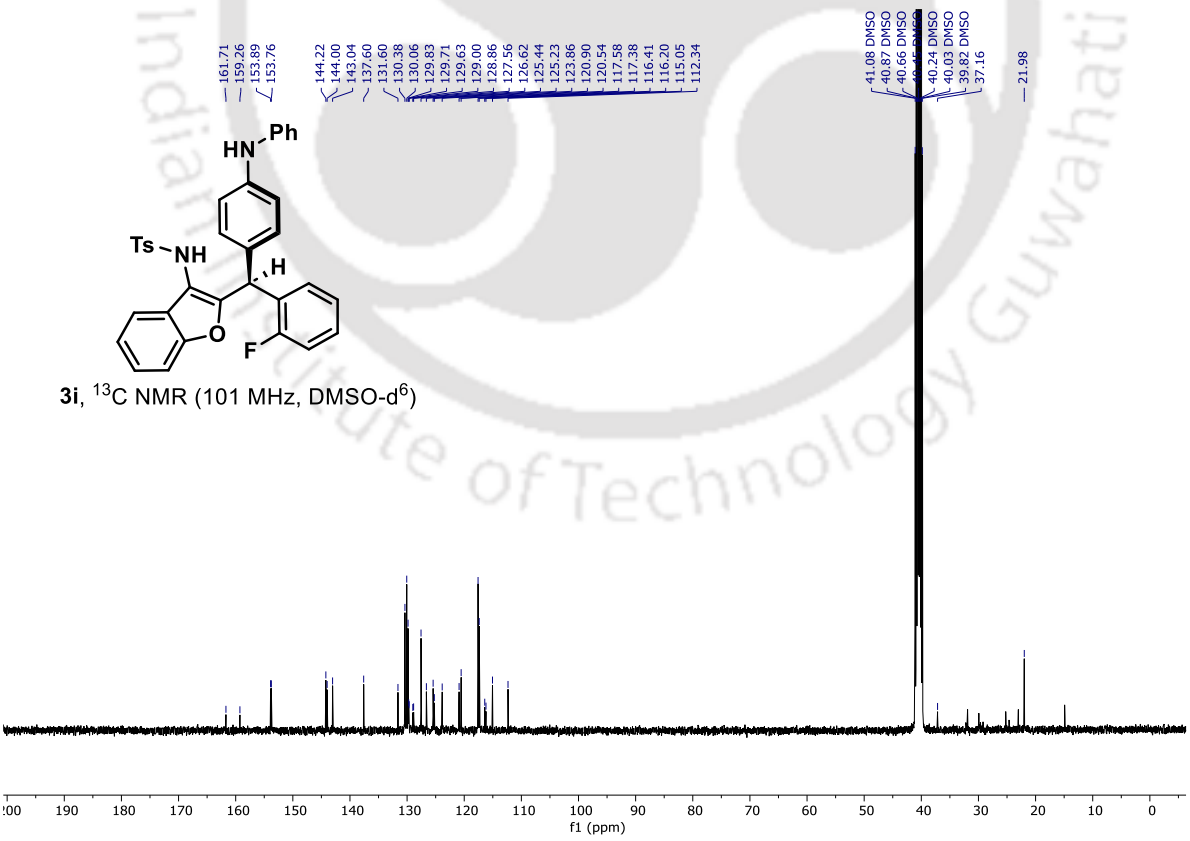

3i, ^{13}C NMR (101 MHz, DMSO-d^{6})

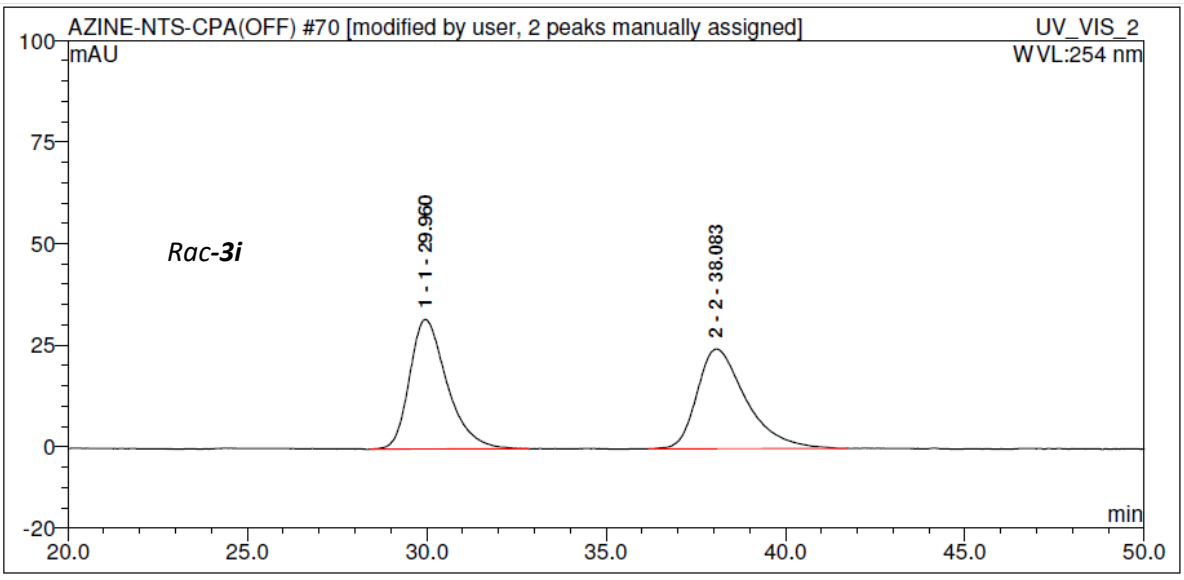

	Peak Name	Ret.Time (detected) min	Area mAU*min	Rel.Area(ident.) %	Height mAU	Amount
1	1	29.96	38.70817	49.99222313	31.90284	n.a.
2	2	38.08333333	38.72021	50.00777687	24.51153	n.a.

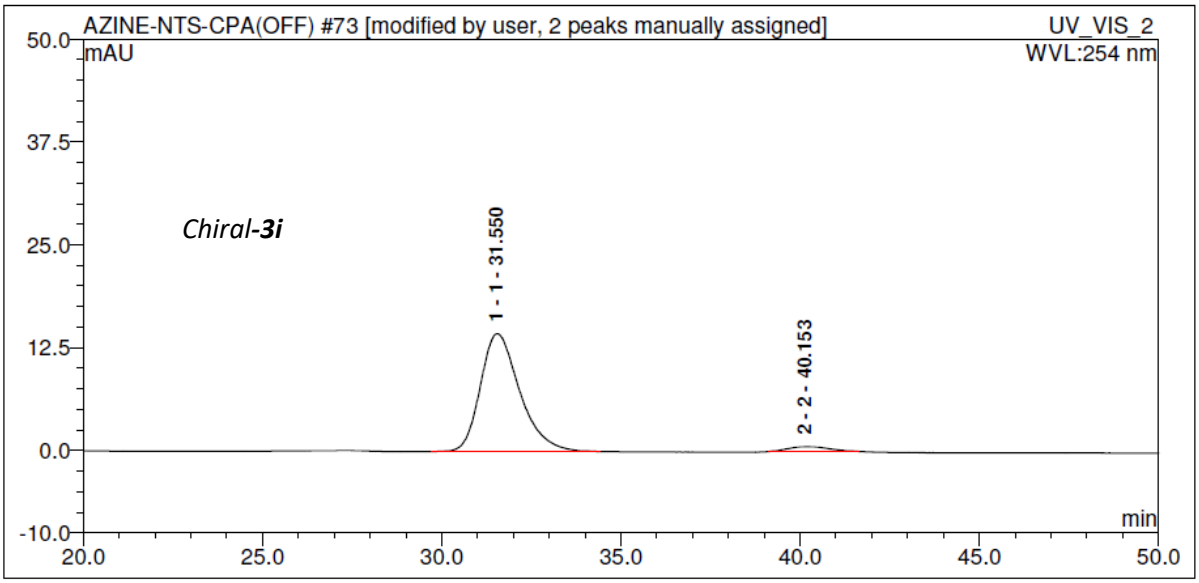

	Peak Name	Ret.Time (detected) min	Area mAU*min	Rel.Area(ident.) %	Height mAU	Amount
1	1	31.55	18.29914	95.86584311	14.34285	n.a.
2	2	40.15333333	0.789139	4.134156891	0.59967	n.a.

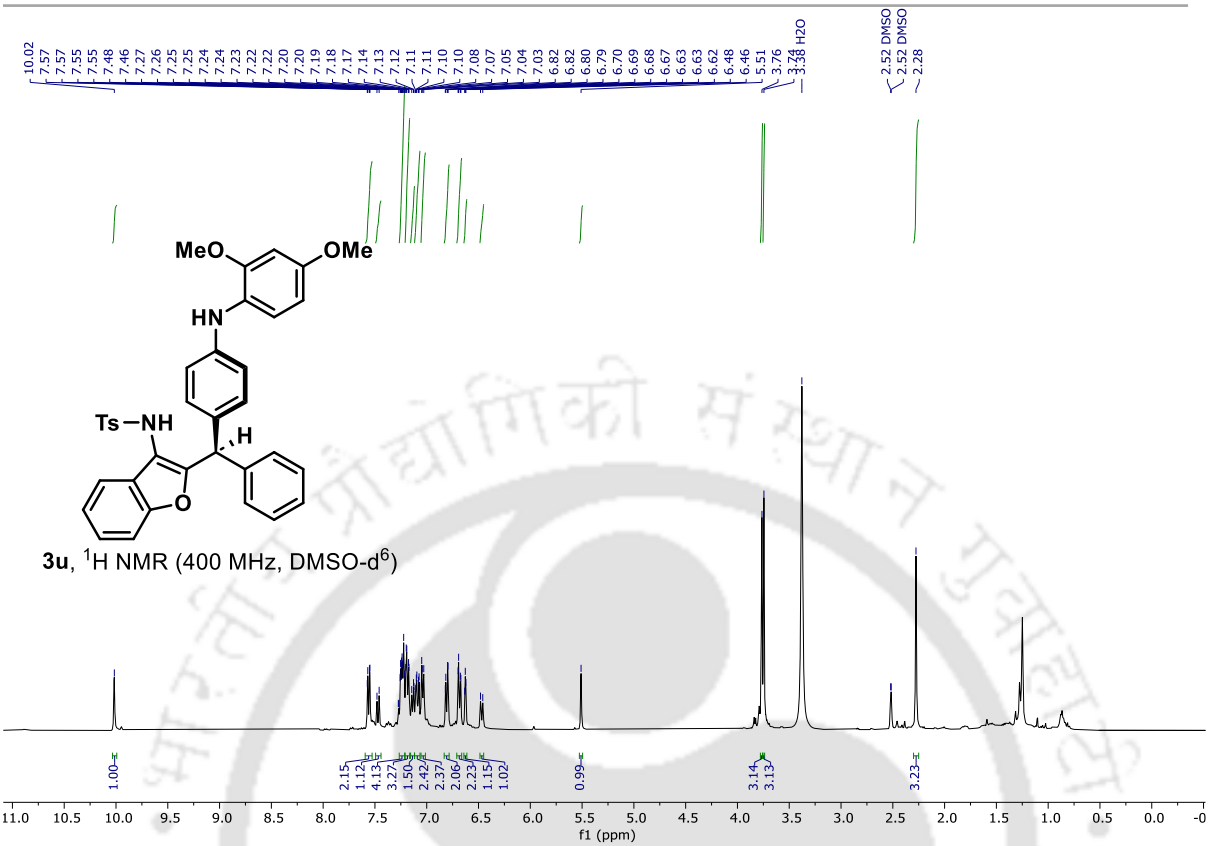

3u, ^{1}H NMR (400 MHz, DMSO-d^{6})

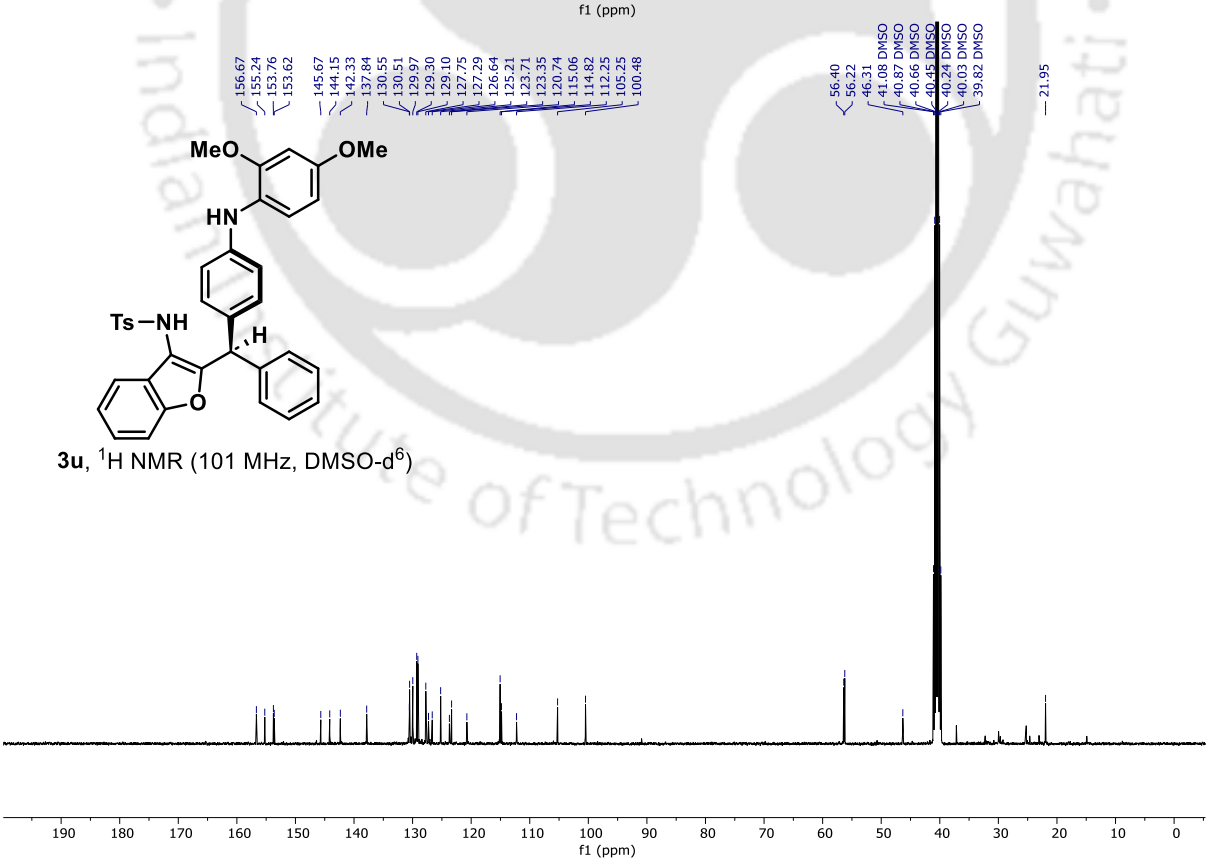

3u, ^{1}H NMR (101 MHz, DMSO-d^{6})

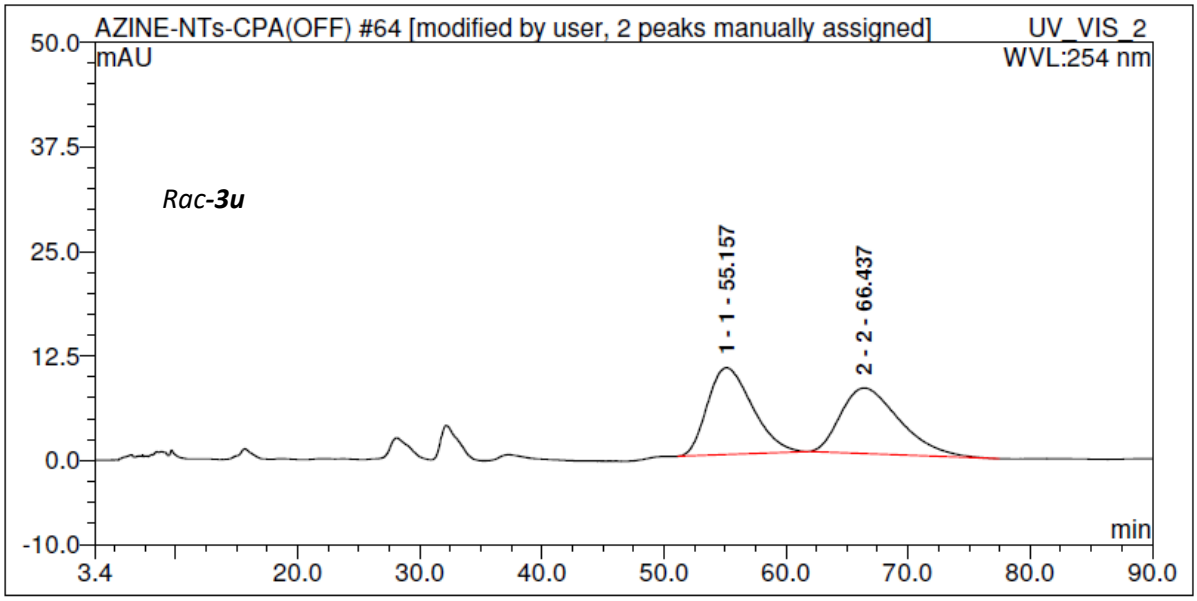

	Peak Name	Ret.Time (detected) min	Area mAU*min	Rel.Area(ident.) %	Height mAU	Amount
1	1	55.16	44.03198	50.24171654	10.36336	n.a.
2	2	66.44	43.608	49.75828346	7.824	n.a.

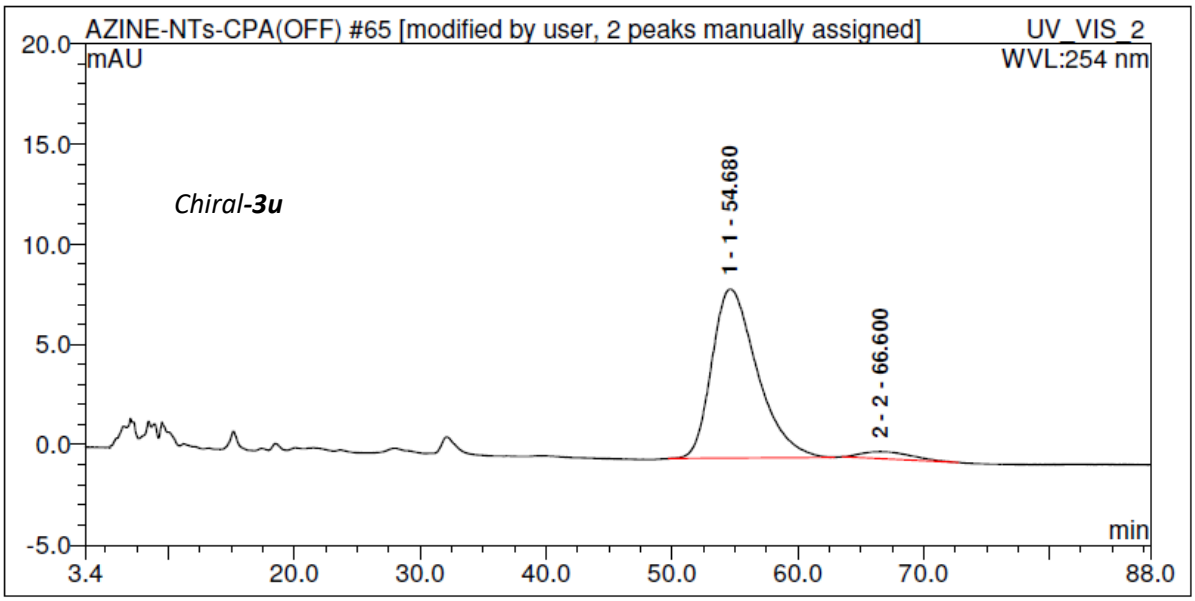

	Peak Name	Ret.Time (detected) min	Area mAU*min	Rel.Area(ident.) %	Height mAU	Amount
1	1	54.68	35.17347	95.61304585	8.42831	n.a.
2	2	66.60	1.614	4.386954151	0.359	n.a.

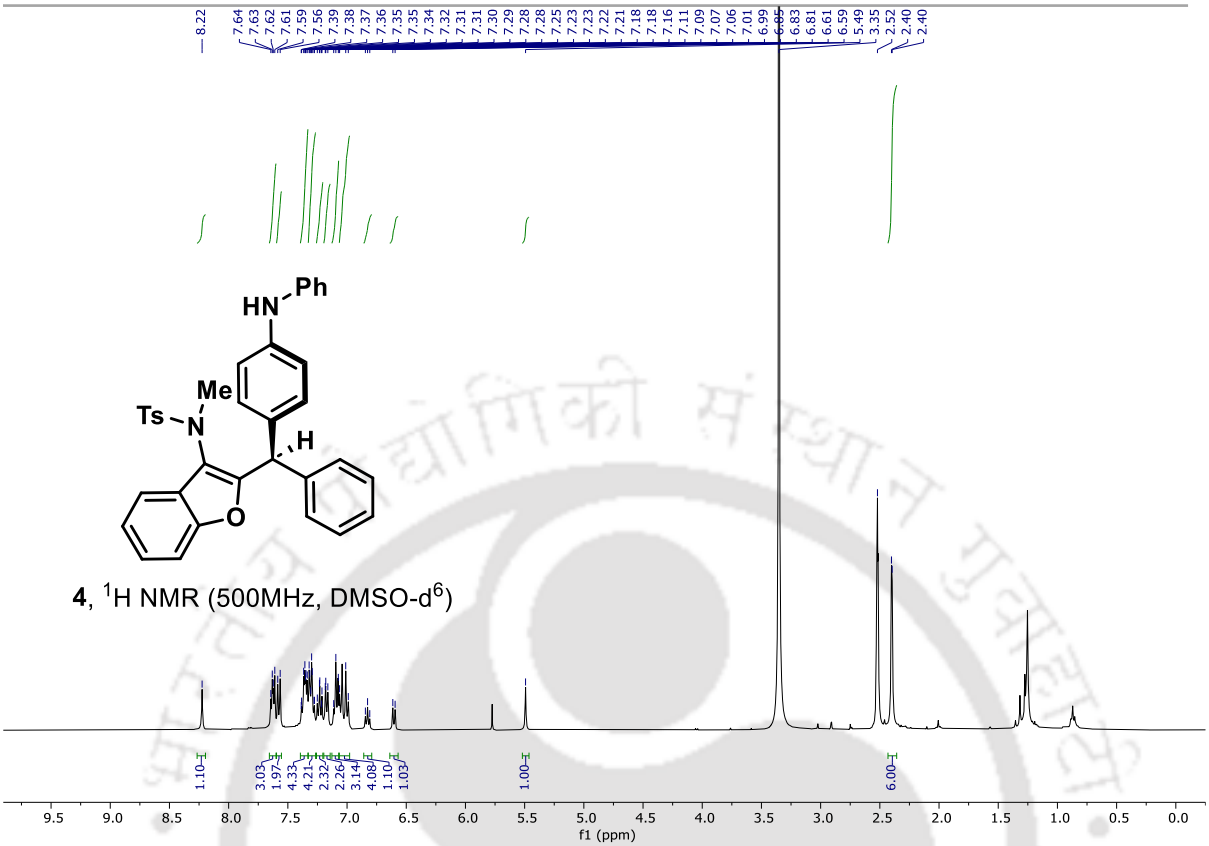

4, ^{1}H NMR (500MHz, DMSO-d^{6})

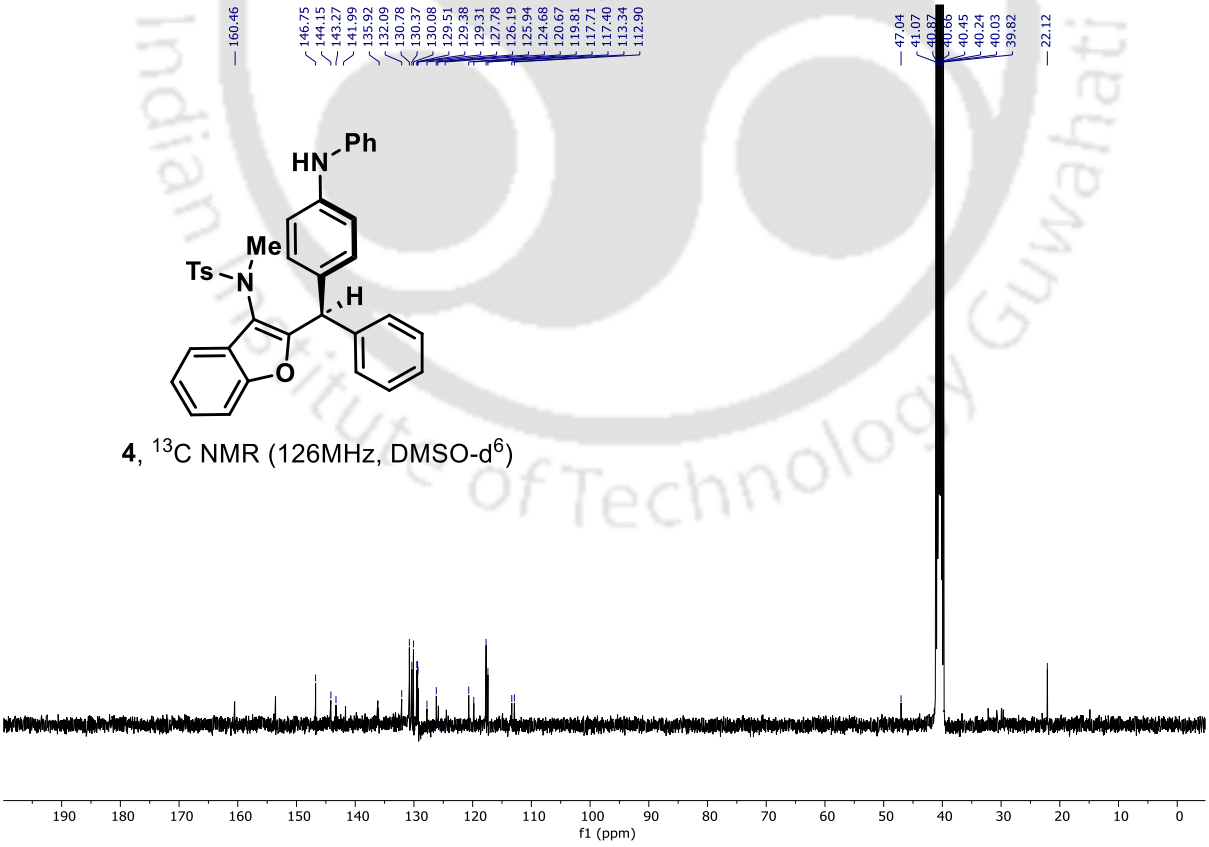

4, ^{13}C NMR (126MHz, DMSO-d^{6})

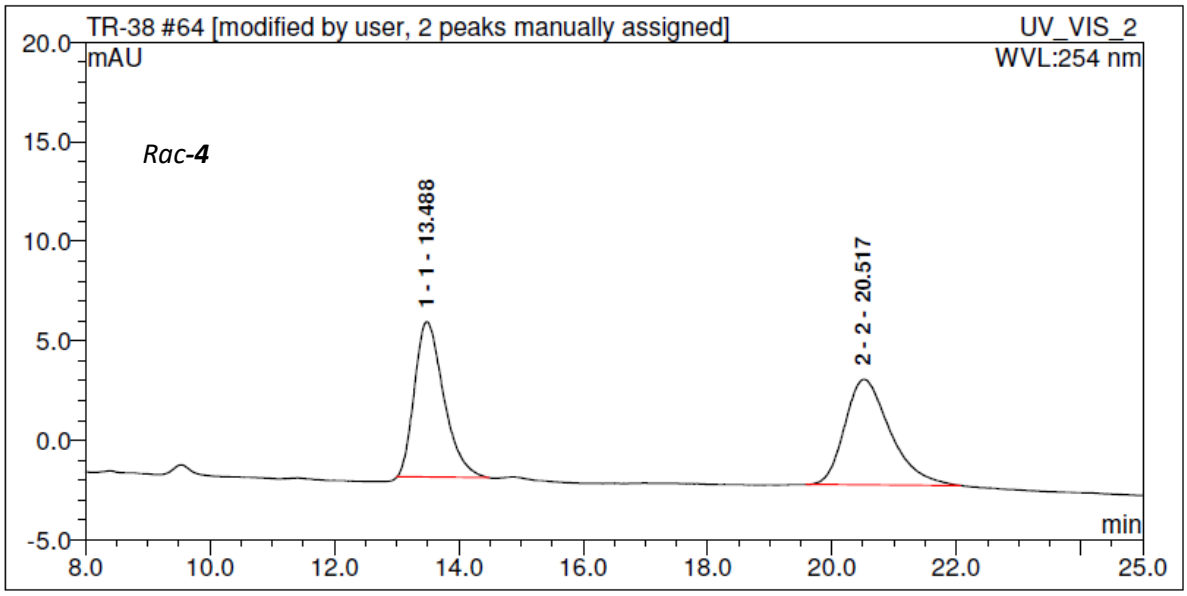

Peak Name	Ret.Time (detected) min	Area mAU*min	Rel.Area(ident.) %	Height mAU	Amount
1 1	13.49	4.259287	48.69296571	7.80147	n.a.
2 2	20.52	4.488	51.30703429	5.293	n.a.

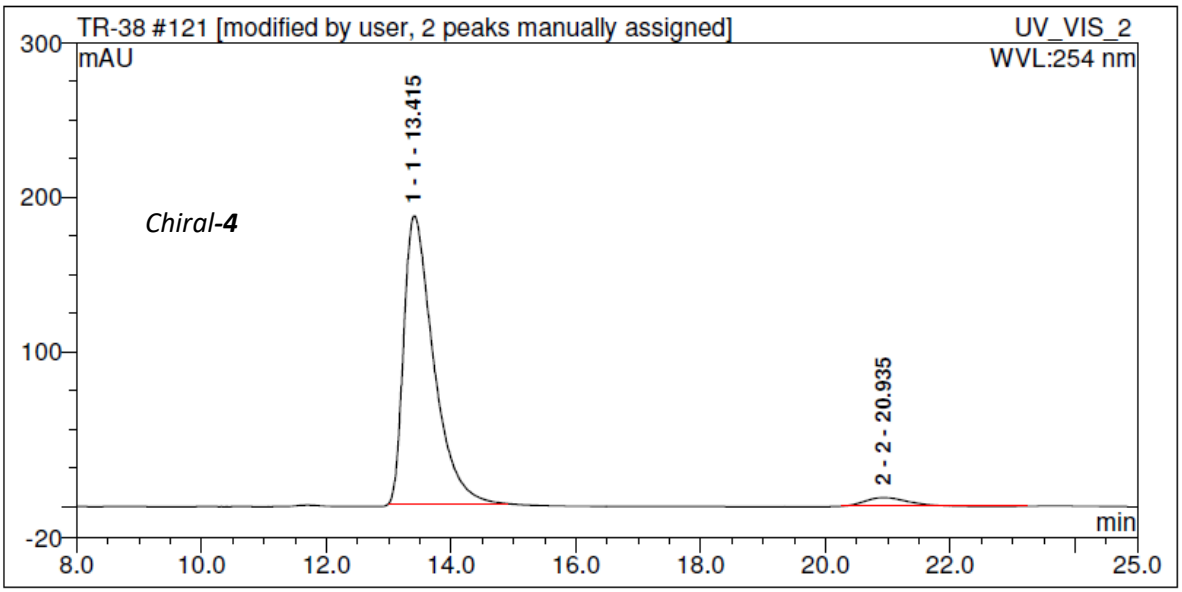

Peak Name	Ret.Time (detected) min	Area mAU*min	Rel.Area(ident.) %	Height mAU	Amount
1 1	13.42	102.5229	95.96243862	185.8448	n.a.
2 2	20.94	4.314	4.037561376	5.571	n.a.

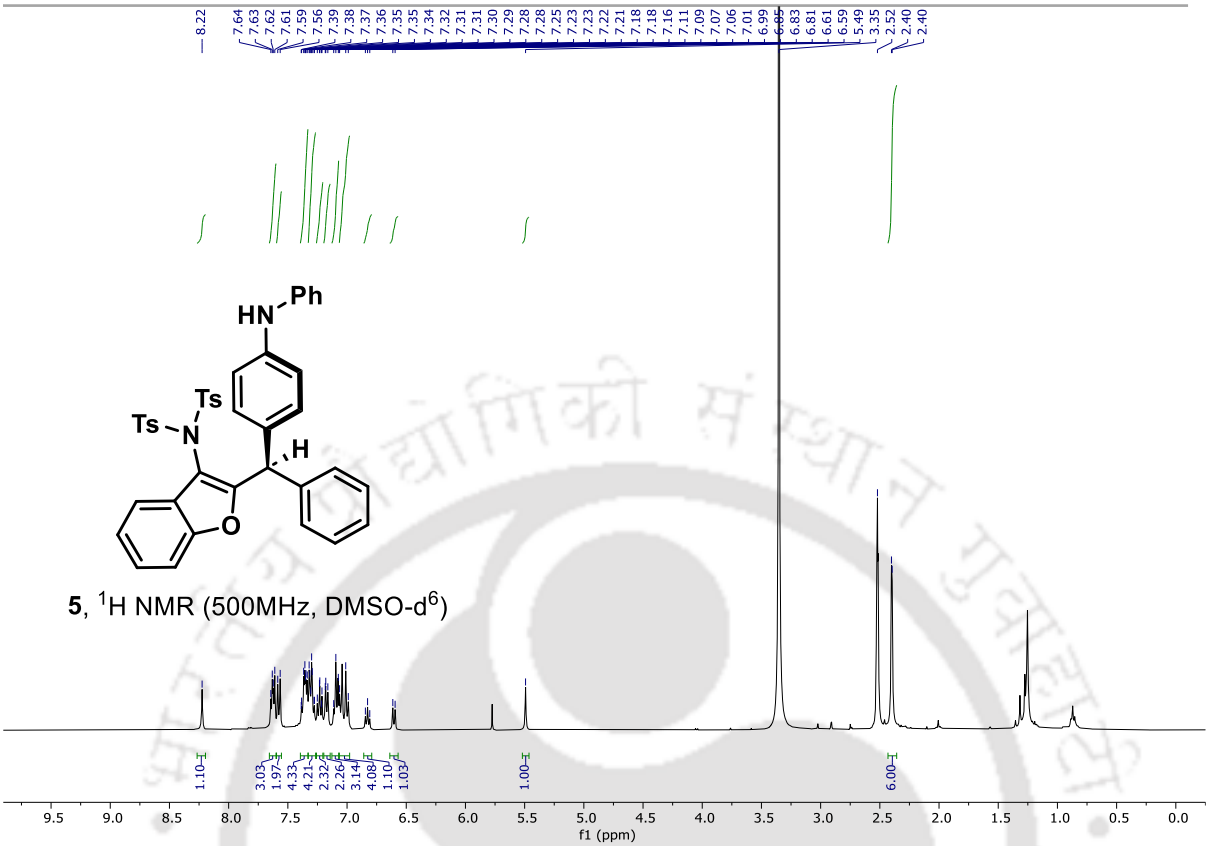

5, ^{1}H NMR (500MHz, DMSO-d^{6})

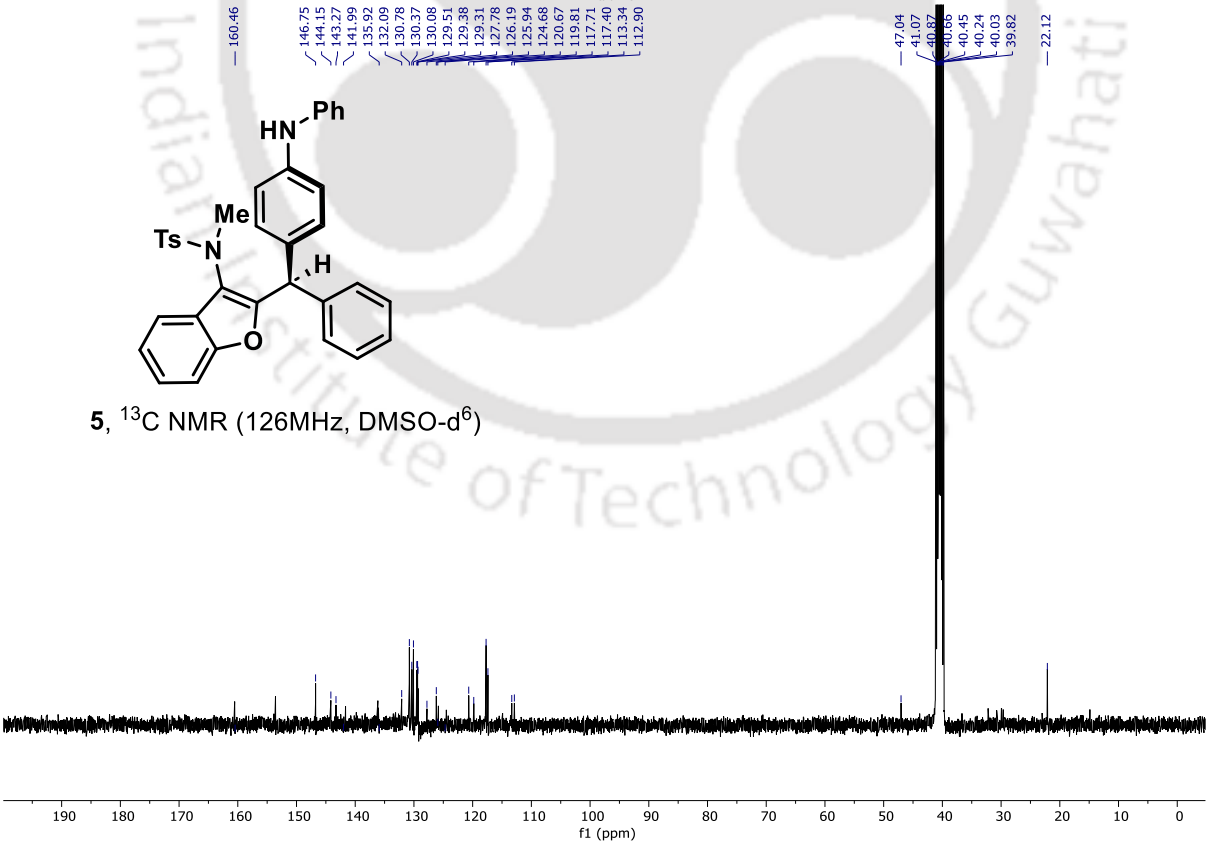

5, ^{13}C NMR (126MHz, DMSO-d^{6})

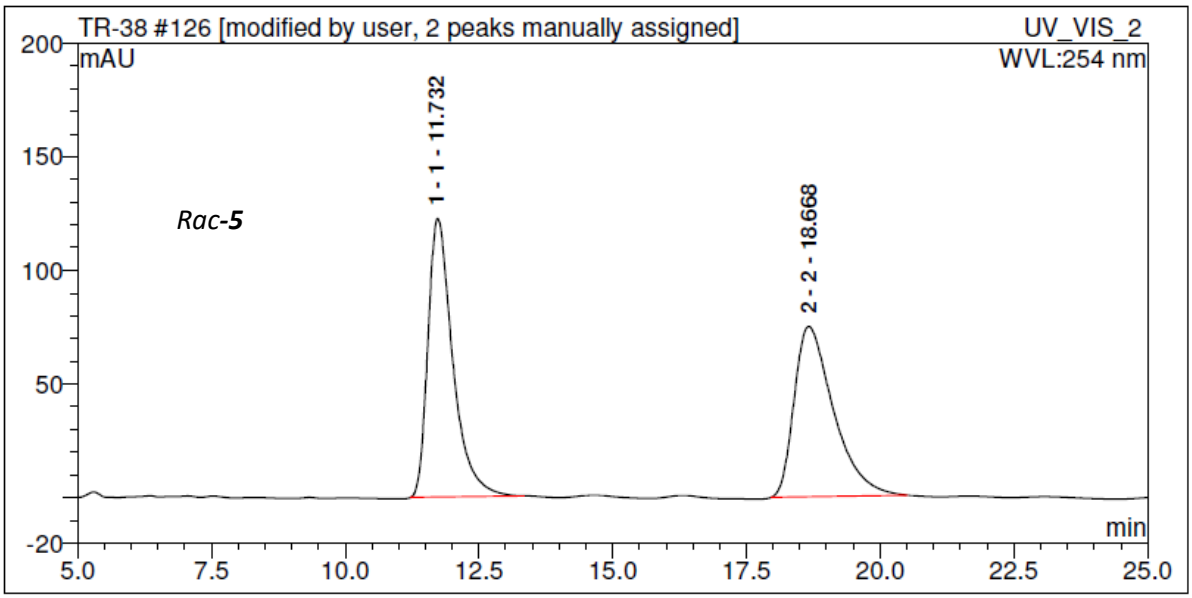

	Peak Name	Ret.Time (detected) min	Area mAU*min	Rel.Area(ident.) %	Height mAU	Amount
1	1	11.73	65.95974	50.83827517	122.3954	n.a.
2	2	18.67	63.785	49.16172483	74.836	n.a.

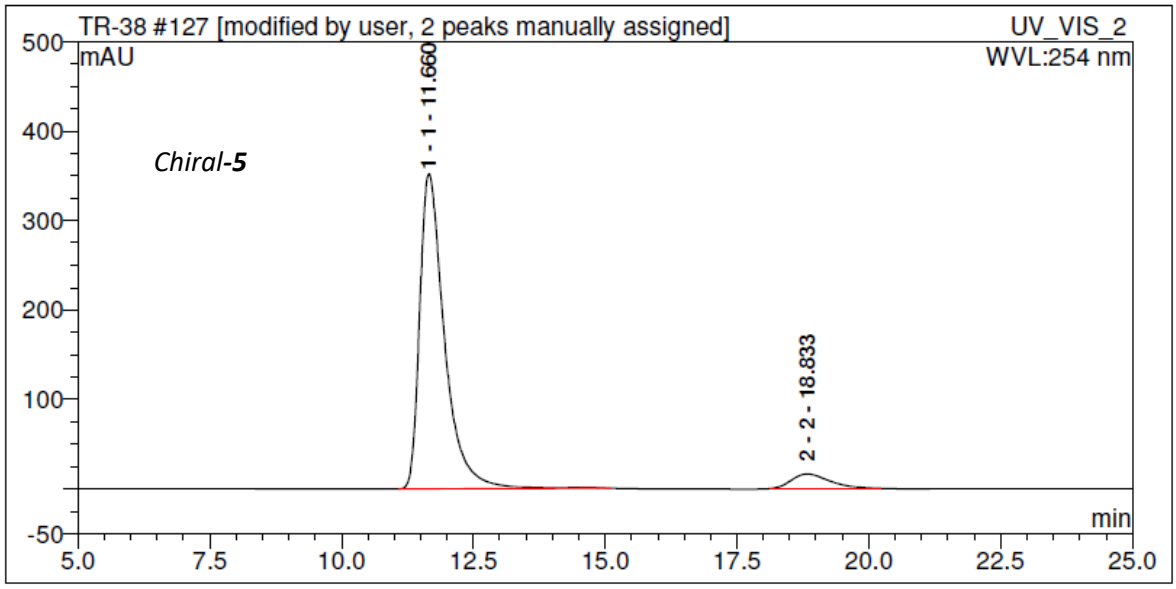

	Peak Name	Ret.Time (detected) min	Area mAU*min	Rel.Area(ident.) %	Height mAU	Amount
1	1	11.66	192.1611	93.3678117	351.8106	n.a.
2	2	18.83	13.650	6.632188304	16.314	n.a.

3.12. References:

1. For selected reviews, see: (a) D. A. Horton, G. T. Bourne, M. L. Smythe, *Chem. Rev.* **2003**, *103*, 893. (b) J. Bariwal, E. Van der Eycken, *Chem. Soc. Rev.* **2013**, *42*, 9283. (c) G. Ulrich, R. Ziessel, A. Harriman, *Angew. Chem., Int. Ed*. **2008**, *47*, 1184. (d) J. A. Bikker, N. Brooijmans, A. Wissner, T. S. Mansour, *J. Med. Chem*. **2009**, *52*, 1493.
2. For a review, see: J. A. Leitch, C. G. Frost, *Synthesis* **2018**, *50*, 2693.
3. For selected recent examples of the *ortho*-C−H functionalization of aniline derivatives, see: (a) F. W. Patureau, F. Glorius, *J. Am. Chem. Soc*. **2010**, *132*, 9982. (b) A. Garcia-Rubia, B. Urones, R. Gomez Arrayas, J. C. Carretero, *Angew. Chem., Int. Ed*. **2011**, *50*, 10927. (c) X. Huang, J. Huang, C. Du, X. Zhang, F. Song, J. You, *Angew. Chem., Int. Ed.* **2013**, *52*, 12970. (d) G. E. M. Crisenza, O. O. Sokolova, J. F. Bower, *Angew. Chem., Int. Ed.* **2015**, *54*, 14866.
4. For selected reviews, see: (a) M. Bandini, A. Melloni, A. Umani-Ronchi, *Angew. Chem., Int. Ed*. **2004**, *43*, 550. (b) T. B. Poulsen, K. A. Jørgensen, *Chem. Rev.* **2008**, *108*, 2903. (c) S.-L. You, Q. Cai, M. Zeng, *Chem. Soc. Rev*. **2009**, *38*, 2190.
5. For examples on N−H functionalization, see: (a) Z. Hou, J. Wang, P. He, J. Wang, B. Qin, X. Liu, L. Lin, X. *Angew. Chem., Int. Ed.* **2010**, *49*, 4763. (b) J. H. Lee, S. Lee, *Chem. Sci*. **2013**, *4*, 2922. (c) C. Du, P.-X. Li, X. Zhu, J.-N. Han, J.-L. Niu, M.-P. Song, *ACS Catal.* **2017**, *7*, 2810. (d) N. J. Adamson, E. Hull, S. J. Malcolmson, *J. Am. Chem. Soc.* **2017**, *139*, 7180. (e) J. M. Dennis, N. A. White, R. Y. Liu, S. L. Buchwald, *J. Am. Chem. Soc*. **2018**, *140*, 4721. For reviews, see: (f) J. F. Hartwig, *Acc. Chem. Res.* **2008**, *41*, 1534. (g) L. Huang, M. Arndt, K. Gooßen, H. Heydt, L. J. Gooßen, *Chem. Rev.* **2015**, *115*, 2596.
6. For selected examples, see: (a) Q. Zhou, H. D. Srinivas, S. Dasgupta, M. P. Watson, *J. Am. Chem. Soc.* **2013**, *135*, 3307. (b) S. C. Matthew, B. W. Glasspoole, P. Eisenberger, C. M. Crudden, *J. Am. Chem. Soc.* **2014**, *136*, 5828. (c) Z.-B. Wang, Y. F. Wong, J.-W. Sun, *Angew. Chem., Int. Ed.* **2015**, *54*, 13711. (d) S.-C. Lu, X.-X. Song, S. B. Poh, H. Yang, M. W. Wong, Y. Zhao, *Chem.- Eur. J.* **2017**, *23*, 2275. (e) F. Jiang, K.-W. Chen, P. Wu, Y.-C. Zhang, Y.-C. Jiao, F. Shi, *Angew. Chem. Int. Ed.* **2019**, *58*, 15104. (f) G.-B. Huang, W.-H. Huang, J. Guo, D.-L. Xu, X.-C. Qu, P.-H. Zhai, X.-H. Zheng, J. Weng, G. Lu, *Adv. Synth. Catal.* **2019**, *361*, 1241. (g) P.-D. Song, L.-L. Hu, T. Yu, J. Jiao, Y.-Q. He, L. Xu, P.-F. Li, *ACS Catal.* **2021**, *11*, 7339. (h) Z.-Y. Han, Y. Zang, C. Liu, W.-G. Guo, H. Huang, J.-W. Sun, *Chem. Commun.* **2022**, *58*, 7128. (i) Q.-L. Yan, M. Duan, C.-E. Chen, Z.-Q. Deng, M.-D. Wu, P.-Y. Yu, M.-L. He, G.-Y. Zhu, K. N. Houk, J.-W. Sun, *Chem. Sci.* **2022**, *13*, 5767. (j) (k) M. Lee, H. M. L. Davies**,** *Org. Lett*. **2023**, *25*, 4000.
7. H. Wulff, B. S. Zhorov, *Chem. Rev*. **2008**, *108*, 174.

8. N. Gathergood, W. Zhuang, K. A. Jørgensen, *J. Am. Chem. Soc*. **2000**, *122*, 12517.
9. N. A. Paras, D. W. C. MacMillan, *J. Am. Chem. Soc*. **2002**, *124*, 7894.
10. Y. Yuan, X. W. Wang, X. Li, K. L. Ding, *J. Org. Chem*. 2004, *69*, 146.
11. S. Shirakawa, R. Berger, J. L. Leighton, *J. Am. Chem. Soc.* **2005**, *127*, 2858.
12. S. Jia, D. Xing, D. Zhang, W. Hu, *Angew. Chem., Int. Ed*. **2014**, *53*, 13098.
13. B. Xu, M.-L. Li, X.-D. Zuo, S.-F. Zhu, Q.-L. Zhou, *J. Am. Chem. Soc.* **2015**, *137*, 8700.
14. J. Chen, L. Zou, C. Zeng, Y. Zhou, B. Fan, *Org. Lett.* **2018**, *20*, 1283.
15. J. Zhou, Z.-H. Li, L. Wang, J.-C. Kang, X.-H. Wang, S.-Y. Zhang, *Org. Lett*. **2021**, *23*, 9353.
16. C. Liu, F.-X. Tan, J. Zhou, H.-Y. Bai, T.-M. Ding, G.-D. Zhu, S.-Y. Zhang, *Org. Lett*. **2020**, *22*, 2173.
17. R.-L. Zhang, B. Liu, K.-X. Qiu, H.-T. Li, H.-N. Zhang, B.-C. Shen, Z.-W. Sun, *Org. Lett*. **2023**, *25*, 1711.
18. For selected very recent examples of the reaction of aurone-derived azadiene, see: (a) B. M. Trost, Z. Zuo, *Angew. Chem., Int. Ed.* **2020**, *59*, 1243. (b) J. Zhou, T.-Z. Li, Y.-W. Sun, B.-X. Du, W. Tan, F. Shi, *ChemCatChem* **2020**, *12*, 4862. (c) S. Frankowski, A. Skrzyńska, L. Sieroń, L. Albrecht, *Adv. Synth. Catal*. **2020**, *362*, 2658. (d) C.-J. Wang, Q.-Q. Yang, M.-X. Wang, Y.-H. Shang, X.-Y. Tong, Y.-H. Deng, Z. Shao, *Org. Chem. Front*. **2020**, 7, 609. (e) B. Jiang, W. Du, Y.-C. Chen, *Chem. Commun.* **2020**, *56*, 7257. (f) J. Yan, X. Li, Y. Chen, Y. Li, W. Chen, R. Zhan, H. Huang, *J. Org. Chem*. **2020**, *85*, 12175. (g) W.-J. Huang, Y.-Y. Ma, L.-X. Liu, B. Wu, G.-F. Jiang, Y.-G. Zhou, *Org. Lett*. **2021**, *23*, 2393. (h) R. Khuntia, S. K. Mahapatra, L. Roy, S. C. Pan, *Chem. Sci*. **2023**, *14*, 10768. (i) S.-S. Qi, J.-Y. Dong, X.-P. Sun, J.-P. Zhai, Y.-B. Sun, Y.-F. Wang, M.-M. Chu, D.-Q. Xu, *J. Org. Chem.* **2024**, *89*, 975. For reviews, see: (j) Q. Deng, X. Meng, *Chem. -Asian J.* **2020**, *15*, 2838. (k) S. K. Saha, A. Bera, S. Singh, N. K. Rana, *Eur. J. Org. Chem*. **2023**, *26*, e202201470.
19. (a) R. Löser, M. Chlupacova, A. Marecek, V. Opletalova, M. Gütschow, *Helv. Chim. Acta*, **2004**, *87*, 2597; (b) M. Morimoto, H. Fukumoto, T. Nozoe, A. Hagiwara, K. Komai, J. Agric, *Food Chem*. **2007**, *55*, 700; (c) Z-Q. Rong, M. Wang, C. H. E. Chow, Y. Zhao, *Chem. Eur. J.* **2016**, *22*, 9483.
20. J. F. Hartwig, M. Kawatsura, S. I. Hauck, K. H. Shaughnessy, L. M. Alcazar-Roman, *J. Org. Chem.* **1999**, *64*, 5575-5580.
21. (a) S. Li, J.-W. Zhang, X.-L. Li, D.-J. Cheng, B. Tan, *J. Am. Chem. Soc*. **2016**, *138*, 16561-16566. b) F. Romanov-Michailidis, L. Guénée, A. Alexakis, *Org. Lett*. **2013**, *15*, 5890-

5893. c) F. Xu, D. Huang, C. Han, W. Shen, X. Lin, Y. Wang, *J. Org. Chem*. **2010**, *75*, 8677-8680. d) I. Čorić, S. Müller, B. List, *J. Am. Chem. Soc*. **2010**, *132*, 17370-17373. e) J.-H. Zhang, J. Liao, X. Cui, K.-B. Yu, J. Zhu, J.-G. Deng, S.-F. Zhu, L.-X. Wang, Q.-L. Zhou, L. W. Chung, T. Ye, *Tetrahedron: Asymmetry* **2002**, *13*, 1363-1366.

Chapter 4

Catalytic Asymmetric de novo Synthesis of Chiral Pyrroles through Desymmetrizing Oxidative [3+2]-Cycloaddition and the Van Leusen Reaction

Abstract: Central chirality in heteroarene derivatives arising from unsymmetrically substituted heteroarene rings is an intriguing but underexplored topic. Herein, we reported the first catalytic enantioselective *de novo* construction of centrally chiral pyrroles through desymmetrizing oxidative [3+2]-cycloaddition by employing silver catalysis. This judicious desymmetrization can produce at least four continuous stereogenic centers without creating any additional stereocenter. Furthermore, to introduce a more diverse set of substituents, we developed the first catalytic asymmetric the Van Leusen reaction with *α*–substituted TosMIC for the synthesis of centrally chiral pyrroles. A wide range of polycyclic 2-substituted, 3,4-fused pyrroles were obtained in high yields and with good to high enantioselectivities. This report includes the elaboration of methanobenzo[*f*]isoindole to synthetically challenging building block chiral isoindole compounds, which are synthesized enantioselectively for the first time.

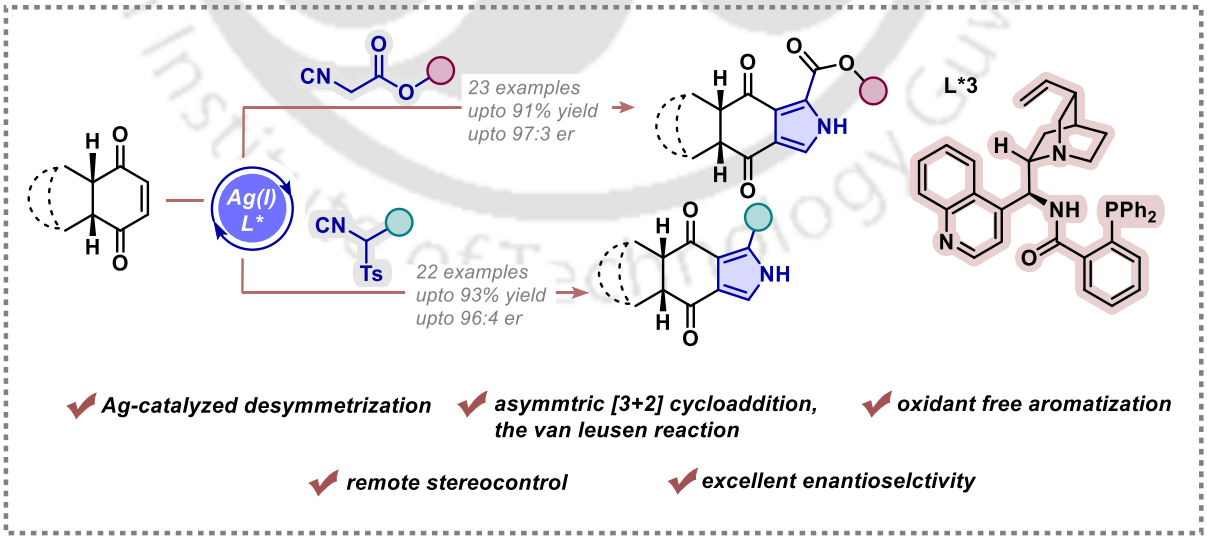

4.1. Introduction:

Pyrrole is one of the most prominent five membered heterocycles which is found in many bioactive natural products and pharmaceuticals.[1] Thus, significant efforts have been given over the years for the synthesis of differently substituted pyrroles.[2] Optically active pyrroles have a wide range of structural and synthetic variations, and the stereogenic centres can appear either close to the heterocyclic unit or remote from the pyrrolic unit.[3] The synthesis of chiral pyrroles fall into four primary categories: (i) chirality is incorporated by substitution at the N-atom; (ii) chirality is incorporated through reactions that take place at the α-position; (iii) chirality is incorporated through reactions that take place at the β-position; and (iv) pyrroles with axial chirality.[3] The first three categories constitute the centrally chiral pyrroles.

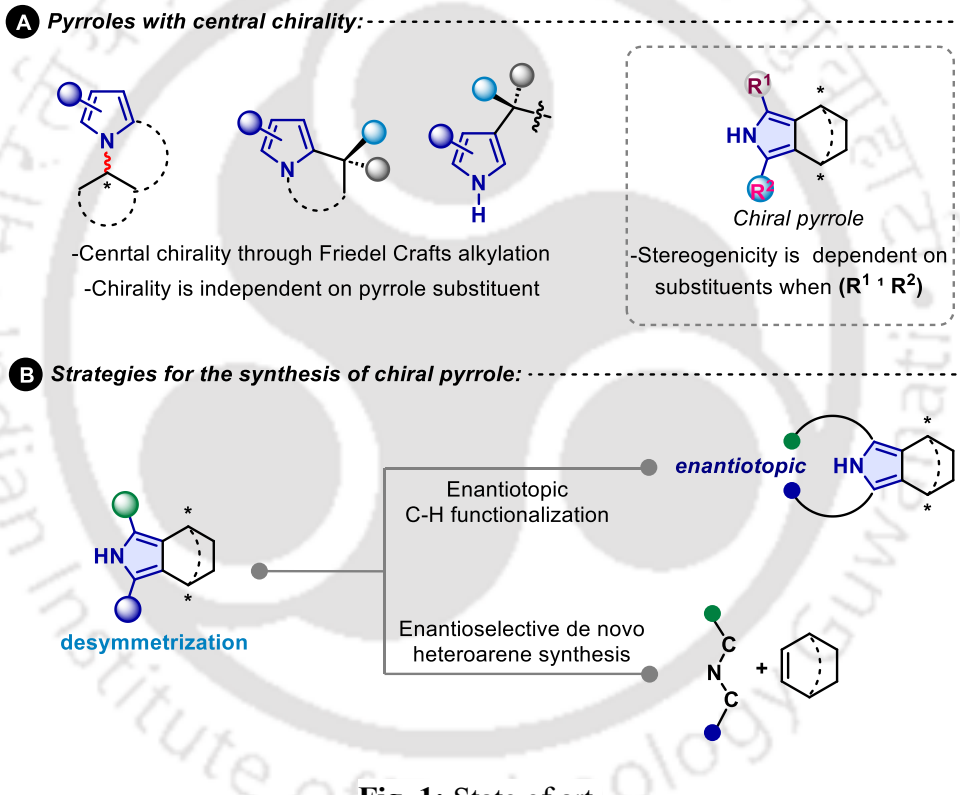

Fig. 1: State of art.

In fact, there are several techniques for the enantioselective synthesis of centrally chiral pyrroles, which are exceedingly prevalent and frequently include one or more chiral centres near to their framework.[4,5] However, in the majority of these instances, the origin of stereogenicity is unrelated to the pyrrole ring substitution pattern (Fig. 1). A fascinating but understudied area is central chirality in pyrrole derivatives resulting from asymmetrical substitution on the pyrrole ring. The substituents in these pyrrole motifs (such as R^1 and R^2, in Fig 1A) not only control their chirality, but they also produce enantiomeric pyrroles when

their positions are switched. Therefore, the enantioselective synthesis of chiral pyrroles presents significant challenges, particularly when attempting to introduce a functional group or substituent to pre-existing symmetrical pyrrole frameworks in an enantioposition-selective manner (Fig. 1B). The lack of functionality on the pyrrole unit in these compounds adds an additional layer of complexity to their enantioselective synthesis. An alternative strategy involves the *de novo* construction of the unsymmetrical pyrrole ring during the enantioselectivity-determining step.

4.2. Previous Study:

4.2.1. Selected examples of catalytic asymmetric *de novo* synthesis of chiral pyrroles:

In 2017, Tan and co-workers reported catalytic asymmetric Paal–Knorr reaction for the synthesis of axially chiral arylpyrroles.[6] High yields and excellent to outstanding enantioselectivities were achieved in the synthesis of a wide variety of C-N axially chiral arylpyrroles (Scheme 1). The authors described, to achieve effective enantiocontrol, a combined-acid catalytic system that includes both a Lewis acid and a chiral phosphoric acid is essential.

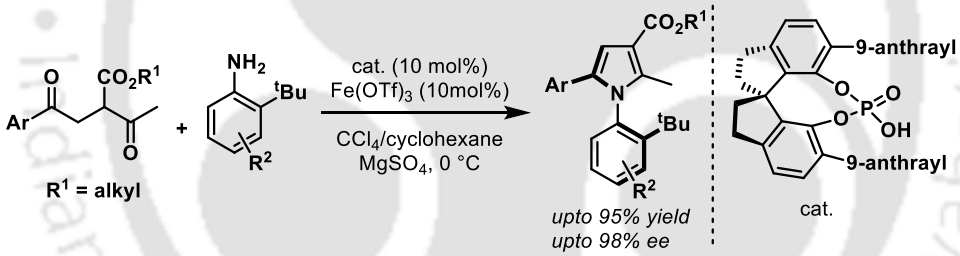

Scheme 1: Asymmetric Paal–Knorr reaction for the synthesis of axially chiral arylpyrroles.

In 2018, Zhu and co-workers described an Ag(I)-chiral phosphine catalyzed synthesis of axially chiral 3-arylpyrroles.[7] The author reported that, under catalytic silver(I) oxide and Cinchona-alkaloid derived phosphine ligand α-isocyanoacetates were reacted chemo-selectively with alkynic ketones gave enantioenriched 3-arylpyrroles in high yields with excellent enantiomeric excesses via *de novo* pyrrole ring construction (Scheme 2).

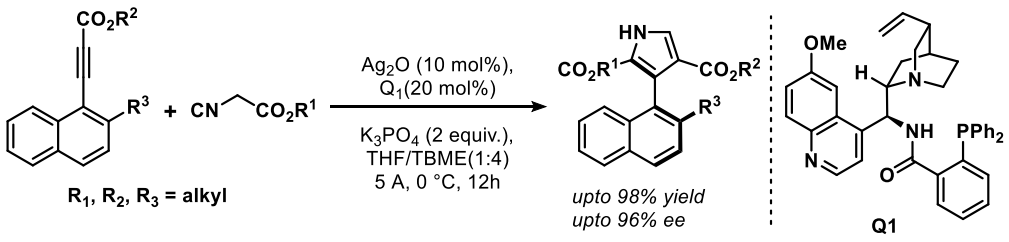

Scheme 2: *De novo* synthesis of axially chiral 3-arylpyrroles from α-isocyanoacetates and alkynic ketones.

In 2019, the same author achieved a breakthrough by developing an epi-quinine thiourea-catalyzed conversion of the Barton–Zard reaction, effectively transforming racemic intermediates into axially chiral 3-arylpyrroles (Scheme 3).[8] Under the optimized catalytic conditions, the (±)-3,4-dihydro-2H-pyrroles underwent a noble kinetic resolution, resulting in the production of (+)-3,4-dihydro-2H-pyrroles and axially chiral (+)-3-arylpyrroles, demonstrating transfer of chirality from the central to axiality. This reaction sequence also incorporates aromatization and HNO_2 syn-elimination.

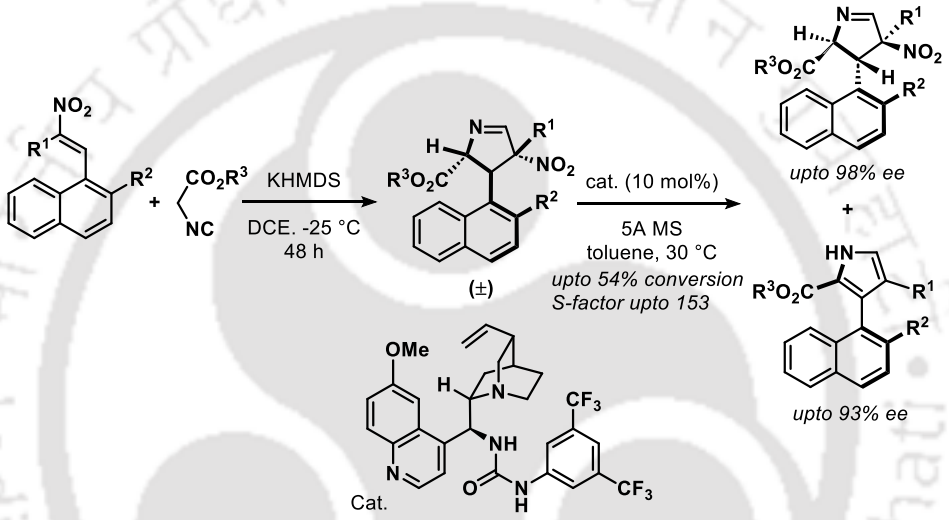

Scheme 3: Kinetic resolution for the synthesis of axially chiral aryl pyrrole.

In 2021, Chen and colleagues made a significant advancement by an Ag(I)-catalyzed atropselective Barton–Zard reaction, effectively enabling the synthesis of axially chiral 3-(hetero)aryl pyrroles through a central-to-axial chirality transfer approach.[9] The authors demonstrated that, under the influence of a quinine-derived phosphine ligand, the Ag(I) catalyst can facilitate the reaction of α-substituted nitroolefins featuring a β-ortho-substituted (hetero)aryl group with α-isocyanoacetate (Scheme 4). This innovative process leads to the formation of axially chiral pyrroles via aromatization, delivering outstanding yields and enantioselectivities.

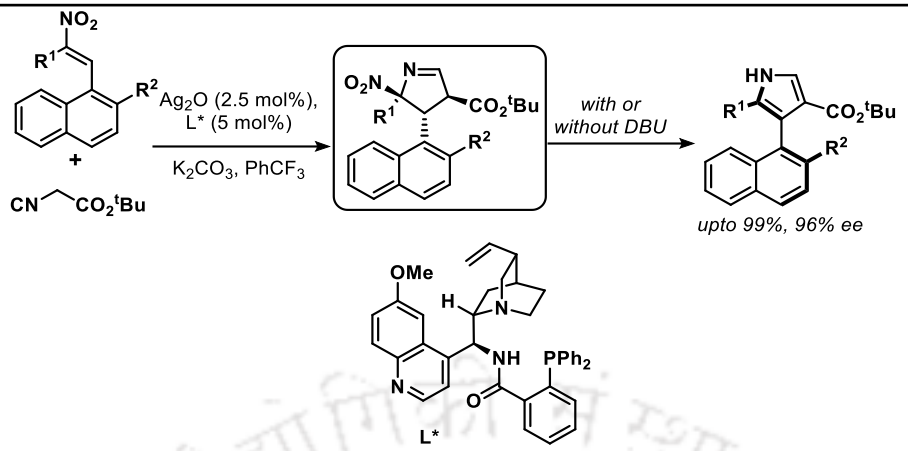

Scheme 4. Ag(I)-catalyzed Barton-Zard reaction for the synthesis of axially chiral 3-(hetero)aryl pyrroles.

In 2019, Tan et al. explored a sequential synthesis of axially chiral 2-arylpyrrole through chirality transfer strategy through cyclization (Scheme 5).[10] Under chiral phase transfer catalysis, an asymmetric N-alkylation afforded highly atropselective alkene which subsequently underwent a chirality transfer via aromatic cyclization to give axially chiral 2-arylpyrroles with excellent yield and ees.

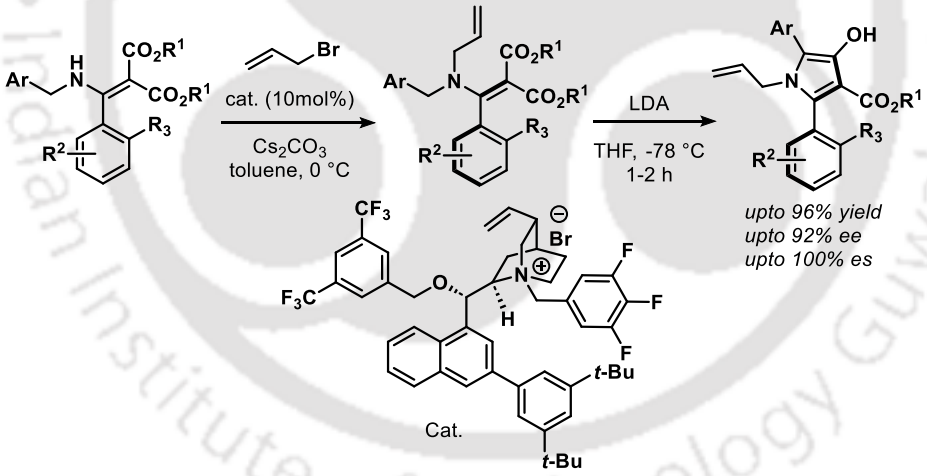

Scheme 5: Chiral PTC catalyzed chirality transfer enabled synthesis of axially chiral pyrrole.

In 2022, the Shi group made a discovery by developing an atropselective Paal–Knorr reaction to synthesize N-N axially chiral pyrroles.[11] Utilizing a catalytic chiral phosphoric acid, they achieved transformation of substituted N-amino indoles and 1,4-diketones into pyrrole rings with outstanding yields and excellent enantioselectivities (Scheme 6). Furthermore, their exploration revealed that several chiral derivatives exhibit potent anti-cancer activity.

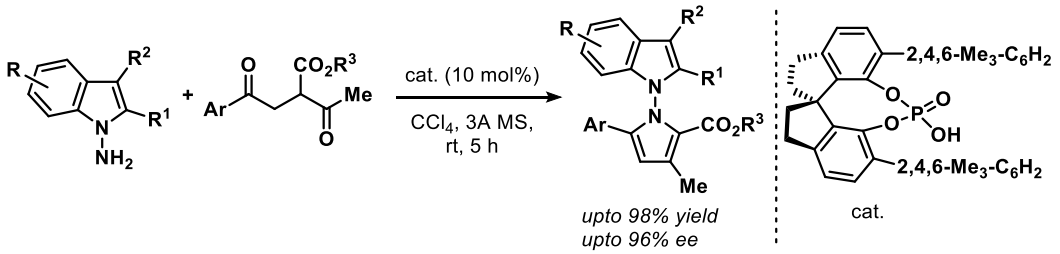

Scheme 6: Catalytic Paal–Knorr reaction for synthesis of N-N axially chiral pyrroles.

In 2023, Ye and co-workers reported a Cu(I)-Chiral phosphine ligand catalyzed atroposelective diyne cyclization for axially chiral pyrroles.[13] Under the optimized catalytic condition, a well-designed substituted diyne gave a vinyl cations which subsequently underwent *de novo* oxidation to afford axially chiral 3arylpyrrole in good yield and excellent ees (Scheme 7).

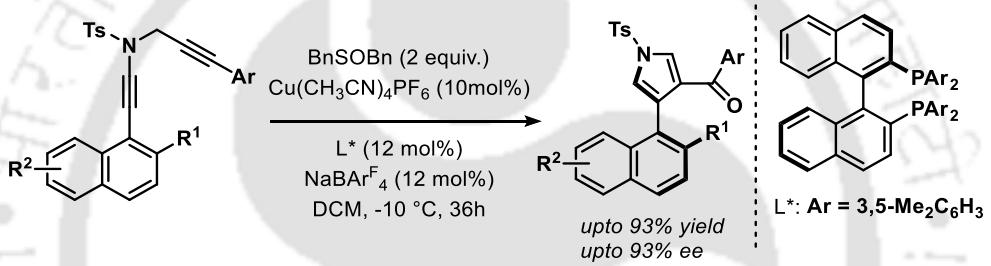

Scheme 7: Catalytic atroposelective diyne cyclization for synthesis of chiral arylpyrrole.

4.2.2. Catalytic asymmetric *de novo* Synthesis of centrally chiral arenes:

In 2019, Chi et al. reported a strategy for synthesizing substituent-dependent, centrally chiral arenes using N-heterocyclic carbene (NHC) catalysis.[14] This method presented a one-step organic catalytic approach that involved an NHC-catalyzed cycloaddition reaction between achiral indanone and α,β-unsaturated aldehydes (Scheme 8). The process enabled the direct construction of benzene and resulted in the formation of optically active 1,3-indandione in high yield and with excellent enantiomeric excess.

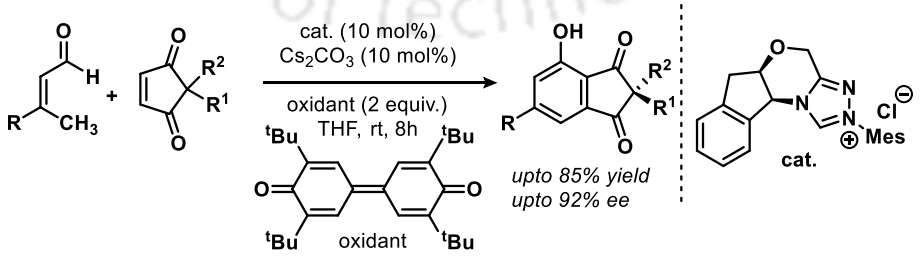

Scheme 8. Chiral NHC catalyzed desymmetrization strategy for chiral arene synthesis.

In the same year, Wang et al. reported the successful initiation of a chiral N-heterocyclic carbene-catalyzed cascade asymmetric desymmetrization reaction involving achiral indanone and α,β-unsaturated aldehydes (Scheme 9).[15] This process was followed by tandem aldol annulation, aromatization, and sequential methylation.

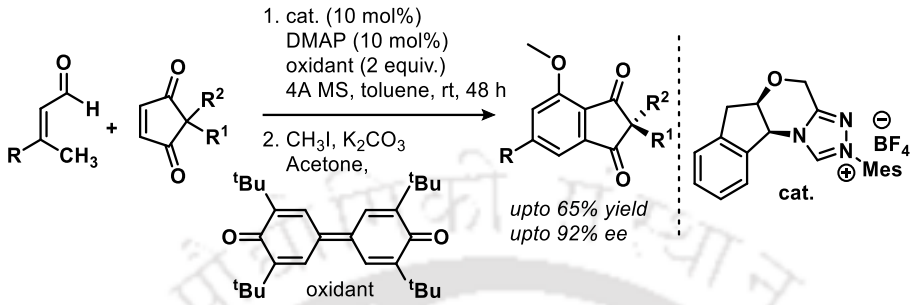

Scheme 9: Sequential NHC catalyzed desymmetization for chiral arene synthesis.

In 2022, Mukherjee and co-workers developed a desymmetizing *de novo* method using diphenylprolinol silyl ether to create centrally chiral arenes (Scheme 10).[16] This process works through a dienamine intermediate, which allows for a [4+2] cycloaddition between polycyclic meso-cyclohexenediones and α,β-unsaturated aldehydes. Then, the Diels-Alder adduct underwent a *de novo* oxidation to afford centrally chiral arenes with high yields and excellent enantiomeric excesses.

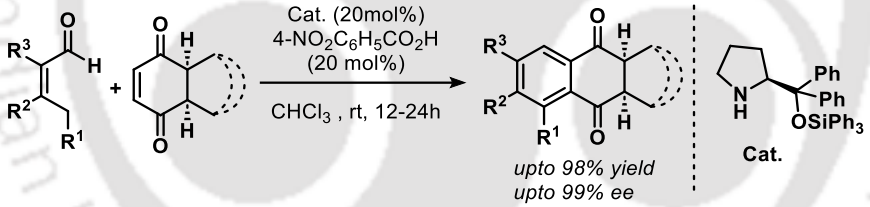

Scheme 10. desymmetrization reaction for chiral arene synthesis via dienamine catalysis.

Later, Mukherjee et al. (2022) introduced a method for atropselective *de novo* arene construction through dienamine catalysis.[17] By employing optimal conditions, prochiral N-aryl maleimides successfully underwent a highly effective desymmetrization reaction with α,β-unsaturated aldehydes (Scheme 11). This approach utilizes a sequential [4+2] cycloaddition followed by aromatization, leading to the formation of axially chiral phthalimides with exceptional yields and excellent enantiomeric excesses.

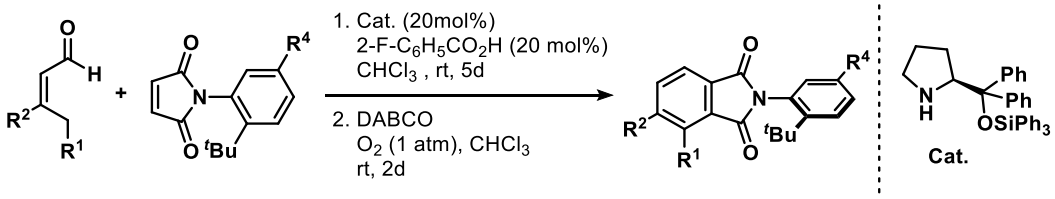

Scheme 11: Synthesis of C-N axial chirality with atroposelective *de novo* arene strategy.

4.3. Objective:

However, the enantioselective *de novo* synthesis of centrally chiral heterocycles via the desymmetrization strategy remains unknown. In 2018, Oh and co-workers elegantly reported silver-catalyzed asymmetric desymmetrization of cyclopentenediones via [3 + 2] cycloaddition with α-substituted isocyanoacetates to deliver pyrrolidine derivativatives (Fig. 2).[18a] Then, in 2022, they developed silver-catalyzed asymmetric desymmetrization of cyclohexadienones via the Van Leusen pyrrole synthesis, however the reaction failed to provide α-substituted pyrroles (Fig. 2).[18b] Thus, enantioselective *de novo* synthesis of centrally chiral heterocycles via the desymmetrization strategy[19] remains unknown.

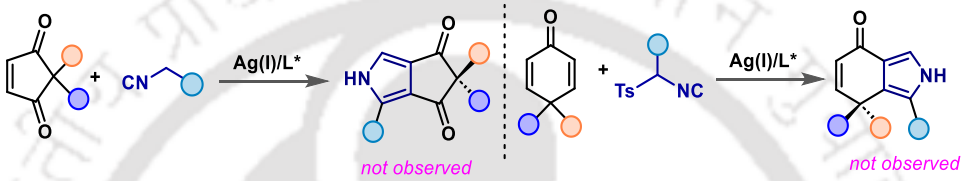

Fig 2. Background of the α-isocyanoacetate and α-substituted TosMIC.

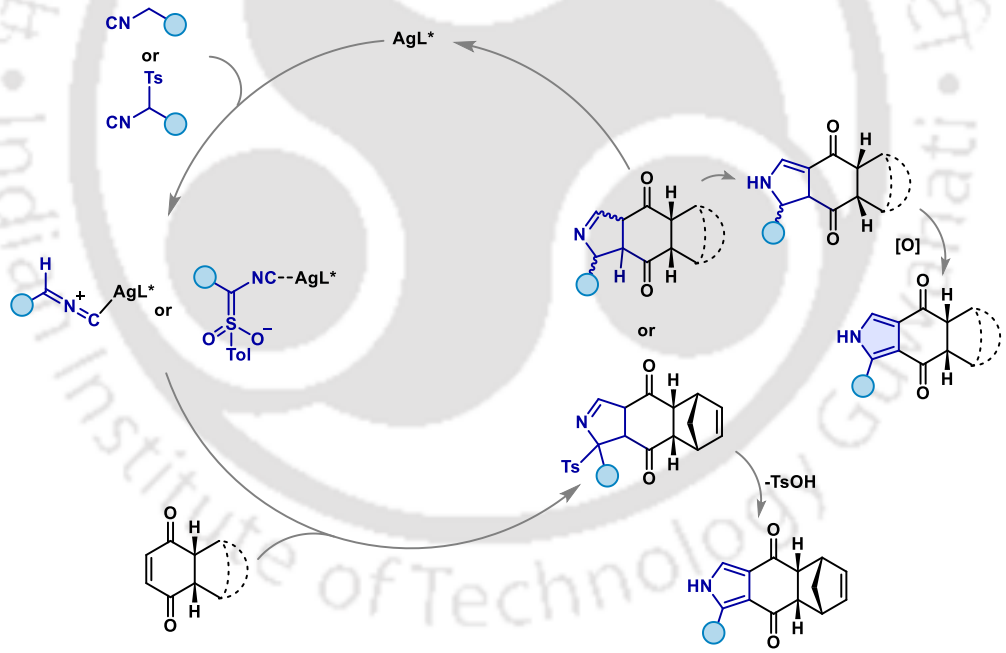

Fig. 3. Catalytic hypothesis for the enantioselective *de novo* construction of chiral pyrrole.

As a proof-of-concept, we have chosen the reaction of polycyclic meso-cyclohexenediones with activated isocyanides,[20] and we envisioned that such a combination may lead to the formation of structurally novel 2-substituted-3,4-fused centrally chiral pyrroles through a [3+2]-cycloaddition/proton shift/oxidation cascade process (Fig. 3).[21] Herein, we describe an operationally simple procedure with silver catalysis[22] to achieve such transformation, leading

to the first catalytic enantioselective *de novo* construction of centrally chiral pyrroles through desymmetrization (Fig. 3). We have also envisaged developing the first asymmetric Van Leusen reaction using the same strategy.

4.4. Results and discussion:

4.4.1. Catalyst, solvent and temperature optimization for *de novo* synthesis of chiral pyrrole:

Table 1: ***Catalyst and solvent optimization for de novo synthesis of chiral pyrrole.***

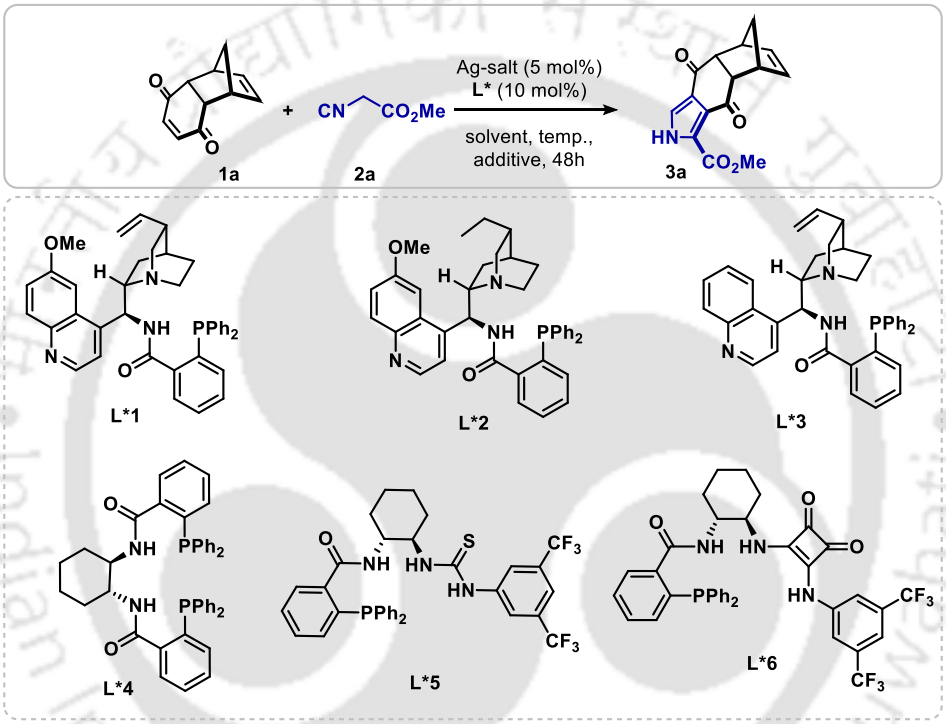

Entry[a]	L*	Ag(I)-salt	Solvent	Additive	Temperature	Yield[b]	ee[c]
1.	**L*1**	Ag_2O	DCE	-	rt	81%	83%
2.	**L*2**	Ag_2O	DCE	-	rt	76%	77%
3.	**L*3**	Ag_2O	DCE	-	rt	73%	88%
4.	**L*4**	Ag_2O	DCE	-	rt	84%	0%
5.	**L*5**	Ag_2O	DCE	-	rt	80%	14%
6.	**L*6**	Ag_2O	DCE	-	rt	82%	8%
7.	**L*3**	Ag_2CO_3	DCE	-	rt	66%	92%
8.	**L*3**	$AgSbF_6$	DCE	-	rt	50%	91%

9.	**L*3**	$AgNO_3$	DCE	-	rt	55%	87%
10.	**L*3**	AgOTf	DCE	-	rt	40%	87%
11.	**L*3**	AgOAc	DCE	-	rt	48%	53%
12.	**L*3**	Ag_2CO_3	DCM	-	rt	65%	92%
13.	**L*3**	Ag_2CO_3	$CHCl_3$	-	rt	68%	91%
14.	**L*3**	Ag_2CO_3	EtOAc	-	rt	71%	93%
15.	**L*3**	Ag_2CO_3	Toluene	-	rt	40%	68%
16.	**L*3**	Ag_2CO_3	THF	-	rt	69%	90%
17.	**L*3**	Ag_2CO_3	EtOAc	4ÅMS	rt	55%	93%
18.	**L*3**	Ag_2CO_3	EtOAc	5ÅMS	rt	40%	92%
19.	**L*3**	Ag_2CO_3	EtOAc	-	0 °C	66%	89%
20.	**L*3**	Ag_2CO_3	EtOAc	-	-10 °C	50%	77%
21.[d,e]	**L*3**	Ag_2CO_3	EtOAc (0.05M)	-	rt	86%	94%

[a] Unless otherwise mentioned, reactions were carried out with 0.1 mmol of **1a** with 0.11 mmol of **2a**, Ag-salt (5 mol%), **L** (10 mol%) in 1 mL solvent at rt for 48h under Ar atmosphere. [b] Isolated yield after silica gel column chromatography. [c] Determined by HPLC. [d] With 2 mL solvent. [e] After 12h, the reaction was stirred in air for 36h.

We started our investigation by conducting a model reaction between endo-norbornenoquinone (**1a)** and methyl isocyanoacetate (**2a**) in 1,2-dichloroethane at room temperature (Table 1). Initially, the combination of silver oxide and readily accessible chiral amino-phosphine precatalysts **L*1–L*3** derived from 9-amino(9-deoxy) epicinchona alkaloids[20b] were checked. Gratifyingly, within 48h, the target reaction proceeded well with **L*1** and silver oxide, delivering the centrally chiral pyrrole product **3a** in high yield with promising enantioselectivity (81% yield, 83% ee, entry 1). Though the enantioselectivity of **3a** got decreased with **L*2**, slight better enantioselectivity was achieved with cinchonidine derived aminophosphine **L*3** (entries 2-3). Then, trans-1,2-diaminocyclohexane derived precatalysts **L*4**–**L*6** were screened but inferior results were observed (entries 4–6). Further investigations of silver salts with **L*3** (entries 7–11) showed that silver carbonate was the optimal one in terms of enantioselectivity (92% ee, entry 7). The subsequent examination of solvents (entries 12–16) revealed that employing ethyl acetate could enhance the reaction's stereoselectivity (93% ee, entry 13). An attempt to improve efficiency by adding additives such as molecular sieves was not successful (entry 17-18). Again, reducing the temperature did not yield positive results (entry 19-20). Better enantioselectivity was detected after lowering the reaction concentration to 0.05 M (94% ee, entry 21). Finally, after 12 hours, the

reaction was stirred in air for 36 hours, and this proved to be beneficial in terms of yield (86% yield) and did not change the enantioselectivity of **3a** (entry 21).

4.4.2. Substrate Scope of [3+2] *de novo* synthesis of chiral pyrrole:

Following the establishment of optimal conditions, the reaction's scope and generality were examined. Initially, different alkyl isocyanoacetates **2** were tested and gratifyingly acceptable results were achieved for a series of chiral pyrrole products (Scheme 12). Ethyl isocyanoacetate **2b** reacted well to provide **3b** in high enantioselectivity. A similar result was detected with *t*-butyl isocyanoacetate **2c** and the product **3c** was isolated in 79% yield with 92% ee (Scheme 12). Then

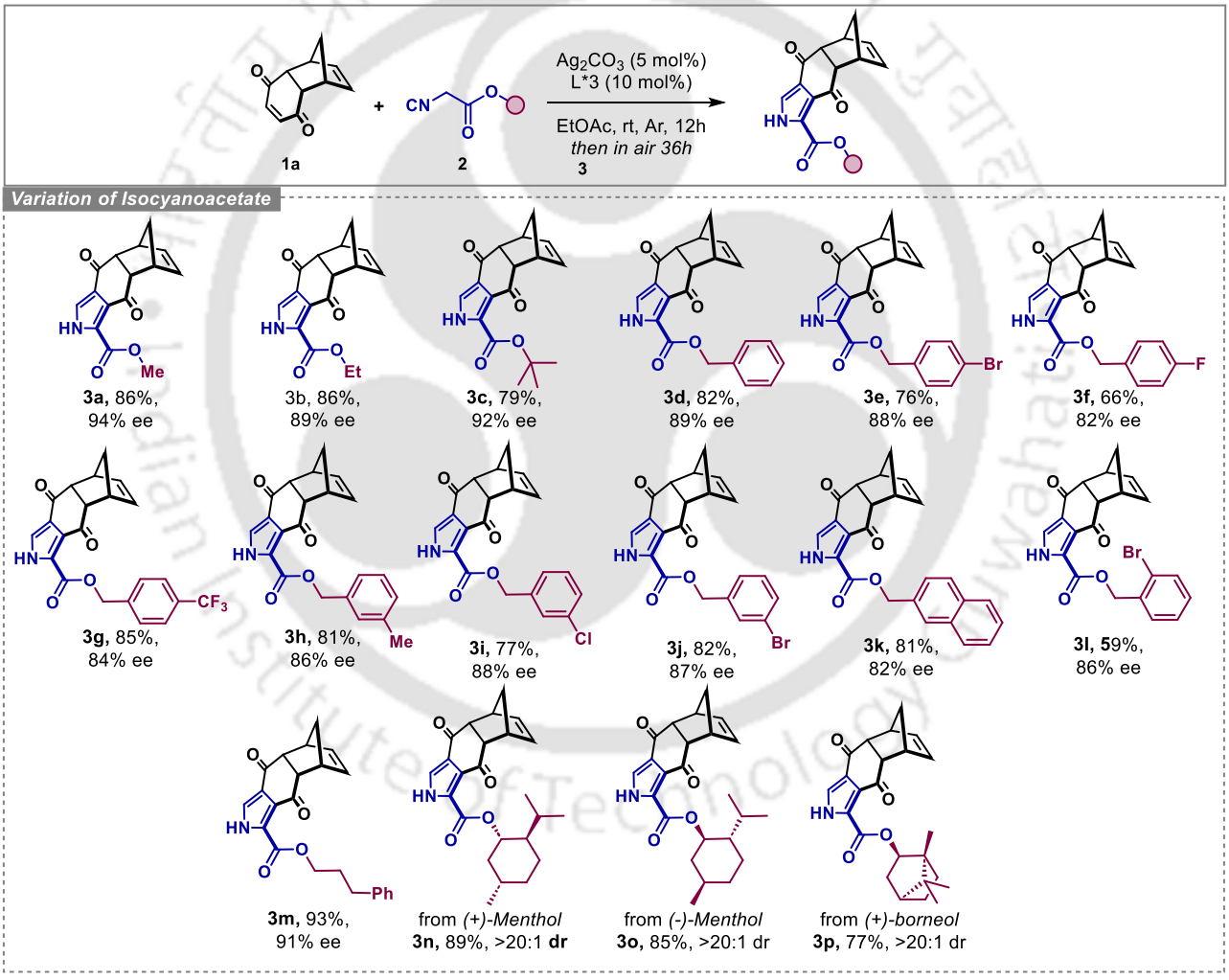

Scheme 12: Scope of isocyanoacetate for [3+2] cycloaddition reaction.

we turned to various benzyl isocyanoacetates (**2d-2j**), resulting in good to high enantioselectivities for the desired products **3d-3j**. For example, unsubstituted benzyl isocyanoacetate **2d** delivered product **3d** in 82% yield with 89% ee. The outcome remained

mostly unchanged with *para*-bromo substituted benzyl isocyanoacetate **2e**. Then *para*-fluoro and *para*-trifluoromethyl substituted benzyl isocyanoacetates **2f** and **2g** were screened and the corresponding products **3f** and **3g** were attained in acceptable yields and enantioselectivities. Additionally, the scope was expanded to include *meta*-substituted benzyl group containing isocyanocetates **2h**-**2j**, and gratifyingly, good results were also obtained there as well. Naphthyl group containing isocyanoacetate **2k** was also tolerated in the reaction and good outcome was detected. 2-Bromo substututed benzyl group containing isocyanoacetate **2l** also participated in the reaction to deliver product **3l** in moderate yield with good enantioselectivity. Better enantioselectivty (91% ee) was obtained with hydrocinnamyl isocyanoacetate 2m. In presence of catalytic Ag_2CO_3/**L*3**, the [3+2] cycloaddition reaction of **1** with enantiopure isocyanoacetates **2n**-**2p** (**2n** derived from L–Menthol, **2o** derived from D-Menthol and **2p** from L-borneol), were engaged in the reaction and the desired products **3n**-**3p** were attained in excellent yield and diastereoselectivities (>20:1 dr).

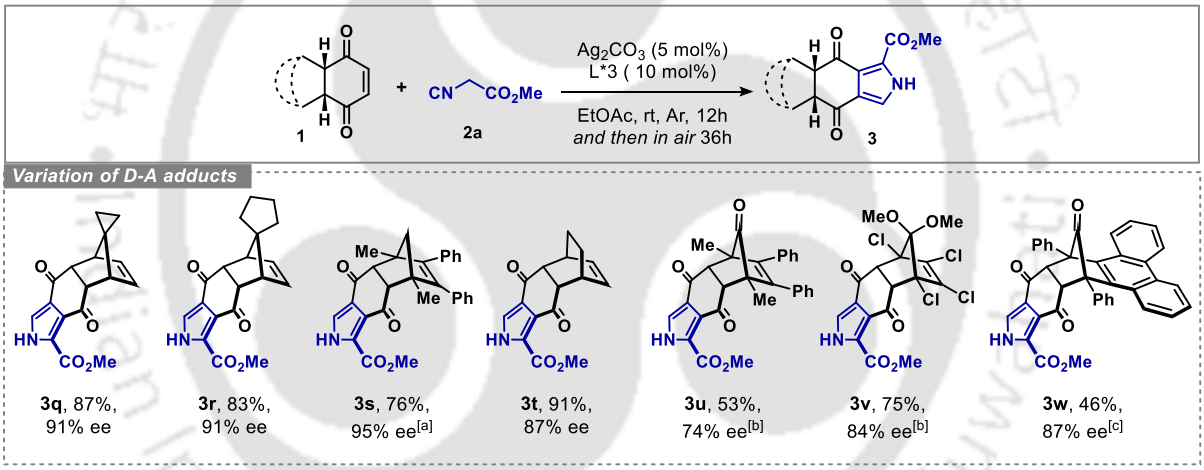

Scheme 13: Scope of D-A adducts for [3+2] cycloaddition reaction, [a] Reaction was run at −10 °C. [b] Reaction was run in 2.5 mL EtOAc. [c] Reaction was run in 2.5 mL $CHCl_3$.

Then a number of polycyclic meso-cyclohexenediones were exposed to this catalytic desymmetrization process (Scheme 13). Among these are endo-DA adducts made from *para*-benzoquinone and a range of cyclic dienes starting from highly substituted and spiro-fused cyclopentadienes to cyclohexadiene, cyclopentadienones and anthracene. Higher substitution was generally associated with improved enantiodiscrimination. Polycyclic pyrroles **3q** and **3r** with spiro-carbacycles were obtained in same enantioselectivity (91% ee). The enantioselectivity got improved for **3s** having higher substitutions and the reaction was run at -10 °C. Then, endo-DA adduct **1e** derived from cyclohexadiene and para-benzoquinone was employed in the reaction and the corresponding product **3t** was attained in acceptable enantioselectivity. Cyclopentadienone derived DA adducts **1f** and **1g** could also be employed

in the reaction, however the products **3u** and **3v** were obtained in slightly lower yields and enantioselectivities. Finally, anthracene group containing DA adduct **1h** was engaged in the reaction and better enantioselectivity for **3w** was detected in chloroform solvent.

4.4.3. Catalyst, solvent and temperature optimization for synthesis of chiral pyrrole with the Van Leusen reaction:

Then we became interested in preparing unsymmetrical pyrroles via the Van Leusen reaction.[23] To the best our knowledge, the Van Leusen reaction was not previously reported with α–substituted TosMIC for chiral pyrrole synthesis. Thus, we started our investigation by conducting

Table 2: Catalyst and solvent optimization for Van leusen reaction

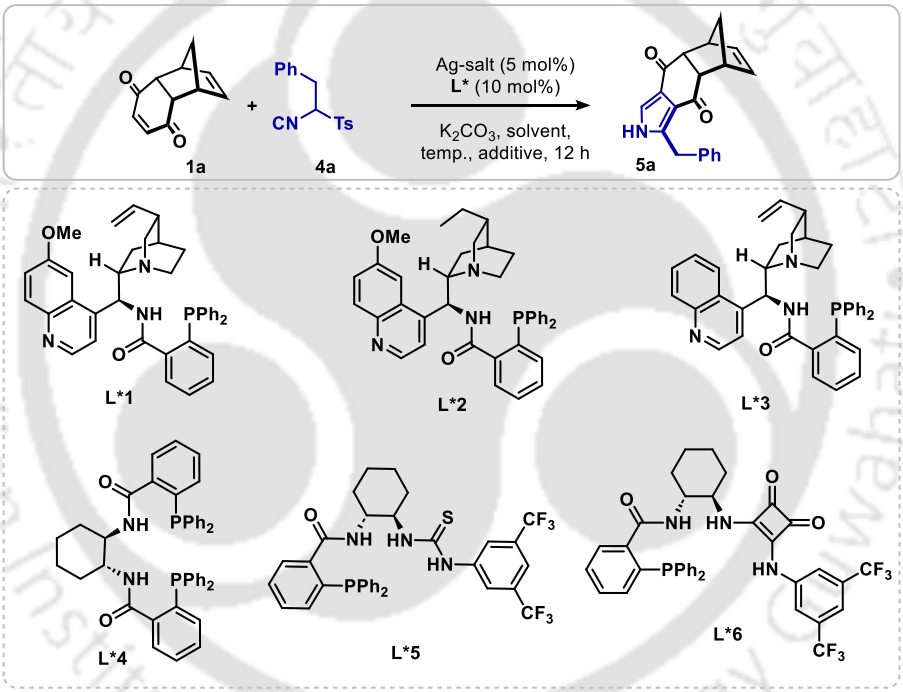

Entr	L*	Ag(I)-salt	Solvent	Additive	Temperatur	Yield[b]	ee[c]
1.	**L*1**	Ag_2O	EtOAc	-	rt	92%	76%
2.	**L*2**	Ag_2O	EtOAc	-	rt	86%	79%
3.	**L*3**	Ag_2O	EtOAc	-	rt	88%	84%
4.	**L*4**	Ag_2O	EtOAc	-	rt	91%	0%
5.	**L*5**	Ag_2O	EtOAc	-	rt	81%	0%
6.	**L*6**	Ag_2O	EtOAc	-	rt	85%	26%
7.	**L*3**	Ag_2CO_3	EtOAc	-	rt	87%	59%

8.	**L*3**	$AgSbF_6$	EtOAc	-	rt	92%	81%
9.	**L*3**	$AgNO_3$	EtOAc	-	rt	81%	80%
10.	**L*3**	AgOTf	EtOAc	-	rt	89%	84%
11.	**L*3**	AgOAc	EtOAc	-	rt	92%	82%
12.	**L*3**	Ag_2O	DCM	-	rt	88%	65%
13.	**L*3**	Ag_2O	$CHCl_3$	-	rt	91%	78%
14.	**L*3**	Ag_2O	Toluene	-	rt	79%	64%
15.	**L*3**	Ag_2O	THF	-	rt	85%	83%
16.	**L*3**	Ag_2O	EtOAc	-	0 °C	89%	84%
17.	**L*3**	Ag_2O	EtOAc	-	-10 °C	85%	84%
18.[d]	**L*3**	Ag_2O	EtOAc	3 Å	rt	90%	84%
19.[d]	**L*3**	Ag_2O	EtOAc	4 Å	rt	92%	87%
20.[d]	**L*3**	Ag_2O	EtOAc	5 Å	rt	96%	82%

[a] Reactions were carried out with 0.1 mmol of **1a** with 0.11 mmol of **4a**, Ag(I)-salt (5 mol%), **L** (10 mol%), K_2CO_3 (0.2 mmol), in 1 mL EtOAc at rt for 12h. [b] Yields calculated after silica gel column chromatography. [c] ees was determined by HPLC. [d] 100mg MS was used.

a model reaction between endo-norbornenoquinone (**1a**), (2-isocyano-2-(phenylsulfonyl)ethyl)benzene (**4a**) and 2 equiv. K_2CO_3 in ethyl acetate at room temperature (Table 2). Initially, the combination of silver oxide and readily accessible chiral amino-phosphine precatalysts **L*1–L*3** derived from 9-amino(9-deoxy) epicinchona alkaloids were checked. Gratifyingly, within 48h, the target reaction proceeded well with **L*1** and silver oxide, delivering the benzyl substituted centrally chiral pyrrole product **5a** in high yield with promising enantioselectivity (92% yield, 76% ee, entry 1). Though the enantioselectivity of **5a** got decreased with **L*2**, slightly better enantioselectivity was achieved with cinchonidine derived aminophosphine **L*3** (entries 2-3). Then, trans-1,2-diaminocyclohexane derived precatalysts **L*4**–**L*6** were screened but inferior results were observed (entries 4–6). Further investigations of silver salts with **L*3** showed no improvement (entries 7-11). The subsequent examination of solvents (entries 11–15) as well as lowering of temperature (entries 16–17) did not enhance the ees. Ultimately, we screened various additives, including molecular sieves. The use of 4Å molecular sieves led to a remarkable improvement, achieving an impressive 87% enantiomeric excess (ee) and a 92% yield of **5a**.

4.4.4. Substrate Scope of the Van-Leusen reaction for synthesis of chiral pyrrole:

Under optimal conditions, we incorporated a range of substitutions on the aromatic ring of **4** and observed the outcomes of the reactions (**Scheme 14**). Initially different *para*-substitutions

were checked and the desired products **5b-5f** were attained in high yields and with good to high enantioselectivities. The halo-substituted products **5c-5e** could be further elaborated via cross-coupling reactions. Similar results were found for the *meta*-substituted products **5g**–**5i**, while **5h** showed a slightly lower yield. *ortho*-Substitutions were also tolerated and the desired products **5j-5k** were isolated in acceptable yields with high enantioselectivities. 2-Naphthyl substituted isocyanide **4l** also participated in the reaction to deliver **5l** in acceptable enantioselectivity. Additionally, our methodology was applied to allyl, prenyl, and geranyl groups containing isocyanates **4m-4o**, yielding good enantioselecities for the corresponding products **5m-5o**.

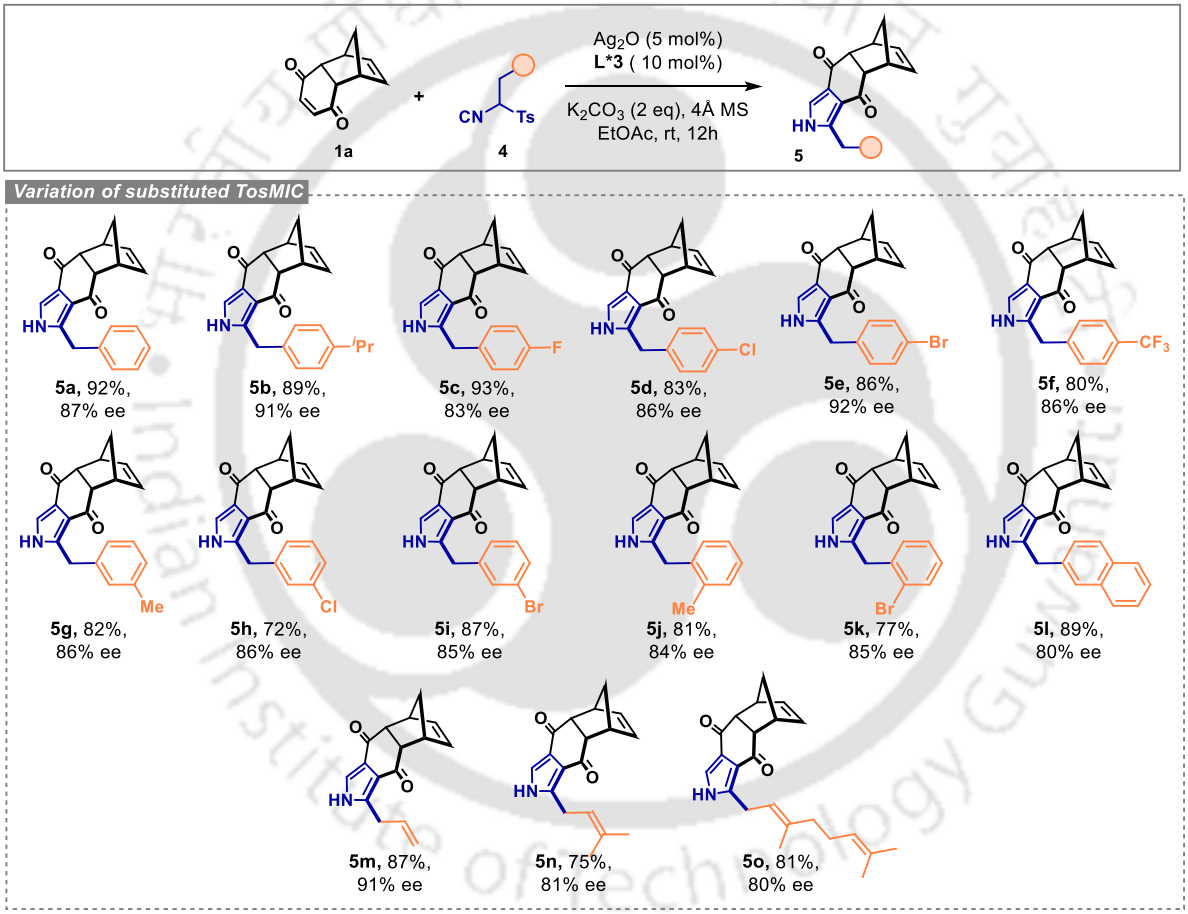

Scheme 14: Scope of α-substituted TosMIC for the Van-Leusen reaction.

In the next stage, a range of polycyclic meso-cyclohexenedionoes **1** with different substitutions were examined (Scheme 15). We were pleased to see positive outcomes for the polycyclic pyrrole products. High enantioselectivities were obtained for polycyclic pyrroles **5p** and **5q** with spiro-carbacycles. Similar enantioselectivity was detected for compound **5r** having highly substituted norbornene motif. After that, the reaction was carried out using the

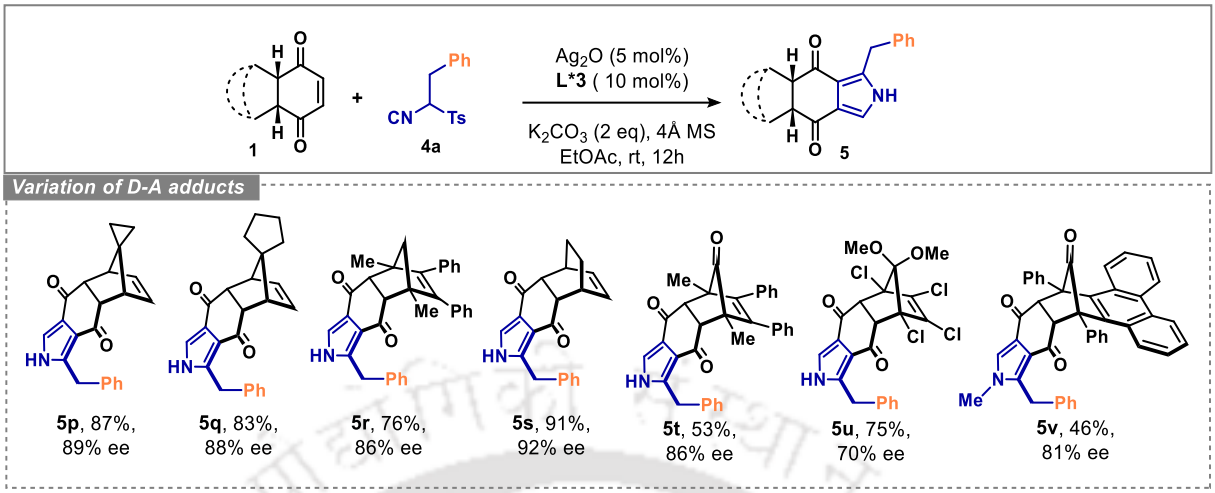

Scheme 15: Scope of D-A adducts for the Van-Leusen reaction.

endo-DA adduct **1e**, and the corresponding product **5s** was obtained with satisfactory enantioselectivity. The DA adducts **1f** and **1g** generated from cyclopentadienone could also be used in the process; however, the yields and enantioselectivities of the products **5t** and **5u** were slightly lower. Finally, anthracene group containing DA adduct **1h** took part in the reaction and moderate yield but high enantioselectivity was detected for product **5v.**

4.5. Determination of absolute configurations:

The absolute configuration of **5m** was determined by single crystal X-ray crystallography. absolute configuration of compound **5m** was determined to be (4a*R*,5*S*,8*R*,8a*S*) by X-ray crystallography (Scheme 16). Thus, other polycyclic pyrroles **3** and **5** are expected to have same configuration.

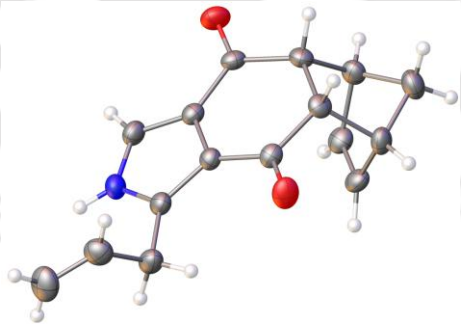

Scheme 16: ORTEP diagram of **5m** with the thermal ellipsoid 30% probability.

4.6. Scale-up reaction and Synthetic transformation:

Then two scale up reactions were performed with 2 mmol of **1a** for the formations of **3a** and **5a** (Scheme 17). In both cases, the reactions progressed smoothly to provide **3a** and **5a** in 78% and 90% yields respectively. To our delight, the enantioselectivities remained constant with

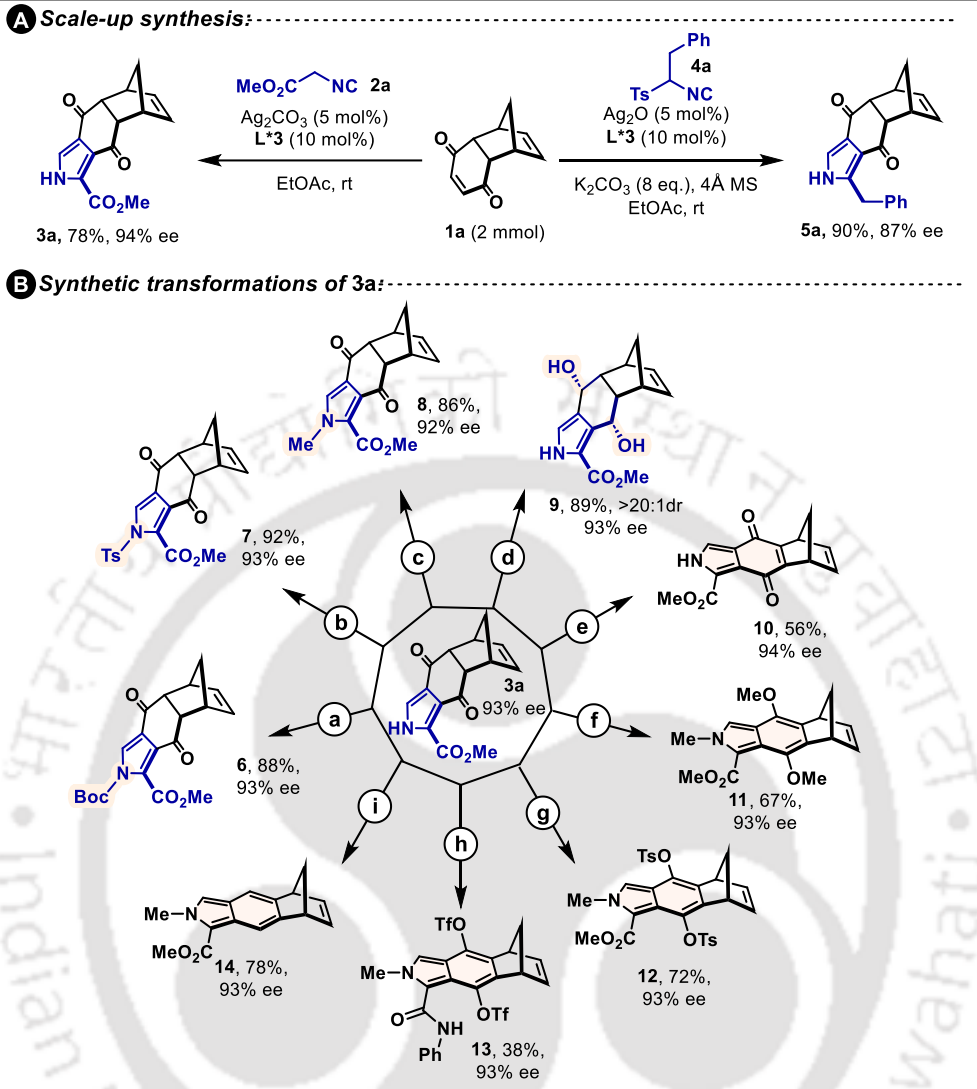

Scheme 17: Scale up reaction and synthetic transformations. Reaction conditions: a) $(Boc)_2O$, DMAP, CH_3CN, rt, 12h; b) TsCl, NH_4HSO_4, KOH, DCM, rt, 30min; c) MeI, K_2CO_3, dioxane, rt, 12h; d) $NaBH_4$, MeOH:DCM, 0 °C, 1h; e) K_2CO_3, CH_3CN, reflux, f) NaH, MeI, THF, 0 °C, 5h; g) MeI, K_2CO_3, DMF, rt, 12h, NaH, TsCl, 0 °C, 5h; h) MeI, K_2CO_3, DMF, rt, 12h; $PhNTf_2$, KHMDS, -78 °C, 1h; LiHMDS, aniline, toluene, rt, 6h; i) MeI, K_2CO_3, DMF, rt, 12h; $PhNTf_2$, KHMDS, -78 °C, 1h; $Pd(OAc)_2$ (5 mol%), DPPP (10 mol%), HCOOH, NEt_3, DMF, 80 °C, 60h.

respect to their initial values. To show the synthetic usefulness of our approach, few transformations were performed on **3a** (Scheme 17). Initially, NH group of **3a** was protected as Boc, Ts and Me groups respectively and compounds **6**, **7** and **8** were formed in high yields. While enantioselectivity was retained in products **6** and **7**, compound **8** showed a small erosion in enantioselectivity. Stereoselective reduction of **3a** with sodium borohydride led to the formation of diol **9** in 89% yield with retention of enantioselectivity. Then compound **10** with dienone motif was formed via the reaction of **3a** with potassium carbonate, and the enantioselectivity remained constant.

Then treatment with sodium hydride and iodomethane led to the formation of compound **11** with N-methylated isoindole motif and the enantioselectivity was unchanged. Similarly, isoindole compound **12** was formed via N-methylation followed by reaction with tosyl chloride in the presence of sodium hydride Then, N-Me protection, enolization, triflate formation and hydrolysis of ester functionality followed by reaction with aniline led to the formation of compound **13** and here also enantioslectivity was preserved. In a similar way, N-Me protection, enolization, triflate formation and reductive cleavage of the triflates with palladium catalyst generated compound **14** with retention of enantiopurity.

4.7. Mechanism:

To understand the mechanism of the reaction, we tried to isolate the intermediate. Thus, we carried out the reaction between **1a** and **2a** at -10 °C under argon atmosphere in dry EtOAc solvent. After 36 hours, an intermediate **A** was found as a precipitate whose structure was determined by 2D NMR. Intermediate **A** is likely to be formed via a catalytic asymmetric [3+2]-cycloaddition/proton shift sequence. Intermediate **A** on oxidation in air gets converted to product **3a**. Based on these experimental results, a possible stereochemical model was proposed for the fo00rmation of **3a**. As shown in Scheme 8, the isocyanide carbon atom of **2a**, carbonyl oxygen of **1a**, phosphorous and amide nitrogen of **L*3** coordinate to the silver(I)

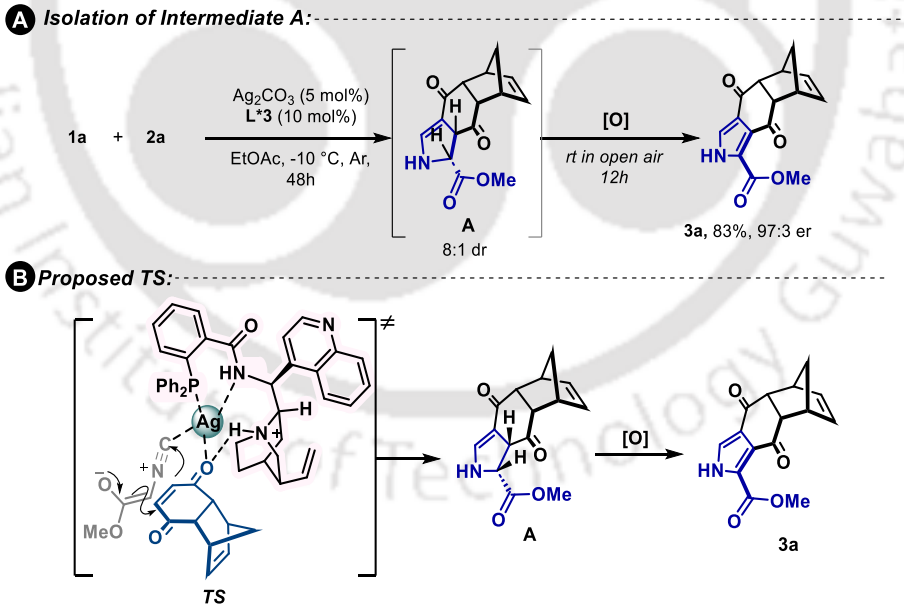

Scheme 16: Isolation of intermediate and the proposed TS.

ion, while the carbonyl oxygen of **1a** further interacts with protonated quinuclidine through hydrogen bonding, thus providing a well-refined stereochemical environment. The (Z)-enolate of **2a** then attacks the unsaturated double bond of **1a** from the less sterically hindered backside to control the stereochemistry of the created stereogenic center and consequently

[3+2]-cycloaddition and proton shift proceeds to generate intermediate **A**. Aerial oxidation of intermediate **A** leads to the formation of **3a**. In a similar fashion compound **5a** is formed where base is required for the elimination of TsH from the [3+2]-cycloadduct.

4.8. Conclusion:

In summary, we have developed the first catalytic enantioselective *de novo* construction of centrally chiral pyrroles through desymmetrizing oxidative [3+2]-cycloaddition using silver catalysis. In addition, we have also described the first catalytic asymmetric Van Leusen reaction for the synthesis of unsymmetrical pyrroles. A series of polycyclic 2-substituted, 3,4-fused pyrroles were obtained in high yields and with good to high enantioselectivities. Mild reaction conditions and 10 mol % of easily available chiral amino-phosphine pre-catalyst along with silver salt were used. The power of this pyrrole construction strategy is described through the elaboration of the products to synthetically challenging polycyclic isoindole compounds–some of which are synthesized enantioselectively for the first time.

4.9. Experimental Section:

4.9.1. General Information:

All dry solvents were dried using activated 4Å molecular sieves and stored under argon. For thin layer chromatography (TLC), silica gel plates with fluorescence indicator 254 nm were used and compounds were visualized by irradiation with UV light and/or iodine and/or Phosphomolybdic acid stain. Celite® 512 medium was used for filtrations. Flash column chromatography was performed using 230-400 mesh silica gel and column chromatography with 100-200 mesh silica gel. Petroleum ether, ethyl acetate, acetone and dichloromethane for column chromatography were acquired from commercial sources and were used without purification. NMR spectra were acquired on a Bruker 400 MHz, 500 MHz and 600 MHz spectrometer. Chemical shifts (δ) are reported in ppm relative to residual solvent signals (Chloroform-d, 7.26 ppm for ^{1}H NMR and 77.23 ppm for ^{13}C NMR respectively. ^{13}C spectra were acquired on a broad band decoupled mode. For ^{1}H-NMR, data are reported as follows: chemical shift, multiplicity (s = singlet, d = doublet, dd = double doublet, ddd = doublet of doublet of doublets, t = triplet, q = quartet, dt = doublet of triplets, m = multiplet), coupling constants (Hz) and integration. Using ESI mode HRMS spectra were recorded. Enantiomeric ratios were determined by HPLC analysis performed on Chiral Columns using a Daicel Chiralpak IA, ID and Phenomenex Lux C4 Column.

4.9.2. General Procedure for synthesis of Diels-Alder adducts:

The derivatives of Diels-Alder adducts were synthesized following reported literature procedure.[24]

4.9.3. General Procedure for synthesis of isocyanoacetates:

The derivatives of isocyanoacetates were synthesized following reported literature procedure.[25]

4.9.4. General Procedure for synthesis of α-Substituted TosMIC:

The derivatives of α-Substituted TosMIC were synthesized following reported literature procedure.[26]

4.9.5. General Procedure for synthesis of various catalyst:

All the catalysts were synthesized according to the reported literature procedure.[27]

4.9.6. General Procedure for the Synthesis of chiral pyrrole via [3+2] cycloaddition:

Method A: Under argon atmosphere, an oven-dried screw cap vial equipped with a magnetic stir bar was charged with Ag_2CO_3 (5 mol%) and **L*3** (10 mol%). Then 2 ml EtOAc was added. After stirring for 30 min, **1** (0.1 mmol, 17.7 mg, 1 equiv.) was added in one portion followed by dropwise addition of **2** (0.1 mmol, 11 mg, 1.1 equiv.) over 15 min at room temperature. The reaction was stirred under this condition until full consumption of starting materials observed. After that, the cap of the vial loosens and stirred the reaction in 'open air' for 36 hr. The solvents were evaporated and purified by column chromatography (DCM : Acetone = 97:3 or petroleum ether : EtOAc = 50:50) to afford product **3.**

Mathod B: Under argon atmosphere, an oven-dried screw cap vial equipped with a magnetic stir bar was charged with Ag_2CO_3 (5 mol%) and **L*3** (10 mol%). Then 2 ml EtOAc was added. After stirring for 30 min, the reaction mixture cooled to -10 °C. To the reaction mixture **1** (0.1 mmol, 17.7 mg, 1 equiv.) was added in one portion followed by dropwise addition of **2** (0.1 mmol, 11 mg, 1.1 equiv.) over 15 min at same temperature. The reaction was stirred at -10 °C until full consumption of starting materials observed. After that, the reaction mixture warm to the room temperature and the cap of the vial loosens and stirred the reaction in 'open air' for 36 hr. The solvents were evaporated and purified by column chromatography (DCM : Acetone = 97:3 or petroleum ether : EtOAc = 50:50) to afford product **3.**

Method C: Under argon atmosphere, an oven-dried screw cap vial equipped with a magnetic stir bar was charged with Ag_2CO_3 (5 mol%) and **L*3** (10 mol%). Then 2.5 ml EtOAc was added. After stirring for 30 min, **1** (0.1 mmol, 17.7 mg, 1 equiv.) was added in one portion followed by dropwise addition of **2** (0.1 mmol, 11 mg, 1.1 equiv.) over 15 min at room temperature. The reaction was stirred under this condition until full consumption of starting materials observed. After that, the cap of the vial loosens and stirred the reaction in 'open air'

for 36 hr. The solvents were evaporated and purified by column chromatography (DCM : Acetone = 97:3 or petroleum ether : EtOAc = 50:50) to afford product **3.**

Method D: Under argon atmosphere, an oven-dried screw cap vial equipped with a magnetic stir bar was charged with Ag_2CO_3 (5 mol%) and **L*3** (10 mol%). Then 2.5 ml $CHCl_3$ was added. After stirring for 30 min, **1** (0.1 mmol, 17.7 mg, 1 equiv.) was added in one portion followed by dropwise addition of **2** (0.1 mmol, 11 mg, 1.1 equiv.) over 15 min at room temperature. The reaction was stirred under this condition until full consumption of starting materials observed. After that, the cap of the vial loosens and stirred the reaction in 'open air' for 36 hr. The solvents were evaporated and purified by column chromatography (DCM : Acetone = 97:3 or petroleum ether : EtOAc = 50:50) to afford product **3.**

4.9.7. General Procedure for the Synthesis of chiral pyrrole via the Van-Leusen reaction:

Under argon atmosphere, an oven-dried screw cap vial equipped with a magnetic stir bar was charged with Ag_2O (5 mol%) and **L*3** (10 mol%). Then 2 ml EtOAc was added. After stirring for 30 min, K_2CO_3 (2equiv.), 4Å MS (100mg), **1** (0.1 mmol, 17.7 mg, 1 equiv.) was added in one portion followed by addition of **4** (0.1 mmol, 11 mg, 1.1 equiv.) at room temperature. The reaction was stirred under this condition until full consumption of starting materials observed. The solvents were evaporated and purified by column chromatography (DCM : Acetone = 95:5) to afford product **5**.

4.9.8. Procedure for the Synthesis of compound 6:

In an oven dried 5ml round bottom flask, compound **3a** (39.0 mg, 0.1 mmol, 1.0 equiv.) was taken and DMAP (0.4 mg, 0.003 mmol, 0.03 equiv.) was added under argon atmosphere. Then 1.0 mL of ACN was added to the reaction mixture. The reaction mixture cooled to 0 °C and Di-tert-butyl dicarbonate (25 µL, 0.11 mmol, 1.1 equiv.) was added dropwise. The mixture was stirred at room temperature, until full consumption of starting materials observed. After that, solvents were evaporated and directly purified by flash chromatography (petroleum ether : ethyl acetate = 80:20) to give **6.**

4.9.9. Procedure for the Synthesis of compound 7:

In an oven dried 10 mL round-bottom flask, **3a** (27.5 mg, 0.1 mmol, 1.0 equiv) in dichloromethane (1 mL), KOH (8.4 mg, 0.15 mmol, 1.5 equiv.) and tetrabutylammonium hydrogensulfate (3.39 mg, 10 mol%) were added, and the mixture was allowed to stir for 15 min followed by addition of a solution of sulfonyl chloride (23 mg, 0.12mmol, 1.2 equiv.) in dichloromethane (0.5 mL), and the mixture was stirred at room temperature until the starting material was consumed. Then, water (20 mL) was added and the aqueous layer was extracted with EtOAc (3 × 20 mL). The combined organic layer was dried (Na_2SO_4) and concentrated,

which upon flash chromatography (petroleum ether : EtOAc = 70:30) gave *N*-sulfonylated pyrroles **7**.

4.9.10. Procedure for the Synthesis of compound 8:

In an oven dried 10 mL round-bottom flask, **3a** (30.3 mg, 0.1 mmol, 1.0 equiv) in DMF (2.5 mL), K_2CO_3 added. The reaction mixture cooled to 0 °C and the mixture was allowed to stir for 5min. Then, methyl iodide was added dropwise at this temperature. The mixture was stirred at room temperature, until full consumption of starting materials observed, H_2O added and extracted with Et_2O. Combined organic layer was washed with brine (3 × 5 mL), dried over anhydrous Na_2SO_4 and concentrated under reduced pressure. The residue was purified by flash column chromatography (petroleum ether : ethyl acetate = 70:30) to give product **8.**

4.9.11. Procedure for the Synthesis of compound 9:

In an oven dried 10 mL round-bottom flask, **3a** (27.5 mg, 0.1 mmol, 1.0 equiv) was taken along with 1.5 mL of MeOH and 1.5 mL of DCM. The resulting solution was cooled to 0 °C in an ice-bath, followed by portion-wise addition of $NaBH_4$ (18.9 mg, 0.5 mmol, 5 equiv). The resulting mixture was stirred at 0 °C. After complete consumption of **3a**, H_2O (5 mL) was added dropwise. The resulting mixture was diluted with 5 mL of DCM. The organic layer was separated, and the aqueous layer was extracted with DCM (3 × 5 mL). Combined organic layer was washed with brine (3 × 5 mL), dried over anhydrous Na_2SO_4 and concentrated under reduced pressure. The residue was purified by flash column chromatography (petroleum ether : ethyl acetate = 70 : 30) to give product **9.**

4.9.12. Procedure for the Synthesis of compound 10:

In an oven and vacuum-dried 10 mL round-bottom flask, equipped with a reflux condenser, K_2CO_3 (82 mg, 0.6 mmol, 6.0 equiv.) and 3a (27.5 mg, 0.1 mmol, 1.0 equiv.) was taken in 2.0 mL of CH_3CN, the resulting suspension was refluxed for 24 h at 85 °C. After 24 h, reaction mixture was cooled to r.t., diluted with 2 mL of sat. NH4Cl solution and 5 mL of CH_2Cl_2. Organic phase was separated from aqueous phase and the aqueous phase was extracted with additional CH_2Cl_2 (2 × 5 mL). Combined organic phase was dried over anhy. Na_2SO_4 and concentrated under reduced pressure. The crude product was purified by silica-gel flash column chromatography (petroleum ether : ethyl acetate = 50:50) to obtain **10.**

4.9.13. Procedure for the Synthesis of compound 11:

In an oven dried 10 mL round-bottom flask, 3a (27.5 mg, 0.1 mmol, 1.0 equiv.) and NaH in 60% mineral oil (57.6 mg, 1.5 mmol, 15.0 equiv) were taken under argon atmosphere. The

resulting mixture was cooled to 0 °C, followed by dropwise addition of 2 mL dry THF. The resulting solution was stirred at 0 °C for 1hr. After that, methyl iodide (50µL, 0.8 mmol, 8.0 equiv) was added dropwise over 10min. The resulting mixture was allowed to stirred at 0 °C for 30 min then stirred at rt for 8hr. After TLC revealed complete consumption of 3a, the reaction mixture was cooled to 0 °C followed by dropwise addition of 3 mL H_2O. The resulting mixture was dilute with 3 mL of CH_2Cl_2. The organic layer was separated, and the aqueous layer was extracted with CH_2Cl_2 (3 × 5 mL). The combined organic layer was washed with brine (3 × 5 mL), dried over anhydrous Na_2SO_4 and evaporated under reduced pressure and flash column chromatography (petroleum ether : Ethyl acetate = 90:10) afforded **11**.

4.9.14. Procedure for the Synthesis of compound 12:

In an oven dried 10 mL round-bottom flask, 3a (27.5 mg, 0.1 mmol, 1.0 equiv) in DMF (1 mL), K2CO3 (20.7 mg, 0.15mmol,1.5 equiv.) was added. The reaction mixture cooled to 0 ℃ and the mixture was allowed to stir for 5min. Then, methyl iodide (7 µL 0.11 mmol, 1.1equiv.) was added dropwise at this temperature. The mixture was stirred at room temperature, until full consumption of starting materials observed, H_2O added and extracted with ethyl acetate. Combined organic layer was washed with brine (3 × 5 mL), dried over anhydrous Na_2SO_4 and concentrated under reduced pressure. Then, the crude mixture and NaH in 60% mineral oil (57.6 mg, 1.5 mmol, 15.0 equiv) were taken in an oven dried 10 ml round-bottom flask under argon atmosphere. The resulting mixture was cooled to 0 °C, followed by dropwise addition of 2 mL dry THF. The mixture stirred for 15min, then 4-Toluenesulfonyl chloride (47.6 mg, 0.25 mmol, 2.5 equiv.) was added in one portion at the same temperature. The reaction was stirred at 0 °C until full consumption of starting material observed. After that, the reaction quenched with H_2O and diluted with 3 mL of CH_2Cl_2. The organic layer was separated, and the aqueous layer was extracted with CH_2Cl_2 (3 × 5 mL). The combined organic layer was washed with brine (3 × 5 mL), dried over anhydrous Na_2SO_4 and evaporated under reduced pressure and flash column chromatography (petroleum ether : Ethyl acetate = 90:10) afforded **12** as a red solid.

4.9.15. Procedure for the Synthesis of compound 13 and 14:

In an oven dried 10 mL round-bottom flask, **3a** (55 mg, 0.2 mmol, 1.0 equiv) in DMF (5 mL), K_2CO_3(41.4 mg, 0.3 mmol, 1.5equiv.) added. The reaction mixture cooled to 0 ℃ and the mixture was allowed to stir for 5 min. Then, methyl iodide (15 µL, 0.24 mmol, 1.2 equiv.) was added dropwise at this temperature. The mixture was stirred at room temperature, until full consumption of starting materials observed, 5ml H_2O added and extracted with Et_2O (3 × 5ml). Combined organic layer was washed with brine (3 × 5 mL), dried over anhydrous

Na_2SO_4 and concentrated under reduced pressure. Then, the crude and $PhNTf_2$ (85.6 mg, 0.24 mmol, 2.4 equiv) were taken in an oven dried 10 ml round-bottom flask under argon atmosphere. To the mixture 2 mL of dry THF was added. The resulting solution was cooled to –78 °C, potassium hexamethyldisilazide (KHMDS) (0.5 M in toluene; 1 ml, 0.5 mmol, 2.5 equiv) was added via a syringe over 10 min, and the resulting mixture was stirred at –78 °C for 3 h. The reaction mixture was poured into water and extracted with Et_2O (3 × 20 mL). The combined organic layer was washed with 1(N) aqueous NaOH solution (3 × 10 mL) and water (2 × 10 mL), dried over anhydrous Na_2SO_4 and concentrated under reduced pressure. The mixture was purified by short silica pad of 100-200 mesh silica gel to give **X** as sticky solid.

Then, in an oven-dried vial equipped with a stirring bar was added **X** (25 mg, 0.042 mmol, 1.00 equiv) and aniline (5.7 µL, 0.063 mmol, 1.50 equiv) under Ar atmosphere. Toluene (0.2 ml) was added, then LiHMDS (1.0 M in THF, 84 µL, 0.084 mmol, 2.0 equiv) was added while vigorous stirring at room temperature, the reaction was stirred at room temperature until full conversion of starting material. After that, the reaction mixture was quenched with NH_4Cl (sat.) until pH < 7, and extracted with EtOAc (2 × 2 mL), the organic layer was washed with water (1 × 2 mL), brine (1 × 2 mL), dried and concentrated. The crude mixture was purified by flash chromatography (petroleum ether : ethyl acetate = 95:5) to afford product **13.**

In an oven dried Schlenk tube, **X** (0.042 mmol, 1.0 equiv), $Pd(OAc)_2$ (0.5 mg, 0.0021 mmol, 0.05 equiv) and 1,3-Bis(diphenylphosphino) propane (dppp) (0.86 mg, 0.0021 mmol, 0.05 equiv) were taken under argon atmosphere, followed by addition of Et_3N (1.4 mL, 1.0 mmol, 24.0 equiv), HCO_2H (26 µL, 0.672 mmol, 16.0 equiv) and 0.25 mL dry DMF. The resulting mixture was heated to 85 °C. After 12 h, the reaction mixture was cooled to ambient temperature, diluted with 5 mL Brine solution and extracted with EtOAc (3 × 5 mL). The combined organic layer was dried over anhydrous Na_2SO_4 and concentrated under reduced pressure, which was purification by flash chromatography (petroleum ether : ethyl acetate = 99:1) to afforded **14** as a white solid.

4.9.16. Isolation of intermediate A:

Under argon atmosphere, an oven-dried screw cap vial equipped with a magnetic stir bar was charged with Ag_2CO_3 (5 mol%) and **L*3** (10 mol%). Then 2 ml degassed EtOAc was added and stirred the mixture at rt for 30min. After that, the mixture cooled to -10 °C for 10min followed by addition of **1a** in one portion. After stirring 5min at this temperature **2a** was added dropwise for 15 min. The reaction allowed to stirred at -10 °C. After 12h a white precipitate form in the reaction mixture. As the precipitate is soluble at rt and unstable in air, solvents

were decanted under Ar atmosphere at -10 °C. The precipitate was quickly transferred to vacuo to remove excess solvent to give intermediate **A** as colourless solid.

4.10. Single crystal X-ray diffraction analysis:

The compound **5m** was dissolved in minimum amount of hot *n*-hexane/ethyl acetate (3:1) and kept the solution at room temperature for 4 days to give needle like crystal. The crystallographic refinement parameters are given below:

CCDC	2373331
Empirical formula	$C_{16}H_{15}NO_2$
Formula weight	253.29
Temperature/K	296.00
Crystal system	tetragonal
Space group	$P4_32_12$
a/Å	12.968(8)
b/Å	12.968(8)
c/Å	15.313(10)
α/°	90
β/°	90
γ/°	90
Volume/Å^3	2575(4)
Z	8
ρ_{calc}g/cm^3	1.307
μ/mm^{-1}	0.086
F(000)	1072.0
Crystal size/mm^3	0.24 × 0.22 × 0.20
Radiation	MoKα (λ = 0.71073)
2Θ range for data collection/°	4.116 to 55.416
Index ranges	$-16 \le h \le 16$, $-16 \le k \le 16$, $-20 \le l \le 20$
Reflections collected	70308
Independent reflections	3004 [R_{int} = 0.0391, R_{sigma} = 0.0143]
Data/restraints/parameters	3004/0/172
Goodness-of-fit on F^2	1.089
Final R indexes [I>=2σ (I)]	R_1 = 0.0369, wR_2 = 0.0863
Final R indexes [all data]	R_1 = 0.0462, wR_2 = 0.0944
Largest diff. peak/hole / e Å^{-3}	0.13/-0.12
Flack parameter	0.3(2)

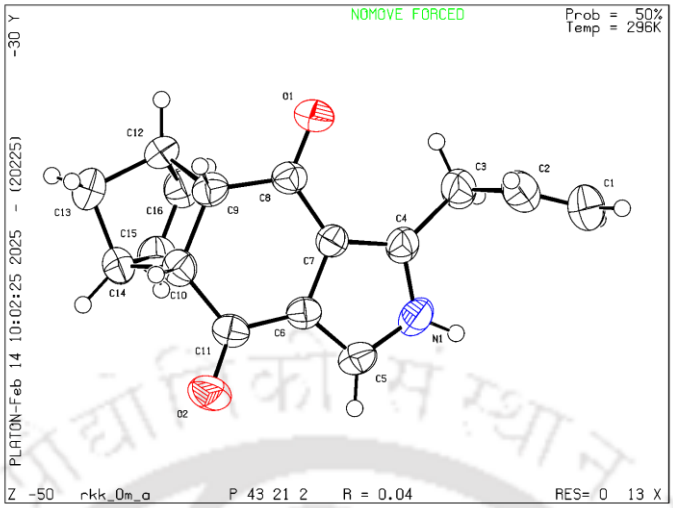

4.11. Characterization of the products:

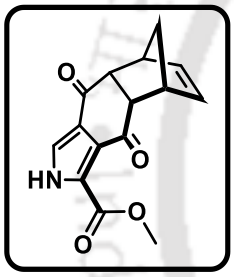

Methyl (4a*R*,5*S*,8*R*,8a*S*)-4,9-dioxo-4,4a,5,8,8a,9-hexahydro-2*H*-5,8-metha nobenzo[*f*]isoindole-1-carboxylate (3a): Product were prepared following '*Method A*, Pale yellow solid, 23.3 mg, 86% yield, 94% ee; R_f = 0.5 (petroleum ether : ethyl acetate = 50:50)

^{1}H NMR (500 MHz, Chloroform-d) δ 10.40 (bs, 1H), 7.49 (d, J = 3.3 Hz, 1H), 6.05 (dd, J = 5.7, 2.9 Hz, 1H), 6.01 (dd, J = 5.7, 2.8 Hz, 1H), 3.95 (s, 3H), 3.61 (s, 1H), 3.58 (s, 1H), 3.40 (dd, J = 8.6, 3.9 Hz, 1H), 3.34 (dd, J = 8.6, 3.9 Hz, 1H), 1.54 (d, J = 8.6 Hz, 1H), 1.48 (d, J = 8.7 Hz, 1H).**^{13}C NMR** (126 MHz, Chloroform-d) δ 195.27, 193.52, 160.68, 135.80, 135.37, 128.27, 125.51, 122.56, 122.17, 52.99, 52.81, 51.72, 49.49, 49.27, 49.05. **HRMS (ESI$^+$) *m/z*:** $[M+Na]^+$ calculated for $C_{15}H_{13}NO_4$: 294.0737, found: 294.0755; **HPLC:** The enantiomeric excess was determined using Phenomenex Lux C4 column (*n*-Hexane/ *i*-PrOH=70:30, flow rate=1.0 mL/min, λ= 254 nm, τ_{major} = 25.4min, τ_{minor} = 53.6 min).

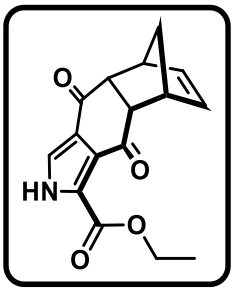

Ethyl (4a*R*,5*S*,8*R*,8a*S*)-4,9-dioxo-4,4a,5,8,8a,9-hexahydro-2*H*-5,8-methanobenzo[*f*]isoindole-1-carboxylate (3b): Product were prepared following '*Method A*', Yellow solid, 23.1 mg, 81% yield, 89% ee; R_f = 0.5 (petroleum ether : ethyl acetate = 50:50)

^{1}H NMR (500 MHz, Chloroform-d) δ 10.34 (bs, 1H), 7.47 (d, J = 3.0 Hz, 1H), 6.05 (dd, J = 5.7, 2.8 Hz, 1H), 6.01 (dd, J = 5.7, 2.8 Hz, 1H), 4.41 (qd, J = 7.1, 5.4 Hz, 2H), 3.62 (s, 1H), 3.58 (s, 1H), 3.40 (dd, J = 8.6, 3.9 Hz, 1H), 3.33 (dd, J = 8.5, 3.9 Hz, 1H), 1.54 (d, J = 8.6 Hz, 1H), 1.48 (d, J = 8.6 Hz, 1H), 1.42 (t, J = 7.1 Hz, 3H).**^{13}C NMR** (126 MHz, Chloroform-d) δ 195.35, 193.30, 160.02, 135.84, 135.35, 128.21, 125.53, 122.63, 122.29, 62.23, 52.80, 51.72, 49.45, 49.18, 48.99, 14.42. **HRMS (ESI$^+$) *m/z*:** $[M+H]^+$ calculated for $C_{16}H_{15}NO_4$: 308.0894, found: 308.0901; **HPLC:** The enantiomeric excess was determined using Phenomenex Lux C4 column (*n*-Hexane/ *i*-PrOH=70:30, flow rate=1.0 mL/min, λ= 220 nm, τ_{major} = 16.7 min, τ_{minor} = 27.8 min).

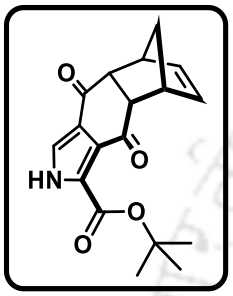

***Tert*-butyl (4a*R*,5*S*,8*R*,8a*S*)-4,9-dioxo-4,4a,5,8,8a,9-hexahydro-2*H*-5,8-methanobenzo[*f*]isoindole-1-carboxylate (3c):** Product were prepared following '*Method A*', pale yellow solid, 25 mg, 79% yield, 92% ee; R_f = 0.5 (petroleum ether : ethyl acetate = 50:50)

^{1}H NMR (500 MHz, Chloroform-d) δ 10.33 (bs, 1H), 7.42 (d, J = 3.2 Hz, 1H), 6.05 (dd, J = 5.7, 2.9 Hz, 1H), 6.00 (dd, J = 5.7, 2.8 Hz, 1H), 3.61 (s, 1H), 3.57 (s, 1H), 1.53 (d, J = 8.7 Hz, 1H), 1.46 (d, J = 8.4 Hz, 1H). **^{13}C NMR** (126 MHz, Chloroform-d) δ 195.55, 192.99, 159.10, 135.85, 135.32, 128.07, 125.22, 124.14, 121.71, 83.59, 52.79, 51.72, 49.41, 49.12, 48.95, 28.40. **HRMS (ESI$^+$) *m/z*:** $[M+Na]^+$ calculated for $C_{18}H_{19}NO_4$: 336.3422, found: 336.3431; **HPLC:** The enantiomeric excess was determined using Phenomenex Lux C4 column (*n*-Hexane/ *i*-PrOH=70:30, flow rate=1.0 mL/min, λ= 254 nm, τ_{major} = 31.5 min, τ_{minor} = 43.3 min).

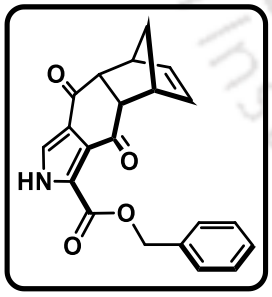

Benzyl (4a*R*,5*S*,8*R*,8a*S*)-4,9-dioxo-4,4a,5,8,8a,9-hexahydro-2*H*-5,8-methanobenzo[*f*]isoindole-1-carboxylate (3d): Product were prepared following '*Method A*', Yellow solid, 28 mg, 82% yield,89% ee; R_f = 0.5 (petroleum ether : ethyl acetate = 50:50)

^{1}H NMR (500 MHz, Chloroform-d) δ 10.45 (s, 1H), 7.47 (d, J = 7.2 Hz, 2H), 7.44 – 7.41 (m, 1H), 7.36 (dd, J = 8.2, 6.2 Hz, 2H), 7.33 – 7.29 (m, 1H), 6.03 (dd, J = 5.7, 2.8 Hz, 1H), 5.99 (dd, J = 5.7, 2.9 Hz, 1H), 5.43 – 5.31 (m, 2H), 3.61 (s, 1H), 3.56 (s, 1H), 3.38 (dd, J = 8.6, 3.9 Hz, 1H), 3.31 (dd, J = 8.6, 3.9 Hz, 1H), 1.53 (d, J = 8.7 Hz, 1H), 1.46 (d, J = 8.6 Hz, 1H).**^{13}C NMR** (126 MHz, Chloroform-d) δ 195.31, 193.21, 159.52, 135.79, 135.47, 135.34, 128.85, 128.67, 128.54, 128.25, 125.99, 122.50, 122.17, 67.66, 52.76, 51.74, 49.50, 49.31, 49.09. **HRMS (ESI$^+$) *m/z*:** $[M+H]^+$ calculated for $C_{21}H_{17}NO_4$: 370.1050, found: 370.1047; **HPLC:** The enantiomeric excess was

determined using Phenomenex Lux C4 column (*n*-Hexane/ *i*-PrOH=70:30, flow rate=1.0 mL/min, λ= 254 nm, τ_{major} = 23.9min, τ_{minor} = 50.3 min).

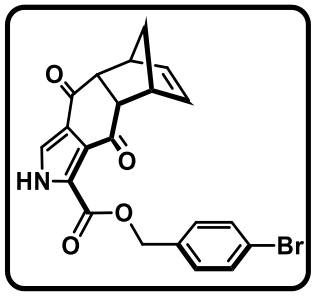

4-bromobenzyl (4a*R*,5*S*,8*R*,8a*S*)-4,9-dioxo-4,4a,5,8,8a,9-hexahydro-2*H*-5,8-methanobenzo[*f*]isoindole-1-carboxylate (3e): Product were prepared following '*Method A*', Yellow solid, 32.4 mg, 76% yield, 88% ee; R_f = 0.5 (petroleum ether : ethyl acetate = 50:50)

^{1}H NMR (600 MHz, Chloroform-d) δ 10.11 (bs, 1H), 7.51 (d, J = 8.0 Hz, 2H), 7.46 (d, J = 3.1 Hz, 1H), 7.40 (d, J = 8.1 Hz, 2H), 6.04 (dd, J = 5.8, 2.8 Hz, 1H), 6.01 (dd, J = 5.9, 2.8 Hz, 1H), 5.40 – 5.28 (m, 2H), 3.62 (s, 1H), 3.58 (s, 1H), 3.40 (dd, J = 8.6, 3.9 Hz, 1H), 3.33 (dd, J = 8.6, 4.0 Hz, 1H), 1.55 (d, J = 8.6 Hz, 1H), 1.48 (d, J = 8.6 Hz, 1H).**^{13}C NMR** (151 MHz, Chloroform-d) δ 195.20, 193.22, 159.66, 135.77, 135.41, 134.44, 132.02, 130.16, 128.37, 125.89, 122.74, 122.53, 121.88, 66.88, 52.78, 51.71, 49.51, 49.32, 49.09. **HRMS (ESI$^+$) *m/z*:** $[M+Na]^+$ calculated for $C_{21}H_{16}BrNO_4$: 448.0155, found: 448.0161; **HPLC:** The enantiomeric excess was determined using Phenomenex Lux C4 column (*n*-Hexane/ *i*-PrOH=70:30, flow rate=1.0 mL/min, λ= 254 nm, τ_{major} = 28.1 min, τ_{minor} = 69.6 min).

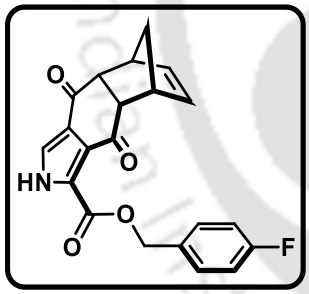

4-fluorobenzyl (4a*R*,5*S*,8*R*,8a*S*)-4,9-dioxo-4,4a,5,8,8a,9-hexahydro-2*H*-5,8-methanobenzo[*f*]isoindole-1-carboxylate (3f): Product were prepared following '*Method A*', Yellow solid, 24.1 mg, 66% yield, 82% ee; R_f = 0.5 (petroleum ether : ethyl acetate = 50:50)

^{1}H NMR (600 MHz, Chloroform-d) δ 10.28 (bs, 1H), 7.51 (dd, J = 8.4, 5.5 Hz, 2H), 7.48 (d, J = 3.3 Hz, 1H), 7.08 (t, J = 8.6 Hz, 2H), 6.06 (dd, J = 5.8, 2.8 Hz, 1H), 6.03 (dd, J = 5.8, 2.8 Hz, 1H), 5.43 – 5.31 (m, 2H), 3.64 (s, 1H), 3.60 (s, 1H), 3.42 (dd, J = 8.6, 3.9 Hz, 1H), 3.35 (dd, J = 8.6, 4.0 Hz, 1H), 1.57 (d, J = 8.2 Hz, 1H), 1.50 (d, J = 8.6 Hz, 1H). **^{13}C NMR** (151 MHz, Chloroform-d) δ 195.25, 193.25, 162.95 (d, $^1J_{C-F}$=246 Hz), 159.62, 135.77, 135.39, 131.3 (d, $^4J_{C-F}$ = 3 Hz), 130.54 (d, $^3J_{C-F}$ = 9 Hz), 128.31, 125.91, 122.52, 122.03, 115.78 (d, $^2J_{C-F}$ = 22.6 Hz), 66.94, 52.77, 51.71, 49.50, 49.30, 49.08. **HRMS (ESI$^+$) *m/z*:** $[M+H]^+$ calculated for $C_{21}H_{16}FNO_4$: 388.0956, found: 388.0958; **HPLC:** The enantiomeric excess was determined using Phenomenex Lux C4 column (*n*-Hexane/ *i*-PrOH=70:30, flow rate=1.0 mL/min, λ= 254 nm, τ_{major} = 14.6min, τ_{minor} = 21.5 min).

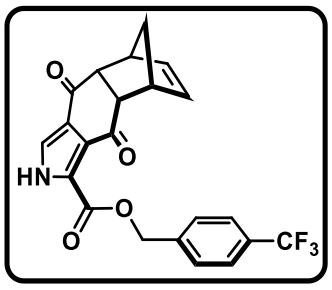

4-(trifluoromethyl)benzyl (4a*R*,5*S*,8*R*,8a*S*)-4,9-dioxo-4,4a,5,8,8a,9-hexahydro-2*H*-5,8-methanobenzo [*f*]isoindole-1-carboxylate (3g): Product were prepared following '*Method A*', Yellow solid, 35.2 mg, 85% yield, 84% ee; R_f = 0.5 (petroleum ether : ethyl acetate = 50:50)

^{1}H NMR (600 MHz, Chloroform-d) δ 10.30 (bs, 1H), 7.65 (d, J = 1.9 Hz, 4H), 7.49 (t, J = 2.5 Hz, 1H), 6.05 (dt, J = 5.1, 2.3 Hz, 1H), 6.01 (dt, J = 5.4, 2.3 Hz, 1H), 5.50 – 5.39 (m, 2H), 3.63 (s, 1H), 3.58 (s, 1H), 3.42 – 3.40 (m, 1H), 3.35 – 3.33 (m, 1H), 1.55 (d, J = 8.6 Hz, 1H), 1.48 (d, J = 8.6 Hz, 1H). **^{13}C NMR** (151 MHz, Chloroform-d) δ 195.23, 193.33, 159.88, 139.39, 135.74, 135.43, 130.79, 130.57, 128.38, 128.29, 125.91, 125.83 (q, J_{CF} = 3 Hz), 122.79, 121.69, 66.69, 52.80, 51.71, 49.51, 49.32, 49.08. **HRMS (ESI$^+$) *m/z*:** $[M+Na]^+$ calculated for $C_{21}H_{16}F_3NO_4$: 438.0924, found: 438.0936; **HPLC:** The enantiomeric excess was determined using Phenomenex Lux C4 column (*n*-Hexane/ *i*-PrOH=70:30, flow rate=1.0 mL/min, λ= 254 nm, τ_{major} = 19.0 min, τ_{minor} = 49.1 min).

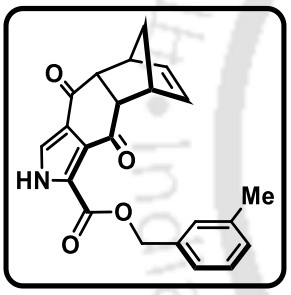

3-methylbenzyl (4a*R*,5*S*,8*R*,8a*S*)-4,9-dioxo-4,4a,5,8,8a,9-hexahydro-2*H*-5,8-methanobenzo[*f*]isoindole-1-carboxylate (3h): Product were prepared following '*Method A*', Yellow solid, 29 mg, 81% yield, 86% ee; R_f = 0.5 (petroleum ether/ethyl acetate = 50:50)

^{1}H NMR (600 MHz, Chloroform-d) δ 10.39 (bs, 1H), 7.42 (s, 1H), 7.28 – 7.23 (m, 3H), 7.13 (d, J = 6.9 Hz, 1H), 6.03 (dd, J = 5.8, 2.7 Hz, 1H), 6.00 – 5.97 (m, 1H), 5.39 – 5.27 (m, 2H), 3.61 (s, 1H), 3.56 (s, 1H), 3.38 (dd, J = 8.6, 3.9 Hz, 1H), 3.30 (dd, J = 8.8, 3.9 Hz, 1H), 2.34 (s, 3H), 1.53 (d, J = 8.5 Hz, 1H), 1.46 (d, J = 8.6 Hz, 1H). **^{13}C NMR** (151 MHz, Chloroform-d) δ 195.35, 193.21, 159.36, 138.54, 135.79, 135.36, 135.31, 129.43, 129.33, 128.76, 128.19, 126.01, 125.68, 122.47, 122.20, 67.67, 52.72, 51.70, 49.49, 49.30, 49.09, 21.57. **HRMS (ESI$^+$) *m/z*:** $[M+Na]^+$ calculated for $C_{29}H_{18}NO_4$: 384.1207, found: 384.1221; **HPLC:** The enantiomeric excess was determined using Phenomenex Lux C4 column (*n*-Hexane/ *i*-PrOH=70:30, flow rate=1.0 mL/min, λ= 254 nm, τ_{major} = 22.0 min, τ_{minor} = 45.7 min).

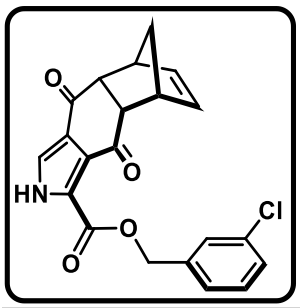

3-chlorobenzyl (4a*R*,5*S*,8*R*,8a*S*)-4,9-dioxo-4,4a,5,8,8a,9-hexa hydro-2*H*-5,8-methanobenzo[*f*]isoindole-1-carboxylate (3i): Product were prepared following '*Method A*', Yellow solid, 22 mg, 77% yield, 88% ee; R_f = 0.5 (petroleum ether : ethyl acetate = 50:50)

^{1}H NMR (500 MHz, Chloroform-d) δ 10.41 (bs, 1H), 7.53 – 7.44 (m, 2H), 7.41 – 7.34 (m, 1H), 7.30 (d, J = 6.0 Hz, 2H), 6.03 – 5.99 (m, 2H), 5.45 – 5.24 (m, 2H), 3.62 (s, 1H), 3.57 (s, 1H), 3.40 (dd, J = 8.5, 4.0 Hz, 1H), 3.33 (dd, J = 8.5, 4.1 Hz, 1H), 1.54 (d, J = 8.7 Hz, 1H), 1.48 (d, J = 8.5 Hz, 1H). **^{13}C NMR** (126 MHz, Chloroform-d) δ 195.29, 193.29, 159.57, 137.48, 135.78, 135.36, 134.71, 130.15, 128.75, 128.38, 128.32, 126.41, 126.07, 122.74, 121.84, 66.64, 52.78, 51.74, 49.53, 49.35, 49.13. **HRMS (ESI$^+$) *m/z*:** $[M+Na]^+$ calculated for $C_{21}H_{16}ClNO_4$: 404.0661, found: 404.0669; **HPLC:** The enantiomeric excess was determined using Phenomenex Lux C4 column (*n*-Hexane/ *i*-PrOH=70:30, flow rate=1.0 mL/min, λ= 254 nm, τ_{major} = 26.4 min, τ_{minor} = 53.3 min).

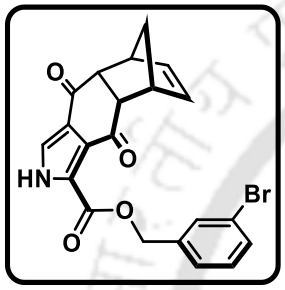

3-bromobenzyl (4a*R*,5*S*,8*R*,8a*S*)-4,9-dioxo-4,4a,5,8,8a,9-hexa hydro-2*H*-5,8-methanobenzo[*f*]isoindole-1-carboxylate (3j): Product were prepared following '*Method A*', Yellow solid, 35 mg, 82% yield, 87% ee; R_f = 0.5 (petroleum ether : ethyl acetate = 50:50)

^{1}H NMR (600 MHz, Chloroform-d) δ 10.34 (bs, 1H), 7.63 (s, 1H), 7.47 (d, J = 3.0 Hz, 1H), 7.46 – 7.42 (m, 2H), 7.24 (t, J = 7.7 Hz, 1H), 6.05 (dd, J = 5.7, 2.8 Hz, 1H), 6.00 (dd, J = 5.9, 2.8 Hz, 1H), 5.40 – 5.29 (m, 2H), 3.62 (s, 1H), 3.58 (s, 1H), 3.41 (dd, J = 8.5, 4.0 Hz, 1H), 3.33 (dd, J = 8.5, 4.0 Hz, 1H), 1.54 (d, J = 8.6 Hz, 1H), 1.48 (d, J = 8.6 Hz, 1H). **^{13}C NMR** (151 MHz, Chloroform-d) δ 195.29, 193.30, 159.49, 137.70, 135.78, 135.35, 131.69, 131.30, 130.44, 128.32, 126.92, 126.06, 122.83, 122.71, 121.80, 66.57, 52.76, 51.72, 49.53, 49.35, 49.13. **HRMS (ESI$^+$) *m/z*:** $[M+Na]^+$ calculated for $C_{21}H_{16}BrNO_4$: 448.0155, found: 448.0158; **HPLC:** The enantiomeric excess was determined using Phenomenex Lux C4 column (*n*-Hexane/ *i*-PrOH=70:30, flow rate=1.0 mL/min, λ= 220 nm, τ_{major} = 18.4 min, τ_{minor} = 25 min).

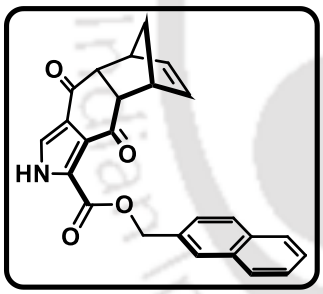

naphthalen-2-ylmethyl (4a*R*,5*S*,8*R*,8a*S*)-4,9-dioxo-4,4a,5,8,8a,9-hexahydro-2*H*-5,8-methanobenzo[*f*] isoindole-1-carboxylate (3k): Product were prepared following '*Method A*', Yellow solid, 32.1 mg, 81% yield, 82% ee; R_f = 0.5 (petroleum ether : ethyl acetate = 50:50).

^{1}H NMR (500 MHz, Chloroform-d) δ 10.31 (bs, 1H), 7.94 (s, 1H), 7.87 – 7.79 (m, 3H), 7.57 (dd, J = 8.4, 1.7 Hz, 1H), 7.50 – 7.47 (m, 2H), 7.41 (d, J = 3.0 Hz, 1H), 6.04 (dd, J = 5.8, 2.8 Hz, 1H), 5.99 (dd, J = 5.7, 2.8 Hz, 1H), 5.59 – 5.47 (m, 2H), 3.61 (s, 1H), 3.56 (s, 1H), 3.37 (dd, J = 8.5, 3.9 Hz, 1H), 3.29 (dd, J = 8.6, 4.0 Hz, 1H), 1.53 (dt, J = 8.6, 2.0 Hz, 1H), 1.46 (d,

J = 8.6 Hz, 1H). **^{13}C NMR** (126 MHz, Chloroform-d) δ 195.30, 193.23, 159.45, 135.79, 135.32, 133.38, 133.34, 132.83, 128.68, 128.24, 128.22, 127.93, 127.90, 126.63, 126.59, 126.14, 125.99, 122.49, 122.12, 67.81, 52.74, 51.70, 49.49, 49.31, 49.08. **HRMS (ESI$^+$) *m/z*:** $[M+Na]^+$ calculated for $C_{25}H_{19}NO_4$: 420.1207, found: 420.1223; **HPLC:** The enantiomeric excess was determined using Phenomenex Lux C4 column (*n*-Hexane/ *i*-PrOH=70:30, flow rate=1.0 mL/min, λ= 254 nm, τ_{major} = 31.0 min, τ_{minor} = 59.0 min).

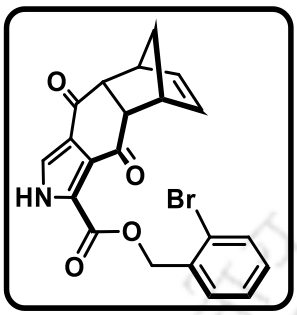

2-bromobenzyl (4a*R*,5*S*,8*R*,8a*S*)-4,9-dioxo-4,4a,5,8,8a,9-hexahydro-2*H*-5,8-methanobenzo[*f*]isoindole-1-carboxylate (3l): Product were prepared following '*Method A*', Yellow solid, 29 mg, 59% yield, 86% ee; R_f = 0.5 (petroleum ether : ethyl acetate = 50:50)

^{1}H NMR (500 MHz, Chloroform-d) δ 10.60 (s, 1H), 7.68 (d, J = 7.6 Hz, 1H), 7.54 (d, J = 7.9 Hz, 1H), 7.48 (d, J = 3.3 Hz, 1H), 7.33 (t, J = 7.5 Hz, 1H), 7.18 (t, J = 7.0 Hz, 1H), 6.04 - 6.03 (m, 1H), 6.02 – 5.97 (m, 1H), 5.47 (d, J = 13.4 Hz, 1H), 5.41 (d, J = 13.3 Hz, 1H), 3.60 (s, 1H), 3.56 (s, 1H), 3.40 - 3.38 (m, 1H), 3.33 - 3.30 (m, 1H), 1.53 (d, J = 8.7 Hz, 1H), 1.46 (d, J = 8.7 Hz, 1H).**^{13}C NMR** (126 MHz, Chloroform-d) δ 195.36, 193.36, 159.24, 135.72, 135.34, 134.79, 132.91, 130.27, 130.04, 128.23, 127.91, 126.11, 123.19, 122.87, 121.87, 67.11, 52.73, 51.71, 49.53, 49.39, 49.15. **HRMS (ESI$^+$) *m/z*:** $[M+Na]^+$ calculated for $C_{21}H_{16}BrNO_4$: 448.0155, found: 448.0161; **HPLC:** The enantiomeric excess was determined using Phenomenex Lux C4 column (*n*-Hexane/ *i*-PrOH=70:30, flow rate=1.0 mL/min, λ= 220 nm, τ_{major} = 24.14 min, τ_{minor} = 66.4 min).

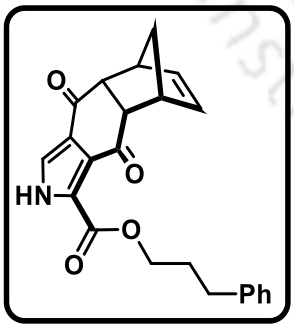

3-phenylpropyl (4a*R*,5*S*,8*R*,8a*S*)-4,9-dioxo-4,4a,5,8,8a,9-hexahydro-2*H*-5,8-methanobenzo[*f*]isoindole-1-carboxylate (3m): Product were prepared following '*Method A*', Yellow solid, 35 mg, 93% yield, 91% ee; R_f = 0.5 (petroleum ether : ethyl acetate = 50:50)

^{1}H NMR (500 MHz, Chloroform-d) δ 9.95 (bs, 1H), 7.40 (d, J = 2.7 Hz, 1H), 7.30 (t, J = 7.5 Hz, 2H), 7.24 (d, J = 7.5 Hz, 2H), 7.21 (t, J = 7.1 Hz, 1H), 6.04 (dd, J = 5.7, 2.8 Hz, 1H), 6.00 (dd, J = 5.8, 2.8 Hz, 1H), 4.37 (td, J = 6.2, 3.7 Hz, 2H), 3.62 (s, 1H), 3.58 (s, 1H), 3.39 (dd, J = 8.5, 3.9 Hz, 1H), 3.33 (dd, J = 8.5, 3.9 Hz, 1H), 2.84 (t, J = 7.4 Hz, 2H), 2.14 (p, J = 6.8 Hz, 2H), 1.54 (d, J = 8.7 Hz, 1H), 1.48 (d, J = 8.6 Hz, 1H). **^{13}C NMR** (126 MHz, Chloroform-d) δ 195.37, 193.12, 159.71, 141.74, 135.76, 135.33, 128.75, 128.71, 128.13, 126.18, 125.66, 122.37, 122.29, 65.64, 52.73, 51.71, 49.48,

49.26, 49.06, 32.63, 30.14. **HRMS (ESI$^+$) *m/z*:** $[M+H]^+$ calculated for $C_{23}H_{22}NO_4$: 376.1544, found: 376.1549; **HPLC:** The enantiomeric excess was determined using Phenomenex Lux C4 column (*n*-Hexane/ *i*-PrOH=70:30, flow rate=1.0 mL/min, λ= 254 nm, τ_{major} = 20.3 min, τ_{minor} = 42.9 min).

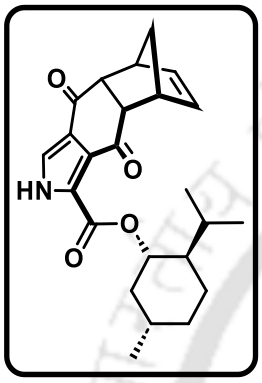

(1*S*,2*R*,5*S*)-2-isopropyl-5-methylcyclohexyl (4a*R*,5*S*,8*R*,8a*S*)-4,9-dioxo-4,4a,5,8,8a,9-hexahydro-2*H*-5,8-methanobenzo[*f*]isoindole-1-carboxylate (3n): Product were prepared following '*Method A*', White sticky solid, 35 mg, 89% yield, >20:1 *dr* ; R_f = 0.5 (petroleum ether/ethyl acetate = 95:5)

^{1}H NMR (500 MHz, Chloroform-d) δ 10.12 (s, 1H), 7.45 (d, J = 2.7 Hz, 1H), 6.01 - 5.99 (m, 2H), 4.93 (td, J = 10.9, 4.5 Hz, 1H), 3.60 (s, 1H), 3.57 (s, 1H), 3.37 (dd, J = 8.5, 3.9 Hz, 1H), 3.32 (dd, J = 8.5, 3.9 Hz, 1H), 2.15 – 2.08 (m, 1H), 1.95 - 1.89 (m, 1H), 1.76 – 1.69 (m, 2H), 1.62 - 1.58 (m,, 2H), 1.53 (d, J = 8.6 Hz, 1H), 1.47 (d, J = 8.7 Hz, 1H), 1.21 – 1.18 (m, 1H), 1.15 – 1.06 (m, 2H), 0.92 (d, J = 6.8 Hz, 6H), 0.77 (d, J = 7.0 Hz, 3H).**^{13}C NMR** (126 MHz, Chloroform-d) δ 195.41, 192.78, 159.31, 135.67, 135.30, 128.29, 125.60, 122.95, 121.97, 76.42, 52.72, 51.78, 49.59, 49.46, 49.28, 47.12, 40.98, 34.31, 31.69, 26.65, 23.78, 22.21, 20.94, 16.75. **HRMS (ESI$^+$) *m/z*:** $[M+Na]^+$ calculated for $C_{24}H_{29}NO_4$: 418.1989, found: 418.1991;

Optical Rotation: $[\alpha]_{25}^{D}$ = +9° (C = 0.2, Chloroform)

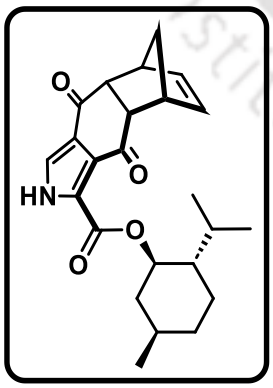

(1*R*,2*S*,5*R*)-2-isopropyl-5-methylcyclohexyl (4a*R*,5*S*,8*R*,8a*S*)-4,9-dioxo-4,4a,5,8,8a,9-hexahydro-2*H*-5,8-methanobenzo[*f*]isoindole-1-carboxylate (3o): Product were prepared following '*Method A*', Pale yellow sticky solid, 34 mg, 85% yield, >20:1 *dr* ; R_f = 0.5 (petroleum ether/ethyl acetate = 95:5)

^{1}H NMR (500 MHz, Chloroform-d) δ 10.12 (s, 1H), 7.45 (d, J = 2.7 Hz, 1H), 6.03 – 5.98 (m, 2H), 4.93 (td, J = 10.9, 4.5 Hz, 1H), 3.60 (s, 1H), 3.57 (s, 1H), 3.37 (dd, J = 8.5, 3.9 Hz, 1H), 3.32 (dd, J = 8.5, 3.9 Hz, 1H), 2.13 – 2.09 (m, 1H), 1.96 – 1.90 (m, 1H), 1.75 – 1.69 (m, 2H), 1.62 –1.58 (m, 2H), 1.53 (d, J = 8.7 Hz, 1H), 1.47 (d, J = 8.7 Hz, 1H), 1.20 – 1.18 (m, 1H), 1.15 – 1.07 (m, 2H), 0.93 (s, 3H), 0.92 (s, 3H), 0.77 (d, J = 7.0 Hz, 3H). **^{13}C NMR** (126 MHz, Chloroform-d) δ 195.41, 192.78, 159.31, 135.67, 135.30, 128.29, 125.60, 122.95, 121.97, 76.42, 52.72, 51.78,

49.59, 49.46, 49.28, 47.12, 40.98, 34.31, 31.69, 26.65, 23.78, 22.21, 20.94, 16.75. **HRMS (ESI$^+$) *m/z*:** $[M+Na]^+$ calculated for $C_{24}H_{29}NO_4$: 418.1989, found: 418.1994;

Optical Rotation: $[\alpha]_{25}^{D} = +29°$ (C = 0.2, Chloroform)

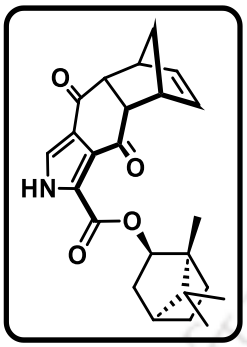

(1*S*,2*R*,5*S*)-2-isopropyl-5-methylcyclohexyl (4a*R*,5*S*,8*R*,8a*S*)-4,9-dioxo-4,4a,5,8,8a,9-hexahydro-2*H*-5,8-methanobenzo[*f*]isoindole-1-carboxylate (3p): Product were prepared following '*Method A*', colourless sticky solid, 30.2 mg, 77% yield, >20:1 *dr* ; R_f = 0.5 (petroleum ether/ethyl acetate = 95:5)

^{1}H NMR (500 MHz, $CDCl_3$) δ 10.24 (s, 1H), 7.46 (s, 1H), 6.09 – 5.95 (m, 2H), 5.11 (dt, J = 9.9, 2.9 Hz, 1H), 3.61 (s, 1H), 3.57 (s, 1H), 3.39 (dd, J = 8.5, 3.9 Hz, 1H), 3.33 (dd, J = 8.5, 3.9 Hz, 1H), 2.47 - 2.41 (m, 1H), 2.26 – 2.20 (m, 1H), 1.83 – 1.75 (m, 2H), 1.54 (d, J = 8.5 Hz, 1H), 1.47 (d, J = 8.6 Hz, 1H), 1.44 – 1.39 (m, 1H), 1.37 – 1.33 (m, 1H), 1.22 – 1.19 (m, 1H), 0.95 (s, 6H), 0.92 (s, 3H). **^{13}C NMR** (126 MHz, Chloroform-d) δ 195.44, 192.84, 160.82, 135.64, 135.36, 128.22, 122.96, 122.07, 82.82, 52.72, 51.83, 49.59, 49.45, 49.30, 49.27, 48.18, 45.12, 36.88, 28.25, 27.34, 19.94, 19.12, 13.85. **HRMS (ESI$^+$) *m/z*:** $[M+Na]^+$ calculated for $C_{24}H_{27}NO_4$: 416.1833, found: 416.1837;

Optical Rotation: $[\alpha]_{25}^{D} = +34°$ (C = 0.2, Chloroform)

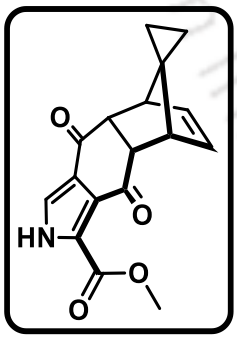

methyl (4a'*R*,5'*S*,8'*R*,8'a*S*)-4',9'-dioxo-4',4a',5',8',8a',9'-hexahydro-2'*H*-spiro[cyclopropane-1,10'-[5,8]methanobenzo[*f*]isoindole]-1'-carboxylate (3q): Product were prepared following '*Method A*', Yellow solid, 26 mg, 87% yield, 91% ee; R_f = 0.5 (petroleum ether : ethyl acetate = 50:50)

^{1}H NMR (500 MHz, Chloroform-d) δ 10.45 (bs, 1H), 7.51 (d, J = 3.1 Hz, 1H), 6.14 (dd, J = 5.9, 2.8 Hz, 1H), 6.10 (dd, J = 5.9, 2.8 Hz, 1H), 3.95 (s, 3H), 3.57 (dd, J = 8.5, 4.0 Hz, 1H), 3.51 (dd, = 8.5, 4.0 Hz, 1H), 2.97 (s, 1H), 2.94 (s, 1H), 0.64 – 0.58 (m, 2H), 0.55 – 0.50 (m, 2H). **^{13}C NMR** (13C NMR (126 MHz, Chloroform-d) δ 195.17, 193.40, 160.65, 135.91, 135.42, 128.47, 125.75, 122.63, 122.19, 54.17, 53.97, 53.68, 53.00, 52.61, 45.18, 8.30, 7.36. **HRMS (ESI$^+$) *m/z*:** $[M+Na]^+$ calculated for $C_{17}H_{15}NO_4$: 320.0894, found: 320.0896; **HPLC:** The enantiomeric excess was determined using Phenomenex Lux C4 column (*n*-Hexane/ *i*-PrOH=70:30, flow rate=1.0 mL/min, λ= 254 nm, τ_{major} = 31.1 min, τ_{minor} = 52.3 min).

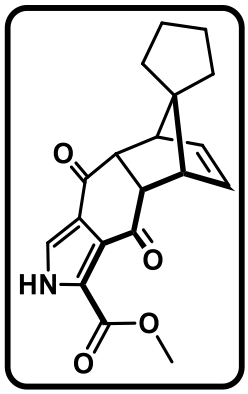

methyl (4a'*R*,5'*S*,8'*R*,8a'*S*)-4',9'-dioxo-4',4a',5',8',8a',9'-hexahydro-2'*H*-spiro[cyclopentane-1,10'-[5,8]methanobenzo[*f*]isoindole]-1'-carboxylate (3r): Product were prepared following '*Method A*', Yellow solid, 27 mg, 83% yield, 91% ee; R_f = 0.5 (petroleum ether : ethyl acetate = 50:50)

^{1}H NMR (500 MHz, Chloroform-d) δ 10.26 (bs, 1H), 7.48 (d, J = 2.8 Hz, 1H), 6.04 (dd, J = 5.9, 2.8 Hz, 1H), 6.01 (dd, J = 5.9, 2.8 Hz, 1H), 3.95 (s, 3H), 3.48 (dd, J = 8.3, 3.9 Hz, 1H), 3.42 (dd, J = 8.3, 3.9 Hz, 1H), 3.19 (s, 1H), 3.16 (s, 1H), 1.65 – 1.59 (m, 2H), 1.54 – 1.47 (m, 6H). **^{13}C NMR** (126 MHz, Chloroform-d) δ 195.71, 193.85, 160.65, 136.70, 136.22, 128.61, 125.85, 122.36, 122.04, 69.23, 56.82, 56.54, 52.99, 52.95, 51.86, 32.29, 31.71, 26.12, 25.60. **HRMS (ESI$^+$) *m/z*:** $[M+Na]^+$ calculated for $C_{19}H_{19}NO_4$: 348.1207, found: 348.1214; **HPLC:** The enantiomeric excess was determined using Phenomenex Lux C4 column (*n*-Hexane/ *i*-PrOH=70:30, flow rate=1.0 mL/min, λ= 254 nm, τ_{major} = 30.9 min, τ_{minor} = 79.7 min).

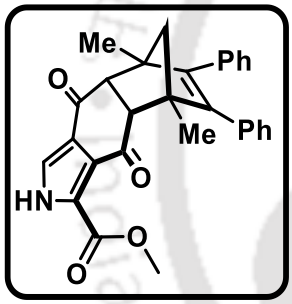

methyl (4a*S*,5*R*,8*S*,8a*R*)-5,8-dimethyl-4,9-dioxo-6,7-diphenyl-4,4a,5,8,8a,9-hexahydro-2*H*-5,8-methanobenzo[*f*]isoindole-1-carboxylate (3s): Product were prepared following '*Method B*', Yellow solid, 34.27 mg, 76% yield, 95% ee; R_f = 0.5 (petroleum ether : ethyl acetate = 50:50)

^{1}H NMR (500 MHz, Chloroform-d) δ 10.15(s, 1H), 7.30 (d, J = 3.1 Hz, 1H), 7.05 - 6.94 (m, 6H), 6.67 (d, J = 7.2 Hz, 2H), 6.53 (d, J = 6.7 Hz, 2H), 3.88 (s, 3H), 3.40 (d, J = 8.4 Hz, 1H), 3.32 (d, J = 8.4 Hz, 1H), 1.85 (d, J = 8.4 Hz, 1H), 1.69 (d, J = 8.4 Hz, 1H), 1.65 (s, 3H), 1.58 (s, 3H). **^{13}C NMR** (126 MHz, Chloroform-d) δ 194.52, 193.29, 160.55, 146.08, 145.47, 135.41, 135.25, 129.78, 129.75, 128.87, 127.79, 127.55, 126.84, 126.57, 126.14, 122.35, 122.06, 65.61, 61.41, 60.55, 59.65, 59.42, 52.81, 18.93, 18.51. **HRMS (ESI$^+$) *m/z*:** $[M+Na]^+$ calculated for $C_{29}H_{25}NO_4$: 474.1676, found: 474.179; **HPLC:** The enantiomeric excess was determined using Phenomenex Lux C4 column (*n*-Hexane/ *i*-PrOH=70:30, flow rate=1.0 mL/min, λ= 254 nm, τ_{major} = 48.3 min, τ_{minor} = 144.3 min).

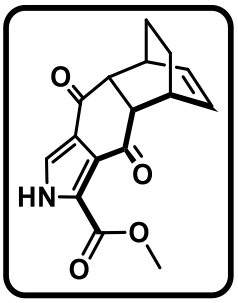

methyl (4a*R*,5*S*,8*R*,8a*S*)-4,9-dioxo-4,4a,5,8,8a,9-hexahydro-2*H*-5,8-ethanobenzo[*f*]isoindole-1-carboxylate (3t): Product were prepared following '*Method A*', Yellow solid, 26 mg, 91% yield, 87% ee; R_f = 0.5 (petroleum ether : ethyl acetate = 50:50)

^{1}H NMR (500 MHz, Chloroform-d) δ 10.19 (s, 1H), 7.51 (d, J = 3.1 Hz, 1H), 6.22 – 6.13 (m, 2H), 3.37 (dd, J = 4.2, 2.1 Hz, 1H), 3.32 (dd, J = 4.1, 2.1 Hz, 1H), 3.13 (dd, J = 9.3, 2.4 Hz, 1H), 3.07 (dd, J = 9.3, 2.4 Hz, 1H), 1.73 (d, J = 8.1 Hz, 2H), 1.38 (dt, J = 8.6, 2.4 Hz, 2H). **^{13}C NMR** (126 MHz, Chloroform-d) δ 195.27, 193.49, 160.59, 134.05, 133.60, 127.68, 125.05, 122.49, 122.19, 53.48, 53.00, 52.28, 35.66, 35.62, 25.31, 25.14. **HRMS (ESI$^+$) *m/z*:** $[M+Na]^+$ calculated for $C_{16}H_{15}NO_4$: 308.0894, found: 308.0901; **HPLC:** The enantiomeric excess was determined using Phenomenex Lux C4 column (*n*-Hexane/ *i*-PrOH=70:30, flow rate=1.0 mL/min, λ= 254 nm, τ_{major} = 21.2 min, τ_{minor} = 73.3 min).

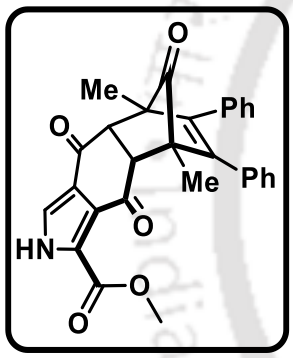

methyl (4a*S*,5*R*,8*S*,8a*R*)-5,8-dimethyl-4,9,10-trioxo-6,7-diphenyl-4,4a,5,8,8a,9-hexahydro-2H-5,8-methanobenzo[f]isoindole-1-carboxylate (3u): Product were prepared following '*Method A*', Yellow solid, 24.6 mg, 53% yield, 74% ee; R_f = 0.5 (petroleum ether : ethyl acetate = 50:50)

^{1}H NMR (500 MHz, $CDCl_3$) δ 10.08 (s, 1H), 7.44 (d, J = 3.0 Hz, 1H), 7.10 - 6.99 (m, 6H), 6.72 - 6.70 (m, 2H), 6.57 – 6.55 (m, 2H), 3.94 (s, 3H), 3.42 (d, J = 9.0 Hz, 1H), 3.35 (d, J = 9.1 Hz, 1H), 1.62 (s, 3H), 1.56 (s, 3H).**^{13}C NMR** (126 MHz, $CDCl_3$) δ 184.82, 184.28, 148.47, 148.22, 140.72, 140.66, 138.50, 138.37, 136.27, 135.95, 135.77, 135.18, 133.28, 130.51, 129.90, 129.40, 127.81, 127.80, 126.59, 124.45, 119.19, 118.98, 32.53, 29.92, 21.47, 21.38. **HRMS (ESI$^+$) *m/z*:** $[M+Na]^+$ calculated for $C_{29}H_{23}NO_5$: 488.1469, found: 488.1469; **HPLC:** The enantiomeric excess was determined using CHIRALPAK IA column (*n*-Hexane/ *i*-PrOH=90:10, flow rate=1.0 mL/min, λ= 254 nm, τ_{major} = 20.4 min, τ_{minor} = 25.7 min).

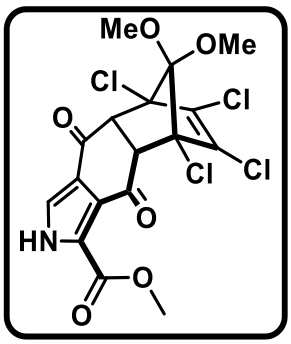

methyl (4a*R*,5*R*,8*S*,8a*S*)-5,6,7,8-tetrachloro-10,10-dimethoxy-4,9-dioxo-4,4a,5,8,8a,9-hexahydro-2*H*-5,8-methanobenzo[*f*]isoindole-1-carboxylate (3v): Product were prepared following '*Method C*', Green solid, 35 mg, 75% yield, 84% ee; R_f = 0.5 (petroleum ether : ethyl acetate = 50:50)

^{1}H NMR (500 MHz, Chloroform-d) δ 10.51 (s, 1H), 7.53 (s, 1H), 3.95 (s, 3H), 3.81 – 3.74 (m, 1H), 3.72 (d, J = 8.2 Hz, 1H), 3.67 (s, 3H), 3.59 (s, 3H).**^{13}C NMR** (126 MHz, Chloroform-d) δ 187.57, 185.89, 160.35, 129.56, 129.29, 127.24, 124.72, 122.98, 122.73, 111.54, 78.14, 78.11, 58.42, 57.53, 53.34, 53.12, 52.34. **^{13}C NMR** (126 MHz, Chloroform-d) δ 199.38, 190.44, 189.37, 159.38, 134.38, 134.28, 134.02, 133.85, 131.47, 131.41, 130.77, 130.72, 129.33, 129.09, 128.78, 128.63, 128.41, 128.26, 128.20, 128.02, 127.42, 127.34, 126.88, 126.75, 126.72, 126.56, 126.28, 126.01, 125.34, 122.97, 122.93, 120.42, 120.12, 66.23, 65.93, 52.36, 51.96, 51.08. **HRMS (ESI$^+$) *m/z*:** $[M+H]^+$ calculated for $C_{17}H_{13}Cl_4NO_6$: 491.9360, found: 491.6359; **HPLC:** The enantiomeric excess was determined using CHIRALPAK IA column (*n*-Hexane/ *i*-PrOH=90:10, flow rate=1.0 mL/min, λ= 220 nm, τ_{major} = 44.5 min, τ_{minor} = 57.4 min).

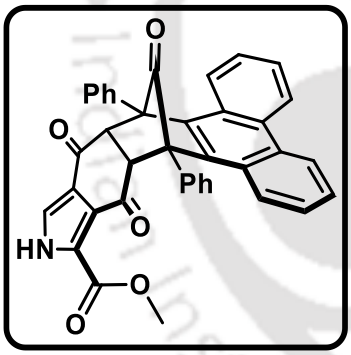

methyl (9*R*,9a*R*,14a*S*,15*S*)-10,14,16-trioxo-9,15-diphenyl-9a,10,12,14,14a,15-hexahydro-9*H*-9,15-methanotriphenyleno[2,3-*f*]isoindole-11-carboxylate (3w): Product were prepared following '*Method D*', Yellow solid, 21.3 mg, 46% yield, 87% ee; R_f = 0.5 (petroleum ether : ethyl acetate = 50:50)

^{1}H NMR (500 MHz, Chloroform-d) δ 9.07 (s, 1H), 8.47 – 8.44 (m,, 4H), 7.71 – 7.66 (m, 2H), 7.48 – 7.41 (m, 4H), 7.36 – 7.32 (m, 2H), 7.25 – 7.20 (m, 3H), 7.18 – 7.11 (m, 3H), 6.25 (d, J = 3.1 Hz, 1H), 4.69 (d, J = 8.4 Hz, 1H), 4.66 (d, J = 8.5 Hz, 1H), 3.55 (s, 3H).**^{13}C NMR** (126 MHz, Chloroform-d) δ 199.38, 190.44, 189.37, 159.38, 134.38, 134.28, 134.02, 133.85, 131.47, 131.41, 130.77, 130.72, 129.33, 129.09, 128.78, 128.63, 128.41, 128.26, 128.20, 128.02, 127.42, 127.34, 126.88, 126.75, 126.72, 126.56, 126.28, 126.01, 125.34, 122.97, 122.93, 120.42, 120.12, 66.23, 65.93, 52.36, 51.96, 51.08. **HRMS (ESI$^+$) *m/z*:** $[M+H]^+$ calculated for $C_{39}H_{25}NO_5$: 610.1625, found: 610.1626; **HPLC:** The enantiomeric excess was determined using CHIRALPAK ID column (*n*-Hexane/ *i*-PrOH=70:30, flow rate=1.0 mL/min, λ= 254 nm, τ_{major} = 38.8 min, τ_{minor} = 47.0 min).

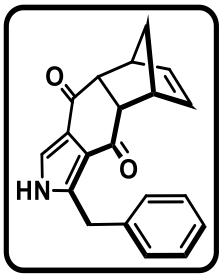

(4a*R*,5*S*,8*R*,8a*S*)-1-benzyl-4a,5,8,8a-tetrahydro-2H-5,8-methanobenzo [f]isoindole-4,9-dione (5a): White solid, 27.9 mg, 92% yield, 87% ee; R_f = 0.5 (petroleum ether : ethyl acetate = 50:50)

^{1}H NMR (500 MHz, Chloroform-d) δ 9.35 (s, 1H), 7.41 (d, J = 8.4 Hz, 2H), 7.13 (d, J = 2.9 Hz, 1H), 7.08 (d, J = 8.4 Hz, 2H), 6.02 - 5.99 (m, 2H), 4.37 – 4.25 (m, 2H), 3.56 (s, 1H), 3.54 (s, 1H), 3.28 – 3.24 (m, 2H)), 1.53 (d, J = 8.6 Hz, 1H), 1.47 (d, J = 8.6 Hz, 1H). **^{13}C NMR** (126 MHz, Chloroform-d) δ 196.16, 196.01, 136.42, 136.24, 135.33, 135.30, 132.28, 130.78, 125.32, 121.27, 119.83, 118.93, 52.31, 52.05, 49.68, 49.26, 49.22, 32.40. **HRMS (ESI$^+$) *m/z*:** $[M+Na]^+$ calculated for $C_{20}H_{17}NO_2$: 326.1152, found: 326.1153; **HPLC:** The enantiomeric excess was determined using Phenomenex Lux C4 column (*n*-Hexane/ *i*-PrOH=70:30, flow rate=1.0 mL/min, λ= 254 nm, τ_{major} = 6.7 min, τ_{minor} = 8.5 min).

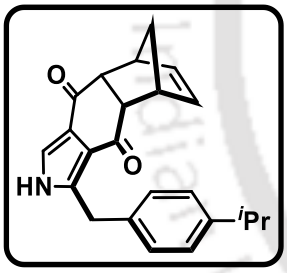

(4a*R*,5*S*,8*R*,8a*S*)-1-(4-isopropylbenzyl)-4a,5,8,8a-tetrahydro-2*H*-5,8-methanobenzo[*f*]isoindole-4,9-dione (5b): White solid, 31 mg, 89% yield, 91% ee; R_f = 0.5 (petroleum ether : ethyl acetate = 50:50)

^{1}H NMR (500 MHz, Chloroform-d) *δ* 9.34 (NH, bs, 1H), 7.16 (d, J = 8.3 Hz, 2H), 7.14 – 7.09 (m, 3H), 6.06 – 5.97 (m, 2H), 4.40 – 4.24 (m, 2H), 3.56 (s, 1H), 3.54 (s, 1H), 3.27 – 3.22 (m, 2H), 2.89 – 2.23 (m, 1H), 1.52 (d, J = 8.6 Hz, 1H), 1.45 (d, J = 8.6 Hz, 1H), 1.22 (s, 3H), 1.20 (s, 3H). **^{13}C NMR** (126 MHz, Chloroform-d) δ 196.13, 196.10, 148.01, 137.56, 135.32, 135.27, 134.43, 129.13, 127.28, 125.25, 119.50, 118.6 9, 52.28, 52.01, 49.64, 49.20, 49.16, 33.91, 32.67, 24.16. **HRMS (ESI$^+$) *m/z*:** $[M+Na]^+$ calculated for $C_{23}H_{23}NO_2$: 368.1621, found: 368.1629; **HPLC:** The enantiomeric excess was determined using Phenomenex Lux C4 column (n-Hexane/ i-PrOH=70:30, flow rate=1.0 mL/min, λ= 254 nm, τ_{major} = 5.7 min, τ_{minor} = 6.4 min).

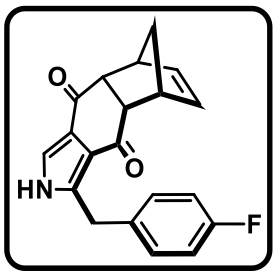

(4a*R*,5*S*,8*R*,8a*S*)-1-(4-fluorobenzyl)-4a,5,8,8a-tetrahydro-2H-5,8-methanobenzo[f]isoindole-4,9-dione (5c): White solid, 30 mg, 93% yield, 83% ee; R_f = 0.5 (petroleum ether : ethyl acetate = 50:50).

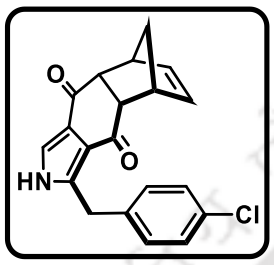

^{1}H NMR (500 MHz, Chloroform-d) *δ* 1H NMR (500 MHz, CDCl3) δ 9.52 (s, 1H), 7.18 (dd, J = 8.7, 5.4 Hz, 2H), 7.13 (d, J = 3.3 Hz, 1H), 6.98 (dt, J = 8.7, 4.4 Hz, 2H), 6.04 – 5.96 (m, 2H), 4.40 – 4.27 (m, 2H), 3.55 (s, 1H), 3.53 (s, 1H), 3.28 – 3.23 (m, 2H), 1.56 – 1.51 (m, 1H), 1.47 (d, J = 8.6 Hz, 1H). **^{13}C NMR** (126 MHz, Chloroform-d) δ 196.15, 196.12, 162.21 (d, $^1J_{CF}$ = 24.5 Hz), 136.91, 135.30, 133.14, 130.60 (d, $^3J_{CF}$ = 9 Hz), 125.30, 119.70, 118.89, 118.86, 116.0 (d, $^2J_{CF}$ = 25.7 Hz), 52.31, 52.05, 49.67, 49.25, 49.20, 32.18. **HRMS (ESI$^+$) *m/z*:** $[M+H]^+$ calculated for $C_{20}H_{16}FNO_2$: 344.1058, found: 344.1069; **HPLC:** The enantiomeric excess was determined using CHIRALPAK ID column (*n*-Hexane/ *i*-PrOH=90:10, flow rate=1.0 mL/min, λ= 274 nm, τ_{major} = 5.5 min, τ_{minor} = 6.3 min).

(4a*R*,5*S*,8*R*,8a*S*)-1-(4-chlorobenzyl)-4a,5,8,8a-tetrahydro-2H-5,8-methanobenzo[f]isoindole-4,9-dione (5d): White solid, 28 mg, 83% yield, 86% ee; R_f = 0.5 (petroleum ether : ethyl acetate = 50:50).

^{1}H NMR (500 MHz, Chloroform-d) δ 9.08 (s, 1H), 7.30 – 7.26 (m, 2H), 7.17 – 7.12 (m, 3H), 6.01 (d, J = 3.4 Hz, 2H), 4.40 – 4.27 (m, 2H), 3.57 (s, 1H), 3.55 (s, 1H), 3.30 – 3.25 (m, 2H), 1.54 (dt, J = 8.6, 2.0 Hz, 1H), 1.47 (d, J = 8.6 Hz, 1H).**^{13}C NMR** (126 MHz, Chloroform-d) δ 196.12, 195.89, 136.27, 135.80, 135.37, 135.31, 133.32, 130.45, 129.38, 125.41, 119.83, 118.82, 52.33, 52.06, 49.69, 49.27, 49.23, 32.39. **HRMS (ESI$^+$) *m/z*:** $[M+Na]^+$ calculated for $C_{20}H_{16}ClNO_2$: 360.0762, found: 360.0773; **HPLC:** The enantiomeric excess was determined using Phenomenex Lux C4 column (*n*-Hexane/ *i*-PrOH=70:30, flow rate=1.0 mL/min, λ= 254 nm, τ_{major} = 5.7 min, τ_{minor} = 7.1 min).

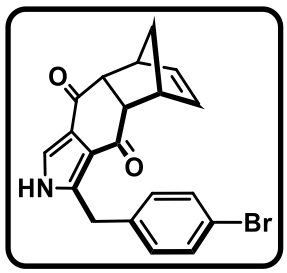

(4a*R*,5*S*,8*R*,8a*S*)-1-(4-bromobenzyl)-4a,5,8,8a-tetrahydro-2H-5,8-methanobenzo[f]isoindole-4,9-dione (5e): White solid, 32.8 mg, 86% yield, 92% ee; R_f = 0.5 (petroleum ether : ethyl acetate = 50:50).

^{1}H NMR (500 MHz, Chloroform-d) δ 9.28 (s, 1H), 7.35 (d, J = 8.4 Hz, 2H), 7.06 (d, J = 2.9 Hz, 1H), 7.02 (d, J = 8.4 Hz, 2H), 5.96 – 5.92 (m, 2H), 4.31 – 4.18 (m, 2H), 3.50 (s, 1H), 3.47 (s, 1H), 3.22 – 3.17 (m, 2H), 1.48 – 1.46 (m, 1H), 1.40 (d, J = 8.6 Hz, 1H). **^{13}C NMR** (126 MHz, Chloroform-d) δ 196.16, 196.01, 136.42, 136.24, 135.33, 135.30, 132.28, 130.78, 125.32, 121.27, 119.83, 118.93, 52.31, 52.05, 49.68, 49.26, 49.22, 32.40. **HRMS (ESI$^+$) *m/z*:** $[M+Na]^+$ calculated for $C_{20}H_{16}BrNO_2$: 404.0257, found: 404.0578; **HPLC:** The enantiomeric excess was determined using Phenomenex Lux C4 column (*n*-Hexane/ *i*-PrOH=70:30, flow rate=1.0 mL/min, λ= 254 nm, τ_{major} = 9.7 min, τ_{minor} = 10.5 min).

(4a*R*,5*S*,8*R*,8a*S*)-1-(4-(trifluoromethyl)benzyl)-4a,5,8,8a-tetrahydro-2H-5,8-methanobenzo[f]isoindole-4,9-dione (5f): White solid, 29.6 mg, 80% yield, 86% ee; R_f = 0.5 (petroleum ether : ethyl acetate = 50:50).

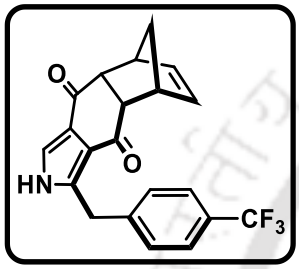

^{1}H NMR (500 MHz, Chloroform-d) δ 9.77 (s, 1H), 7.53 (d, J = 8.2 Hz, 2H), 7.32 (d, J = 8.2 Hz, 2H), 7.13 (d, J = 2.9 Hz, 1H), 5.99 (dt, J = 8.4, 4.2 Hz, 2H), 4.45 (d, J = 16.0 Hz, 1H), 4.39 (d, J = 16.0 Hz, 1H), 3.55 (s, 1H), 3.52 (s, 1H), 3.30 – 3.21 (m, 2H), 1.53 (d, J = 8.7 Hz, 1H), 1.46 (d, J = 8.6 Hz, 1H). **^{13}C NMR** 13C NMR (126 MHz, Chloroform-d) δ 196.19, 196.17, 141.78, 135.78, 135.28, 129.72, 129.47, 129.27, 126.01 (q, J = 3.9 Hz, CF_3), 125.31, 123.13, 120.06, 119.13, 52.30, 52.08, 49.68, 49.27, 49.23, 32.65. **HRMS (ESI$^+$) *m/z*:** $[M+Na]^+$ calculated for $C_{21}H_{16}F_3NO_2$: 394.1026, found: 394.1027; **HPLC:** The enantiomeric excess was determined using Phenomenex Lux C4 column (*n*-Hexane/ *i*-PrOH=90:10, flow rate=1.0 mL/min, λ= 254 nm, τ_{major} = 12.16 min, τ_{minor} = 14.8 min).

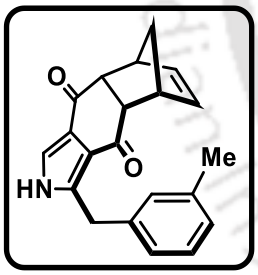

(4a*R*,5*S*,8*R*,8a*S*)-1-(3-methylbenzyl)-4a,5,8,8a-tetrahydro-2H-5,8-methanobenzo[f]isoindole-4,9-dione (5g): White solid, 26 mg, 82% yield, 86% ee; R_f = 0.5 (petroleum ether : ethyl acetate = 50:50).

^{1}H NMR (500 MHz, Chloroform-d) δ 8.64 (s, 1H), 7.22 (t, J = 7.5 Hz, 1H), 7.12 (d, J = 2.9 Hz, 1H), 7.09 (d, J = 7.8 Hz, 1H), 7.01 (d, J = 8.4 Hz, 2H),6.07 – 6.02 (m, 2H), 4.41 – 4.25 (m, 2H), 3.60 (s, 1H), 3.57 (s, 1H), 3.29 (t, J = 3.6 Hz, 2H), 2.32 (s, 3H), 1.54 (dd, J = 8.6, 2.0 Hz, 1H), 1.48 (d, J = 8.6 Hz, 1H).**^{13}C NMR** (126 MHz, Chloroform-d) δ 196.04, 195.86, 139.16, 137.14, 136.81, 135.36, 130.07, 129.27, 128.27, 126.32, 125.41, 119.54, 118.45, 52.33, 52.04, 49.67, 49.26, 49.22, 33.14, 21.60. **HRMS (ESI$^+$) *m/z*:** $[M+na]^+$ calculated for $C_{21}H_{19}NO_2$: 340.1308, found: 340.1316; **HPLC:** The enantiomeric excess was determined

using Phenomenex Lux C4 column (*n*-Hexane/ *i*-PrOH=80:20, flow rate=1.0 mL/min, λ= 254 nm, τ_{major} = 11.3 min, τ_{minor} = 15.3 min).

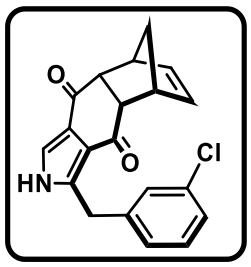

(4a*R*,5*S*,8*R*,8a*S*)-1-(3-chlorobenzyl)-4a,5,8,8a-tetrahydro-2H-5,8-methanobenzo[f]isoindole-4,9-dione (5h): White solid, 24.2 mg, 72% yield, 86% ee; R_f = 0.5 (petroleum ether : ethyl acetate = 50:50).

^{1}H NMR (500 MHz, Chloroform-d) δ 9.98 (NH, bs, 1H), 7.22 – 7.15 (m, 3H), 7.13 (d, J = 2.5 Hz, 1H), 7.09 (d, J = 6.8 Hz, 1H), 6.02 – 5.97 (m, 2H), 4.38 – 4.27 (m, 2H), 3.57 – 3.48 (m, 2H), 3.24 (s, 2H), 1.52 (d, J = 8.6 Hz, 1H), 1.45 (d, J = 8.8 Hz, 1H). **^{13}C NMR** (126 MHz, Chloroform-d) δ 196.08, 139.49, 135.97, 135.09, 134.64, 130.13, 128.82, 127.19, 126.97, 125.04, 119.74, 118.98, 52.13, 51.90, 49.52, 49.11, 49.07, 32.26. **HRMS (ESI$^+$) *m/z*:** $[M+Na]^+$ calculated for $C_{20}H_{16}ClNO_2$: 360.0762, found: 360.0762; **HPLC:** The enantiomeric excess was determined using Phenomenex Lux C4 column (*n*-Hexane/ *i*-PrOH=70:30, flow rate=1.0 mL/min, λ= 254 nm, τ_{major} = 5.9 min, τ_{minor} = 7.1 min).

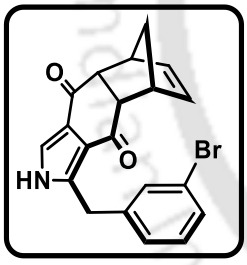

(4a*R*,5*S*,8*R*,8a*S*)-1-(3-bromobenzyl)-4a,5,8,8a-tetrahydro-2H-5,8-methanobenzo[f]isoindole-4,9-dione (5i): White solid, 33.2 mg, 87% yield, 85% ee; R_f = 0.5 (petroleum ether : ethyl acetate =50:50).

^{1}H NMR (500 MHz, Chloroform-d) δ 9.85 (s, 1H), 7.36 – 7.31 (m, 2H), 7.17 – 7.11 (m, 3H), 6.04 – 5.97 (m, 2H), 4.39 – 4.28 (m, 2H), 3.57 – 3.50 (m, 2H), 3.28 – 3.21 (m, 2H), 1.52 (d, J = 8.6, 1H), 1.46 (d, J = 8.6 Hz, 1H). **^{13}C NMR** (126 MHz, Chloroform-d) δ 196.28, 196.26, 139.95, 136.15, 135.30, 131.89, 130.65, 130.35, 127.66, 125.25, 123.10, 119.92, 119.18, 52.32, 52.08, 49.72, 49.31, 49.27, 32.43. **HRMS (ESI$^+$) *m/z*:** $[M+Na]^+$ calculated for $C_{20}H_{16}BrNO_2$: 404.0257, found: 404.055; **HPLC:** The enantiomeric excess was determined using Phenomenex Lux C4 column (*n*-Hexane/ *i*-PrOH=70:30, flow rate=1.0 mL/min, λ= 254 nm, τ_{major} = 5.7 min, τ_{minor} = 7.1 min).

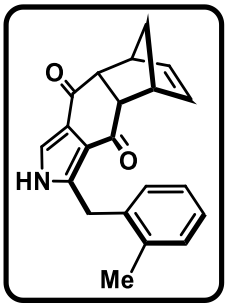

(4a*R*,5*S*,8*R*,8a*S*)-1-(2-methylbenzyl)-4a,5,8,8a-tetrahydro-2H-5,8-methanobenzo[f]isoindole-4,9-dione (5j): White solid, 25.7 mg, 81% yield, 84% ee; R_f = 0.5 (petroleum ether : ethyl acetate =50:50).

1H NMR (500 MHz, Chloroform-d) δ 9.42 (s, 1H), 7.18 (t, J = 7.4 Hz, 1H), 7.11 (d, J = 2.9 Hz, 1H), 7.04 (d, J = 7.5 Hz, 1H), 6.99 (d, J = 8.3 Hz, 2H), 6.06 – 5.95 (m, 2H), 4.39 – 4.24 (m, 2H), 3.55 (s, 1H), 3.53 (s, 1H) 3.24 (q, J = 2.6 Hz, 2H), 2.28 (s, 3H), 1.52 (d, J = 8.6 Hz, 1H), 1.45 (d, J = 8.6 Hz, 1H). **^{13}C NMR** (126 MHz, Chloroform-d) δ 196.15, 196.12, 138.94, 137.36, 137.15, 137.12, 135.29, 135.26, 129.91, 129.09, 128.07, 126.16, 125.22, 119.54, 118.78, 118.76, 52.28, 52.01, 49.64, 49.22, 49.18, 32.97, 21.56. **HRMS (ESI$^+$) *m/z*:** $[M+H]^+$ calculated for $C_{21}H_{19}NO_2$: 340.1308, found: 340.1312; **HPLC:** The enantiomeric excess was determined using Phenomenex Lux C4 column (*n*-Hexane/ *i*-PrOH=70:30, flow rate=1.0 mL/min, λ= 254 nm, τ_{major} = 6.4 min, τ_{minor} = 8.2 min).

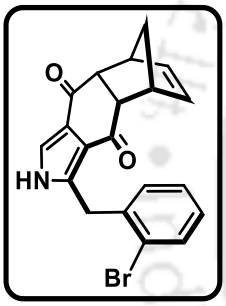

(4a*R*,5*S*,8*R*,8a*S*)-1-(2-bromobenzyl)-4a,5,8,8a-tetrahydro-2H-5,8-methanobenzo[f]isoindole-4,9-dione (5k): White solid, 29.4 mg, 77% yield, 85% ee; R_f = 0.5 (petroleum ether : ethyl acetate =50:50).

^{1}H NMR (500 MHz, Chloroform-d) δ 9.05 (s, 1H), 7.56 (d, J = 8.0 Hz, 1H), 7.38 (d, J = 7.8 Hz, 1H), 7.26 (d, J = 15.1 Hz, 1H), 7.16 (d, J = 2.9 Hz, 1H), 7.13 (t, J = 7.7 Hz, 1H), 6.01 (s, 2H), 4.58 – 4.47 (m, 2H), 3.59 (s, 1H), 3.56 (s, 1H), 3.32 – 3.24 (m, 2H), 1.53 (d, J = 8.6 Hz, 1H), 1.47 (d, J = 8.6 Hz, 1H). **^{13}C NMR** (126 MHz, Chloroform-d) δ 196.12, 195.65, 137.59, 135.57, 135.38, 135.28, 133.26, 131.63, 129.22, 128.44, 125.28, 124.39, 119.82, 118.81, 52.35, 52.03, 49.65, 49.28, 32.84. **HRMS (ESI$^+$) *m/z*:** $[M+Na]^+$ calculated for $C_{20}H_{16}$ $BrNO_2$: 404.0257, found: 404.0258; **HPLC:** The enantiomeric excess was determined using Phenomenex Lux C4 column (*n*-Hexane/ *i*-PrOH=70:30, flow rate=1.0 mL/min, λ= 254 nm, τ_{major} = 5.2 min, τ_{minor} = 5.7 min).

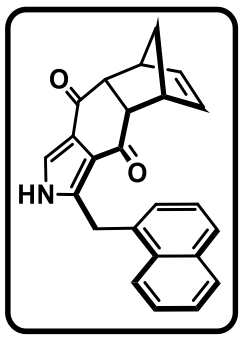

(4a*R*,5*S*,8*R*,8a*S*)-1-(naphthalen-1-ylmethyl)-4a,5,8,8a-tetrahydro-2H-5,8-methanobenzo[f]isoindole-4,9-dione (5l): White solid, 31.4 mg, 89% yield, 80% ee; R_f = 0.5 (petroleum ether : ethyl acetate =50:50).

^{1}H NMR (500 MHz, Chloroform-d) δ 8.77 (s, 1H), 7.89 – 7.81 (m, 2H), 7.78 (d, J = 8.2 Hz, 1H), 7.48 - 7.44 (m, 2H), 7.44 – 7.39 (m, 1H), 7.37 (d, J = 6.7 Hz, 1H), 6.96 (d, J = 2.9 Hz, 1H), 6.09 – 6.08 (m, 1H), 6.02 – 5.99 (m, 1H), 4.80 (s, 2H), 3.61 (s, 1H), 3.53 (s, 1H), 3.30 (dd, J = 8.4, 3.9 Hz, 1H), 3.23

(dd, J = 8.4, 4.1 Hz, 1H), 1.54 (d, J = 8.7 Hz, 1H), 1.46 (d, J = 8.6 Hz, 1H). **^{13}C NMR** (126 MHz, Chloroform-d) δ 196.39, 195.83, 136.80, 135.40, 135.22, 134.29, 133.15, 131.98, 128.98, 128.57, 127.75, 127.01, 126.42, 125.82, 125.16, 124.04, 119.28, 118.76, 52.37, 52.00, 49.68, 49.32, 49.29, 30.81. **HRMS (ESI$^+$) *m/z*:** $[M+Na]^+$ calculated for $C_{24}H_{19}NO_2$: 376.1308, found: 376.1312; **HPLC:** The enantiomeric excess was determined using Phenomenex Lux C4 column (*n*-Hexane/ *i*-PrOH=70:30, flow rate=1.0 mL/min, λ= 254 nm, τ_{major} = 5.7 min, τ_{minor} = 7.1 min).

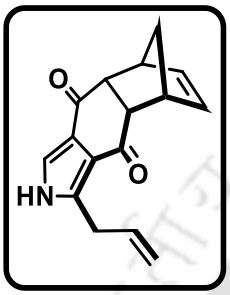

(4a*R*,5*S*,8*R*,8a*S*)-1-allyl-4a,5,8,8a-tetrahydro-2H-5,8-methanobenzo[f]isoindole-4,9-dione (5m): White solid, 22 mg, 87% yield, 91% ee; R_f = 0.5 (petroleum ether : ethyl acetate =50:50).

^{1}H NMR (500 MHz, Chloroform-d) δ 9.49 (NH, bs, 1H), 7.21 (d, J = 2.9 Hz, 1H), 6.01 (d, J = 2.4 Hz, 2H), 5.96 – 5.88 (m, 1H), 5.23 – 5.14 (m, 2H), 3.85 – 3.73 (m, 2H), 3.56 (s, 2H), 3.29 – 3.25 (m, 2H), 1.52 (d, J = 8.6 Hz, 1H), 1.46 (d, J = 8.4 Hz, 1H). **^{13}C NMR** (126 MHz, Chloroform-d) δ 196.02, 136.09, 135.35, 135.25, 133.37, 125.47, 119.53, 118.78, 118.61, 52.29, 52.04, 49.64, 49.22, 49.16, 31.23. **HRMS (ESI$^+$) *m/z*:** $[M+Na]^+$ calculated for $C_{16}H_{15}NO_2$: 276.0995, found: 276.0995; **HPLC:** The enantiomeric excess was determined using Phenomenex Lux C4 column (*n*-Hexane/ *i*-PrOH=70:30, flow rate=1.0 mL/min, λ= 254 nm, τ_{major} = 19.7 min, τ_{minor} = 23.7 min).

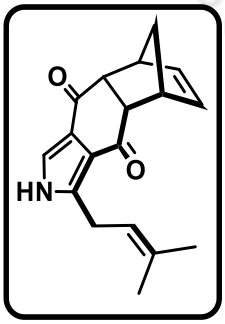

(4a*R*,5*S*,8*R*,8a*S*)-1-(3-methylbut-2-en-1-yl)-4a,5,8,8a-tetrahydro-2H-5,8-methanobenzo[f]isoindole-4,9-dione (5n): White solid, 21 mg, 75% yield, 81% ee; R_f = 0.5 (petroleum ether : ethyl acetate =50:50).

^{1}H NMR (500 MHz, Chloroform-d) δ 9.35 (s, 1H), 7.16 (d, J = 2.9 Hz, 1H), 6.01 (s, 2H), 5.30 (t, J = 7.5 Hz, 1H), 3.77 (dd, J = 17.5, 7.5 Hz, 1H), 3.69 (dd, J = 17.4, 7.4 Hz, 1H), 3.55 (s, 2H), 3.26 (s, 2H), 1.76 (s, 3H), 1.68 (s, 3H), 1.52 (d, J = 8.6 Hz, 1H), 1.45 (d, J = 8.6 Hz, 1H). **^{13}C NMR** (126 MHz, Chloroform-d) δ 196.11, 195.96, 137.96, 137.32, 135.38, 135.23, 125.46, 119.00, 118.21, 118.19, 118.14, 52.26, 52.01, 49.62, 49.17, 49.09, 25.95, 25.93, 18.14. **HRMS (ESI$^+$) *m/z*:** $[M+Na]^+$ calculated for $C_{18}H_{19}NO_2S$: 304.1308, found: 304.1309; **HPLC:** The

enantiomeric excess was determined using Phenomenex Lux C4 column (*n*-Hexane/ *i*-PrOH=70:30, flow rate=1.0 mL/min, λ= 254 nm, τ_{major} = 20.5 min, τ_{minor} = 22.8 min).

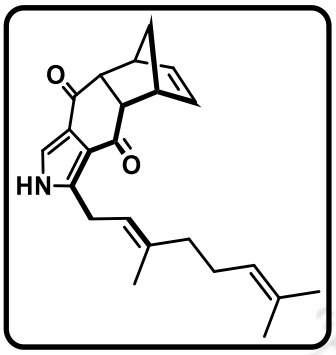

(4a*R*,5*S*,8*R*,8a*S*)-1-((E)-3,7-dimethylocta-2,6-dien-1-yl)-4a,5,8,8a-tetrahydro-2H-5,8-methanobenzo[f]isoindole-4,9-dione (5o): White solid, 28.3 mg, 81% yield, 80% ee; R_f = 0.5 (petroleum ether : ethyl acetate =50:50).

^{1}H NMR (500 MHz, $CDCl_3$) δ 9.28 (s, 1H), 7.14 (s, 1H), 6.00 (s, 2H), 5.30 (s, 1H), 5.08 (s, 1H), 3.78 - 3.66 (m, 2H), 3.56 (s, 2H), 3.26 (s, 2H), 2.21 – 2.08 (m, 4H), 1.71 (s, 3H), 1.62 (s, 3H), 1.60 (s, 3H), 1.51 (d, J = 8.7 Hz, 1H), 1.45 (d, J = 8.7 Hz, 1H). **^{13}C NMR** (126 MHz, $CDCl_3$) δ 196.19, 195.88, 144.16, 142.48, 137.48, 135.18, 135.03, 132.45, 124.39, 118.74, 117.92, 114.05, 52.03, 51.80, 49.45, 49.00, 48.91, 39.45, 26.14, 25.81, 25.72, 17.79, 15.97. **HRMS (ESI$^+$) *m/z*:** $[M+Na]^+$ calculated for $C_{23}H_{27}NO_2$: 372.1934, found: 372.1949; **HPLC:** The enantiomeric excess was determined using Phenomenex Lux C4 column (*n*-Hexane/ *i*-PrOH=95:5, flow rate=1.0 mL/min, λ= 254 nm, τ_{major} = 46.9 min, τ_{minor} = 53.6 min).

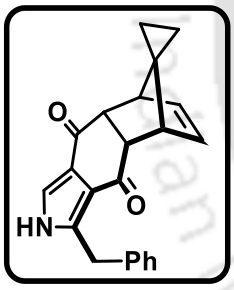

(4a'*R*,5'*S*,8'R,8'a*S*)-1'-benzyl-4a',5',8',8a'-tetrahydro-2'*H*-spiro[cyclopropane-1,10'-[5,8]methanobenzo[*f*]isoindole]-4',9'-dione (5p): Yellow solid, 28.6 mg, 87% yield, 89% ee; R_f = 0.5 (petroleum ether/ethyl acetate = 50:50)

^{1}H NMR (500 MHz, Chloroform-d) δ 9.10 (s, 1H), 7.31 (t, J = 7.4 Hz, 2H), 7.25 (d, J = 5.5 Hz, 2H), 7.20 (d, J = 7.5 Hz, 2H), 7.12 (d, J = 3.3 Hz, 1H), 6.14 – 6.09 (m, 2H), 4.41 (d, J = 16.6 Hz, 1H), 4.33 (d, J = 16.6 Hz, 1H), 3.49 – 3.40 (m, 2H), 2.92 (d, J = 9.6 Hz, 2H), 0.63 – 0.55 (m, 2H), 0.53 – 0.49 (m, 2H). **^{13}C NMR** (126 MHz, Chloroform-d) δ 195.92, 195.83, 137.19, 137.11, 135.45, 135.40, 129.28, 129.21, 127.41, 125.59, 119.91, 118.72, 54.17, 54.11, 53.24, 52.96, 45.28, 33.12, 8.29, 7.39. **HRMS (ESI$^+$) *m/z*:** $[M+Na]^+$ calculated for $C_{22}H_{19}NO_2$: 352.1208, found: 352.1214; **HPLC:** The enantiomeric excess was determined using Phenomenex Lux C4 column (*n*-Hexane/ *i*-PrOH=70:30, flow rate=1.0 mL/min, λ= 274 nm, τ_{major} = 7.14min, τ_{minor} = 9.9 min).

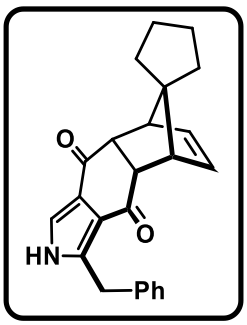

(4a'*R*,5'*S*,8'*R*,8'a*S*)-1'-benzyl-4a',5',8',8a'-tetrahydro-2'H-spiro[cyclopentane-1,10'-[5,8]methanobenzo[f]isoindole]-4',9'-dione (3q): Yellow solid, 29.6 mg, 83% yield, 88% ee; R_f = 0.5 (petroleum ether/ethyl acetate = 95:5)

^{1}H NMR (1H NMR (500 MHz, Chloroform-d) δ 9.19 (NH, bs, 1H), 7.32 (t, J = 7.4 Hz, 2H), 7.29 – 7.24 (m, 1H), 7.22 (d, J = 7.2 Hz, 2H), 7.12 (d, J = 3.0 Hz, 1H), 6.06 – 6.01 (m, 2H), 4.45 – 4.30 (m, 2H), 3.39 – 3.34 (m, 2H), 3.17 – 3.14 (m, 2H), 1.66 – 1.60 (m, 2H), 1.57 – 1.47 (m, 6H). **^{13}C NMR** (126 MHz, Chloroform-d) δ 196.52, 196.50, 137.24, 136.94, 136.16, 136.10, 129.24, 129.19, 127.36, 125.65, 119.98, 118.54, 69.27, 56.79, 52.43, 52.16, 33.09, 32.23, 31.74, 26.10, 25.60. **HRMS (ESI$^+$) *m/z*:** $[M+Na]^+$ calculated for $C_{24}H_{23}NO_2$: 380.1621, found: 380.1622; **HPLC:** The enantiomeric excess was determined using Phenomenex Lux C4 column (*n*-Hexane/ *i*-PrOH=70:30, flow rate=1.0 mL/min, λ= 254 nm, τ_{major} = 7.8 min, τ_{minor} = 10.0 min).

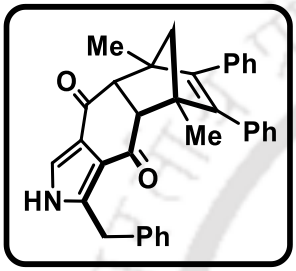

(4a*S*,5*R*,8*S*,8a*R*)-1-benzyl-5,8-dimethyl-6,7-diphenyl-4a,5,8,8a-tetrahydro-2H-5,8-methanobenzo[f]isoindole-4,9-dione (5r): Yellow solid, 43.8 mg, 91% yield, 96% ee; R_f = 0.5 (petroleum ether/ethyl acetate = 95:5)

^{1}H NMR (500 MHz, Chloroform-d) δ 8.65 (s, 1H), 7.34 – 7.27 (m, 3H), 7.17 – 7.12 (m, 2H), 7.11 – 6.94 (m, 7H), 6.72 - 6.68 (m, 4H), 4.37 (d, J = 17.0 Hz, 1H), 3.98 (d, J = 17.0 Hz, 1H), 3.33 (s, 2H), 1.84 (d, J = 8.4 Hz, 1H), 1.72 – 1.70 (m, 4H), 1.62 (s, 3H).**^{13}C NMR** (126 MHz, Chloroform-d) δ 195.73, 195.48, 146.48, 145.74, 136.70, 136.62, 135.88, 135.83, 129.84, 129.69, 129.42, 129.35, 127.71, 127.70, 127.49, 126.61, 126.48, 125.85, 120.29, 118.42, 65.78, 60.70, 60.54, 59.19, 59.04, 33.19, 19.18, 18.79. **HRMS (ESI$^+$) *m/z*:** $[M+H]^+$ calculated for $C_{34}H_{29}NO_2$: 506.2091, found: 506.2112; **HPLC:** The enantiomeric excess was determined using Phenomenex Lux C4 column (*n*-Hexane/ *i*-PrOH=70:30, flow rate=1.0 mL/min, λ= 254 nm, τ_{major} = 7.2 min, τ_{minor} = 9.2 min).

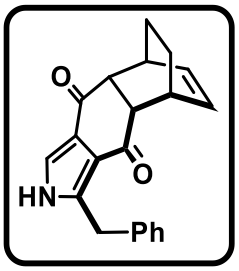

(4a'*R*,5'S,8'*R*,8'a*S*)-1-benzyl-4a,5,8,8a-tetrahydro-2H-5,8-ethanobenzo[f]isoindole-4,9-dione (5s): Yellow solid, 43.8 mg, 91% yield, 92% ee; R_f = 0.5 (petroleum ether/ethyl acetate = 95:5)

^{1}H NMR (500 MHz, Chloroform-d) δ 9.23 (s, 1H), 7.30 (t, J = 7.4 Hz, 2H), 7.25 (d, J = 6.7 Hz, 1H), 7.20 (d, J = 7.9 Hz, 2H), 7.13 (d, J = 2.9 Hz, 1H), 6.21 – 6.15 (m, 2H), 4.46 – 4.28 (m, 2H), 3.36 – 3.27 (m, 2H), 2.98 (s, 2H), 1.72 (d, J = 7.5 Hz, 2H), 1.37 (dd, J = 8.9, 2.6 Hz, 2H).**^{13}C NMR** (126 MHz,

Chloroform-d) δ 196.17, 196.14, 137.17, 137.16, 133.73, 133.67, 129.24, 129.20, 127.36, 124.57, 119.04, 118.76, 52.95, 52.68, 35.92, 35.85, 33.15, 25.40, 25.36. **HRMS (ESI$^+$) *m/z*:** $[M+Na]^+$ calculated for $C_{21}H_{19}NO_2$: 340.1308, found: 340.1321; **HPLC:** The enantiomeric excess was determined using Phenomenex Lux C4 column (*n*-Hexane/ *i*-PrOH=70:30, flow rate=1.0 mL/min, λ= 254 nm, τ_{major} = 6.3 min, τ_{minor} = 9.4 min).

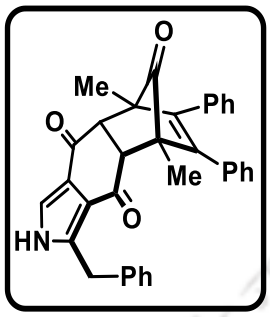

(4a*S*,5*R*,8*S*,8a*R*)-1-benzyl-5,8-dimethyl-6,7-diphenyl-4a,5,8,8a-tetrahydro-2H-5,8-methanobenzo[f]isoindole-4,9,10-trione (5t): Yellow solid, 26.3 mg, 53% yield, 86% ee; R_f = 0.5 (petroleum ether/ethyl acetate = 95:5)

^{1}H NMR (400 MHz, Chloroform-d) *δ* 7.58 (d, *J* = 7.3 Hz, 2H), 7.55 – 7.52 (m, 3H), 7.50 (s, 1H), 7.48 – 7.43 (m, 1H), 7.38 (d, *J* = 8.2 Hz, 1H), 7.33 (t, *J* = 7.6 Hz, 2H), 7.29 – 7.23 (m, 2H), 7.21 (d, *J* = 7.8 Hz, 2H), 7.17 – 7.13 (m, 5H), 7.09 (d, *J* = 7.3 Hz, 1H), 7.07 – 7.03 (m, 3H), 6.05 (d, *J* = 13.1 Hz, 1H), 5.92 (s, 1H), 4.88 (d, *J* = 13.1 Hz, 1H), 2.42 (s, 3H).**^{13}C NMR** (126 MHz, Chloroform-d) *δ* 201.13, 158.44, 154.88, 152.64, 144.85, 137.64, 136.98, 136.57, 136.21, 130.36, 130.22, 130.04, 129.95, 129.35, 129.11, 128.53, 128.35, 128.26, 127.51, 127.34, 126.88, 126.26, 125.31, 123.23, 120.54, 119.29, 112.24, 54.23, 49.51, 21.85. **HRMS (ESI$^+$) *m/z*:** $[M+Na]^+$ calculated for $C_{34}H_{27}NO_3$: 520.1884, found: 520.1892; **HPLC:** The enantiomeric excess was determined using CIRALPAK IA column (*n*-Hexane/ *i*-PrOH=80:20, flow rate=1.0 mL/min, λ= 254 nm, τ_{minor} = 5.15 min, τ_{major} = 5.76 min).

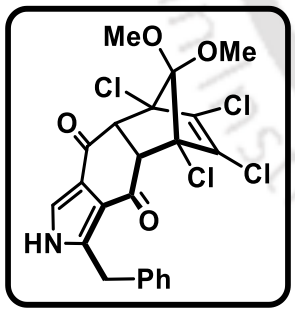

(4a*R*,5*R*,8*S*,8a*S*)-1-benzyl-5,6,7,8-tetrachloro-10,10-dimethoxy-4a,5,8,8a-tetrahydro-2H-5,8-methanobenzo[f]isoindole-4,9-dione (5u): Yellow solid, 37.6 mg, 75% yield, 70% ee; R_f = 0.5 (petroleum ether/ethyl acetate = 95:5)

^{1}H NMR (500 MHz, Chloroform-d) δ 9.01 (s, 1H), 7.32 (t, J = 7.2 Hz, 2H), 7.28 (d, J = 7.0 Hz, 1H), 7.22 - 7.20 (m, 3H), 4.35 (s, 2H), 3.69 - 3.67 (m, 5H), 3.61 (s, 3H).**^{13}C NMR** (126 MHz, Chloroform-d) δ 188.18, 187.98, 138.18, 136.57, 129.39, 129.35, 129.33, 127.61, 124.28, 119.61, 119.04, 111.34, 78.27, 78.17, 57.56, 57.39, 53.33, 52.31, 33.01. **HRMS (ESI$^+$) *m/z*:** $[M+H]^+$ calculated for $C_{22}H_{17}Cl_4NO_4$: 523.9775, found: 523.9786; **HPLC:** The enantiomeric excess

was determined using Phenomenex Lux C4 column (*n*-Hexane/ *i*-PrOH=70:30, flow rate=1.0 mL/min, λ= 254 nm, τ_{major} = 5.15 min, τ_{minor} = 5.76 min).

(9*R*,9a*R*,14a*S*,15*S*)-11-benzyl-12-methyl-9,15-diphenyl-9,9a,14a,15-tetrahydro-10H-9,15-methanotriphenyleno[2,3-f]isoindole-10,14,16(12H)-trione (5v): After following general method, the reaction mixture was filtered, and solvents were evaporated. Then, 1ml DMF and K_2CO_3 (2 equiv.) was added to the mixture. After that, methyl iodide (1.5 equiv.) was added at 0 °C and stirred for 12 h. Solvents were evaporated and purified by flash chromatography to give **3v** as Yellow solid, 29 mg, 53% yield, 81% ee; R_f = 0.5 (petroleum ether/ethyl acetate = 70:30).

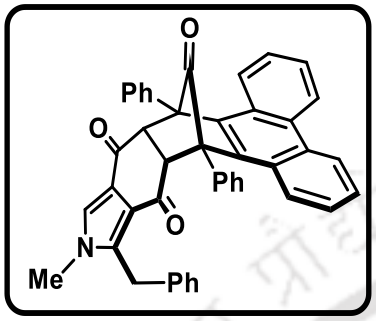

^{1}H NMR (500 MHz, Chloroform-d) δ 8.63 (d, J = 8.4 Hz, 1H), 8.58 (d, J = 8.4 Hz, 1H), 8.47 (d, J = 7.9 Hz, 1H), 8.43 (d, J = 7.9 Hz, 1H), 7.69 – 7.63 (m, 2H), 7.56 (t, J = 7.7 Hz, 1H), 7.49 (t, J = 7.7 Hz, 1H), 7.46 – 7.40 (m, 3H), 7.34 – 7.29 (m, 3H), 7.25 – 7.19 (m, 3H), 7.11 (d, J = 7.9 Hz, 1H), 7.07 (d, J = 7.8 Hz, 1H), 6.96 (d, J = 8.4 Hz, 2H), 6.37 (d, J = 8.2 Hz, 2H), 6.28 (s, 1H), 4.77 – 4.64 (m, 2H), 3.55 (s, 2H), 2.90 (s, 3H). **^{13}C NMR** (126 MHz, Chloroform-d) δ 190.88, 190.12, 135.68, 135.06, 134.75, 134.36, 131.57, 131.49, 131.00, 130.88, 129.33, 129.17, 129.11, 128.92, 128.82, 128.11, 127.98, 127.24, 127.04, 127.00, 126.85, 126.72, 126.43, 126.39, 123.62, 122.89, 122.81, 122.75, 121.27, 66.59, 66.54, 51.04, 50.59, 34.29, 22.92. **HRMS (ESI$^+$) *m/z*:** $[M+H]^+$ calculated for $C_{45}H_{31}NO_3$: 656.2197, found: 656.2212; **HPLC:** The enantiomeric excess was determined using Phenomenex Lux C4 column (*n*-Hexane/ *i*-PrOH=70:30, flow rate=1.0 mL/min, λ= 254 nm, τ_{major} = 20.3 min, τ_{minor} = 22.8 min).

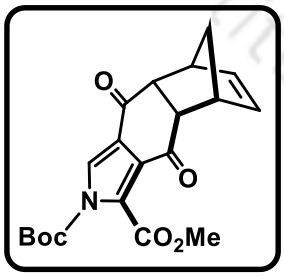

6: colourless liquid (32.6 mg, 88 % yield, 93% ee); **^{1}H NMR** (500 MHz, Chloroform-d) δ 7.70 (s, 1H), 6.06 (dd, *J*=5.7, 2.8 Hz, 1H), 6.02 (dd, *J*=5.8, 2.7 Hz, 1H), 3.98 (s, 3H), 3.58 (s, 2H), 3.35–3.28 (m, 2H), 1.58 (s, 9H), 1.53 (d, *J*=8.7 Hz, 1H), 1.46 (d, *J*=8.8 Hz, 1H). **^{13}C NMR** (126 MHz, Chloroform-d) δ 194.75, 194.04, 161.89, 146.82, 135.69, 135.45, 125.95, 124.42, 124.28, 121.86, 88.47, 53.64, 52.13, 52.09, 49.69, 49.60, 49.55, 27.86. **HRMS (ESI$^+$) *m/z*:** $[M+H]^+$ calculated for $C_{20}H_{22}NO_6$: 372.1442, found: 372.1450; **HPLC:** The enantiomeric excess was determined using CHIRALPAK IA column (*n*-Hexane/ *i*-PrOH=95 : 5, flow rate=1.0 mL/min, λ= 254 nm, τ_{minor}=20.17 min, τ_{major}=22.0 min).

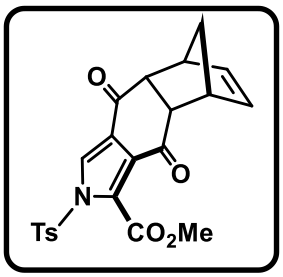

7: Yellow solid (32 mg, 92 % yield, 93% ee); **^{1}H NMR** (600 MHz, Chloroform-d) δ 7.92 (d, *J*=8.1 Hz, 2H), 7.69 (s, 1H), 7.38 (d, *J*=8.1 Hz, 2H), 6.03 (dd, *J*=5.8, 2.8 Hz, 1H), 5.99 (dd, *J*=5.8, 2.8 Hz, 1H), 4.02 (s, 3H), 3.56 (s, 1H), 3.54 (s, 1H), 3.31–3.25 (m, 2H), 2.44 (s, 3H), 1.51 (d, *J*=8.5 Hz, 1H), 1.43 (d, *J*=8.7 Hz, 1H). **^{13}C NMR** (151 MHz, Chloroform-d) δ 194.35, 193.61, 161.26, 147.51, 135.77, 135.45, 133.59, 130.55, 128.91, 125.89, 125.03, 124.58, 122.45, 54.01, 52.20, 52.07, 49.56, 49.38, 49.33, 22.05. **HRMS (ESI$^+$) *m/z*:** $[M+Na]^+$ calculated for $C_{22}H_{19}NO_6S$: 448.0826, found: 448.0827; **HPLC:** The enantiomeric excess was determined using Phenomenex Lux C4 column (*n*-Hexane/ *i*-PrOH=70 : 30, flow rate=1.0 mL/min, λ= 254 nm, τ_{major}=21.1 min, τ_{minor}=27.2 min).

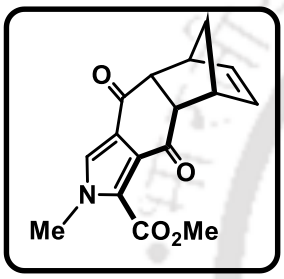

8: Yellow solid (24.5 mg, 86 % yield, 92% ee); **^{1}H NMR** (500 MHz, Chloroform-d) δ 7.24 (s, 1H), 6.04 (dd, *J*=5.7, 2.8 Hz, 1H), 5.99 (dd, *J*=5.7, 2.8 Hz, 1H), 3.94 (s, 3H), 3.86 (s, 3H), 3.57 (s, 1H), 3.55 (s, 1H), 3.34 (dd, *J*=8.5, 3.8 Hz, 1H), 3.29 (dd, *J*=8.5, 3.9 Hz, 1H), 1.53 (d, *J*=8.7 Hz, 1H), 1.46 (d, *J*=8.6 Hz, 1H). **^{13}C NMR** (126 MHz, Chloroform-d) δ 194.70, 193.21, 161.52, 135.84, 135.32, 127.10, 126.51, 125.31, 123.74, 52.79, 52.67, 51.73, 49.41, 48.93, 48.88, 37.76. **HRMS (ESI$^+$) *m/z*:** $[M+Na]^+$ calculated for $C_{16}H_{15}NO_4$: 308.0894, found: 308.0900; **HPLC:** The enantiomeric excess was determined using Phenomenex Lux C4 column (*n*-Hexane/ *i*-PrOH=70 : 30, flow rate=1.0 mL/min, λ= 254 nm, τ_{major}=37.2 min, τ_{minor}=42.8 min).

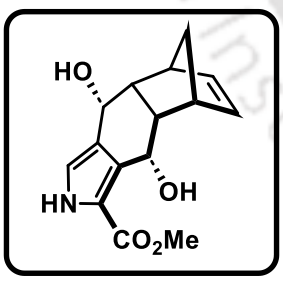

9: Sticky solid (24.5 mg, 89 % yield, >20 : 1 dr, 93% ee); **^{1}H NMR** (500 MHz, Chloroform-d) δ 8.88 (s, 1H), 6.71 (d, *J*=2.9 Hz, 1H), 5.93 (dd, *J*=5.5, 3.0 Hz, 1H), 5.84 (dd, *J*=5.6, 2.9 Hz, 1H), 5.26 (d, *J*=6.0 Hz, 1H), 4.88 (d, *J*=6.0 Hz, 1H), 3.85 (s, 3H), 3.08 (s, 1H), 2.96 (s, 1H), 2.81 (ddd, *J*=9.9, 6.1, 3.4 Hz, 1H), 2.73 (ddd, *J*=10.0, 6.1, 3.3 Hz, 1H), 1.43 (d, *J*=7.7 Hz, 1H), 1.39 (d, *J*=8.0 Hz, 1H). **^{13}C NMR** (126 MHz, Chloroform-d) δ 162.42, 134.59, 133.74, 132.37, 127.46, 117.90, 117.08, 65.24, 64.65, 51.98, 51.55, 46.99, 46.64, 45.73, 45.34. **HRMS (ESI$^+$) *m/z*:** $[M+Na]^+$ calculated for $C_{15}H_{17}NO_4$: 298.1050, found: 298.1049; **HPLC:** The enantiomeric excess was determined using Phenomenex Lux C4 column (*n*-Hexane/ *i*-PrOH=70 : 30, flow rate=1.0 mL/min, λ= 254 nm, τ_{major}=8.9 min, τ_{minor}=11.53 min).

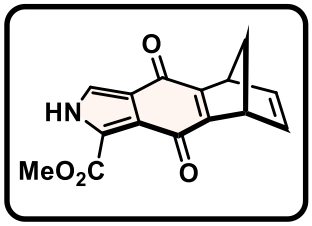

10: Bright yellow solid (15 mg, 56 % yield, 93% ee); **^{1}H NMR** (500 MHz, Chloroform-d) δ 9.74 (s, 1H), 7.47 (d, *J*=2.4 Hz, 1H), 6.87 (t, *J*=1.9 Hz, 2H), 4.18 (s, 1H), 4.16 (s, 1H), 4.00 (s, 3H), 2.32 (d, *J*=7.0 Hz, 1H), 2.28 (d, *J*=7.1 Hz, 1H).**^{13}C NMR** (126 MHz, Chloroform-d) δ 178.98, 177.91, 165.71, 162.73, 160.67, 142.83, 142.73, 125.66, 123.20, 123.00, 122.47, 73.49, 53.00, 48.87, 48.42. **HRMS (ESI^{+}) *m/z*:** $[M+Na]^{+}$ calculated for $C_{15}H_{11}NO_4$: 292.0581, found: 292.0592; **HPLC:** The enantiomeric excess was determined using Phenomenex Lux C4 column (*n*-Hexane/ *i*-PrOH=70 : 30, flow rate=1.0 mL/min, λ= 254 nm, τ_{major}=9.5 min, τ_{minor}=12.1 min).

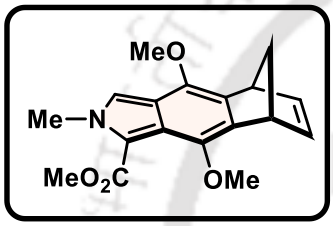

11: Yellow solid (21 mg, 67 % yield, 93% ee). **^{1}H NMR** (500 MHz, Chloroform-d) δ 7.22 (s, 1H), 6.70–6.67 (m, 2H), 4.24 (s, 1H), 4.19 (s, 1H), 4.10 (s, 3H), 4.00 (s, 3H), 3.94 (s, 3H), 3.77 (s, 3H), 2.18 (d, *J*=7.5 Hz, 1H), 2.09 (d, *J*=7.4 Hz, 1H). **^{13}C NMR** (126 MHz, Chloroform-d) δ 162.87, 142.34, 141.30, 141.27, 141.10, 139.36, 127.35, 122.99, 120.85, 120.26, 63.71, 62.10, 60.77, 51.40, 47.05, 46.17, 39.37. **HRMS (ESI^{+}) *m/z*:** $[M+Na]^{+}$ calculated for $C_{18}H_{19}NO_4$: 336.1207, found: 336.1208; **HPLC:** The enantiomeric excess was determined using Phenomenex Lux C4 column (*n*-Hexane/ *i*-PrOH=90 : 10, flow rate=1.0 mL/min, λ= 254 nm, τ_{major}=9.6 min, τ_{minor}=10.5 min).

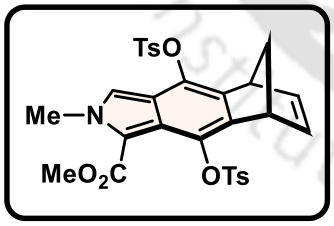

12: Red solid (43 mg, 72 % yield, 93% ee). **^{1}H NMR** (500 MHz, Chloroform-d) δ 7.74 (d, *J*=8.1 Hz, 2H), 7.61 (d, *J*=8.0 Hz, 2H), 7.32 (d, *J*=8.0 Hz, 2H), 7.25 (d, *J*=7.5 Hz, 2H), 6.79 (s, 1H), 6.27 (dd, *J*=5.3, 3.1 Hz, 1H), 6.12 (dd, *J*=5.3, 3.1 Hz, 1H), 3.97 (s, 3H), 3.93 (s, 3H), 3.65 (s, 1H), 3.47 (s, 1H), 2.46 (s, 3H), 2.41 (s, 3H), 1.79 (d, *J*=7.9 Hz, 1H), 1.50 (d, *J*=7.8 Hz, 1H). **^{13}C NMR** (126 MHz, Chloroform-d) δ 162.04, 145.76, 145.31, 141.94, 141.33, 141.11, 136.70, 133.14, 133.06, 132.79, 129.99, 129.82, 128.96, 128.86, 119.74, 119.51, 113.58, 63.79, 51.95, 47.74, 46.93, 39.16, 21.90, 21.82. **HRMS (ESI^{+}) *m/z*:** $[M+Na]^{+}$ calculated for $C_{30}H_{27}NO_8S_2$: 616.1071, found: 616.1082; **HPLC:** The enantiomeric excess was determined using Phenomenex Lux C4 column (*n*-Hexane/ *i*-PrOH=70 : 30, flow rate=1.0 mL/min, λ= 254 nm, τ_{major}=28.8 min, τ_{minor}=37.1 min).

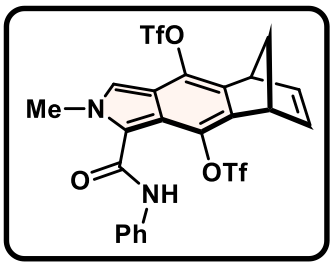

13: Orenge solid (23 mg, 38 % yield, 93% ee). **^{1}H NMR** (500 MHz, Chloroform-d) δ 12.71 (s, 1H), 7.83 (d, *J*=8.0 Hz, 2H), 7.38 (t, *J*=7.7 Hz, 2H), 7.33 (s, 1H), 7.15 (t, *J*=7.4 Hz, 1H), 6.92 (t, *J*=4.1 Hz, 1H), 6.89 (t, *J*=4.0 Hz, 1H), 4.22 (s, 1H), 4.18 (s, 1H), 4.14 (s, 3H), 2.38 (d, *J*=7.1 Hz, 1H), 2.33 (d, *J*=7.1 Hz, 1H). ^{13}C NMR (126 MHz, Chloroform-d) δ 181.24, 178.34, 164.92, 164.42, 157.84, 142.75, 142.73, 138.58, 129.96, 129.75, 129.24, 124.64, 123.67 (−OCF_3, *J*=395.6 Hz), 120.80, 120.50, 73.66, 48.96, 48.63, 40.26. **HRMS (ESI$^+$) *m/z*:** $[M+Na]^+$ calculated for $C_{23}H_{16}F_6N_2O_7S_2$: 633.0196, found: 633.0201; **HPLC:** The enantiomeric excess was determined using CHIRALPAK ID column (*n*-Hexane/ *i*-PrOH=70 : 30, flow rate=1.0 mL/min, λ= 220 nm, τ_{major}=6.3 min, τ_{minor}=9.4 min).

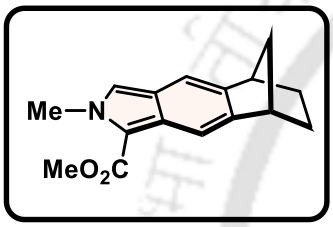

14: white solid (18.9 mg, 78 % yield, 94% ee). **^{1}H NMR** (500 MHz, Chloroform-d) δ 7.79 (s, 1H), 7.25 (s, 1H), 7.20 (s, 1H), 4.19 (s, 3H), 3.95 (s, 3H), 3.41 (s, 1H), 3.34 (s, 1H), 1.98–1.89 (m, 2H), 1.77 (d, *J*=8.8 Hz, 1H), 1.62–1.59 (m, 1H), 1.32–1.29 (m, 2H).**^{13}C NMR** (126 MHz, Chloroform-d) δ 162.76, 147.82, 143.99, 129.25, 123.13, 122.72, 111.23, 110.00, 50.89, 47.74, 43.95, 43.39, 38.80, 28.25, 28.13. **HRMS (ESI$^+$) *m/z*:** $[M+Na]^+$ calculated for $C_{16}H_{17}NO_2$: 278.1152, found: 278.1162; HPLC: The enantiomeric excess was determined using Phenomenex Lux C4 column (*n*-Hexane/ *i*-PrOH=70 : 30, flow rate=1.0 mL/min, λ= 254 nm, τ_{major}=8.6 min, τ_{minor}=9 min).

4.12. NMR Spectra and HPLC chromatogram:

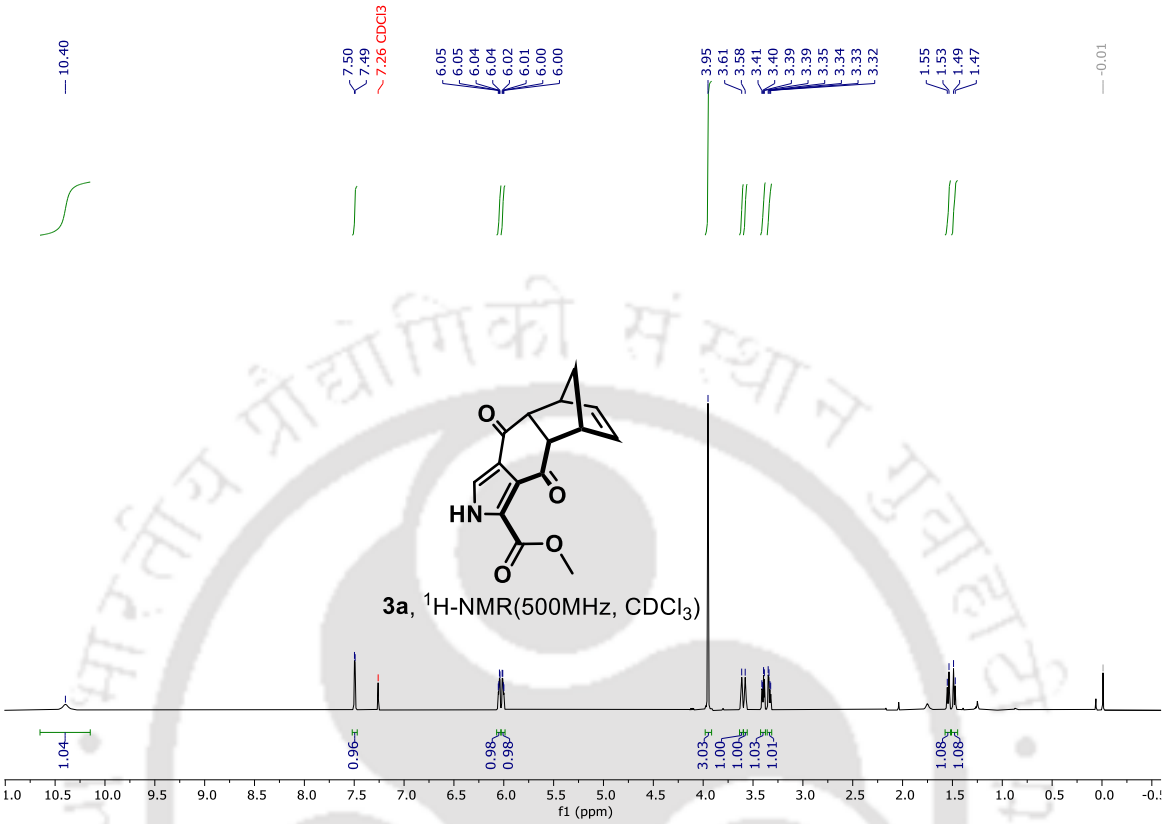

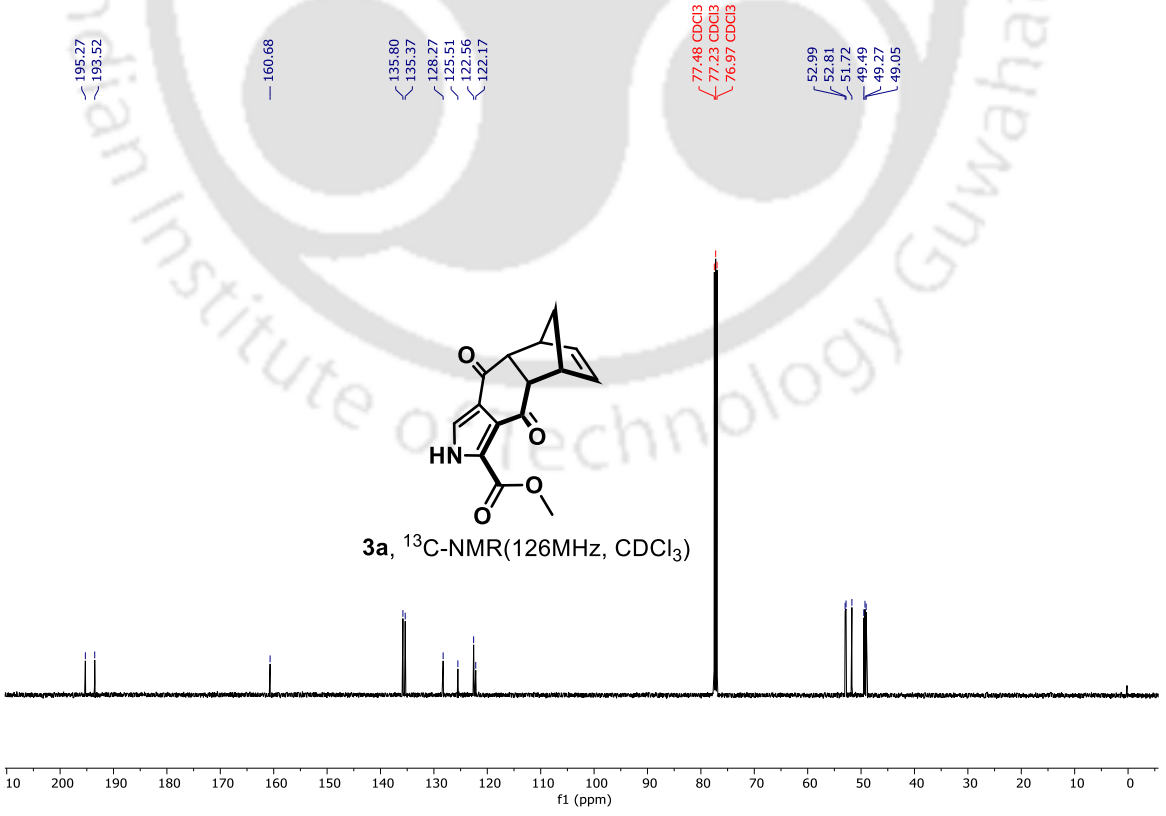

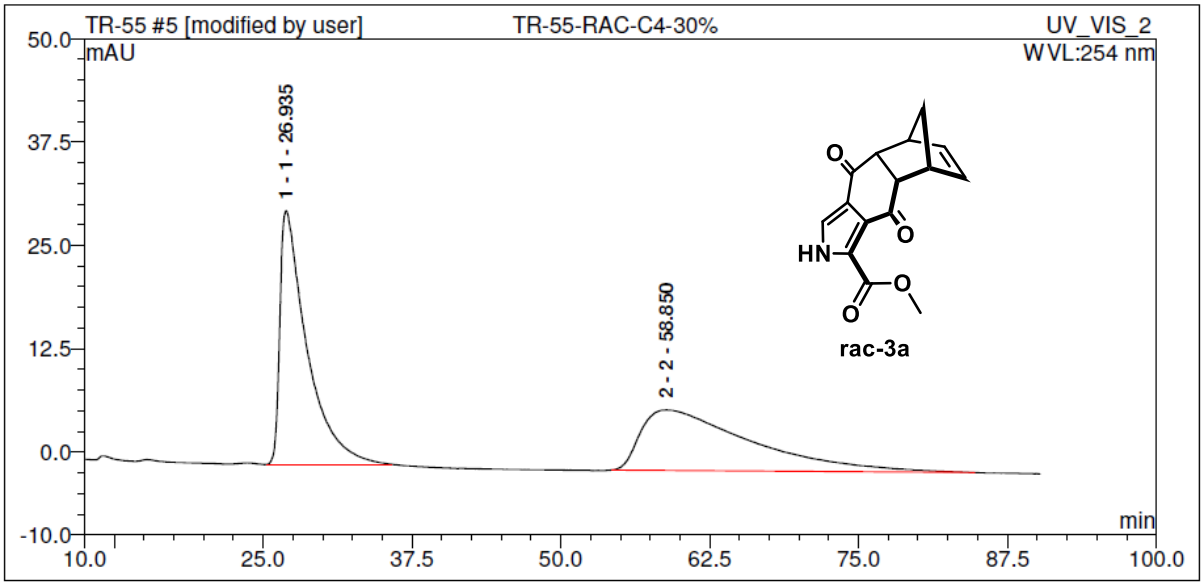

	Peak Name	Ret.Time (detected) min	Area mAU*min	Rel.Area(ident.) %	Height mAU	Amount
1	1	26.935	80.43954	50.80001212	30.6771	n.a.
2	2	58.85	77.90597	49.19998788	7.32499	n.a.

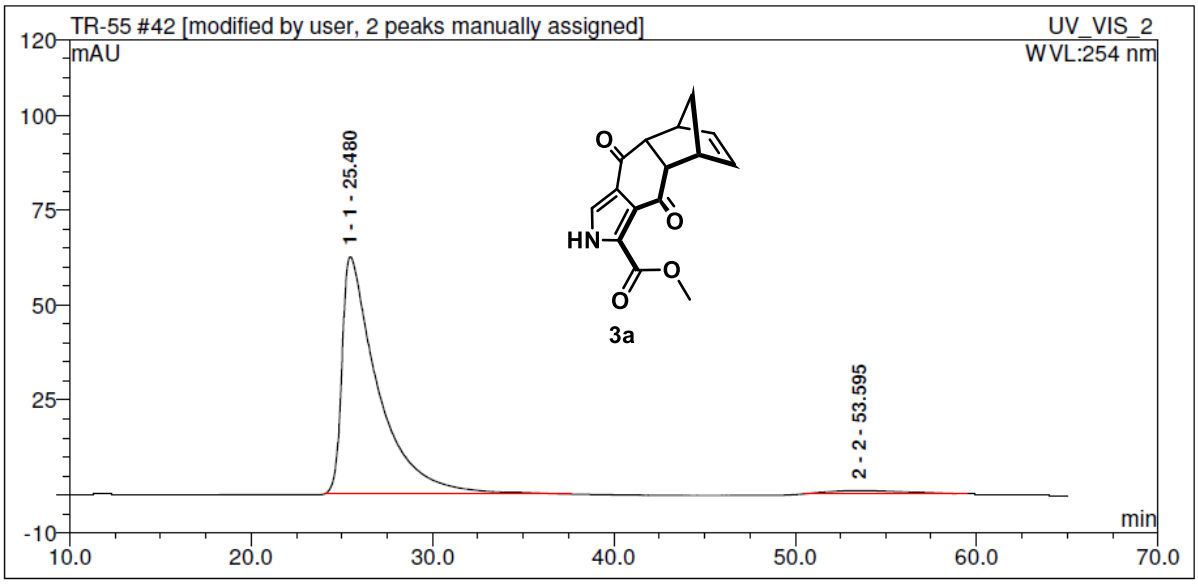

	Peak Name	Ret.Time (detected) min	Area mAU*min	Rel.Area(ident.) %	Height mAU	Amount
1	1	25.48	144.715	96.9803767	62.4756	n.a.
2	2	53.595	4.505908	3.019623299	0.89425	n.a.

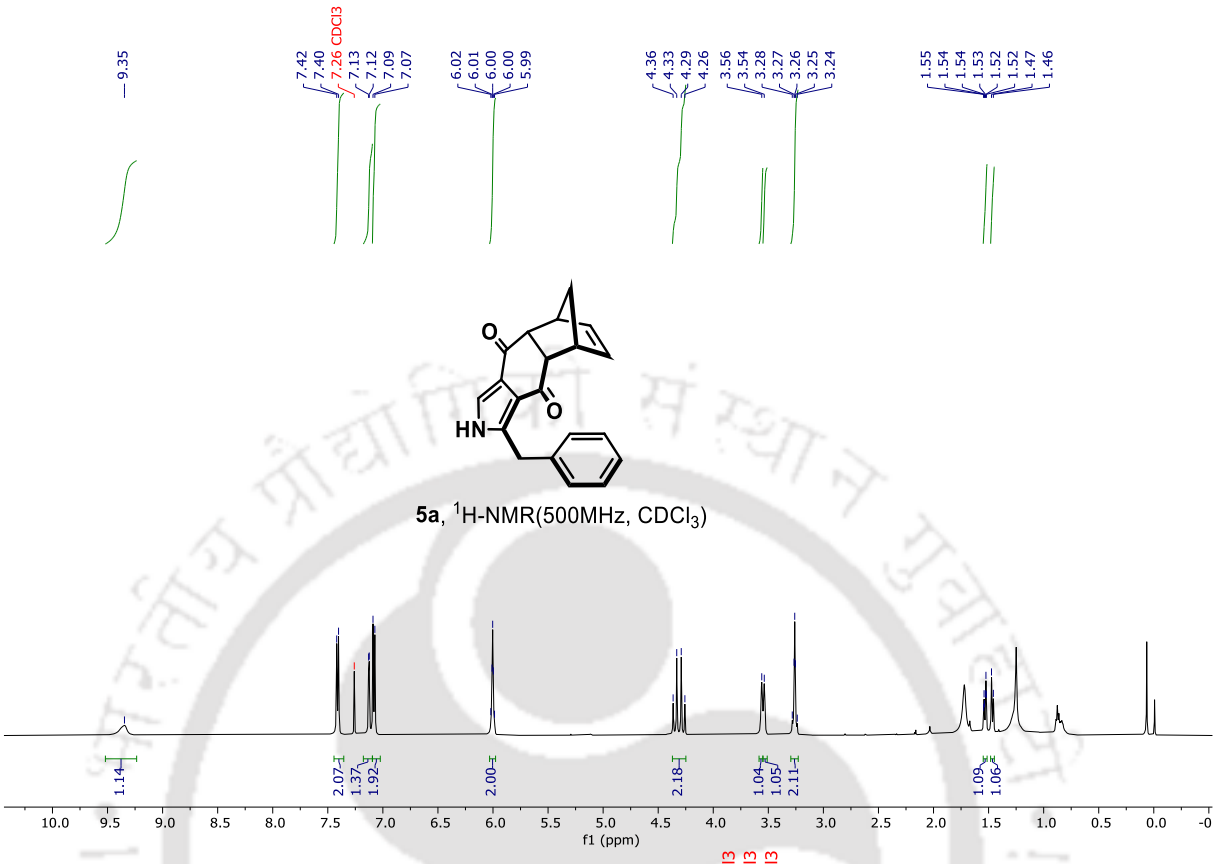

5a, ^{1}H-NMR(500MHz, $CDCl_3$)

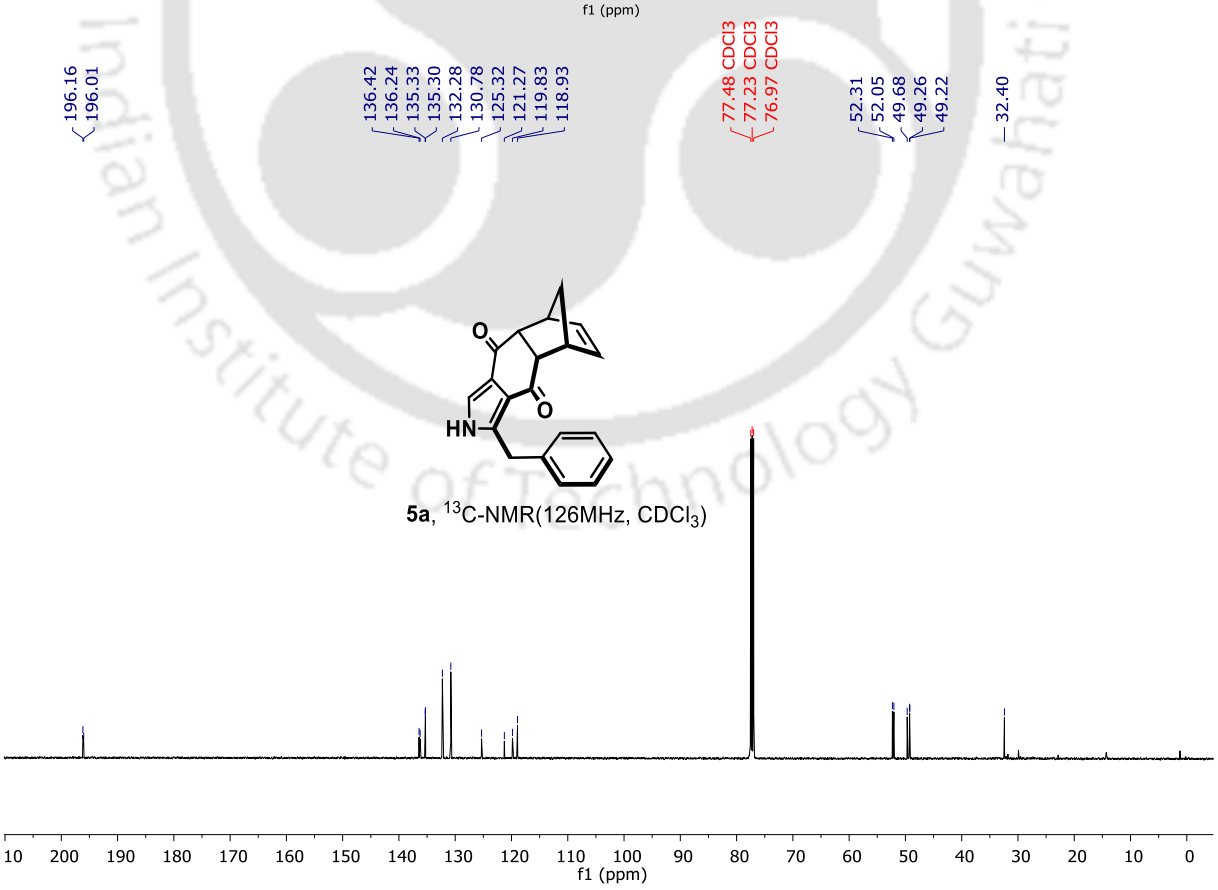

5a, ^{13}C-NMR(126MHz, $CDCl_3$)

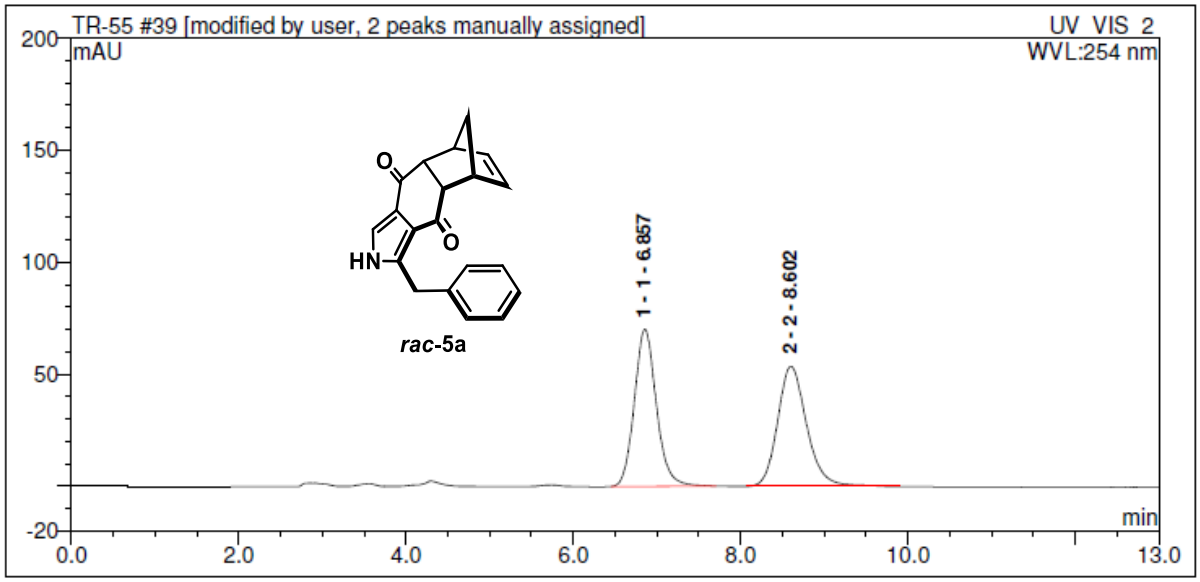

No.	Peak Name	Ret.Time (detected) min	Area mAU*min	Rel.Area(ident.) %	Height mAU	Amount
1	1	6.856666667	21.4242	49.81432638	70.09702	n.a.
2	2	8.601666667	21.58391	50.18567362	53.58348	n.a.

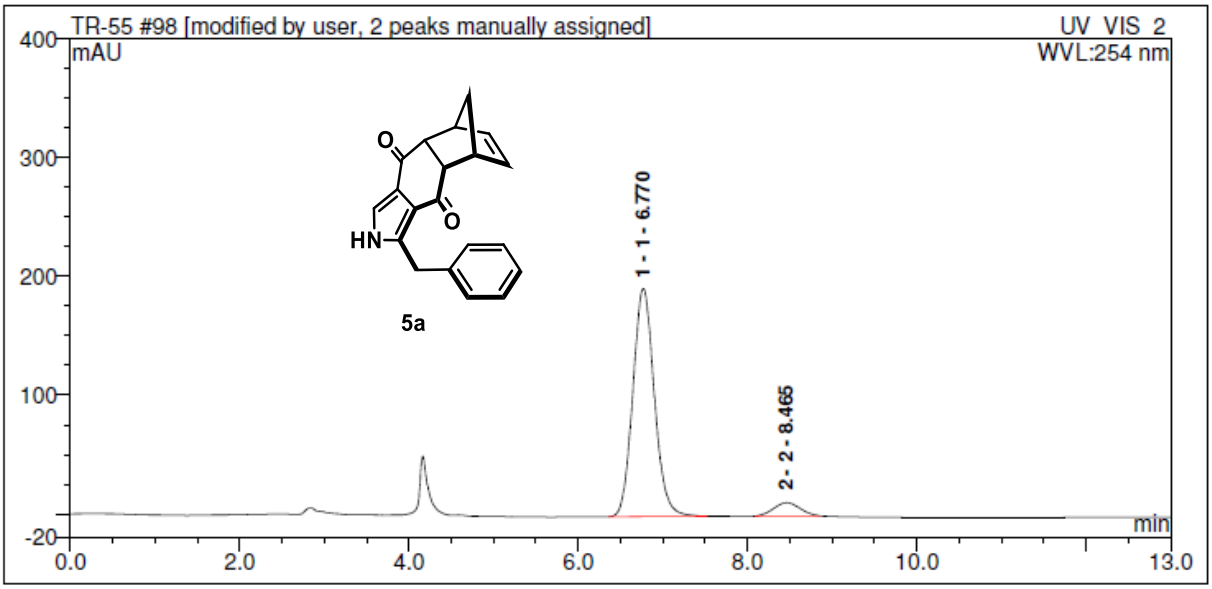

No.	Peak Name	Ret.Time (detected) min	Area mAU*min	Rel.Area(ident.) %	Height mAU	Amount
1	1	6.77	56.43566	93.45168813	191.6545	n.a.
2	2	8.465	3.954539	6.548311869	11.0913	n.a.

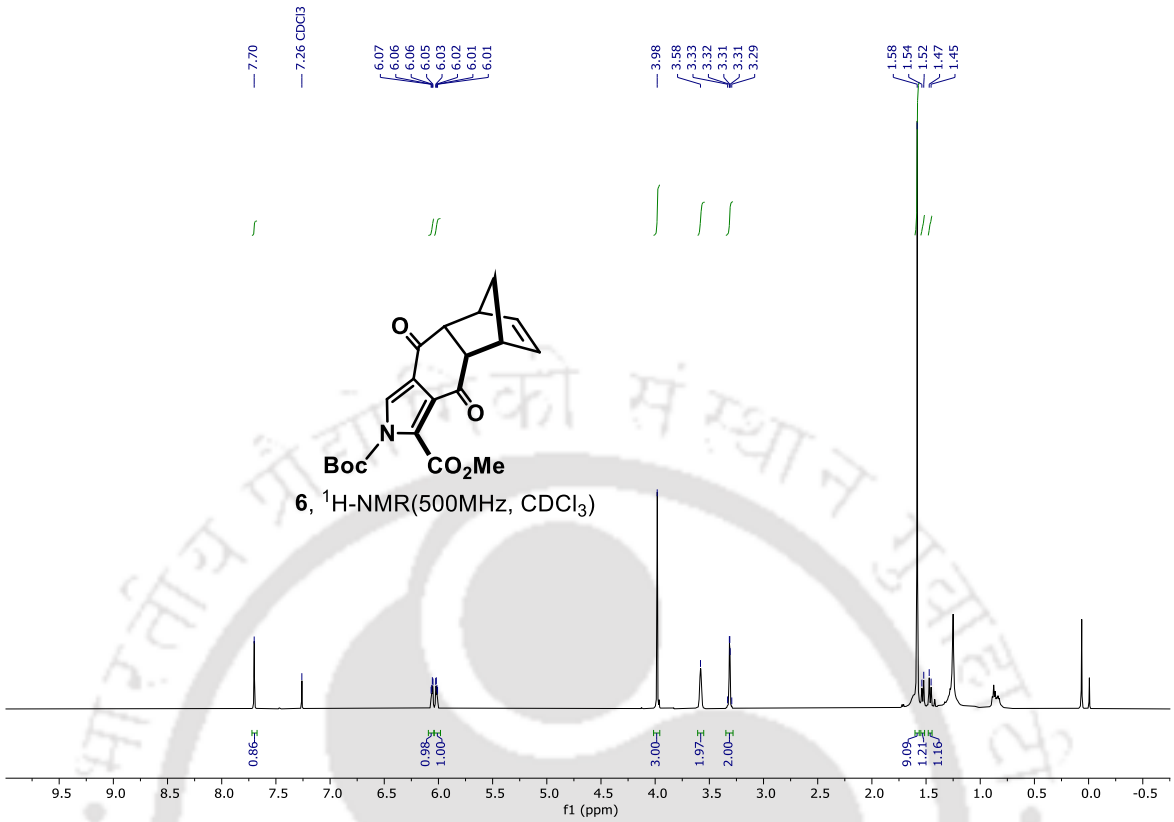

6, ^{1}H-NMR(500MHz, $CDCl_3$)

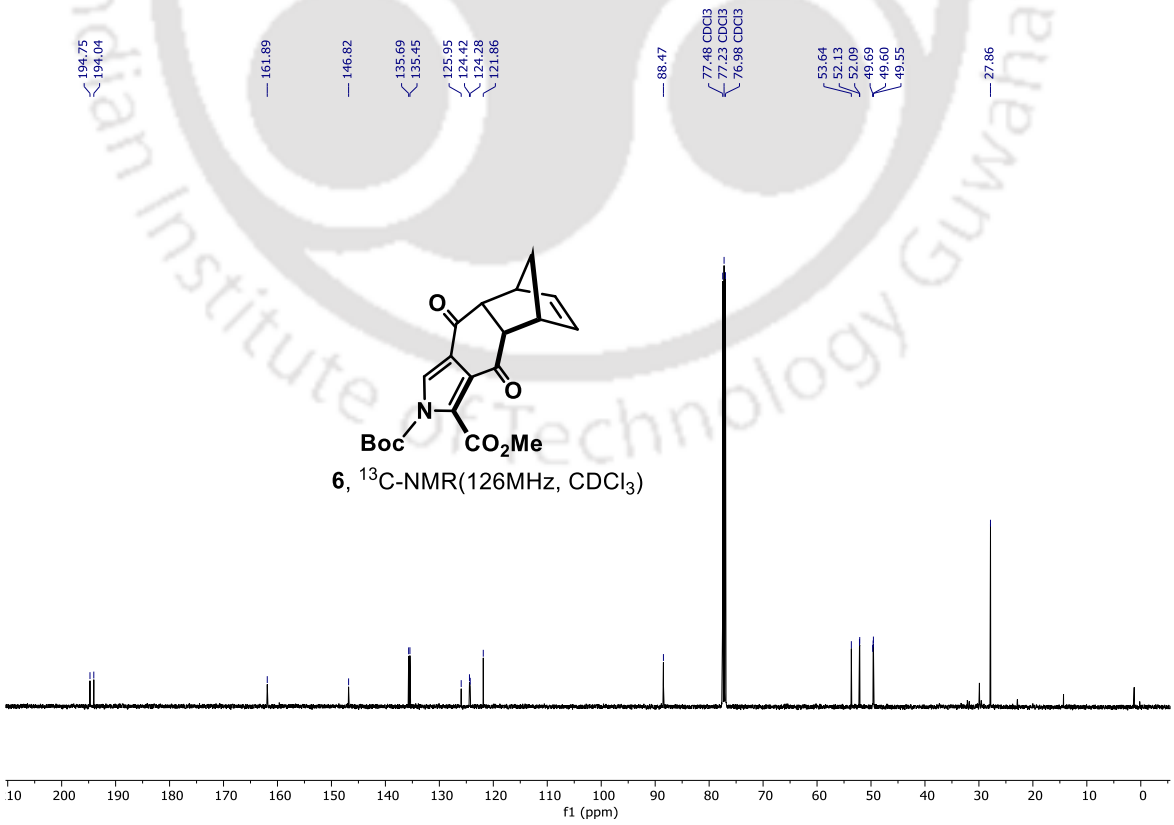

6, ^{13}C-NMR(126MHz, $CDCl_3$)

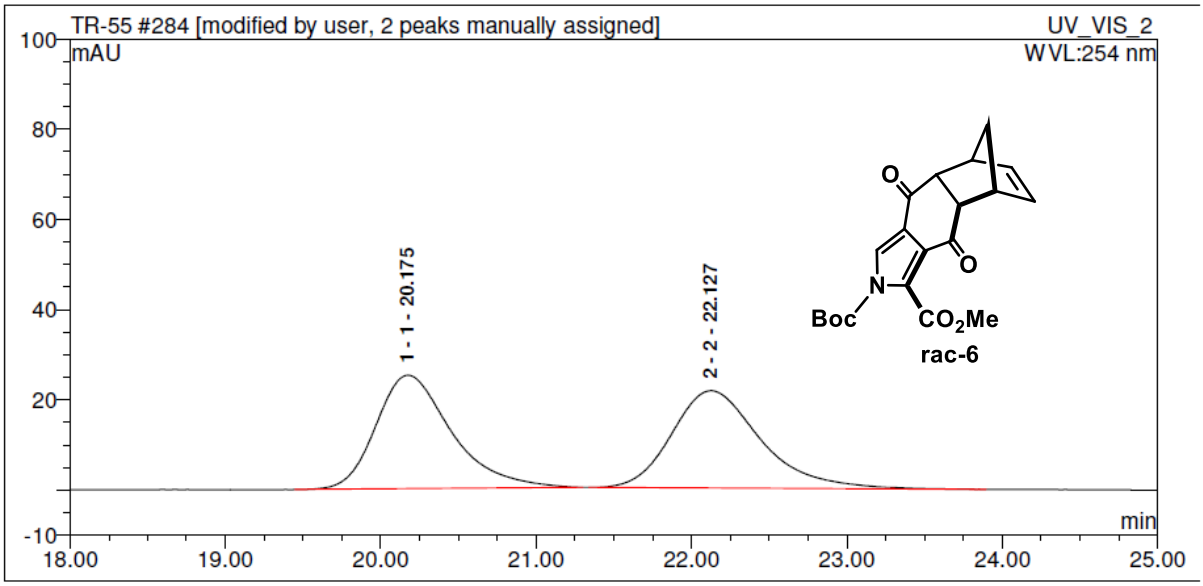

	Peak Name	Ret.Time (detected) min	Area mAU*min	Rel.Area(ident.) %	Height mAU	Amount
1	1	20.175	14.19589	49.76858968	25.16338	n.a.
2	2	22.12666667	14.3279	50.23141032	21.56406	n.a.

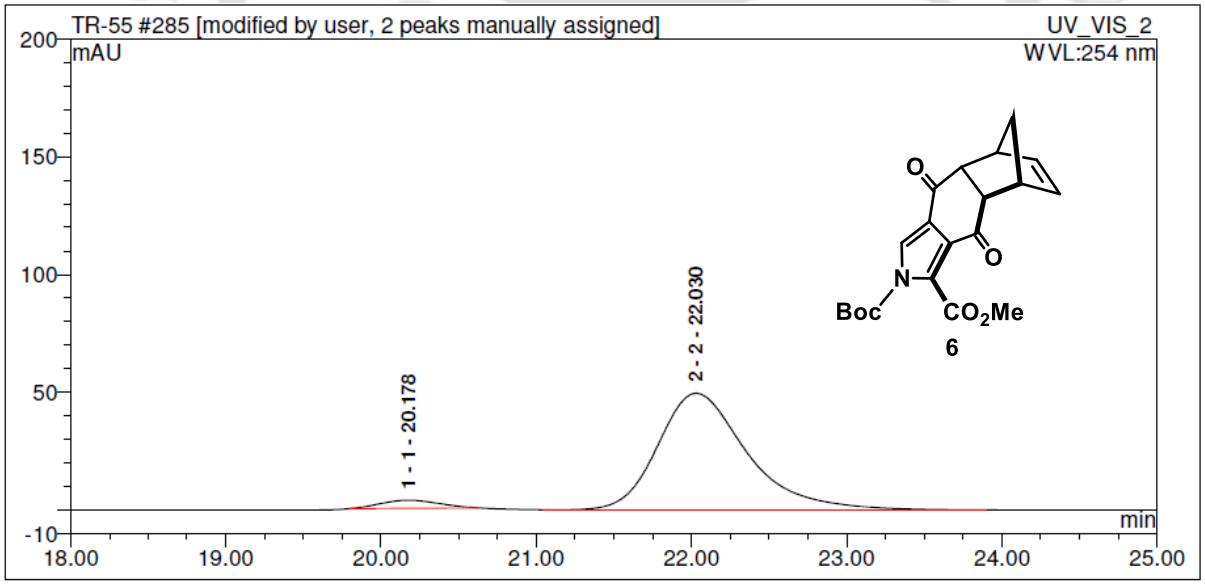

	Peak Name	Ret.Time (detected) min	Area mAU*min	Rel.Area(ident.) %	Height mAU	Amount
1	1	20.17833333	1.48704	4.330204242	3.38597	n.a.
2	2	22.03	32.85406	95.66979576	49.36466	n.a.

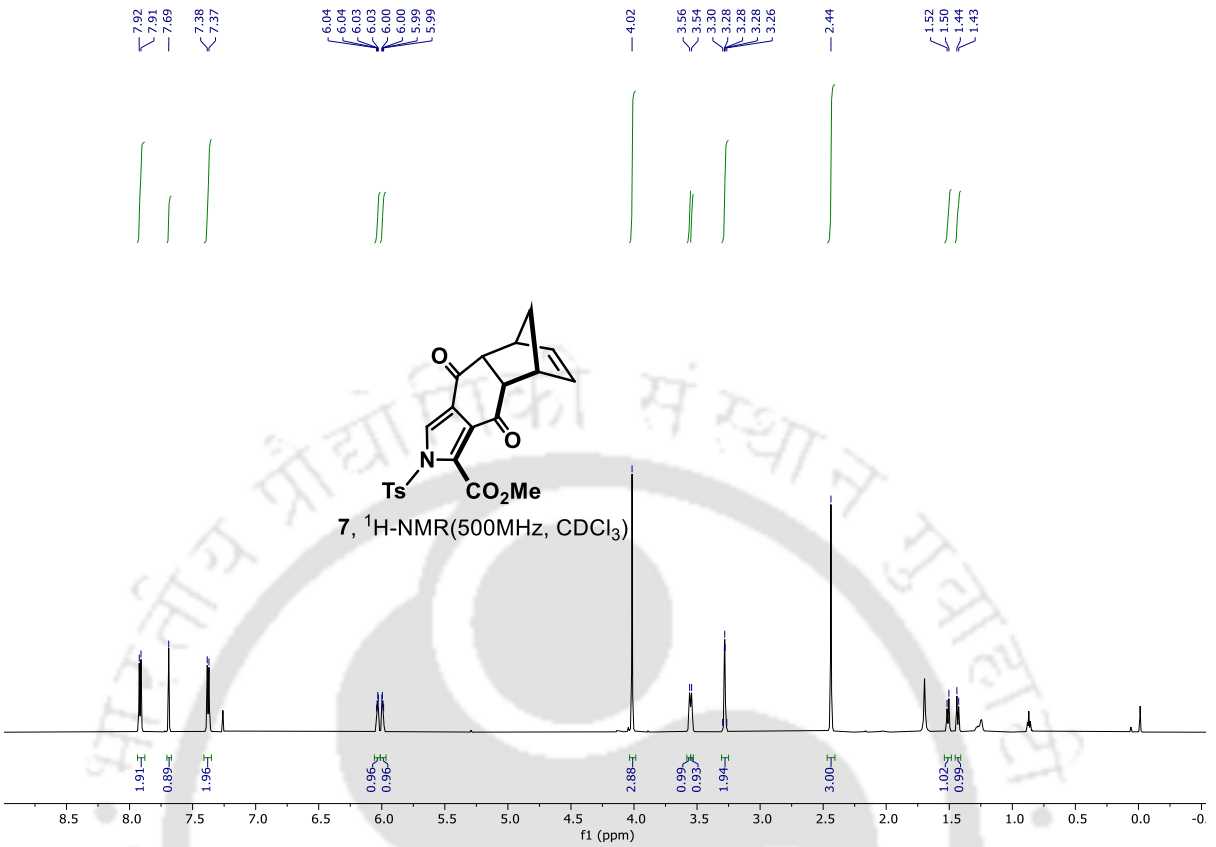

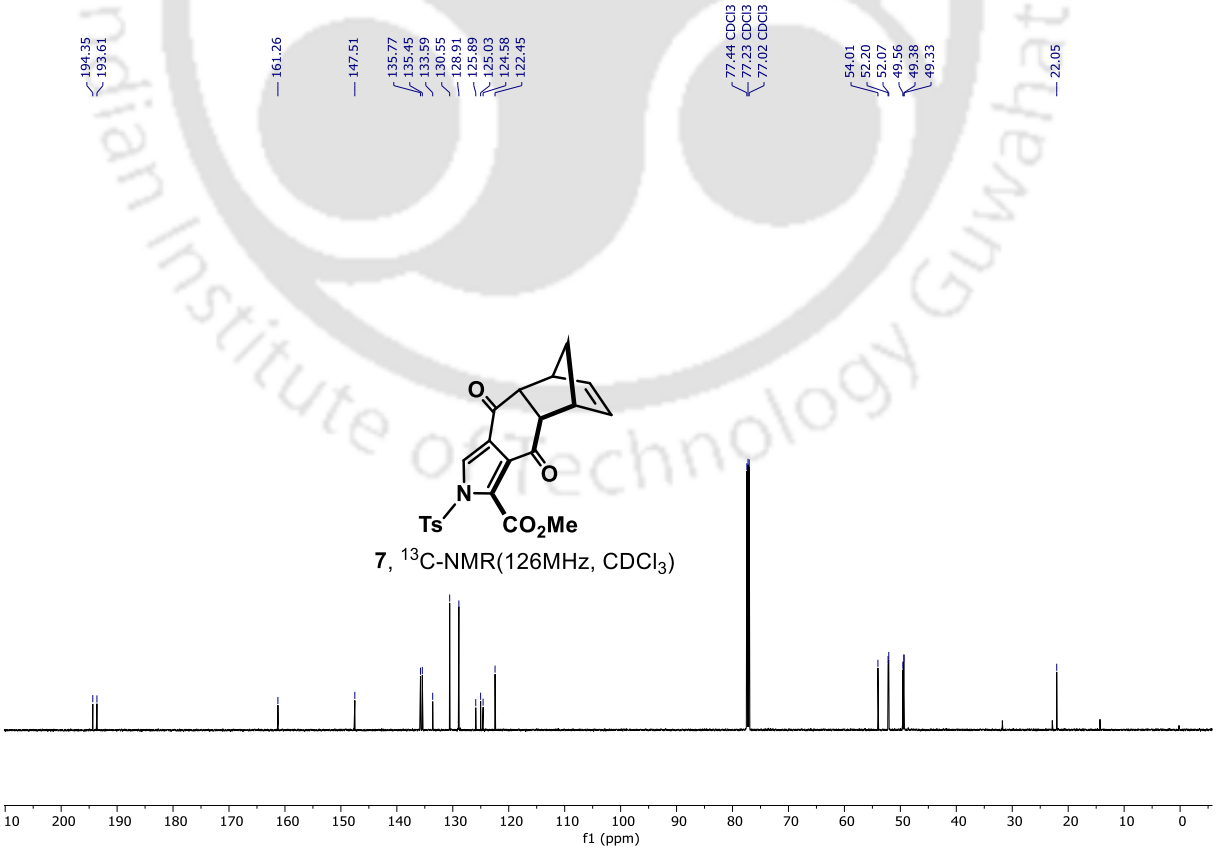

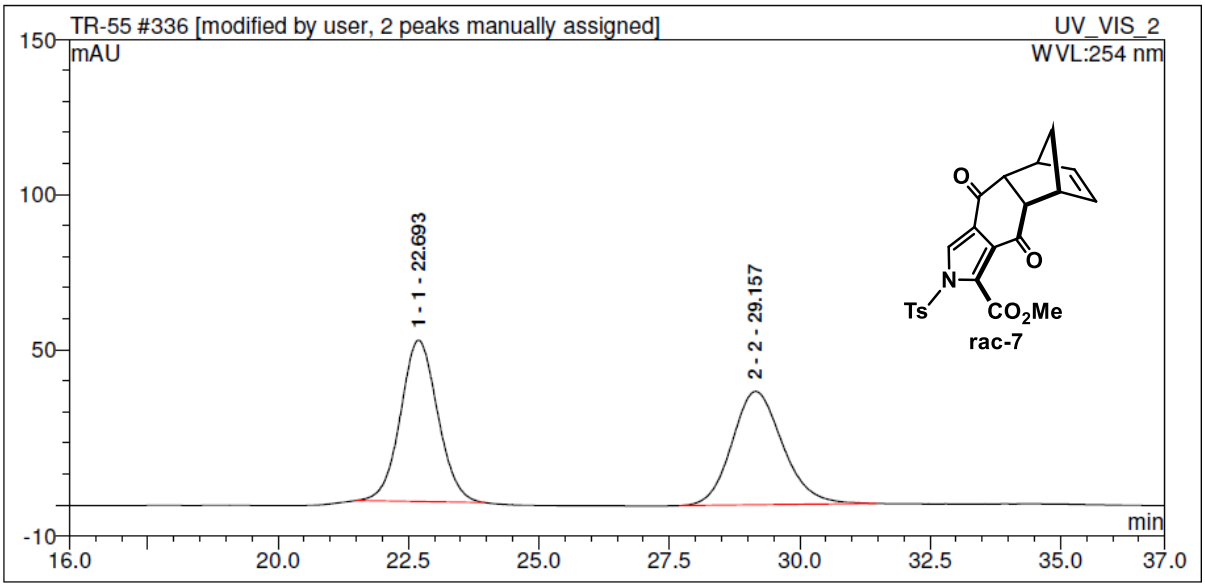

	Peak Name	Ret.Time (detected) min	Area mAU*min	Rel.Area(ident.) %	Height mAU	Amount
1	1	22.69333333	43.08901	51.07294587	51.93802	n.a.
2	2	29.15666667	41.27858	48.92705413	36.50659	n.a.

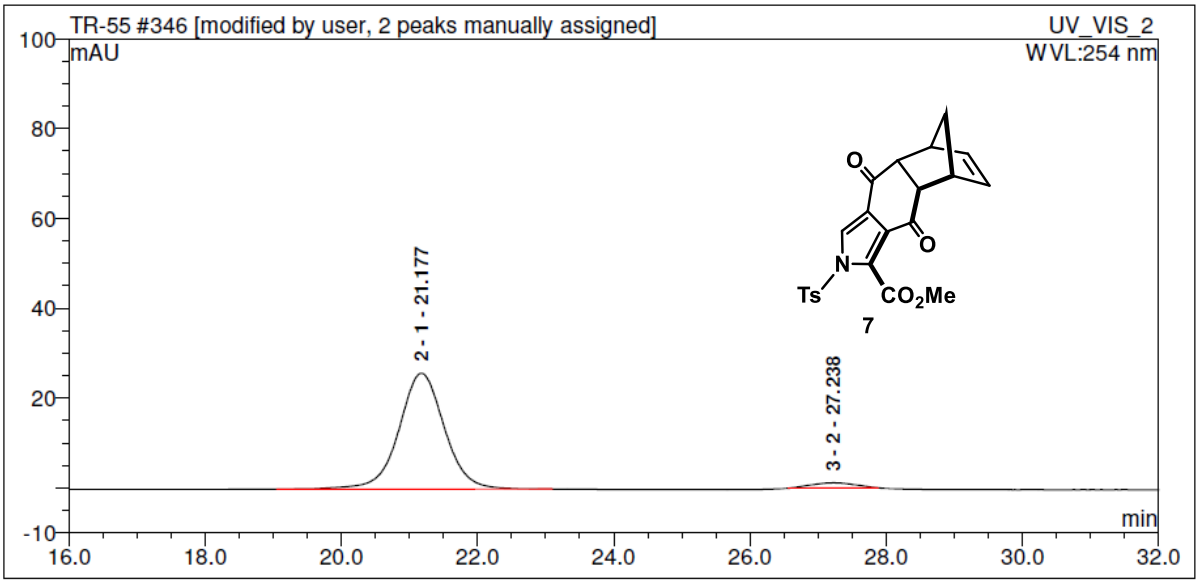

	Peak Name	Ret.Time (detected) min	Area mAU*min	Rel.Area(ident.) %	Height mAU	Amount
2	1	21.17666667	20.17009	96.00260967	25.83139	n.a.
3	2	27.23833333	0.839763	3.996977748	1.13043	n.a.

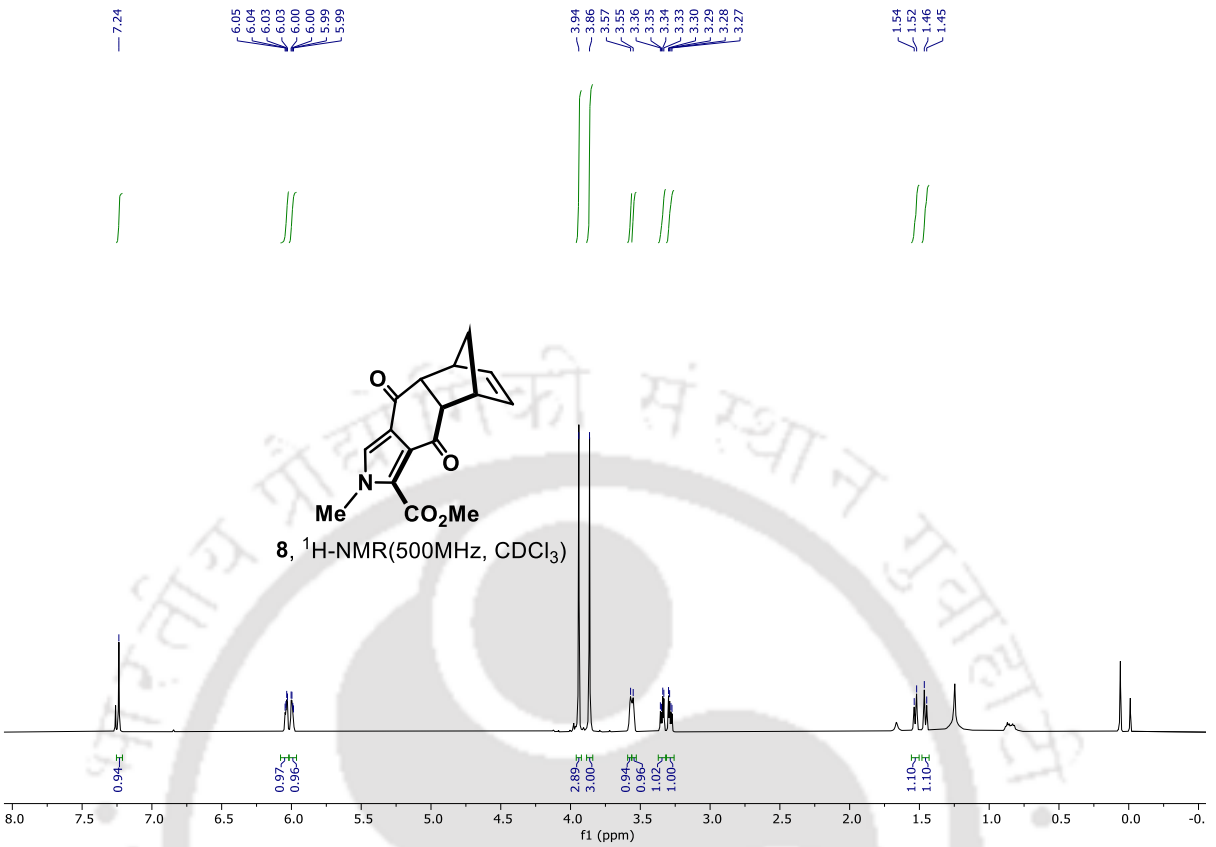

8, ^{1}H-NMR(500MHz, $CDCl_3$)

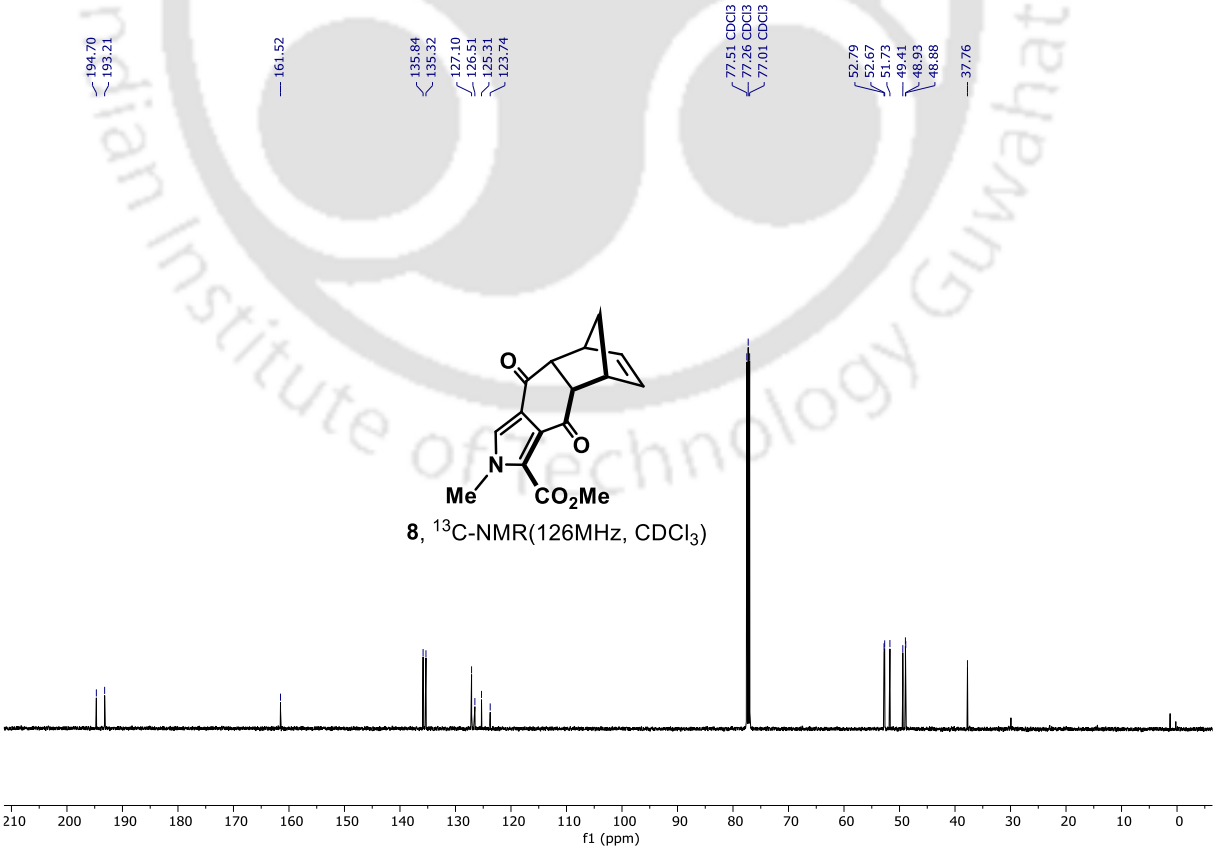

8, ^{13}C-NMR(126MHz, $CDCl_3$)

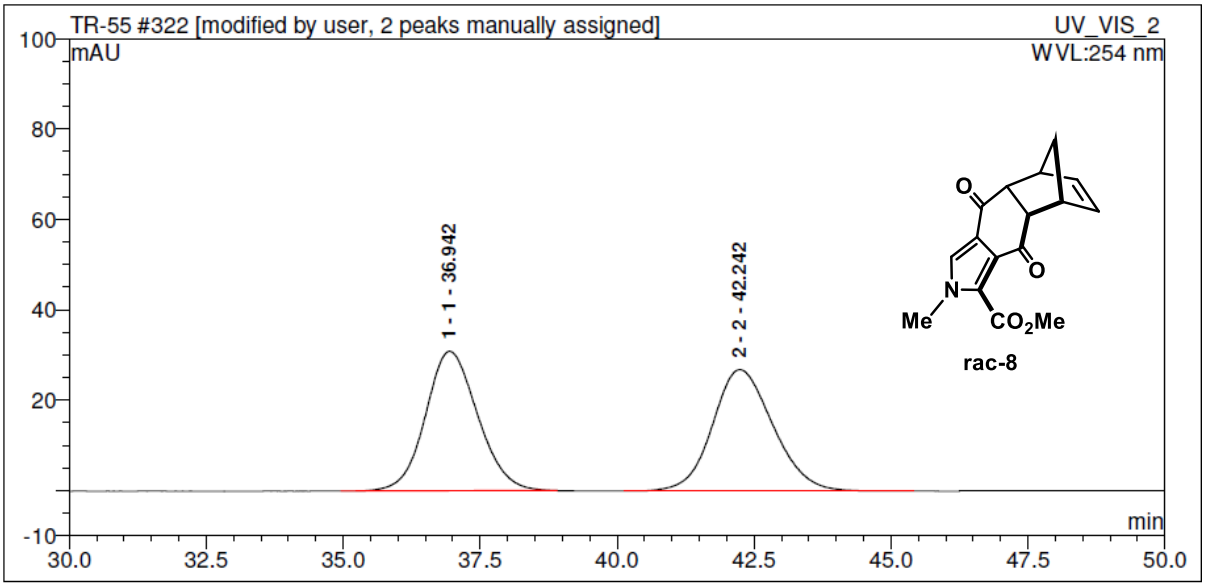

	Peak Name	Ret.Time (detected) min	Area mAU*min	Rel.Area(ident.) %	Height mAU	Amount
1	1	36.94166667	34.18248	49.71669011	30.88055	n.a.
2	2	42.24166667	34.57205	50.28330989	26.895	n.a.

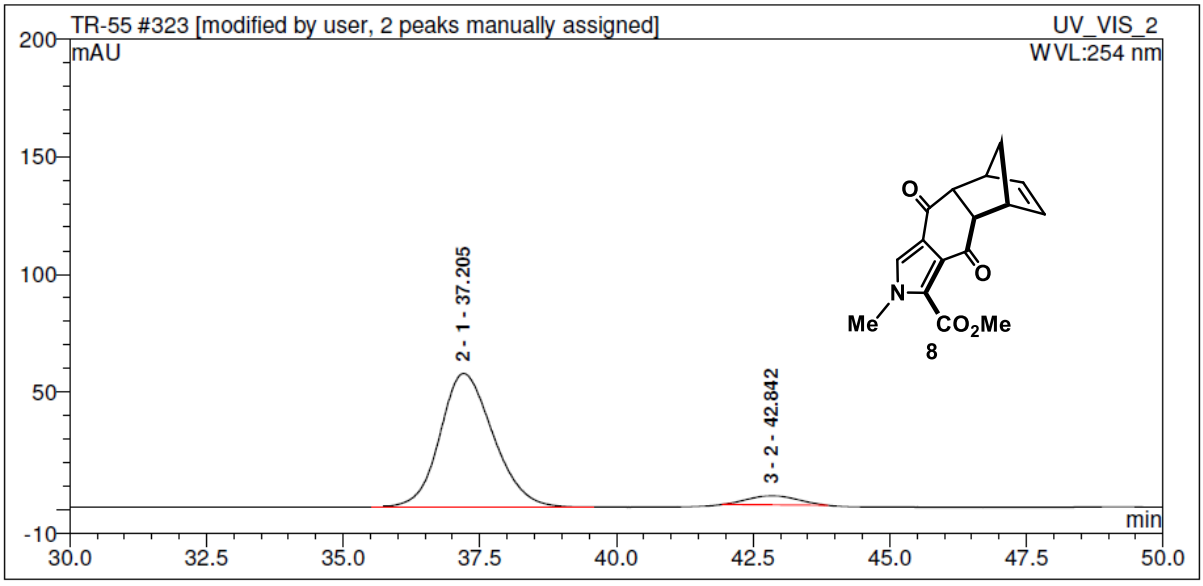

	Peak Name	Ret.Time (detected) min	Area mAU*min	Rel.Area(ident.) %	Height mAU	Amount
2	1	37.205	64.2641	94.15369743	56.70418	n.a.
3	2	42.84166667	3.990363	5.846302499	3.81703	n.a.

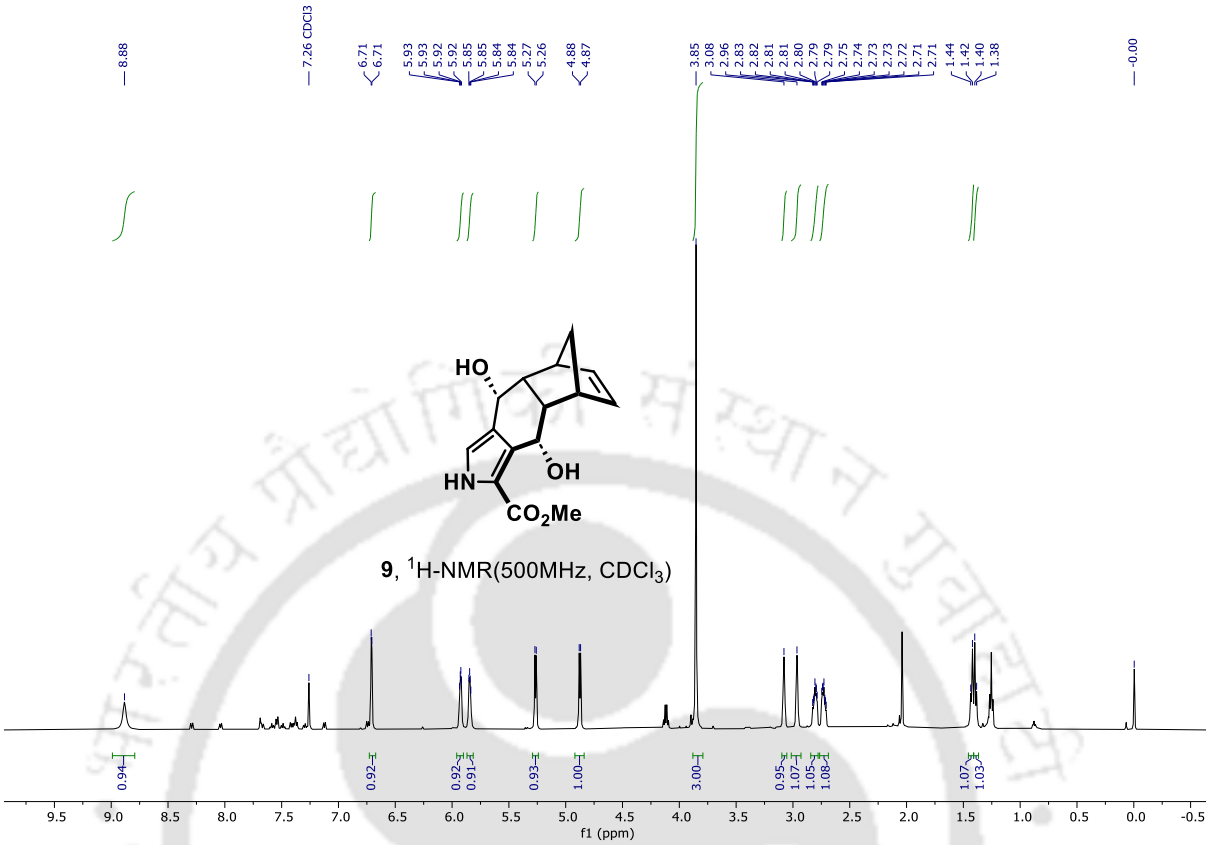

9, ^{1}H-NMR(500MHz, $CDCl_3$)

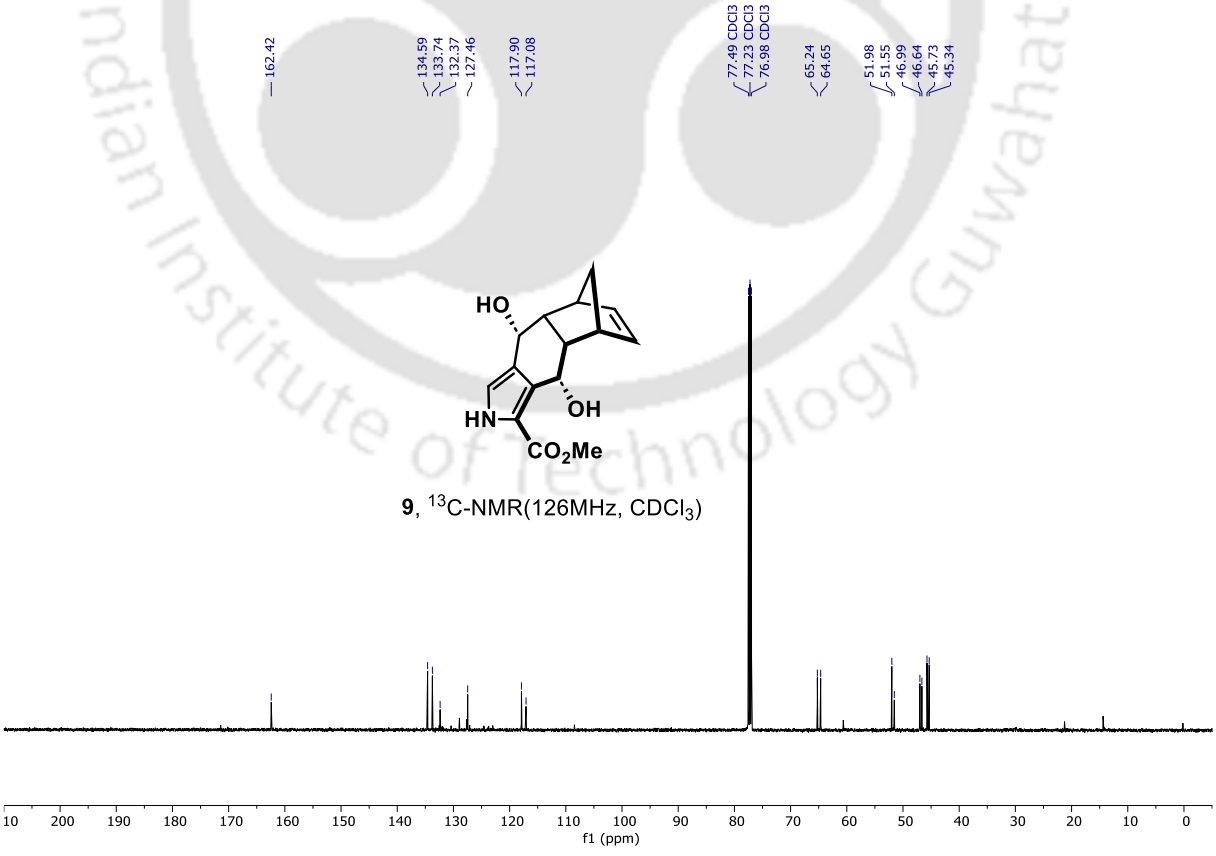

9, ^{13}C-NMR(126MHz, $CDCl_3$)

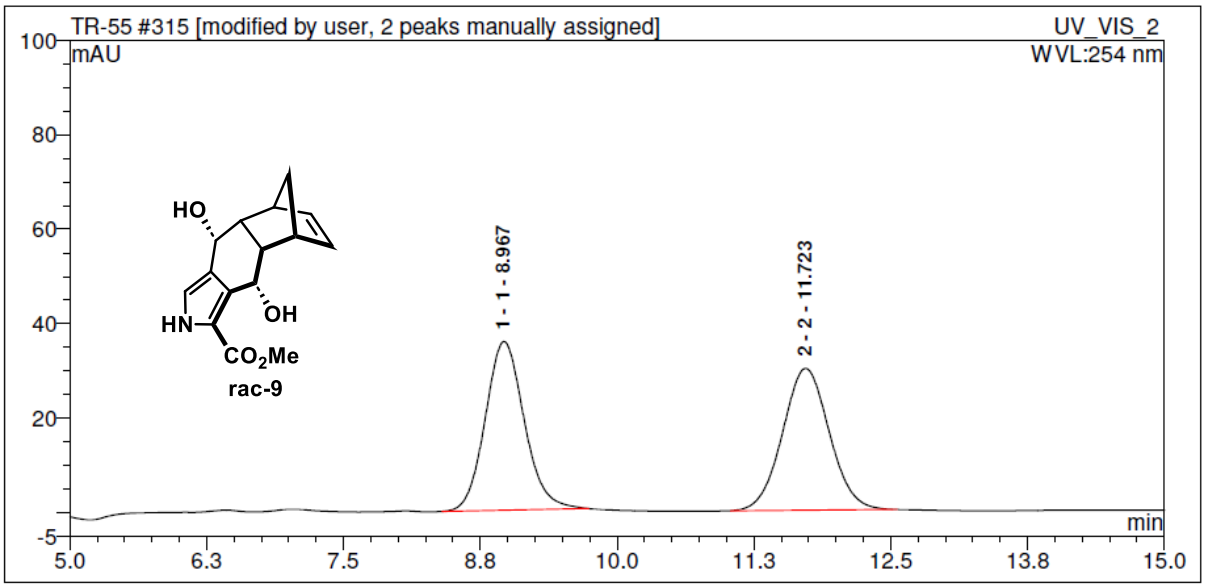

	Peak Name	Ret.Time (detected) min	Area mAU*min	Rel.Area(ident.) %	Height mAU	Amount
1	1	8.966666667	14.73806	49.77346804	35.65788	n.a.
2	2	11.72333333	14.87221	50.22653196	29.97582	n.a.

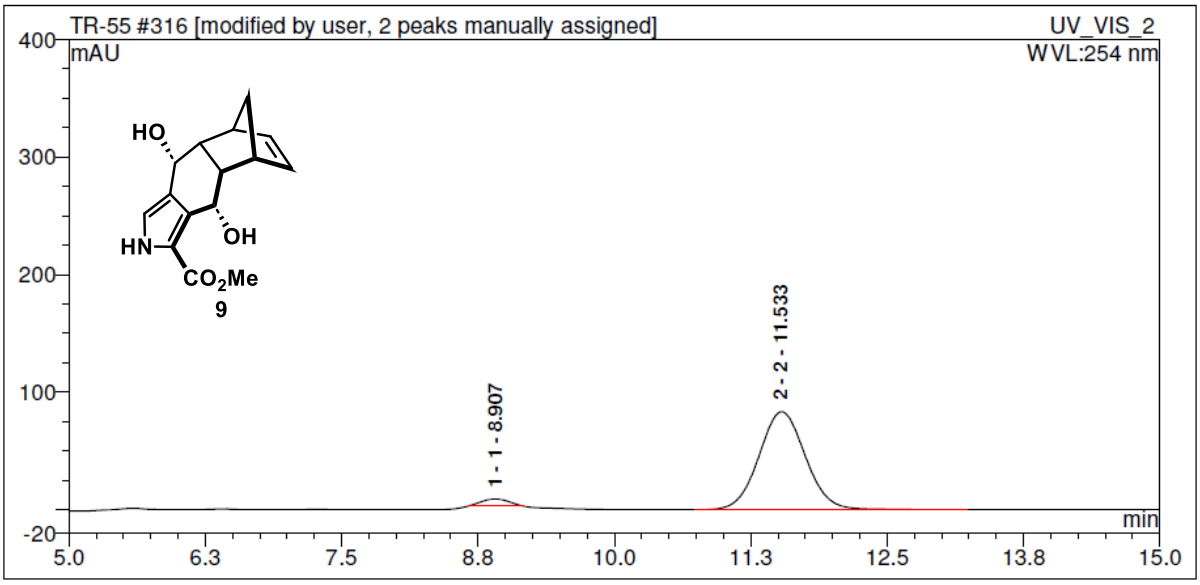

	Peak Name	Ret.Time (detected) min	Area mAU*min	Rel.Area(ident.) %	Height mAU	Amount
1	1	8.906666667	1.796782	4.180195425	6.08592	n.a.
2	2	11.53333333	41.18642	95.81980458	83.17469	n.a.

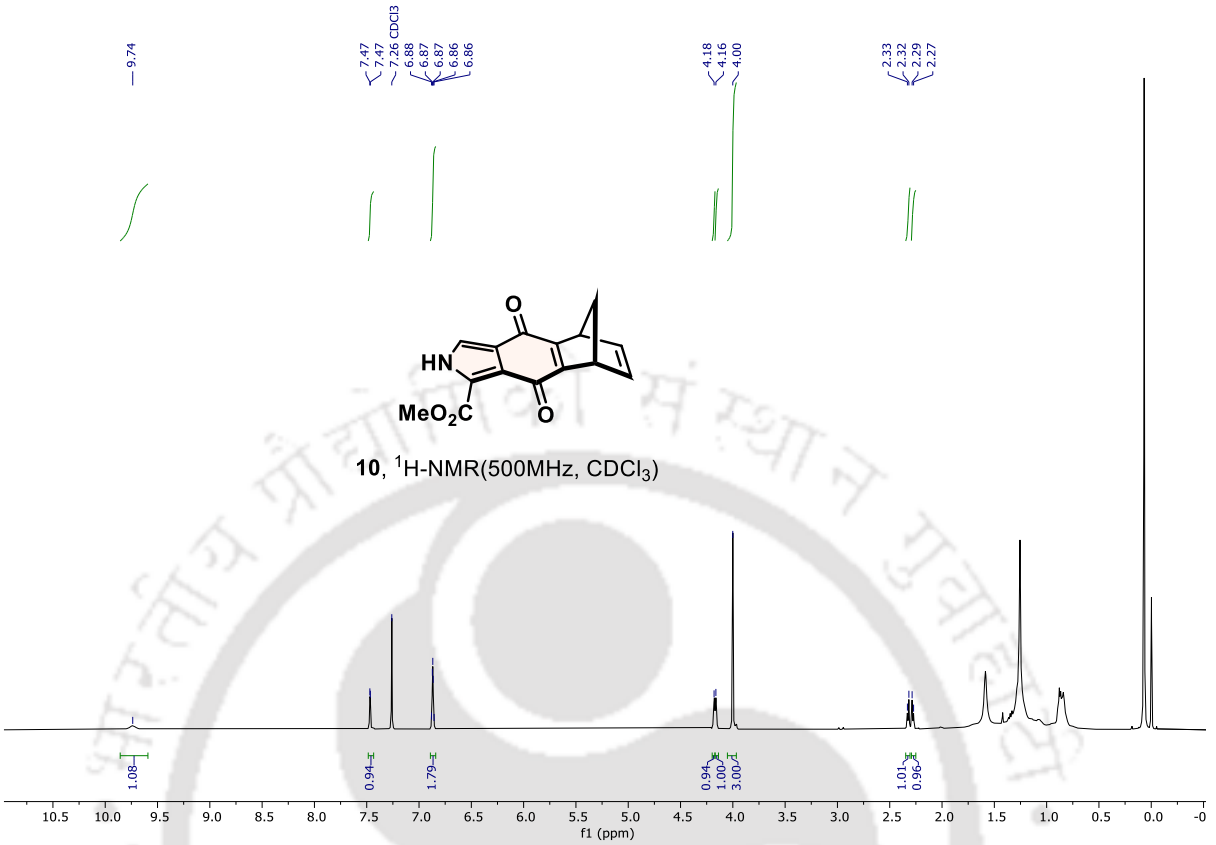

10, ^{1}H-NMR(500MHz, $CDCl_3$)

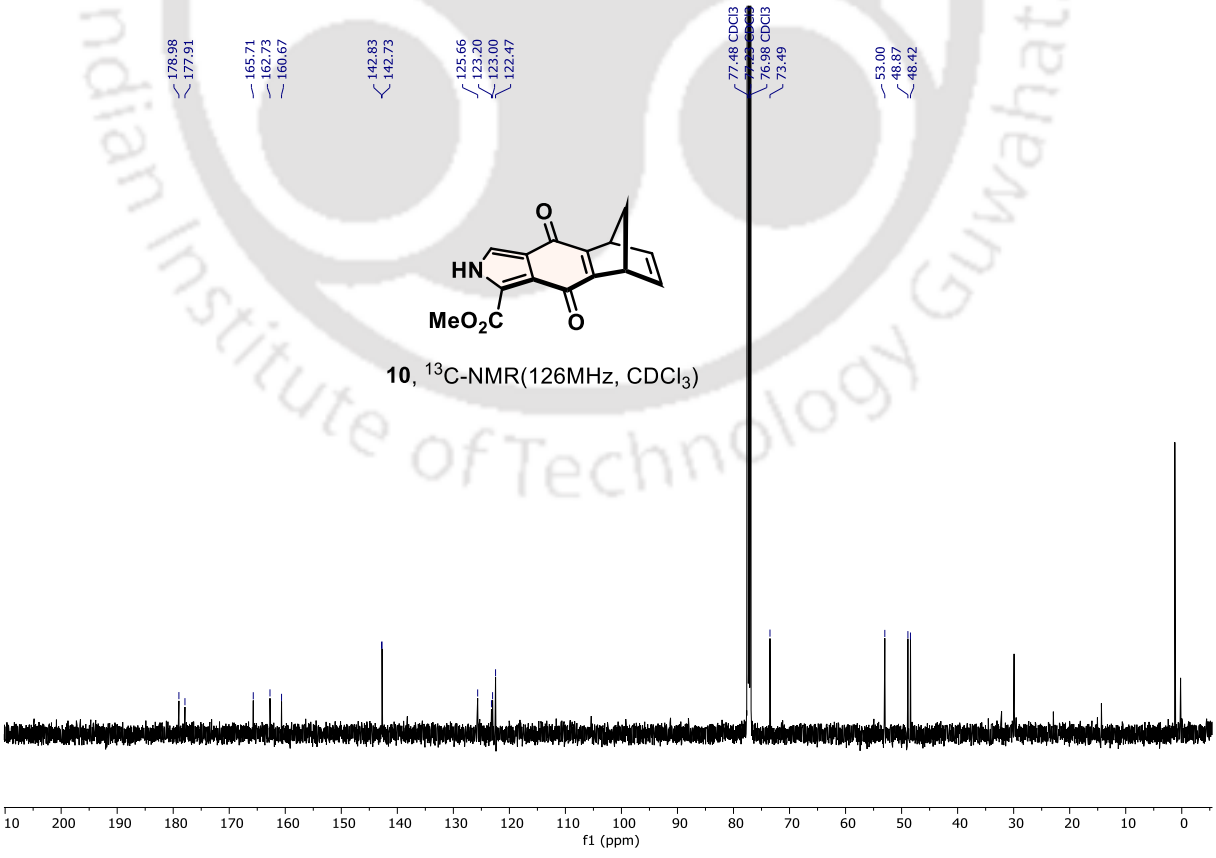

10, ^{13}C-NMR(126MHz, $CDCl_3$)

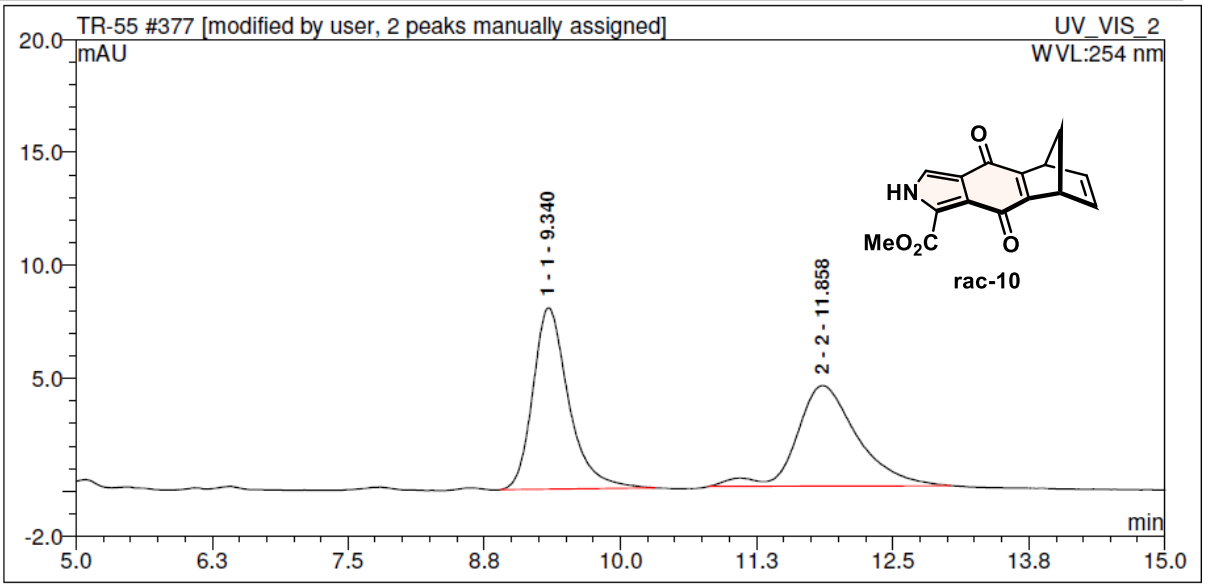

	Peak Name	Ret.Time (detected) min	Area mAU*min	Rel.Area(ident.) %	Height mAU	Amount
1	1	9.34	3.057771	51.47239097	8.02521	n.a.
2	2	11.85833333	2.882833	48.52760903	4.44214	n.a.

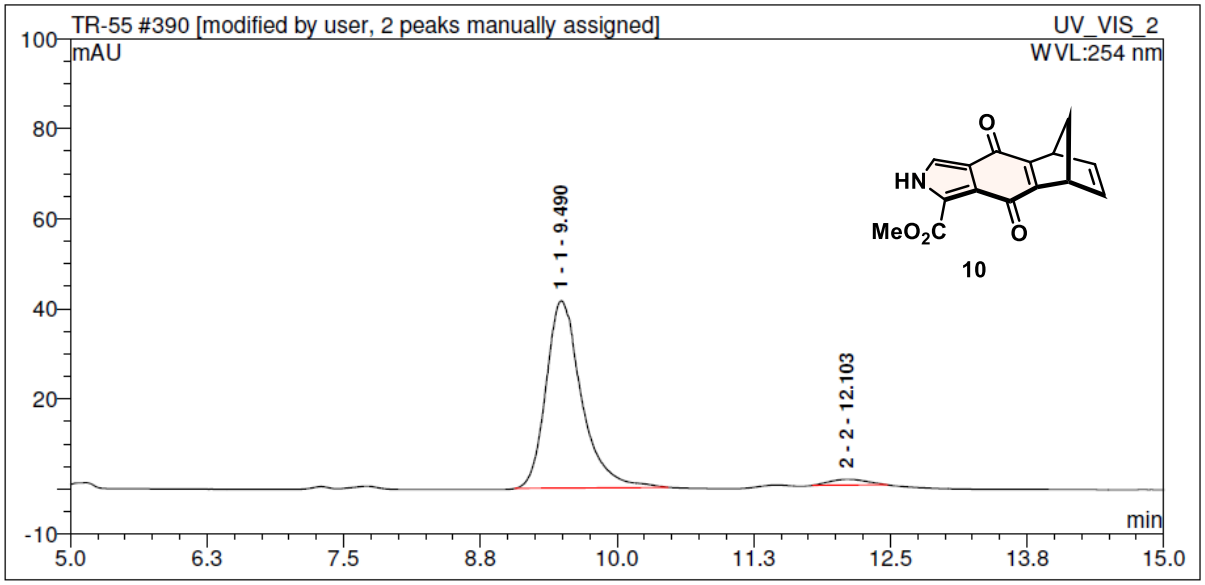

	Peak Name	Ret.Time (detected) min	Area mAU*min	Rel.Area(ident.) %	Height mAU	Amount
1	1	9.49	15.68279	96.93501526	41.57924	n.a.
2	2	12.10333333	0.495873	3.064984743	1.25515	n.a.

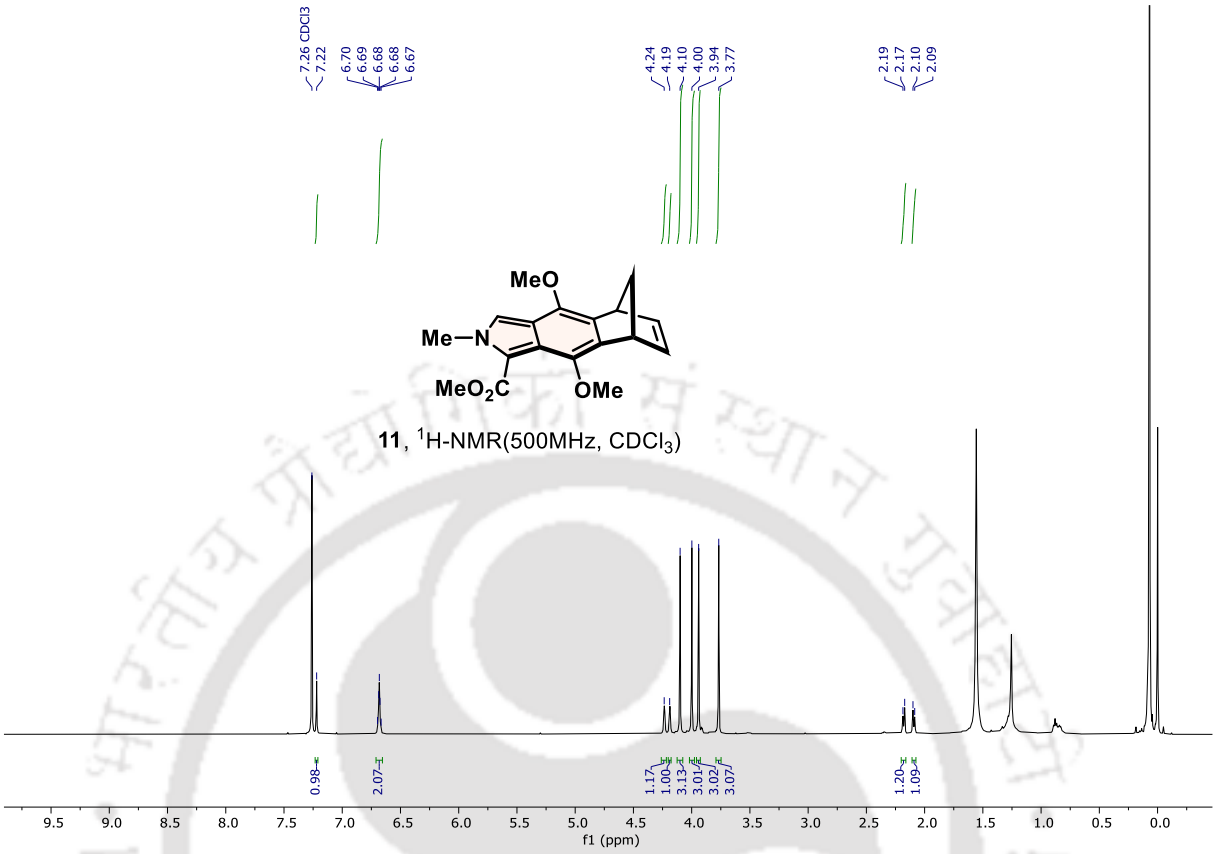

11, ^{1}H-NMR(500MHz, $CDCl_3$)

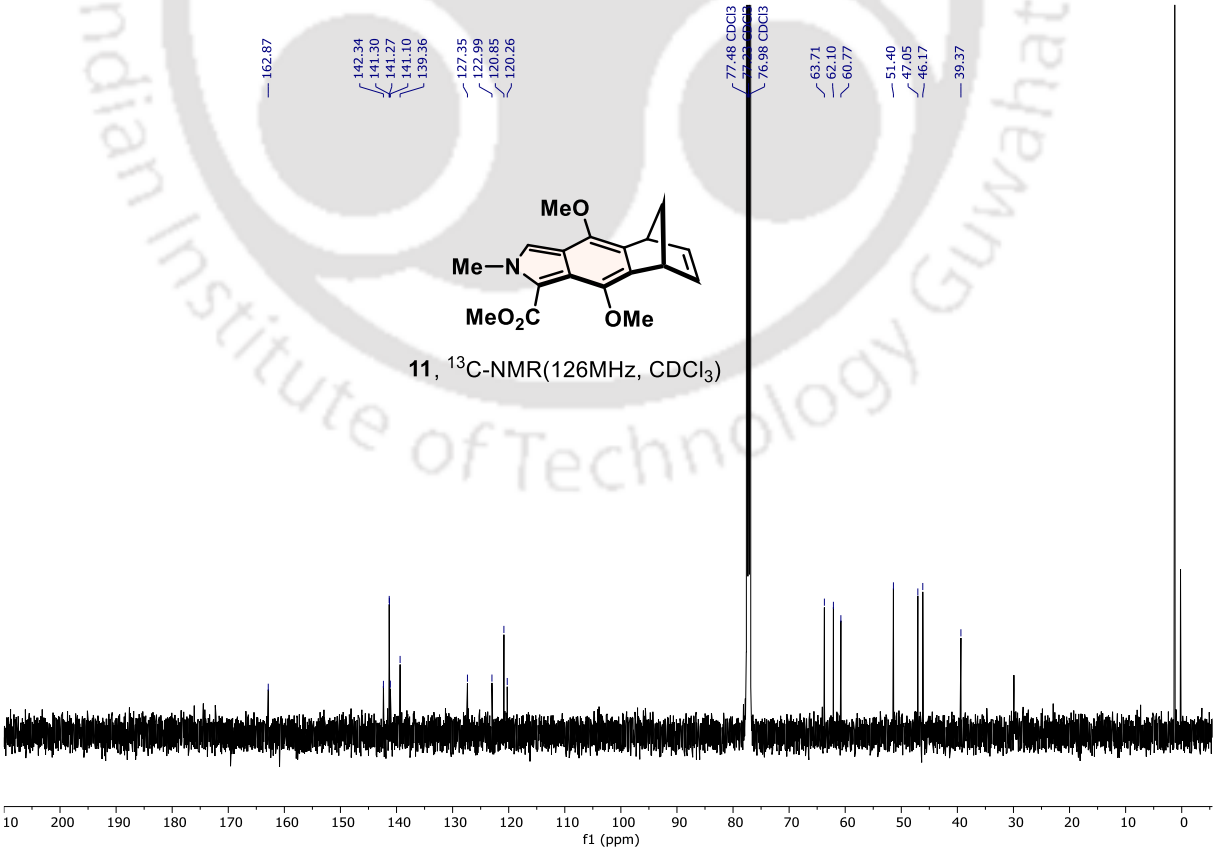

11, ^{13}C-NMR(126MHz, $CDCl_3$)

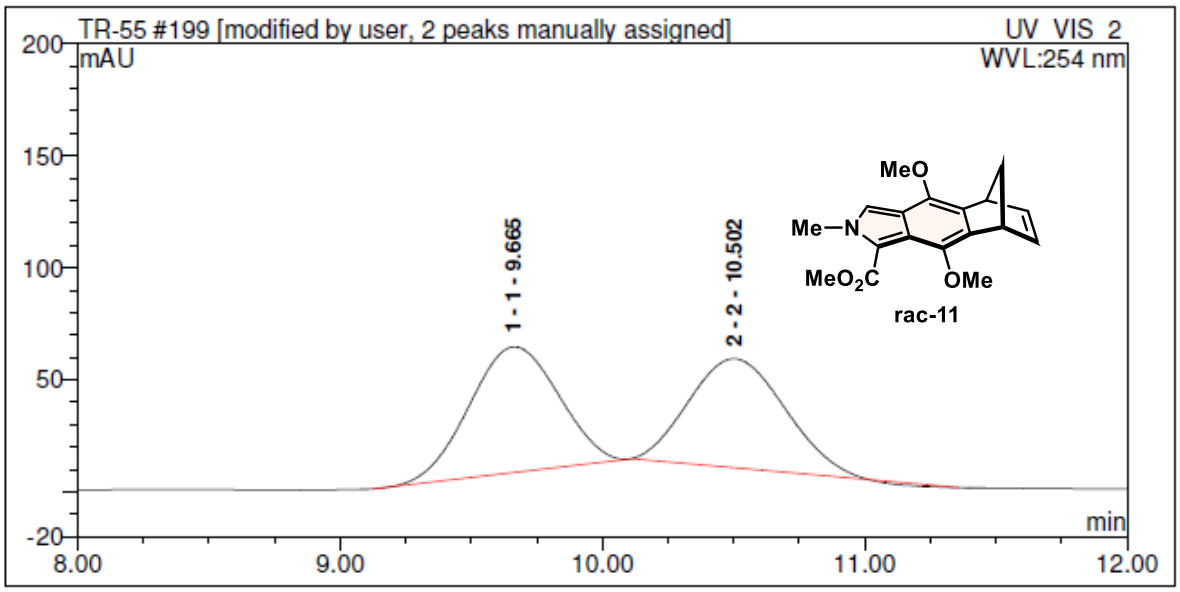

	Peak Name	Ret.Time (detected) min	Area mAU*min	Rel.Area(ident.) %	Height mAU	Amount
1	1	9.67	22.06906	51.77476602	56.024	n.a.
2	2	10.50	20.556	48.22523398	48.688	n.a.

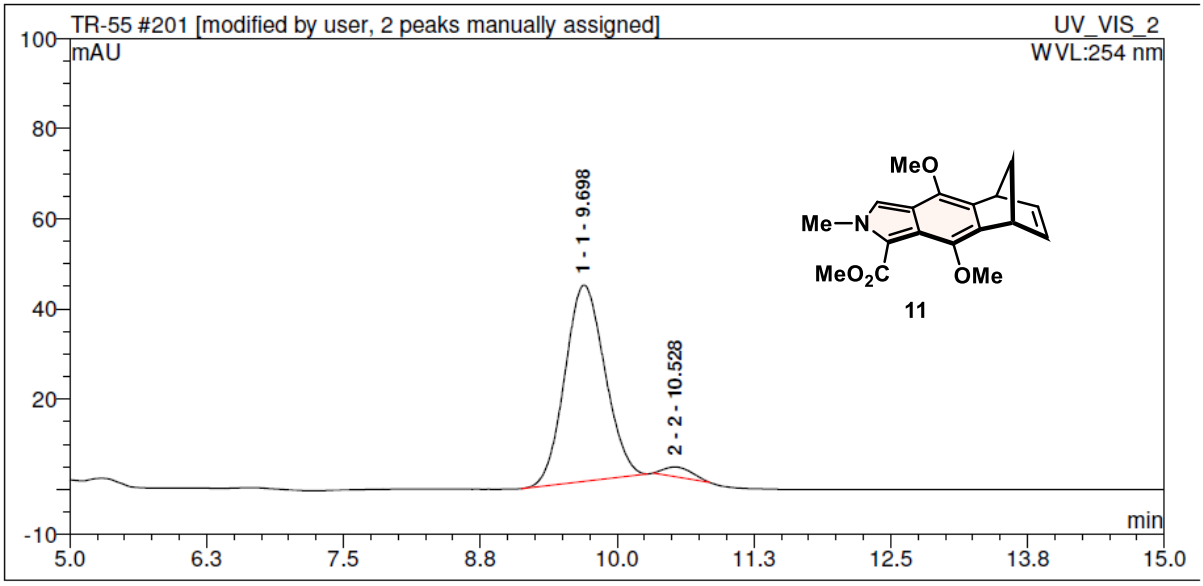

	Peak Name	Ret.Time (detected) min	Area mAU*min	Rel.Area(ident.) %	Height mAU	Amount
1	1	9.698333333	18.38709	96.60180877	43.49881	n.a.
2	2	10.52833333	0.646808	3.398191233	2.11878	n.a.

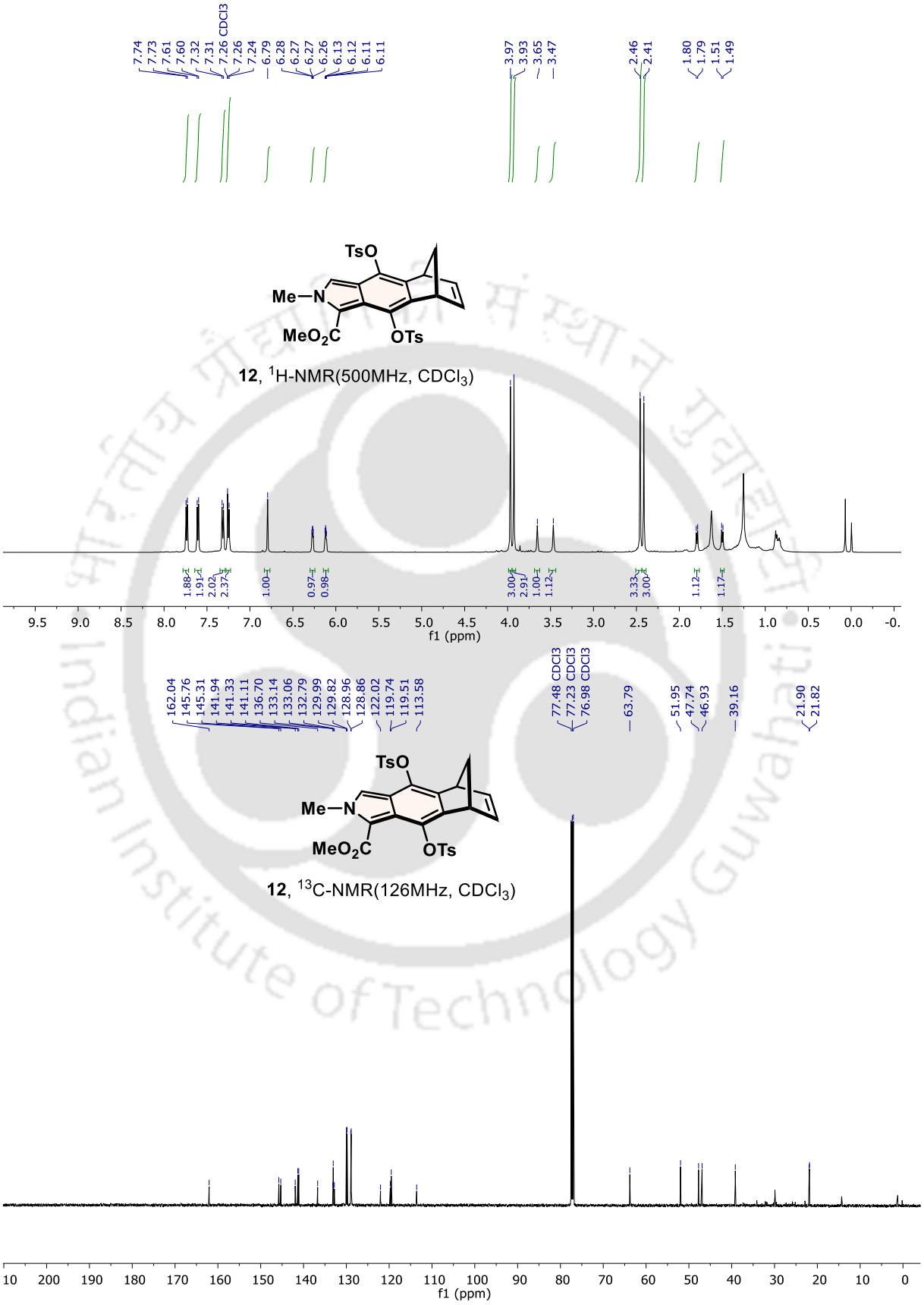

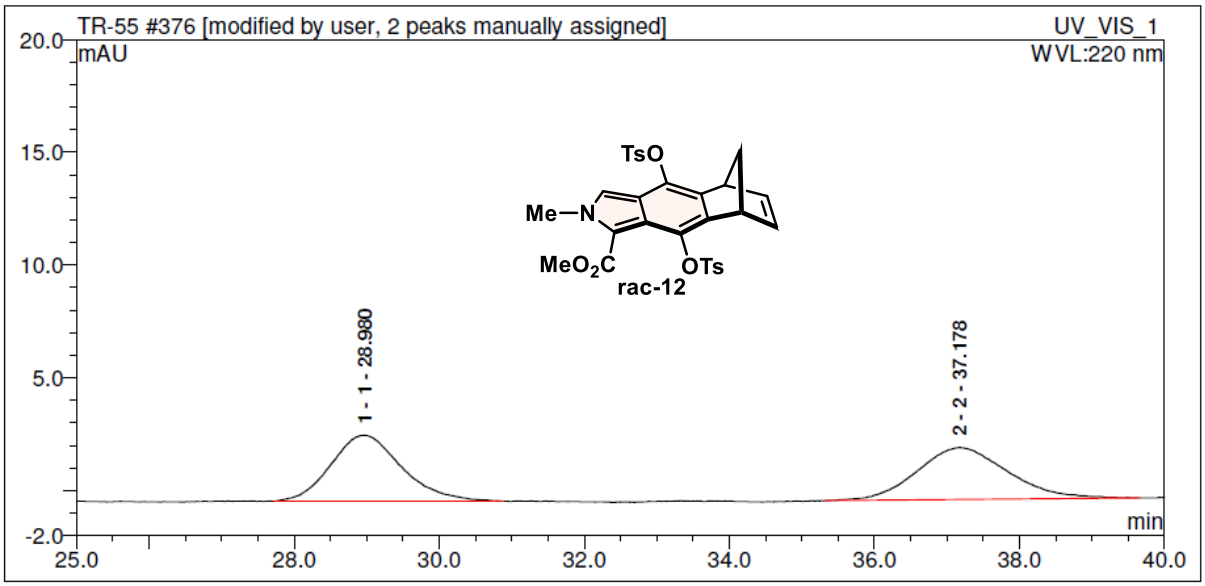

	Peak Name	Ret.Time (detected) min	Area mAU*min	Rel.Area(ident.) %	Height mAU	Amount
1	1	28.98	3.324138	49.88791569	2.92758	n.a.
2	2	37.17833333	3.339075	50.11208431	2.30765	n.a.

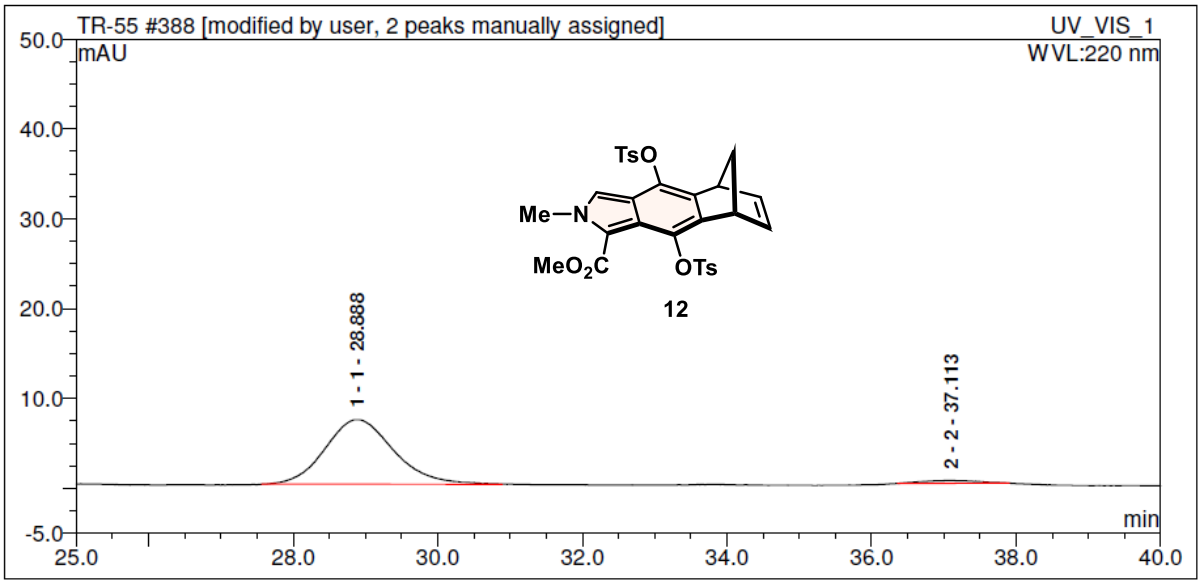

	Peak Name	Ret.Time (detected) min	Area mAU*min	Rel.Area(ident.) %	Height mAU	Amount
1	1	28.88833333	7.8974	96.47091402	7.18229	n.a.
2	2	37.11333333	0.288902	3.529085977	0.32083	n.a.

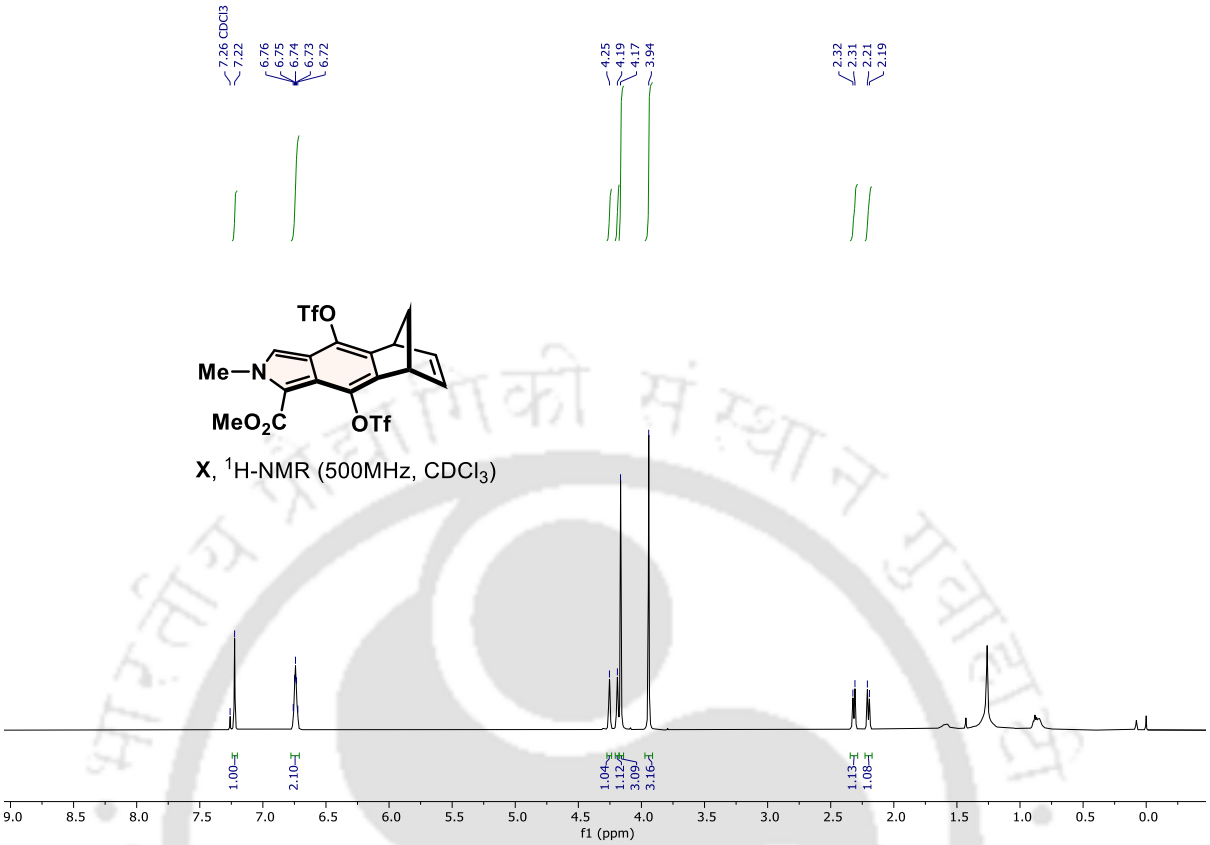

X, ^{1}H-NMR (500MHz, $CDCl_3$)

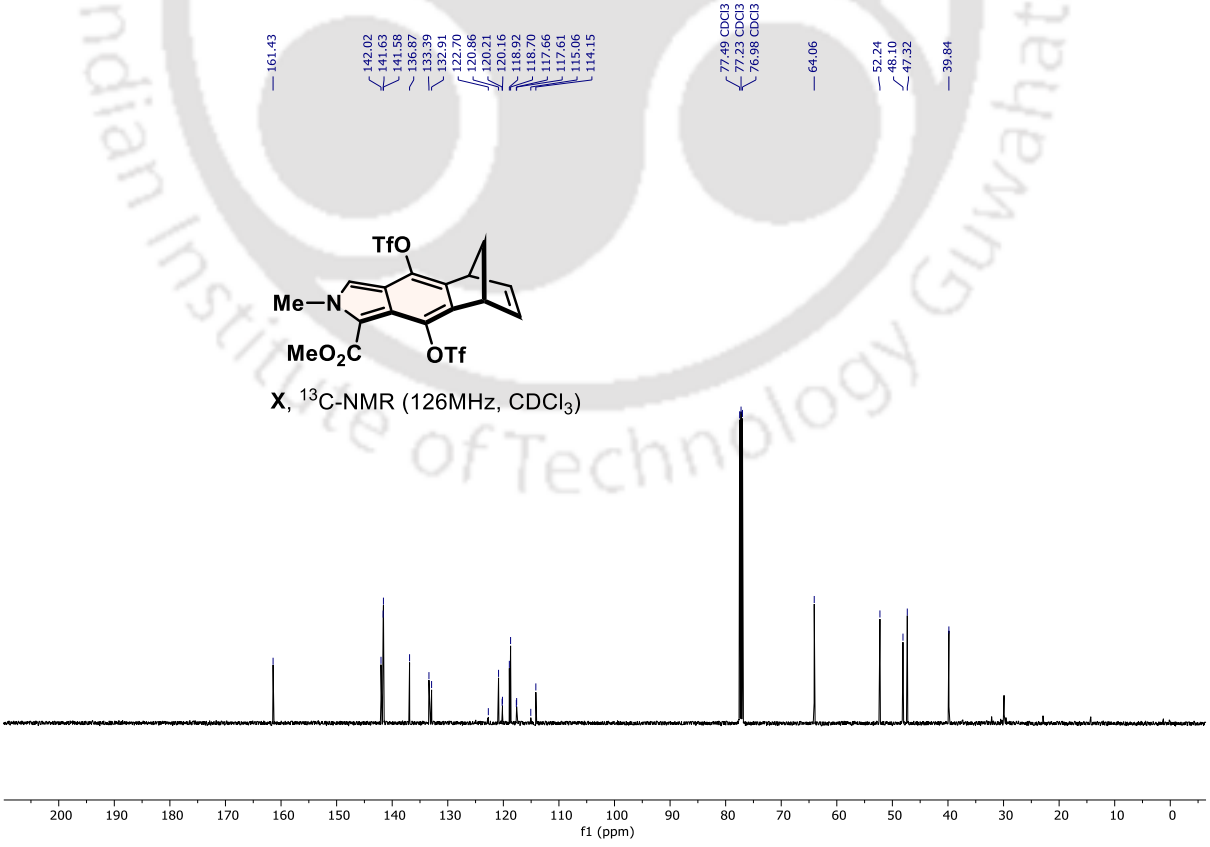

X, ^{13}C-NMR (126MHz, $CDCl_3$)

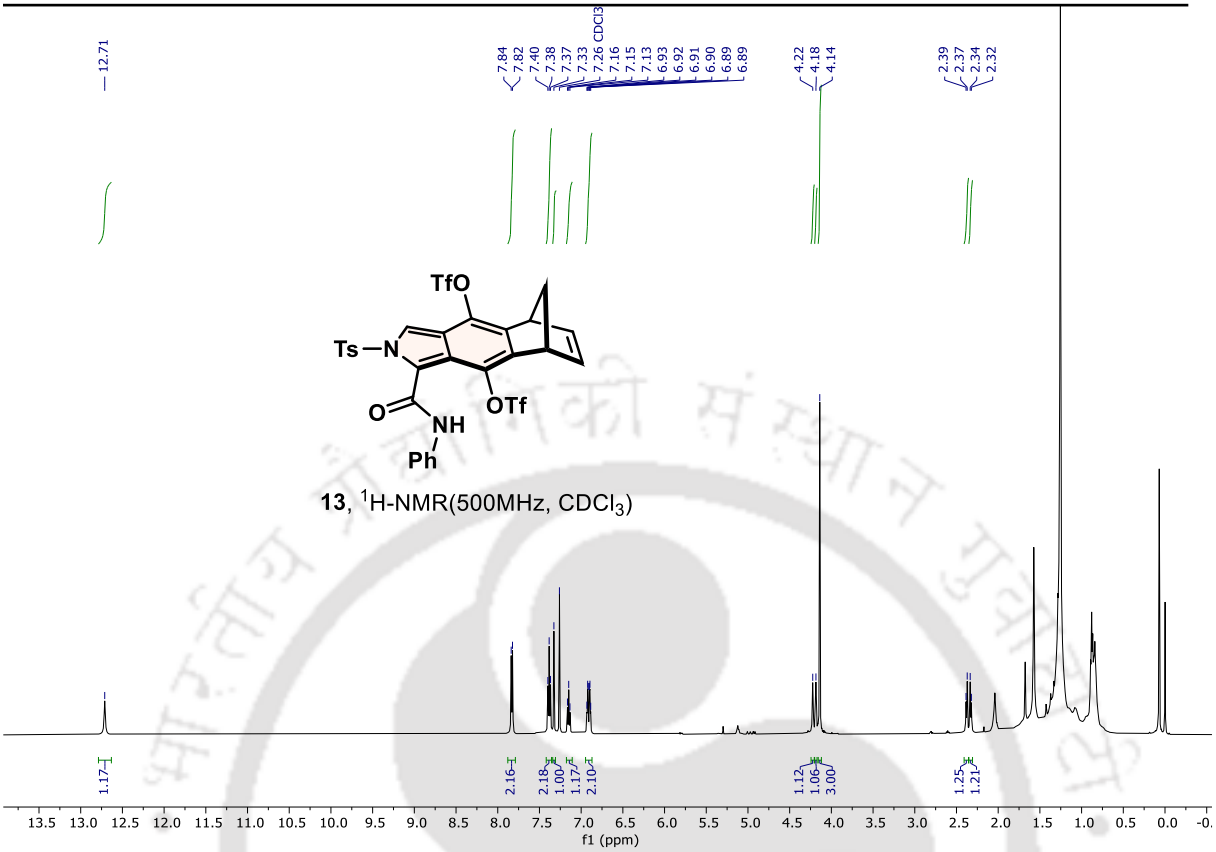

13, ^{1}H-NMR(500MHz, $CDCl_3$)

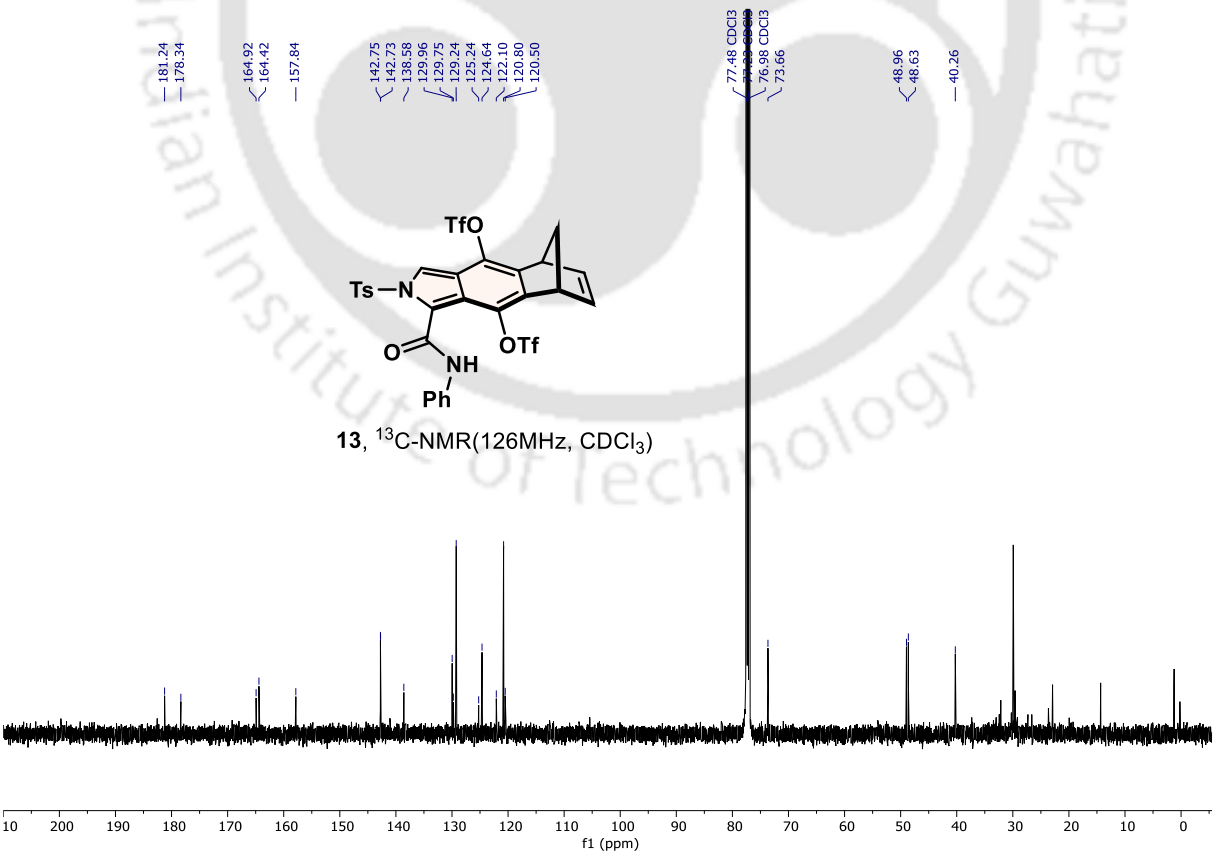

13, ^{13}C-NMR(126MHz, $CDCl_3$)

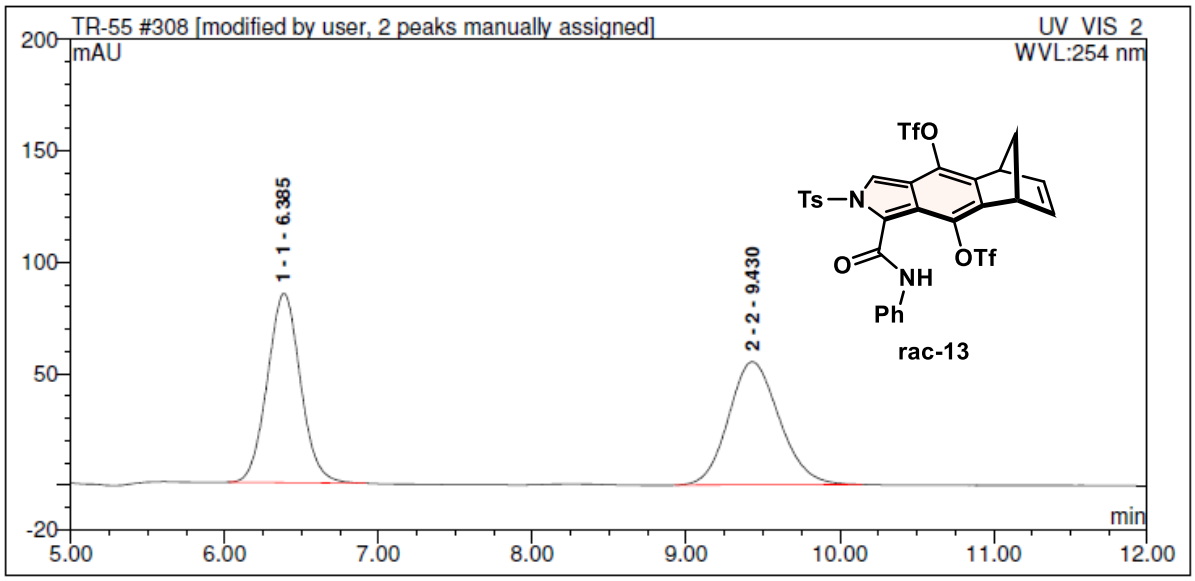

Peak Name	Ret.Time (detected) min	Area mAU*min	Rel.Area(ident.) %	Height mAU	Amount
1 1	6.385	21.19492	50.06884712	84.77203	n.a.
2 2	9.43	21.13663	49.93115288	55.13567	n.a.

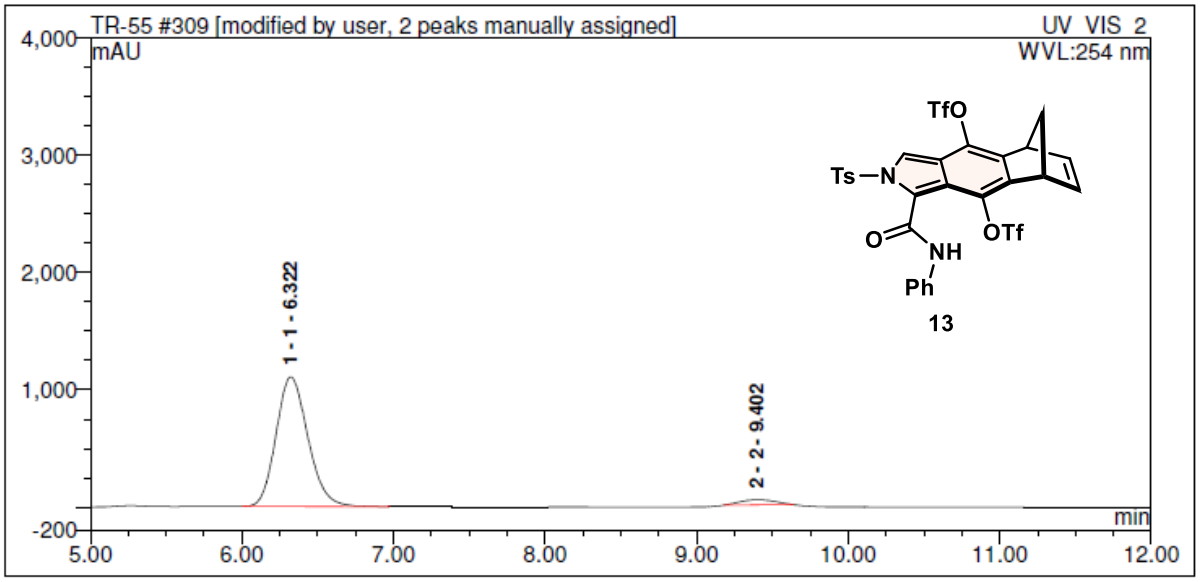

Peak Name	Ret.Time (detected) min	Area mAU*min	Rel.Area(ident.) %	Height mAU	Amount
1 1	6.321666667	269.4786	95.86254511	1103.954	n.a.
2 2	9.401666667	11.63077	4.137454892	43.96718	n.a.

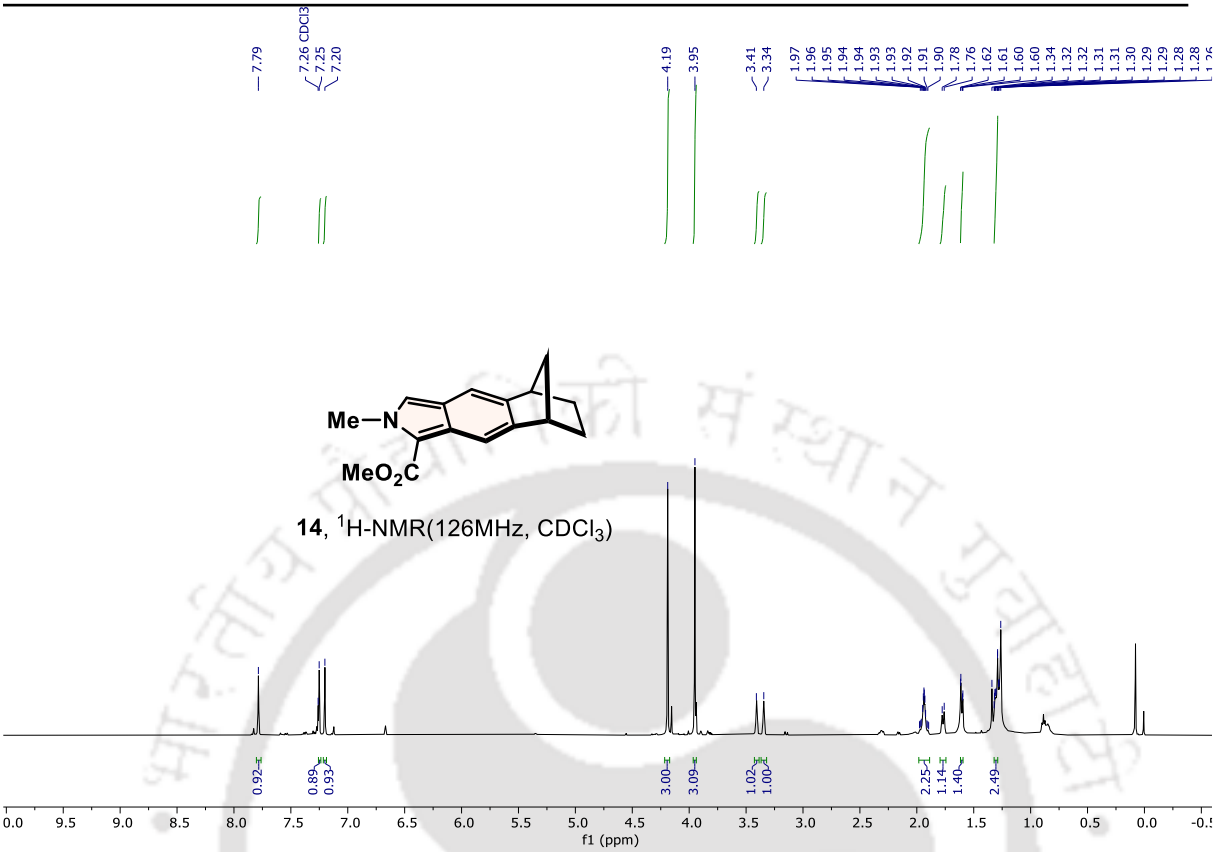

14, ^{1}H-NMR(126MHz, $CDCl_3$)

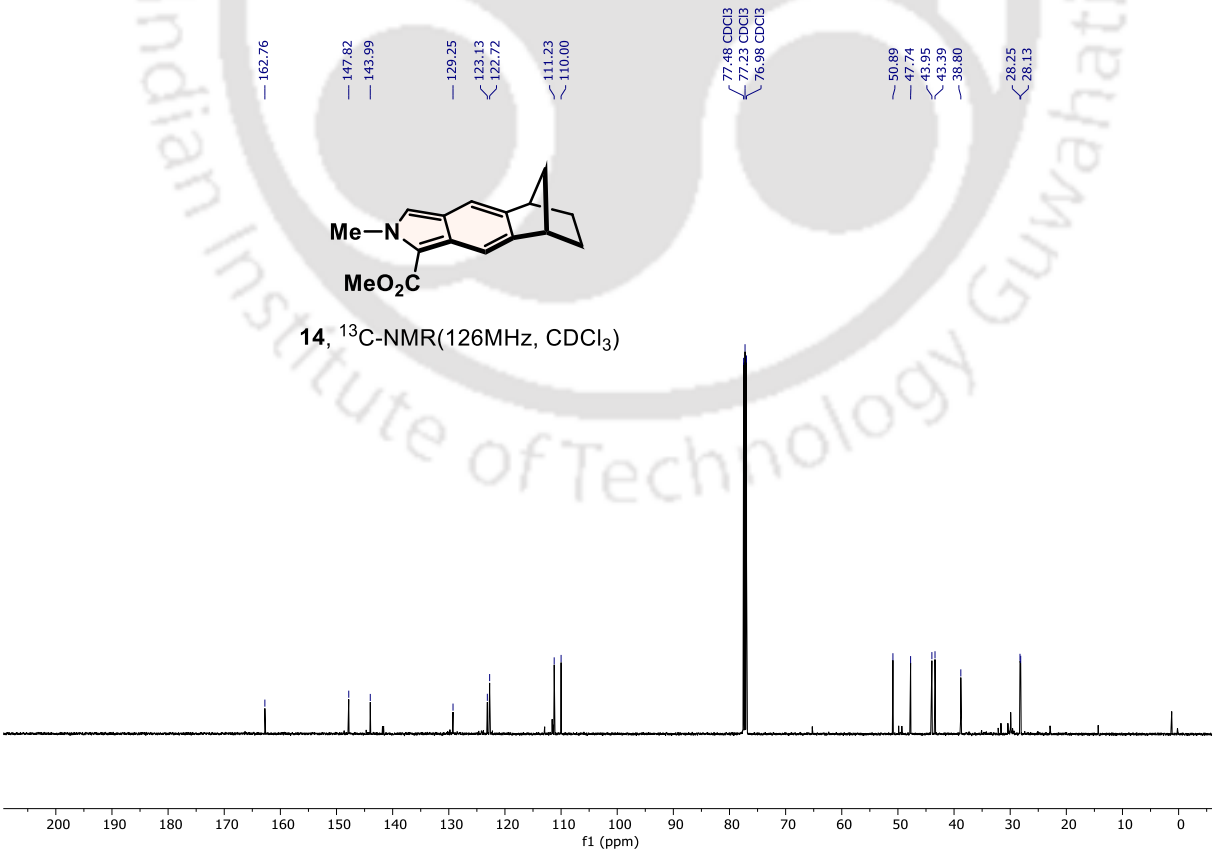

14, ^{13}C-NMR(126MHz, $CDCl_3$)

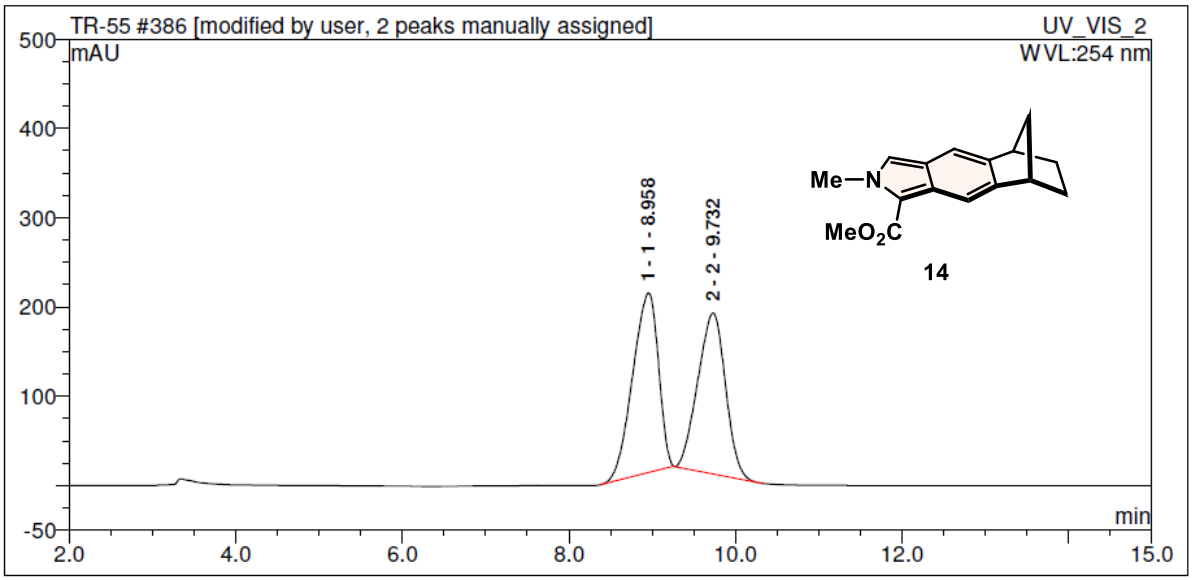

	Peak Name	Ret.Time (detected) min	Area mAU*min	Rel.Area(ident.) %	Height mAU	Amount
1	1	8.958333333	72.1049	50.93589631	201.1795	n.a.
2	2	9.731666667	69.45519	49.06410369	180.3602	n.a.

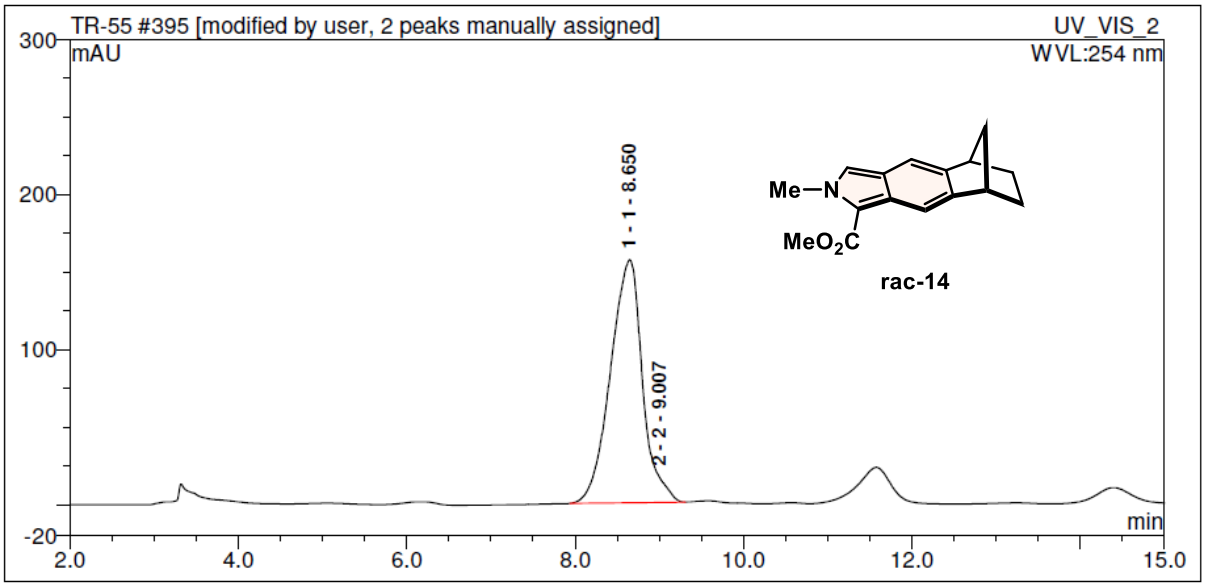

	Peak Name	Ret.Time (detected) min	Area mAU*min	Rel.Area(ident.) %	Height mAU	Amount
1	1	8.65	67.11382	97.43814141	156.5116	n.a.
2	2	9.006666667	1.764567	2.561858585	15.88611	n.a.

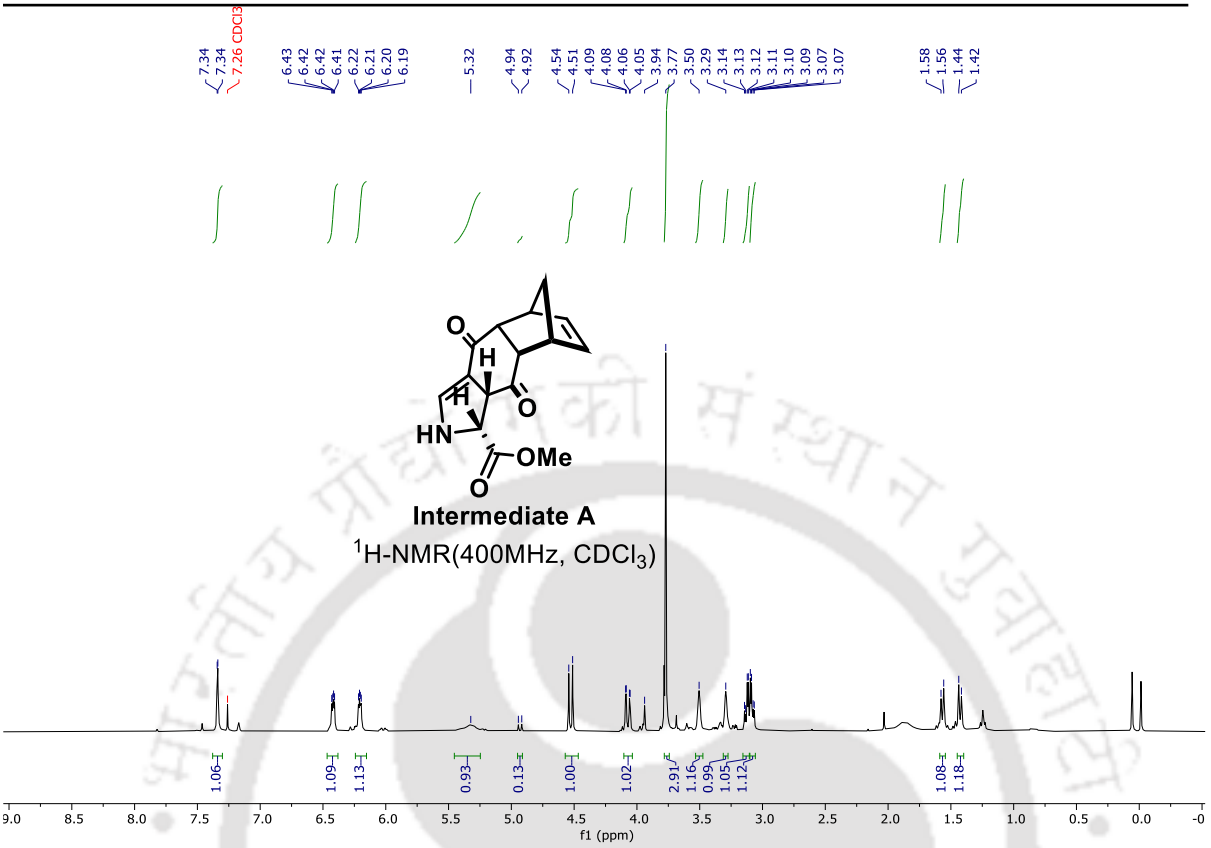

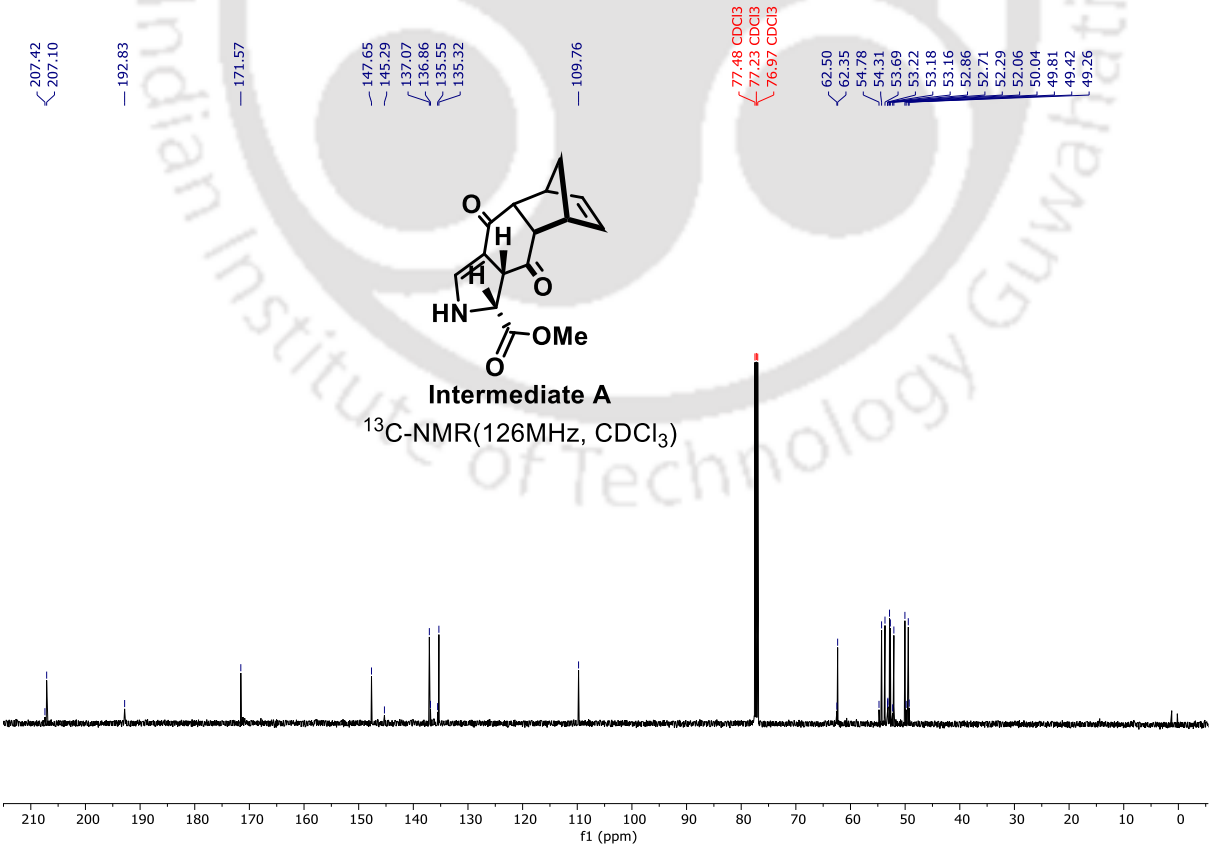

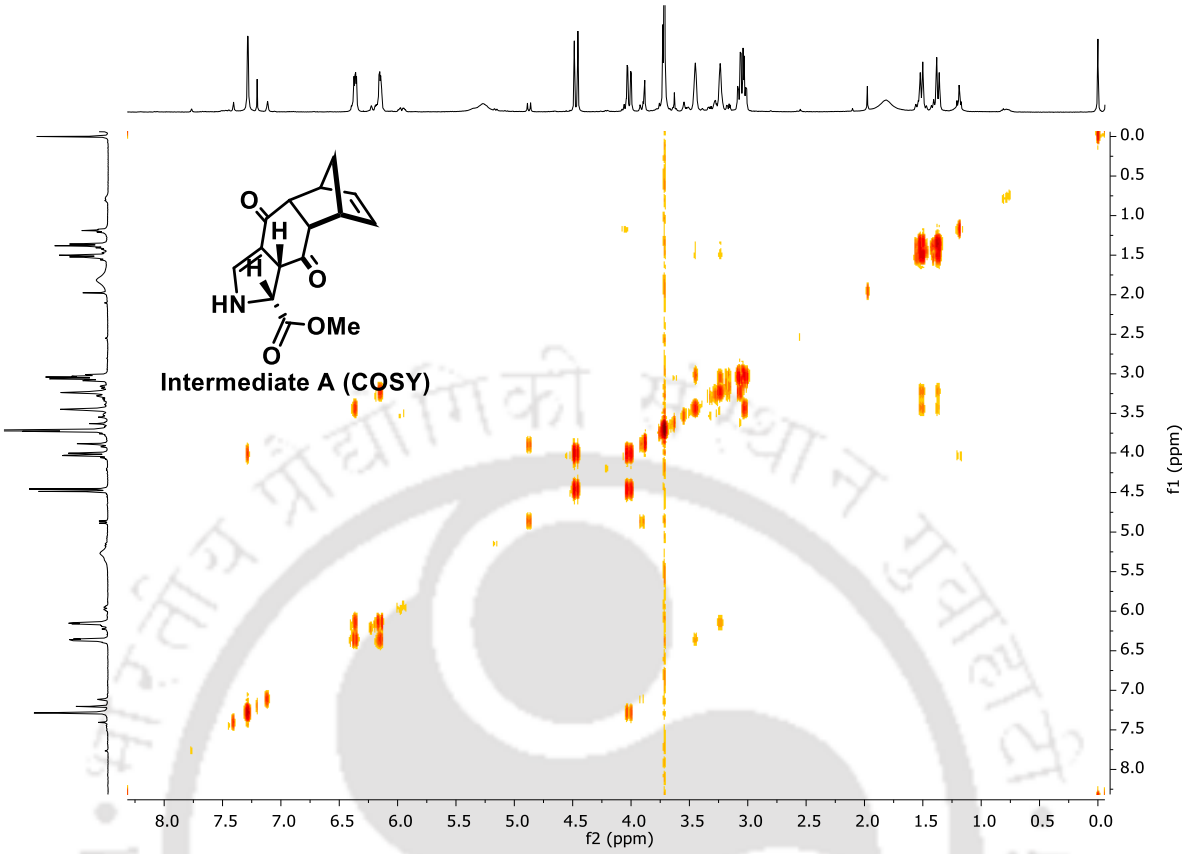

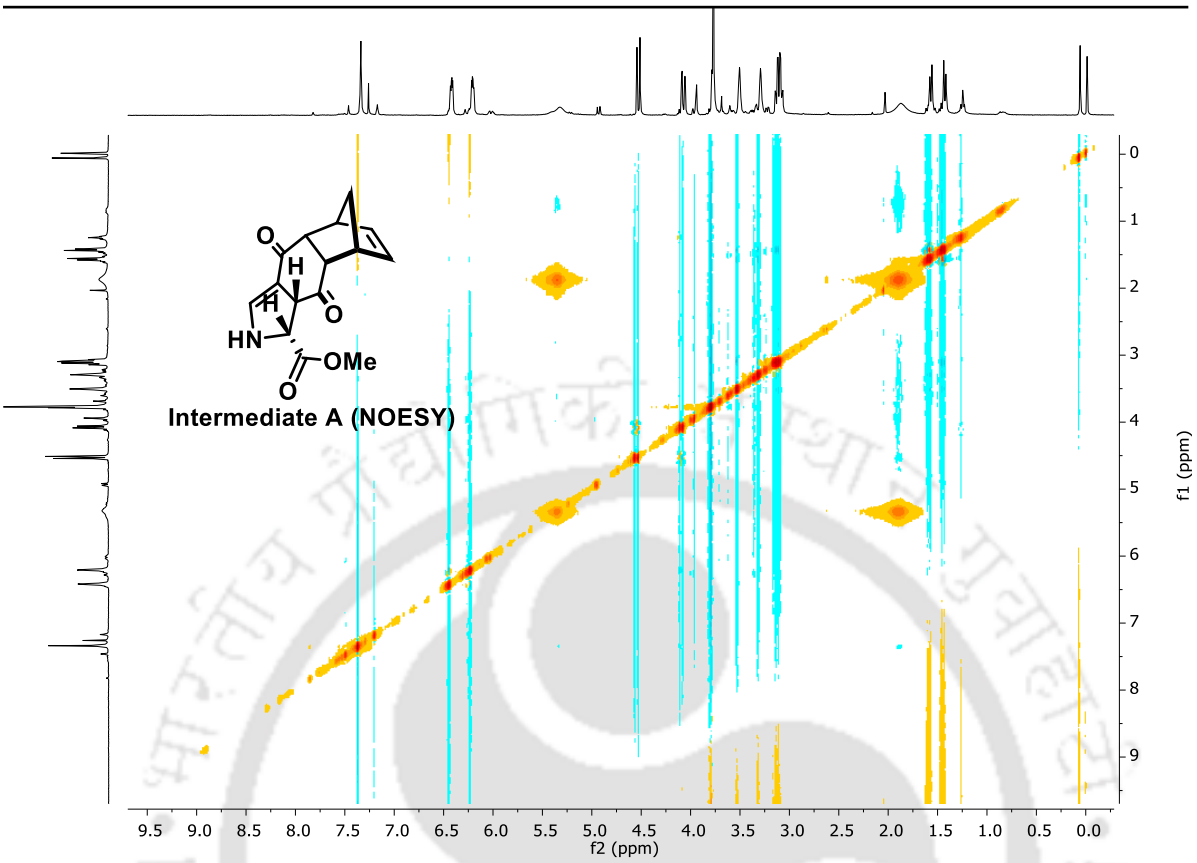

4.13. References:

1. (a) M. J. F. Calvete, S. M. Pinto, *Curr. Org. Synth*. **2017**, *14*, 704; (b) S. Ahmad, O. Alam, Mohd. J. Naim, M. Shaquiquzzaman, M. M. Alam, M. Iqbal, *Eur. J. Med. Chem*. **2018**, *157*, 527–561.
2. For selected recent reviews, see:a) B. Borah, K. D. Dwivedi, L. R. Chowhan, *RSC Adv.* **2021**, *11*, 13585–13601; b) I. V. Efimov, L. N. Kulikova, A. R. Miftyakhova, M. D. Matveeva, L. G. Voskressensky, *ChemistrySelect* **2021**, *6*, e202103486; c) T. Shi, G. Yin, X. Wang, Y. Xiong, Y. Peng, S. Li, Y. Zeng, Zhen Wang, *Green Synth. Catal*. **2023**, *4*, 20.
3. For a review, see: S. Thirumalairajan, B. M. Pearce, A. Thompson, Chem. Commun. **2010**, 46, 1797.
4. For selected transition metal catalysed examples, see: (a) Z. Cao, Y. Liu, Z. Liu, X. Feng, M. Zhuang, H. Du, *Org. Lett*. **2011**, *13*, 2164; (b) C.-X. Zhuo, Q.-F. Wu, Q. Zhao, Q.-L. Xu, S.-L. You, *J. Am. Chem. Soc*. **2013**, *135*, 8169; (c) C.-X. Zhuo, Q. Cheng, W.-B. Liu, Qi. Zhao, S.-L. You, *Angew. Chem. Int. Ed*. **2015**, *54*, 847; (d) T. Das, P. Saha, V. K. Singh, *Org. Lett*. **2015**, *17*, 5088; (e) C.-X. Zhuo, X. Zhang, S.-L. You, *ACS Catal*. **2016**, *6*, 5307; (f) L. Huang, Y. Cai, C. Zheng, L.-X. Dai, S.-L. You, *Angew. Chem. Int. Ed*.

2017, *56*, 1054; (g) S. Iwase, Y. Suzuki, S. Tanaka, M. Kitamura, *Org. Lett.* **2020**, *22*, 1929; (h) L. Huang, J.-H. Xie, Y. Cai, C. Zheng, X.-L. Hou, L.-X. Dai, S.-L. You, *Chem. Commun*. **2021**, *57*, 5390.

5. For selected organocatalytic examples, see: (a) N. A. Paras, D. W. C. MacMillan, *J. Am. Chem. Soc*. **2001**, *123*, 437; (b) G. Li, G. B. Rowland, E. B. Rowland, J. C. Antilla, *Org. Lett.* **2007**, *9*, 4065; (c) I. T. Raheem, P. S. Thiara, E. N. Jacobsen, *Org. Lett* **2008**, *10*, 1577; (d) Q. Yin, S.-L. You, *Chem. Sci*. **2011**, 2, 1344; (e) S.-G. Wang, S.-L. You, *Angew. Chem. Int. Ed.* **2014**, *53*, 2194; (f) G. P. Y. Kok, P.-L. Shao, J.-Y. Liao, S. N. F. B. S. Ismail, W. Yao, Y. Lu, Y. Zhao, *Chem.-Eur. J* **2018**, *24*, 10513; (g) Y. You, W.-Y. Lu, K.- X. Xie, J.-Q. Zhao, Z.-H. Wang, W.-C. Yuan, *Chem Commun*. **2019**, *55*, 8478; (h) M. Hatano, k. Toh, K. Ishihara, *Org. Lett*. **2020**, *22*, 9614; (i) T. Uchikura, K. Aruga, R. Suzuki, T. Akiyama, *Org. Lett.* **2022**, *24*, 4699. For a review, see: (j) D. Gaviña, M. Escolano, J. Torres, G. Alzuet-Piña, M. Sánchez-Roselló, C. del Pozo, *Adv. Synth Catal*. **2021**, *363*, 3439.
6. L. Zhang, J. Zhang, J. Ma, D.-J. Cheng, B. Tan, *J. Am. Chem. Soc*. **2017**, *139*, 1714.
7. S.-C. Zheng, Q. Wang, J. Zhu, *Angew. Chem. Int. Ed*. **2019**, *58*, 1494.
8. S.-C. Zheng, Q. Wang, J. Zhu, *Angew. Chem. Int. Ed*. **2019**, *58*, 9215.
9. X.-L. He, H.-R. Zhao, X. Song, B. Jiang, W. Du, Y.-C. Chen, *ACS Catal.* **2019**, *9*, 4374.
10. Y.-B. Wang, Q.-H. Wu, Z.-P. Zhou, S.-H. Xiang, Y. Cui, P. Yu, B. Tan, *Angew. Chem. Int. Ed*. **2019**, *58*, 13443.
11. K.-W. Chen, Z.-H. Chen, S. Yang, S.-F. Wu, Y.-C. Zhang, F. Shi, *Angew. Chem. Int. Ed.* **2022**, *61*, e202116829.
12. C. X. A. Tan, R. Li, F. Zhang, L. Dai, N. Ullah, Y. Lu, *Angew. Chem. Int. Ed.* **2022**, *61*, e202209494.
13. Y.-B. Chen, L.-G. Liu, C.-M. Chen, Y.-X. Liu, B. Zhou, X. Lu, Z. Xu, L.-W. Ye, *Angew. Chem. Int. Ed*. **2023**, *62*, e202303670.
14. T. Zhu, Y. Liu, M. Smetankova, S. Zhuo, C. Mou, H. Chai, Z. Jin, Y. R. Chi, *Angew. Chem. Int. Ed.* **2019**, *58*, 15778;
15. J.-M. Hu, J.-Q. Zhang, B.-B. Sun, J.-B. Chen, J.-Q. Yu, X.-P. Yang, H.-P. Lv, Z. Wang, X.-W. Wang, *Org. Lett*. **2019**, *21*, 8582.
16. B. Ghosh, M. S. Harariya, S. Mukherjee, *Angew. Chem. Int. Ed.* **2022**, *61*, e202204523;
17. S. Mondal, S. Mukherjee, *Org. Lett.* **2022**, *24*, 8300.
18. (a) J. George, H. Y. Kim, K. Oh, *Org. Lett*. **2018**, *20*, 2249; b) M. A. Abozeid, H. Y. Kim, K. Oh, *Org. Lett.* **2022**, *24*, 1812.
19. For selected recent reviews, see: (a) A. Borissov, T. Q. Davies, S. R. Ellis, T. A. Fleming, M. S. W. Richardson, D. J. Dixon, *Chem. Soc. Rev*. **2016**, *45*, 5474; (b) X.-P. Zeng, Z.-Y.

Cao, Y.-H. Wang, F. Zhou, J. Zhou, *Chem. Rev*. **2016**, *116*, 7330; (c) M. A. Horwitz, J. S. Johnson, *Eur. J. Org. Chem*. **2017**, *11*, 1381; (d) M. D. Díaz De Villegas, J. A. Gálvez, P. Etayo, R. Badorrey, P. López-Ram-De-Víu, *Chem. Soc. Rev*. **2011**, *40*, 5564; (e) Y. Xu, T.-Y. Zhai, Z. Xu, L.-W. Ye, *Trends Chem.* **2022**, *4*, 191; (f) C. Nájera, F. Foubelo, J. M. Sansano, M. Yus, *Tetrahedron* **2022**, 106–107, 132629.

20. For selected examples, see: (a) C. Guo, M.-X. Xue, M.-K. Zhu, L.-Z. Gong, *Angew. Chem. Int. Ed.* **2008**, *47*, 3414; (b) F. Sladojevich, A. Trabocchi, A. Guarna, D. J. Dixon, *J. Am. Chem. Soc.* **2011**, *133*, 1710; (c) H. Y. Kim, K. Oh, *Org. Lett*. **2011**, *13*, 1306; (d) M.-X. Zhao, H. Zhou, W.-H. Tang, W.-S. Qu, M. Shi, *Adv. Synth. Catal*. **2013**, *355*, 1277; (e) M. Wang, X.-H. Liu, P. He, L.-L. Lin, X.-M. Feng, *Chem. Commun*. **2013**, *49*, 2572; (f) P.-L. Shao, J.-Y. Liao, Y. A. Ho, Y. Zhao, *Angew. Chem. Int. Ed*. **2014**, *53*, 5435; (g) M. Hayashi, M. Iwanaga, N. Shiomi, D. Nakane, H. Masuda, S. Nakamura, *Angew. Chem. Int. Ed*. **2014**, *53*, 8411; (h) R. de la Campa, I. Ortin, D. J. Dixon, *Angew. Chem. Int. Ed*. **2015**, *54*, 4895; (i) J.-Y. Liao, P.-L. Shao, Y. Zhao, *J. Am. Chem. Soc*. **2015**, *137*, 628; (j) A. R. Keeri, A. Gualandi, A. Mazzanti, J. Lewinski, P. G. Cozzi, *Chem. Eur. J.* **2015**, *21*, 18949; (k) W.-W. Luo, X. Yuan, L.-L. Lin, P.-F. Zhou, X.-H. Liu, X.-M. Feng, *Chem. Sci*. **2016**, *7*, 4736; (l) P. Martínez-Pardo, G. Blay, M. C. Munoz, J. R. Pedro, A. S. Marco, C. Vila, *Chem. Commun*. **2018**, *54*, 2862; (m) B. Xu, Z.-M. Zhang, L.- J. Zhou, J.-L. Zhang, *Org. Lett*. **2018**, *20*, 2716; (n) Z.-P. Wang, Q. Wu, J. Jiang, Z.-R. Li, X.-J. Peng, P.-L. Shao, Y. He, *Org. Chem. Front*. **2018**, *5*, 36; (o) Q. Wan, J.-H. Xie, C. Zheng, Y.-F. Yuan, S.-L. You, *Angew. Chem. Int. Ed.* **2021**, *60*, 19730; (p) L.-F. Tao, S. Zhang, F. Huang, W.-T. Wang, Z.-H. Luo, L. Qian, J.-Y. Liao, *Angew. Chem. Int. Ed.* **2022**, *61*, e202202679; (q) B. Das, N. Chakraborty, H. N. Dhara, P. Bhattacharya, B. K. Patel, *J. Org. Chem*. 2024, *89*, 1331; For a review, see: (r) J. Luo, G.-S. Chen, S.-J. Chen, Z.-D. Li, Y.-L. Liu, *Chem. Eur. J.* **2021**, *27*, 6598.
21. For selected recent examples on catalytic asymmetric [3+2]-cycloadditions: (a) P. Wu, W.-T. Zhang, J.-X. Yang, X.-Y. Yu, S.-F. Ni, W. Tan, F. Shi, *Angew. Chem. Int. Ed.* **2024**, *63*, e202410581; (b) S.-J. Liu, T.-Z. Li, N.-Y. Wang, Q. Cheng, Y. Jiao, Y.-C. Zhang, F. Shi, *Org. Chem. Front.* **2024**, *11*, 4812; For recent reviews on catalytic asymmetric cycloadditions: (c) W. Tan, J.-Y. Zhang, C.-H. Gao, F. Shi, *Sci. China Chem*. **2023**, *66*, 966; (d) Z.- Q. Zhu, T.-Z. Li, S.-J. Liua, F. Shi, *Org. Chem. Front*. **2024**, *11*, 5573.
22. For reviews, see: (a) H. Pellissier, *Chem. Rev*. **2016**, *116*, 14868; (b) M. Li, W. Wu, H. Jiang, *ChemCatChem* **2020**, *12*, 5034.
23. For a review, see: Z. Ma, Z. Ma, D. Zhang, *Molecules* **2018**, *23*, 2666.
24. (a) R. Sarkar, S. Mukherjee, *Org. Lett*. **2016**, *18*, 6160; (b) C. J. C. Lamb, F. Vilela, A-L. Lee, *Org. Lett.* **2019**, *21*, 8689.

25. (a) W. Liang, K. Nakajima, K. Sakata, Y. Nishibayashi, *Angew. Chem. Int. Ed*. **2019**, *58*, 1168; (b) M. G. Ricardo, J. F. Marrrero, O. ValdØs, D. G. Rivera, L. A. Wessjohann, *Chem. Eur. J*. **2019**, *25*, 769. (c) A. Franchino, P. Jakubec, D. J. Dixon, *Org. Biomol. Chem*., **2016**, *14*, 93.
26. L. Wang, A. Studer, *Org. Lett*. **2017**, *19*, 5701.
27. (a) F. Sladojevich, A. Trabocchi, A. Guarna, D. J. Dixon, J. Am. Chem. Soc. **2011**, *133*, 1710-1713; (b) P.-L. Shao, J.-Y. Liao, Y. A. Ho, Y. Zhao, *Angew. Chem. Int. Ed*. **2014**, *53*, 5435-5439; (c) Y. Xiong, Z. Du, H. Chen, Z. Yang, Q. Tan, C. Zhang, L. Zhu, Y. Lan, M. Zhang, *J. Am. Chem. Soc*. **2019**, *141*, 961-971.

Chapter 5

Organocatalytic Asymmetric Desymmetrizing Friedel-Crafts Reaction of Prochiral 3,4-Fused Pyrroles

Abstract: An interesting but little-studied topic is central chirality in heteroarene derivatives originating from unsymmetrically substituted heteroarene rings. Herein, we have demonstrated the first catalytic enantioselective desymmetrizing Friedel-Crafts reaction of prochiral 3,4-fused pyrroles. The electrophiles used are allenamides and an easily available phosphoric acid was employed as the catalyst. At least four continuous stereogenic centers can be produced by this careful desymmetrization without producing any extra stereocentres. High yields and good to high enantioselectivities were obtained for a variety of polycyclic 2-substituted, 3,4-fused pyrroles.

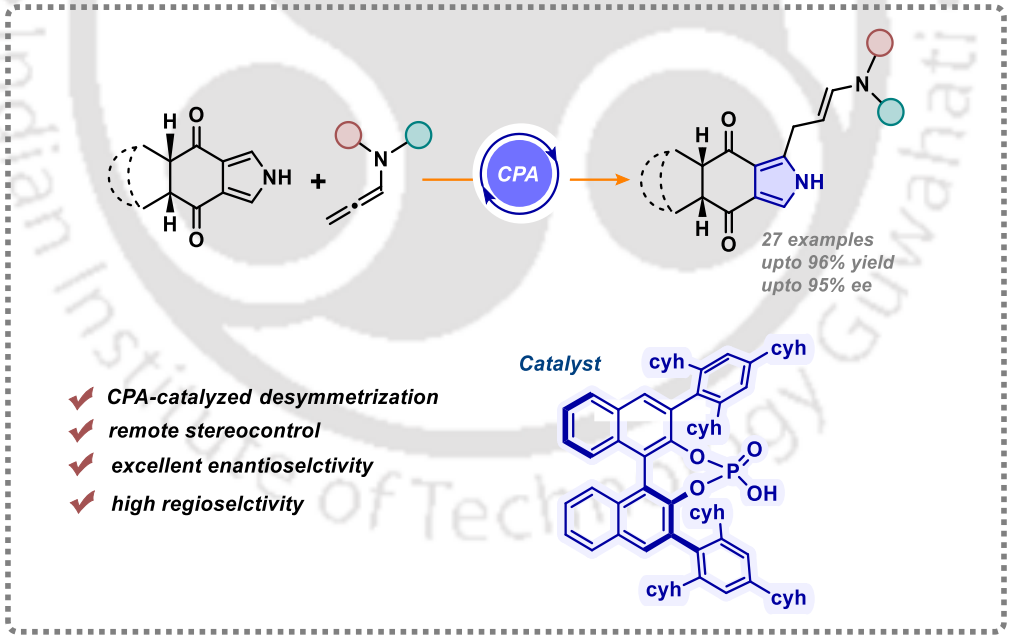

5.1. Introduction:

Pyrrole is a notable five-membered heterocycle that is present in a variety of pharmaceuticals and bioactive natural products. [1] As a result, much effort has been made over time to synthesize pyrroles with diverse substitutions.[2] Many structural and synthetic variations exist in optically active pyrroles, and the stereogenic centers may be located near or far from the heterocyclic unit. There are six main types of chiral pyrrole synthesis. (i) chirality at the α-position; (ii) chirality at the β-position; (iii) chirality at the nitrogen atom; (iv) chirality of pyrroles annulated through the α-position and nitrogen atom; (v) chirality of pyrroles annulated through the α- and β-positions; and (vi) axially chiral pyrroles.[3] The centrally chiral pyrroles fall into the first five categories. The enantioselective synthesis of centrally chiral pyrroles, which are very common and usually contain one or more chiral centers close to their framework, can be accomplished in a number of ways. [4-6] But in most of these cases, the pyrrole ring substitution pattern has little to do with the formation of

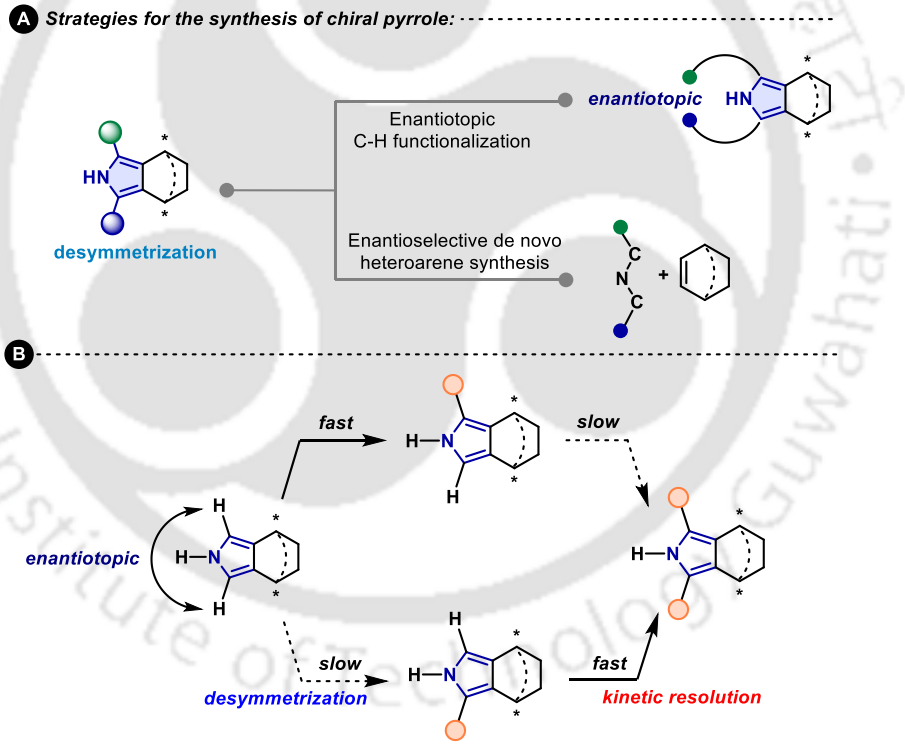

Fig. 1: Desymmetrization Strategy.

stereogenicity. Central chirality in pyrrole derivatives resulting from asymmetrical substitution on the pyrrole ring is an intriguing but little-studied topic. These pyrrole motifs' substituents not only regulate their chirality but also, when their locations are changed, generate enantiomeric pyrroles. Consequently, it is quite challenging to synthesize such chiral pyrroles in an enantioselective manner, particularly when a functional group or substituent is

added to the pre-existing symmetrical pyrrole frameworks in an enantioposition-selective way, e.g enantioselective desymmetrizing Friedel Crafts reaction (Fig. 1a). Another strategy involves creating the de novo construction of unsymmetrical pyrrole ring in the enantioselectivity-determining step.[7] In this context, desymmetrizing pre-existing symmetrical pyrroles is the most challenging because of regioselectivity. The enantioselctivity of this enantiotropic pyrroles depends on two process one by desymmetrization or another combined desymmetrization/kinetic resolution process (Fig. 1b).

5.2. Previous Study:

In 2001, McMillan et al., reported organocatalyzed first F-C alkylation of pyrroles.[8] Under iminium catalysis, α,β-unsaturated aldehydes reacted with N-methyl pyrroles to afford chiral pyrroles in high yields and excellent ees (Scheme 1).

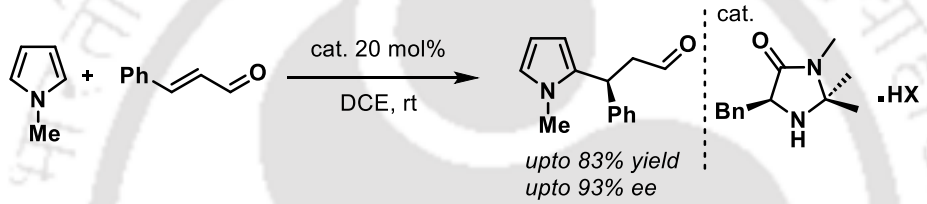

Scheme 1: First asymmetric Friedel−Crafts alkylation of pyrroles.

In 2005, Palomo and co-worker reported Cu-complex catalyzed F-C alkylation of N-methyl pyrroles with unsaturated ketones. The authors clarified that unsaturated ketones' carbonyl group and free alcohol play a crucial role in catalyst binding to enable an enantioselective 1,4-addition (Scheme2).[9] Under optimal conditions, the F-C alkylation products were obtained in good yields and excellent ees.

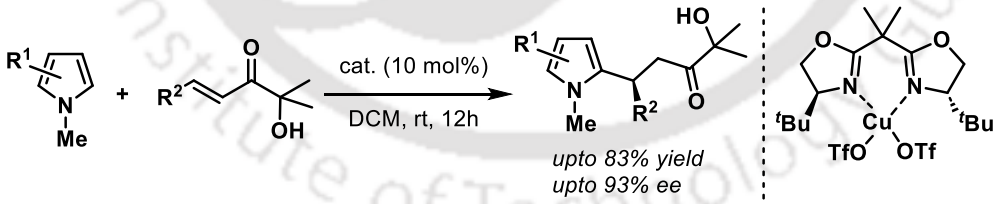

Scheme 2: Chiral Cu(I)-complex catalyzed Friedel−Crafts alkylation of pyrrole.

Then, in 2008, Muller at al. described Friedel−Crafts alkylation of pyrroles with nitroalkenes using a dinuclear zinc-complex chiral catalyst (Scheme 3). In this method, N-H in pyrroles initially binds with chiral Zn-complex, which underwent a stereoselective F-C alkylation to coordinated nitroalkenes and the products were isolated in excellent yields and ees.[10]

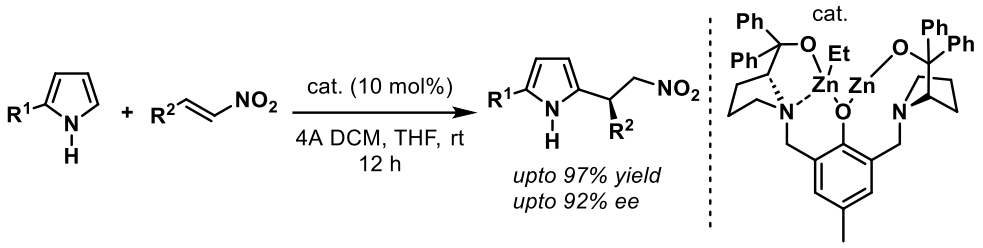

Scheme 3: Chiral dinuclear zinc-complex catalysed F-C reaction of pyrrole.

In 2009, similar Friedel−Crafts alkylation of pyrroles with nitroalkenes was reported by Li group. Pyrroles and nitroalkenes underwent a dual H-bonding activation to process the asymmetric Friedel-Crafts reaction using phosphoric acid generated from BINOL (Scheme 4). Under the optimal conditions, the reaction gave chiral pyrroles in excellent yields and ees.[11]

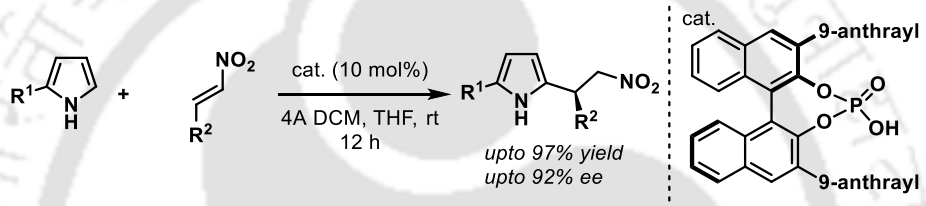

Scheme 4: Chiral phosphoric acid catalyzed F-C reaction of pyrrole and nitroalkenes.

Then, in 2016, Ohara et al. reported an aza-Friedel−Crafts alkylation reaction with pyrroles by organocatalysis.[12] This aza F-C synthesis produced a quaternary center containing chiral N-aryl amines in outstanding yields and ees under the catalysis of chiral imidazolinephosphoric acid (Scheme 5).

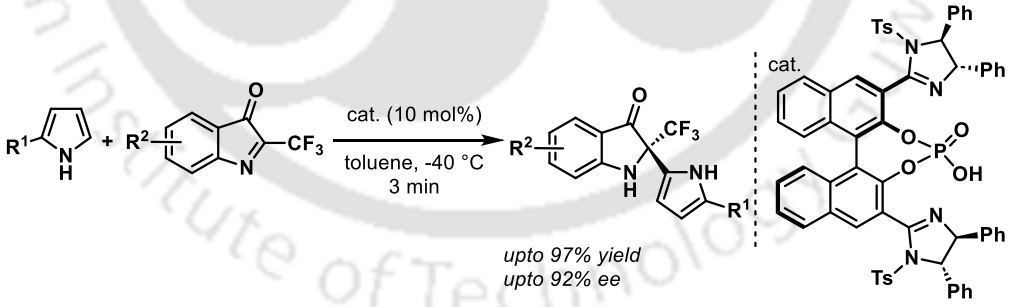

Scheme 5: Chiral Bronsted acid catalyzed aza-F-C reaction of pyrrole.

Then, Lin et al. explored chiral phosphoric acid catalyzed F-C reaction of pyrroles with CF_3-bearing imines (Scheme 6).. Trifluoromethyl benzoxazinone experienced dual H-bonding activation and acted as an H-bonding acceptor (driven by the CF_3 moiety) when mixed with an appropriate BINOL-based phosphoric acid. This resulted in a quaternary center bearing chiral N-aryl amines in outstanding yields and ees. [13]

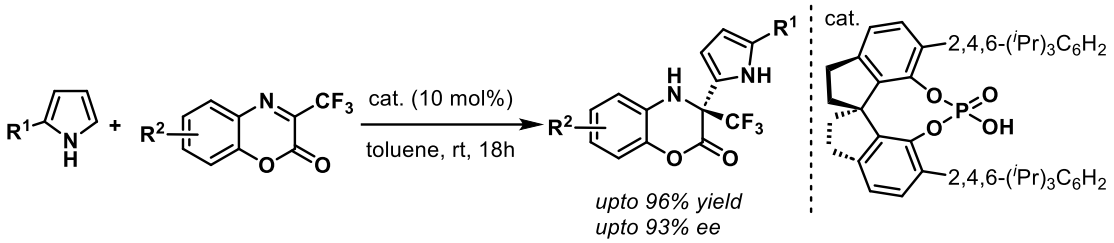

Scheme 6: Chiral Bronsted acid catalyzed F-C reaction of pyrrole and trifluoromethyl benzoxazinone.

In 2019, Jiang et al. reported the first asymmetric intramolecular ring-closing alkylation of inert pyrroles with α,β-unsaturated ketones, and it is catalyzed by chiral Brønsted acid. This process offers a range of 4-phenyl-4,5-dihydro-6H-benzo[f]pyrrolo[1,2-a]azepin-6-ones in mild reaction conditions, with high yields and good enantioselectivities (Scheme 7). [14]

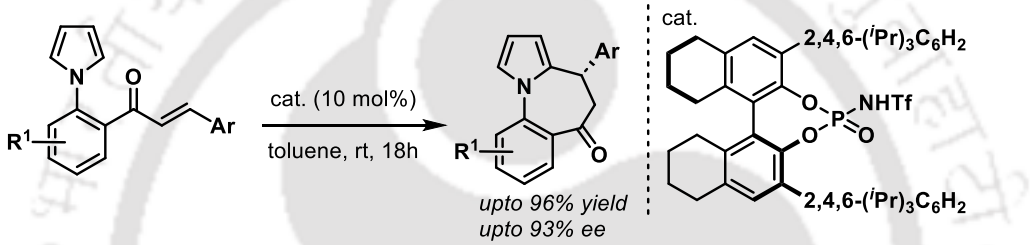

Scheme 7: Chiral Bronsted acid catalyzed ring closing F-C reaction of pyrrole.

In 2020, Ishihara and co-workers described a chiral BINOL-derived bis(phosphoric acid) catalyzed enantioselective aza-Friedel–Crafts reaction of pyrroles with acyclic α-ketimino esters (Scheme 8). [15] With a catalyst loading of 0.2 mol%, the reaction yielded quaternary carbon center containing products in high yields and enantioselectivities. A preliminary mechanism for this method points to a hydrogen bonding with potential π–π interactions as the cause of strereoselctivity.

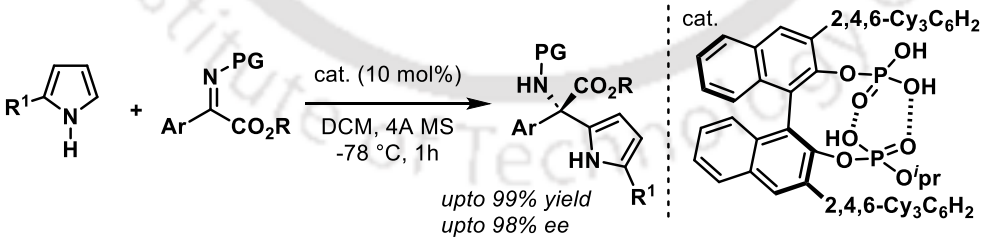

Scheme 8: Aza-F-C reaction catalyzed by Chiral bis(phosphoric acid) F-C reaction of pyrrole.

Wang et al. reported a chiral spiro phosphoric acid catalyzed enantioselective reaction involving ketenes and N-H pyrroles.[16] The asymmetric synthesis of C-acylated pyrroles with α-stereogenic carbon centers is made possible by this process. Friedel-Crafts-like acylation of pyrroles and enantioselective protonation of ketenes or α-diazoketones are the subsequent reactions (Scheme 9).

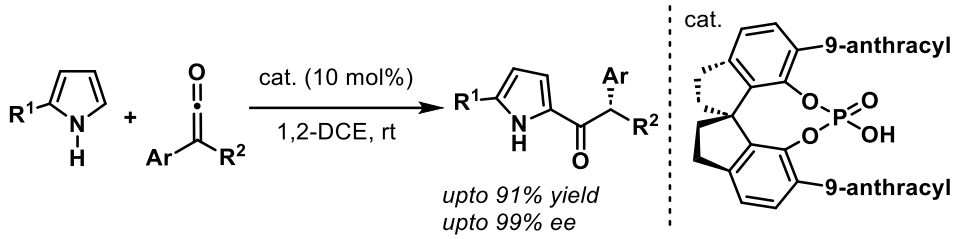

Scheme 9: Asymmetric Friedel-Crafts-like acylation of pyrroles with ketene.

Then, in 2022, Akiyama et al. reported chiral phosphoric acid catalysed Friedel–Crafts alkylation of N-unprotected alkynyl trifluoromethyl ketimines with pyrroles, in order to synthesize α-2-pyrrolyl, α-trifluoromethyl primary propargylic amines with high enantioselectivities (Scheme 10). [17]

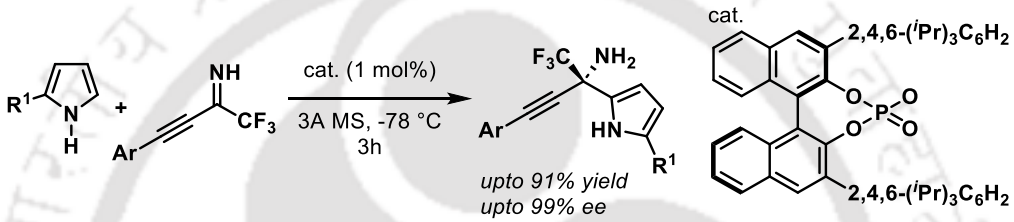

Scheme 10: Asymmetric Friedel-Crafts-like acylation of pyrroles with ketene.

The Friedel–Crafts alkylation procedure of C2/C5-disubstituted pyrroles at the β-(C3) position with isoindolinone-derived ketimines was developed by Gredičak et al. in 2023 using chiral phosphoric acid as a catalyst. 2-Monosubstituted pyrroles can also undergo this transformation, producing α-(C5) functionalized pyrroles (Scheme 11). [18] According to the control experiments, H-bonding interactions between the catalyst and the substrates are essential for the reaction's successful completion.

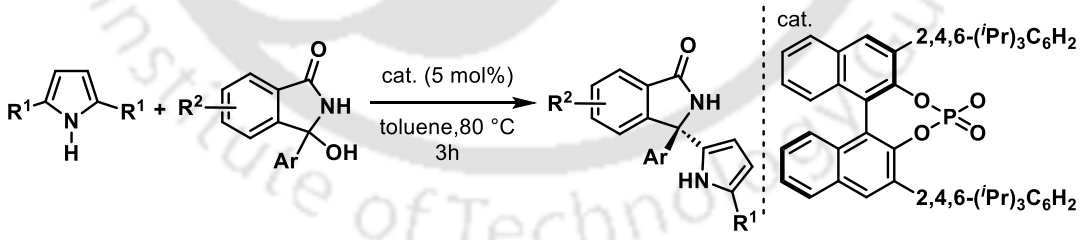

Scheme 11: Asymmetric Friedel-Crafts-like reaction of pyrroles with ketimines.

Muller and colleagues discovered a new technique for the bromination-based desymmetrization of diarylmethylamido bis(phenols) by employing tetrapeptides with tertiary amine motifs as catalysts.[19] Enantiotopic arenes were desymmetrized with N-bromo succinimide producing chiral diaryl amines with moderate yields and good ee (Scheme 12). To find out how much the secondary resolution affected product enantioselectivity, the authors performed a kinetic resolution experiment. The results demonstrated that the primary

source of enantioselectivity in this desymmetrization process is the differentiation of enantiotopic arenes enabled by the peptide.

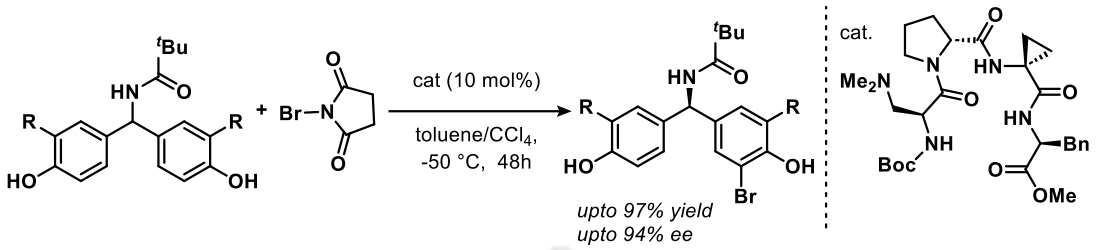

Scheme 12: Chiral peptide catalyzed desymmetrization of diarylmethylamido bis(phenols).

Whereas, in 2020 Tse and Yeung reported desymmetrizing catalytic asymmetric halogenation of BPOL (bisphenol) with NBS as the halogen source.[20] According to the authors, the bifunctional catalyst (S)-BINOL-amine derivative uses intermolecular hydrogen bonds to increase the hydroxyl proton's acidity. By forming hydrogen bonds with the acidic proton, this amino organocatalyst can simultaneously activate the halogen source and the phenol substrate, enabling the halogen atom to be delivered in enantioselective fashion (Scheme 13). Here, the kinetic resolution process reveals, the enantioselectivity determined only by desymmetrization.

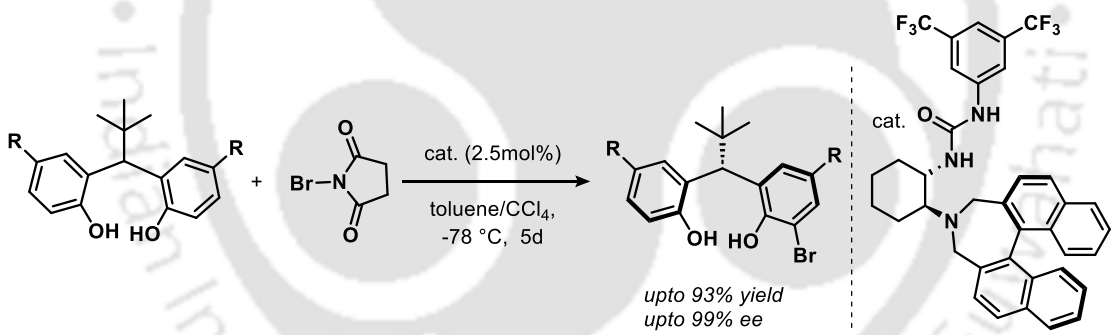

Scheme 13: Chiral peptide catalyzed desymmetrization of BPOL via F-C bromination.

5.3. Objective:

It has been shown that the catalytic asymmetric Friedel-Crafts (FC) alkylation of five-membered heteroaromatic compounds, like pyrroles and indoles, with electron-deficient olefins is a very effective and cost-effective method to create synthetically versatile chiral heteroaromatic-substituted compounds.[21] The inherent instability of pyrroles toward an acidic environment, however, limits study on the catalytic asymmetric FC alkylation of pyrroles with electron-deficient olefins, in stark contrast to the substantial studies dedicated to indoles.[22] To the best of our knowledge a desymmetrizing enantioselective Friedel-Crafts reaction with olefins is still not known. We developed an desymmetrization F-C reaction of enantiotopic pyrroles with allenamides [23, 24].

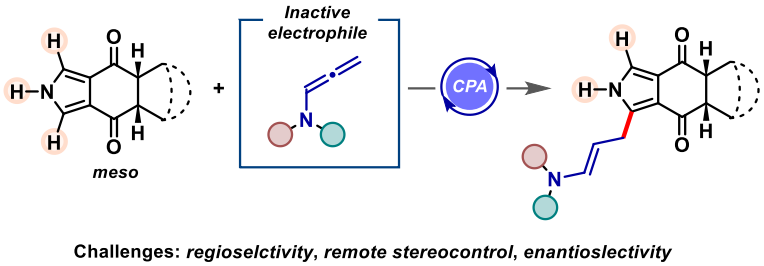

Fig. 2: Objective.

5.4. Results and discussion:

5.4.1. Catalyst, solvent and temperature optimization of the reaction:

Table 1: Catalyst, solvent and temperature optimization:

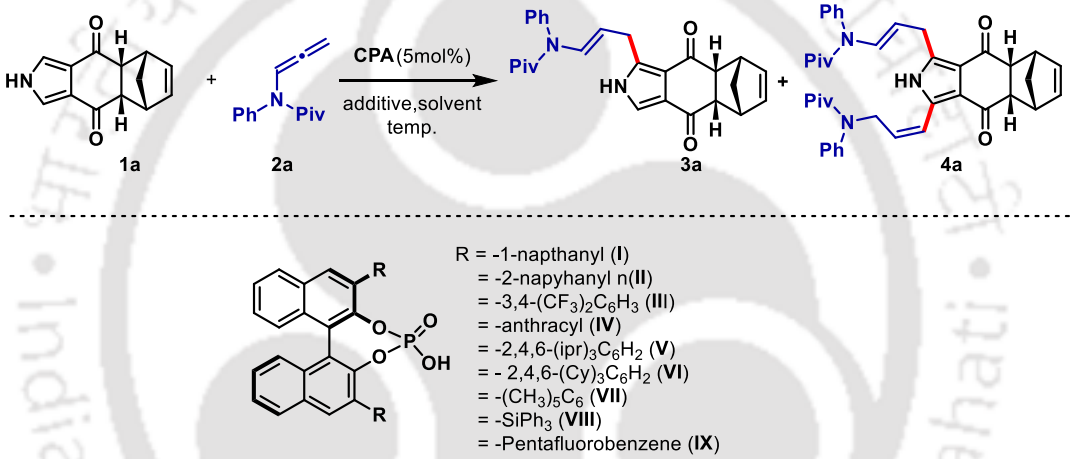

Entry[a]	Catalyst	Solvent	Additive/temp.	%Yield(3a/4a)[b]	% ee[c]
1.	**I**	toluene	- / rt	40/23	2%
2.	**II**	toluene	- / rt	43/12	7%
3.	**III**	toluene	- / rt	59/16	28%
4.	**IV**	toluene	- / rt	60/17	41%
5.	**V**	toluene	- / rt	68/<5	69%
6.	**VI**	toluene	- / rt	61/15	84%
7.	**VII**	toluene	- / rt	53/19	16%
8.	**VIII**	toluene	- / rt	trace	-
9.	**IX**	toluene	- / rt	23/<5	6%
10.	**VI**	DCM	- / rt	32/21	38%
11.	**VI**	$PhCF_3$	- / rt	57/15	70%
12.	**VI**	cyclohexane	- / rt	23/21	81%
13.	**VI**	benzene	- / rt	64/12	78%
14.	**VI**	*o*/*p*-xylene	- / rt	73/19	84%

15.	**VI**	*o*-xylene	- / rt	42/15	86%
16.	**VI**	*p*-xylene	- / rt	53/29	83%
17.	**VI**	mesitylene	- / rt	42/22	84%
18.[d]	**VI**	*o*-xylene	3Å/rt	68/10	79%
19.[e]	**VI**	*o*-xylene	4Å /rt	55/12	81%
20.[f]	**VI**	*o*-xylene	5Å /rt	45/<5	82%
21.[f]	**VI**	*o*-xylene	5Å /0 °C	67/<5	88%
22.[f]	**VI**	*o*-xylene	5Å /-10 °C	51/<5	82%
23.[f,g]	**VI**	*o*-xylene	5Å /0 °C/0.5M	69/<5	92%

[a] Unless otherwise mentioned, reactions were carried out with 0.1 mmol of 1a with 0.2 mmol of 2a, 5 mol% catalyst in 1 mL solvent at rt for 8h in argon atmosphere. [b] Isolated yield after silica gel column chromatography. [c] Determined by HPLC. [d] with 100mg 3 Å MS. [e] with 100mg 4 Å MS. [f] with 100mg 5 Å MS. [g] Reaction was run at 0 °C for 12h in 0.5 M o-xylene.

To begin our study, we performed a model reaction at room temperature between 4a,5,8,8a-tetrahydro-2H-5,8-methanobenzo[f]isoindole-4,9-dione (**1a**) and allenamide (**2a**)[16-17] in toluene (Table 1). Initially, 1-naphthyl substituted chiral phosphoric acid **I** was checked in the reaction. In addition to the formation of the desired mono-substituted product **3a**, bis-substituted meso-compound **4a** was also detected (entry 1). The reaction with 2-naphthyl substituted chiral phosphoric acid **II** was next examined, and a similar outcome was discovered (entry 2). Slightly higher enantioselectivities were attained with catalysts **III** and **IV** having 3,5-di triflurometh ylphenyl substituents and anthracenyl substituents respectively (entries 3-4). Then TRIP catalyst **V** was screened in the reaction and to our delight, the formation of **4a** was minimized and compound **3a** was isolated in 68% yield with 69 (entry 5). With catalyst **VI** containing 2,4,6-tricyclohexylphenyl substituents, better enantioselectivity was observed (entry 6). However, lower enantioselectivity for **3a** was detected with catalyst **VII** having pentamethyl phenyl substituents and poor yield was found with catalyst **VIII** having triphenylsilyl substituents (entries 7-8). Also, use of pentafluorobenzene substituent catalyst **X** was not fruitful (entry 9). Next, we focused on using catalyst **VI** for solvent optimization. Moderate enantioselectivities were found in dichloromethane and triflouorotoluene (entries 10-11). Then cyclohexane, benzene, mesitylene and *ortho*-xylene were checked, and gratifyingly good results were found in *ortho*-xylene (entries 12-17). Molecular sieves were then introduced to the process, further reducing the production of **4a** (entries 18-20). Lowering of temperature was done, at 0 °C, ee increased to 88% (entry 21-22). Finally, the reaction was run at 0 °C for 12 hours with 5Å in 0.5 M solvent and the compound **3a** was obtained in 69% yield with 92% ee (entry 23).

5.4.2. Scope of the reaction:

Following the establishment of optimal conditions, the reaction's scope and generality were tested. Initially, different polycyclic meso-3,4-fused pyrroles were examined in the catalytic

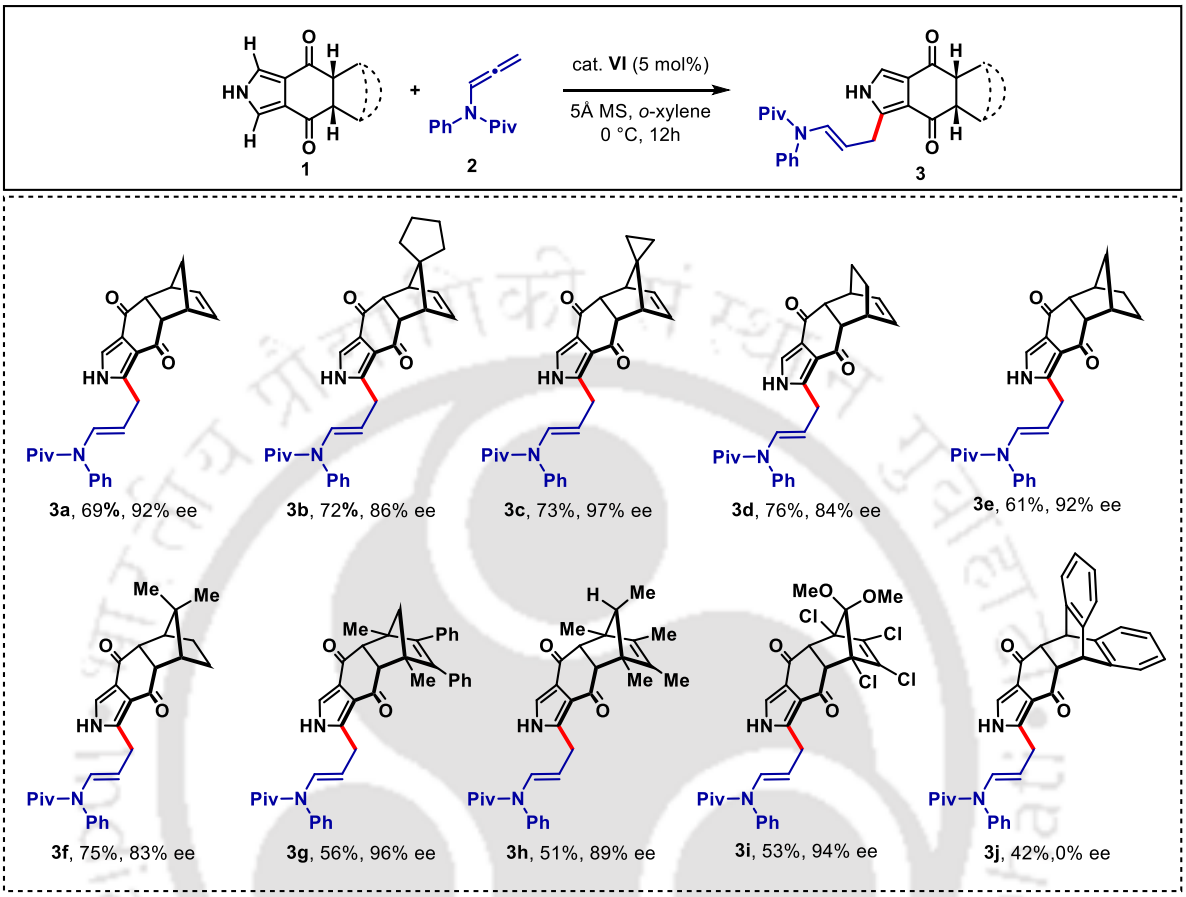

Scheme 14: Scope of enantiotopic pyrroles.

desymmetrizing Friedel-Crafts reaction and good results were detected (Scheme 14). For example, fused pyrrole **1b** derived from the Diels-Alder (DA) adduct of *para*-benzoquinone and spiro-fused cyclopentadiene reacted smoothly to deliver product **3b** in 72% yield with 86% ee. Similar result was observed for product **3c** having a spiro-fused cyclopropyl group. The procedure also produced product **3d** in 76% yield with 84% ee using fused pyrrole **1c**, which was produced from the DA adduct of *para*-benzoquinone and cyclohexadiene. High enantioselectivity was detected for compound **3e** having norboryl motif. Interestingly, the enatioselectivity slightly reduced for product **3f** having a quaternary centre with geminal dimethyl group. The Friedel-Crafts reaction was next examined using pyrrole **1g**, which was obtained from the highly substituted cyclopentadiene and *para*-benzoquinone DA adduct (Scheme 14). To our delight product **3g** was obtained in 56% yield with 96% ee. The results of product **3h** with pentamethyl substitution were observed with 51% yield and 89% ee. The pyrrole **1i** obtained from a highly substituted cyclopentadiene and *para*-benzoquinone DA

adduct was next examined. Gratifyingly better enantioselecitivity was attained for product **3i**. Lastly, the pyrrole **1j**, which is generated from the DA adduct of *para*-benzoquinone and anthracene, was screened. However, no enantioselectivity was detected for product **3j**.

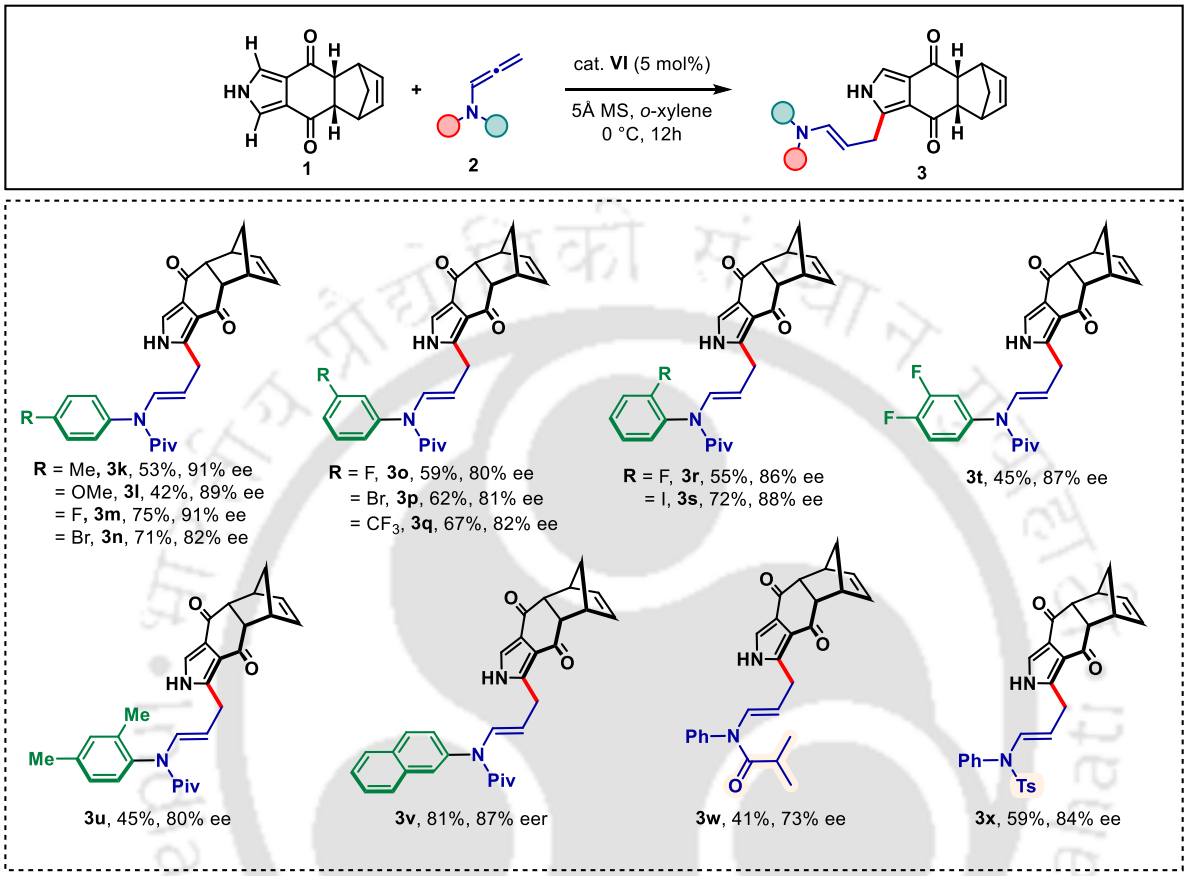

Scheme 15: Scope of various allenamides.

Then we became interested to check the scope of allenamide **2** in the reaction (Scheme 15). Initially allenamides **2** with various substitutions on the aryl group were prepared and engaged in the reaction with **1a**. Allenamides **2b** and **2c** having tolyl and *para*-anisyl groups respectively reacted smoothly to deliver products **3k** and **3l** in 91% er and 89% ee respectively. Different halo-substitutions were also tolerated. While fluoro-containing product **3m** achieved high enantioselectivity, bromo-containing product **3n** showed slightly lower enantioselectivity. Then different *meta*-substitutions were checked and here also good results were observed. For example, decent enantioselectivities were detected for compounds **3o** and **3p** having 3-fluoro and 3-bromo substitutions respectively. Additionally, trifluoromethyl group was tolerated, and product **3q** was produced with good enantioselectivity. (Scheme 15). After that, *ortho*-substituted allenamides **2i** and **2j** having 2-fluoro and 2-iodo substitutions respectively were screened in the reaction and good results were observed for the products **3r** and **3s**. Then, disubstituted aryl group containing allenamides **2k** and **2l** took part in the

reaction to deliver the products **3t** and **3u** in 87% and 80% enantioselectivity respectively. Then, we used allenamides **2m** and **2n** in the process by substituting isobutyryl and tosyl groups for the pivaloyl group. The reactions progressed smoothly to afford products **3w** and **3x** in good enantioselectivities.

Then, different important scaffolds containing substituents were incorporated, and the corresponding allenamides were checked in the reaction (Scheme 16). Initially, geraniol-derived substrate **2y** was employed in the reaction, product **3y** was obtained with 79% yield and 80% ee. Then, (-)-perillyl alcohol derived allenamide **2z** progressed the reaction well to provide product **3z'** as a single diastereomer in 61% yield. The reaction also proceeded smoothly with substrate **2z'** having a (-)-menthol motif, affording product **3z'** in >20:1 dr.

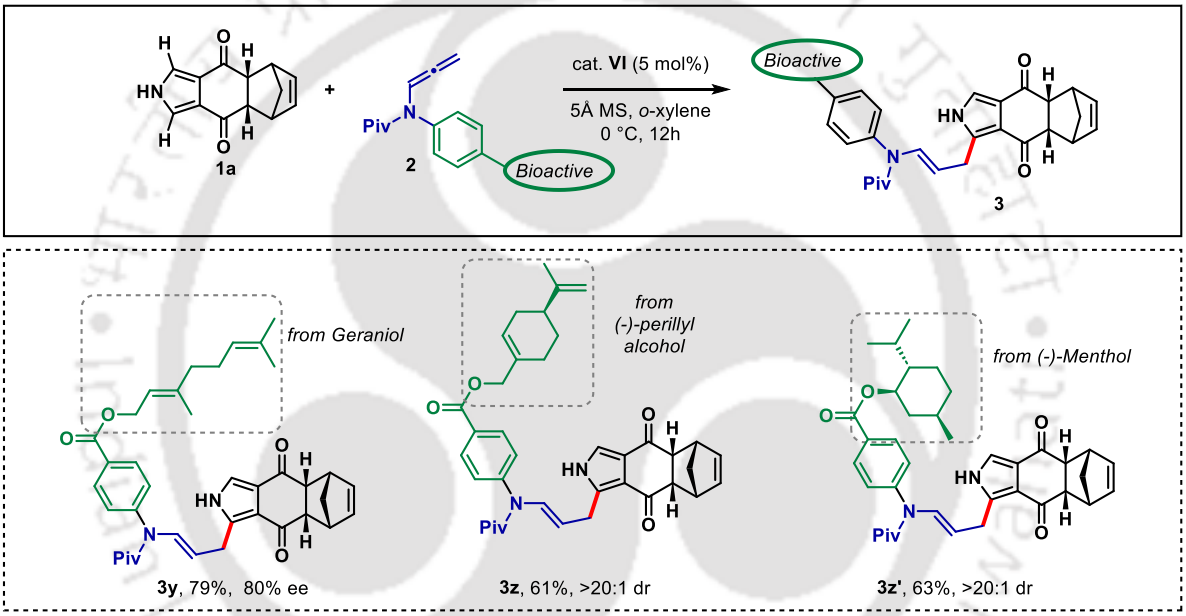

Scheme 16: Scope of various allenamides containing bioactive molecules.

5.5. Mechanism

5.5.1. Control experiment:

To get insight of the reaction mechanism, several control experiments were performed. Initially, the reaction of enantiotopic pyrrole **1a** and allenamide **2b** was carried out under the standard conditions with 0.75 equivalent of **2b** and provided the centrally chiral pyrrole **3a** in 39% yield with 92% ee, accompanied with a trace amount of disubstituted product **4a**, which indicated that desymmetrization is a key contributor for stereocontrol. Racemic compound **3a** was treated with 0.55 equivalent of **2b** under standard conditions and produced unreacted **3a** in 32% yield with 0% ee and disubstituted product **4a** in 28% yield (Scheme 17b), indicating that the enantioselectivity was solely due to CPA-catalyzed desymmetrization.

Then, a reaction was performed with N-methyl protected **1a** and **5** was obtained with 41% yield and 28% ee. The Freidel-crafts reaction of **1a** and **12** afforded **3r** in 53% yield and 74% ee, indicating an ion-pair mechanism.

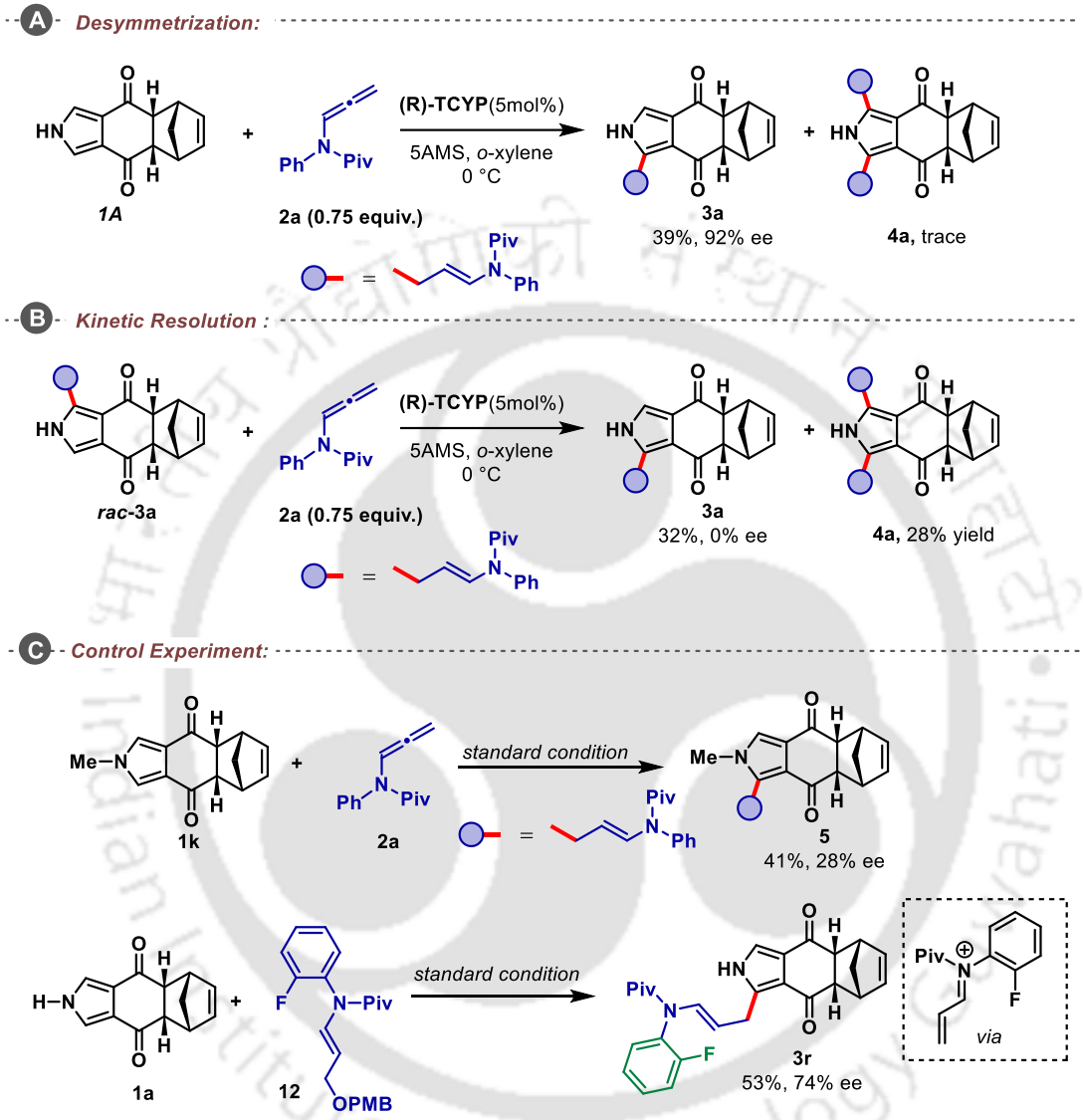

Scheme 17: a) desymmetrization, b) kinetic resolution, c) Control experiments.

5.5.2. Proposed mechanism:

Based on control experiments, catalytic mechanism was proposed in Scheme 18. The first role of CPA is the facile addition with the allenamide **2a** to form the allyl phosphate adduct intermediate **INT- A**. The covalent phosphate **INT -A** would undergo the facile E1cB -type elimination to give the α-β -unsaturated iminium ion **INT-B** paired with the corresponding chiral phosphate anion. Then Friedel-crafts addition and conjugate addition of the **INT-B** takes place with **1a** under the influence of chiral phosphate anion. The hydrogen bonding

between **1a** with the P=O moiety of phosphate **INT-C** was believed to be crucial. Consequently, the attack of **1a** to the α,β-unsaturated iminium ion under the dual-activation of the phosphate anion afforded the product **3a**.

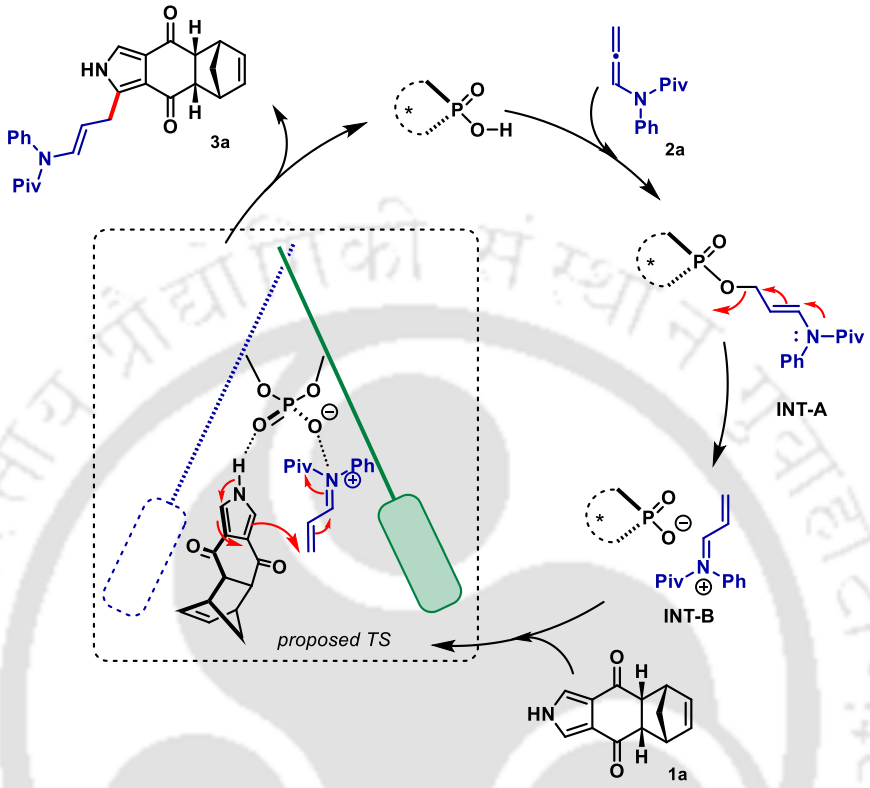

Scheme 18: Proposed catalytic cycle.

5.6. Conclusion:

In summary, we have developed the first catalytic enantioselective construction of centrally prochiral 3,4-fused pyrroles through desymmetrizing F-C reaction with allenamides using chiral phosphoric acid catalysis. A series of polycyclic 2-substituted, 3,4-fused pyrroles were obtained in high yields and with good to high enantioselectivities. The control experiment suggested that the servocontrol governed by desymmetrization only. Also, an ion-pair transition state proposed for the desymmetrization reaction.

5.7. Experimental Section:

5.7.1. General Information:

All dry solvents were dried using activated 4Å molecular sieves and stored under argon. For thin layer chromatography (TLC), silica gel plates with fluorescence indicator 254 nm were used and compounds were visualized by irradiation with UV light and/or iodine and/or Phosphomolybdic acid stain. Celite® 512 medium was used for filtrations. Column

chromatography was performed using 100-200 mesh silica gel. Hexane, ethyl acetate, acetone and dichloromethane for column chromatography were acquired from commercial sources and were used without purification. NMR spectra were acquired on a Bruker 400 MHz, 500 MHz and 600 MHz spectrometer. Chemical shifts (δ) are reported in ppm relative to residual solvent signals (Chloroform-d, 7.26 ppm for ^{1}H NMR and 77.23 ppm for ^{13}C NMR respectively. ^{13}C spectra were acquired on a broad band decoupled mode. For ^{1}H-NMR, data are reported as follows: chemical shift, multiplicity (s = singlet, d = doublet, dd = double doublet, ddd = doublet of doublet of doublets, t = triplet, q = quartet, dt = doublet of triplets, m = multiplet), coupling constants (Hz) and integration. Using ESI positive mode HRMS spectra was recorded. Enantiomeric excesses were determined by HPLC analysis performed on Chiral Columns using a Daicel Chiralpak IA, AD-H and Phenomenex Lux C4 Column.

5.7.2. General Procedure for synthesis of prochiral pyrrole:

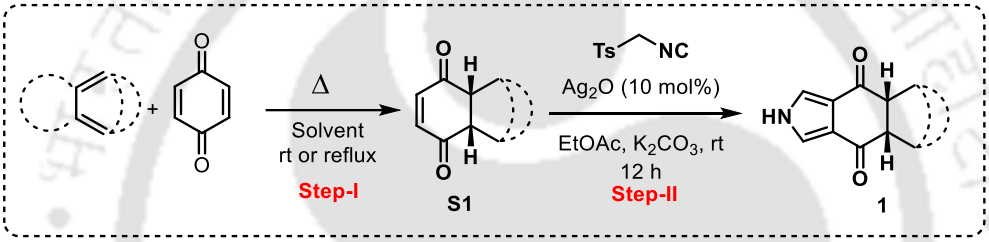

Step-I: In an oven dried 50ml round-bottom flask p-benzoquinone was taken and purged with argon atmosphere. Then solvent was added. After that, desired Diene was added at rt. The mixture was stirred at rt or refluxed to get the desired meso-derivative in good yield (**S1**).

Step-II: Under argon atmosphere, an oven-dried 100ml round bottom flask, equipped with a magnetic stir bar was charged with Ag_2O (0.6 mmol, 10 mol%), K_2CO_3 (18 mmol, 3 equiv.) and **S1** (6 mmol, 1equiv.). Then, 50 ml EtOAc was added. After stirring for 15 min, TosMIC (6.6 mmol, 1.1 equiv.) was added in one portion. The solvents were evaporated and purified by column chromatography (pet ether : EtOAc = 50:50) to give products. The product again, purified by recrystallization in hot DCM, to give **1a – 1j** in good to excellent yield.

5.7.3. General Procedure for synthesis of allenamide:

The derivatives of ynone were synthesized following reported literature procedure.[23g]

5.7.4. General Procedure for synthesis of various catalyst:

All the catalysts were synthesized according to the reported literature procedure.[23g]

5.7.5. General Procedure for the Synthesis of chiral triarylmethane derivatives:

Under argon atmosphere, an oven-dried screw cap vial equipped with a magnetic stir bar was charged with **1**(0.1 mmol, 1 equiv.), **VI** catalyst (0.005 mmol, 5 mol%), and 5Å MS (100 mg). Then, 0.5ml *o*-xylene was added in the mixture and cooled to 0 °C. After 15min, allenamide **2** (0.12mmol, 1.2 equiv.) was added to the mixture and stirred at the same temperature. After 8h, allenamide **2** (0.08 mmol, 0.8 equiv.) added to the mixture and stirred for another 4h. Then, the crude mixture was loaded in column chromatography (petroleum ether : EtOAc = 50:50) to afford **3**.

5.8. Characterization data of the products:

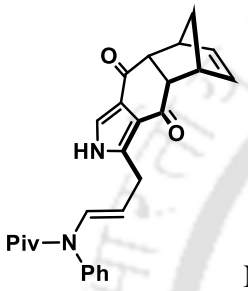

N-((E)-3-(4,9-dioxo-4,4a,5,8,8a,9-hexahydro-2H-5,8-methanobenzo[f]isoindol-1-yl)prop-1-en-1-yl)-N-phenylpivalamide (3a): yellow solid, 29.5 mg, 69% yield, 92% ee; R_f = 0.5 (petroleum ether : ethyl acetate = 50:50)

^{1}H NMR (500 MHz, Chloroform-d) δ 9.67 (s, 1H), 7.55 (d, J = 14.4 Hz, 1H), 7.44 - 7.38 (m, 3H), 7.18 - 7.16 (m, 3H), 5.99 – 5.96 (m, 1H), 5.95 – 5.91 (m, 1H), 4.42 - 4.37 (m, 1H), 3.73 (dd, J = 16.4, 7.4 Hz, 1H), 3.66 (dd, J = 16.3, 7.5 Hz, 1H), 3.54 (s, 1H), 3.51 (s, 1H), 3.24 - 3.19 (m, 2H), 1.49 (d, J = 8.5 Hz, 1H), 1.43 (d, J = 8.9 Hz, 1H), 1.05 (s, 9H). **^{13}C NMR** (126 MHz, Chloroform-d) δ 195.96, 195.81, 177.25, 139.89, 136.76, 135.30, 135.27, 134.88, 130.50, 129.66, 129.06, 125.32, 119.17, 118.77, 109.79, 52.25, 51.96, 49.60, 49.16, 49.10, 41.52, 29.48, 27.48.**HRMS (ESI$^+$) *m/z*:** $[M+H]^+$ calculated for $C_{27}H_{28}N_2O_3$: 429.5395, found: 429.5390; **HPLC:** The enantiomeric excess was determined using Phenomenex Lux C4 column (*n*-Hexane/ *i*-PrOH=80:20, flow rate=1.0 mL/min, λ= 254 nm, τ_{minor} = 17.7 min, τ_{major} = 22.3 min).

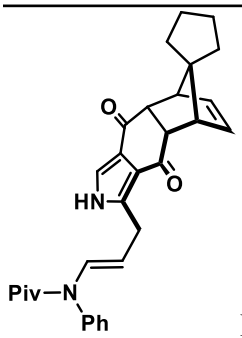

N-((E)-3-(4',9'-dioxo-4',4a',5',8',8a',9'-hexahydro-2'H-spiro[cyclopentane-1,10'-[5,8]methanobenzo[f]isoindol]-1'-yl)prop-1-en-1-yl)-N-phenylpivalamide (3b): Pale yellow solid, 34.7 mg, 72% yield, 86% ee; R_f = 0.5 (petroleum ether : ethyl acetate = 50:50)

^{1}H NMR (400 MHz, Chloroform-d) δ 9.82 (s, 1H), 7.54 (d, J = 14.3 Hz, 1H), 7.46 – 7.36 (m, 3H), 7.19 - 7.15 (m, 3H), 5.97 (dd, J = 5.9, 3.0 Hz, 1H), 5.92 (dd, J = 5.9, 3.0 Hz, 1H), 4.43 - 4.36 (m, 1H), 3.78 – 3.60 (m, 2H), 3.33 - 3.26 (m, 2H), 3.12 (s, 1H), 3.08 (s, 1H), 1.63 - 1.56 (m, 2H), 1.52 - 1.44 (m, 6H), 1.04 (s, 9H). **^{13}C NMR** (101 MHz, Chloroform-d) δ 196.37, 196.30, 177.28, 139.85, 136.60, 136.12, 136.04, 134.78, 130.49, 129.64, 129.05, 125.59, 119.49, 118.68, 109.99, 69.19, 56.72, 56.67, 52.36, 52.06, 41.49, 32.20, 31.79, 31.76, 29.48, 27.48, 26.09, 25.60. **HRMS (ESI$^+$) *m/z*:** $[M+H]^+$ calculated for $C_{31}H_{34}N_2O_3$: 483.6315, found: 483.6321; **HPLC:** The enantiomeric excess was determined using Phenomenex Lux C4 column (*n*-Hexane/ *i*-PrOH=80:20, flow rate=1.0 mL/min, λ= 254 nm, τ_{minor} = 21.5 min, τ_{major} = 25.9 min).

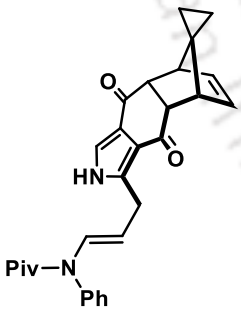

N-((E)-3-(4',9'-dioxo-4',4a',5',8',8a',9'-hexahydro-2'H-spiro[cyclopropane-1,10'-[5,8]methanobenzo[f]isoindol]-1'-yl)prop-1-en-1-yl)-N-phenylpivalamide (3c): yellow solid, 33.2 mg, 73% yield, 97% ee; R_f = 0.5 (petroleum ether : ethyl acetate = 50:50)

^{1}H NMR (400 MHz, Chloroform-d) δ 9.53 (s, 1H), 7.47 (d, J = 14.3 Hz, 1H), 7.40 – 7.36 (m, 1H), 7.36 – 7.30 (m, 2H), 7.16 – 7.10 (m, 3H), 6.02 (dd, J = 5.4, 2.4 Hz, 1H), 5.98 (dd, J = 5.4, 2.3 Hz, 1H), 4.33 (dt, J = 14.5, 7.4 Hz, 1H), 3.73 – 3.56 (m, 2H), 3.37 – 3.27 (m, 2H), 2.84 (s, 1H), 2.81 (s, 1H), 0.98 (s, 9H), 0.54 – 0.48 (m, 2H), 0.46 – 0.38 (m, 2H). **^{13}C NMR**

(101 MHz, Chloroform-d) δ 195.86, 195.63, 139.87, 136.73, 135.42, 135.35, 135.08, 130.47, 129.67, 129.07, 125.52, 119.37, 118.82, 109.83, 54.08, 53.99, 53.15, 52.83, 45.21, 41.52, 29.91, 29.48, 8.24, 7.34. **HRMS (ESI$^+$) *m/z*:** $[M+H]^+$ calculated for $C_{29}H_{30}N2O_3$: 455.5775, found: 483.6315; **HPLC:** The enantiomeric excess was determined using Phenomenex Lux C4 column (*n*-Hexane/ *i*-PrOH=80:20, flow rate=1.0 mL/min, λ= 254 nm, τ_{minor} = 27.1 min, τ_{major} = 40.1 min).

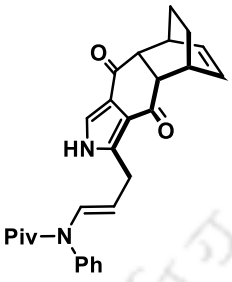

N-((E)-3-(4,9-dioxo-4,4a,5,8,8a,9-hexahydro-2H-5,8-ethanobenzo[f]isoindol-1-yl)prop-1-en-1-yl)-N-phenylpivalamide (3d): yellow solid, 33.6 mg, 76% yield, 84% ee; R_f = 0.5 (petroleum ether : ethyl acetate = 50:50)

^{1}H NMR (500 MHz, Chloroform-d) δ 10.00 (s, 1H), 7.56 (d, J = 14.3 Hz, 1H), 7.43 - 7.37 (m, 3H), 7.19 -7.17 (m, 3H), 6.15 - 6.08 (m, 2H), 4.43 - 4.38 (m, 1H), 3.76 - 3.65 (m, 2H), 3.29 (s, 1H), 3.25 (s, 1H), 2.96 - 2.91 (m, 2H), 1.69 (d, J = 7.9 Hz, 2H), 1.33 (d, J = 8.6 Hz, 2H), 1.04 (s, 9H). **^{13}C NMR** (126 MHz, Chloroform-d) δ 195.97, 177.22, 139.80, 136.86, 134.64, 133.71, 133.61, 130.49, 129.63, 129.05, 124.49, 118.93, 118.55, 110.01, 52.89, 52.60, 41.48, 35.85, 35.76, 29.48, 27.56, 25.37. **HRMS (ESI$^+$) *m/z*:** $[M+H]^+$ calculated for $C_{28}H_{30}N_2O_3$: 443.5665, found: 443.5671; **HPLC:** The enantiomeric excess was determined using Phenomenex Lux C4 column (*n*-Hexane/ *i*-PrOH=80:20, flow rate=1.0 mL/min, λ= 254 nm, τ_{minor} = 17.7 min, τ_{major} = 24.7 min).

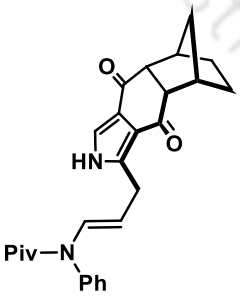

N-((E)-3-((4aS,5R,8R)-4,9-dioxo-4,4a,5,6,7,8,8a,9-octahydro-2H-5,8-methanobenzo[f]isoindol-1-yl)prop-1-en-1-yl)-N-phenylpivalamide (3e): yellow solid, 26.2 mg, 61% yield, 92% ee; R_f = 0.5 (petroleum ether : ethyl acetate = 50:50).

^{1}H NMR (400 MHz, Chloroform-d) δ 10.08 (s, 1H), 7.52 (d, J = 14.2 Hz, 1H), 7.39 – 7.30 (m, 3H), 7.19 (d, J = 2.8 Hz, 1H), 7.15 – 7.10 (m, 2H), 4.38 (dt, J = 14.5, 7.4 Hz, 1H), 3.77 –

3.62 (m, 2H), 2.93 - 2.85 (m, 2H), 2.83 (s, 1H), 2.80 (s, 1H), 1.46 – 1.34 (m, 2H), 1.34 – 1.25 (m, 2H), 1.16 - 1.09 (m, 2H), 0.98 (s, 9H). **^{13}C NMR** (101 MHz, Chloroform-d) δ 196.97, 196.91, 177.13, 139.59, 136.48, 134.51, 130.29, 129.46, 128.88, 125.17, 119.10, 118.53, 109.92, 52.92, 52.61, 43.01, 42.95, 41.31, 39.50, 29.30, 27.39, 24.67, 24.64. **HRMS (ESI$^+$) *m/z*:** $[M+H]^+$ calculated for $C_{27}H_{30}N_2O_3$: 431.5555, found: 231.5538; **HPLC:** The enantiomeric excess was determined using Chiralapk IE column (*n*-Hexane/ *i*-PrOH=85:15, flow rate=1.0 mL/min, λ= 254 nm, τ_{minor} = 38.6 min, τ_{major} = 48.5 min).

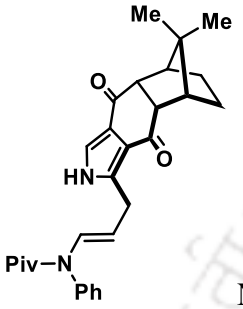

N-((E)-3-(10,10-dimethyl-4,9-dioxo-4,4a,5,6,7,8,8a,9-octahydro-2H-5,8-methanobenzo[f]isoindol-1-yl)prop-1-en-1-yl)-N-phenylpivalamide (3f): Pale yellow solid, 34.4 mg, 75% yield, 88% ee; R_f = 0.5 (petroleum ether : ethyl acetate = 50:50)

^{1}H NMR (500 MHz, Chloroform-d) δ 9.67 (s, 1H), 7.55 (d, J = 14.4 Hz, 1H), 7.44 - 7.38 (m, 3H), 7.18 - 7.16 (m, 3H), 4.42 - 4.37 (m, 1H), 3.73 (dd, J = 16.4, 7.4 Hz, 1H), 3.66 (dd, J = 16.3, 7.5 Hz, 1H), 3.54 (s, 1H), 3.51 (s, 1H), 3.24 - 3.19 (m, 2H), 1.34 – 1.25 (m, 2H), 1.16 - 1.09 (m, 2H), 1.05 (s, 9H), 0.93 (s, 3H), 0.91 (s, 3H). **^{13}C NMR** (126 MHz, Chloroform-d) δ 195.96, 195.81, 177.25, 139.89, 136.76, 135.30, 135.27, 134.88, 130.50, 129.66, 129.06, 125.32, 119.17, 52.25, 51.96, 49.60, 49.16, 49.10, 41.52, 29.48, 27.48, 26.38, 26.32, 24.67, 24.64. **HRMS (ESI$^+$) *m/z*:** $[M+H]^+$ calculated for $C_{29}H_{34}N2O_3$: 459.6059, found: 459.6036; **HPLC:** The enantiomeric excess was determined using Phenomenex Lux C4 column (*n*-Hexane/ *i*-PrOH=80:20, flow rate=1.0 mL/min, λ= 254 nm, τ_{minor} = 17.7 min, τ_{major} = 22.3 min).

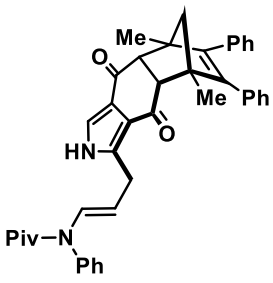

N-((E)-3-(5,8-dimethyl-4,9-dioxo-6,7-diphenyl-4,4a,5,8,8a,9-hexahydro-2H-5,8-methanobenzo[f]isoindol-1-yl)prop-1-en-1-yl)-N-phenylpivalamide (3g): Pale yellow solid, 34.1 mg, 56% yield, 96% ee; R_f = 0.5 (petroleum ether : ethyl acetate = 50:50)

^{1}H NMR (500 MHz, Chloroform-d) δ 9.58 (s, 1H), 7.48 (d, J = 14.3 Hz, 1H), 7.45 – 7.36 (m, 3H), 7.16 (d, J = 7.3 Hz, 2H), 7.12 (d, J = 2.8 Hz, 1H), 7.03 – 6.95 (m, 3H), 6.89 (t, J = 7.4 Hz, 1H), 6.79 (t, J = 7.7 Hz, 2H), 6.71 – 6.64 (m, 2H), 6.48 (d, J = 7.6 Hz, 2H), 4.34 - 4.29 (m, 1H), 3.58 (dd, J = 16.5, 7.4 Hz, 1H), 3.39 (dd, J = 16.6, 7.5 Hz, 1H), 3.26 (d, J = 8.3 Hz, 1H), 3.21 (d, J = 8.3 Hz, 1H), 1.77 (d, J = 8.3 Hz, 1H), 1.64 (d, J = 8.3 Hz, 1H), 1.61 (s, 3H), 1.56 (s, 3H), 1.03 (s, 9H). **^{13}C NMR** (151 MHz, Chloroform-d) δ 195.81, 195.23, 177.34, 146.66, 145.36, 139.95, 136.34, 135.85, 135.80, 135.14, 130.44, 129.80, 129.69, 129.60, 129.02, 127.66, 127.46, 126.52, 126.37, 125.72, 119.93, 118.72, 109.64, 65.72, 60.69, 60.45, 59.19, 58.89, 41.52, 29.49, 27.24, 19.16, 18.70. **HRMS (ESI$^+$) *m/z*:** $[M+H]^+$ calculated for $C_{41}H_{40}N2O_3$: 609.3112, found: 609.3101; **HPLC:** The enantiomeric excess was determined using Phenomenex Lux C4 column (*n*-Hexane/ *i*-PrOH=80:20, flow rate=1.0 mL/min, λ= 254 nm, τ_{minor} = 15.8 min, τ_{major} = 35 min).

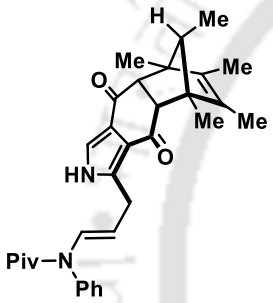

N-((E)-3-(5,6,7,8,10-pentamethyl-4,9-dioxo-4,4a,5,8,8a,9-hexahydro-2H-5,8-methanobenzo[f]isoindol-1-yl)prop-1-en-1-yl)-N-phenylpivalamide (3h): Pale yellow solid, 25.4 mg, 51% yield, 92% ee; R_f = 0.5 (petroleum ether : ethyl acetate = 50:50)

^{1}H NMR (400 MHz, Chloroform-d) δ 9.59 (s, 1H), 7.55 (d, J = 14.2 Hz, 1H), 7.41 (q, J = 7.5, 7.1 Hz, 3H), 7.16 (d, J = 6.4 Hz, 2H), 7.09 (d, J = 2.8 Hz, 1H), 4.38 (dt, J = 14.3, 7.3 Hz, 1H), 3.64 (dd, J = 7.5, 2.8 Hz, 2H), 2.85 (p, J = 7.0, 6.1 Hz, 2H), 1.40 (q, J = 6.4 Hz, 1H), 1.31 (s, 3H), 1.27 (s, 3H), 1.22 (s, 3H), 1.10 (s, 3H), 1.04 (s, 9H), 0.56 (d, J = 6.4 Hz, 3H).**^{13}C NMR** (101 MHz, Chloroform-d) δ 195.97, 177.22, 139.80, 136.86, 134.64, 133.71, 133.61, 130.49, 129.63, 129.05, 124.49, 118.93, 118.55, 110.01, 52.89, 52.60, 41.48, 35.85, 35.76, 29.48, 27.56, 25.37, 24.93, 14.72, 11.25,. **HRMS (ESI$^+$) *m/z*:** $[M+H]^+$ calculated for $C_{32}H_{39}N2O_3$: 499.6745, found: 499.6745; **HPLC:** The enantiomeric excess was determined using Phenomenex Lux C4 column (*n*-Hexane/ *i*-PrOH=80:20, flow rate=1.0 mL/min, λ= 254 nm, τ_{minor} = 17.7 min, τ_{major} = 22.3 min).

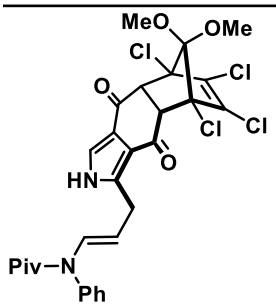

N-phenyl-N-((E)-3-(5,6,7,8-tetrachloro-10,10-dimethoxy-4,9-dioxo-4,4a,5,8,8a,9-hexahydro-2H-5,8-methanobenzo[f]isoindol-1-yl)prop-1-en-1-yl)pivalamide (3i): Pale yellow solid, 33.2 mg, 53% yield, 94% ee; R_f = 0.5 (petroleum ether : ethyl acetate = 50:50)

^{1}H NMR (600 MHz, Chloroform-d) δ 9.99 (s, 1H), 7.57 (d, J = 14.2 Hz, 1H), 7.44 - (m, 3H), 7.24 (d, J = 2.8 Hz, 1H), 7.18 (d, J = 7.5 Hz, 2H), 4.42 - 4.37 (m, 1H), 3.75 - 3.71 (m, 1H), 3.65 (s, 3H), 3.64 - 3.59 (m, 3H), 3.58 (s, 3H), 1.04 (s, 9H). **^{13}C NMR** (151 MHz, Chloroform-d) δ 188.01, 187.84, 177.33, 139.72, 138.01, 134.57, 130.50, 129.70, 129.29, 129.27, 129.16, 124.24, 119.74, 118.48, 111.28, 109.88, 78.23, 78.15, 57.48, 57.34, 53.29, 52.27, 41.55, 29.51, 27.59. **HRMS (ESI$^+$) *m/z*:** $[M+H]^+$ calculated for $C_{29}H_{28}Cl_4N_2O_5$: 627.0796, found: 627.0799; **HPLC:** The enantiomeric excess was determined using Phenomenex Lux C4 column (*n*-Hexane/ *i*-PrOH=80:20, flow rate=1.0 mL/min, λ= 254 nm, τ_{minor} = 32.3 min, τ_{major} = 49.7 min).

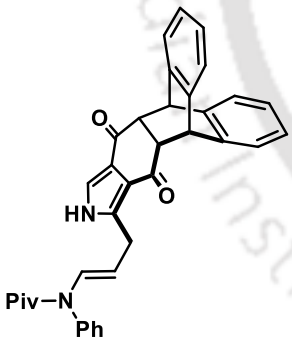

N-((E)-3-(4,11-dioxo-4,4a,5,10,10a,11-hexahydro-2H-5,10-[1,2]benzenonaphtho[2,3-f]isoindol-1-yl)prop-1-en-1-yl)-N-phenylpivalamide (3j): Pale yellow solid, 22.7 mg, 42% yield, 0% ee; R_f = 0.5 (petroleum ether : ethyl acetate = 50:50)

^{1}H NMR (600 MHz, Chloroform-d) δ 9.39 (s, 1H), 7.47 – 7.40 (m, 4H), 7.40 – 7.37 (m, 2H), 7.19 – 7.16 (m, 2H), 7.15 - 7.13 (m, 3H), 7.06 (d, J = 7.3 Hz, 1H), 7.03 (d, J = 2.8 Hz, 1H), 6.90 (t, J = 7.4 Hz, 1H), 6.85 (t, J = 7.4 Hz, 1H), 4.98 (d, J = 2.6 Hz, 1H), 4.94 (d, J = 2.6 Hz, 1H), 4.33 - 4.28 (m, 1H), 3.64 (dd, J = 16.4, 7.4 Hz, 1H), 3.57 (dd, J = 16.3, 7.5 Hz, 1H), 3.15 (dd, J = 9.4, 2.5 Hz, 1H), 3.12 (dd, J = 9.4, 2.6 Hz, 1H), 1.04 (s, 9H). **^{13}C NMR** (151 MHz, Chloroform-d) δ 194.06, 193.87, 177.43, 142.97, 142.93, 140.75, 140.73, 139.93, 136.69,

135.06, 130.46, 129.67, 129.07, 126.39, 126.23, 126.17, 124.78, 124.62, 124.21, 123.94, 118.77, 118.27, 109.74, 52.48, 52.22, 49.07, 49.05, 41.54, 29.49, 27.33. **HRMS (ESI$^+$) *m/z*:** $[M+H]^+$ calculated for $C_{36}H_{32}N_2O_3$: 541.2486, found: 541.2482; **HPLC:** The enantiomeric excess was determined using Phenomenex Lux C4 column (*n*-Hexane/ *i*-PrOH=80:20, flow rate=1.0 mL/min, λ= 254 nm, τ_{minor} = 17.9 min, τ_{major} = 37.8 min).

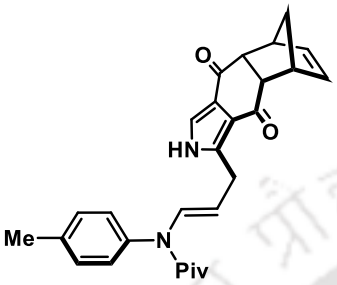

N-((E)-3-(4,9-dioxo-4,4a,5,8,8a,9-hexahydro-2H-5,8-methanobenzo[f]isoindol-1-yl)prop-1-en-1-yl)-N-(p-tolyl)pivalamide (3k): Pale yellow solid, 23.4 mg, 53% yield, 91% ee; R_f = 0.5 (petroleum ether : ethyl acetate = 50:50)

^{1}H NMR (600 MHz, Chloroform-d) δ 9.76 (s, 1H), 7.54 (d, J = 14.2 Hz, 1H), 7.21 (d, J = 8.2 Hz, 2H), 7.16 (d, J = 2.8 Hz, 1H), 7.05 (d, J = 8.3 Hz, 2H), 5.98 (dd, J = 5.7, 3.0 Hz, 1H), 5.93 (dd, J = 5.7, 2.8 Hz, 1H), 4.43 - 4.38 (m, 1H), 3.73 (dd, J = 16.6, 7.8 Hz, 1H), 3.66 (dd, J = 16.6, 7.2 Hz, 1H), 3.54 (s, 1H), 3.51 (s, 1H), 3.21 (qd, J = 8.3, 3.8 Hz, 2H), 2.38 (s, 3H), 1.49 (d, J = 8.4 Hz, 1H), 1.43 (d, J = 8.4 Hz, 1H), 1.04 (s, 9H). **^{13}C NMR** (151 MHz, Chloroform-d) δ 195.98, 195.81, 177.39, 139.10, 137.13, 136.88, 135.29, 135.27, 134.96, 130.25, 130.22, 125.27, 119.12, 118.80, 109.68, 52.25, 51.95, 49.59, 49.15, 49.08, 41.48, 29.51, 27.43, 21.38. **HRMS (ESI$^+$) *m/z*:** $[M+H]^+$ calculated for $C_{28}H_{30}N2O_3$: 443.2330, found: 443.2331; **HPLC:** The enantiomeric excess was determined using Phenomenex Lux C4 column (*n*-Hexane/ *i*-PrOH=80:20, flow rate=1.0 mL/min, λ= 254 nm, τ_{minor} = 21 min, τ_{major} = 25.2 min).

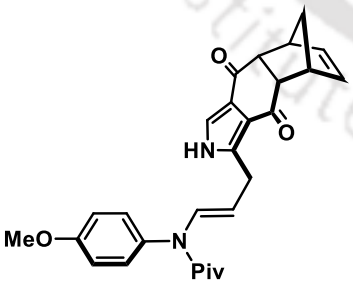

N-((E)-3-(4,9-dioxo-4,4a,5,8,8a,9-hexahydro-2H-5,8-methanobenzo[f]isoindol-1-yl)prop-1-en-1-yl)-N-(4-methoxyphenyl)pivalamide (3l): Product were prepared following '*Method A*, Pale yellow solid, 19.2 mg, 42% yield, 89% ee; R_f = 0.5 (petroleum ether : ethyl acetate = 50:50)

^{1}H NMR (400 MHz, Chloroform-d) δ 9.72 (s, 1H), 7.54 (d, J = 14.3 Hz, 1H), 7.17 (d, J = 2.8 Hz, 1H), 7.08 (d, J = 8.9 Hz, 2H), 6.92 (d, J = 8.9 Hz, 2H), 5.99 (dd, J = 5.7, 2.8 Hz, 1H), 5.95 (dd, J = 5.7, 2.7 Hz, 1H), 4.41 (dt, J = 14.4, 7.4 Hz, 1H), 3.83 (s, 3H), 3.78 – 3.62 (m, 2H), 3.54 (s, 1H), 3.51 (s, 1H), 3.26 - 3.18 (m, 2H), 1.50 (d, J = 8.5 Hz, 1H), 1.43 (d, J = 8.6 Hz, 1H), 1.05 (s, 9H). **^{13}C NMR** (101 MHz, Chloroform-d) δ 195.86, 195.65, 177.36, 159.57, 136.66, 135.11, 135.08, 134.94, 132.05, 131.32, 125.04, 118.90, 118.63, 114.53, 109.37, 55.51, 52.05, 51.73, 49.40, 48.95, 48.89, 41.21, 29.30, 27.17. **HRMS (ESI$^+$) *m/z*:** $[M+H]^+$ calculated for $C_{28}H_{30}N2O_4$: 459.2279, found: 459.2288; **HPLC:** The enantiomeric excess was determined using Phenomenex Lux C4 column (*n*-Hexane/ *i*-PrOH=80:20, flow rate=1.0 mL/min, λ= 254 nm, τ_{minor} = 22.5 min, τ_{major} = 27.9 min).

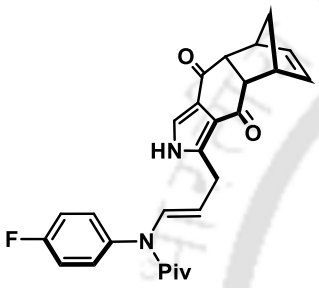

N-((E)-3-(4,9-dioxo-4,4a,5,8,8a,9-hexahydro-2H-5,8-methanobenzo[f]isoindol-1-yl)prop-1-en-1-yl)-N-(4-fluorophenyl)pivalamide (3m): Pale yellow solid, 33.5 mg, 75% yield, 91% ee; R_f = 0.5 (petroleum ether : ethyl acetate = 50:50).

^{1}H NMR (600 MHz, Chloroform-d) δ 9.66 (s, 1H), 7.53 (d, J = 14.1 Hz, 1H), 7.21 – 7.14 (m, 3H), 7.13 - 7.11 (m, 2H), 5.98 (dd, J = 5.7, 2.9 Hz, 1H), 5.94 (dd, J = 5.8, 2.9 Hz, 1H), 4.42 - 4.38 (m, 1H), 3.73 (dd, J = 16.3, 7.3 Hz, 1H), 3.66 (dd, J = 16.2, 7.5 Hz, 1H), 3.54 (s, 1H), 3.51 (s, 1H), 3.24 - 3.20 (m, 2H), 1.50 (d, J = 8.4 Hz, 1H), 1.44 (d, J = 8.5 Hz, 1H), 1.06 (s, 9H). **^{13}C NMR** (151 MHz, Chloroform-d) δ 195.96, 195.80, 177.13, 163.38, 161.73, 136.56, 135.81, 135.78, 135.29, 135.28, 134.68, 132.23, 132.17, 125.36, 119.26, 118.75, 116.82, 116.67, 109.79, 52.26, 51.97, 49.61, 49.17, 49.11, 41.44, 29.47, 27.46. **HRMS (ESI$^+$) *m/z*:** $[M+H]^+$ calculated for $C_{27}H_{27}FN_2O_3$: 447.2079, found: 447.2087; **HPLC:** The enantiomeric excess was determined using Chiralpak IA column (*n*-Hexane/ *i*-PrOH=95:5, flow rate=1.0 mL/min, λ= 254 nm, τ_{major} = 40.5 min, τ_{minor} = 47.7 min).

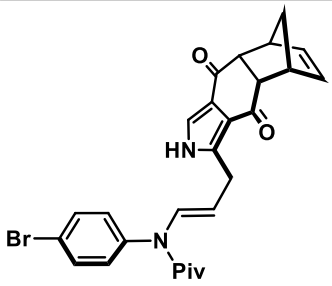

N-(4-bromophenyl)-N-((E)-3-(4,9-dioxo-4,4a,5,8,8a,9-hexahydro-2H-5,8-methanobenzo[f]isoindol-1-yl)prop-1-en-1-yl)pivalamide (3n): Pale yellow solid, 35.9 mg, 72% yield, 82% ee; R_f = 0.5 (petroleum ether : ethyl acetate = 50:50)

^{1}H NMR (400 MHz, Chloroform-d) δ 9.96 (s, 1H), 7.55 (d, J = 8.6 Hz, 2H), 7.49 (d, J = 14.3 Hz, 1H), 7.16 (d, J = 2.8 Hz, 1H), 7.06 (d, J = 8.5 Hz, 2H), 5.97 (dd, J = 5.7, 2.8 Hz, 1H), 5.93 (dd, J = 5.6, 2.8 Hz, 1H), 4.41 (dt, J = 14.4, 7.3 Hz, 1H), 3.76 - 3.62 (m, 2H), 3.53 - 3.51(m, 2H), 3.26 – 3.18 (m, 2H), 1.50 (d, J = 8.5 Hz, 1H), 1.44 (d, J = 8.7 Hz, 1H), 1.06 (s, 9H). **^{13}C NMR** (101 MHz, Chloroform-d) δ 195.80, 195.74, 176.81, 138.72, 136.36, 135.09, 135.06, 134.09, 132.82, 131.93, 125.05, 122.80, 119.07, 118.72, 109.99, 52.05, 51.77, 49.42, 48.96, 48.90, 41.28, 29.27, 27.27. **HRMS (ESI$^+$) *m/z*:** $[M+H]^+$ calculated for $C_{27}H_{27}BrN_2O_3$: 507.1278, found: 507.1277; **HPLC:** The enantiomeric excess was determined using Phenomenex Lux C4 column (*n*-Hexane/ *i*-PrOH=80:20, flow rate=1.0 mL/min, λ= 254 nm, τ_{minor} = 15.8 min, τ_{major} = 20.3 min).

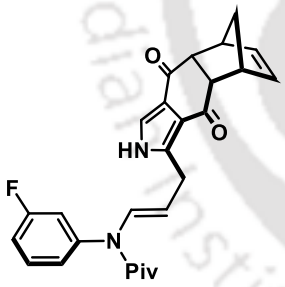

N-((E)-3-(4,9-dioxo-4,4a,5,8,8a,9-hexahydro-2H-5,8-methanobenzo[f]isoindol-1-yl)prop-1-en-1-yl)-N-(3-fluorophenyl)pivalamide (3o): Product were prepared following '*Method A*, Pale yellow solid, 26.3 mg, 59% yield, 80% ee; R_f = 0.5 (petroleum ether : ethyl acetate = 50:50).

^{1}H NMR (600 MHz, Chloroform-d) δ 9.47 (s, 1H), 7.54 (d, J = 14.2 Hz, 1H), 7.45 (d, J = 7.5 Hz, 1H), 7.31 – 7.26 (m, 2H), 7.25 – 7.18 (m, 2H), 6.02 (dd, J = 5.6, 2.9 Hz, 1H), 5.98 (dd, J = 5.9, 2.8 Hz, 1H), 4.49 - 4.44 (m, 1H), 3.79 - 3.70 (m, 2H), 3.58 (s, 1H), 3.55 (s, 1H), 3.28 - 3.23 (m, 2H), 1.53 (d, J = 8.5 Hz, 1H), 1.47 (d, J = 8.5 Hz, 1H), 1.12 (s, 9H). **^{13}C NMR** (151 MHz, Chloroform-d) δ 195.97, 195.74, 177.11, 159.57, 157.91, 136.58, 135.30, 133.67, 132.31, 131.29, 131.24, 127.86, 127.78, 125.40, 125.15, 125.13, 119.19, 118.71, 117.30, 117.17, 108.36, 52.26, 51.95, 49.60, 49.16, 49.10, 41.32, 28.77, 27.30. **HRMS (ESI$^+$) *m/z*:**

$[M+H]^+$ calculated for $C_{27}H_{27}FN_2O_3$: 447.2079, found: 447.2091; **HPLC:** The enantiomeric excess was determined using Chiralapk IA column (*n*-Hexane/ *i*-PrOH=95:5, flow rate=1.0 mL/min, λ= 254 nm, τ_{major} = 41.3min, τ_{minor} = 49.2 min).

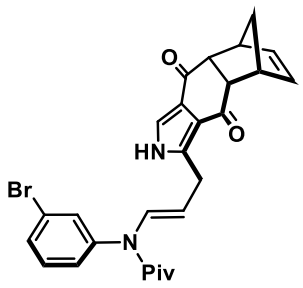

N-(3-bromophenyl)-N-((E)-3-(4,9-dioxo-4,4a,5,8,8a,9-hexahydro-2H-5,8-methanobenzo[f]isoindol-1-yl)prop-1-en-1-yl)pivalamide (3p): yellow solid, 31.4 mg, 62% yield, 81% ee; R_f = 0.5 (petroleum ether : ethyl acetate = 50:50)

^{1}H NMR (600 MHz, Chloroform-d) δ 9.85 (s, 1H), 7.54 (d, J = 8.2 Hz, 1H), 7.46 (d, J = 14.2 Hz, 1H), 7.35 (s, 1H), 7.31 (t, J = 8.0 Hz, 1H), 7.17 (d, J = 2.7 Hz, 1H), 7.14 (d, J = 7.9 Hz, 1H), 5.99 (dd, J = 5.7, 2.8 Hz, 1H), 5.95 (dd, J = 5.8, 2.8 Hz, 1H), 4.45 (dt, J = 14.5, 7.3 Hz, 1H), 3.70 (qd, J = 16.2, 7.3 Hz, 2H), 3.53 (d, J = 13.5 Hz, 2H), 3.22 (qd, J = 8.4, 3.5 Hz, 2H), 1.50 (d, J = 8.5 Hz, 1H), 1.44 (d, J = 8.5 Hz, 1H), 1.07 (s, 9H). **^{13}C NMR** (151 MHz, Chloroform-d) δ 196.01, 195.87, 177.07, 141.29, 136.45, 135.30, 135.29, 134.38, 133.48, 132.20, 130.90, 130.48, 129.17, 125.30, 122.82, 119.30, 118.92, 110.40, 52.26, 51.97, 49.61, 49.16, 49.10, 41.51, 29.45, 27.43. **HRMS (ESI$^+$) *m/z*:** $[M+H]^+$ calculated for $C_{27}H_{27}BrN_2O_3$: 507.1278, found: 507.1283; **HPLC:** The enantiomeric excess was determined using Phenomenex Lux C4 column (*n*-Hexane/ *i*-PrOH=80:20, flow rate=1.0 mL/min, λ= 254 nm, τ_{minor} = 15.9 min, τ_{major} = 20.3 min).

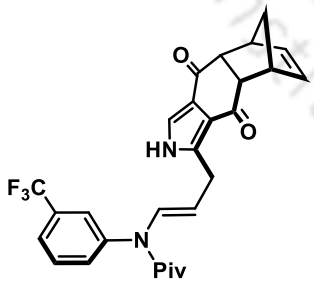

N-((E)-3-(4,9-dioxo-4,4a,5,8,8a,9-hexahydro-2H-5,8-methanobenzo[f]isoindol-1-yl)prop-1-en-1-yl)-N-(3-(trifluoromethyl)phenyl)pivalamide (3q): Pale yellow solid, 33.2 mg, 67% yield, 82% ee; R_f = 0.5 (petroleum ether : ethyl acetate = 50:50)

^{1}H NMR (600 MHz, Chloroform-d) δ 10.04 (s, 1H), 7.67 (d, J = 8.2 Hz, 1H), 7.58 (t, J = 7.9 Hz, 1H), 7.47 (d, J = 14.2 Hz, 1H), 7.45 (s, 1H), 7.39 (d, J = 8.0 Hz, 1H), 7.16 (d, J = 2.9 Hz,

1H), 5.97 (dd, J = 5.8, 2.9 Hz, 1H), 5.91 (dd, J = 5.8, 2.9 Hz, 1H), 4.43 - 4.38 (m, 1H), 3.72 (dd, J = 16.1, 7.3 Hz, 1H), 3.66 (dd, J = 16.2, 7.3 Hz, 1H), 3.53 (s, 1H), 3.50 (s, 1H), 3.23 (dd, J = 8.3, 3.9 Hz, 1H), 3.20 (dd, J = 8.3, 3.8 Hz, 1H), 1.49 (d, J = 8.5 Hz, 1H), 1.43 (d, J = 8.5 Hz, 1H), 1.05 (s, 9H). **^{13}C NMR** (151 MHz, Chloroform-d) δ 196.00, 195.95, 177.10, 140.68, 136.36, 135.25, 134.27, 133.88, 132.50, 132.28, 130.39, 127.40, 127.38, 127.35, 125.79, 125.77, 125.25, 124.44, 122.64, 119.34, 118.99, 110.68, 52.23, 51.97, 49.60, 49.15, 49.08, 41.41, 29.36, 27.44. **HRMS (ESI$^+$) *m/z*:** $[M+H]^+$ calculated for $C_{28}H_{27}F_3N2O_3$: 497.2047, found: 497.2047; **HPLC:** The enantiomeric excess was determined using Phenomenex Lux C4 column (*n*-Hexane/ *i*-PrOH=80:20, flow rate=1.0 mL/min, λ= 254 nm, τ_{minor} = 14.8 min, τ_{major} = 18.9 min).

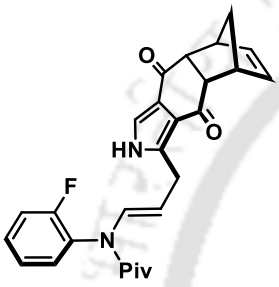

N-((E)-3-(4,9-dioxo-4,4a,5,8,8a,9-hexahydro-2H-5,8-methanobenzo[f]isoindol-1-yl)prop-1-en-1-yl)-N-(2-fluorophenyl)pivalamide (3r): Pale yellow solid, 24.5 mg, 55% yield, 86% ee; R_f = 0.5 (petroleum ether : ethyl acetate = 50:50)

^{1}H NMR (600 MHz, Chloroform-d) δ 9.64 (s, 1H), 7.49 (d, J = 14.2 Hz, 1H), 7.41 (q, J = 8.2 Hz, 1H), 7.17 (d, J = 2.8 Hz, 1H), 7.12 (td, J = 8.3, 2.7 Hz, 1H), 7.00 (d, J = 7.9 Hz, 1H), 6.93 (d, J = 9.1 Hz, 1H), 5.99 (dd, J = 5.7, 2.9 Hz, 1H), 5.94 (dd, J = 5.8, 2.8 Hz, 1H), 4.45 (dt, J = 14.4, 7.3 Hz, 1H), 3.73 (dd, J = 16.5, 7.4 Hz, 1H), 3.67 (dd, J = 16.5, 7.6 Hz, 1H), 3.54 (s, 1H), 3.52 (s, 1H), 3.25 - 3.20 (m, 2H), 1.50 (d, J = 8.6 Hz, 1H), 1.44 (d, J = 8.4 Hz, 1H), 1.08 (s, 9H). **^{13}C NMR** (151 MHz, Chloroform-d) δ 195.99, 195.80, 177.02, 163.93, 162.27, 141.46, 141.40, 136.46, 135.31, 135.28, 134.41, 130.85, 130.79, 126.34, 126.32, 125.35, 119.28, 118.81, 117.97, 117.83, 116.35, 116.21, 110.05, 52.26, 51.97, 49.61, 49.17, 49.11, 41.58, 29.44, 27.45. **HRMS (ESI$^+$) *m/z*:** $[M+H]^+$] calculated for $C_{27}H_{27}FN_2O_3$: 447.2079, found: 447.2083; **HPLC:** The enantiomeric excess was determined using Phenomenex Lux C4 column (*n*-Hexane/ *i*-PrOH=80:20, flow rate=1.0 mL/min, λ= 254 nm, τ_{minor} = 15.3 min, τ_{major} = 19.8 min).

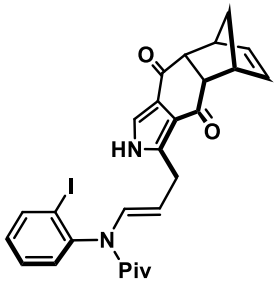

N-((E)-3-(4,9-dioxo-4,4a,5,8,8a,9-hexahydro-2H-5,8-methanobenzo[f]isoindol-1-yl)prop-1-en-1-yl)-N-(2-iodophenyl)pivalamide (3s): Pale yellow solid, 39.9 mg, 72% yield, 84% ee; R_f = 0.5 (petroleum ether : ethyl acetate = 50:50).

^{1}H NMR (500 MHz, Chloroform-d) δ 9.85 (s, 1H), 7.54 (d, J = 8.2 Hz, 1H), 7.46 (d, J = 14.2 Hz, 1H), 7.35 (s, 1H), 7.31 (t, J = 8.0 Hz, 1H), 7.17 (d, J = 2.7 Hz, 1H), 7.14 (d, J = 7.9 Hz, 1H), 5.99 (dd, J = 5.7, 2.8 Hz, 1H), 5.95 (dd, J = 5.8, 2.8 Hz, 1H), 4.45 (dt, J = 14.5, 7.3 Hz, 1H), 3.70 (qd, J = 16.2, 7.3 Hz, 2H), 3.53 (d, J = 13.5 Hz, 2H), 3.22 (qd, J = 8.4, 3.5 Hz, 2H), 1.50 (d, J = 8.5 Hz, 1H), 1.44 (d, J = 8.5 Hz, 1H), 1.07 (s, 9H). **^{13}C NMR** (151 MHz, Chloroform-d) δ 196.01, 195.87, 177.07, 141.29, 136.45, 135.30, 135.29, 134.38, 133.48, 132.20, 130.90, 130.48, 129.17, 125.30, 122.82, 119.30, 118.92, 110.40, 52.26, 51.97, 49.61, 49.16, 49.10, 41.51, 29.45, 27.43. **HRMS (ESI$^+$) *m/z*:** $[M+H]^+$ calculated for $C_{27}H_{27}IN2O_3$: 555.1140, found: 555.1142; **HPLC:** The enantiomeric excess was determined using Phenomenex Lux C4 column (*n*-Hexane/ *i*-PrOH=85:15, flow rate=1.0 mL/min, λ= 254 nm, τ_{minor} = 19 min, τ_{major} = 25.3 min).

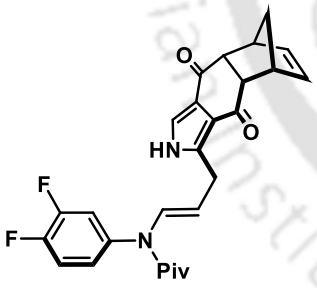

N-(3,4-difluorophenyl)-N-((E)-3-(4,9-dioxo-4,4a,5,8,8a,9-hexahydro-2H-5,8-methanobenzo[f]isoindol-1-yl)prop-1-en-1-yl)pivalamide (3t): Pale yellow solid, 20.9 mg, 53% yield, 87%; R_f = 0.5 (petroleum ether : ethyl acetate = 50:50)

^{1}H NMR (500 MHz, Chloroform-d) δ 9.44 (s, 1H), 7.45 (d, J = 14.2 Hz, 1H), 7.23 (t, J = 8.8 Hz, 1H), 7.19 (s, 1H), 7.05 (t, J = 8.7 Hz, 1H), 6.96 (d, J = 8.7 Hz, 1H), 6.00 (d, J = 5.7 Hz, 1H), 5.96 (d, J = 5.6 Hz, 1H), 4.49 – 4.40 (m, 1H), 3.75 (dd, J = 16.5, 7.2 Hz, 1H), 3.67 (dd, J = 16.4, 7.4 Hz, 1H), 3.55 - 3.53 (m, 2H), 3.31 – 3.18 (m, 2H), 1.51 (d, J = 8.8 Hz, 1H), 1.45 (d, J = 8.7 Hz, 1H). **^{13}C NMR** (126 MHz, Chloroform-d) δ 196.02, 195.73, 177.00, 136.20, 135.35, 135.27, 134.43, 125.41, 119.91, 119.77, 119.36, 118.77, 118.24, 118.10, 110.02, 52.28, 51.97, 49.63, 49.18, 49.12, 41.50, 29.41, 27.37. **HRMS (ESI$^+$) *m/z*:** $[M+H]^+$ calculated

for $C_{27}H_{27}F_2N2O_3$: 465.1985, found: 465.1999; **HPLC:** The enantiomeric excess was determined using Phenomenex Lux C4 column (*n*-Hexane/ *i*-PrOH=80:20, flow rate=1.0 mL/min, λ= 254 nm, τ_{minor} = 17.7 min, τ_{major} = 22.3 min).

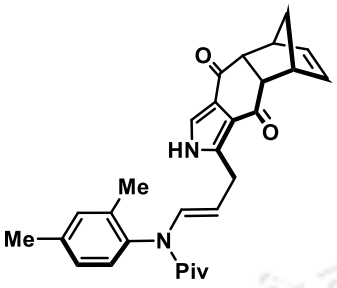

N-(2,4-dimethylphenyl)-N-((E)-3-(4,9-dioxo-4,4a,5,8,8a,9-hexahydro-2H-5,8-methanobenzo[f]isoindol-1-yl)prop-1-en-1-yl)pivalamide (3u): Pale yellow solid, 20.5mg, 45% yield, 80% ee; R_f = 0.5 (petroleum ether : ethyl acetate = 50:50)

^{1}H NMR (500 MHz, Chloroform-d) **^{1}H NMR** (600 MHz, Chloroform-d) δ 9.64 (s, 1H), 7.49 (d, J = 14.2 Hz, 1H), 7.17 (d, J = 2.8 Hz, 1H), 7.12 (s, 1H), 7.00 (d, J = 7.9 Hz, 1H), 6.93 (d, J = 9.1 Hz, 1H), 5.99 (dd, J = 5.7, 2.9 Hz, 1H), 5.94 (dd, J = 5.8, 2.8 Hz, 1H), 4.45 (dt, J = 14.4, 7.3 Hz, 1H), 3.73 (dd, J = 16.5, 7.4 Hz, 1H), 3.67 (dd, J = 16.5, 7.6 Hz, 1H), 3.54 (s, 1H), 3.52 (s, 1H), 3.25 - 3.20 (m, 2H), 2.23 (s, 3H), 2.20 (s, 3H), 1.50 (d, J = 8.6 Hz, 1H), 1.44 (d, J = 8.4 Hz, 1H), 1.08 (s, 9H). **^{13}C NMR** (126 MHz, Chloroform-d) δ 195.80, 195.74, 176.81, 138.72, 136.36, 135.09, 135.06, 134.09, 132.82, 131.93, 125.05, 122.80, 119.07, 118.72, 109.99, 52.05, 51.77, 49.42, 48.96, 48.90, 41.28, 29.27, 27.27, 23.45, 23.41. **HRMS (ESI$^+$) *m/z*:** $[M+H]^+$ calculated for $C_{29}H_{32}N2O_3$: 457.2486, found: 457.24105; **HPLC:** The enantiomeric excess was determined using Phenomenex Lux C4 column (*n*-Hexane/ *i*-PrOH=85:15, flow rate=1.0 mL/min, λ= 254 nm, τ_{minor} = 27.5 min, τ_{major} = 37.1 min).

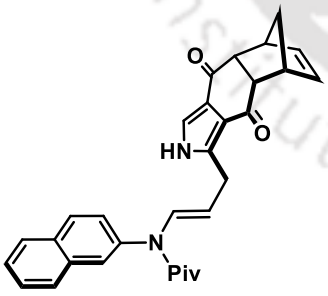

N-((E)-3-(4,9-dioxo-4,4a,5,8,8a,9-hexahydro-2H-5,8-methanobenzo[f]isoindol-1-yl)prop-1-en-1-yl)-N-(naphthalen-2-yl)pivalamide (3v): Pale yellow solid, 38.7 mg, 81% yield, 87% ee; R_f = 0.5 (petroleum ether : ethyl acetate = 50:50)

^{1}H NMR (600 MHz, Chloroform-d) δ 9.70 (s, 1H), 7.93 – 7.86 (m, 2H), 7.82 (d, J = 7.7 Hz, 1H), 7.66 (s, 1H), 7.61 – 7.50 (m, 3H), 7.27 (d, J = 6.1 Hz, 1H), 7.16 (d, J = 3.0 Hz, 1H), 5.95 (dd, J = 5.8, 3.0 Hz, 1H), 5.88 (dd, J = 5.7, 2.9 Hz, 1H), 4.41 (dt, J = 14.5, 7.4 Hz, 1H), 3.73

(dd, J = 16.3, 7.3 Hz, 1H), 3.67 (dd, J = 16.6, 7.5 Hz, 1H), 3.52 (s, 1H), 3.46 (s, 1H), 3.20 (dd, J = 8.4, 3.8 Hz, 1H), 3.16 (dd, J = 8.3, 3.9 Hz, 1H), 1.47 (d, J = 8.6 Hz, 1H), 1.40 (d, J = 8.4 Hz, 1H), 1.07 (s, 9H). **^{13}C NMR** (151 MHz, Chloroform-d) δ 195.94, 195.80, 177.62, 137.13, 136.65, 135.30, 135.21, 134.92, 133.40, 133.03, 129.75, 129.11, 128.18, 128.09, 128.06, 127.46, 127.17, 125.26, 119.18, 118.78, 110.20, 52.22, 51.93, 49.56, 49.12, 49.05, 41.57, 29.56, 27.41. **HRMS (ESI$^+$) *m/z*:** $[M+H]^+$ calculated for $C_{31}H_{30}N2O_3$: 479.2330, found: 479.2341; **HPLC:** The enantiomeric excess was determined using Phenomenex Lux C4 column (*n*-Hexane/ *i*-PrOH=80:20, flow rate=1.0 mL/min, λ= 254 nm, τ_{minor} = 21.6 min, τ_{major} = 26.5 min).

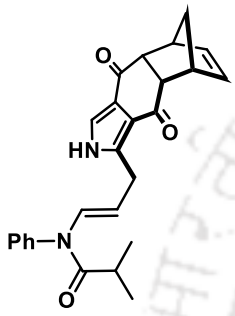

N-((E)-3-(4,9-dioxo-4,4a,5,8,8a,9-hexahydro-2H-5,8-methanobenzo[f]isoindol-1-yl)prop-1-en-1-yl)-N-phenylisobutyramide (3w): Pale yellow solid, 17 mg, 41% yield, 73% ee; R_f = 0.5 (petroleum ether : ethyl acetate = 50:50)

^{1}H NMR (400 MHz, Chloroform-d) δ 9.86 (s, 1H), 7.61 (d, J = 14.4 Hz, 1H), 7.49 - 7.39 (m, 3H), 7.20 – 7.14 (m, 3H), 5.98 (dd, J = 5.6, 2.8 Hz, 1H), 5.93 (dd, J = 5.7, 2.8 Hz, 1H), 4.52 (dt, J = 14.6, 7.4 Hz, 1H), 3.73 (qd, J = 16.1, 7.4 Hz, 2H), 3.54 (s, 1H), 3.51 (s, 1H), 3.25 – 3.15 (m, 2H), 2.46 – 2.33 (m, 1H), 1.49 (d, J = 8.5 Hz, 2H), 1.43 (d, J = 8.6 Hz, 2H), 1.25 (s, 9H), 1.03 (d, J = 6.7 Hz, 6H). **^{13}C NMR** (101 MHz, Chloroform-d) δ 196.06, 195.87, 176.53, 139.20, 136.72, 135.31, 131.74, 130.42, 129.17, 128.89, 125.29, 119.17, 118.85, 110.34, 52.26, 51.96, 49.63, 49.18, 49.12, 29.94, 27.50, 19.83. **HRMS (ESI$^+$) *m/z*:** $[M+H]^+$ calculated for $C_{26}H_{26}N2O_3$: 415.2017, found: 415.2015; **HPLC:** The enantiomeric excess was determined using Phenomenex Lux C4 column (*n*-Hexane/ *i*-PrOH=85:15, flow rate=1.0 mL/min, λ= 254 nm, τ_{minor} = 31.9 min, τ_{major} = 38.2 min).

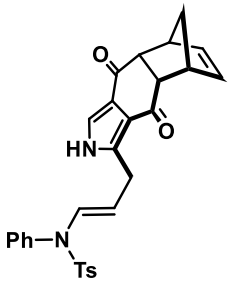

N-((E)-3-(4,9-dioxo-4,4a,5,8,8a,9-hexahydro-2H-5,8-methanobenzo[f]isoindol-1-yl)prop-1-en-1-yl)-4-methyl-N-phenylbenzenesulfonamide (3x): colourless solid, 29 mg, 59% yield, 91% ee; R_f = 0.5 (petroleum ether : ethyl acetate = 50:50).

^{1}H NMR (600 MHz, Chloroform-d) δ 9.64 (s, 1H), 7.49 (d, J = 14.2 Hz, 1H), 7.41 (q, J = 8.2 Hz, 1H), 7.17 (d, J = 2.8 Hz, 1H), 7.12 (td, J = 8.3, 2.7 Hz, 1H), 7.00 (d, J = 7.9 Hz, 1H), 6.93 (d, J = 9.1 Hz, 1H), 5.99 (dd, J = 5.7, 2.9 Hz, 1H), 5.94 (dd, J = 5.8, 2.8 Hz, 1H), 4.45 (dt, J = 14.4, 7.3 Hz, 1H), 3.73 (dd, J = 16.5, 7.4 Hz, 1H), 3.67 (dd, J = 16.5, 7.6 Hz, 1H), 3.54 (s, 1H), 3.52 (s, 1H), 3.25 - 3.20 (m, 2H), 2.41 (s, 3H), 1.50 (d, J = 8.6 Hz, 1H), 1.44 (d, J = 8.4 Hz, 1H). **^{13}C NMR** (151 MHz, Chloroform-d) δ 195.99, 195.80, 163.93, 162.27, 141.46, 141.40, 136.46, 135.31, 135.28, 134.41, 130.85, 130.79, 126.34, 126.32, 125.35, 119.28, 118.81, 117.97, 117.83, 116.35, 116.21, 110.05, 52.26, 51.97, 49.61, 49.17, 49.11, 41.58, 24.35. **HRMS (ESI$^+$) *m/z*:** $[M+Na]^+$ calculated for $C_{29}H_{26}N2O_4S$: 499.1687, found: 499.1688; **HPLC:** The enantiomeric excess was determined using Phenomenex Lux C4 column (*n*-Hexane/ *i*-PrOH=80:20, flow rate=1.0 mL/min, λ= 254 nm, τ_{minor} = 17.7 min, τ_{major} = 22.3 min).

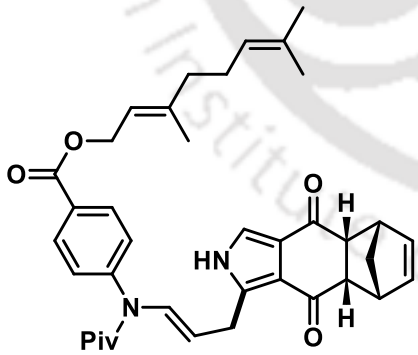

3y : Sticky solid, 48 mg, 79% yield, 80% ee; R_f = 0.5 (petroleum ether : ethyl acetate = 50:50)

^{1}H NMR (500 MHz, Chloroform-d) δ 9.96 (s, 1H), 7.55 (d, J = 8.6 Hz, 2H), 7.49 (d, J = 14.3 Hz, 1H), 7.16 (d, J = 2.8 Hz, 1H), 7.06 (d, J = 8.5 Hz, 2H), 5.97 (dd, J = 5.7, 2.8 Hz, 1H), 5.93 (dd, J = 5.6, 2.8 Hz, 1H), 5.30 (s, 1H), 5.18 (s, 2H), 5.08 (s, 1H), 4.45 (dt, J = 14.4, 7.3 Hz, 1H), 3.73 (dd, J = 16.5, 7.4 Hz, 1H), 3.67 (dd, J = 16.5, 7.6 Hz, 1H), 3.54 (s, 1H), 3.52 (s, 1H),

3.25 - 3.20 (m, 2H), 2.21 – 2.08 (m, 4H), 1.71 (s, 3H), 1.62 (s, 3H), 1.60 (s, 3H), 1.50 (d, J = 8.6 Hz, 1H), 1.44 (d, J = 8.4 Hz, 1H), 1.08 (s, 9H). **^{13}C NMR** (126 MHz, Chloroform-d) δ 195.27, 193.52, 160.68, 135.80, 135.37, 128.27, 125.51, 122.56, 122.17, 52.99, 52.81, 51.72, 49.49, 49.27, 49.05. **HRMS (ESI$^+$) *m/z*:** $[M+H]^+$ calculated for $C_{38}H_{44}N2O_3$: 609.3323, found: 609.3327. **HPLC:** The enantiomeric excess was determined using Phenomenex Lux C4 column (*n*-Hexane/ *i*-PrOH=95:5, flow rate=1.0 mL/min, λ= 254 nm, τ_{major} = 46.9 min, τ_{minor} = 53.6 min).

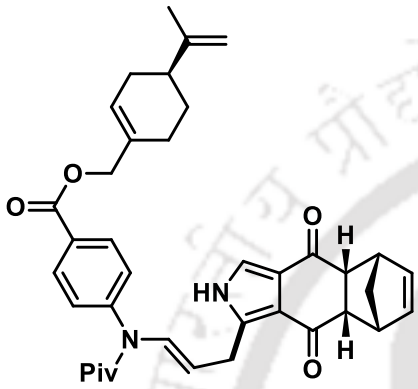

3z : Orenge solid, 37 mg, 61% yield, >20:1 dr; R_f = 0.5 (petroleum ether : ethyl acetate = 50:50).

^{1}H NMR (500 MHz, Chloroform-d) δ 9.72 (s, 1H), 7.54 (d, J = 14.3 Hz, 1H), 7.17 (d, J = 2.8 Hz, 1H), 7.08 (d, J = 8.9 Hz, 2H), 6.92 (d, J = 8.9 Hz, 2H), 5.99 (dd, J = 5.7, 2.8 Hz, 1H), 5.95 (dd, J = 5.7, 2.7 Hz, 1H), 5.84 (s, 1H), 4.72 (d, J = 6.6 Hz, 2H), 4.40 (s, 2H), 4.41 (dt, J = 14.4, 7.4 Hz, 1H), 3.83 (s, 3H), 3.78 – 3.62 (m, 2H), 3.54 (s, 1H), 3.51 (s, 1H), 3.26 - 3.18 (m, 2H), 2.17 (q, J = 9.9, 6.3 Hz, 4H), 1.90 – 1.83 (m, 1H), 1.74 (s, 3H), 1.52 (dt, J = 11.9, 6.0 Hz, 1H), 1.50 (d, J = 8.5 Hz, 1H), 1.43 (d, J = 8.6 Hz, 1H), 1.05 (s, 9H). **^{13}C NMR** (126 MHz, Chloroform-d) δ 196.02, 195.73, 166.43, 177.00, 136.20, 135.35, 135.27, 134.43, 125.41, 119.91, 119.77, 119.36, 118.77, 118.24, 118.10, 110.02, 52.28, 82.0, 72.5, 51.97, 49.63, 49.18, 49.12, 41.50, 41.0, 30.6, 29.41, 27.37, 26.42, 20.93. **HRMS (ESI$^+$) *m/z*:** $[M+H]^+$ calculated for $C_{38}H_{44}N_2O_5$: 607.3167, found: 607.3167.

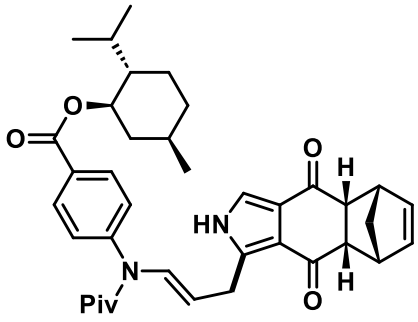

3z' : White solid, 38.4 mg, 61% yield, >20:1 dr; R_f = 0.5 (petroleum ether : ethyl acetate = 50:50)

^{1}H NMR (400 MHz, Chloroform-d) δ 9.79 (s, 1H), 8.08 (d, J = 8.0 Hz, 2H), 7.50 (d, J = 14.2 Hz, 1H), 7.25 (d, J = 4.5 Hz, 2H), 7.15 (d, J = 2.8 Hz, 1H), 5.96 (dd, J = 5.8, 2.8 Hz, 1H), 5.91 (dd, J = 5.9, 2.8 Hz, 1H), 4.94 (td, J = 10.9, 4.5 Hz, 1H), 4.39 (dt, J = 14.4, 7.3 Hz, 1H), 3.68 (qd, J = 16.1, 7.2 Hz, 2H), 3.52 (s, 1H), 3.49 (s, 1H), 3.20 (tt, J = 8.5, 4.3 Hz, 2H), 2.12-2.09 (m, 1H),

2.04 – 1.87 (m, 2H), 1.74-1.69 (m, 2H), 1.59-1.50 (m, 2H), 1.48 (d, J = 8.9 Hz, 1H), 1.42 (d, J = 8.9 Hz, 1H), 1.30 – 1.20 (m, 2H), 1.06 (s, 9H), 0.91 (d, J = 6.9 Hz, 6H), 0.79 (d, J = 6.9 Hz, 3H). **^{13}C NMR** (101 MHz, Chloroform-d) δ 195.74, 176.81, 165.07, 143.79, 136.25, 134.18, 135.06, 131.21, 130.79, 130.27, 125.10, 119.07, 118.63, 110.16, 75.50, 52.04, 51.76, 49.39, 48.94, 48.87, 47.24, 41.38, 40.97, 34.26, 31.46, 29.28, 27.29, 26.44, 23.52, 22.02, 20.83, 16.43. **HRMS (ESI$^+$) *m/z*:** $[M+H]^+$ calculated for $C_{15}H_{13}NO_4$: 611.3480, found: 611.3481.

5.9. NMR spectra and HPLC chromatogram:

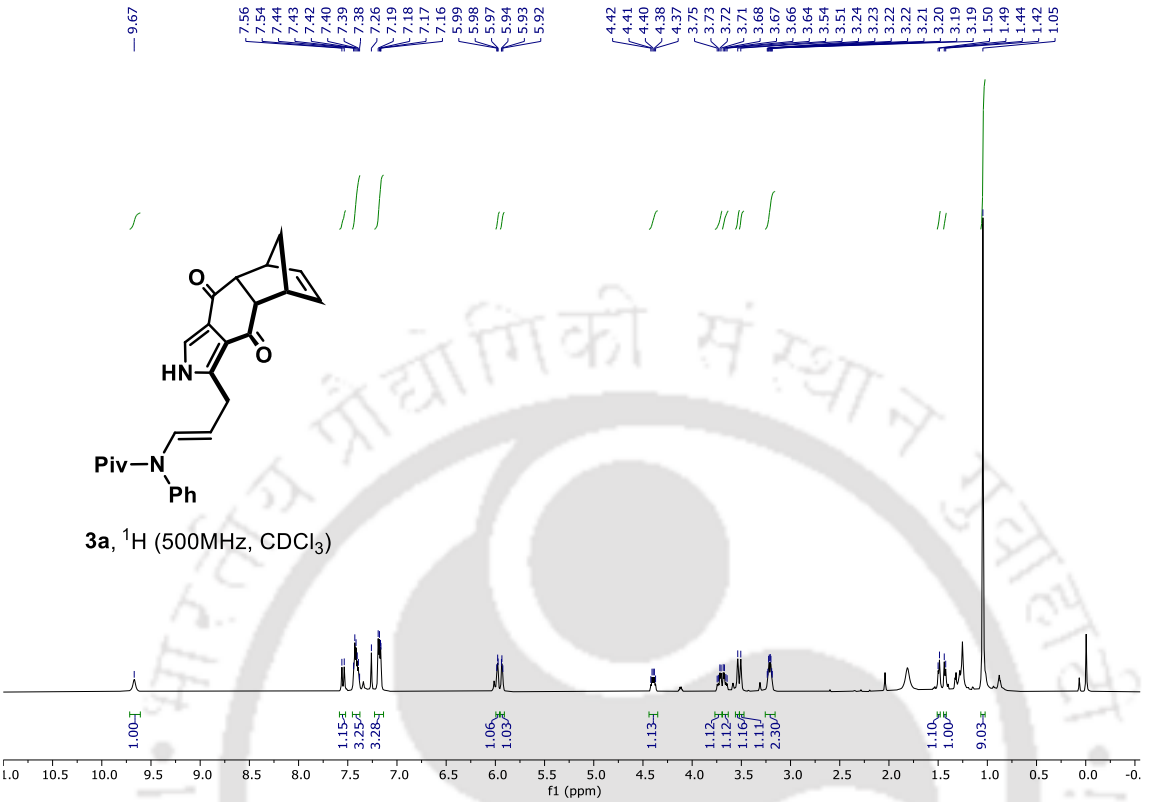

3a, ^{1}H (500MHz, $CDCl_3$)

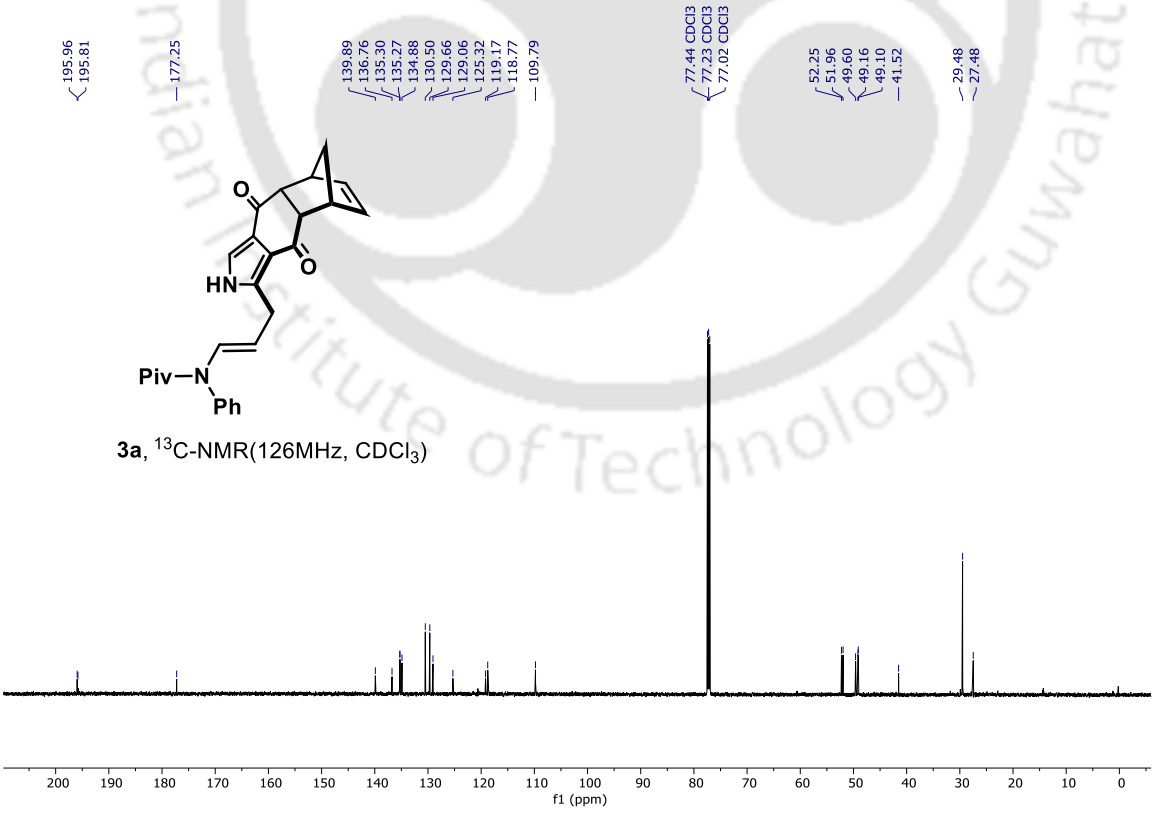

3a, ^{13}C-NMR(126MHz, $CDCl_3$)

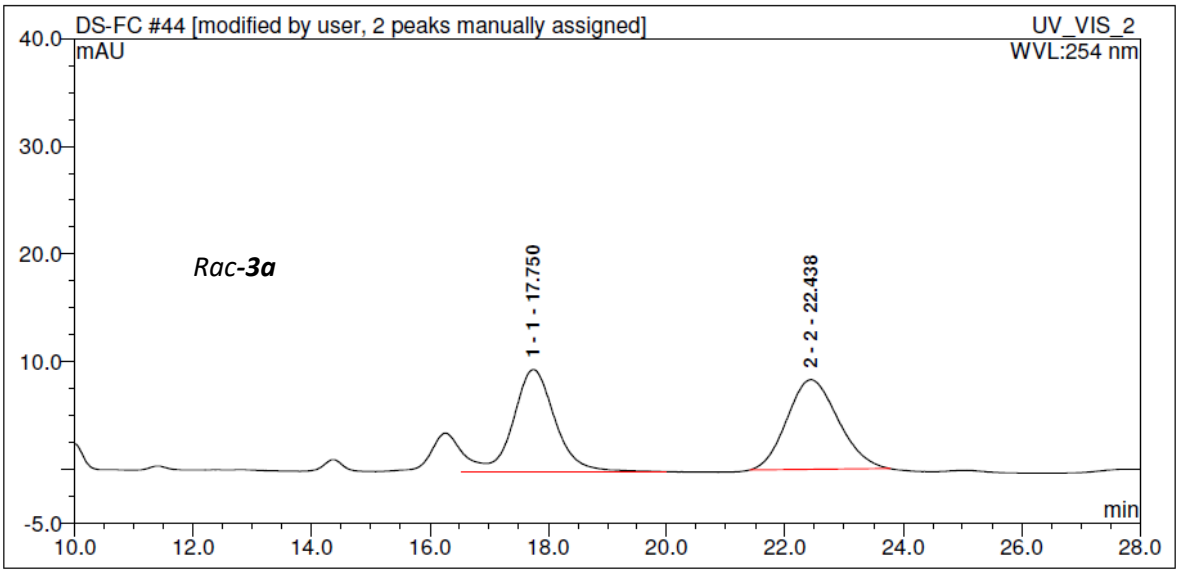

	Peak Name	Ret.Time (detected) min	Area mAU*min	Rel.Area(ident.) %	Height mAU	Amount
1	1	17.75	8.056602	49.1702814	9.48567	n.a.
2	2	22.43833333	8.328502	50.8297186	8.31641	n.a.

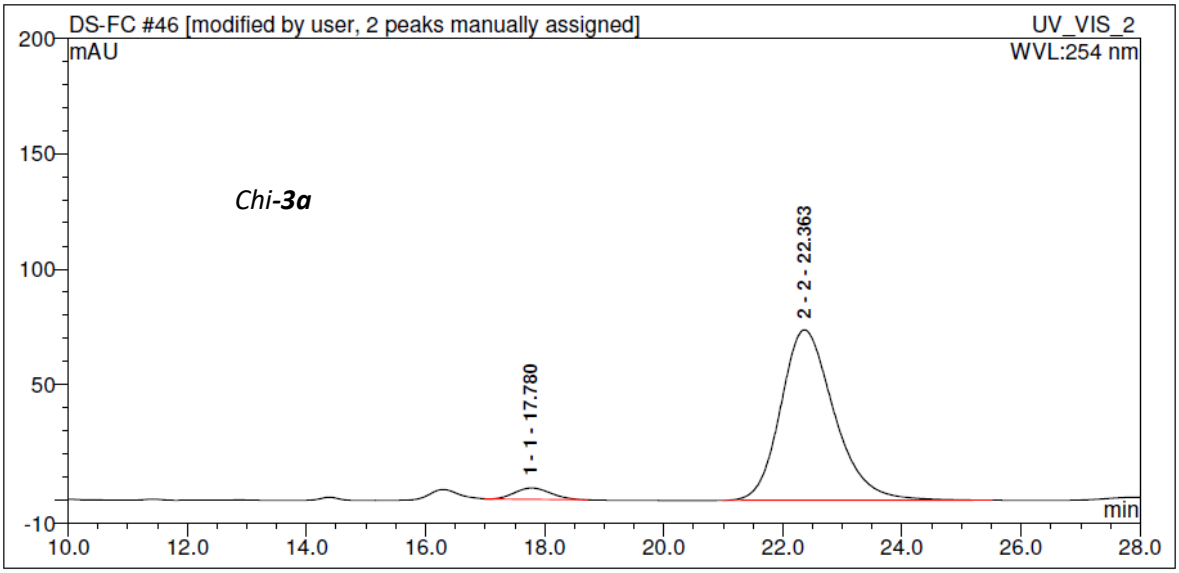

	Peak Name	Ret.Time (detected) min	Area mAU*min	Rel.Area(ident.) %	Height mAU	Amount
1	1	17.78	3.409413	4.2520568	4.87762	n.a.
2	2	22.36333333	76.77327	95.7479432	73.72404	n.a.

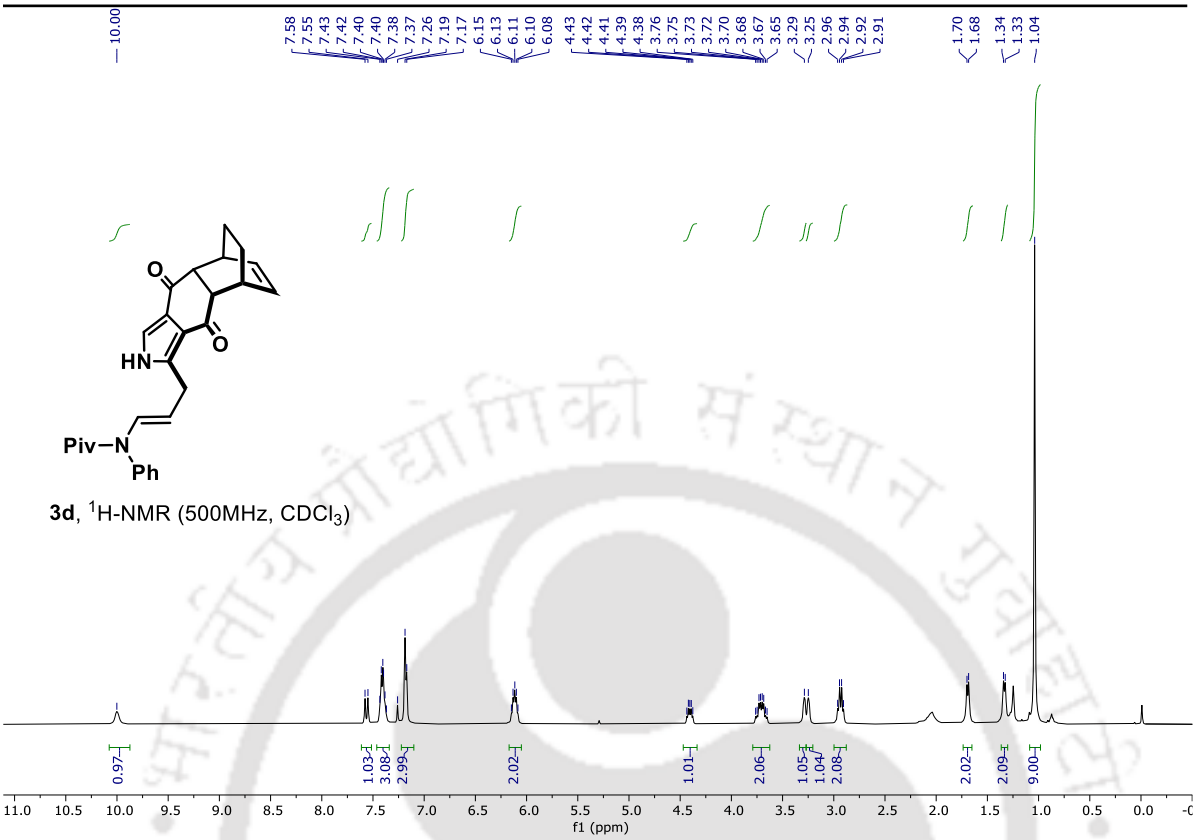

3d, ^{1}H-NMR (500MHz, $CDCl_3$)

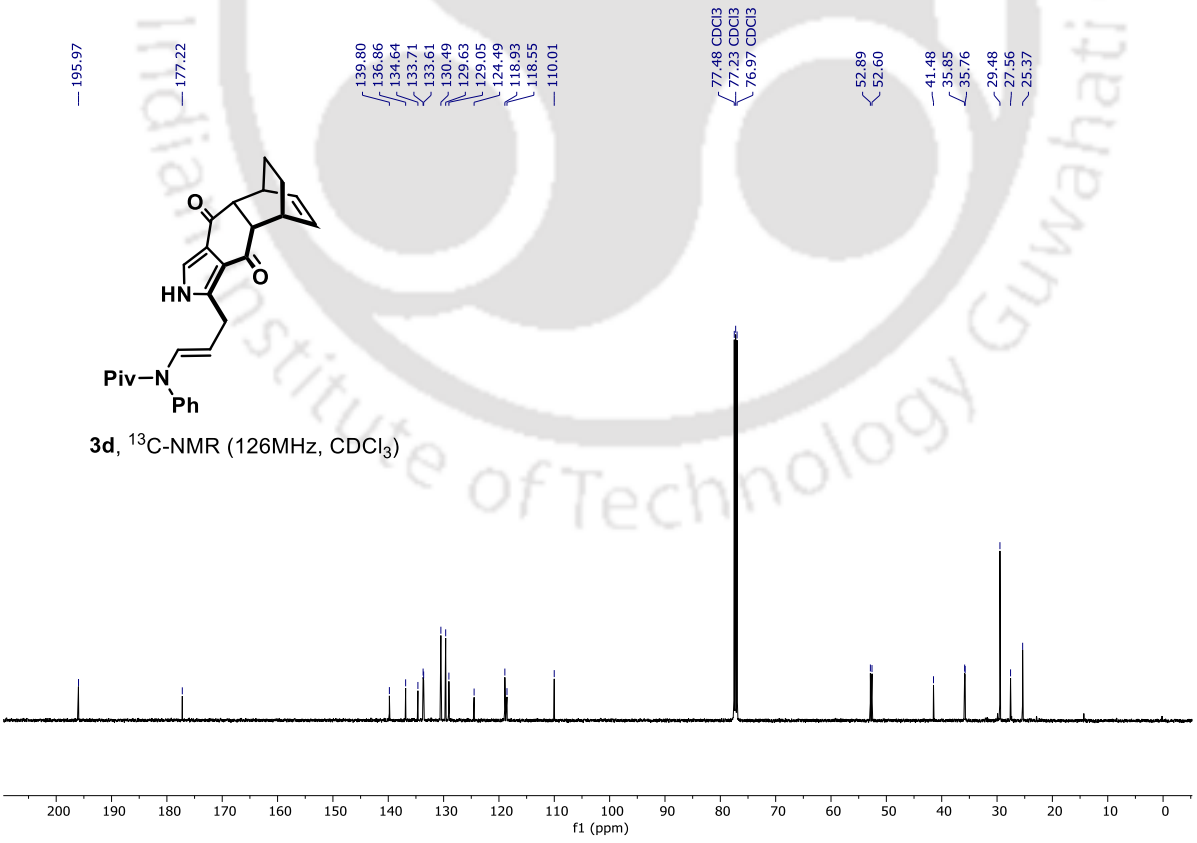

3d, ^{13}C-NMR (126MHz, $CDCl_3$)

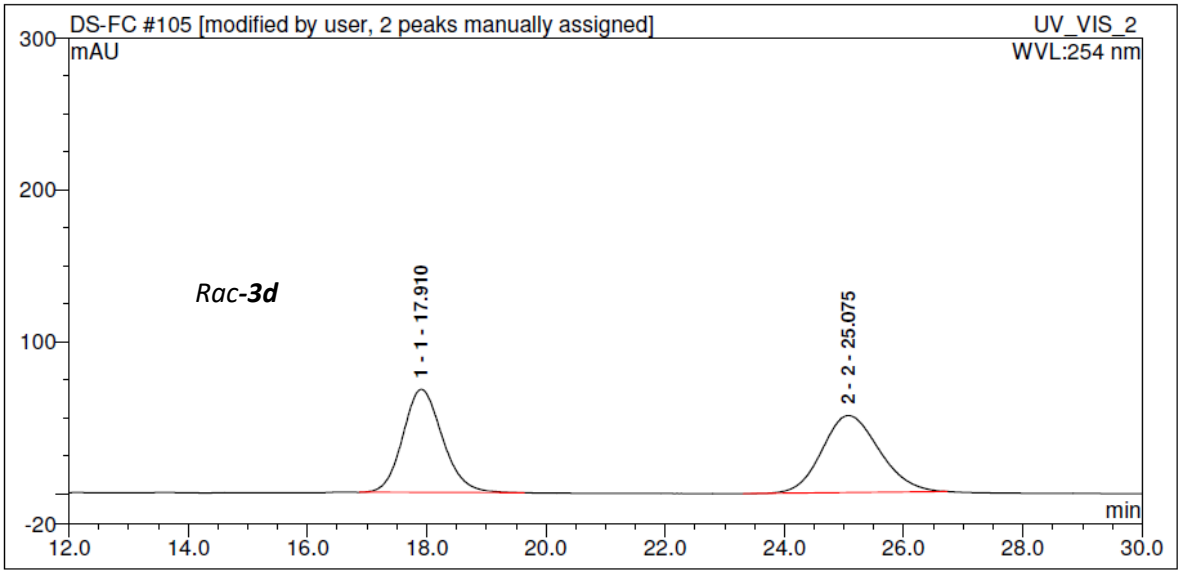

	Peak Name	Ret.Time (detected) min	Area mAU*min	Rel.Area(ident.) %	Height mAU	Amount
1	1	17.91	52.30217	48.12074367	67.81444	n.a.
2	2	25.075	56.38728	51.87925633	50.65882	n.a.

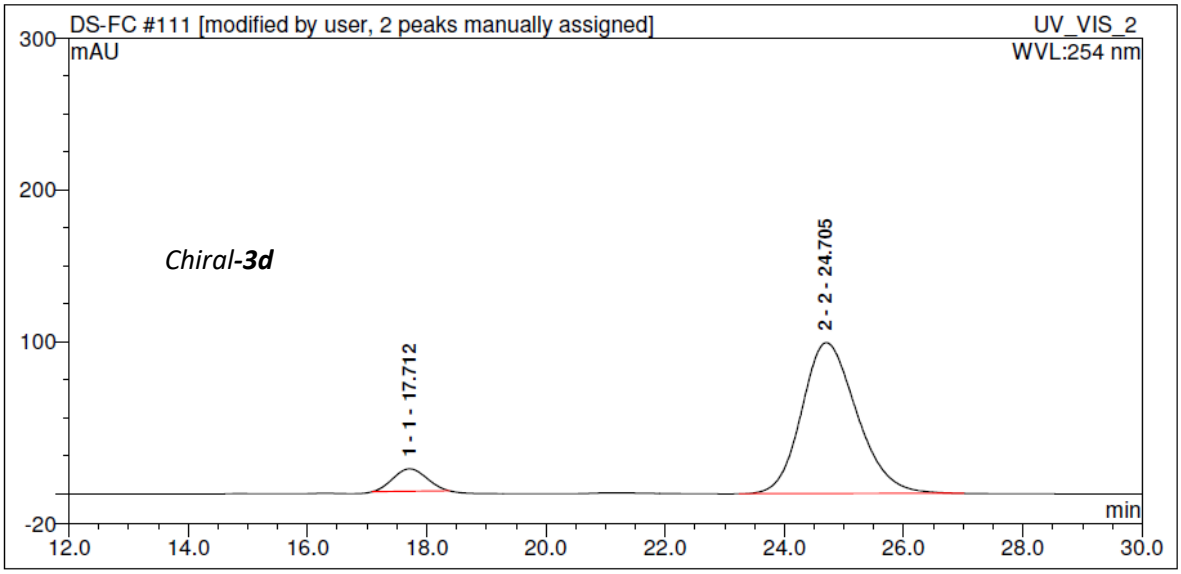

	Peak Name	Ret.Time (detected) min	Area mAU*min	Rel.Area(ident.) %	Height mAU	Amount
1	1	17.71166667	9.623323	8.271039115	14.81102	n.a.
2	2	24.705	106.7263	91.72896088	99.3511	n.a.

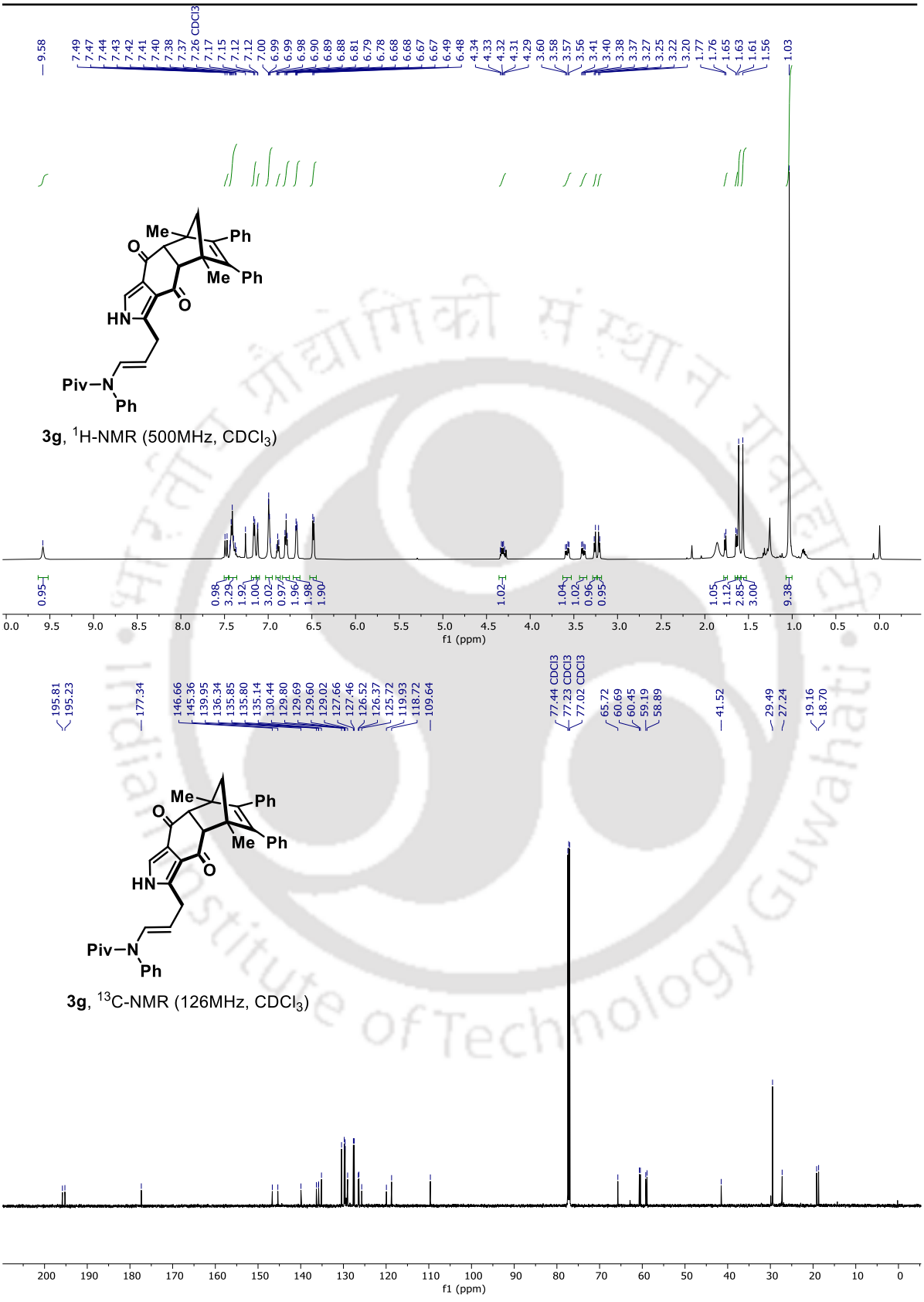

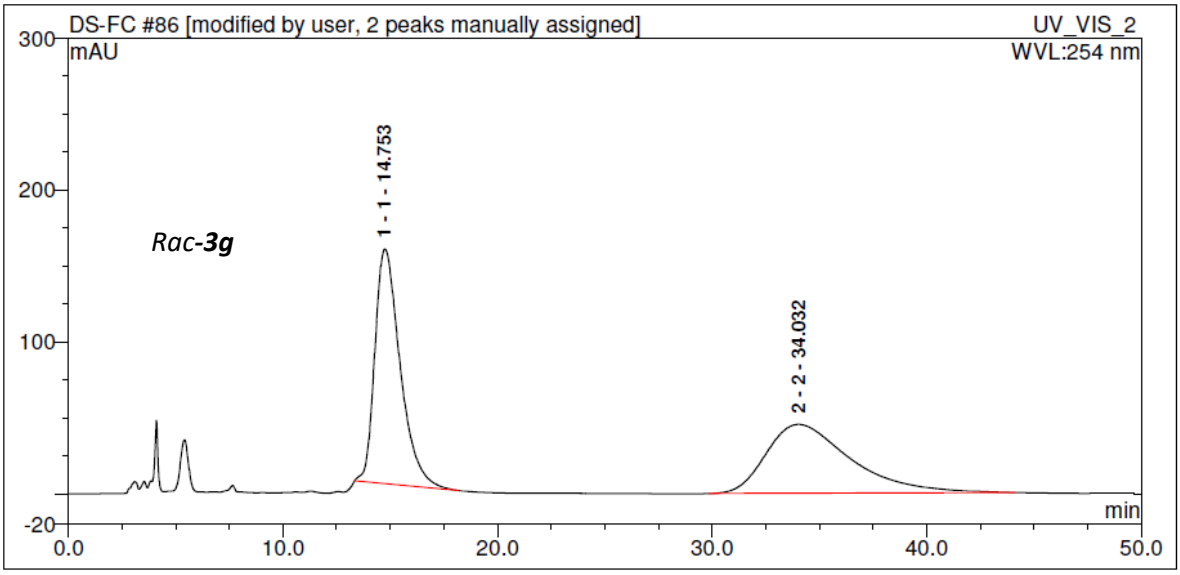

	Peak Name	Ret.Time (detected) min	Area mAU*min	Rel.Area(ident.) %	Height mAU	Amount
1	1	14.75333333	211.1139	50.53764187	154.5478	n.a.
2	2	34.03166667	206.622	49.46235813	45.2921	n.a.

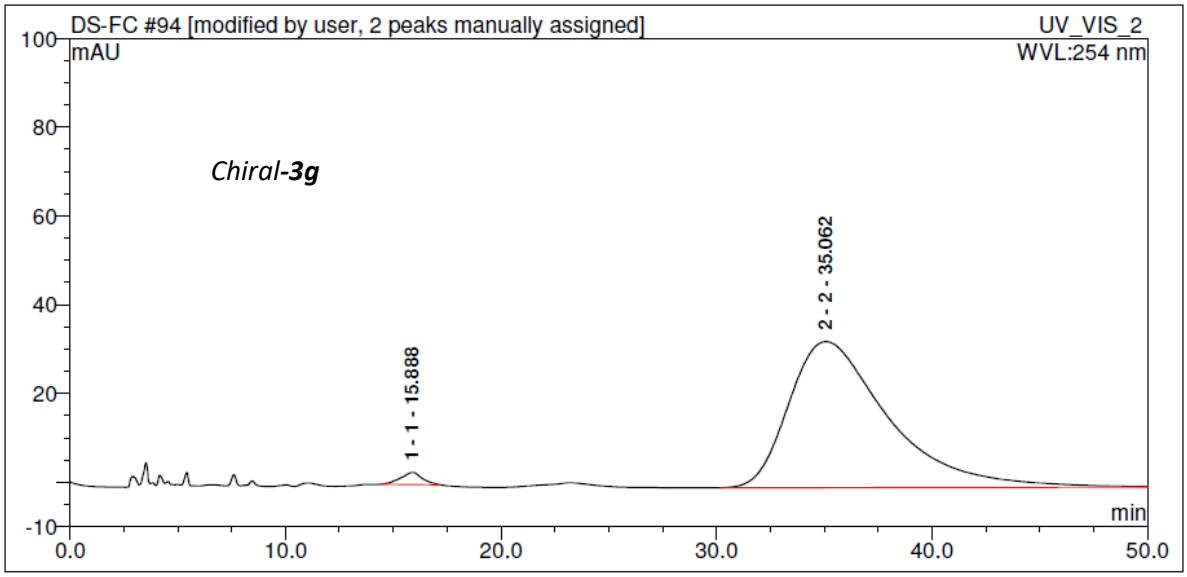

	Peak Name	Ret.Time (detected) min	Area mAU*min	Rel.Area(ident.) %	Height mAU	Amount
1	1	15.88833333	3.161897	1.761902115	2.74774	n.a.
2	2	35.06166667	176.2974	98.23809788	32.88531	n.a.

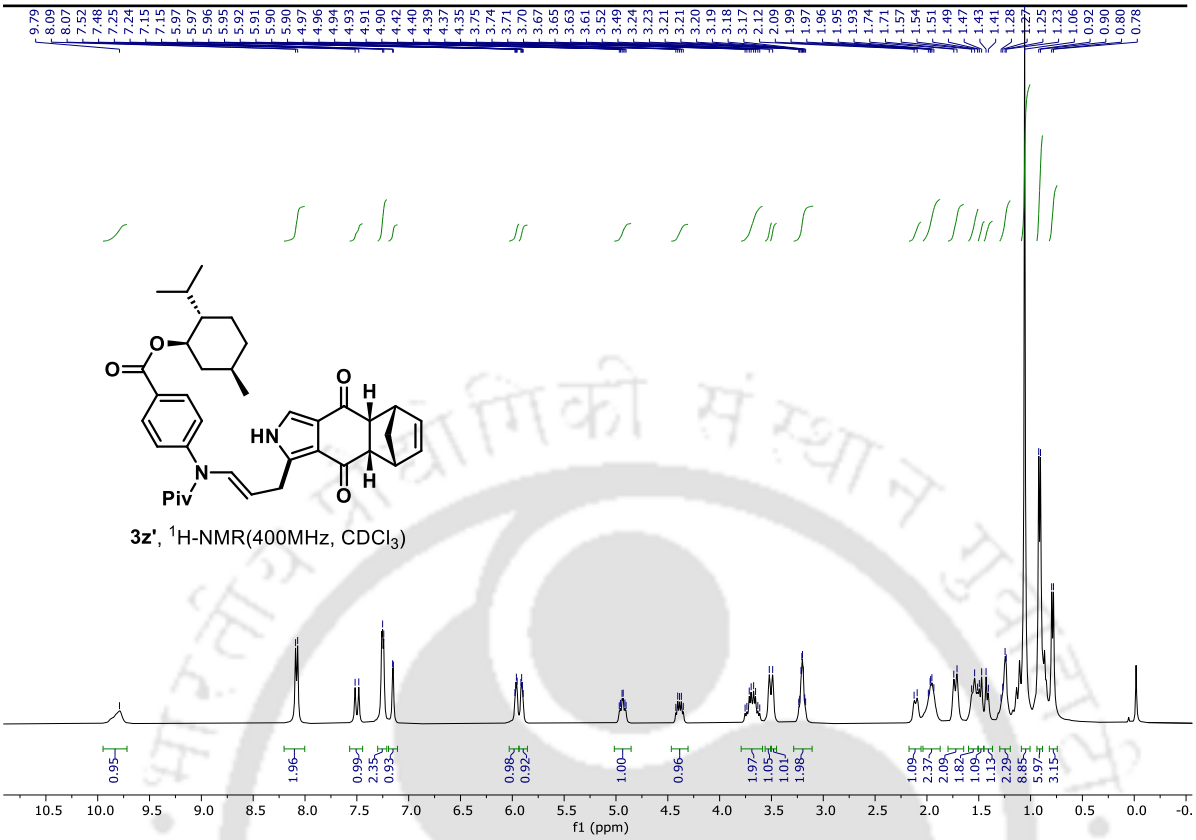

3z', ^{1}H-NMR(400MHz, $CDCl_3$)

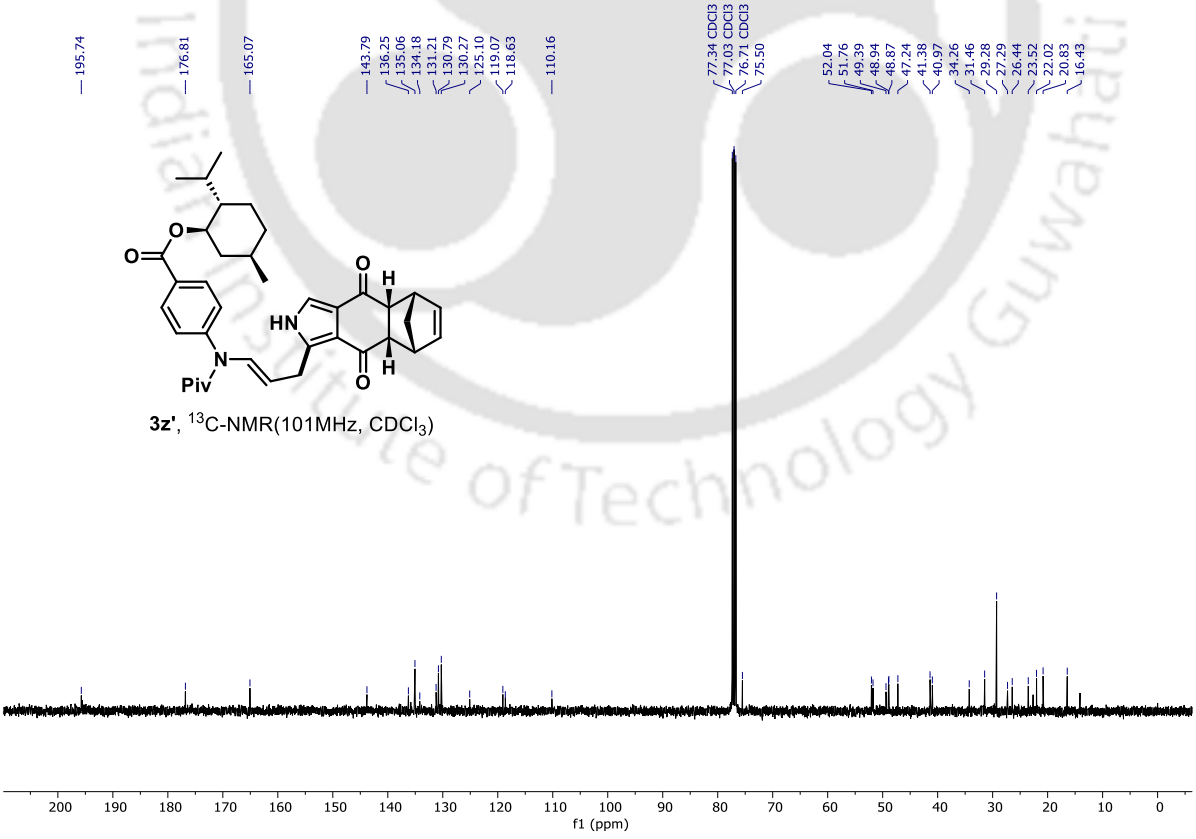

3z', ^{13}C-NMR(101MHz, $CDCl_3$)

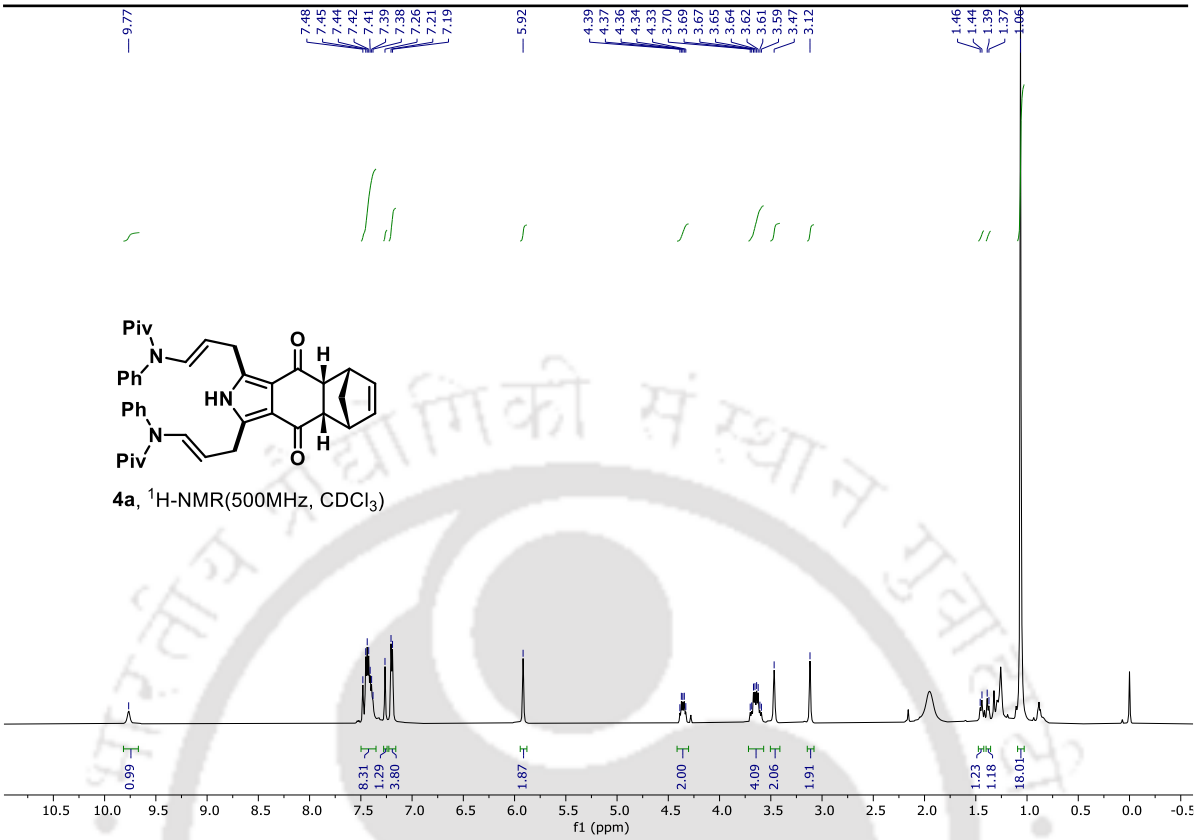

4a, ^{1}H-NMR(500MHz, $CDCl_3$)

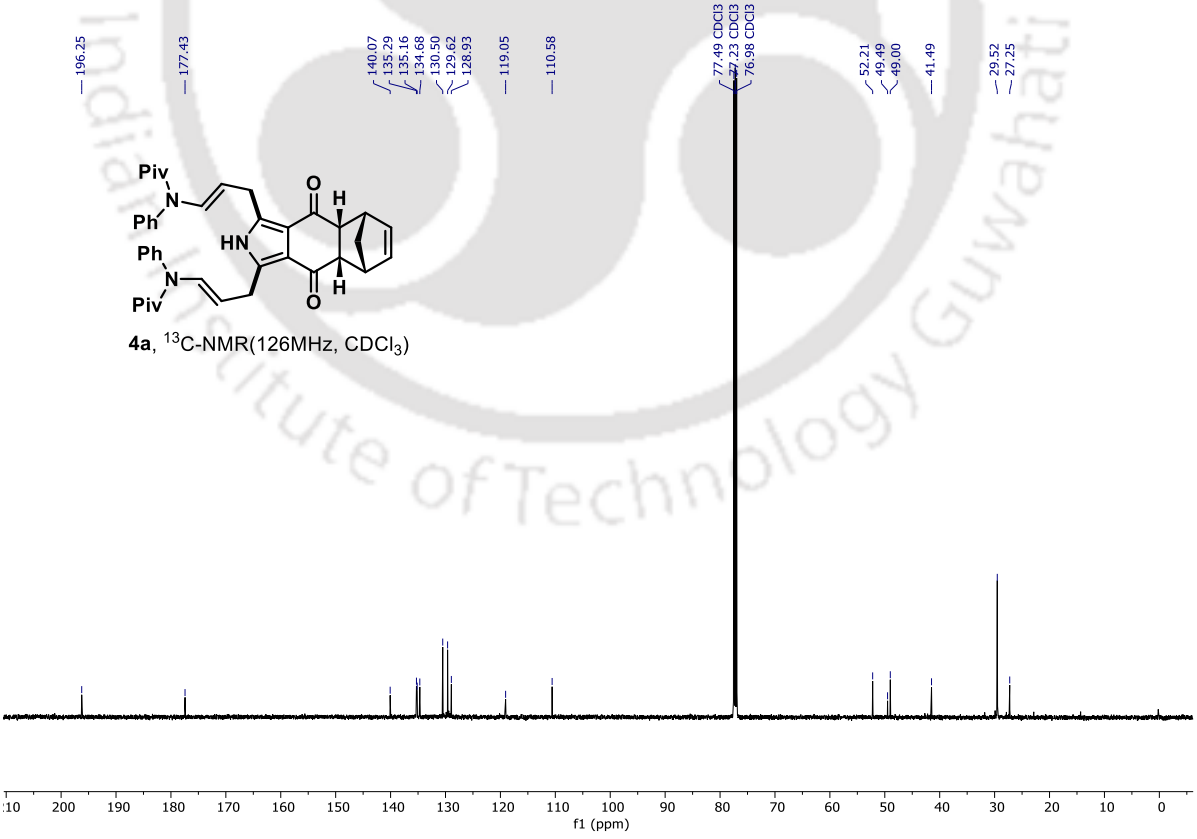

4a, ^{13}C-NMR(126MHz, $CDCl_3$)

5.10. References:

1. M. J. F. Calvete, S. M. Pinto, *Curr. Org. Synth.* **2017**, *14*, 704; b) S. Ahmad, O. Alam, Mohd. J. Naim, M. Shaquiquzzaman, M. M. Alam, M. Iqbal, *Eur. J. Med. Chem.* **2018**, *157*, 527–561.
2. For selected recent reviews, see: a) B. Borah, K. D. Dwivedi, L. R. Chowhan, *RSC Adv.* **2021**, *11*, 13585–13601; b) I. V. Efimov, L. N. Kulikova, A. R. Miftyakhova, M. D. Matveeva, L. G. Voskressensky *ChemistrySelect* **2021**, *6*, e202103486; c) T. Shi, G. Yin, X. Wang, Y. Xiong, Y. Peng, S. Li, Y. Zeng, Zhen Wang, *Green Synthesis and Catalysis* **2023**, *4*, 20.
3. For reviews, see: a) S. Thirumalairajan, B. M. Pearce, A. Thompson, *Chem. Commun*. **2010**, *46*, 1797; b) J. W. Campbell, M. J. Cotnam, F. R. Annan, J. W. Hilborn, A. Thompson, *Chem. Commun.*, **2024**, 60, 11385.
4. For selected transition metal catalysed examples, see: a) Z. Cao, Y. Liu, Z. Liu, X. Feng, M. Zhuang, H. Du, *Org. Lett.* **2011**, *13*, 2164; (b) C.-X. Zhuo, Q.-F. Wu, Q. Zhao, Q.-L. Xu, S.-L. You, *J. Am. Chem. Soc*. **2013**, *135*, 8169; (c) C.-X. Zhuo, Q. Cheng, W.-B. Liu, Qi. Zhao, and S.-L. You, *Angew. Chem. Int. Ed*. **2015**, *54*, 847; (d) T. Das. P. Saha and V. K. Singh, *Org. Lett*. **2015**, *17*, 5088; (e) C.-X. Zhuo, X. Zhang, and S.-L. You, *ACS Catal*. **2016**, *6*, 5307; (f) L. Huang, Y. Cai, C. Zheng, L.-X. Dai and S.-L. You *Angew. Chem. Int. Ed*. **2017**, *56*, 1054; (g) S. Iwase, Y. Suzuki, S. Tanaka, and M. Kitamura, *Org. Lett*. **2020**, *22*, 1929; (h) L. Huang, J.-H. Xie, Y. Cai, C. Zheng, X.-L. Hou, L.-X. Dai and S.-L. You, *Chem. Commun*. **2021**, *57*, 5390.
5. For selected organocatalytic examples, see: a) N. A. Paras, D. W. C. MacMillan, *J. Am. Chem. Soc*. **2001**, *123*, 437; b) G. Li, G. B. Rowland, E. B. Rowland, J. C. Antilla, *Org. Lett*. **2007**, *9*, 4065; (c) I. T. Raheem, P. S. Thiara, E. N. Jacobsen, *Org. Lett*. **2008**, *10*, 1577; (d) Q. Yin, S.-L. You, *Chem. Sci*. **2011**, *2*, 1344; (e) S.-G. Wang, S.-L. You, *Angew. Chem. Int. Ed.* **2014**, *53*, 2194; (f) G. P. Y. Kok, P.-L. Shao, J.-Y. Liao, S. N. F. B. S. Ismail, W. Yao, Y. Lu, Y. Zhao, *Chem.-Eur. J.* **2018**, *24*, 10513; (g) Y. You, W.-Y. Lu, K.-X. Xie, J.-Q. Zhao, Z.-H. Wang, W.-C. Yuan, *Chem Commun*. **2019**, *55*, 8478; (h) M. Hatano, k. Toh, K. Ishihara, *Org. Lett*. **2020**, *22*, 9614; (i) M. A. Abozeid, H. Y. Kim, K. Oh, *Org. Lett*. **2022**, *24*, 1812; (j) T. Uchikura, K. Aruga, R. Suzuki, T. Akiyama, *Org. Lett*. **2022**, *24*, 4699. For a review, see: (k) D. Gaviña, M. Escolano, J. Torres, G. Alzuet-Piña, M. Sánchez-Roselló, C. del Pozo, *Adv. Synth Catal*. **2021**, *363*, 3439.
6. For synthesis of axially chiral pyrroles, see: a) L. Zhang, J. Zhang, J. Ma, D.-J. Cheng, B. Tan, *J. Am. Chem. Soc.* **2017**, *139*, 1714; b) S.-C. Zheng, Q. Wang, J. Zhu, *Angew. Chem. Int. Ed.* **2019**, *58*, 1494; c) S.-C. Zheng, Q. Wang, and J. Zhu, *Angew. Chem. Int. Ed*. **2019**,

58, 9215; d) X.-L. He, H.-R. Zhao, X. Song, B. Jiang, W. Du, Y.-C. Chen, *ACS Catal*. **2019**, *9*, 4374; e) Y.-B. Wang, Q.-H. Wu, Z.-P. Zhou, S.-H. Xiang, Y. Cui, P. Yu, B. Tan, *Angew. Chem. Int. Ed*. **2019**, *58*, 13443; f) K.-W. Chen, Z.-H. Chen, S. Yang, S.-F. Wu, Y.-C. Zhang, F. Shi, *Angew. Chem. Int. Ed*. **2022**, *61*, e202116829; g) C. X. A. Tan, R. Li, F. Zhang, L. Dai, N. Ullah, Y. Lu, *Angew. Chem. Int. Ed*. **2022**, *61*, e202209494; h) Y.-B. Chen, L.-G. Liu, C.-M. Chen, Y.-X. Liu, B. Zhou, X. Lu, Z. Xu, L.-W. Ye, *Angew. Chem. Int. Ed.* **2023**, *62*, e202303670.

7. For the reports on the de novo synthesis of chiral arenes, see: a) T. Zhu, Y. Liu, M. Smetankova, S. Zhuo, C. Mou, H. Chai, Z. Jin, Y. R. Chi, Angew. Chem. Int. Ed. 2019, 58, 15778; b) J.-M. Hu, J.-Q. Zhang, B.-B. Sun, J.-B. Chen, J.-Q. Yu, X.-P. Yang, H.-P. Lv, Z. Wang, X.-W. Wang, Org. Lett. 2019, 21, 8582; c) B. Ghosh, M. S. Harariya, S. Mukherjee, Angew. Chem. Int. Ed. 2022, 61, e202204523; d) S. Mondal, S. Mukherjee, Org. Lett. 2022, 24, 8300.
8. N. A. Paras, D. W. C. MacMillan, *J. Am. Chem. Soc.* **2001**, *123*, 4370.
9. C. Palomo, M. Oiarbide, B. G. Kardak, J. M. Garcia, A. Linden, J. *Am. Chem. Soc.* **2005**, *127*, 4154.
10. B. M. Trost, C. Muller, *J. Am. Chem. Soc*. **2008**, *130*, 2438.
11. Y.-F. Sheng, Q. Gu, A.-J. Zhang, S.-L. You, *J. Org. Chem*. **2009**, *74*, 6899
12. S. Nakamura, N. Matsuda, M. Ohara, *Chem. Eur. J.* **2016**, *22*, 9478
13. H. Lou, Y. Wang, E. Jin, X. Lin, *J. Org. Chem.* **2016**, *81*, 2019
14. Z. Wei, J. Zhang, H. Yang, G. Jiang. *Adv. Synth. Catal.* **2019**, *361*, 3694.
15. Manabu Hatano, Kohei Toh, Kazuaki Ishihara, *Org. Lett*. **2020**, *22*, 9614.
16. Q.-Y. Wang, T.-F. Liu, L.-F. Chu, Y. Yao, C.-D. Lu, *Chem. Commun*. **2021**, *57*, 11992.
17. T. Uchikura, K. Aruga, R. Suzuki, T. Akiyama, *Org. Lett*. **2022**, *24*, 4699.
18. A. Beriša, M. Gredičak, *Org. Biomol. Chem*. **2023**, *21*, 3381.
19. A. E. Hurtley, E. A. Stone, A. J. Metrano, S. J. Miller, *J. Org. Chem*. **2017**, *82*, 11326.
20. X. Xiong, T. Zheng, X. Wang, Y.-L. S. Tse, Y.-Y. Yeung, *Chem* **2020**, *6*, 919.
21. M. Bandini, A. Umanie-Ronchi, *Catalytic Asymmetric Friedel-Crafts Alkylations*; Wiley-VCH: Weinheim, Germany, 2009.
22. For selected reviews, see: a) T. B. Poulsen, K. A. Jorgensen, *Chem. Rev*. **2008**, *108*, 2903; b) V. Terrasson, R. M. de Figueiredo, J. M. Campagne, *Eur. J. Org. Chem*. **2010**, 2635; c) M. Zeng, S. L. You, *Synlett* **2010**, 1289; d) T. Ahmad, S. Khan, N. Ullah, *ACS Omega* **2022**, *7*, 35446.

23. For selected examples, see: a) C. Romano, M. Jia, M. Monari, E. Manoni, M. Bandini, *Angew. Chem. Int. Ed*. **2014**, *53*, 13854; b) E. Manoni, A. Gualandi, L. Mengozzi, M. Bandini, P. G. Cozzi, *RSC Adv*. **2015**, *5*, 10546; c) X. Yang, F. D. Toste, *Chem. Sci*. **2016**, *7*, 2653; d) L. Villar, U. Uria, Jose I. Martinez, L. Prieto, E. Reyes, L. Carrillo, J. L. Vicario, *Angew. Chem. Int. Ed*. **2017**, *56*, 10535; e) K. Yang, X. Bao, S. Liu, J. Xu, J. Qu, B. Wang, *Eur. J. Org. Chem*. **2018**, 6469; e) B. Yang, X. Zhai, S. Feng, D. Hu, Y. Deng, Z. Shao, *Org. Lett.* **2019**, *21*, 330; f) R. Blieck, S. Lemouzy, A. van der Lee, M. Taillefer, F. Monnier, *Org. Lett*. **2021**, *23*, 9199; g) J. Wang, F. He, X. Yang, *Nature Commun*. **2021**, *12*, 6700; h) J. Wei, J. Zhang, J. K. Cheng, S.-H. Xiang, B. Tan, *Nature Chem*. **2023**, *15*, 647.

24. For reviews, see: a) X. Li, Y. Liu, N. Ding, X. Tan, Z. Zhao, *RSC Adv*. **2020**, *10*, 36818; b) E. Manoni, M. Bandini, *Eur. J. Org. Chem*. **2016**, 3135.

➢ **Publication:**

1. **Rupkumar Khuntia**, Sanat Kumar Mahapatra, Lisa Roy, Subhas Chandra Pan*, Structurally divergent enantioselective synthesis of benzofuran fused azocine derivatives and spiro-cyclopentanone benzofurans enabled by sequential catalysis. *Chem. Sci*., **2023**, *14*, 10768–10776.

2. **Rupkumar Khuntia**, Diptendu Maity, Subhas Chandra Pan*. Catalytic Asymmetric De Novo Synthesis of Chiral Pyrroles Through Desymmetrizing Oxidative [3+2]-Cycloaddition and the Van Leusen Reaction. *Chem. Eur. J.* **2025**, *31*, e202404511.

3. **Rupkumar Khuntia**, Subhrajit Karmakar, Koyal Roy, Kalishankar Bhattacharyya and Subhas Chandra Pan*. Organocatalytic Regio- and Enantioselective Friedel-Crafts Alkylation of N-Aryl Anilines with Aurone-Derived Azadienes: Access to Benzofuran Embedded Triarylmethanes. *Chem Asian J*. **2025**, *20*, e00722.

4. **Rupkumar Khuntia**, Subhas Chandra Pan*. Organocatalytic Asymmetric Desymmetrizing Friedel-Crafts Reaction of Prochiral 3,4-Fused Pyrroles. (*Org. Lett*. **2025**, accepted)

5. **Rupkumar Khuntia**, Chandan Gharui, Subhas Chandra Pan*. Handbook of CH-functionalization: Organocatalytic Allylic and Benzylic C-H Bond Functionalization, Wiley. **2022**. DOI: 10.1002/9783527834242.chf0212.

➢ **Conferences:**

1. Participated in poster presentation in **Frontiers in Chemical Sciences** (December 2022) at IIT Guwahati.
2. Participated in poster presentation in **JNOST-XVIII** (October 2023) at IISER Pune.
3. Participated in poster presentation in **North-East Research Conclave** (May 2022) at IIT Guwahati.